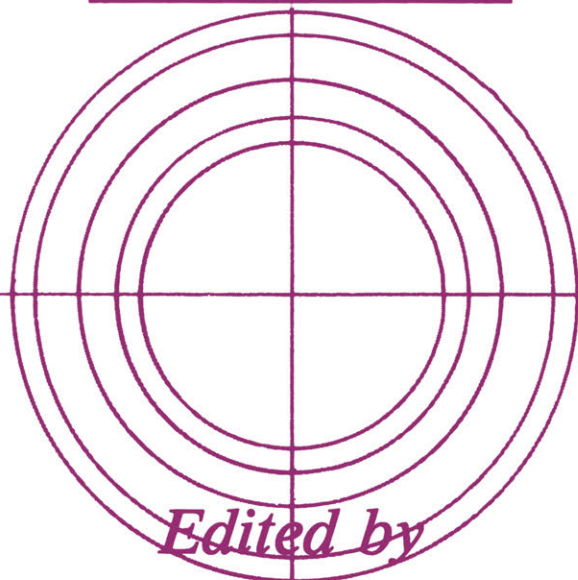


MODERN ANALYTICAL CHEMISTRY

Mass Spectrometry

Clinical and Biomedical Applications

Volume 1



Edited by

Dominic M. Desiderio

Mass Spectrometry

Clinical and Biomedical Applications

Volume 1

MODERN ANALYTICAL CHEMISTRY

Series Editor: David M. Hercules
University of Pittsburgh

ADVANCES IN COAL SPECTROSCOPY

Edited by Henk L. C. Meuzelaar

APPLIED ATOMIC SPECTROSCOPY

Volumes 1 and 2

Edited by E. L. Grove

CHEMICAL DERIVATIZATION IN ANALYTICAL CHEMISTRY

Edited by R. W. Frei and J. F. Lawrence

Volume 1: Chromatography

Volume 2: Separation and Continuous Flow Techniques

COMPUTER-ENHANCED ANALYTICAL SPECTROSCOPY

Volume 1: Edited by Henk L. C. Meuzelaar and Thomas L. Isenhour

Volume 2: Edited by Henk L. C. Meuzelaar

Volume 3: Edited by Peter C. Jurs

ION CHROMATOGRAPHY

Hamish Small

ION-SELECTIVE ELECTRODES IN ANALYTICAL CHEMISTRY

Volumes 1 and 2

Edited by Henry Freiser

LIQUID CHROMATOGRAPHY/MASS SPECTROMETRY

Techniques and Applications

Alfred L. Yergey, Charles G. Edmonds, Ivor A. S. Lewis, and Marvin L. Vestal

MASS SPECTROMETRY

Clinical and Biomedical Applications

Volume 1

Edited by Dominic M. Desiderio

MODERN FLUORESCENCE SPECTROSCOPY

Volumes 1–4

Edited by E. L. Wehry

PRINCIPLES OF CHEMICAL SENSORS

Jiří Janata

TRANSFORM TECHNIQUES IN CHEMISTRY

Edited by Peter R. Griffiths

A Continuation Order Plan is available for this series. A continuation order will bring delivery of each new volume immediately upon publication. Volumes are billed only upon actual shipment. For further information please contact the publisher.

Mass Spectrometry

Clinical and Biomedical Applications
Volume 1

Edited by

Dominic M. Desiderio

Departments of Neurology and Biochemistry
The University of Tennessee, Memphis
Memphis, Tennessee

SPRINGER SCIENCE+BUSINESS MEDIA, LLC

Library of Congress Cataloging-in-Publication Data

Mass spectrometry / edited by Dominic M. Desiderio.

p. cm. -- (Modern analytical chemistry)

Includes bibliographical references and index.

Contents: v. 1. Clinical and biomedical applications.

1. Mass spectrometry. 2. Biomolecules--Analysis. I. Desiderio, Dominic M. II. Series.

[DNLM: 1. Chemistry, Clinical--instrumentation. 2. Chemistry, Clinical--methods. 3. Spectrum Analysis, Mass. QC 454.M3 M41421] QP519.9.M3M352 1992

616.07'56--dc20

DNLM/DLC

for Library of Congress

92-49302

CIP

Grateful acknowledgment is made to Henry Holt & Company for permission to reprint an excerpt from "The Road Not Taken," in *The Poetry of Robert Frost*, New York: Holt, Rinehart and Winston, 1979.

ISBN 978-1-4899-1175-9

ISBN 978-1-4899-1173-5 (eBook)

DOI 10.1007/978-1-4899-1173-5

© Springer Science+Business Media New York 1992

Originally published by Plenum Press, New York in 1992

Softcover reprint of the hardcover 1st edition 1992

All rights reserved

No part of this book may be reproduced, stored in a retrieval system, or transmitted, in any form or by any means, electronic, mechanical, photocopying, microfilming, recording, or otherwise, without written permission from the Publisher

Contributors

Donald H. Chace, Division of Genetics and Metabolism and Department of Pediatrics, Duke University Medical Center, Durham, North Carolina 27710

Dominic M. Desiderio, Departments of Neurology and Biochemistry, Charles B. Stout Neuroscience Mass Spectrometry Laboratory, University of Tennessee–Memphis, Tennessee 38163

Charles G. Edmonds, Chemical Methods and Separations Group, Chemical Sciences Department, Pacific Northwest Laboratory, Richland, Washington 99352

Kym F. Faull, The Neuropsychiatric Institute and Department of Psychiatry and Biobehavioral Sciences, UCLA School of Medicine, Los Angeles, California 90024

John B. Fenn, Department of Chemical Engineering, Yale University, New Haven, Connecticut 06520

David J. Harvey, Department of Pharmacology, University of Oxford, Oxford OX1 3QT, England

Tomiko Kuhara, Division of Human Genetics, Medical Research Institute, Kanazawa Medical University, Uchinada, Ishikawa 920-02, Japan

Joseph A. Loo, Chemical Methods and Separations Group, Chemical Sciences Department, Pacific Northwest Laboratory, Richland, Washington 99352

Matthias Mann, European Molecular Biology Laboratory, 6900 Heidelberg, Germany.

Isamu Matsumoto, Division of Human Genetics, Medical Research Institute, Kanazawa Medical University, Uchinada, Ishikawa 920-02, Japan

David S. Millington, Division of Genetics and Metabolism and Department of Pediatrics, Duke University Medical Center, Durham, North Carolina 27710

Diane Rindgen, Department of Chemistry and The Barnett Institute of Chemical Analysis and Materials Science, Northeastern University, Boston, Massachusetts 02115

Kunihiko Saito, Department of Medical Chemistry, Kansai Medical University, Moriguchi, Osaka 570, Japan

Richard D. Smith, Chemical Methods and Separations Group, Chemical Sciences Department, Pacific Northwest Laboratory, Richland, Washington 99352

Paul Vouros, Department of Chemistry and The Barnett Institute of Chemical Analysis and Materials Science, Northeastern University, Boston, Massachusetts 02115

Preface

Two roads diverged in a wood, and I—
I took the one less traveled by,
And that has made all the difference.

Robert Frost

The purpose of this book is to collect recent developments in the use of mass spectrometry in the field of clinical and biomedical research. Several broad areas of research are described, including electrospray ionization, metabolism, physiology, neuronal systems, and structural modifications of proteins. More specifically, the principles and applications of electrospray ionization are described, and the use of mass spectrometry in the study of amino acids, platelet-activating factor, muscle relaxants, acylcarnitines, neurotransmitters and neuropeptides, cannabinoids, and glycoproteins is described.

This volume was prompted by the continuing use of mass spectrometry in an expanding variety of research areas in the clinical and biomedical sciences that require the combination of the efficient ionization of large and polar biomolecules with the high level of detection sensitivity and molecular specificity that mass spectrometry and tandem mass spectrometry offer to those areas of research. The chapters in this book continue to define the concepts of clinical and biomedical mass spectrometry, and the data reported by the authors in this volume reflect the very careful attention to experimental detail, the interaction of mass spectroscopists with biological and clinical scientists, and the continued development of mass spectrometric methodologies.

It has been a pleasure to work with this group of contributors, and I wish to express my appreciation to them for writing their chapters and describing the research done in their laboratories.

This book collects the state-of-the-art mass spectrometry research in the areas of clinical and biomedical sciences into one volume, and it is hoped that a newcomer to these fields of research will find this volume helpful to his or her research.

Dominic M. Desiderio

Memphis, Tennessee

Contents

Chapter 1

Electrospray Mass Spectrometry: Principles and Methods

Matthias Mann and John B. Fenn

1. Introduction	1
1.1. History	1
1.2. Electrospray vis-à-vis Other Ionization Methods	3
1.3. How ESMS Is Performed	6
2. The Component Processes of ESMS	7
2.1. Charged Droplets by Electrospray Dispersion	8
2.2. Ion Formation from Charged Droplets	13
2.3. Ion Transport	22
2.4. Analysis of ES Ions	24
3. Some Practical Considerations	30
3.1. Sample Preparation and Introduction	30
3.2. Fouling Problems	30
3.3. Performance Diagnosis	31
3.4. Data Systems and Software	31
4. Summary and Conclusions	32
References	33

Chapter 2

The Analysis of Biomolecules by Electrospray Ionization–Mass Spectrometry and Tandem Mass Spectrometry

Richard D. Smith, Joseph A. Loo, and Charles G. Edmonds

1. Introduction	37
2. Experimental Methods and Considerations	39
2.1. The Electrospray Source	39
2.2. The Atmosphere–Vacuum Interface	41

3. ESI–MS of Large Biomolecules	43
3.1. Molecular Weight Determination	43
3.2. Positive-Ion Spectra of Large Polypeptides and Proteins	45
3.3. Higher-Order Protein Structure Effects	52
3.4. Negative-Ion Spectra of Large Polypeptides and Proteins	58
4. ESI–Tandem Mass Spectrometry of Polypeptides and Proteins	64
4.1. General Considerations	64
4.2. Melittin	64
4.3. Ribonuclease A	73
4.4. Serum Albumins	76
5. Combined Separations and ESI–MS of Polypeptides and Proteins	84
6. Conclusions	91
Summary	91
References	92

Chapter 3

The Analysis of Muscle Relaxants by Mass Spectrometric Methods

Diane Rindgen and Paul Vouros

1. Introduction	99
2. Chemical Analysis	102
2.1. Other Analytical Techniques	102
2.2. Mass Spectrometric Techniques	103
3. Conclusions	127
References	129

Chapter 4

Quantitative Analytical Mass Spectrometry of Endogenous Neuropeptides in Human Pituitaries

Dominic M. Desiderio

1. Introductory Comments and Overview	133
2. Qualitative Analytical Mass Spectrometry	135
3. Quantitative Analytical Mass Spectrometry	136
4. Basic Principles of the Analytical Method	138
4.1. Tissue Acquisition	139
4.2. Extraction	140
4.3. Reversed-Phase High-Performance Liquid Chromatography	140
4.4. Fast Atom Bombardment Ionization	141
4.5. Scan Modes	142
4.6. Internal Standard	148
4.7. Calibration Curves	148
4.8. Electrospray Ionization	151

5. Examples of Measurements of Opioid Peptides in a Single Human Pituitary	152
5.1. Method Development: Measurement of ME in 11 Human Pituitaries	152
5.2. Pituitaries: Control versus Tumors	154
5.3. Electrospray	156
6. Conclusions	156
6.1. Detection Sensitivity	160
6.2. Nomenclature	160
6.3. Molecular Specificity	161
6.4. Endogenous Neuropeptide Systems	161
References	162

Chapter 5

Neurotransmitters

Kym F. Faull

1. Introduction	167
1.1. History of the Recognition of Neurotransmitters	167
1.2. Neurotransmitters and Their Role in Information Transfer	168
1.3. Characteristics of Synaptic Vesicles	171
1.4. Anatomic Localization	171
1.5. The Correlation between Sites of Release and Receptor Density	173
1.6. The Relationship between Neurotransmitters and Clinical Medicine	176
2. Chemical Nature of Neurotransmitters	181
2.1. Comparison between the Nonpeptide and Peptide Neurotransmitters	182
2.2. Neurotransmitter Biosynthesis and Processing	182
3. Mass Spectrometric Characterization of Neurotransmitters	183
3.1. The Nonpeptide Neurotransmitters	185
3.2. The Peptide Neurotransmitters	196
References	199

Chapter 6

Cannabinoids

David J. Harvey

1. Introduction	207
2. Mass Spectrometric Characteristics of Natural Cannabinoids	210
2.1. Tetrahydrocannabinols	211
2.2. Cannabinol	213

2.3. Cannabidiol	214
2.4. Minor Cannabinoids	214
3. GC/MS Studies on Natural Cannabinoids	216
4. Cannabinoid Metabolites	219
4.1. General Method for the Identification of Hepatic Metabolites	224
4.2. Metabolic Studies on Specific Cannabinoids	234
5. Quantitative Studies	247
5.1. Measurement of Delta-9-THC in Physiological Fluids	247
5.2. Metastable Ion Monitoring	250
6. Conclusions	252
References	253

Chapter 7

Inborn Errors of Amino Acid and Organic Acid Metabolism

Isamu Matsumoto and Tomiko Kuhara

1. Introduction	259
2. Profiling Procedure	260
2.1. Analytical Methods	260
2.2. Gas Chromatographic and Mass Spectrometric Analysis	262
3. Amino Acid and Organic Acid Metabolic Disorders	262
3.1. Disorders of Aromatic Amino Acid and Organic Acid Metabolism	262
3.2. Disorders of Branched-Chain Amino Acid Metabolism	271
3.3. Disorders of Multienzyme Defects	289
4. Problems Underlying the Chemical Diagnosis	292
5. Conclusion	293
References	294

Chapter 8

Carnitine and Acylcarnitines in Metabolic Disease Diagnosis and Management

David S. Millington and Donald H. Chace

1. Introduction and Background	299
1.1. Biochemical Role of Carnitine	299
1.2. Carnitine Deficiency	301
1.3. Carnitine Therapy	301
1.4. Role of Mass Spectrometry	302
2. Methods for the Analysis of Carnitine	302
2.1. Enzymatic Assays	302
2.2. Tandem Mass Spectrometric Assay	303

3. Methods for the Analysis of Specific Acylcarnitines	305
3.1. High-Performance Liquid Chromatographic Methods	305
3.2. GC/MS Methods	307
3.3. Tandem Mass Spectrometry Techniques	308
4. Synthesis, Characterization, and Handling of Standards	314
5. Summary	315
References	316

Chapter 9

Platelet-Activating Factor and Related Compounds

Kunihiko Saito

1. Introduction	319
2. Biochemical Background	320
3. Mass Spectrometry of PAF	321
3.1. Gas Chromatography-MS	323
3.2. Fast Atom Bombardment MS	327
3.3. Fast Atom Bombardment MS/MS	328
4. Preparation of PAF from Animal Tissues	332
4.1. A Combination of Column Chromatography and Thin-Layer Chromatography	333
4.2. High-Performance Liquid Chromatography	333
4.3. Procedures for Vinyl PAF from Rat Heart	333
5. Discussion	335
References	339

<i>Index</i>	345
--------------------	-----

Electrospray Mass Spectrometry

Principles and Methods

Matthias Mann and John B. Fenn

1. INTRODUCTION

The objective in this chapter is to introduce the principles and methods of electrospray mass spectrometry (ESMS), a relatively new technique for the analysis of complex, polar, and labile molecules. Based on electrospray (ES) ionization at atmospheric pressure of solute species in volatile solvents, ESMS has attracted widespread interest only since 1988, when it was shown capable of producing and weighing intact ions of very large biomolecules (1). Along with laser desorption (LD) (2–5), ES has now become an ionization method of choice for MS analysis of molecules in the mass range above 10 kDa. It is also finding increasing application in the analysis of smaller species and seems destined to become an indispensable tool in the emerging discipline of biological mass spectrometry (6). In this account we describe the essential features of ESMS in an attempt to provide some perspectives on how it works and how it can be used. The interested reader is referred to several recent reviews (7–10) for additional information on results that have been obtained, comparisons with other methods, and references to the literature.

1.1. History

The term *electrospray* refers to the dispersion of a liquid into small charged droplets by electrostatic fields. This phenomenon was observed as early as the

Matthias Mann • European Molecular Biology Laboratory, 6900 Heidelberg, Germany. *John B. Fenn* • Department of Chemical Engineering, Yale University, New Haven, Connecticut 06520.

18th century and is today the basis of technology used in applications ranging from applying pesticides to painting cars (11). Not until the late 1960s was it first proposed and tried by Malcolm Dole and his colleagues as a method for producing ions of large molecules for mass spectrometric analysis. Their original pioneering experiments were with samples of narrowly dispersed oligomers of polystyrene ranging in molecular weight (M_p) from 50 to 500,000 (12–15). Solutions of these samples in a volatile solvent were passed through a hypodermic needle into a cylindrical chamber through which flowed a bath gas (nitrogen) at atmospheric pressure. A potential of several kilovolts was maintained between the needle and the chamber walls to provide an intense electric field at the needle tip that dispersed the emerging liquid into a fine spray of small charged droplets. Dole recognized that evaporation of the solvent would increase the charge density on a droplet surface until the so-called Rayleigh limit would be reached at which electrostatic repulsion would be of the same magnitude as the surface tension of the droplet liquid. The consequent strong instability would result in disruption of the droplet into a progeny of smaller droplets by a process often referred to as a *Coulomb explosion*.

Dole further argued that if the original solution of macromolecules were sufficiently dilute, a sequence of such explosions would result in ultimate droplets so small that they would on average contain only one of the original solute macromolecules. As the last of the solvent evaporated, those single macromolecules would retain some charge on their containing droplets, thus giving rise to a dispersion of macroions in the bath gas. A portion of this gaseous dispersion of macroions could then be expanded as a supersonic free jet into a vacuum system for mass analysis of the ions.

Because the ions he hoped to produce were much too heavy for weighing by available analyzers, Dole sought to determine their masses by measuring the potential required to prevent them from reaching a Faraday cup collecting electrode in series with a sensitive electrometer. An ion's mass could be deduced from this measure of its kinetic energy together with a value of its velocity based on the assumption that during free jet expansion into the vacuum system it reached the readily calculable velocity of the bath gas. The results of these ingenious experiments were intriguing and in some cases seemed to produce plausible values of ion mass. However, the perspective of recent experience raises serious questions about the interpretation of those results. It now seems unlikely that the detected ions actually comprised individual charge-bearing macromolecules (7). Moreover, evidence is accumulating that Dole's charged residue model (CRM) for ion formation from charged droplets applies only in relatively rare circumstances. The ion evaporation model (IEM) of Iribarne *et al.* (16–18) to be described later is much more widely accepted. Even so, Dole deserves full credit for planting the seeds from which modern ESMS has grown.

Because of various experimental difficulties, Dole abandoned his MS ex-

periments in the early 1970s. In spite of his intriguing preliminary results, the technique failed to attract other investigators, so that for nearly a decade there were no published papers on the subject. Activity in ESMS was renewed in the early 1980s by Alexandrov and his collaborators in Leningrad (19) and independently by our group at Yale (20,21). A few years later the groups of Smith at Battelle (22) and Henion at Cornell (23) also began experimenting with the technique. During the initial stages of this revival of interest in ESMS the focus was on solute species whose ions had masses small enough for analysis by conventional analyzers (quadrupole mass filters and magnetic sector instruments). Then in 1987 our laboratory reported that ES could produce ions from oligomers of poly (ethylene glycols) (PEGs) with M_r s up to at least 20,000 (24). Moreover, because of extensive multiple charging, the mass/charge (m/z) values of even the largest of these ions were always less than 1500, well within the range of modest quadrupole analyzers. Even so, interest in ESMS remained at a low level until a year later, when a report of analogous results with proteins having M_r s as high as 40,000 sparked the explosive increase in interest and activity that is largely responsible for the inclusion of this chapter in this volume.

1.2. Electrospray vis-à-vis Other Ionization Methods

We have previously suggested (7) that the various ionization methods that have been developed for labile and nonvolatile compounds could be conveniently divided into two classes: (a) those depending on rapid addition of energy to molecules of such species dispersed in or on the surface of a condensed phase and (b) those based on the use of strong electric fields to extract ionic species from a substrate. The idea behind the former or "energy-sudden" methods is that sufficiently rapid energy addition to ("heating" of) complex molecules can result in vaporization and ionization before intramolecular energy transfer can bring about decomposition. The rapid energy deposition is usually achieved by dispersing the analyte molecules on a surface or in a suitable matrix and then exposing them to an incident flux of high-energy species: atoms in fast atom bombardment (FAB); ions in fast ion bombardment (FIB), also known as liquid secondary ion mass spectrometry (LSIMS); radioactive decay products of 252-californium in plasma desorption (PD); and photons in laser desorption (LD). All of these energy-sudden methods have played an important role in the development of mass spectrometry for analysis of large molecules and still enjoy widespread use. They generally suffer from one or more of such disadvantages as small analyte ion currents, which, except for LD, decrease to the vanishing point at M_r s above 40,000 or less, high degrees of internal excitation in the product ions, relatively high mass/charge ratios, chemical noise from matrix ions, and difficult sample preparation.

Quite different in principle and practice from the violent energy-sudden

ionization techniques are the more reversible methods that use strong electric fields to desorb ions from a substrate. It is convenient to distinguish these field methods in terms of whether they are carried out in vacuum or in gas at or near atmospheric pressure. The vacuum methods include field desorption (FD) ionization and electrohydrodynamic (EH) ionization. In FD the analyte is applied to an array of sharp points or “whiskers” on a wire that is then placed at high potential in a vacuum system. At the right combination of voltage and wire temperature, the high fields at the sharp points desorb analyte species as ions. In EH a solution of analyte in a nonvolatile liquid such as glycerol is introduced into the vacuum system through a small hypodermic needle maintained at high potential relative to nearby surfaces. The resulting field at the needle tip disperses the emerging liquid into “droplets” or clusters so small that many of them are actually individual analyte ions with or without one or more molecules of solvation. In FD the preparation of arrays of points and dosing them with analyte is tedious. Moreover, the right combination of voltage and temperature is difficult to achieve because it lies within a very narrow range and differs from species to species. In EH it is often hard to find a liquid that is a good solvent for the analyte, has a vapor pressure low enough to avoid “freeze-drying,” and provides an electrical conductivity high enough to produce useful ion currents. Moreover, a substantial fraction of the ions produced are more or less highly solvated. In both FD and EH the absence of any moderating bath gas means that the voltages used to produce the required fields result in ion energies so high that very expensive magnetic sector instruments are the only suitable analyzers. For these and other reasons neither FD nor EH has become widely used.

The second category of ionization techniques based on electric fields comprises what might be called the *spray methods* in which the field strengths required for ion desorption are obtained by the evaporation of charged droplets. The three important members of this family are thermospray (TS), aerospray (AS), and electrospray (ES). Ion formation in all three seems to be based on the field desorption mechanism embodied in the IEM of Iribarne and Thomson. The techniques differ primarily in the method of droplet production.

In TS, ion-containing sample liquid flows at a rate of about 1 ml/min through a tube with walls hot enough to vaporize 90% or more of the solvent (25–27). The resulting rapid expansion disperses the remaining liquid into small droplets entrained in superheated vapor that emerges as a supersonic free jet into a heated chamber maintained at a few millibars. Because of statistical fluctuations in the distribution of cations and anions, the droplets carry a net charge that is positive in half of them and negative in the other half. The chamber is hot enough to maintain the vapor in a superheated state so that solvent evaporates from the droplets, thus increasing their surface charge so that they can undergo a sequence of Coulomb explosions to produce very small droplets in the manner described by Dole and outlined above.

In AS the droplets are produced by the pneumatic nebulization effect used in perfume atomizers and, as in TS, are charged by statistical fluctuations in the distribution of cations and anions among the droplets (16–18). The ion currents produced in pure AS are so small that a polarizing electrode at high voltage is placed near the nebulizing region to provide a field that increases ion currents and causes the charge on all the droplets to have the same sign, positive or negative, depending on the polarity of electrode potential. Thus, AS as practiced can be considered a hybrid of ES and pure AS. In addition to depending on aerodynamic forces for nebulization, this technique differs from ES in that the polarizing electrode provides a field but is not part of the circuit. That is to say, the field it provides is not strong enough to drive the ions to the electrode. Instead, they follow the streamlines of the gas flow to a downstream location where an orifice admits some of them into a vacuum system containing the mass analyzer. For whatever reason, the ion currents are always much smaller in AS than in ES.

A somewhat different hybrid of ES and AS uses a configuration of elements very similar to that shown for ES in Fig. 1.1 with the difference that a nebulizing gas flow is introduced coaxially around the emerging liquid stream. This variation on the ES–AS hybrid theme was called *ion spray* (IS) by its originators (28), a somewhat unfortunate choice of name because its two implications, that ions are sprayed and that a new ionization mechanism is involved, are both misleading. In our view a term like *aeroelectrospray* (AES) would more nearly reflect what it really is. We believe that much confusion could be avoided if the names given to techniques were carefully chosen to reflect their operational charac-

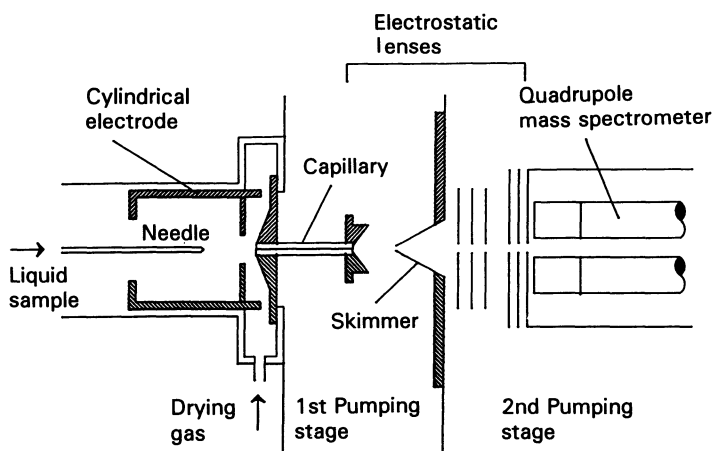


Figure 1.1. Schematic representation of an electrospray mass spectrometry apparatus. See text for details of operation.

teristics more faithfully than is often the case. In this perspective, SIMS, for example, is an acronym for a kind of mass spectrometry, not an ionization method that might better be called fast ion bombardment (FIB), as we noted earlier. Similarly, what we have here called AS was dubbed by its inventors *atmospheric pressure ion evaporation* (APIE), a term still widely used even though it does not clearly identify any particular technique because it relates to a mechanism of ion formation common to three different ones, TS, AS, and ES.

1.3. How ESMS Is Performed

Because ES is the central theme of this chapter, its operation and use in MS is outlined in somewhat more detail than was the case for the other ionization methods. To provide a framework for the discussion that follows, we identify the essential features of the technique with reference to the ESMS apparatus that is schematically displayed in Fig. 1.1 and has been previously described in detail (7,8). Solution containing the analyte species of interest is injected, typically at a rate of a few microliters per minute through the sharp-tipped hypodermic needle into a countercurrent flow of drying gas, typically a few liters per minute of warm dry nitrogen. The end wall of the chamber contains a glass capillary tube with a length of several centimeters and a bore of a few tenths of a millimeter. The metalized front face of the tube is maintained at a potential difference of several kilovolts below the grounded needle in order to provide an electrostatic field at the needle tip sufficiently strong to disperse the emerging sample solution into a fine spray of charged droplets. Driven by the potential gradient, the droplets migrate toward the capillary inlet against the countercurrent flow of bath gas, shrinking as they go as a result of evaporation of solvent into the bath gas. In the manner described earlier, this shrinking increases a droplet's surface charge density until the Rayleigh limit is reached, at which time electrostatic repulsion overcomes the surface tension and a Coulomb explosion breaks up the droplet into a multiplicity of smaller droplets. A sequence of one or more of these explosions finally produces droplets so small that the combination of charge density and radius of curvature at the droplet surface produces an electric field intense enough to desorb solute ions from the droplets into the ambient gas. These ions also migrate down the potential gradient toward the capillary entrance where some of them are entrained in a stream of gas that enters the capillary to emerge at the exit end as a supersonic free jet into the first stage of the vacuum system. A core portion of that jet passes through the skimmer into the second stage of the vacuum system that contains the mass analyzer.

Clearly, the ions entering the capillary are in a potential well whose depth equals the potential difference between the grounded needle and the metalized front face of the capillary. We have found that if the exit end of the capillary is at ground, the drift velocity of the ions from the potential gradient in the capillary is much less than the flow velocity of the gas relative to the capillary walls.

Consequently, the ions are lifted by the gas flow out of the potential well at the capillary inlet back up to ground potential at the capillary exit. Indeed, they can be raised to the 10 kV or more above ground potential that may be required for injection into a magnetic sector analyzer (29). Sometimes the aperture admitting the ion-bearing gas into the vacuum system is a simple flat plate orifice instead of a glass capillary. In that case the needle must be maintained at several kilovolts above ground, thus posing a hazard to an operator. Any source of sample liquid, e.g., a liquid chromatograph, must also be at the needle potential unless the conduit leading from it to the needle has a combination of length, bore, and solution conductivity providing an electrical resistance high enough so that the current leak to ground will not overheat the sample liquid or overload the power supply. It is noteworthy that in some commercial sources, for example, those supplied by Analytica of Branford, CT, one or more preliminary vacuum stages between the capillary exit and the high-vacuum chambers remove much of the free jet gas at relatively high pressure with mechanical rotary pumps. Thus, a much larger flux of ion-bearing gas can be admitted to the vacuum system with a consequent increase in useful ion currents by factors of up to 100 or more.

The apparatus of Fig. 1.1 performs the same functions as did the original apparatus of Dole and is similar in many ways. An important difference, apart from the use of the glass capillary and conventional mass analysis, is the flow direction of the bath or drying gas. In Dole's apparatus the flow was concurrent with the motion of the charged droplets and ions, i.e., from left to right. In the apparatus of Fig. 1.1, that flow is from right to left, countercurrent to the motion of charged droplets and ions, and thus sweeps all material except pure bath gas and high mobility ions out of the system at the back end of the apparatus. This arrangement greatly increases the rate and effectiveness of solvent evaporation from both droplets and ions and decreases fouling of the vacuum system and its analyzer. More importantly, the absence of solvent vapor in the bath gas entering the glass capillary avoids resolution of the ions by the substantial cooling that occurs during free jet expansion into vacuum. Such resolution must have occurred in Dole's experiments and is one of the reasons for concern about his results. It can be avoided, and solvent vaporization achieved, without recourse to countercurrent flow if the system temperatures are high enough to insure that any vapor is always superheated when ions or charged droplets are present. All TS sources depend on high temperatures for this purpose, as do some ES sources now on the market, but they are more prone to fouling than when a counter current gas flow is used in the desolvation region.

2. THE COMPONENT PROCESSES OF ESMS

It should be clear from this description of ESMS operation that it comprises four principal steps or processes in succession: (a) formation of charged droplets

by ES dispersion of sample liquid, (b) formation of ions from the charged droplets by desolvation, (c) the transport of the ions from their origin at atmospheric pressure to the mass analyzer in its vacuum chamber, and (d) mass analysis of the ions. Each of these steps is discussed in the following sections.

2.1. Charged Droplets by Electrospray Dispersion

Although the ability of electrostatic fields to disperse liquids was observed as early as the 18th century, the first serious experimental study of the phenomenon was by Zeleny (30). In a series of communications beginning in 1914, he provided a remarkably detailed description of the phenomenon, many features of which have since been “rediscovered” by investigators who haven’t bothered to read his papers. The configuration in Zeleny’s experiments was functionally similar to that section of Fig. 1.1 in which liquid at a flow rate of a few microliters per minute is passed through a small tube, e.g., a hypodermic needle with a bore of 0.1 mm. If the needle is maintained at high potential relative to a nearby counterelectrode, the resulting electrostatic field at the needle tip shapes the emerging liquid into a conical meniscus. Zeleny was first to observe such menisci and clearly recognized that they resulted from the balance of electrostatic and surface tension forces. Many years later an analysis by G. I. Taylor (31) predicted that the surface of a static dielectric liquid in a strong electric field would assume a conical shape. His analysis does not really apply to a streaming conducting liquid dispersing into droplets, as in the experiments of Zeleny and in all subsequent applications of the electrospray phenomenon including ESMS. Even so, the conical menisci that are observed at the needle tip in all these cases are usually referred to as Taylor cones.

Some features of the structure and behavior of Taylor cones that could not be discerned in Zeleny’s results have been revealed in recent flash photographs by Takashi Nohmi in our laboratory and in much more extensive photographic studies of ES characteristics by Gomez and Tang, also at Yale (32). Figure 1.2A is a photograph by Nohmi of the cone at the tip of a stainless steel hypodermic needle at a potential of 4 kV relative to a grounded plane electrode to the right of the needle and outside the field of view. The needle has a bore of 0.2 mm through which a very dilute solution of polyethylene glycol in 1 : 1 methanol–water is flowing at about 2 $\mu\text{L}/\text{min}$. The picture clearly shows a filament or jet of liquid emerging from the tip of the cone with a diameter of 2.9 μm and extending for several tens of jet diameters before breaking up. As described in Rayleigh’s classical analysis of laminar jets of uncharged liquids (33) and clearly shown in the camcorder pictures by Gomez and Tang of flows emerging from somewhat larger tubes and higher flow rates, varicose waves appear on the surface of these jets and increase in amplitude until they disrupt the jet into a sequence of nearly monodisperse droplets having a diameter about twice that of the jet. For the ES

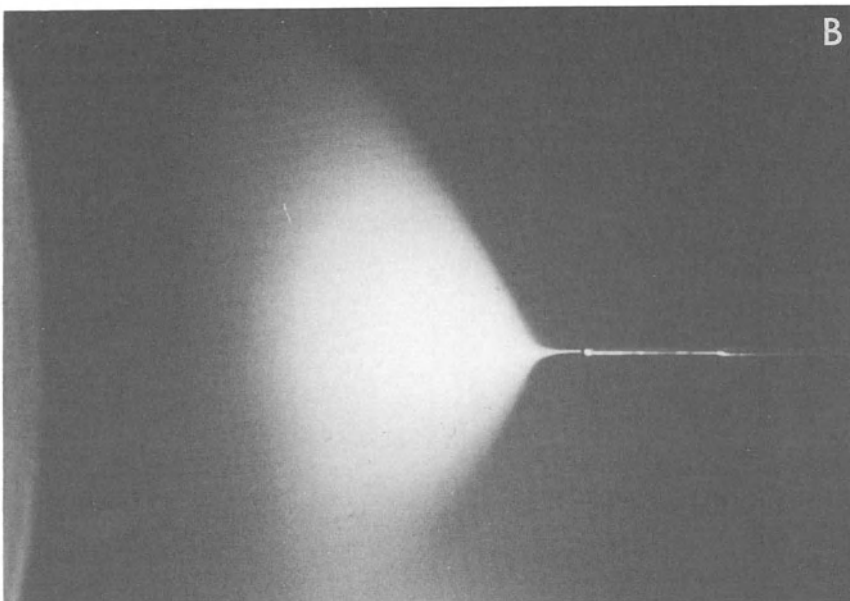
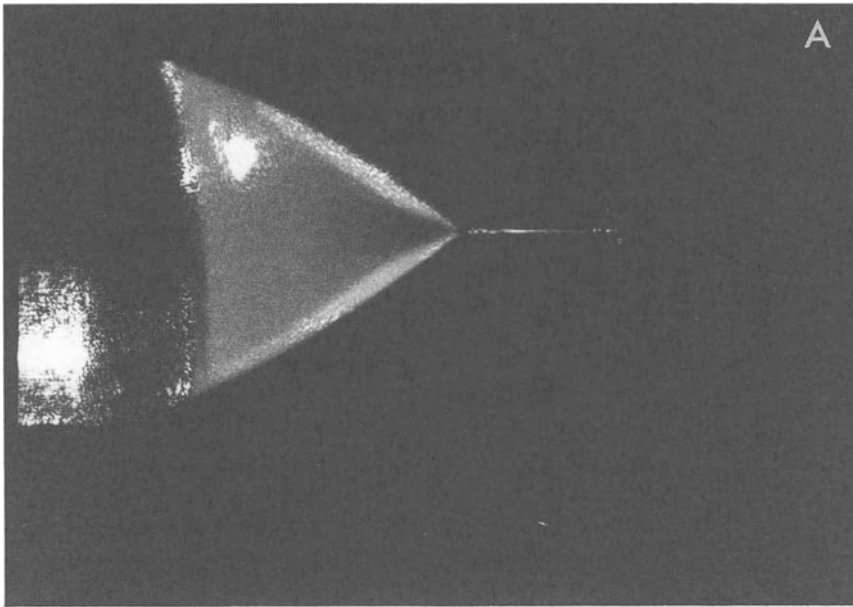


Figure 1.2. Photographs illustrating some facets of electrospray dispersion of liquids. Panel A is 10-nsec flash photomicrograph of the region at the tip of a liquid injection with a bore of 0.2 mm, which is the diameter of the base of the Taylor cone. The diameter of the liquid jet issuing from the cone tip is $2.8\ \mu\text{m}$, and the beginning of its break-up into a spray is hardly visible at the edge of the picture. Panel B is a several-second exposure of a fully developed spray.

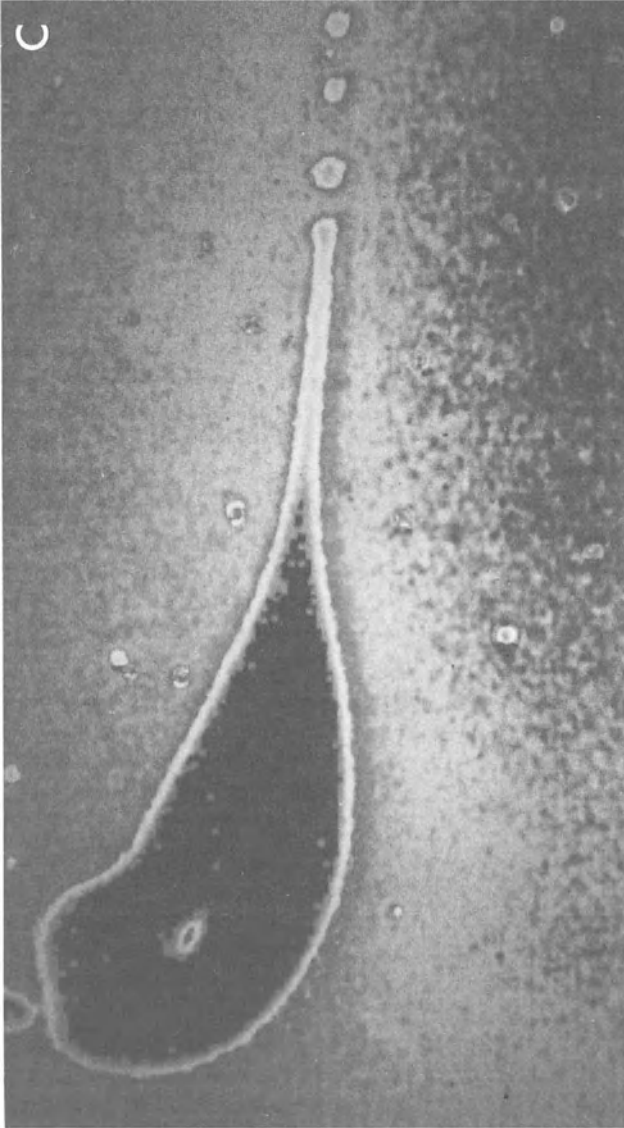


Figure 1.2. (Continued) Panel C shows the Coulomb explosion of a heptane droplet with a diameter of about $60\ \mu\text{m}$. Note that on the right-hand side the droplet liquid seems to have formed a Taylor cone, from the tip of which a jet of liquid emerges and breaks up into droplets. This behavior is reminiscent of what occurs at the needle tip, as shown in A.

case the droplets are charged so that Coulomb forces cause their trajectories to diverge, thus forming a conical spray. The beginning of this divergence is barely visible in the picture in Fig. 1.2A, but the whole spray is clearly portrayed in Fig. 1.2B, which was taken with white-light illumination and an exposure of several seconds.

Figure 1.2C shows a droplet at near the Rayleigh limit in the process of undergoing a Coulomb explosion, a phenomenon mentioned earlier that is discussed further in the section on Mechanisms of Ion Formation. To our knowledge, this photograph by Gomez and Tang represents the first visualization of an actual droplet caught in the act of breaking up as the result of the instability caused by a near balance between electrostatic and surface tension forces. The droplet in this case had a diameter of about 60 μm and was produced by electrospraying heptane made slightly conductive by the addition of some anti-static agent.

The characteristics of these sprays and their behavior depend strongly on a number of variables including the properties of the liquid, especially its conductivity, surface tension, and flow rate. The strength and configuration of the electric field are also very important and are determined by the potential applied to the needle along with such geometric factors as the shapes of the tube tip and the counterelectrode as well as the distance between them. Stable sprays can be maintained only when the values of these variables are within an interdependent range of values. In general, to maintain spray stability with a particular needle size, flow rate must decrease as liquid conductivity increases, and field strength (applied voltage) must increase as flow rate and/or surface tension increases. The upper limit to field strength is determined by the onset of a corona discharge that distorts the field at the needle tip and destroys the stability of the spray. As is well known, a corona discharge will occur at a lower field strength when the needle is at a negative rather than a positive polarity. Thus, to produce negative ions, it is helpful to introduce near the needle tip a small auxiliary flow of a gas having a high electron affinity, e.g., oxygen or sulfur hexafluoride, to scavenge free electrons and suppress the onset of corona (21).

The best MS results are obtained when the spray is operating in a stable *fog mode*, in which it looks like a cone of white mist, as shown in Fig. 1.2B. A special case of the fog mode is the *rainbow mode*, so called because of the colors that appear under illumination by white light. These colors are characteristic of higher-order Tyndall spectra (HOTS) and indicate that the droplets are fairly monodisperse, with diameters of around 2 μm or less. The rainbow mode is characterized by a spray current somewhat higher than in the fog mode and is most often achieved at the highest field strengths (applied voltages) that can be reached without breakdown to corona. Once started, however, it can usually be maintained at voltages below the onset value. It is important to realize that the current in a stable spray, which is the total net charge per unit time available for

ionizing analyte molecules, cannot be freely chosen by the operator. For a particular liquid and electrode geometry, it is in effect a property of the spray and is fairly constant in the region of stability, having only a small dependence on the applied voltage or the liquid flow rate. For a particular solution, electrode configuration, and flow rate, the current in a stable spray reaches a maximum value when the spray is in the rainbow mode.

Because spray stability depends on so many interacting variables, it sometimes happens that the combination of properties presented by a sample solution are such that a stable spray cannot be maintained by conventional ES practice. This problem is most often encountered when ESMS is used for species-specific detection with separation systems. The flow rates are often too high in liquid chromatography (LC) and too low in capillary zone electrophoresis (CZE) to permit stable sprays. The mobile phase in either technique may have a conductivity and/or surface tension that is too high.

Various methods have been evolved to enhance sprayability in these difficult cases. The pneumatic assist to nebulization used in the ionspray technique (23) provides stable sprays with flow rates as high as 200 $\mu\text{l}/\text{min}$ and with solution conductivities much greater than ES alone can tolerate. Vestal and co-workers (34) have reported that good results can be obtained with solutions having high flow rates and conductivities by raising the temperature of the needle and its surroundings. Another effective approach is the use of a sheath flow of a "well-behaved" liquid around a core flow of sample liquid as introduced by Smith et al. (22) for ESMS detection in CZE. The original purpose was to provide a good electrical connection with the liquid emerging from the quartz capillary in which the electrophoresis takes place. It turned out that the electric field at the needle tip can effectively disperse the mixture of sheath and core flow of sample liquid even when a stable spray cannot be formed from the sample liquid alone. Moreover, dilution with sheath liquid increases the total rate of liquid flow to convenient values when the CZE flow alone is too small to provide a stable spray. Some investigators claim that advantages can often be realized by combining the sheath-flow and pneumatic-assist techniques.

By one or another of these devices it is now possible to practice effective ESMS over a wide range of conditions with sample solutions embracing a wide variety of properties. Even pure water containing trifluoroacetic acid, a long-time challenge to ESMS, can now be effectively accommodated. However, concentrations of nonvolatile buffers above 10 mM or so can still present difficulties, as they do in all other ionization methods with the possible exception of LD. The problem may be that such high solute concentrations prevent the evaporating droplets from reaching dimensions small enough to allow ion formation. Also to be noted is that these techniques for enhancing the sprayability of refractory liquids generally exact a cost in the form of decreased analytical sensitivity, but this cost is often tolerable because the innate sensitivity of ESMS is so high.

2.2. Ion Formation from Charged Droplets

As yet there is no satisfactory theoretical description of the formation of gas-phase ions from solute species in charged liquid droplets. Indeed, as may have been inferred from the previous discussion, the basic mechanism is still in dispute. In the absence of a satisfactory theory we have been dependent almost entirely on experimental observations to provide some insight on various aspects of the ionization process. In what follows we attempt to summarize what has emerged from these experimental observations.

2.2.1. The Nature of ES Ions

In conventional ionization methods an initially neutral atom or molecule becomes a positive ion by losing an electron, or a negative ion by attaching one, usually as the result of a gas-phase encounter with an electron, a photon, an electronically excited atom, or another ion. An ES ion, on the other hand, comprises a species that is already an anion or cation in the droplet solution or is an adduct of such an ion with an ordinarily neutral solute species. Such charged adducts, for example, a peptide or protein with one or more adduct protons or a glycol molecule with an adduct Na^+ , are often called *quasimolecular ions*.

2.2.2. Electrospray is “Extra Soft”

One of the most striking features of ES ionization is the absence of decomposition for the most fragile of species, even those held together by weak non-covalent bonds. Whatever the mechanism by which the ion and solvent are separated, it does not involve excitation of the ion to a suprathreshold energy state. Its temperature in the droplet and after desolvation is never higher than the maximum bath gas temperature, usually less than 350°K. Sometimes, during free jet expansion, ES ions are deliberately accelerated by an applied field and become heated by collisions with bath gas molecules in order to enhance desolvation. Such collisions can be sufficiently energetic to cause rupture of the strongest covalent bonds, but they are not inherent or necessary in the ion formation process. Recent findings indicate that conditions in the droplet are so benign that proteins retain their tertiary structure up to the moment of desolvation (35).

2.2.3. Multiple Charging and Mass Range

Another characteristic and valuable feature of ES ionization is its ability to produce intact ions with extensive multiple charging from large molecules. A rule of thumb is that ES ions comprise roughly 1 kDa of mass for every charge, but mass/charge (m/z) ratios from half to twice that value have been encoun-

tered. It also happens that in a population of multiply charged ions of a parent species the distribution of charges is always such that between some minimum and maximum number of charges per ion every possible charge state is represented. Thus, the mass spectrum of such a population comprises a sequence of peaks, the ions of each peak differing by a single charge from those of adjacent peaks. Figure 1.3 shows some examples of such spectra for several proteins. It is noteworthy that the distribution of peak heights is roughly Gaussian (more nearly Gaussian on a z/m scale) and that the number of charge states increases with increasing M_r of the parent species. Also noteworthy is that both the width and location of the m/z range spanned by the peaks can vary substantially from species to species, but results to date indicate that the maximum m/z values are always less than about 3000. Consequently, an analyzer with only a modest mass range (for singly charged ions) can weigh the ES ions of parent species that are very large indeed.

However, the m/z scale of the ordinate is not linear in z , the number of charges per ion. Consequently, the distance between peaks on that scale decreases as the number of charges per ion increases. It follows that as the M_r of the parent species increases, the analyzer needs higher resolution (to distinguish between adjacent peaks) but not higher mass range. Recent results showed that intact ES ions can be formed from poly(ethylene glycol)s with M_r s up to 5,000,000 (36). Because these very large ions had up to 4000 or more charges, they could be weighed with a quadrupole analyzer having an upper limit to m/z of only 1500. Unfortunately, the spectrum comprised a broad band of peaks that could not be resolved, in part because adjacent peaks for the same oligomer are so close together and in part because of congestion resulting from the superposition of a distribution of charge states for each oligomer on a distribution of oligomer masses for each charge state.

2.2.4. Ionization Efficiency

In any consideration of efficiency it is important to distinguish between situations in which the supply of charge might be a limiting factor and those in which it is not. Clearly, it could well be limiting when there are more prospective charge sites on the analyte molecules in a spray than there are charges in the spray. Under typical operating conditions the solution flow rate might be 1 $\mu\text{l}/\text{min}$, and the spray current on the order of 100 nA. If, as noted above, the analyte molecules can retain about one elementary charge per kilodalton, then charge limitation might be expected when the sample solution contains around 0.1 g/liter of analyte. In this charge-limited case, the ES ionization efficiency can be conveniently defined as the ratio of the total number of charges on all the analyte ions to the number of charges in the spray, i.e., the fraction of charge supplied to the source that leaves in the form of analyte ions. This ratio or fraction can vary from zero in the worst case to unity in the best.

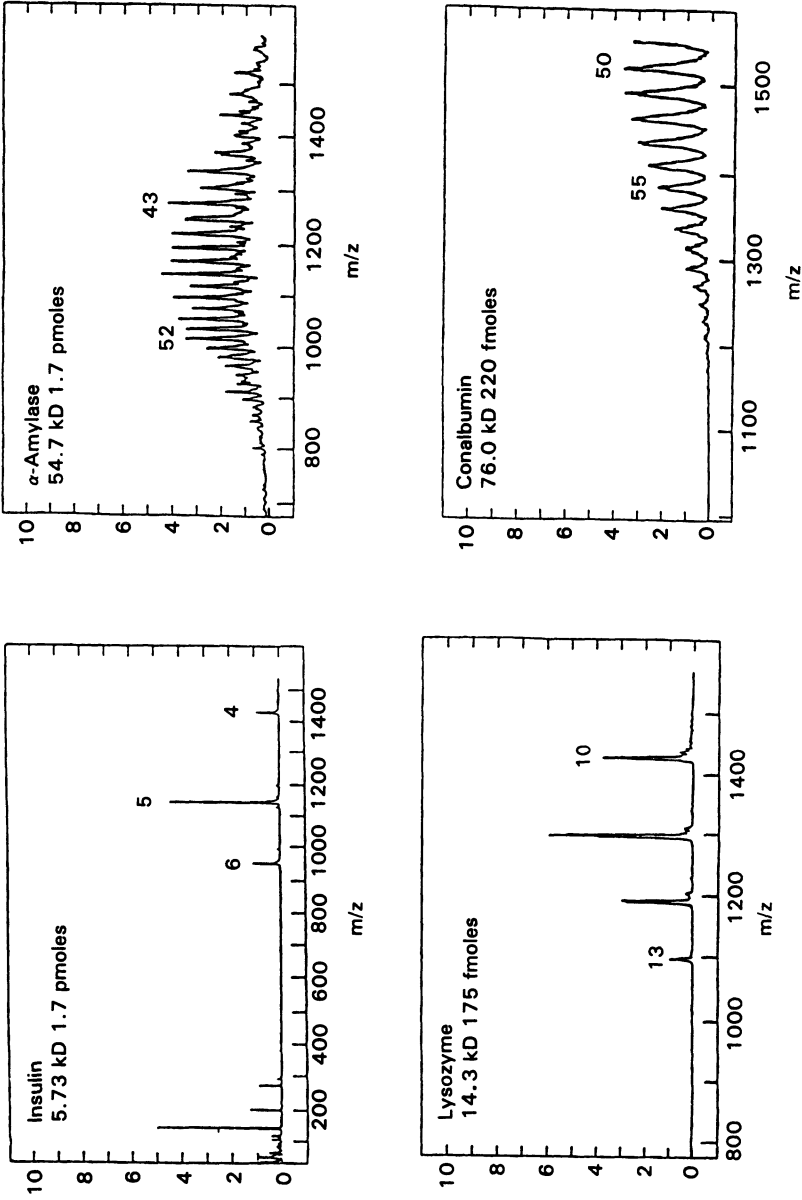


Figure 1.3. Representative ES mass spectra for several proteins: insulin, M_r 5730; lysozyme, M_r 14,300; α -amylase, M_r 54,700; and conalbumin, M_r 26,000.

On the other hand, when the supply of charge is not a limiting factor, a more appropriate definition of efficiency would be the fraction of analyte molecules entering the source that becomes ions. Although careful measurements of these quantities have not often been made, experience in several laboratories suggests that both of these efficiencies can be very high, up to substantial fractions of unity for species that are ionized in solution. In practice, the determining factor in analytical sensitivity is the fraction of ions produced in the source that can be delivered to the analyzer. Values of this *transport efficiency* as low as 0.0001 have been reported for systems now in use (9). For sources with multistage pumping mentioned earlier, values as high as 0.003 have been achieved. Clearly, increasing this transport efficiency offers the greatest opportunity for improvement in performance.

2.2.5. Sensitivity and Dynamic Range

For analytical purposes it is important to know the dynamic range and the linearity of a system's response to the amount of sample introduced. Figure 1.4 shows the measured ESMS signal for doubly charged ions of the peptide gramicidin S and its dependence on liquid flow rate and analyte concentration. The indicated behavior for a given flow rate in Fig. 1.4A, noted early on (37) and typical of essentially all analyte species, shows that the signal is linear over about four decades in concentration up to some critical value at which there is a rather abrupt change in the slope of the curve. On the other hand, as Fig. 1.4B shows, at a given analyte concentration, the signal is almost independent of flow rate. It follows that detectability, in terms of minimum total amount of material, becomes maximal when liquid flow rate and analyte concentration are at the lowest possible values. It also follows that the most informative measure of ESMS sensitivity is the minimum detectable concentration of analyte.

To provide some perspective we cite an example of results routinely achieved by S. Shen (personal communication), who obtained a spectrum of myoglobin with a signal/noise ratio of 30 in a 15-sec scan over the entire m/z range of the quadrupole (0 to 1500) during injection of a 0.8 nM solution in methanol-water at a rate of 1 $\mu\text{l}/\text{min}$. These numbers translate into the consumption of 200 amol of analyte while the spectrum was being recorded. By using ion counting instead of analogue detection and inserting another stage of pumping, one could hope to improve this sensitivity by another one or two powers of ten. If the application were such that single-ion monitoring of one or two peaks would suffice for detection, or if array detection were to be used with a magnetic sector instrument, then another ten- or 100-fold increase in sensitivity might be expected. Ultimately, in a Fourier transform ion cyclotron resonance (FTICR) instrument, one could obtain a spectrum with perhaps 100 ions or less in the cell because each ion has so many charges. Of course, these estimates of ultrahigh sensitivities are based on the amount of material introduced into the instrument

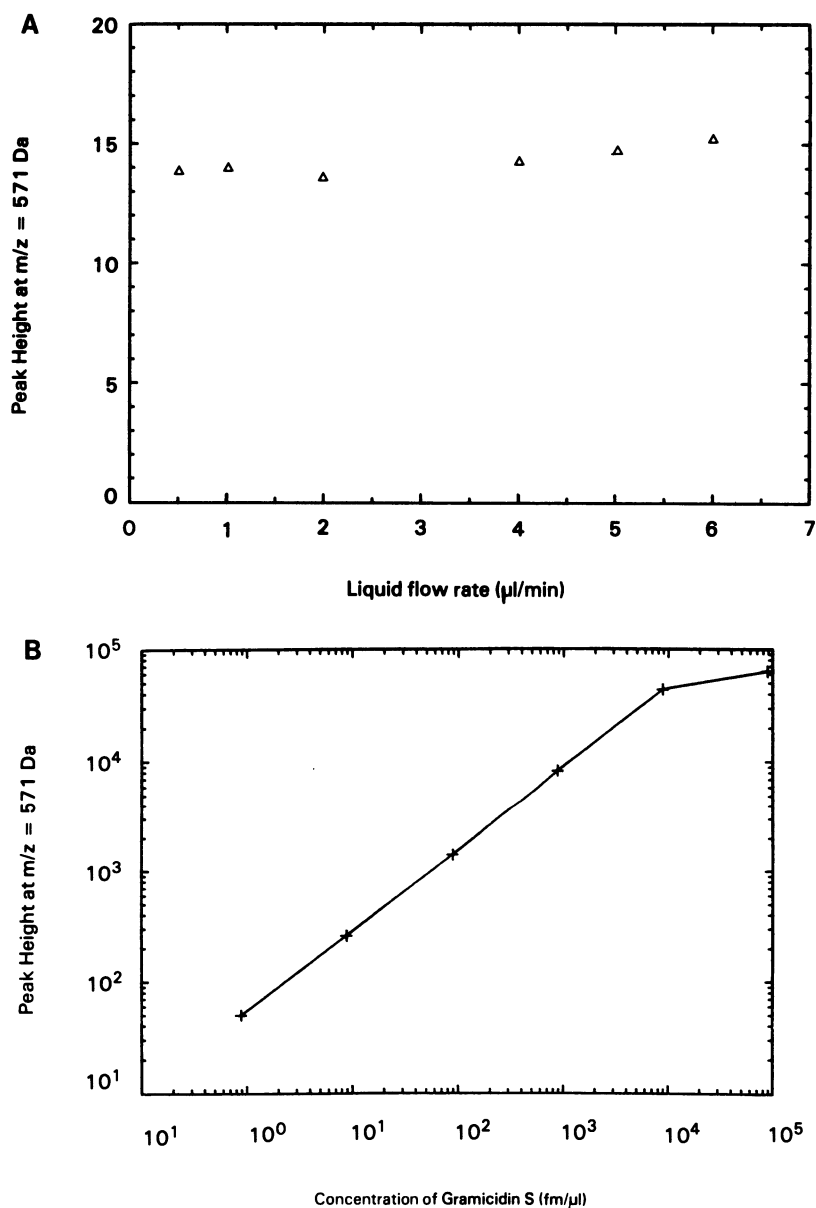


Figure 1.4. The effects of liquid flow rate (A) and analyte concentration (B) on the ESMS signal for the peptide gramicidin S in a 50:50 methanol–water solution.

while the spectrum is being recorded. Much more material is generally needed to carry out an actual analysis because of handling losses in preparing and transferring the sample to the instrument, e.g., by adsorption on tubing walls. Indeed, the practical limits of sensitivity in ESMS are generally determined by the extent of such handling losses during sample preparation and processing, not by the inherent sensitivity of ion formation and mass analysis.

2.2.6. Selectivity

Investigations of the types of molecules that ES can transform into ions have not been sufficiently systematic or comprehensive to permit definitive predictions of ionizability in any particular case. However, experience has revealed some patterns that are helpful in making educated guesses. All ES ions that have thus far been identified comprise species that are already ions in the sample solution or are adducts of such ions with nonionic solute species. Because ion-dipole interactions are the most likely source of adduct-bonding force, one would surmise that nonionic species must have a relatively high polarizability if they are to form strong attachments to prospective adduct ions. Available experimental results strongly support this expectation. Most species ordinarily considered to be nonionic that have been found to form ES ions by attaching other ions, for example, poly (ethylene glycols), are in fact polar. Indeed, in our view the appearance of such nonionic molecules in ESMS spectra as adducts with other solute ions constitutes direct evidence that the "adduction" takes place in solution, so that these species are already ions before ES dispersion of the solution into charged droplets.

Van Berkel *et al.* have recently shown that charge transfer agents can make possible the formation of ES ions from nonpolar compounds (38). For example, they found that polyaromatic hydrocarbons in solution could donate electrons to acceptors with a strong electron affinity such as some quinones and thus give rise to positive ES ions. The many implications of this intriguing result remain to be explored. Meanwhile, for the purposes of this book, the species that can readily and effectively be transformed by ES into "free" ions *in vacuo* fortunately include most important classes of biomolecules including peptides and proteins, nucleotides, carbohydrates, and glycoproteins. In general, it seems that almost any species having a sufficient number of polar charge-bonding sites to result in m/z values under 3000 can form ES ions for mass analysis. However, no positive evidence has yet appeared that ions with even larger m/z values cannot be produced.

2.2.7. Interference Effects

It is early for firm conclusions, but results thus far suggest that interference between components of analyte mixtures is less likely in ES ionization than in

some other techniques, e.g., FAB and PD. A fair amount of evidence does suggest that when the number of charges on a droplet is less than the total number of accessible charge sites on solute species in the droplet, those available charges attach to the sites on the most polarizable of those solute species. As a general rule for species of similar composition, polarizability increases with size. Thus, for example, background peaks from impurities of small mass in an injected solvent will disappear when an analyte species of high M_r is added to the solution. Moreover, interaction might occur in solution between one analyte species and another; for example, a chemical reaction that consumes one or both of them. In that event ES ions could not be expected for the species that is no longer present when formation of “free” gas-phase ions begin. Much remains to be learned about such interference effects and the possible suppression of ion formation from one species by the presence of another.

2.2.8. Cluster Formation

At high initial concentrations of some analyte species, an ES mass spectrum shows peaks corresponding to cluster ions, aggregates containing more than one analyte molecule per charge. We have found that such clustering can be extensive with amino acids and nucleotides. For example, cluster ions containing up to 24 arginine molecules with up to four charges (H^+) have been observed (39). The extent of clustering depends very much on the solvent as well as the analyte species. Moreover, the presence of some cosolutes can have a strong effect. Addition of small quantities of NaCl or HCl to the initial solution completely suppresses the clustering of arginine, whereas similar amounts of NaOH or NaAc have little or no effect. Other complexes held together by noncovalent bonds have been observed. We recently found that when cyclosporin A and gramicidin S were cosolutes in methanol–water, the dominant ions were doubly charged mixed dimers of the two species. Henion *et al.* have identified spectral peaks of enzyme–substrate complexes and have obtained information on the reaction kinetics by monitoring the time dependence of the peak height in samples from enzyme digests of the substrate (40).

2.2.9. Mechanisms of Ion Formation

We indicated earlier that unanimity has not yet been reached on the mechanism of ES ion formation from charged droplets. Most investigators identify themselves with one of two main schools of thought on how the ions are produced. One school holds that the charged residue model (CRM) originally proposed by Dole (12–15) embodies the essential features of what really happens. According to that model, the evaporation of solvent from the droplets leads to one or more Coulomb explosions that ultimately produce droplets small enough to contain only one analyte molecule. As the last of the solvent evaporates from

its containing droplet, that molecule retains some of the droplet's charge to become an ion.

The other principal school of thought believes that a more satisfactory explanation of observed behavior is embodied in the ion evaporation model (IEM) of Iribarne and Thomson (16–18). This model presumes the Dole scenario for the production of very small charged droplets by a combination of solvent evaporation and Coulomb explosions, but it does not require production of droplets containing only one analyte molecule. Instead, it holds that solvent evaporation increases surface charge density, thus producing a strong electrostatic field at the droplet surface. When the droplet size becomes small enough, the combination of small radius of curvature and high charge density produces a field sufficiently strong to overcome the solvation forces holding an ion to the droplet and to “lift” it from the surface into the ambient gas. After a substantial fraction of the net charge on the droplet has been carried off in this way, the remaining analyte molecules and other involatile solutes form a weakly charged residue as the last of the solvent evaporates.

We cannot engage here in a detailed discussion on the pros and cons of the two models but point out that in the IEM model the number of charges required to desorb an ion from the droplet depends only on the structure of the ion and the properties of the solution gas interface, including its radius of curvature and surface charge density. Therefore, within a fairly broad range of variation, the average charge state of the desorbed ions should not depend appreciably on the flow rate or the analyte concentration in the solution. Experiment confirms this and other implications of the desorption model that the charged residue model is hard put to account for. The main objections to the IEM stem from the fact that observed analyte ion currents are much higher than can be accounted for by calculated rates of ion desorption (41,42). Such rate calculations depend on the magnitude of the free energy change for the desorption process, and those that have been carried out thus far use a value for the free energy change estimated by Iribarne and Thomson for small ions like Na^+ that are very hydrophilic (16–18). Peaks for such ions do occasionally appear in ES mass spectra, but only under very special circumstances and always with very small amplitudes. In our view the much larger currents that are obtained for ions of the bigger and more complex species of biological interest are not evidence of shortcomings in the IEM. They simply reflect smaller free energies of desorption than are assumed in the calculations. In sum, we believe that the available experimental evidence seems to favor the desorption mechanism of the IEM for ion formation. However, the details of the process remain shrouded in mystery.

2.2.10. Molecule-Ion Charge Capacity

A very natural question with implications as to ionization mechanism concerns the maximum number of charges that can be retained by an isolated analyte

molecule in the gas phase. An analysis has been carried out for poly (ethylene glycols) (PEGs) that relates this maximum number to a balance between the Coulomb forces repelling a charge from the ion and the ion-dipole forces binding it to a site (24). The essence of that analysis is that the maximum number of charges is reached when the energy of that ion-dipole bond equals the electrostatic repulsion energy of the centermost charge on the ion, i.e., the one for which the repulsion energy is greatest. For a PEG oligomer with Na^+ as the adduct charge, the site is an oxygen atom, and the bonding energy is 2.05 eV. It is assumed that the electrostatic repulsion forces stretch the molecule into its so-called zig-zag configuration, for which the distance between oxygen atoms is known to be 0.35 nm. The solid curve in Fig. 1.5 shows that for oligomers with molecular weights above up to 20,000 this model leads to a nearly linear dependence of the maximum number of charges on oligomer mass. The experimental data indicated by the square points also show a linear dependence of charge number on mass in this size range but are only about 60% of model predictions.

We believe the reason for this difference is that an oligomer ion desorbs from the droplet before the surface charge density is high enough to deposit all the charges the oligomer can hold. This speculation finds support in recent experiments with PEGs having molecular weights up to 5 million (36). The results showed that these very large oligomers could form ES ions only with solutions so dilute that each initially formed droplet had a diameter of about 2.8 μm and contained only a single oligomer. When stretched out, that oligomer

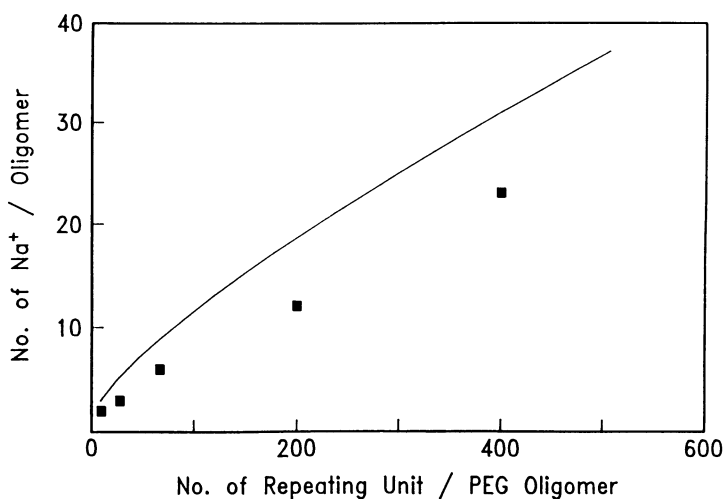


Figure 1.5. The dependence of charge state on molecular weight for oligomers of poly (ethylene glycols). The solid line shows the predictions of the electrostatic model for the maximum number of charges that an oligomer can hold. The points are measured values.

would have a length of about 40 μm , so it had to be highly folded in order to fit in the droplet.

Even more interesting and provocative was the finding by mass analysis that the actual number of charges on these very large oligomer ions was almost exactly equal to the maximum number predicted by the model. Because the initial droplet had about ten times that many charges, enough charges were always present to “saturate” the oligomer’s charge-holding capacity. Thus, as the last of the solvent evaporated, the oligomer simply retained all the charges it could hold, the excess charges being dissipated in the ambient gas, probably in the form of charged solvent clusters. Such charged solvent clusters are always found when “pure” solvent is electrosprayed and indeed constituted most of the ions that were observed in the first bona fide mass spectra of ES ions (20,21). On the other hand, as suggested above, the smaller oligomer ions were able to desorb as soon as they acquired enough charges to lift them from the droplet surface, apparently about 60% of the number they could hold. The most straightforward rationalization of these observations is that the very large oligomer ions are formed by the charged-residue mechanism of Dole. The small oligomer ions, on the other hand, are formed by the ion-evaporation mechanism of Iribarne and Thomson. In the former case, solvent abandons the ion. In the latter, the ion deserts the solvent. In sum, ES ions can be produced by either the IEM or the CRM, but the former applies in most cases.

2.3. Ion Transport

When ions are formed at atmospheric pressure, whether by ES or any other technique, they must somehow be transported through a billionfold or so change in pressure into the vacuum environment required for mass analysis. Any aperture that will pass ions into the vacuum system will also pass the neutral gas in which they are dispersed, and that gas must be removed by the system’s pumps. The pressure ratio across that aperture will almost inevitably greatly exceed the critical value required to reach sonic velocity (between 2 and 3, depending on C_p/C_v for the gas) so the gas enters the vacuum system as a supersonic free jet in which the temperature, density, and pressure drop very rapidly. The distribution of gas properties in such a jet is scaled by the diameter of its source orifice or aperture. Thus, at an axial distance of ten diameters, the ratios of jet gas temperature and density to their stagnation (source) values are, respectively, about 0.015 and 0.002 for a monatomic gas, 0.08 and 0.001 for a diatomic gas. In order to avoid exorbitant pumping speed requirements, one must use aperture diameters that are generally less than 1 mm. Consequently, the jet gas reaches the ambient pressure in a very short distance. It is noteworthy that the jet characteristics are essentially the same whether the aperture is a sharp-edged orifice, the throat of a contoured nozzle, or the exit end of a long tube or capillary, so

long as its minimum diameter (where the flow velocity equals the local speed of sound) is at the exit plane. If there is any diverging section downstream of this minimum diameter where the flow goes supersonic, a viscous boundary layer of thermalized gas grows very rapidly, filling the diverging section and destroying the isentropic character of the flow. The only way to avoid such boundary layer effects in small nozzles is to allow unconfined, "free" expansion by dispensing with a diverging section on the nozzle.

In single-stage systems, the jet expands directly into the high-vacuum chamber housing the mass analyzer, where the ambient pressure must be no higher than a few tens of microrrns. In this situation even a very small orifice admits enough gas to require very large pumping speeds. For example, the Sciex TAGA 6000E uses cryopumping speeds of 20,000 liters/sec or more in order to accommodate the flow through an orifice having a diameter of only 0.10 to 0.15 μm . Alternatively, one may resort to staged pumping systems in which a conical *skimmer* passes only a core portion of the free jet from the first vacuum chamber into one or more successive stages. In this way much of the jet gas can be removed from the first stages at pressures substantially higher than could be tolerated by the mass analyzer. In the system of Fig. 1.2, for example, each of the two stages is exhausted by a baffled diffusion pump with an effective speed of about 1000 liters/sec.

If the ratio of ions to neutrals remains constant during transport from the ES chamber to the mass analyzer, i.e., is the same in the gas entering the mass spectrometer chamber as it was in the gas leaving the ionization chamber, then the ion current into the analyzer chamber is determined only by the amount of gas entering that chamber. Therefore, staging would offer no advantages because analytical sensitivity would be determined by the pumping speed in the last chamber no matter how many stages may have preceded it. However, ions entering one stage can be focused by judicious arrangement of electrostatic fields so that gas leaving for the next stage is richer in ions than when it entered. Thus, in the three-stage systems based on ES sources produced by Analytica of Branford, CT, most of the ion-bearing gas leaving the electrospray chamber through a glass capillary with a bore of 0.4 mm (see Fig. 1.1) is removed at relatively high pressure in a first vacuum stage by rotary mechanical pumps. The second and third vacuum stages are each pumped by small (350 liters/sec) turbo pumps. Because ion focusing in the first two stages is so effective, up to one of every 500 ions produced in the ES chamber is delivered to the analyzer chamber. In the one-stage system described above, only one in 10,000 of the ions formed makes it that far, even though the pumping speed in the analyzer chamber is 20,000 liters/sec (9).

In addition to its role in ion transport, the free jet expansion can perform another useful function. Application of a potential difference between the source aperture and the skimmer accelerates the ions, bringing about collisions with the

unaccelerated neutral carrier gas molecules. The energy of such a collision is determined by the kinetic energies and masses of the ion and its neutral collision partner. In turn, the kinetic energy of the ion is determined by the distance it travels between collisions (its mean free path) and the strength of the field. The latter depends on the voltage difference between aperture and skimmer, which can be readily varied over a wide range. Thus, one can choose collision energies just sufficient to desolvate ions or high enough to break chemical bonds and produce offspring fragment ions for MS–MS studies of identity and structure with a single analyzer (43). Such collisional excitation in the free jet can also be used to advantage for “preheating” large ions so that they can be collisionally dissociated after selection by the first analyzer (see Chapter 2). It is noteworthy that this collisional heating and/or dissociation can be carried out at jet densities high enough to bring about very rapid thermalization of the ion translational energies almost immediately after they enter the skimmer and “escape” the field. Consequently, the effective injection energy of an ion entering the analyzer is determined by the potential of the skimmer relative to the analyzer and is independent of any fields upstream of the skimmer.

2.4. Analysis of ES Ions

The new and unique feature of ES ions is the extensive multiple charging that can occur when their molecular weights rise substantially above 1000. To generations of mass spectrometrists accustomed to dealing with singly charged ions, the implications of multiple charging have sometimes seemed surprising and confusing. In this section we examine some of these strange and wonderful implications.

2.4.1. Mass Analyzers

Quadrupole mass filters have been the workhorse analyzers responsible for the majority of ESMS results thus far reported. This analyzer–ion combination has been a “natural,” in part because quadrupoles are relatively inexpensive, easy to use, capable of excellent mass accuracy, and, therefore, by far the most common analyzers in laboratories throughout the world. Moreover, quadrupoles are relatively easy to interface with high-pressure sources, and the disadvantage of their relatively limited nominal mass range was overcome by the multiple charging of ES ions. For these same reasons quadrupoles will no doubt continue to be the most popular analyzers for some time to come. However, they suffer from limited resolution as well as from the inefficiency inherent in all dispersion instruments because of their small effective duty cycle. These handicaps have stimulated an increasing use of other kinds of analyzers for ES ions.

In the past 2 years ES sources have been successfully coupled to double-

focusing magnetic sector instruments (44–46). Interface design is somewhat more complicated in these combinations because the high acceleration voltages required for ion injection make it difficult to avoid corona discharges in the regions of intermediate pressure that are always encountered between the source chamber at atmospheric pressure and the analyzer chamber at relatively high vacuum. Sector instruments offer much higher resolution than quadrupoles. Figure 1.6 comprises a portion of the spectrum for bovine insulin showing clearly resolved isotope peaks for the quintuply charged ions. This spectrum was obtained with a sector instrument and exhibits a resolution of 10,000 (P. Dobberstein, personal communication). Also noteworthy is that, when used with array detectors, sector instruments can detect and distinguish ions of different mass simultaneously, thus avoiding some of the “waste” of signal inherent in purely dispersive instruments. Ion trajectories are longer in sector machines than in quadrupoles, and it has emerged that the large, multiply charged ions provided by ES seem to have large cross sections for collisional dissociation at the high

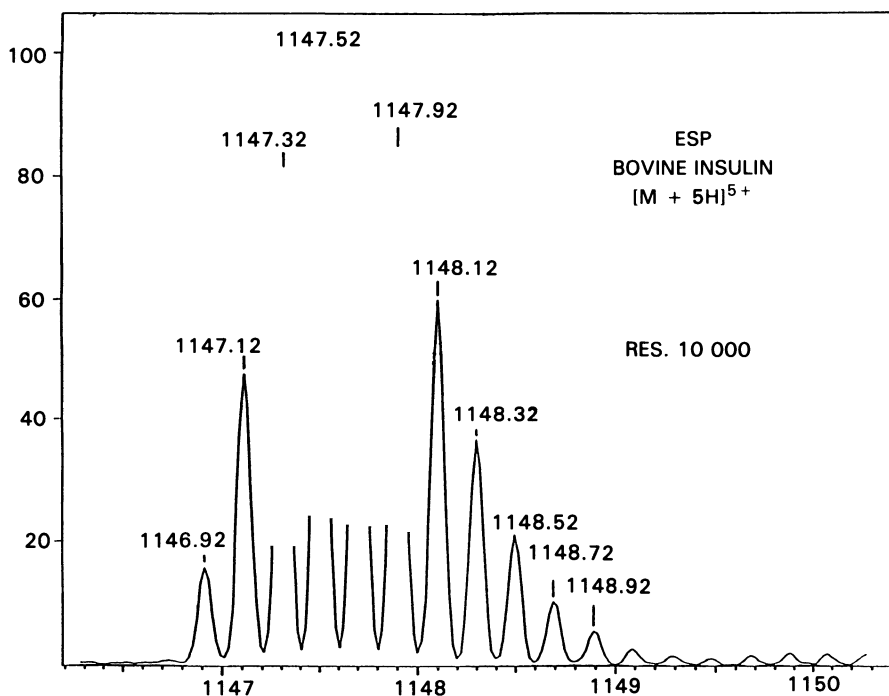


Figure 1.6. A portion of an ES mass spectrum for bovine insulin showing the quintuply charged ions. Peaks for molecules with differing numbers of carbon-13 peaks are clearly resolved. The spectrum was recorded with a magnetic sector analyzer having a resolution of 10,000. (Courtesy of P. Dobberstein, Finnigan-MAT.)

energies used for injection into magnetic analyzers. Consequently, vacuum requirements are more stringent in sector instruments than in quadrupoles or ion traps.

The quadrupole ion trap, or *quistor*, is a relative of the conventional quadrupole that operates by trapping and storing a batch of ions by means of RF fields having a combination of frequency and amplitude that maintains all the ions in stable orbits. An operator can destabilize the orbits of ions with progressively increasing values of m/z , for example, by scanning the amplitude of the fields, thus releasing them successively to an external detector to produce a spectrum. By this procedure all the ions stored in the trap contribute to the spectrum. Clearly, the overall analytical sensitivity thus depends on the fraction of the ions produced that become trapped. If ion production is batchwise on a schedule that can be synchronized with the schedule of filling and scanning times, then the analytical sensitivity can be quite high and will depend largely on the efficiency of capture. Internal batchwise production, for example, by laser desorption, seems to be most promising in this regard. Ion production by ES, on the other hand, is inherently continuous and must be external to the trap. Even so, the combination of ES ionization with an ion-trap mass analysis has already provided some impressive results (47). Long considered to be a low-resolution analyzer for ions with m/z values of 600 or less, the ion trap has shown an ability to extend its mass range to m/z values of 70,000 and to achieve resolutions of 30,000 or more. Because its hardware is simple and inexpensive, and its vacuum requirements are modest, many investigators believe that the ion trap is destined to become the most widely used analyzer of all. However, problems with mass accuracy, dynamic range, and software development remain to be solved before its promise can be fully realized.

In terms of resolution and sensitivity, analyzers based on Fourier transform ion cyclotron resonance (FTICR) seem to promise the ultimate in performance (48). Time-of-flight (TOF) instruments may well emerge as the simplest and most economical of analyzers (49). Both have been used for analysis of ES ions, but results thus far are very preliminary, and it seems a bit early to speculate on how important a role either of them may play in the future.

2.4.2. The Nature and Interpretation of ES Mass Spectra

As has already been discussed, ES ions consist of analyte molecules with varying numbers of small “adduct” charges attached. Thus, a substance of molecular weight M_r will give rise to a spectrum that is a sequence of peaks at positions K_i on the m/z scale such that:

$$\begin{aligned} K_i &= (M_r + im_\alpha)/i = M_r/i + m_\alpha \\ (K_i - m_\alpha) &= K' = M_r/i \end{aligned} \quad (1.1)$$

where m_α is the mass of an adduct charge and i is the number of such adducts on the ion. It is clear from the second part of Eq. 1.1 that the symbolism becomes simpler if the adduct ion mass is subtracted from the mass scale, i.e., if the K_i values are replaced by their K'_i counterparts. To determine M_r in Eq. 1.1, one must first determine i , the charge states (number of adduct charges) of the ions giving rise to the peaks. This determination is readily achieved by simultaneous solution of Eq. 1.1 for any two peaks. If the difference between the charge states of the two peaks is represented by j (e.g., $j = +2$ for a peak whose ions have $i + 2$ charges, i.e., the second peak to the left of the peak whose ions have i charges), the solution is:

$$i = j + K'_{i+j}/(K'_i - K'_{i+j}) \quad (1.2)$$

That is to say, we know *ab initio* that the ions of any one peak differ by one charge from those of either adjacent peak, so long as those adjacent peaks represent ions of the same parent species. It follows that the adduct ion mass m_α can in principle be determined from Eq. 1.1 after i has been determined. However, the value of the peak location K_i must be measured with very high accuracy to obtain an acceptable value of m_α . Consequently, it is often convenient to assume a value. For proteins and peptides the adduct charges are usually protons, but not always. For other species they can vary substantially, depending on the nature of the species and the composition of the solution. When the identity, and therefore the mass, of m_α is in doubt, one can assume an identity and then "spike" the solution with some of the assumed species and consider what happens to the spectrum. If no change occurs in peak positions, then the guess was right. If the peaks shift, or if new peaks appear, one can frequently deduce the value of m_α in the original spectrum from the magnitude of the shift or from the displacement of the new peaks relative to those in the original spectrum.

Having determined i from Eq. 1.2 and having arrived at or assumed a value of m_α , one can then estimate M_r from Eq. 1.1:

$$M_r = (1/n_o) \sum_i (i K_i) \quad (1.3)$$

that is to say, by straightforward averaging of the values obtained from each of the n_o individual peaks that have been considered. Experience with proteins of known M_γ reveals that the estimate of M_γ from one of the peaks in the middle of the sequence is often better than one obtained from peaks at either end. The reason is, of course, that the K'_i values for the peaks in the middle have a higher signal/noise ratio. To obtain the best possible mass estimate, it is therefore advantageous to weight the contributions of the peaks, for example, by their relative height. A more reliable weighting makes use of the coherence of the

sequence. It is clear from Eq. 1.1 that the K'_i values of any two peak locations must be a ratio of small integers. This feature can be used to weight the contribution of a peak by its proximity to a straight line defined by:

$$1/i = (1/j)[(K'_i/K'_{i+j}) - 1] \quad (1.4)$$

which comes from solving Eq. 1.1 for any two peaks. Mann *et al.* (50) describe an algorithm for obtaining such a weighted average. (Note that Eq. 6 in that paper should read: $w_i^{-1} = \dots$ and that the second part of the formula is simply a statement that the sum of the weighting factors must be unity.) Similar algorithms can be devised to identify the peaks belonging to the sequence for a particular parent species in the apparent hodge-podge of peaks that sometimes characterized the spectrum of a mixture of such species.

Another way to extract information on M_γ is to “deconvolute” the spectrum (50). In this procedure one resorts to a mathematical function that transforms the sequence of peaks from ions of a single species and maps it into a single peak that would have been obtained if all the ions had the mass of the parent species and the adduct charge had zero mass. Figure 1.7 shows the application of this algorithm to the mass spectrum of the protein cytochrome C (horse heart). To perform the deconvolution one must assume a value for the mass of the adduct ion, taken to be a proton in this case. Such processing of spectral data is

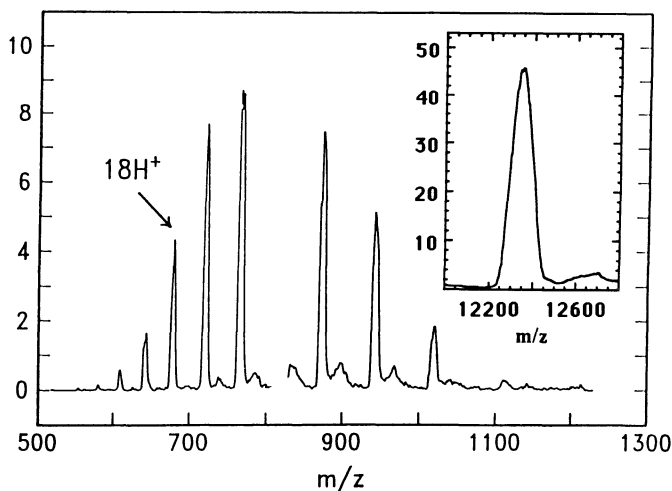


Figure 1.7. An ES mass spectrum for cytochrome C (horse heart). The insert shows the result of a deconvolution procedure that transforms the multiple peaks of the measured spectrum into a single peak that would be obtained if all ions had comprised the parent molecule with a single adduct charge with negligible mass. Note that the ordinates of both spectra have the same scale.

particularly useful for analyzing mixtures because in their spectra it can be very difficult to identify visually the peaks belonging to particular components, especially if those components are numerous and unknown *a priori*. This ability to resolve mixtures has been very helpful in identifying carbohydrate adducts in glycoproteins (I. Jardin, personal communication).

Also noteworthy is that the algorithm sums contributions to signal only at m/z values that match the coherence of the sequence of peaks from a particular species. Therefore, it discriminates against random contributions so that the signal/noise ratio is higher in the deconvoluted spectrum than in the measured one. Several groups have made refinements in the original algorithm that improve its performance, for example, by suppressing side bands. One new version even avoids the need to assume a value for the adduct ion mass m_α . Instead, it treats m_α as an independent variable so that the deconvoluted spectrum becomes a three-dimensional surface (51). Maximum entropy methods have also recently been applied to the interpretation of ESMS spectra (52). Although a twofold increase in resolution is claimed, experience with this approach is not yet sufficient to determine whether the improvement that this interesting development can provide will be worth what it costs in complexity and time of computation (52).

One of the attractive features of ESMS (partly shared by LDMS) is the ability to determine M_r values with high accuracy even for large species. Previous techniques such as gel electrophoresis could achieve an accuracy of no better than 5% for unsequenced proteins. Electrospray MS spectra typical of those that can be obtained with a good quadrupole analyzer provide a precision of 0.01% and on occasion have determined M_r for proteins to within one unit at values of 20,000 or more. Reasons for this remarkable precision include the absence of fragmentation and the multiplicity of peaks for a single species. The m/z value of the ions for each peak constitutes an independent measure of the parent ion mass. Consequently, averaging these m/z values substantially decreases the random error. In contrast to the case of FAB and other energy-sudden techniques, there seem to be no losses of small neutral fragments that can lead to distortion of peak shapes.

Another reason for the precision is the fact that the ions always have relatively low m/z values, for which measurements and calibrations are easier. In addition, random errors are reduced by the averaging of m/z values for several peaks in the same spectrum. On the other hand, to achieve accuracies commensurate with achievable precision requires very exact calibration of the m/z scale because an error in absolute peak location is multiplied by the number of charges on the ion. For example, a systematic error of only 0.05 units on the m/z scale becomes a 5-unit error in M_r if the median number of charges on the ions is 100. Comparison of values obtained from different peaks can provide an estimate of random error, but the absolute error includes contributions from both random and

calibration errors. This still-new ability to achieve high accuracy in M_r is rapidly finding practical applications. For example, a single and nearly instantaneous ESMS determination of M_r for a batch of recombinant protein could confirm the identity of the product and provide information on the masses and, therefore, the identities of contaminants.

3. SOME PRACTICAL CONSIDERATIONS

For routine use of ESMS in analysis of biological samples, it might be valuable for an investigator to understand its principles, but it is imperative that he or she observe some practical rules that have evolved from experience. Unfortunately, there is yet very little literature available on what constitutes good ESMS practice, but we will briefly mention some things to be kept in mind.

3.1. Sample Preparation and Introduction

In selecting reagents, one should take the same precautions that have been found effective in HPLC. Solvents should be of HPLC grade and degassed to avoid bubble formation during passage through the injection needle, which may have been heated somewhat by contact with warm bath gas. It is now possible to maintain stable sprays with liquids having high surface tensions, conductivities, and flow rates, but when other constraints permit, solutions with low surface tensions, conductivities, and flow rates are easier to work with. Because low flow rates are desirable and often used, special care must be exercised to minimize dead volume in fittings and injection valves in order to avoid broadening of LC or CZE peaks as well as memory effects. Because ESMS is so sensitive, the small quantities of sample that adsorb on walls of inlet tubes and fittings can give rise to persistent memory effects. Removal is usually achieved quite simply by “washing” the walls with a flow of appropriate solvent, e.g., mild acid in the case of proteins. In the case of small samples one must be concerned that much or all of some analyte species may be “lost” to these wall effects. Also to be remembered is that the small conduits often used are prone to plugging by small particles that may be present initially or be precipitated from solution en route to the spray zone. Liquid injection flow should be pulse-free and constant. Positive-displacement syringe pumps are more satisfactory than double-barrel plunger pumps.

3.2. Fouling Problems

Sample liquids having high concentrations of analyte or nonvolatile buffers can cause spray instabilities by forming insulating deposits that accumulate

charge and distort the distribution of electric fields. These deposits can form at the tip of the needle, on the inside walls of the spray chamber, and in the intermediate vacuum stages. In systems using a glass capillary as in Fig. 1.1, incomplete evaporation of droplets can sometimes result in wetting of the inside surface of the capillary, making it conductive so that the MS signal drops, sometimes very rapidly. We attribute this signal loss to the discharging of analyte ions on the conducting wall. However, such an explanation loses some credibility in the face of the successful use of heated metal tubes by Chait's group to transfer ions from the source into the vacuum system (53). The susceptibility of ESMS systems to these kinds of fouling problems varies widely and is apparently less of a problem when a countercurrent flow of bath gas is used to sweep out nonionic material. In our experience, sources that are well designed and carefully operated can be down for cleaning as little as 1% of the time. Poor design and careless operation can keep a system out of use for as much as half the time or more. Sources that are prone to foul easily should at least be easy to clean.

3.3. Performance Diagnosis

It is a great advantage to be able to monitor the spray by visual inspection and/or by measuring the spray current. For example, if the spray is stable and the analyte is known to behave well, one should start troubleshooting on the MS end of the apparatus. Conversely, if the spray is unstable, the trouble is likely to be found in the spray chamber. Especially useful is the ability to check spray behavior during operation under unfamiliar conditions, as with new solvents or flow rates. An ideal system would allow one to isolate each operating stage so that spray behavior, ion formation, ion transport, and mass analysis could be diagnosed independently.

3.4. Data Systems and Software

In practice, an especially important feature of an ESMS apparatus is its data system, because in principle hundreds of samples can be analyzed per day. In a well-designed and well-behaved system, only a small fraction of operating time and effort would be required for introducing samples. A much larger fraction would be required for interpreting results. Thus, the system for collecting and processing data should be very fast, efficient, and user-friendly. Data-system capability will become increasingly important as MS analysis becomes more widely applied and carried out by operators who are not experienced mass spectrometrists. In the particular case of ESMS, the data system should at least be able to deconvolute a multiple peak spectrum for a single species and provide its M_r value "on line." Indeed, the ability to acquire and interpret the complex spectra for mixtures of species, rapidly and efficiently, has been demonstrated so

often that one should probably refrain from purchasing an ESMS instrument for which such capability is not at least prospectively available. Effective data processing and operating systems are becoming so vital for the effective use of modern instruments that a system's software may be on its way to becoming more important than its hardware.

4. SUMMARY AND CONCLUSIONS

We have attempted to describe the principles and methods of ESMS, an analytical technique that comprises four principal component processes or steps, each with its own challenges and opportunities for improvement. (a) The first is the spraying or dispersion of the liquid into charged droplets. This step determines compatibility with sample sources. Methods have been developed that can provide stable spray operation over a wide range of flow rates and compositions. (b) The second step is the formation of analyte ions from charged droplets. Experiments have established that ions are formed intact from a wide variety of polar and parent species, efficiently and in relative abundance. A unique feature is the ability of ES to produce from very large and fragile parent species ions that have extensive multiple charging. An important consequence of this multiple charging is that the mass spectrum for a single species comprises a coherent sequence of peaks whose number and charge state depend on the size and chemical nature of the parent. (c) The third step is transport of ions from the atmospheric pressure environment in which they are formed to the high-vacuum environment of the mass analyzer. The efficiency of this transport step plays a major role in determining the analytical sensitivity of the system. (d) Mass analysis of the ions and interpretation of the spectra follow. All types of mass analyzers can be used, including quadrupole filters, magnetic sector instruments, ion traps, Fourier-transform ion cyclotron resonance, and time-of-flight instruments. More experience has been accumulated with the first three of these types of analyzers, but there is no reason to believe that use of the last two will not increase substantially. The ESMS spectra are unique in that multiple peaks are obtained for large species so that the spectra are complex. Data-processing procedures have been developed that greatly simplify the interpretation process and promise to become increasingly user-friendly.

Up to now, ES ionization has been more rapidly embraced by the community of manufacturers and users of mass spectrometers than has laser desorption (LD) ionization. This apparent "preference" may well be transient and seems largely to result from the greater availability of ESMS systems. In turn, that availability results in part from the fact that ES sources can be readily adapted to the types of mass analyzers that are most familiar and have the greatest sales volume. It seems highly likely that LD will grow rapidly as the TOF analysis

methods to which it is best adapted become perfected. The really large-volume markets await the development of robust "benchtop" systems that can provide the advantages of mass spectrometric analysis at moderate cost. It will be interesting to see which type of system will capture that market.

REFERENCES

1. Meng, C. K., Mann, M., and Fenn, J. B., 1988, Of protons or proteins—A beam's a beam for a' that, *Z. Phys.* **D10**:361–368.
2. Tanaka, K., Waki, H., Ido, Y., Akita, S., Yoshida, Y., and Yoshida, T., 1988, Protein and polymer analyses up to m/z 100,000 by laser ionization time-of-flight mass spectrometry, *Rap. Commun. Mass Spectrom.* **2**:151–153.
3. Karas, M., and Hillenkamp, F., 1988, in *Proceedings 11th International Mass Spectrometry Conference, Bordeaux*.
4. Karas, M., and Hillenkamp, F., 1989, Ultraviolet laser desorption of proteins up to 120,000 daltons, *Adv. Mass Spectrom.* **11A**:416–417.
5. Karas, M., and Hillenkamp, F., 1988, Laser desorption ionization of proteins with molecular masses exceeding 100,000 daltons, *Anal. Chem.* **60**:2299–2301.
6. Burlingame, A. L., Millington, D. S., Norwood, D. L., and Russel, D. H., Mass spectrometry, *Anal. Chem.* **62**:268R–303R.
7. Fenn, J. B., Mann, M., Meng, C. K., Wong, S. F., and Whitehouse, C. M., 1990, Electrospray ionization—Principles and practice, *Mass Spectrom. Rev.* **9**:37–70.
8. Fenn, J. B., Mann, M., Meng, C. K., Wong, S. F., and Whitehouse, C. M., 1989, Electrospray ionization for mass spectrometry of large biomolecules, *Science* **246**:64–71.
9. Smith, R. D., Loo, J. A., Edmonds, C. K. G., Barinaga, C. J., and Udseth, H. R., 1990, New developments in biochemical mass spectrometry: Electrospray ionization, *Anal. Chem.* **62**:882–889.
10. Mann, M., 1990, Electrospray: Its potential and limitations as an ionization method for biomolecules, *Org. Mass Spectrom.* **25**:575–587.
11. Bailey, A. G., 1988, *Electrostatic Spraying of Liquids*, Research Studies Press, Taunton, and John Wiley & Sons, New York.
12. Dole, M., Mach, L. L., Hines, R. L., Mobley, R. C., Ferguson, L. P., and Alice, M. B., 1968, Molecular beams of macroions, *J. Chem. Phys.* **49**:2240.
13. Mach, L. L., Kralik, P., Rheude, A., and Dole, M., 1970, Molecular beams of macroions, II, *J. Chem. Phys.* **52**:4977–4986.
14. Clegg, G. A., and Dole, M., 1971, Molecular beams of macroions, III, *Biopolymers* **20**:821–826.
15. Teer, D., and Dole, M., 1975, *J. Polym. Sci.* **13**:985.
16. Iribarne, J. V., and Thomson, B. A., 1976, Evaporation of small ions from charged droplets, *J. Chem. Phys.* **64**:2287–2294.
17. Thomson, B. A., and Iribarne, J. V., 1979, Field-induced ion evaporation from liquid surfaces at atmospheric pressure, *J. Chem. Phys.* **71**:4451–4463.
18. Iribarne, J. V., Dziedzic, P. J., and Thomson, B. A., 1983, Atmospheric-pressure ion evaporation mass spectrometry, *Int. J. Mass Spectrom. Ion Phys.* **50**:331–347.
19. Alexandrov, M. L., Gall, L. N., Krasnov, M. V., Nikolaev, V. I., and Shkurov, V. A., 1985, Mass-spectrometric analysis of thermally unstable compounds of low volatility by the extraction of ions from solution at atmospheric pressure, *Zh. Anal. Khim.* **40**:1227–1236.

20. Yamashita, M., and Fenn, J. B., 1984, Electro spray ion-source—Another variation on the free-jet theme, *J. Phys. Chem.* **88**:4451–4459.
21. Yamashita, M., and Fenn, J. B., 1984, Negative-ion production with the electro spray ion-source, *J. Phys. Chem.* **88**:4671–4675.
22. Smith, R. D., Barinaga, C. J., and Udseth, H. R., 1988, Improved electro spray ionization interface for capillary zone electrophoresis-mass spectrometry, *Anal. Chem.* **60**:1948–1952.
23. Bruins, A. P., Covey, T. R., and Henion, J. D., 1987, Ion spray interface for combined liquid chromatography/atmospheric pressure ionization mass spectrometry, *Anal. Chem.* **59**:2642–2646.
24. Wong, S. F., Meng, C. K., and Fenn, J. B., 1988, Multiple charging in electro spray ionization of poly (ethylene glycols), *J. Phys. Chem.* **92**:546–550.
25. Blakley, C. R., McAdams, M. J., and Vestal, M. L., 1978, Crossed-beam liquid chromatograph-mass spectrometer combination, *J. Chromatogr.* **158**:261–276.
26. Blakley, C. R., Carmody, J. J., and Vestal, M. L., 1980, Combined liquid chromatograph/mass spectrometer for involatile biological samples, *Clin. Chem.* **26**:1467–1473.
27. Blakley, C. R., Carmody, J. J., and Vestal, M. L., 1980, A new soft ionization technique for mass spectrometry of complex molecules, *J. Am. Chem. Soc.* **102**:5931–5933.
28. Bruins, A. P., Weidolf, L. O. G., and Henion, J. D., 1987, Determination of sulfonated azo dyes by liquid chromatography/atmospheric pressure ionization/mass spectrometry, *Anal. Chem.* **59**:2647–2652.
29. Whitehouse, C. M., Yamashita, M., Meng, C. K., and Fenn, J. B., 1985, in: *Proceedings of the 14 International Symposium Rarefied Gas Dynamics* (H. Oguchi, ed.), University of Tokyo Press, Tokyo, p. 857.
30. Zeleny, J., 1917, Instability of electrified liquid surfaces, *Phys. Rev.* **10**:1.
31. Taylor, G. I., 1964, Disintegration of water drops in an electrical field, *Proc. R. Soc. A* **280**:383–397.
32. Gomez, A., and Tang, K., 1992, Fission of charged droplets in electrostatic sprays, *Nature* (submitted).
33. Rayleigh, Lord, 1882, On the equilibrium of liquid conducting masses charged with electricity, *Phil. Mag.* **14**:184.
34. Allen, M. H., Field, F. H., and Vestal, M. L., 1990, Design and performance of a new electro spray interface, *Proceedings of the 38th ASMS Conference on Mass Spectrometry and Allied Topics*, ASMS, Tucson, pp. 431–432.
35. Chowdhury, S. K., Katta, V., and Chait, B. T., 1990, Probing conformational changes in proteins by mass spectrometry, *J. Am. Chem. Soc.* **112**:9012–9013.
36. Nohmi, T., and Fenn, J. B., in press, Electro spray mass spectrometry of poly (ethylene glycols) with molecular weights up to five million, *J. Am. Chem. Soc.* **114**:3241.
37. Whitehouse, C. M., Dreyer, R. N., Yamashita, M., and Fenn, J. B., 1985, Electro spray interface for liquid chromatographs and mass spectrometers, *Anal. Chem.* **57**:675–679.
38. Van Berkel, G. J., McCluckey, S. L., and Glish, G. L., 1991, Preforming ions in solution via charge-transfer complexation for analysis by electro spray ionization mass spectrometry, *Anal. Chem.* **63**:2064–2068.
39. Meng, C. K., and Fenn, J. B., 1991, Formation of charged clusters during electro spray ionization of organic solute species, *Org. Mass Spectrom.* **26**:542–549.
40. Ganem, B., Yu Tsyri Li, and Henion, J. D., 1991, Detection of noncovalent receptor ligand complexes by mass spectrometry, *J. Am. Chem. Soc.* **113**:6294–6296.
41. Roellgen, F. W., Bramer-Wegner, E., Butfering, L., 1987, Field-ion emission from liquid solutions—Ion evaporation against electrohydrodynamic disintegration, *J. Phys.* **48**:253–256.
42. Schmelzeisen-Redeker, G., Butfering, L., and Roellgen, F. W., 1989, Desolvation of ions and molecules in thermospray mass spectrometry, *Int. J. Mass Spectrom. Ion Processes* **90**:139–150.

43. Katta, V., Chowdhury, S. K., and Chait, B. T., 1991, Use of single-quadrupole mass spectrometer for collision-induced dissociation studies of multiply charged peptide ions produced by electrospray ionization, *Anal. Chem.* **63**:174–178.
44. Allen, M. H., and Lewis, I. A. S., 1989, Electrospray on magnetic instruments, *Rapid Commun. Mass Spectrom.* **3**:225–258.
45. Meng, C. K., McEwen, C. N., and Larsen, B. S., 1990, Electrospray ionization on a high-performance magnetic-sector mass spectrometer, *Rapid Commun. Mass Spectrom.* **4**:147–150.
46. Gallagher, R. T., Chapman, J. R., and Mann, M., 1990, Design and performance of an electrospray ionization source for a doubly focusing magnetic sector mass spectrometer, *Rapid Commun. Mass Spectrom.* **4**:329–372.
47. Van Berkel, G. J., Glish, G. L., and McLuckey, S. A., 1990, Electrospray ionization combined with ion trap mass spectrometry, *Anal. Chem.* **62**:1284–1295.
48. Henry, K. D., Williams, E. R., Wang, B. H., McLafferty, F. W., Shabanowitz, J., and Hunt, D. F., 1989, Fourier-transform mass spectrometry of large molecules by electrospray ionization, *Proc. Natl. Acad. Sci. U.S.A* **86**:9075–9078.
49. Boyle, J. G., Whitehouse, C. M., and Fenn, J. B., 1991, An ion-storage time-of-flight mass spectrometer for analysis of electrospray ions, *Rapid Commun. Mass Spectrom.* **5**:400–405.
50. Mann, M., Meng, C. K., and Fenn, J. B., 1989, Interpreting mass spectra of multiply charged ions, *Anal. Chem.* **61**:1702–1708.
51. Labowsky, M., Whitehouse, C. M., and Fenn, J. B., 1992, Three dimensional analysis of mass spectra for multiply charged ions, *Rapid Commun. Mass Spectrom.* (submitted).
52. Reinhold, B., and Reinhold, V., 1992, Electrospray ionization mass spectrometry: Deconvolution by an entropy-based algorithm. *J. Am. Soc. Mass Spectrom.* **3**:207.
53. Chowdhury, S. K., Katta, V., and Chait, B. T., 1990, An electrospray-ionization mass spectrometer with new features, *Rapid Commun. Mass Spectrom.* **4**:81–87.

The Analysis of Biomolecules by Electrospray Ionization–Mass Spectrometry and Tandem Mass Spectrometry

Richard D. Smith, Joseph A. Loo, and Charles G. Edmonds

1. INTRODUCTION

Electrospray ionization–mass spectrometry (ESI–MS) has its origins in research that long preceded the current flurry of activity. The study of electrospray phenomena extends back over perhaps two and one-half centuries to the work of Bose (1) and certainly to that of Zeleny early in this century (2). The seminal research into the use of electrospray as an ionization method was done by Malcom Dole and co-workers (3,4), who, more than 20 years ago, performed extensive studies into the electrospray process and defined many of the important experimental parameters. The purpose of Dole’s studies was to use ESI to produce gas-phase macroions. Dole’s approach was largely an adaptation of the electrospray studies performed in the 1930s by Chapman, who conducted ion mobility studies of low-molecular-weight salts formed from the evaporation of charged droplets (5). Experimental evidence was presented for ionization of zein ($M_r \sim 50,000$) (6) and lysozyme (7). Interpretation of Dole’s results was problematic, however, because a mass spectrometer was not available, and only ion retardation (3,4,6) and ion mobility (7) measurements were obtained. However,

Richard D. Smith, Joseph A. Loo, and Charles G. Edmonds • Chemical Methods and Separations Group, Chemical Sciences Department, Pacific Northwest Laboratory, Richland, Washington 99352.

the importance of Dole's contributions cannot be overstated; his research clearly presaged the ESI-MS of macromolecules, arguably the multiple charging phenomenon, as well as many of the instrumental methods currently utilized (3,4,6-8). In 1984 ESI-MS experiments were reported essentially simultaneously by both Yamashita and Fenn (9) and Aleksandrov *et al.* (10,11). Fenn and co-workers also demonstrated ESI-MS in the negative-ion mode (12), building on the original negative-ion work by Dole and co-workers (3,4,6). Using a magnetic sector instrument, the Russian researchers independently demonstrated the on-line combination with liquid chromatography in 1984 (11) and over the next few years applied ESI-MS to oligosaccharides (13) and intact polypeptides with M_r to 1500 Da (14) and developed chemical-digestion-based methods for their sequence determination (15).

The multiple charging of lysozyme by ESI was deduced by Dole on the basis of ion mobility measurements (7), but difficulties in data interpretation led them to suggest a level of charging substantially lower than that shown by subsequent MS studies. In 1985 Fenn and co-workers (16) and Aleksandrov *et al.* (13,14,17) reported dominant contributions of multiply charged molecular ions for polypeptides. Later, Fenn and co-workers reported the ionization of polyethylene glycols of average molecular weights up to 17,500 with as many as 23 charges (from associated sodium ions) (18). Because the polyethylene glycol samples had relatively broad molecular weight distributions, only unresolved "humps" of ions from $m/z \sim 550$ to >1400 were observed for higher-molecular-weight samples. In 1988, Fenn and co-workers (19) first reported ESI-MS spectra of intact multiply protonated molecular ions of proteins up to 40 kDa having as many as 45 positive charges. Fenn's initial results were quickly duplicated and extended by our group (20,21) and Covey *et al.* (22).

Since its introduction in 1988 as a tool for the ionization of large biomolecules, the practice of ESI-MS has grown impressively. Although its inception was nearly simultaneous with the introduction of matrix-assisted laser desorption/ionization (MALDI) methods for similar applications (23), the number of ESI-MS applications has been substantially greater. One reason for this difference is the speed with which commercial instrumentation became available, and particularly the ease of retrofitting existing quadrupole instruments. Such was not the case for MALDI methods, and commercial instrumentation has been slower to appear. Although it is not yet possible to compare ESI and MALDI quantitatively, it appears that MALDI may well have sensitivity advantages for high-molecular-weight proteins. However, ESI has clear advantages for analysis of liquids, particularly the effluents from microscale or "nanoscale" capillary separation methods. In addition, tandem mass spectrometry has been shown to be useful for dissociation studies of the multiply charged biomolecules produced by ESI, allowing much greater dissociation efficiencies than for singly charged molecules (24,25). The combination of these capabilities potentially constitutes

an enabling technology capable of profoundly affecting the practice of mass spectrometry and its role in significant areas of biochemical research.

2. EXPERIMENTAL METHODS AND CONSIDERATIONS

The following discussion is divided into two parts based on the functional components of the ESI-MS instrumentation. These factors are the electrospray source, or *tip*, where electrostatic nebulization of a liquid stream occurs, and the atmosphere-vacuum interface, where the droplets and resulting ions are desolvated and transferred from near atmospheric pressure to the vacuum environment of the mass spectrometer.

2.1. The Electrospray Source

The ESI source may be simply a metal capillary (e.g., stainless steel hypodermic needle) at elevated voltage relative to a counterelectrode having an orifice where ions and/or charged droplets entrained in a flow of gas enter the mass spectrometer. Liquid flow is generated by infusion syringes, separation devices, or other liquid sources. The ESI source requires production of a high electric field at the capillary tip. The electric field causes charge to accumulate on the liquid surface at the capillary terminus and disrupts the liquid surface. The ESI liquid nebulization process can be pneumatically assisted (5) using a high-velocity annular flow of gas at the capillary terminus, as originally described by Dole and co-workers (3).

Our interest in coupling high-resolution capillary electrophoresis (CE) separation methods with ESI-MS led to the development of the liquid sheath electrospray source (26). An organic liquid sheath (often pure methanol, methoxyethanol, or acetonitrile, but frequently augmented by small proportions of acetic acid, water, and/or other reagents), flows through the annular space between a $\sim 200\text{-}\mu\text{m}$ o.d. fused silica capillary, which delivers analyte solution to the ion source, and a stainless steel capillary ($\geq 250\ \mu\text{m}$ i.d.). A detailed view of a recent version of the interface in a configuration developed and optimized for combined CE-MS is shown in Fig. 2.1; a $300\text{-}\mu\text{m}$ i.d. fused silica capillary surrounds the smaller-diameter CE analytical capillary. For positive-ion ESI, a voltage of +4 to +6 kV is applied indirectly to the sheath liquid from which the fused silica tube protrudes approximately 0.2 mm. For experiments in which sample solution is directly infused to the ESI source, syringe pumps deliver controlled flows of analyte and sheath liquids at rates of $0.1\text{--}1\ \mu\text{l}/\text{min}$ and $2\text{--}5\ \mu\text{l}/\text{min}$, respectively. Potential problems from the formation of bubbles in the connecting lines are minimized by the inclusion of a trapping volume. Additional stability is obtained by degassing the organic solvents used in the sheath and by minimizing heating

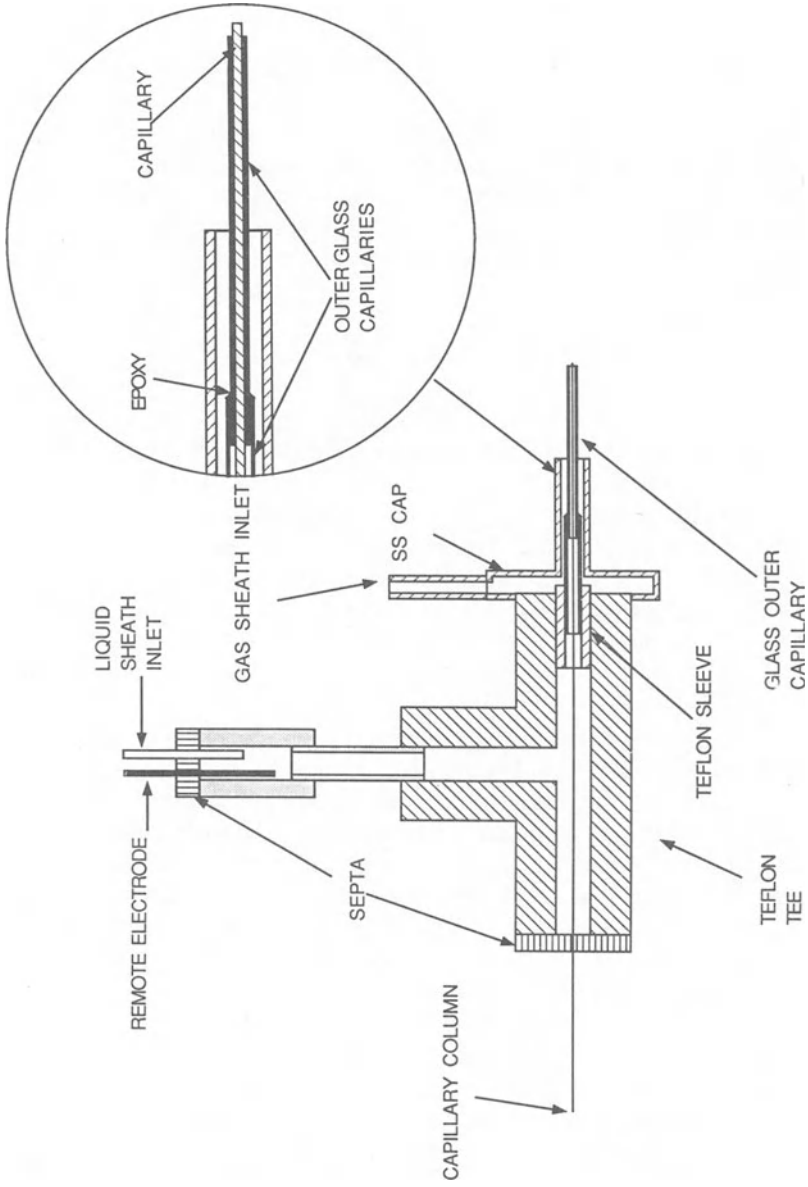


Figure 2.1. Detailed schematic of the sheath liquid electrospray source developed for ESI-MS (26). Inset shows detail for the capillary tip.

(e.g., due to the countercurrent gas flow). These steps are particularly useful for CE-MS, as are cooling of the entire assembly to $\sim 15^{\circ}\text{C}$ (27) and the use of less volatile sheath solvents such as methoxyethanol (28).

For the positive-ion mode, sample solutions of proteins and peptides are typically prepared in 1–5% v/v acetic acid in good-quality ($>16\text{ M}\Omega/\text{cm}$) deionized water. For the negative-ion mode, good performance has often been obtained with sample solutions prepared in 1–2% ammonium hydroxide/water or in deionized water (if strongly acidic groups are present). In addition, an electron scavenger is generally required to inhibit electrical discharge at the capillary terminus (29,30). Sulfur hexafluoride has proven particularly useful for suppressing corona discharges and improving the stability of negative-ion production. Introduction of this gas is most effectively accomplished using gas flow ($\sim 100\text{--}250\text{ ml/min}$) through an annular volume surrounding the sheath liquid (Fig. 2.1).

Greater flow rates of more highly conductive liquids lead to unstable performance (“spitting”) and larger droplet sizes. The dependence of ESI ion current (I) on solution conductivity (σ) is relatively weak ($I \propto \sigma^{0.22}$) (30). The ESI currents for a typical water/methanol/5% acetic acid solution are in the range of 0.1–0.3 μA .

Evidence exists that heating is useful for manipulating the electrospray process. For example, slight heating allows aqueous solutions to be readily electrosprayed (31), presumably because of the decreased viscosity and surface tension. Thermally assisted (32) and pneumatically assisted (33) electrosprays allow higher liquid flow rates but decrease the extent of droplet charging. Studies with conventional and “electrically assisted” thermospray indicate that on electrical “assistance” the extent of multiple charging for large molecules increases (32). Thus, the average charge state may be continuously adjustable between the limiting cases of electrospray ionization (electric field, no heating) and thermospray ionization (heating, no electric field). The maximum extent of charging likely results from the pure electrospray process, and any method aimed at “assisting” ESI is expected to decrease charging (34).

2.2. The Atmosphere–Vacuum Interface

The formation of macromolecular ions requires conditions promoting solvent evaporation from the initial droplet population. This evaporation can be accomplished at near-atmospheric pressure by a countercurrent flow of dry gas at moderate temperatures ($\sim 80^{\circ}\text{C}$), by heating during transport through the interface, and by (particularly in the case of ion-trapping methods) energetic collisions at relatively low pressure. Droplets shrink to the point at which repulsive Coulombic forces approach the level of droplet cohesive forces (e.g., surface tension). There is also direct evidence that small droplets emit “microjets” of smaller droplets as they become unstable (35). On the basis of light scattering and residual particle measurements, an initial droplet size of $\sim 1\text{ }\mu\text{m}$ has been

deduced. Evidence for “second-generation” droplets in the 0.01- to 0.1- μm size range has also been obtained (36). As we suggested earlier (37), a process yielding jets of very small droplets by Rayleigh fission may be mechanistically indistinguishable from a process involving the field evaporation of highly solvated ions.

An important attribute of an ion source operating at atmospheric pressure is the efficiency of sampling and transport of ions into the mass spectrometer. The simplest method utilizes a 100- to 130- μm orifice to a vacuum region maintained by a single stage of high-speed cryopumping (Sciex, Thornhill, Ontario, Canada). Charged droplets formed by ESI drift against a countercurrent flow of dry N_2 , which serves to speed desolvation and exclude large droplets and particles. As the ions pass through the orifice into the vacuum, further desolvation is accomplished by collisions as the ions are accelerated into a radiofrequency-only focusing quadrupole region of the mass spectrometer.

Alternatively, many instruments have been developed based on differentially pumped interfaces. The capillary inlet-skimmer interface developed by Fenn and co-workers (34) is widely used and is commercially available (Analytica, Branford, CT). A countercurrent flow of bath gas (typically N_2 at a pressure slightly above atmospheric) assists solvent evaporation and sweeps away high- m/z residual particles and solvent vapor from the mass spectrometer inlet. Ions migrate toward the sampling orifice, where some fraction of them are entrained in the gas flow entering a glass capillary (metalized at both ends to establish well-defined electric fields). Although some loss occurs, ions can be transmitted through capillaries with good efficiency. Ions emerge from the capillary, in the first differentially pumped stage, as a component of a free jet expansion. A fraction of the ions is then transmitted through a skimmer and additional ion optics into the m/z analyzer. The electrically insulating nature of the glass capillary provides considerable flexibility because ion transmission does not depend strongly on the voltage gradient between the conducting ends of the capillary.

An alternative approach to droplet desolvation relies solely on heating during droplet transport through a heated metal (38) or glass capillary (34,39). A countercurrent gas flow is not essential and, in fact, may decrease obtainable ion currents. The electrospray source is positioned nearer to the sampling capillary orifice (typically 0.3 to 1.0 cm). The charged droplets are swept into the heated capillary, which provides effective ion desolvation, particularly when augmented by a capillary-skimmer voltage gradient. The disadvantage of this approach, and of all sources not using a gas “curtain” or countercurrent flow, is that much more solvent and residual material (i.e., solute particles) enter the mass spectrometer. Advantages of the heated capillary, however, are the ease with which it can be adapted to a variety of MS configurations, potentially higher transport efficiency (which arises from the proximity to the electrospray tip), and the ability to heat ions for either desolvation or dissociation (40) in a manner largely independent of m/z .

Considerable doubts remain concerning the detailed mechanism of ESI, particularly related to the identity of the charged species desorbed, evaporated, or "ejected" from the surface of the highly charged and rapidly evaporating droplets. Such questions are difficult to resolve using mass spectrometry because only the end result is observed and only after transport through, and perturbation by, the atmosphere–vacuum interface. However, an advantage of ESI interfaces using countercurrent gas flow is that the dry nitrogen environment will minimize the condensation effects caused by cooling when gas expands into the vacuum. With this approach, differences between the detected ion population and that present at atmospheric pressure (e.g., the extent of desolvation) will generally be caused by the greater activation (i.e., temperature) of the former.

The greatest success to date with ESI–MS has been obtained using quadrupole mass spectrometers. The combination with magnetic instruments was accomplished several years ago by Russian researchers (10,11,13–15) and more recently by others (41–51). Initial results with time-of-flight instrumentation have been reported and suggest that improved sensitivity (by ion storage and accumulation) will be necessary to yield results comparable to quadrupole instruments (52). Such improved sensitivity appears practical in designs utilizing orthogonal extraction, where most of the ions may be effectively utilized. Quadrupole ion-trap (i.e., ITMS) results appear particularly encouraging, although the mass measurement accuracy is currently much poorer than with quadrupole mass spectrometers (53–57). The ITMS sensitivity is comparable to or better than quadrupole mass spectrometers, suggesting very efficient injection and trapping, and significant advantages in tandem MS (MS/MS) sensitivity appear obtainable. McLafferty and co-workers have pioneered the combination of ESI with Fourier transform-ion cyclotron resonance mass spectrometry (FT-ICR) (58–60). Laude and co-workers have demonstrated that substantial gains in sensitivity are obtainable by having the ESI interface in the high magnetic field of an ICR superconducting magnet (61). The potential for higher-order mass spectrometry, MS^n ($n \geq 3$), and perhaps efficient photodissociation is promising. High resolving power at moderate m/z , a capability of ion-trapping devices, has been demonstrated for proteins and appears to have considerable potential, although technical difficulties remain to be solved. At least for the next few years, it appears that quadrupole mass spectrometers will be the most widely used analyzers with ESI because of factors that include lower cost and ease of interfacing.

3. ESI–MS OF LARGE BIOMOLECULES

3.1. Molecular Weight Determination

Molecular weight measurements for biopolymers can be obtained because ESI mass spectra generally consist of a distribution of molecular ion charge states

without contributions from dissociation (unless induced during transport into the MS vacuum). The envelope of charge states for proteins, arising generally from protonation, yields a distinctive pattern of peaks because of the discrete nature of the electronic charge; i.e., adjacent peaks vary by addition or subtraction of one charge. As first reported by Fenn and co-workers (19,62), the relative molecular mass, M_r , of a macromolecule may be determined from mass spectra, given several assumptions. One often assumes for proteins that charging is caused by protonation of the molecular ion. Although this process is not invariably the case, it has been found correct for most proteins studied to date. It is also generally assumed that ESI is an extremely “soft” ionization technique and will yield, under appropriate conditions, intact molecular ions. In the case of noncovalently bonded species, such as multimeric proteins, mass spectra are typically obtained under conditions in which only the individual subunits are observed.

Equation 2.1 describes the relationship (for positive ESI-MS) between a multiply charged ion at m/z p_1 with charge z_1 and M_r :

$$p_1 z_1 = M_r + M_a z_1 = M_r + 1.0079 z_1 \quad (2.1)$$

where the charge-carrying species (M_a) is a proton. The molecular weight of a second multiply protonated ion at m/z p_2 (where $p_2 > p_1$) that is j peaks away from p_1 (e.g., $j = 1$ for two adjacent peaks) is given by:

$$p_2(z_1 - j) = M_r + 1.0079(z_1 - j) \quad (2.2)$$

Equations 2.1 and 2.2 can be solved for the charge of p_1 :

$$z_1 = j(p_2 - 1.0079)/(p_2 - p_1) \quad (2.3)$$

The molecular weight is obtained by taking z_1 as the nearest integer value. Additional measurements derive from each peak in the distribution. For example, thioredoxin from *E. coli* (37) gives $(M + 9H)^{9+}$ to $(M + 13H)^{13+}$ molecular ions at m/z 1298.0, 1168.27, 1062.27, 973.74, and 898.88, respectively. A calculated M_r of $11,672.9 \pm 0.5$ Da is in close agreement with the expected M_r of 11,673.4.

Similarly, for negative ESI-MS:

$$z_1 = j(p_2 + 1.0079)/(p_2 - p_1) \quad (2.4)$$

As shown by C. M. Whitehouse (personal communication), the approach to M_r determination can be generalized to include the mass of the added charged species, M_a (e.g., H^+ , Na^+ , K^+). Automated approaches for deconvolution of ESI-MS spectra have been developed that give increased accuracy if adducted species are resolved.

Measurements of M_r for proteins greater than 100 kDa have been demonstrated, and in favorable cases precisions better than 0.005% have been obtained, far superior to more traditional techniques such as denaturing gel electrophoresis (5–10%). High accuracy is required for >20-kDa proteins to differentiate single-residue mutations that produce, for example, 1-Da mass differences (e.g., Asp and Asn, Leu/Ile, and Asn, Glu, and Gln). Feng *et al.* (63) have demonstrated 0.001% (10 ppm) M_r precision (i.e., M_r 10,000 \pm 0.1) by a Gaussian curve-fitting method.

The majority of the reported ESI–MS results have utilized relatively low-resolution quadrupole analyzers. With higher resolution, charge state assignment in even complex mass spectra is possible by measurement of isotopic peak separations. Henry *et al.* (60) have demonstrated resolving powers >60,000 with a 2.8 Tesla FT-ICR instrument, readily resolving up to the 18+ charge state for equine myoglobin and the 16+ charge state for equine cytochrome C, with a precision and mass accuracy of 0.1 Da. This combination of high resolution and high accuracy may be particularly useful for identification of unknowns and for analysis of complex mixtures. Accuracies on the order of 1 ppm (0.0001%) or better should eventually be obtainable by a combination of ESI with double-focusing or FT-ICR mass spectrometers.

3.2. Positive-Ion Spectra of Large Polypeptides and Proteins

The net number of charged sites under solvation conditions appears to be one of the principal factors affecting the maximum extent of charging observed in ESI mass spectra. For most proteins (prepared in aqueous solution, pH < 4), an approximately linear correlation is observed between the maximum number of charges and the number of basic amino acid residues (e.g., arginine, lysine, and histidine) plus the N (amino) terminus (37,64) for protein standards. Under typical acidic solution conditions used for ESI, most if not all basic residues will be protonated in solution. For example, methionyl-human growth hormone (MethGH, M_r 22,256) contains 11 arginines, 3 histidines, 9 lysines, and the N-terminal methionine residue, for a total of 24 likely protonation sites in solution. Correspondingly, the $(M + 24H)^{24+}$ molecular ion at m/z 928 is the most highly charged species observed by ESI–MS. The acidic residues can be deprotonated in solution at pH greater than \sim 5, and such conditions would be expected to lower the observed ESI positive charge state distribution.

Many proteins contain disulfide bridges in their native state that significantly affect higher-order structure. Native bovine α -lactalbumin (M_r 14,175) has 17 basic residues and four cysteine–cysteine disulfide bridges, yet a maximum of only 13 charges is observed in the ESI mass spectrum. As shown in Fig. 2.2b, reduction of disulfide bonds with 1,4-dithiothreitol (DTT, Cleland's reagent) results in molecular ions up to 19+. The number of disulfide bonds can be determined by the increase in M_r on reduction. For α -lactalbumin, an 8-Da

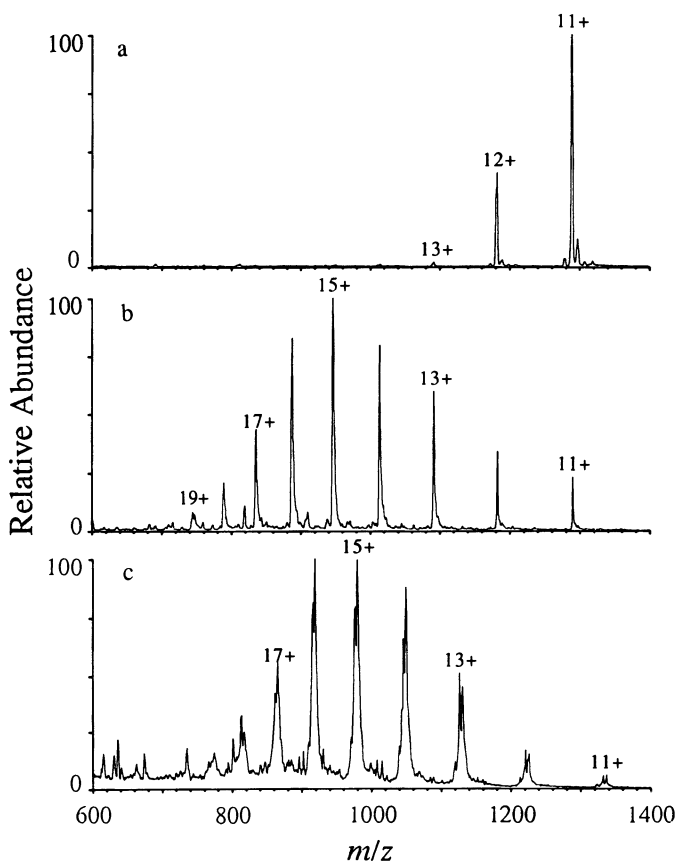


Figure 2.2. Electrospray ionization mass spectrum of bovine α -lactalbumin (a) before and (b) after reduction with DTT and (c) mass spectrum of the reduced/carboxymethylated form.

increase is consistent with four Cys–Cys bonds. Carboxymethylation of Cys residues (after DTT reduction) with iodoacetate results in the expected 472-Da increase in M_r for α -lactalbumin (64) as well as a similar extent of protonation (Fig. 2.2c). As found in other cases, the maximum number of charges observed in the ESI mass spectra exceeds the number expected on the basis of the number of highly basic residues (37,63). Bojesen's data (65) indicate that glutamine has a similar gas-phase proton affinity as lysine. Lactalbumin contains five such Gln residues as possible protonation sites. More recent results (66,67) are supportive of our earlier speculation (64) that glutamine residues may contribute to the extensive protonation observed.

Another example of “overcharging” is demonstrated in Fig. 2.3. Proinsulin is the precursor to insulin with an additional C peptide joining the A and B

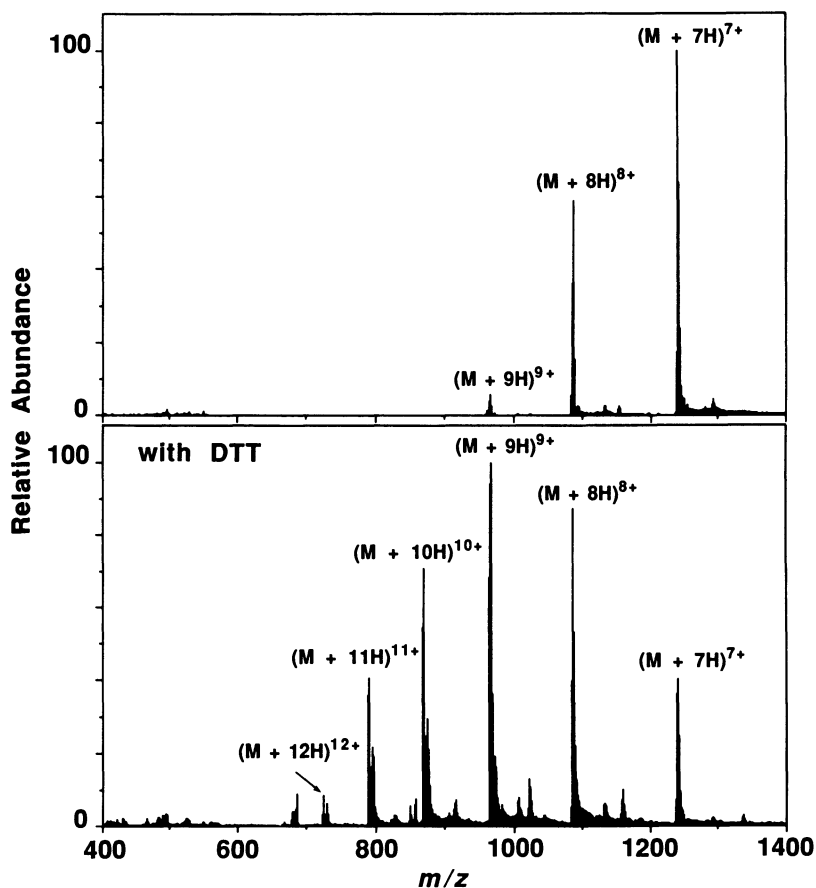


Figure 2.3. ESI-MS spectra of bovine proinsulin (M_r 8681): native protein (top) and after the reduction of disulfide bonds with 1,4-dithiothreitol (DTT) (bottom).

chains. The polypeptide from the bovine species is composed of 81 residues (M_r 8680.8) and three disulfide bonds linking residues 7–67, 19–80, and 66–71. Thus, the majority of the polypeptide chain is enclosed by disulfide bonds, with the exception of the first six residues from the N terminus and the C-terminal asparagine residue. A measured molecular weight of 8680.5 ± 0.46 agrees closely with that expected from its sequence. Reduction of the three disulfide bonds with DTT leads to the appearance of more highly charged molecular ions extending to the 12+ state. The experimentally measured M_r of 8686.4 ± 0.67 is consistent with the reduced form of proinsulin (M_r 8686.9). Again, although the primary structure of bovine proinsulin contains only nine basic amino acid sites (four Arg, two His, two Lys, and the N terminus), protonation at other sites (e.g., glutamine residues) apparently contributes upon disulfide reduction.

The ESI mass spectra of noncovalently bound protein subunits generally show multiply charged ions characteristic of their respective subunits. Lactate dehydrogenase from rabbit muscle ($M_r \sim 140$ kDa) is an enzyme composed of four identical 36-kDa subunits. Over 50 positive charges indicative of the subunit molecular weight are detected by ESI-MS. Similarly, human hemoglobin is a tetrameric protein consisting of two α and two β chains; its ESI mass spectrum shows multiply charged ions for the α (M_r 15,126) and the β (M_r 15,867) chain units.

The ESI mass spectra of noncovalently bound heme-containing proteins obtained under typical acidic conditions generally do not exhibit molecular ions for the heme-polypeptide complex. Such an iron-porphyrin group is associated with hemoglobin; however, ions characteristic of only the subunit minus the heme are found. The same is true for myoglobin from lower-pH solutions (68), but under certain solution conditions the noncovalently bound heme-peptide complex is observed (68,69). The 5% aqueous acetic acid (pH = 2.4) solution used for ESI-MS of myoglobin yields only multiply protonated molecular ions for the polypeptide chain (i.e., apomyoglobin). An additional peak for heme⁺ is observed in 1 : 1 H₂O/alcohol solutions with 5% acetic acid. Myoglobin in unbuffered aqueous solution yields contributions of $(M + \text{heme} + (n - 1)H)^{n+}$ and apomyoglobin molecular ions in addition to heme⁺, with relative abundances depending strongly on interface conditions. The dependence on solution conditions appears to be correlated to changes in protein structure; certain conditions (including lower pH) result in denaturation and loss of the heme (see the following section). At low pH, myoglobin is known to unfold in solution, expelling the heme group (70). At more basic pH, myoglobin remains globular, partially retaining the heme in the negative-ion spectra (see Section 3.4) (71). In contrast, the heme-protein cytochrome *c* is covalently linked to the iron-porphyrin group through thioether bonds to two cysteine residues. Thus, the M_r determined by ESI-MS is consistent with the polypeptide-heme species.

The utility of ESI-MS for larger proteins can be illustrated by examining the results obtained for a range of serum albumins: acidic, stable, 66-kDa monomeric proteins that are among the most studied in biochemistry (72). Complete sequences are available for human, bovine, rat (72), sheep (73), and porcine (74) albumin, and partial amino acid sequences (typically the N-terminal residues) are known for other species. Albumin amino acid sequence alignment is well conserved between species: 63% total conservation is maintained among the sequences for human, rat, and bovine albumins. Relative molecular weights with precisions on the order of 0.01% or better can be obtained, as shown in Table 2.1 for ten different albumin species (75). Although precision was similar to that determined for smaller polypeptides and proteins, some M_r measurements were high by as much as 0.27% compared to values based on reported sequences. The purity of the commercial albumins may be as high as 96% based on the nitrogen

Table 2.1
Molecular Weights and Peak Widths from ESI-MS Spectra
of Serum Albumins

Species	M_r (exptl.)	M_r (seq.) ^a	FWHH (50+) ^b
Bovine	66,443 ± 5	66,430	4.3
Human	66,605 ± 7	66,438	8.2
Rat	66,000 ± 6	65,870	5.0
Porcine	66,770 ± 5	66,731	4.3
Sheep	66,385 ± 6	66,293	5.0
Horse	65,667 ± 6	—	8.7
Rabbit	66,148 ± 6	—	4.0
Dog	65,854 ± 7	—	10.7
Goat	66,304 ± 5	—	(8.9)
	66,578 ± 8		
Guinea pig	65,962 ± 8	—	(15.8)
	66,284 ± 8		
	66,586 ± 7		

^aAverage molecular weights calculated from available complete amino acid (or nucleotide) sequences.

^bFull width in m/z units at half the peak height for the $(M+50H)^{50+}$ multiply charged molecule. Values in parentheses indicate that more than one molecular ion component is partially resolved in the peak cluster.

content. However, heterogeneity may still arise from various contributions, including adducts (fatty acids, bilirubin, glycans, etc.), structural modifications, cleavages by traces of proteolytic enzymes in the preparation, and amino acid modifications (72). Moreover, errors in sequence determination may occur; Hirayama *et al.* (76) recently corrected the amino acid sequence of bovine serum albumin, giving an M_r in close agreement with the measured value (63,75).

The relative purity of the serum albumins can be qualitatively assessed with ESI-MS based on the molecular ion peak width. This assessment requires that spectra be obtained under conditions that result in sufficient collisional activation to remove residual solvent and noncovalently associated molecules. Table 2.1 lists the measured widths (in m/z units) at half the height of the peak maxima for the $(M + 50H)^{50+}$ species (between m/z 1310 and 1340) for ten albumins. Porcine albumin, which gave the closest agreement with the measured molecular weight, also gave one of the narrowest peak widths. A few of the albumins, notably goat and guinea pig albumin, showed additional partially resolved components (75). Figure 2.4 compares a portion of the ESI spectra for porcine and guinea pig albumin, showing the greater heterogeneity of the latter (where at least three components are evident). Because the reported M_r measurements are based on peak maxima, sample microheterogeneity can cause a shift in peak maxima sufficient to partially explain the difference from M_r values based on the sequence. Thus, a properly deconvoluted peak shape (i.e., corrected for instru-

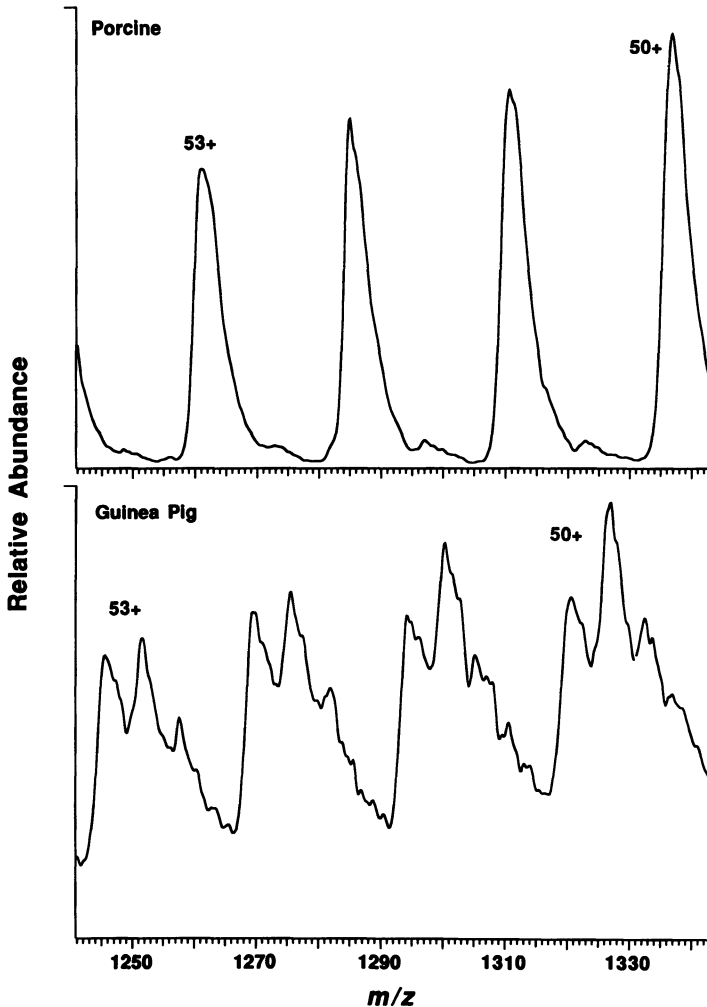


Figure 2.4. Partial mass spectra of porcine (top) and guinea pig (bottom) albumins illustrating the greater microheterogeneity of the latter.

mental contributions) may provide information on purity or heterogeneity. A recent ESI-MS study by Geisow and co-workers (77) of commercial and recombinant human albumin samples also showed similar M_r values. However, the spectrum for the recombinant form showed much narrower peak widths (~ 2 m/z units versus ~ 7 m/z units for the commercial sample).

In biotechnology, protein purity (and impurity) determination is crucial for certification and control of product potency, stability, and safety. The presence of

trace protein contaminants at the part-per-million level may cause a biological immune response in the recipient. Impurities may also include DNA, residual host proteins, proteolytic clips, and residual cellular proteins (78). Additionally, "a concern in the recombinant DNA manufacture of proteins is the potential for a single point mutation or mistranslation of the complementary DNA, which would cause single or multiple amino acid substitutions in a protein" (79).

The ESI-MS technique has already found application for the molecular weight determination of recombinant proteins such as human growth hormone, interleukin-2, and interferon- γ . A protein with M_r 131 Da higher than expected because of an N-terminal methionine is often detected in the protein products. This modification arises from the start codon (AUG for methionine in eukaryotes) used for the translation process. Van Dorsselaer *et al.* (80) applied ESI-MS to verify the identity of recombinant proteins up to 44 kDa. Analysis of HIV proteins (15–26 kDa) has shown cleavage products and proteins (with loss of C-terminal residues) in addition to the expected proteins. Acetylation of the N terminus and truncated products were easily identified for α_1 -antitrypsin variants expressed in *E. coli* and *Saccharomyces cerevisiae* (80). M_r measurement accuracy of 0.01% allows for evaluation of such mixture products from a single ESI mass spectrum.

As noted for albumins, the relative heterogeneity of protein preparations can be qualitatively evaluated by ESI-MS. Witkowska and co-workers (81) determined the purity of their preparation of thioesterase II, an enzyme used to hydrolyze acyl chains of intermediate-length fatty acids. Two products were detected, one in which the full-length protein (263 residues, M_r 29,513) has an N-terminal acetylmethionine residue and a second in which the C terminus is truncated (261 residues, M_r 29,299) and the N terminus is also acetylated.

Electrospray ionization MS has also been used to examine proteins isolated from biological matrices. Lens crystallins, structural proteins found in the eye lens, were subjected to ESI-MS for detection of possible posttranslational modifications (82). Spectra from HPLC fractions of β -bovine lens crystallins (M_r 20,000 to 25,000) have indicated acetylation of the N-terminus (83). Protein variants of trypsin (84) and hemoglobin (85–87) have been studied by ESI-MS. Over 400 variants of human hemoglobin chains (α , β , δ , γ) are known, many of which arise as a result of a single nucleotide base substitution, and variants have been identified by M_r measurement with accuracy routinely within ± 1 Da (at $M_r \sim 15$ kDa).

Structure analysis of glycoproteins and their many possible carbohydrate structural isomers is a major analytical challenge (88,89). Several examples of electrospray ionization of glycopeptides and glycoproteins exist. Although ESI mass spectra for glycoproteins such as ribonuclease B, ovalbumin, and transferrin have been reported, the difficulty in analysis and lack of sensitivity for many glycoproteins have previously been noted (90). Many glycoproteins do not yield

interpretable mass spectra. Peptide mapping by LC/MS/MS of enzymatic digests of glycoproteins has been successfully used to determine the sites and identity of carbohydrate binding (91–93). Gillece-Castro and co-workers (94) reported the mass spectra of bovine fetuin and DNase, but only after removal of N-linked and O-linked oligosaccharides with enzymes such as neuraminidase, N-glycosidase F (PNGase F), and O-glycanase. Several other groups (95,96) have reported moderate success in glycoprotein analysis by ESI.

It is clear that the extent of charging of the protein in the ESI process is generally constrained by the number of charge sites in solution. Solution conditions (e.g., other possible charged species, charged adducts) likely play a role, but mechanisms have not yet been well defined. The maximum extent of charging in the gas phase is ultimately limited by Coulombic forces, but much less in solution, where the relatively high dielectric constant of the solvent can effectively shield and optimally distribute charge. The highly basic amino acids rarely account for more than 20% to 25% of a protein (which would correspond to $m/z \sim 500$ for full protonation). Coulombic repulsion makes charging of adjacent residues less favored in the gas phase and could substantially lower barriers to proton transfer from such sites. Coulombic effects might even increase to a level such that deprotonation will occur during desolvation. It is now established that higher charge states of proteins are more reactive to proton transfer and may more readily undergo dissociation (37,97).

3.3. Higher-Order Protein Structure Effects

Information on higher-order structure (secondary, tertiary, quaternary) is fundamental to biological research. Protein conformation in solution depends in a complex fashion on the intramolecular forces dictated by amino acid sequences. The native state of a protein is typically folded into a well-defined three-dimensional structure by relatively weak intramolecular forces (e.g., hydrogen bonding). Protein function in biological systems generally involves interactions of specific structural conformations essential for activity (98). X-ray crystallography, nuclear magnetic resonance, and various spectroscopic methods have been used to probe such conformational changes. Mass spectrometry potentially offers greater speed and sensitivity in qualitatively evaluating changes in higher-order structure.

According to our present understanding, the charge distribution observed for proteins by ESI-MS is related to the solution phase structure. However, the details of this relationship are unclear because details are uncertain concerning how ESI and subsequent gas-phase processes, such as proton transfer during desolvation, may alter this initial charge distribution. As first demonstrated by Loo *et al.* (64) and shown for proinsulin in Fig. 2.3, protein charging depends dramatically on higher-order protein structure. Reductive cleavage of disulfide

bonds between cysteine residues alters the higher-order structure of the protein. The native disulfide-bridged conformation may have basic amino acid sites in the internal volume of the globular structure that are less readily protonated. Repulsive Coulombic forces are also greater for the more compact native structure, and charge sites may be more labile in the gas phase to reactions (e.g., proton transfer). Disulfide-cleavage reactions allow the protein to “relax” or unfold into more extended conformations, allowing greater protonation of otherwise “buried” sites. The consequence of this behavior is demonstrated by comparisons of spectra for disulfide-containing proteins and their disulfide-reduced forms. Bovine serum albumin is composed of 585 amino acids, 35 of which are cysteine residues that compose 17 disulfide bridges. Its ESI mass spectrum in Fig. 2.5 (top) shows the $(M + 67H)^{67+}$ ion as approximately the most highly charged species. On disulfide bond reduction with DTT, up to 89 charges are observed (Fig. 2.5, bottom), compared to 100 expected on the basis of the number of basic

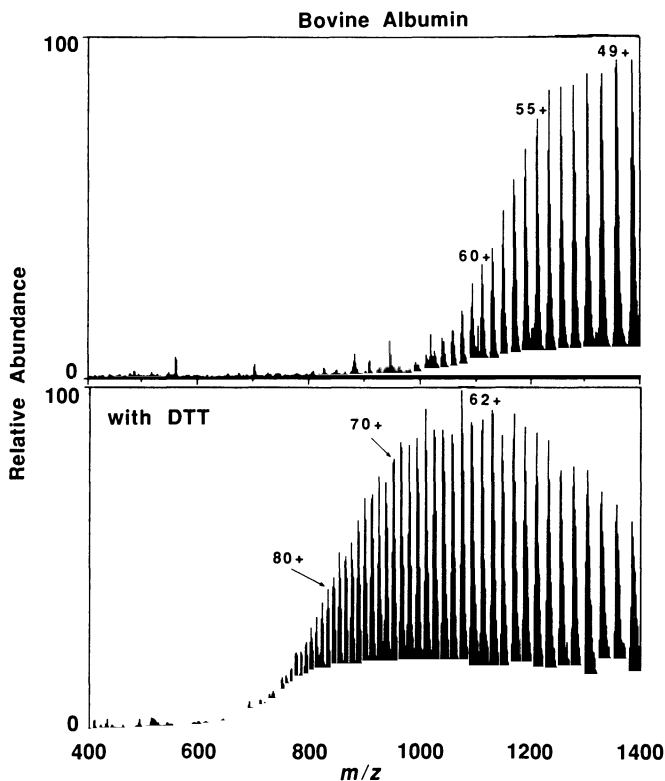


Figure 2.5. Mass spectra of bovine serum albumin (M_r 66 kDa): native form (top) and after disulfide reduction with DTT (bottom).

residues. Similar results were obtained for the covalently bound bovine albumin dimer (64).

In the case of proteins containing disulfide bonds, it is clear that disulfide reduction will alter solution and gas-phase structure and, perhaps implicitly, the extent of charging. The three-dimensional protein structure in solution is generally governed by relatively weak noncovalent interactions. It is unclear to what extent higher-order protein structure will be preserved through the electrospray process and influence the observed ESI charge state distribution.

Changes in protein environment, such as changes in pH, temperature, addition of reagents (such as guanidine hydrochloride or urea), or other solvent conditions may cause the protein to unfold or denature. Chait and co-workers have demonstrated a dramatic effect of pH on the ESI spectrum of cytochrome *c* (99). Similar behavior, i.e., a bimodal charge state distribution reflecting a mixture of conformers, is also observed on addition of acetic acid to an aqueous solution of hen-egg lysozyme (M_r 14,306) (100). Cytochrome *c* and lysozyme have been shown to denature from a compact folded conformation to a random coil state when the pH is lowered from 3.3 to 1.6 (99–101). Thus, the higher charge state distribution (at lower m/z) may represent the contribution from the random coil state. Feng and co-workers have reported similar results for papain (102), suggesting that the different charge state distributions observed for different pH conditions are consistent with the known structural changes.

The use of organic solvents, such as those generally used for ESI, can also cause protein denaturation (103,104). A dramatic example of such behavior is found for bovine ubiquitin (M_r 8565) (100). Figure 2.6 shows the ESI mass spectra of ubiquitin in various water–acetonitrile solvent mixtures (with 5% acetic acid). For higher fractions of organic solvent, the ESI mass spectra show charging extending to the $(M + 13H)^{13+}$ molecular ion, consistent with the 13 basic residues (Fig. 2.6a). For a highly aqueous sample (>90%, but using a liquid sheath of acetonitrile), a bimodal charge distribution is evident, with the 7+ and 8+ molecular ions dominating the spectrum (Fig. 2.6c). In spite of the bimodal distribution, m/z measurements are consistent with a single M_r value. Increasing the fraction of organic solvent shifts the charge state distribution to the higher charge (lower m/z) (Fig. 2.6b). The native structure of ubiquitin is known to be globular in an aqueous environment (105,106). It is also known that perturbation of the aqueous medium, such as by addition of organic solvents or urea, causes unfolding of the polypeptide chain from its compact native form (98,103,104,107,108). Lowering the dielectric constant of the solution by increasing the alcohol content has been shown to increase the α -helical form of the denatured protein by alcohol binding to hydrophobic sites (108), consistent with other protein studies (103,107). The native globular form for ubiquitin dominates, yielding the 7+ and 8+ species in aqueous solution (Fig. 2.6c). (A small contribution from the denatured α -helix structure giving the 10+ to 13+ charge

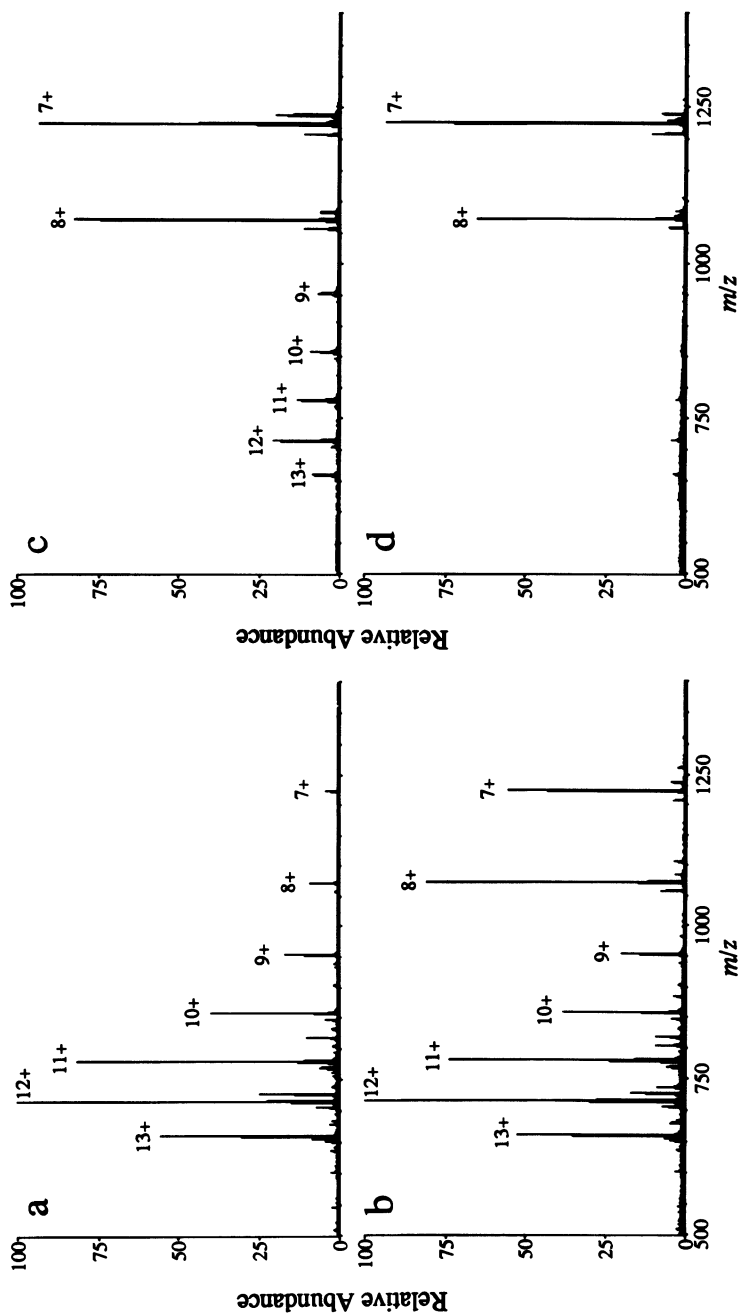


Figure 2.6. Electrospray ionization mass spectra of bovine ubiquitin (M_r 8565) in (a) 18:77:5, (b) 12:83:5, and (c) 0:95:5 acetonitrile: water: acetic acid solvent mixtures with an acetonitrile liquid sheath. The same conditions as in (c) were used to generate (d), except that water was used for the liquid sheath.

states is ascribed to denaturation by contact with the acetonitrile sheath liquid used in the ESI source.) Denaturation can be nearly eliminated by replacing the acetonitrile sheath with an aqueous sheath, as evident in Fig. 2.6d by the nearly complete absence of the 9+ to 13+ charge states. Increasing the acetonitrile content of the analyte solution to 12% results in a substantial contribution ascribed to the α -helix structure (Fig. 2.6b). Further addition of acetonitrile to 18% (and higher) results in primarily the denatured state.

Another approach for probing higher-order solution-phase structure exploits hydrogen/deuterium (H/D) isotopic exchange in solution, as shown by Chait and Katta (109). D_2O is substituted for H_2O , and H/D exchange is allowed to occur over a period of minutes to hours. The extent of H/D exchange depends on higher-order solution structure because of the variable accessibility of labile hydrogens. Consistent with expectations, much greater H/D exchange was observed for some denatured forms of globular proteins (109).

It is difficult to resolve all of the factors contributing to the ESI charge state distribution. Changes in physical parameters such as pH, dielectric constant, and surface tension may have important effects on the desorption/ionization event(s) and may ultimately affect the observed charge state distribution. Available results suggest that multiple conformation states can be qualitatively monitored in some cases using the ESI mass spectrum. Although the charge state distribution from ESI is at least partially governed by solution-phase conformations, it is uncertain how liquid-phase structure is related to the relevant gas-phase structure(s). Even if the charge state distribution is "locked in" by factors that include solution-phase structure, the actual gas-phase three-dimensional structure may be altered by the heating required to complete desolvation and likely assisted by repulsive Coulombic forces once the protein is stripped of the mediating effects of the dielectric solvent.

Evidence is increasing that relatively weak noncovalent bonds can influence gas-phase structure of multiply charged proteins. A relatively common observation in polypeptide mass spectra is the appearance of noncovalently bound dimers, particularly for samples prepared at high concentration. Generally, such contributions to ESI spectra are relatively small, particularly because interface conditions are selected (intentionally or otherwise) to provide sufficient excitation for desolvation. Under such conditions, one would generally expect noncovalently associated species to dissociate. However, dissociation of noncovalently bound species may not always occur, as in the myoglobin positive-ion ESI spectra at near-neutral pH (data not shown) and the negative-ion spectra at higher pH (Fig. 2.7), where the heme group is clearly retained for a substantial fraction of the molecules. The negative-ion spectra of oxidized A-chain insulin and the positive-ion spectra of B-chain insulin show abundant dimer ion peaks under certain conditions, as shown in Fig. 2.8. Intact insulin is known to form dimers and larger multimers under broad ranges of solution conditions (110). The

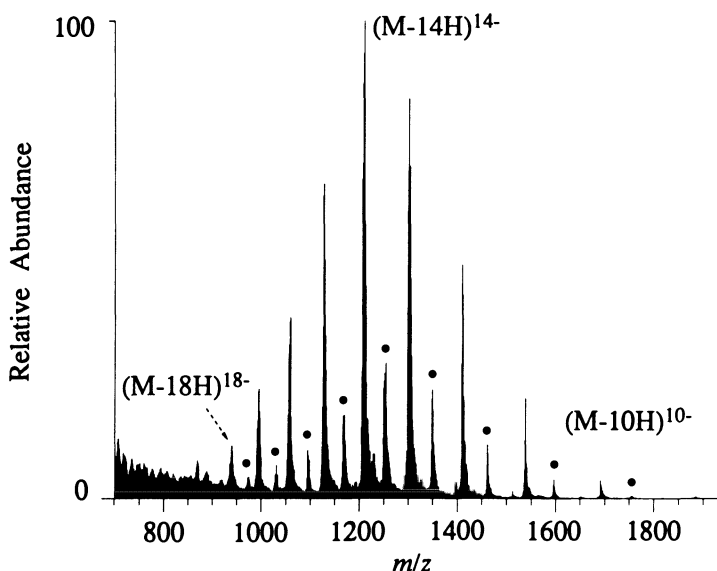


Figure 2.7. Negative-ion ESI spectrum of horse heart myoglobin in 1% NH_4OH aqueous solution. The peaks labeled with dots represent the intact polypeptide-heme complex.

MS/MS studies of the suspected dimer species yield the expected monomers of higher and lower m/z . It is highly unlikely that dimers are formed in the gas phase because of the considerable Coulombic barrier. It is now apparent that such dimeric species were unsuspected contributors to some of our initial MS/MS studies of proteins (24,25). Figure 2.9 shows low-resolution collision-induced dissociation (CID) spectra for the 9+ to 12+ charge states of cytochrome *c* obtained in one of our earliest studies (24). Each charge state selected for MS/MS study was “contaminated” by about 1% of the dimer (at the same m/z but twice the charge). The dissociation of the dimer forms the monomer with charge states having approximately half the charge of the dimer. Noncovalently bonded dimers in the gas phase will most likely be observed at higher m/z , where Coulombic repulsive forces are lower.

These results suggest that noncovalently associated multimers of larger proteins may also be detectable by ESI-MS under appropriate solution and interface conditions. The recent observation of noncovalent enzyme-substrate and receptor-ligand complexes (111) is consistent with this expectation. A complex between the cytoplasmic receptor, human FK binding protein (M_r 11,812), a member of the immunosuppressant binding protein family, and the recently discovered immunosuppressant FK506 (M_r 804) was observed in the ESI mass spectrum. Similarly, the enzymatic reaction of hen egg-white lysozyme (HEWL) with N-acetylglucosamine (NAG) oligosaccharides was monitored by detecting

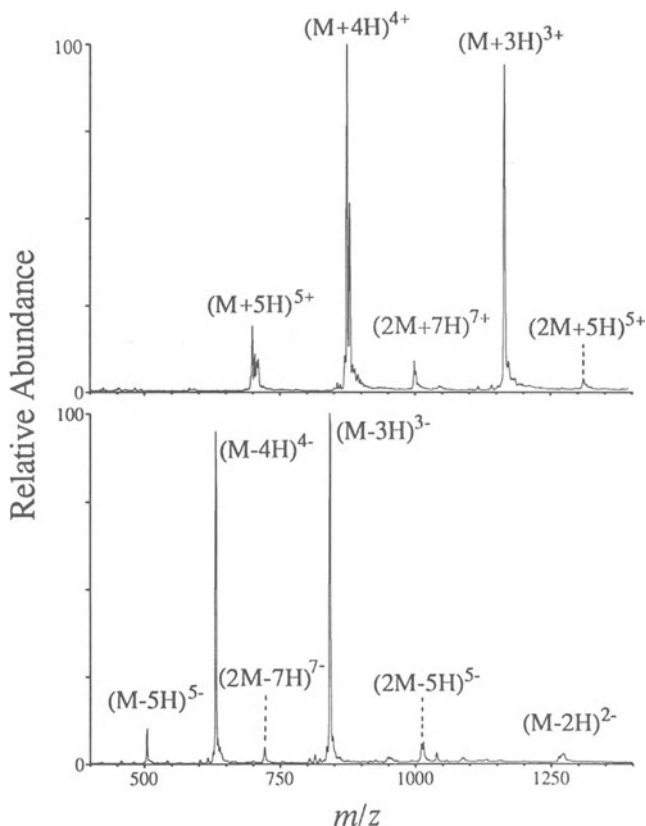


Figure 2.8. Electrospray ionization mass spectrum of bovine B-chain insulin (M_r 3496) in 5% acetic acid (top) and negative-ion mass spectrum of bovine A-chain insulin (oxidized, M_r 2531) in H_2O (bottom).

the HEWL–NAG_{*n*} complexes (112). The hydrolysis of NAG₆ by HEWL produces predominantly NAG₄ and NAG₂. A solution containing HEWL and NAG₆ yields multiply charged ions corresponding to the HEWL–NAG₆ and HEWL–NAG₄ complexes.

The ESI–MS technique should prove useful for probing other noncovalent binding interactions. On the basis of such preliminary observations, broad assumptions concerning the gas-phase structure of biopolymer ions from ESI (i.e., that large ions will necessarily be “extended” in the gas phase) are premature.

3.4. Negative-Ion Spectra of Large Polypeptides and Proteins

The ESI–MS analysis of polypeptides and proteins has generally been performed in the positive ionization mode. The more basic sites of the amino acid

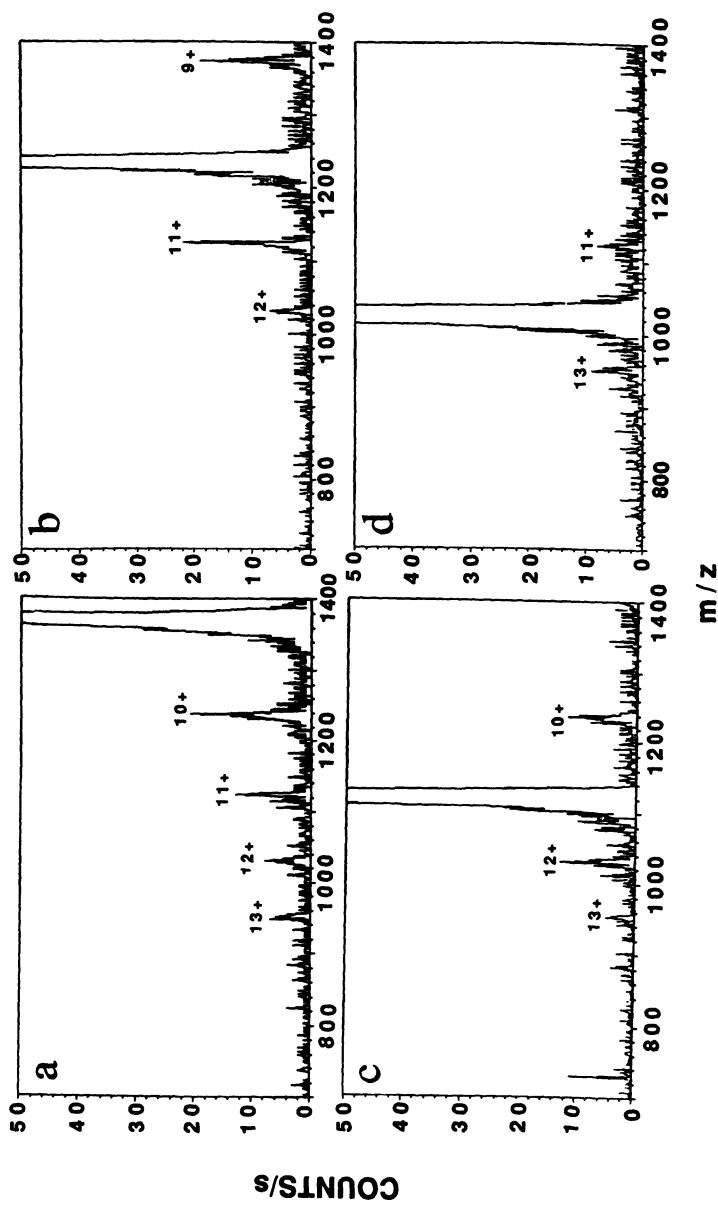


Figure 2.9. MS/MS spectra for the (a) 9+, (b) 10+, (c) 11+, and (d) 12+ protonated ions and the dimer species at the same m/z [i.e., $(2M + 18H)^{18+}$, etc.] for cytochrome *c* obtained under similar CID conditions. The small fraction (<2%) of noncovalently bound dimer dissociates readily to yield monomers.

residues (arginine, lysine, histidine, and the N-terminus) have sufficiently large pK values to ensure that proteins will be multiply protonated in acidic solutions. Negative-ion ESI has been demonstrated for a variety of small molecules with acidic functionalities such as carboxylic, phosphoric, and sulfonic acid groups (113–115). Also, ESI mass spectra of mono- and oligonucleotides have been reported (22,37,69,116,117), and a distribution of multiply charged molecular anions for transfer RNAs with M_r to 25 kDa has also been observed (37,117). We have also observed that polystyrene sulfonates extending to >1 MDa can be efficiently ionized. However, very few negative-ion ESI mass spectra of polypeptides have been reported; one early example was the negative-ion ESI mass spectrum from an aqueous solution of bovine A-chain insulin (M_r 2533) (37) in which the four cysteine residues had been oxidized. Multiple charging to the 5– deprotonated charge state was observed (Fig. 2.8). Most proteins in neutral and acidic aqueous solutions do not produce multiply charged anions because acidic residues such as glutamic acid (Glu) and aspartic acid (Asp) typically have pK_a s of around 5; i.e., the protein often retains a net positive charge in solution because of the protonated basic residues.

However, as first shown by Loo *et al.* (71), multiply charged (deprotonated) molecules can be produced by ESI in basic pH aqueous solution (e.g., 1–3% ammonium hydroxide), where basic residues are generally uncharged. Horse heart myoglobin in aqueous 1% NH_4OH solution (pH \sim 11.3) yields an electrospray ionization mass spectrum with a bell-shaped multiple charge state distribution extending up to approximately the $(M - 19H)^{19-}$ charge state, as shown in Fig. 2.7. Horse myoglobin has 13 Glu and 7 Asp residues, corresponding closely to the maximum negative charge state observed. Myoglobin spectra also show a less-intense series of ions corresponding to the noncovalently attached protoporphyrin IX heme cofactor (71).

Similarly, A-chain bovine insulin (oxidized, M_r 2531.6) yields multiple charging to the 5– charge state in aqueous solution (Fig. 2.8, bottom). However, in 1% NH_4OH , the observed multiple charging extends to the 7– charge state, presumably because of the deprotonation of the two glutamic acid residues (71).

Figure 2.10 shows the negative-ion ESI mass spectrum for an aspartic proteinase found in gastric juice, pepsin (porcine, M_r 34.5 kDa). Pepsin does not afford a positive-ion ESI mass spectrum (with limited m/z -range quadrupole instrumentation), and only limited success for pepsin has been reported with californium-252 plasma desorption (118,119) and MALDI (120). Porcine pepsin has only two Arg, one Lys, and one His basic residues, apparently insufficient for production of multiply protonated molecules below m/z 2000. However, the 29 Asp and 13 Glu acidic amino acid residues permit multiple charging in the negative ionization mode up to $(M - 42H)^{42-}$ from an aqueous 1% NH_4OH solution.

The effects of pH and cationic substitution are illustrated in Fig. 2.11 for porcine pepsin. The 1% (0.15 M) NH_4OH solution utilized for Fig. 2.10 con-

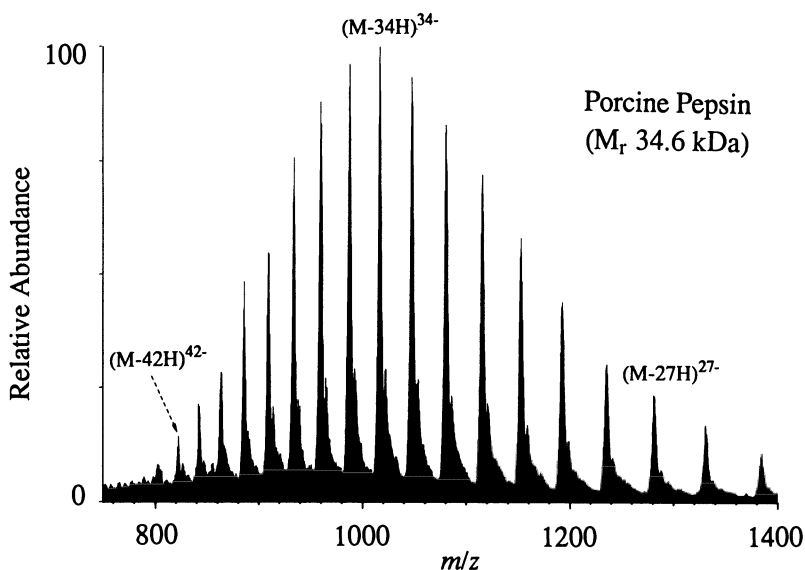


Figure 2.10. Negative-ion ESI mass spectrum of porcine pepsin (M_r 34.5 kDa) in 1% NH_4OH (aq.) solution.

trasts significantly with results obtained for porcine pepsin in 5×10^{-2} , 5×10^{-3} , and 5×10^{-4} M NaOH. At the 5×10^{-4} M NaOH concentration (pH ~ 10.7), signal intensities for molecular ions are substantially reduced, and tailing is noted on the high- m/z side of each peak because of sodium–hydrogen exchange (Fig. 2.11, bottom). The extent of charging observed in this case is reduced compared to that shown in Fig. 2.10; this reduction may be attributed to the slightly lower pH (71). Slightly more charging, to the 51– charge state, is observed for pepsin in a 5×10^{-3} M NaOH (pH = 11.7) aqueous solution, as shown in Fig. 2.11 (middle). Cysteine and tyrosine residues may also deprotonate in high-pH solutions because they have expected $\text{p}K_a$ ranges in proteins of 8.5 to 8.9 and 9.6 to 10.0, respectively (121). The phenolic hydroxy group of tyrosine may ionize under these conditions as well. We have observed formation of triply charged anions from basic solutions of the hexapeptide Tyr-Tyr-Tyr-Tyr-Tyr-Tyr, and it appears reasonable that some of the 16 tyrosine amino acids of pepsin may be deprotonated under these experimental solution conditions (71). Compared to lower NaOH concentration, a much greater extent of sodium adduction is also observed. Higher charge states ($>45^-$) show only small amounts of Na substitution, and the extent of Na substitution increases approximately linearly with decreasing charge. An unresolved distribution of sodium adducts is found for each charge state, such that the lower charge states (higher m/z) show more sodium substitution than ions of higher charge. The m/z of each charge state shifts substantially because the most probable species contains numerous Na

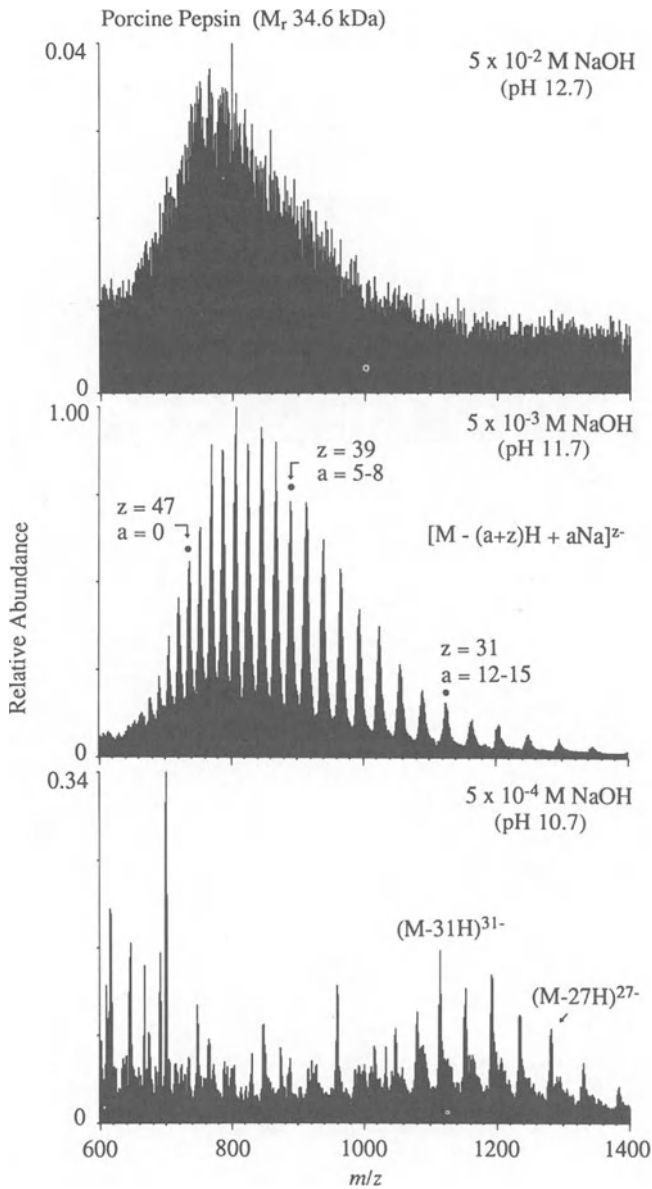


Figure 2.11. Electrospray ionization mass spectrum of porcine pepsin in 5×10^{-2} M (top), 5×10^{-3} M (middle), and 5×10^{-4} M NaOH (bottom).

substitutions, i.e., $[M - (a + z)H + aNa]^z-$. A similar situation applies to negative ESI mass spectra of large oligonucleotides (37). M_r calculations for conditions where cation adduction is not resolved are limited to $\sim 0.5\%$ precision and accuracy because each charge state contains a different (and unknown) average number of sodium counterions. At higher concentrations of NaOH, 5×10^{-2} M (pH ~ 12.7), signal intensity is severely attenuated. In addition to a possibly greater extent of sodium substitution, the protein may be degraded by hydrolysis.

More than 50 negative charges were observed in the negative-ion spectrum of disulfide-reduced sheep albumin (Fig. 2.12), which has 100 total Glu and Asp residues. No multiply charged deprotonated molecules were detected below m/z 2000 for native sheep albumin with disulfide linkages intact (i.e., native sheep albumin does not charge to over 33 $-$). These results are qualitatively consistent with positive ESI spectra for albumins (37,64). However, the amount of charging in the negative-ionization mode for sheep albumin is only half of that observed by positive ESI. One hundred basic residues occur in the sequence of sheep albumin. Approximately 69+ and 96+ (maximum) charges were observed for the native and disulfide-reduced forms of the protein (75). The role that different conformations of reduced albumin at acidic and alkaline pH play in the observed

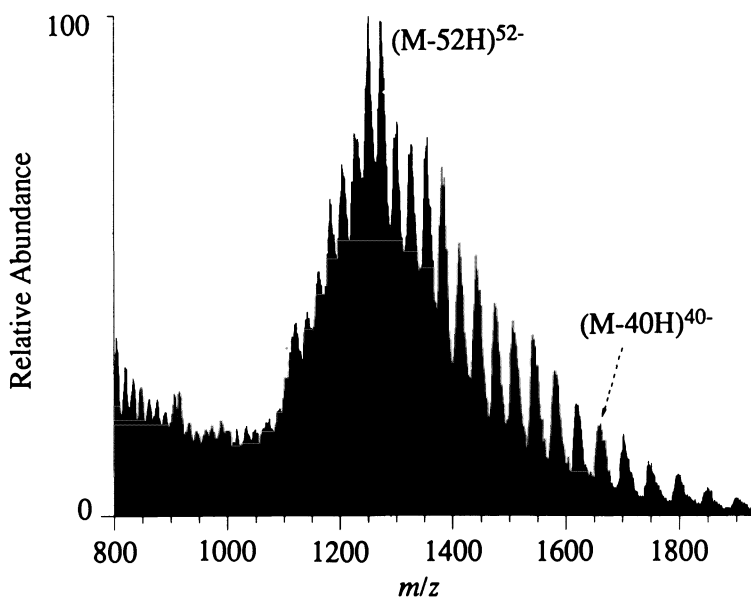


Figure 2.12. Negative-ion ESI mass spectrum of disulfide-reduced sheep serum albumin in 1% NH_4OH (aq.).

variations in charging is unknown. Clearly, however, the ability to obtain both positive- and negative-ion ESI spectra extends the utility of these methods and may provide new qualitative insights related to protein structure in solution.

4. ESI-TANDEM MASS SPECTROMETRY OF POLYPEPTIDES AND PROTEINS

4.1. General Considerations

An important development related to ESI-MS has been the demonstration that large, multiply charged ions can be efficiently dissociated by multiple low-energy collisions with a neutral target gas (24,25,37,97). However, because the CID products are often multiply charged, data interpretation presents special difficulties if product charge states are unknown. Higher resolution or the use of ion-molecule reactions to manipulate product ion charge state or mass can be useful for charge-state determination. Lacking sufficient resolution to separate the isotopic contribution, tandem MS is most straightforward for doubly charged ions. For example, in the case of doubly charged peptides generated from the specific proteolytic digestion of proteins by trypsin, two charges are generally expected to reside on opposite ends of the molecule (an arginine or lysine residue at the C terminus and the N-terminal basic site). Thus, CID results primarily in singly charged fragment ions. It is clear that ESI-MS/MS of doubly charged ions has extended the molecular weight range for which complete polypeptide sequence information can be obtained.

As molecular weight increases, complete sequence information becomes more difficult to obtain. Although the upper M_r value practical for obtaining complete sequence information is uncertain, it is clear that such a capability, based on the techniques currently used, must break down at some point. Nonetheless, qualitatively useful information (i.e., regarding posttranslational modifications, limited sequence information from the termini, etc.) can be obtained, even at relatively high M_r . As mass spectrometric capabilities become more sensitive and sophisticated (perhaps based upon MS^n , utilizing ICR or ITMS instrumentation), the feasibility of analyzing and sequencing higher-molecular-weight polypeptides and other applications should continue to advance. The current status of ESI-MS/MS is illustrated below in the context of three "case studies" of multiply charged polypeptides spanning a wide M_r range: melittin (M_r 2845), ribonuclease A (M_r 13,682), and serum albumins ($M_r \sim 66$ kDa).

4.2. Melittin

Melittin was one of the first polypeptides to be studied by ESI-MS/MS (122). As we have previously described (21,97), manipulation of the nozzle-

skimmer bias voltage (ΔNS) allows for efficient CID of ESI-generated molecular ions formed at atmospheric pressure. As pressure drops through the interface, ions can be accelerated, allowing numerous low-energy collisions. Figure 2.13 (top) gives the ESI mass spectrum for melittin, a polypeptide with 26 amino acid residues that is dominated by the 3+ to 6+ multiply protonated molecules.

Increasing ΔNS from 85 V to 285 V causes sufficient collisional “heating” to induce dissociation of most molecular ions, yielding the spectrum given in Fig. 2.13 (bottom). The various dissociation products, distributed across the

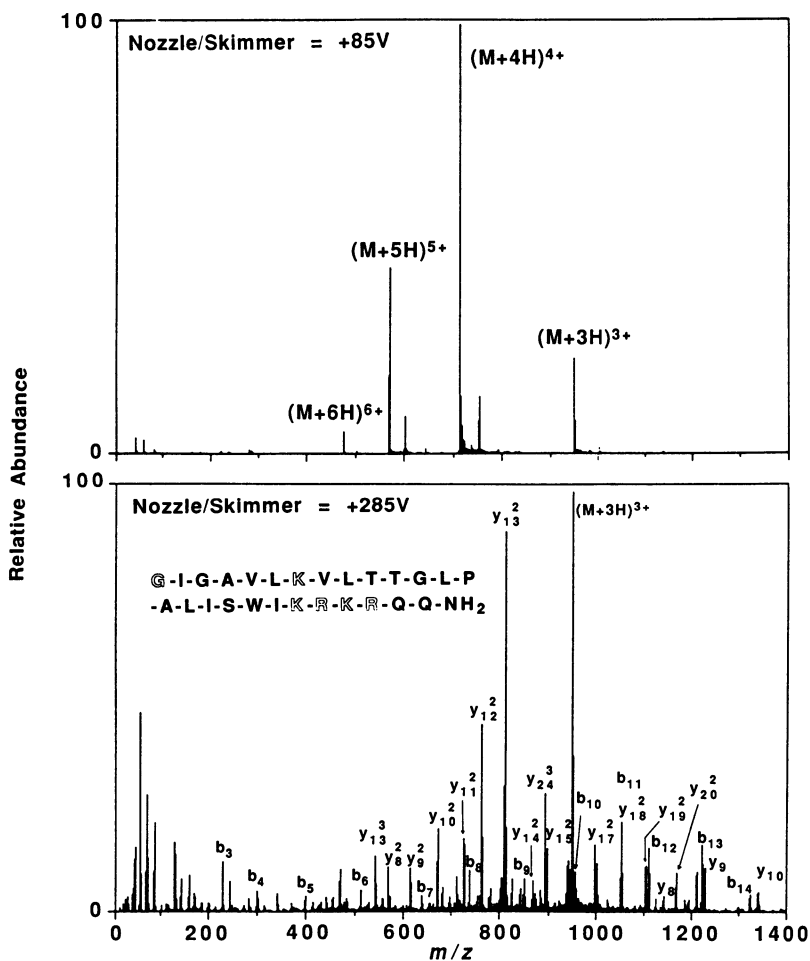


Figure 2.13. ESI/MS spectrum for melittin at low ΔNS (+85 V, top) and high ΔNS (+285 V, bottom). The superscripts on the sequence assignments refer to the charge state of the ions. The likely charge sites in solution are indicated by the outlined letters in the single-letter sequence.

entire m/z range, have been assigned using the conventional notation (123,124) augmented by a superscript that indicates the charge state (absence of a superscript signifies a singly charged ion). Figure 2.13 (bottom) also shows significant contributions at low m/z that are attributed to individual amino acid residues and other singly charged dissociation products likely arising from sequential CID processes.

The CID spectra for the 3+, 4+, 5+, and 6+ protonated molecules of melittin are shown in Fig. 2.14 and provide a striking qualitative comparison of the effect of parent ion charge state. Nearly all peaks in the various product-ion spectra may be readily attributed to reasonable sequence-related fragments (122). The major qualitative observations based on these results include (a) increasing CID efficiency with increasing charge-state and (b) spectra dominated by multiply charged fragments for the higher-charge-state parents. Because $E = z \cdot V$, the center-of-mass collision energy (E_{cm}) obtainable with quadrupole instruments extends to the 5- to 10-eV range. Consideration of the collision gas thickness and the large collision cross section estimated for melittin molecular ions suggests that the average number of collisions was approximately five to ten (122).

The intensities of the 2+, 3+, and 4+ multiply charged y_{13} products and the abrupt termination of the “b” series at b_{13} indicate that the N-terminal peptide bond of proline is significantly more labile than other peptide bonds. This facile cleavage at a proline residue has been observed for CID of other peptides (125,126).

Tandem MS studies of the peaks at m/z 812 and m/z 542, formed by dissociation in the interface (Fig. 2.13) and attributed to the y_{13}^2 and y_{13}^3 species, give the CID spectra shown in Fig. 2.15 (97). Such results support the assignments in Figs. 2.13 (bottom) and 2.14 and provide sequence information for portions of the molecule unprobed for the intact molecular ion.

It is obvious that higher charge states of polypeptides are less stable under typical CID conditions. Results such as those shown in Fig. 2.14 also indicate significant changes in the relative abundances of dissociation products. However, it is difficult to resolve quantitatively the role of Coulombic repulsion on parent ion dissociation rates. To analyze that factor, one must be assured that the different charge states are excited to the same extent; i.e., the “temperature” for each charge state population must be the same. However, depending on interface conditions, differing degrees of collisional excitation will result, and each charge state will be characterized by different quasithermal distributions. Because of the wide variation in pressure through the length of the interface and the uncertain extent of cooling in the expansion, it is an extremely difficult task to select conditions that ensure similar excitation.

We have recently introduced the technique of thermally induced dissociation (TID) to provide similar levels of excitation for all charge states (40). In TID, a heated metal capillary is used to dissociate ions introduced from the atmospheric

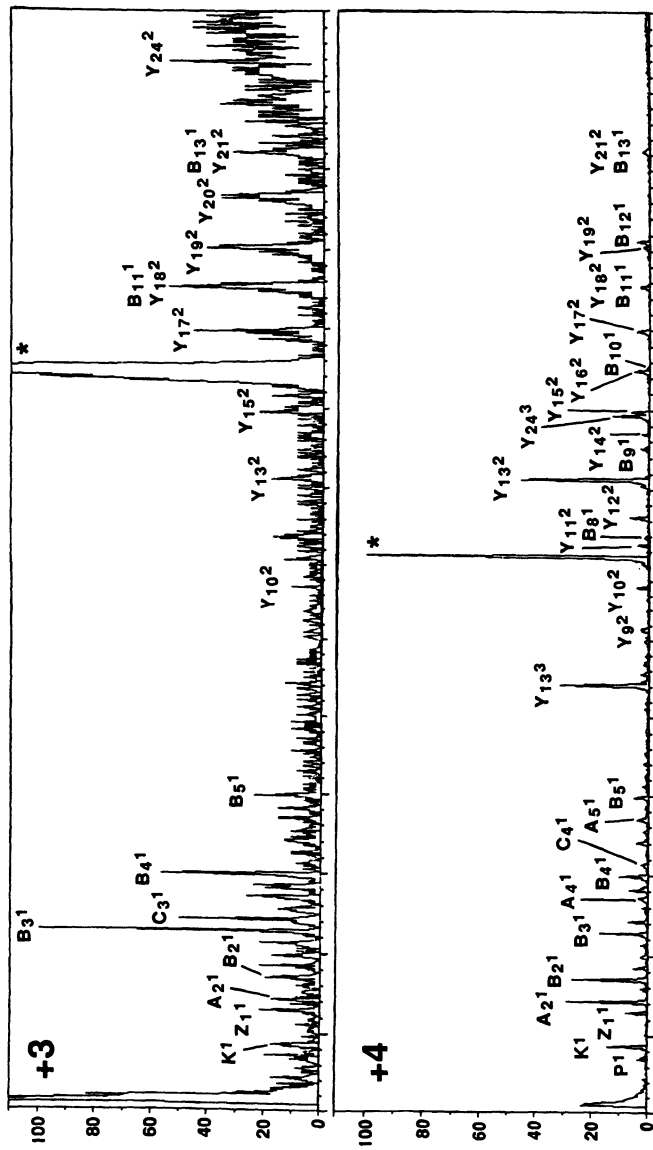
pressure ESI source, thus acting as a thermal reactor. In this manner, electric fields that normally cause collisional excitation in the interface are eliminated, and cooling on expansion should rapidly and efficiently quench reaction processes. Figure 2.16a shows a spectrum of melittin obtained under conditions of moderate heating, which is similar to that obtained with the nozzle–skimmer interface (Fig. 2.13, top). Figures 2.16b and 2.16c show spectra of melittin with progressively greater heating. Extensive dissociation is evident from the attenuation of the parent ion peaks and the appearance of the labeled “y-mode” TID products. The range of temperatures covered in Fig. 2.16 is approximately from 200°C to 400°C. Similar to the higher-energy (tandem) CID studies, the most abundant product ions correspond to various charge states of ions resulting from cleavage between residues 13 and 14 (i.e., y_{13}).

The more highly charged (protonated) ions are especially labile to TID (40). Figure 2.16c shows that the 6+ to 4+ molecular ions are absent from the spectrum, whereas the 3+ species remains. (At higher temperature, the 3+ ion dissociates.) The TID in the capillary may also be combined with subsequent collisional activation in the capillary–skimmer interface (induced by voltage gradients, ΔNS) to produce nearly any desired degree of fragmentation. It is not yet clear how much of the internal energy gained by thermal activation in the capillary persists after cooling early in the expansion and contributes to subsequent CID.

The most likely polypeptide sites to be protonated in solution, and their relative basicities, can differ substantially from rankings based on the relative proton affinities (PA) of amino acid residues in the gas phase. In the gas phase, one expects higher-PA sites to be protonated first (i.e., the preferred sites for lower charge states). The most basic amino acid residues have the greatest PA, with a relative ranking of arginine > histidine > lysine (127). Experimental results clearly show that other peptide sites can be protonated. The relative ranking of these residues is expected to be tryptophan > proline > glutamine, on the basis of ICR equilibrium studies (127). This order contrasts with a relative ranking of glutamine > tryptophan > glutamic acid on the basis of metastable dissociation of protonated dimers (65).

A factor of considerable importance to ESI–MS is the role of Coulombic forces because of the increased repulsion among charge sites. As molecular charge state increases, one also expects an increased proclivity for proton transfer (and other reaction processes) from Coulombic contributions. In addition to increased CID efficiency, Coulombic effects may lower the “effective PA” of the amino acid residues and, depending on ion structure, influence the probability of protonation at a specific site. Studies of proton transfer reactions of multiply charged polypeptides are consistent with this expectation (128–130).

In the case of melittin, where five highly basic residues occur in addition to the amino terminus (see the single-letter sequence in Fig. 2.13), some educated



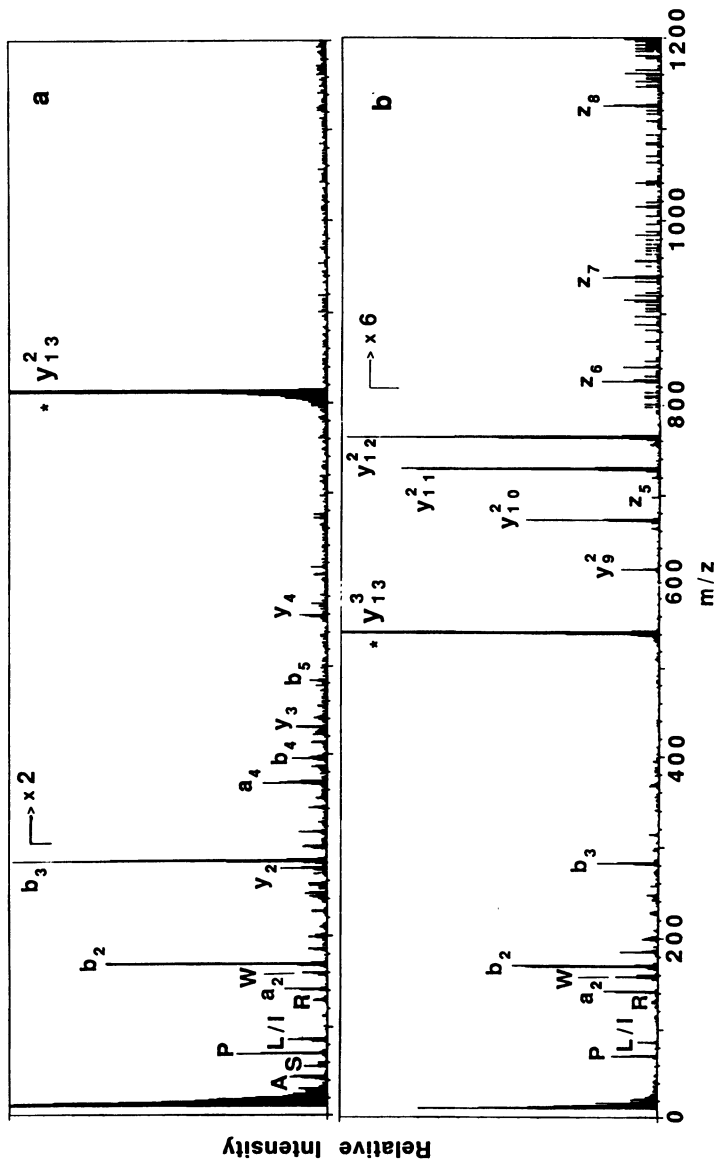


Figure 2.15. Tandem mass spectra of the (a) Y_{13}^2 (doubly charged) and (b) Y_{13}^3 (triply charged) product ions selected from dissociation of melittin in the atmosphere-vacuum interface at $\Delta NS = +285$ V.

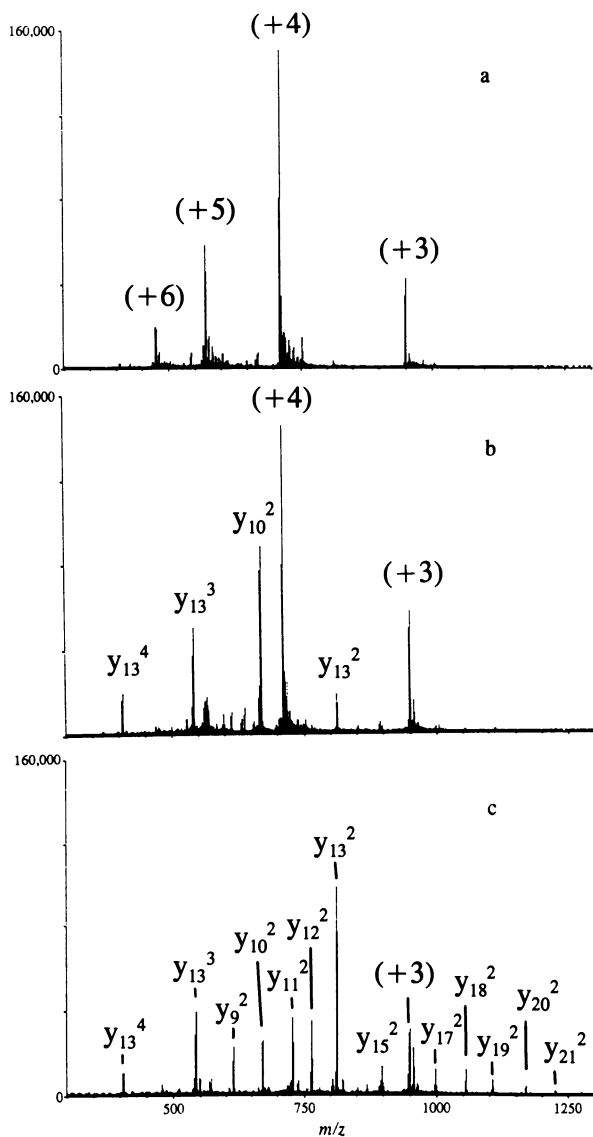


Figure 2.16. Thermally induced dissociation (TID) of melittin in a heated metal capillary at increasing levels of heating from (a) 25 W (heater power applied to capillary) to (b) 37 W to (c) 49 W.

guesses can be made as to where the protons reside in the gas phase. The high dielectric constant of the solvent allows adjacent residues to be protonated in solution. As the solvent is removed, Coulombic effects will increase. For melittin, which has four adjacent, highly basic residues, it is highly probable that protons will migrate to other sites, perhaps by a solvent-mediated process before complete desolvation. The CID of melittin molecular ions (Fig. 2.14) indicates that four protonation sites reside in the y_{13} (and possibly y_{11}) fragment, which encompasses not only the four adjacent highly basic arginine and lysine residues but also two glutamine and one tryptophan residues. However, fragmentation in the highly basic region is not observed for melittin (except from CID/MS/CID/MS experiments in Fig. 2.15) in spite of the very strong Coulombic contribution expected if these sites were charged. Intramolecular proton transfer to tryptophan and glutamine residues would greatly increase ion stability and allow at least one uncharged residue between protonated residues.

Although direct evidence for such intramolecular proton transfer does not yet exist, ion-molecule studies provide some circumstantial support (128–131). Although they do not explicitly consider this possibility, McLuckey and co-workers (129,131) have shown that the $(M + 3H)^{3+}$ ion for melittin is unreactive, whereas the $(M + 4H)^{4+}$ ion undergoes proton transfer and/or cluster formation on reaction with 1,6-diaminohexane (PA = 239 kcal/mol) and “proton sponge” [1,8-bis(dimethylamine) naphthalene, PA > 239 kcal/mol (132)], respectively. The $(M + 4H)^{4+}$ species would likely require protonation of at least two of the four adjacent highly basic sites in solution (if the N terminus and a lysine at residue 7 are also protonated). However, the amino terminus is less likely to be protonated in solution, suggesting that three of the four adjacent highly basic residues will be protonated initially. This conjecture is supported by the fact that an intense y_{13}^3 fragment is observed on CID of the 4^+ species. The y_{13}^3 was also the only fragment of the $(M + 4H)^{4+}$ species observed to react with 1,6-diaminohexane in the ITMS (129). The y_{13}^2 species is unreactive. The quadruply protonated molecule's substantially greater reactivity compared to the triply charged molecule may be attributed either to strong Coulombic contributions (perhaps arising from protonation of adjacent residues) or to protonation of less basic residues. Clearly, one must also consider Coulombic effects in assigning likely protonation sites.

The implication of these studies is that a large amount of information regarding polypeptide structure can be obtained or deduced from dissociation and reaction studies. The role of Coulombic forces in CID and reaction processes appears to be significant. Although CID processes are useful for probing primary structure (i.e., peptide sequence), reaction processes should have much greater potential for probing higher-order structure in the gas phase. Reaction studies can be conducted at low levels of internal excitation, whereas the stepwise activation to internal energies required for CID (on the order of 10^2 – 10^3 eV for proteins) is likely to cause loss of labile structural elements.

4.3. Ribonuclease A

Bovine pancreatic ribonuclease A (RNase A) (M_r 13,682) is composed of 124 amino acid residues and four disulfide bonds that link Cys residues 26 to 87, 40 to 95, 58 to 110, and 65 to 72 (133). Much literature has been devoted to this molecule as a model for protein folding (134). The ESI mass spectra of RNase A and its disulfide-reduced form show typical bell-shaped distributions of multiply charged molecules. The $(M + 15H)^{15+}$ ion is the most highly charged species observed for native RNase A; however, on reduction, the distribution extends to the $(M + 23H)^{23+}$ species (135).

The CID product ion mass spectra obtained for the 12^+ and 13^+ charge states of native and reduced RNase A reveal higher relative intensities for product ions of the disulfide-reduced parent species (Fig. 2.17). For example, the ratio of the m/z 872 (y_8) ion to the parent ion intensity is more than a factor of 2 greater than for the native protein for both charge states. The y_8 ion, or its doubly charged version (y_8^2), is formed by cleavage of the Val¹¹⁶–Pro¹¹⁷ peptide bond (with a single charge retained on the C-terminal fragment). Other intense peaks were ascribed to cleavage of the N-terminal amide bond of a Pro residue (Asn¹¹³–Pro¹¹⁴ at m/z 617) or y_{11} . For the reduced state, the $[y_8]/[(M + nH)^{n+}]$ ratio gradually increases from 0.08 for $n = 12$ to 0.27 for $n = 17$. The more highly charged molecule might be expected to have a more extended conformation because of the mutual electrostatic repulsion of charge sites (64,136,137). The presence of disulfide bridges prevents highly extended conformations. A more extended (gas-phase) structure, as expected for the reduced protein, would have a reduced Coulombic contribution, which may explain the observed differences in dissociation pathways (135).

Complementary ion pairs (which in sum account for the entire molecular ion) are a major feature of the reduced RNase A CID mass spectra (135). For example, for the $(M + 13H)^{13+}$ molecular ion of reduced RNase A, the complement of the singly charged y_8 ion is the 12^+ species, b_{116}^{12} . The y_{11} – b_{113}^{12} and y_{11}^2 – b_{113}^{11} pairs are also prominent. Spectra for other charge states studied (up to 17^+) display peaks consistent with these assignments. Ions corresponding to y_8 , y_8^2 , and y_{11}^2 are also present in the CID spectra along with their complements, b_{116}^{n-1} , b_{116}^{n-2} , and b_{113}^{n-2} , respectively. The region below m/z 400 contains small b- and y-mode contributions from dissociation occurring near the N and C termini in addition to immonium ions indicative of the presence of particular single amino acid residues (138). A series of triply charged b_{14}^3 to b_{24}^3 ions (Asp¹⁴ to Asn²⁴) is observed between m/z 500 and 850 in the CID spectra for all parent charge states studied (135).

Dissociation in the atmosphere–vacuum interface yields spectra that show similarities and differences between the reduced and native forms. For the reduced state (and presumably more extended conformation), bond cleavage from the N-terminal (b_{21}^3 – b_{24}^3) region occurs closer to the Cys²⁶ residue; C-terminal

singly charged sequence ions, y_8 to y_{11} , are also observed in both forms of the protein along with some of the major complementary ions also observed in the CID spectra (Fig. 2.18).

Confirmation of product ion assignments arising from dissociation in the atmosphere–vacuum interface can be obtained by MS/MS, as demonstrated for the peak at m/z 872, attributed to a prominent y_8 species occurring in all CID spectra of RNase A (135). As shown in Fig. 2.19, ions below m/z 872 are caused by conventional sequence-specific fragmentation for the putative octapeptide (residues 117 to 124). No product ions were observed above m/z 872, as would be expected for the parent species being singly charged. Tandem mass spectra of

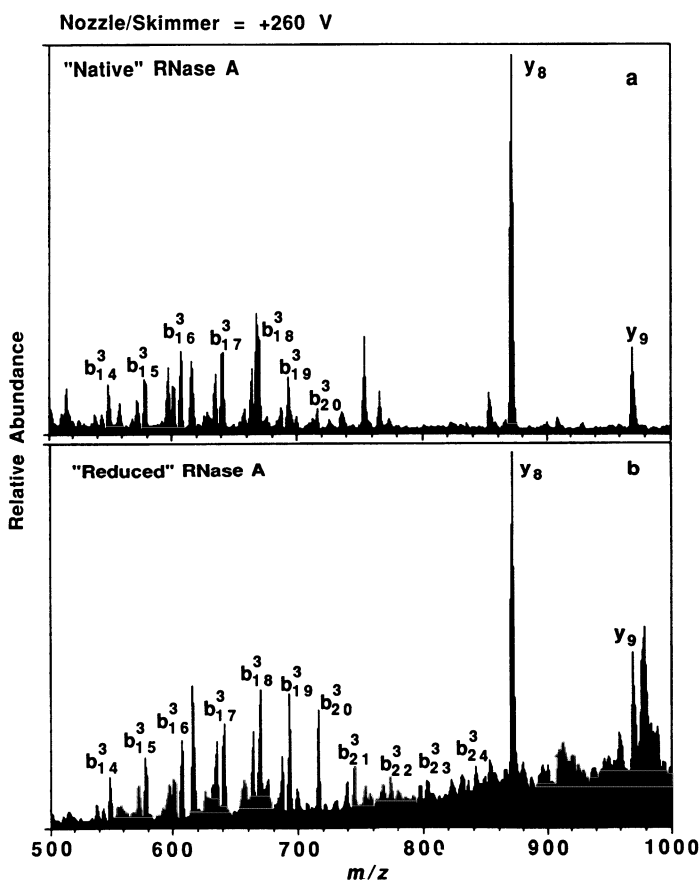


Figure 2.18. Electrospray ionization mass spectra of (a) native RNase A and its disulfide-reduced state (b) at $\Delta NS = +260$ V. Sufficient collisional heating of the molecular ions has occurred to induce dissociation of most of the multiply charged molecular ions to form the sequence-specific ions labeled in the spectra.

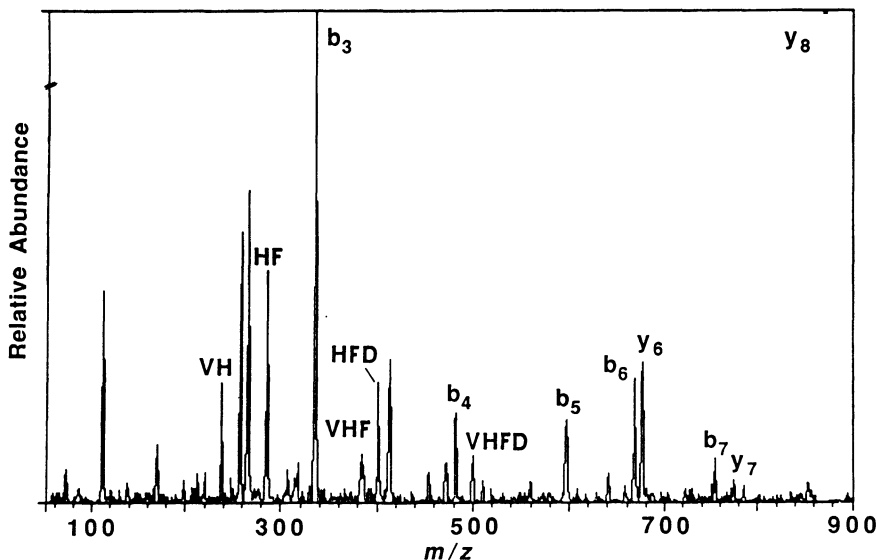


Figure 2.19. Collision-induced dissociation mass spectrum of the m/z 872 fragment ion of RNase A generated by CID in the atmosphere–vacuum interface ($\Delta NS = +235$ V). The resulting mass spectrum is consistent with the assignment of the m/z 872 ion as a y_8 singly charged species of RNase A.

other fragment parent ions shown in Fig. 2.18 confirmed tentative CID assignments.

The study of RNase A CID processes highlights an important point: protein structure and charge location are strongly interactive. At a minimum, changes in structure will generally correspond to different distributions of charge sites. Thus, in the case of RNase A, the reduced form is more likely to have protonation sites toward the center (or more hydrophobic regions) of the globular structure. Comparison of CID mass spectra for similar charge states of the native and reduced forms results in dissociation products that have different charge states. Whether higher-order structure by itself influences the probability of cleavage at a particular site likely depends on whether structural differences are still meaningful after the multiple-collision excitation process. In any event, in cases where structure is constrained by covalent disulfide bonds, it is clear that significant differences in dissociation products can result.

4.4. Serum Albumins

An advantage of conducting dissociation in the ESI–MS interface is that there yet appears to be no upper limit to the ability to induce efficient dissocia-

tion. The problems that arise with increasing molecular weight can be attributed to spectrum complexity and the limited intensities that result for specific CID product ions. Limited resolution and uncertainties in charge state assignments combine to cause increasing difficulties for the interpretation of large-molecule CID spectra.

Serum albumins represent the largest molecules extensively studied thus far using CID in the interface and conventional MS/MS methods (75). Figure 2.20 shows dissociation spectra obtained in the interface for dog, sheep, and horse albumins. Nearly all the more intense product ion peaks detected have been assigned as multiply charged “b” ions arising from fragmentation within the first 30 residues from the N terminus. These spectra are dominated by dissociation of a range of charge states defined at lower m/z by the envelope of molecular ion charge states (i.e., those observed at low ΔNS) and at higher m/z by decreased activation efficiency. For native albumins, the range of charge states that dissociate typically extends from 60+ to perhaps 40+ for the conditions used.

Our sequence assignments are facilitated by factors such as the expected low probability of observing products of bond cleavage from regions enclosed by disulfide bonds (62% of the amino acid sequence of bovine albumin is enclosed by its 17 Cys–Cys bonds) and the assumption that dissociation products occur from similar regions of the molecule for all albumin species. Particularly helpful is the fact that the albumins, as a class of proteins, exhibit a high level of sequence homology. At least two overlapping product ion charge state distributions were observed for all albumin species, providing additional support for our assignments. For example, dissociation of the Asn¹⁸–Phe¹⁹ bond (giving the b_{18} ion) of sheep albumin is represented by products at m/z 1048 (doubly charged) and m/z 699 (triply charged). Cleavage of the Ala²⁶–Phe¹⁷ bond (b_{26} ion) of horse serum albumin is indicated by product ions at m/z 982 (3+), 737 (4+), and 590 (5+). This distribution of product charge states may result from the dissociation of parent ions with a variety of charge states. Parent species of the same total charge may also have their charges distributed differently throughout the molecule, leading to a similar result. Interpretation of such spectra might be approached by adapting the deconvolution algorithms used for distributions of multiply charged molecular ions (62).

Subtle differences in the degree of charging for the fragment ions were also observed and found to be consistent with the spectral assignments. In a 5% acetic acid solution, most if not all basic groups should be protonated in solution. Horse, bovine, and rat albumin each have seven basic amino acid residues (lysine, arginine, and histidine) within the first 28 residues in addition to the possible N-terminal charge site, and we observe multiple charging for product ions up to the 5+ state. On the other hand, the most highly charged product is 4+ for dog, sheep, rabbit, porcine, goat, and human albumins, which contain either five or six basic sites within the initial 28 residues.

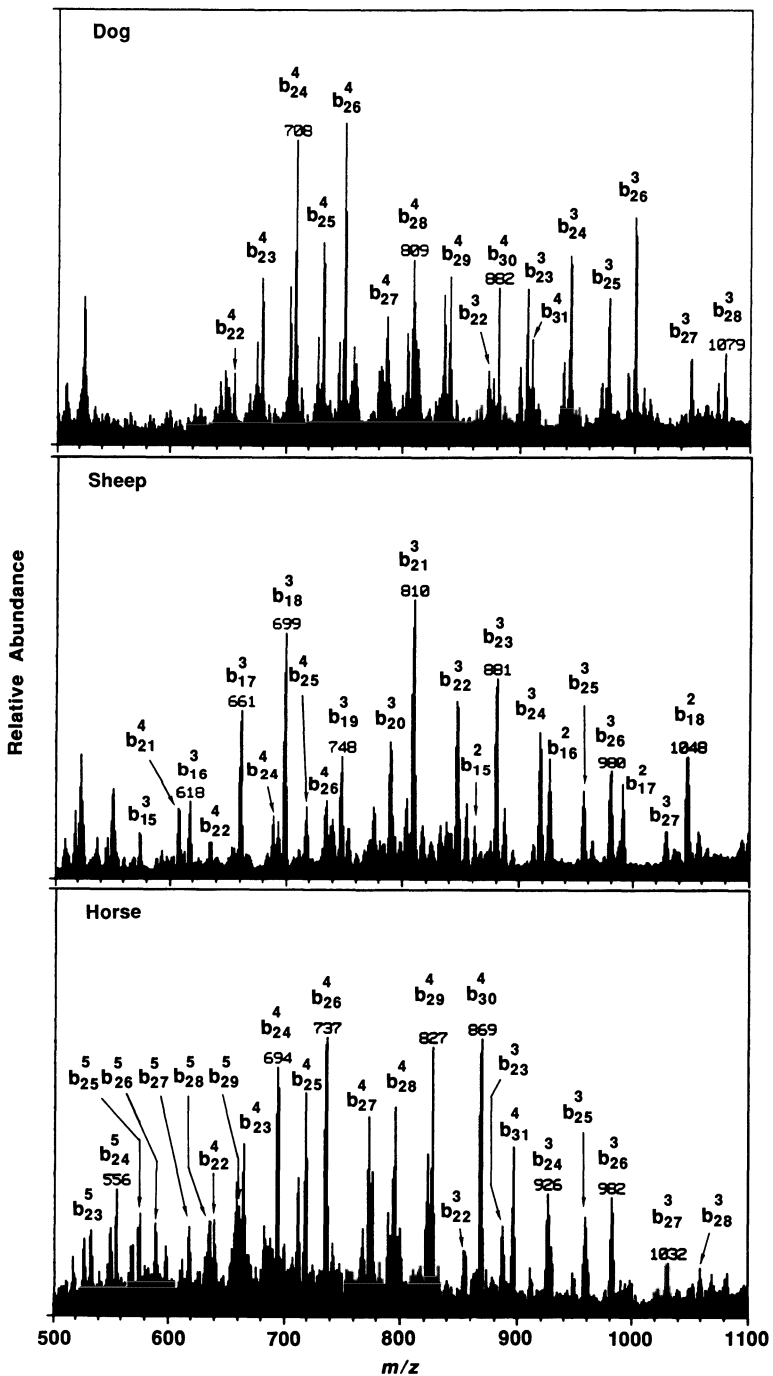


Figure 2.20. Electrospray ionization mass spectra of (top) dog, (middle) sheep, and (bottom) horse serum albumins with $\Delta NS = +335$ V.

Distinctive mass spectra were obtained for the albumin species by collisional dissociation in the interface. These data permitted detailed verification of reported sequences for residues between position ~ 18 to ~ 28 from the N terminus, depending on the albumin species, and indicated a few errors in reported sequences (75). For example, goat serum albumin yielded similar ESI mass spectra to sheep albumin at high ΔNS values. Although conventional Edman degradation sequence analysis indicates one difference in the initial 30 residues between goat and sheep albumin, the mass spectra indicate otherwise. Asparagine resides at position 18 in the case of sheep albumin, whereas histidine is reputed to be present at this site for goat albumin. Thus, a 23-Da shift should be observed and easily identified in the collision spectra for the two species. Instead, identical product ion spectra were obtained, indicating Asn at position 18 for goat albumin. Peptide-mapping experiments from tryptic digestion followed by separate HPLC analysis and ESI-MS also revealed similarities in their primary structure for the samples examined (75).

Similarly, in the case of dog serum albumin, only the first 24 residues are known from the literature (139). Along with known sequence homologies, the experimentally observed product ions allowed prediction of the sequence for residues 25–31. Ions b_{22} to b_{24} were assigned from calculations for all possible m/z values based on the available amino acid sequence. Remaining products were assigned as sequential b-mode dissociation products starting from b_{24} . For example, the ion at m/z 708.3 was assigned as b_{24}^4 with a mass of 2,830 Da. The next major ion at higher m/z is m/z 733.1; its mass for a 4+ ion would be 2,929.2 Da, or an increase of 99 Da, corresponding to a valine residue (b_{25}^4). An overlapping suite of triply charged ions is also present and was used for confirmation of the assignments. As ion at m/z 977.0 is assigned at the b_{25}^3 product, and so forth to b_{31}^3 . For dog albumin, it was not possible to distinguish the presence of lysine versus glutamine (0.04 Da difference) at position 29, or leucine versus isoleucine at position 31 (75). The major fragmentation between residues 18 and 28 for the serum albumins also allows a limited verification of residues 1–17 by comparing the M_r of the smallest product ion to the expected value. For example, the smallest M_r fragment ion observed for dog serum albumin (b_{22}) is in good agreement with the M_r calculated for the first 22 residues.

Results for tandem MS of the $(M + 49H)^{49+}$ ion of sheep albumin are shown in Fig. 2.21. These CID studies used argon as the neutral target and a laboratory-frame translational energy of 6.86 keV. The fragment ions identified were generally of the same m/z values produced by dissociation in the nozzle-skimmer interface.

In addition to the product ions at lower m/z , CID studies of most albumins analyzed (75) gave product ions near the parent species (m/z 1329 and 1384 for sheep albumin) as shown in Fig. 2.21. Their m/z values correspond closely to

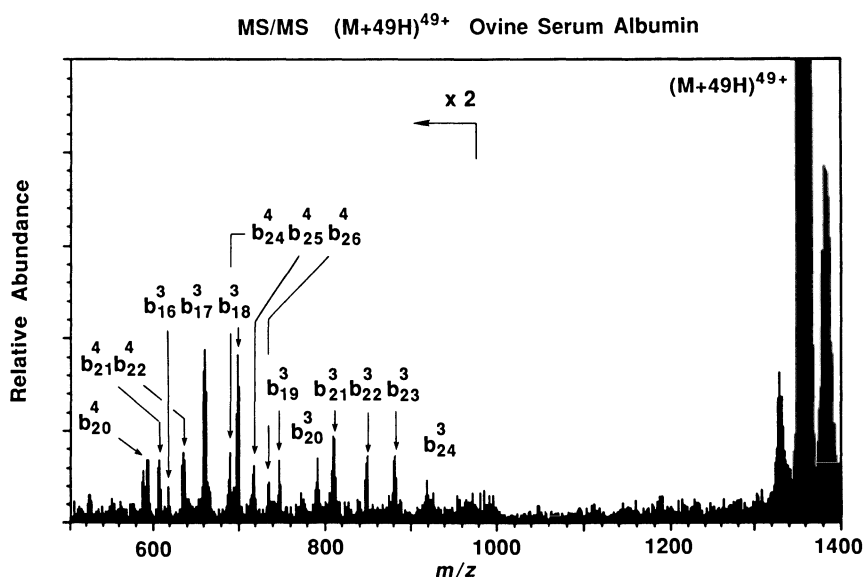


Figure 2.21. Tandem mass spectrum of the (M + 49H)⁴⁹⁺ molecule of sheep albumin with $E_{\text{lab}} = 6860$ V (argon collision target).

intact molecular ions with 50+ and 48+ charges, respectively. Most likely, these ions arise from dissociation of a noncovalently bound dimer [i.e., (2M + 98H)⁹⁸⁺, whose m/z position would be the same as the (M + 49H)⁴⁹⁺ ion]. Such a dimer species appears to be present in low abundance (~5% of the monomer for porcine albumin, as suggested by Fig. 2.4, top) (75) and has been observed in greater abundance at higher m/z (63).

Dissociation of reduced sheep albumin (which gives low- Δ NS spectra similar to that for reduced bovine albumin, shown in Fig. 2.5, bottom) in the interface resulted in an unresolved signal extending to $m/z < 700$. This result is partly attributed to large numbers of unresolved product ions that originate from the many available dissociation pathways and charge states. However, dissociations near the N terminus still appear to constitute energetically favored processes.

The CID MS/MS results for reduced albumin are shown in Fig. 2.22 and indicate that the location of charge sites is different for the native and reduced forms. Dissociation of the (M + 49H)⁴⁹⁺ molecular ion of disulfide-reduced sheep albumin produces fragmentation similar to that shown in Fig. 2.21 under identical Δ NS and E_{lab} conditions, but without the prominent 4+ charge state products. Product ions extending slightly further into the sequence (to residue 26), compared to the native state, are evident along with a rising base line extending to higher m/z , which we attribute to additional unresolved fragmenta-

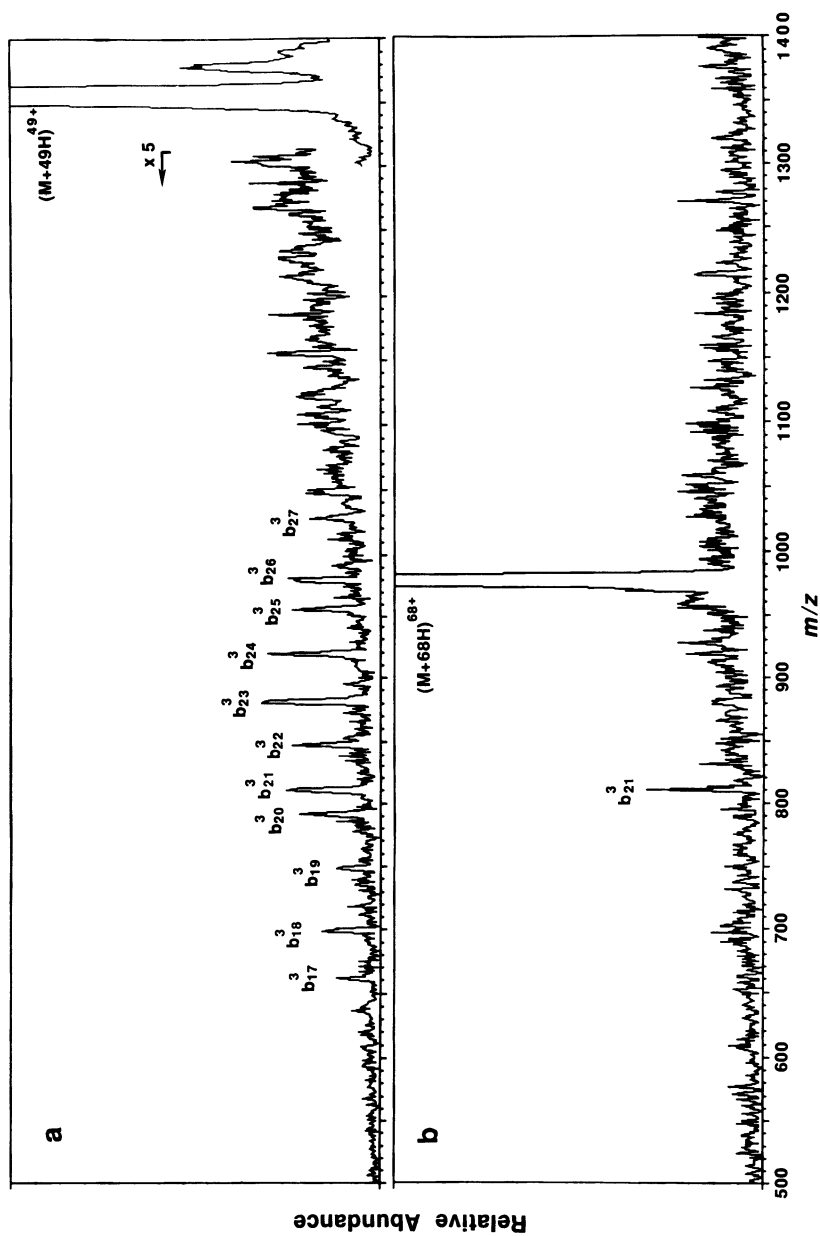


Figure 2.22. MS/MS spectra of the (a) $(M + 49H)^{49+}$ and (b) $(M + 68H)^{68+}$ parent ions from disulfide-reduced sheep albumin.

tion processes. The $(M + 49H)^{49+}$ ion for the reduced form might be expected to have fewer charges on the N-terminal region, leading to the observed lowering of product charge states.

To compare CID of different charge states for the reduced albumin, the ΔNS was adjusted such that collision energy was similar for the 49+ and 68+ molecular ions in the atmosphere–vacuum region and collision quadrupole. The MS/MS of the $(M + 68H)^{68+}$ molecular ion (Fig. 2.22b) produces a weak peak, tentatively assigned as the b_{21}^3 ion, as the only resolvable product species on top of a broad “hump,” which again is attributed to many additional unresolved CID products.

The increased Coulombic effects for more highly charged molecules may also give rise to larger dissociation rates and alter the relative abundances of dissociation products. A theoretical evaluation of possible Coulombic effects (137) shows that doubling of the charge state can lead to dramatic increases in dissociation rates. The effect is greatest when charge is evenly distributed between the two fragments, where the Coulombic interactions effectively lower the barrier to dissociation to the greatest extent. The importance of Coulombic effects depends on the internal energy of the molecular ions; at high levels of excitation, branching ratios are increasingly determined by the preexponential “frequency factor” associated with the dissociation pathway (137). Bunker and Wang (140) have previously shown that, for uncharged (or singly charged) molecules, in the absence of Coulombic effects, the frequency factor is greatest for cleavage near the chain termini. At the large-molecule limit, the frequency factor approaches 0 for particular cleavages near the chain center (although the summation of all possible cleavages for the “interior” can still be large). Calculations (137) indicate that Coulombic forces can reverse this situation if a sufficiently high charge state is obtained. Thus, higher charge states may dissociate more rapidly and, more importantly, may dissociate more readily to yield products of cleavages nearer the molecule’s center. This rationale may explain, at least in part, the fact that CID products evident for $(M + 49H)^{49+}$ are not prominent for $(M + 68H)^{68+}$, even though total CID efficiency is greater.

For the albumin species, most of the prominent fragmentation is centered near residue 20 from the N terminus, with the various multiply charged products providing information on a series of ~ 10 sequential residues. MS/MS studies of fragment ions produced at an elevated ΔNS bias can again provide additional information. CID/MS/CID/MS experiments for sheep albumin were performed on the triply charged b_{18} and b_{21} fragments with $\Delta NS = +335$ V (Fig. 2.23). Doubly charged b_{16} to b_{19} , b_{18}^3 , and singly charged b_2 to b_4 and y_2 to y_3 are found for the b_{21}^3 parent ion. CID of b_{18}^3 yields b_{13}^2 to b_{17}^2 , b_{16}^3 to b_{17}^3 , and b_3 to b_4 products along with weak signals attributed to internal fragmentation.

CID/MS/CID/MS experiments were also used to provide support for peptide sequence assignments for rabbit serum albumin. The ESI mass spectrum of

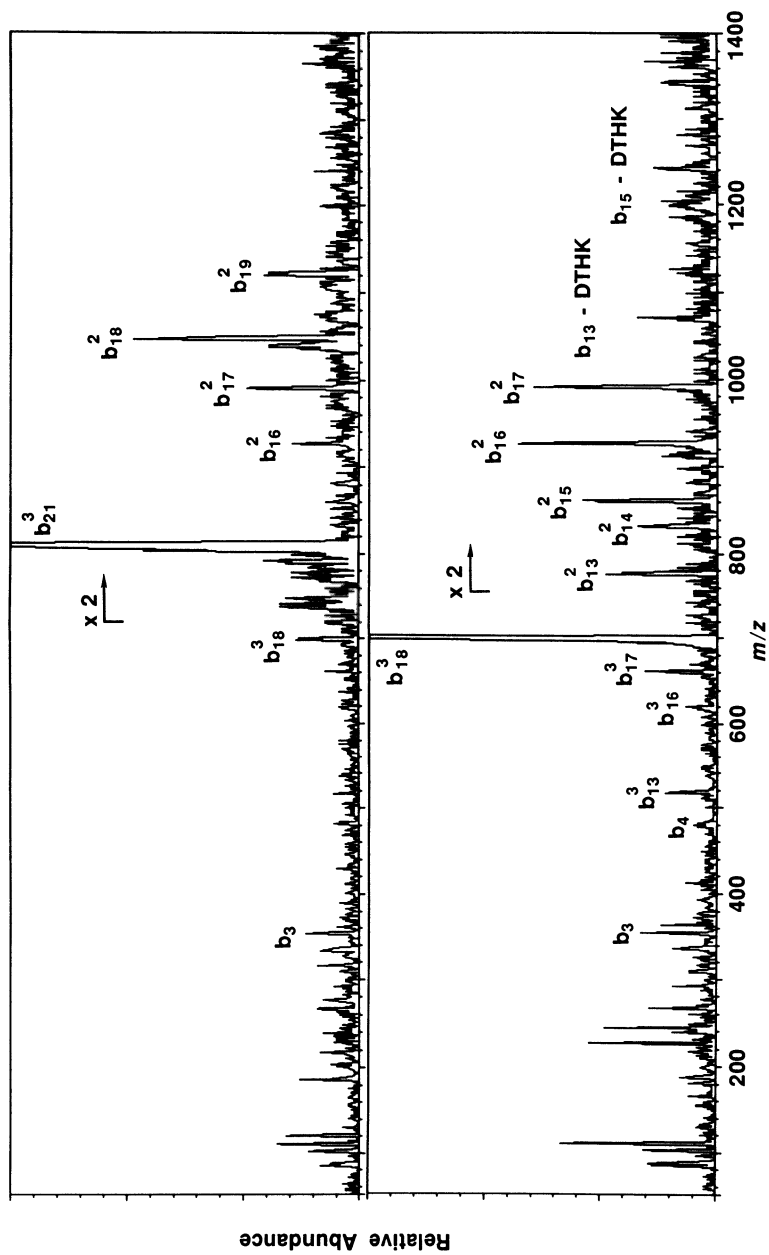


Figure 2.23. Collision-induced dissociation mass spectra of the b_{21}^3 (top) and b_{18}^3 (bottom) product ions of sheep albumin with $\Delta NS = +335$ V and $E_{lab} = 420$ eV.

rabbit serum albumin at high Δ NS (75) shows that most of the intense peaks between m/z 500–1000 occur at lower m/z than predicted, based on amino acid sequence (141). Triply charged ions corresponding to b_{18}^3 and b_{19}^3 of the published sequence were found. However, b_{20}^3 – b_{26}^3 and b_{20}^4 – b_{25}^4 ions appeared to be ~ 15 Da too low, suggesting the possibility that residue 20 is not Lys (incremental mass = 128 Da) as expected for its reported sequence but, rather, an alternative residue of mass ~ 113 Da such as Ile or Leu. Interestingly, position 20 (Lys) is homologous for seven species examined and for hamster albumin reported by Vötsch *et al.* (141). These results suggested an error in the previously suggested sequence. This conclusion was also supported by an additional study involving further dissociation of the b_{22}^3 product ion, which results in doubly charged b_{16} – b_{18} ions and triply charged a_{18} – a_{22} and b_{18} – b_{21} products at m/z values consistent with Ile/Leu at position 20.

These results demonstrate that useful structural information can be obtained for multiply charged molecules of at least 66 kDa, a factor at least 10 larger than reported for singly charged ions. It is conceivable that ESI–MS/MS may also have utility for rapid detection of genetic variants. Over 30 different human serum albumin variants, mostly from single-point mutations in the albumin gene, are known. Although the sequence information obtained is limited for molecules of such size, further progress may be expected. We note that the MS/CID/MS and CID/MS/CID/MS spectra suggest an abundance of lower-intensity dissociation processes that cannot be suitably examined at present because of limited sensitivity and spectral “congestion” (arising from the range of potential products and charge states). In addition, it is also likely that important fragmentation products from regions more interior of the molecule fall outside our current m/z range (1400).

An exciting possibility of ESI is the future use of more sensitive and higher-resolution MS methods that might allow more extensive sequence information to be obtained. It may be possible that ITMS and FT-ICR methods allowing sequential MS^n analyses may provide much more extensive primary structure information in only a fraction of time required by conventional methodologies. MS^4 spectra for multiply charged ions from small peptides have recently been obtained with ESI–ion trap MS (52,142). With higher-resolution methods, charge state assignments from either resolved isotopic peaks or unresolved isotopic envelopes are possible (60).

5. COMBINED SEPARATIONS AND ESI–MS OF POLYPEPTIDES AND PROTEINS

A high-resolution separation prior to mass spectral analysis of biological materials is highly desirable because nearly all systems of interest are comprised

of mixtures of varying complexity. Even proteins in a highly “purified” state are often mixtures because of naturally occurring microheterogeneity, or are converted to mixtures before analysis by chemical or enzymatic processes. Sample sizes may be limited, and multiple purification stages are often precluded. Practical incentives exist to conduct biochemical research on the smallest scale possible. It is not surprising, therefore, that combined separation–MS analysis is of broad interest and that greater sensitivity is almost always desired.

Liquid chromatography (LC) and, increasingly, capillary electrophoresis (CE) are widely used in the separation of proteins and peptides and have been interfaced to mass spectrometers using ESI. Flow rates of 1–10 $\mu\text{l}/\text{min}$ are generally used for unassisted ESI (as opposed to the somewhat higher flow rates for “ion spray”), depending somewhat on solution composition (37,143). If the buffer or additive concentration is less than 10^{-2} M, an approximately linear response with analyte concentration can be obtained (143–145). It is possible to couple LC or CE with ESI–MS over a limited range of flow rates and buffer compositions, and the first ESI–MS interface with CE was accomplished in this manner (146,147). Uncoupling the properties of the sprayed solution from that used for the separation is often desirable. Second-generation interfaces provide for postcolumn mixing of the column eluent with a suitable solution to uncouple the separation and ESI steps and increase the flexibility of the combined system (26,148,149).

The use of reverse-phase LC–ESI for the analysis of peptide mixtures, particularly enzymatic digests of proteins, is rapidly growing. Historically, LC has been most widely used at flow rates of ~ 1 ml/min for conventional packed columns (4.6 mm i.d.) and, more recently, approximately 50 $\mu\text{l}/\text{min}$ for “microbore” columns (1 mm i.d.). These flow rates are too large for unassisted ESI, but this limitation can be sufficiently reduced using high-volume gas flow over the electrospray tip to pneumatically assist the ESI process (22,115,148,149). With this “ion spray” interface, the entire eluent from a 1-mm i.d. column can be sprayed, whereas a split (usually $\sim 20 : 1$) is used with flow rates from conventional columns. Tryptic digests have been examined with this interface with an ITMS (54) and compared to results using continuous flowing fast atom bombardment (CF-FAB) interfaces on a triple quadrupole MS (91). Recent results have shown a number of methods for operation at higher flow rates involving flow splitting, ultra-sonic assistance, or splitting of the electrospray droplet plume.

The performance of conventional 4 to 5-mm and 1-mm i.d. columns with a triple quadrupole instrument has also been reported (150). The conditions varied somewhat in these experiments, but in general a gradient elution starting from 100% H_2O to up to 90% acetonitrile was used with a constant trifluoroacetic acid content of $\sim 0.15\%$. Approximately 10–50 pmol per component injected into the interface is required for practical full-scan mass spectrometry, and typical peak widths are 15 to 30 sec.

Packed capillary LC has also been coupled to mass spectrometry using both pneumatically assisted and unassisted ESI (151,152). Capillary diameters as small as 50 μm , with flow rates of only a few microliters per minute, have been used. Useful full-scan mass spectrometry was reported from 25 pmol per component for a tryptic digest of dephosphorylated β -casein (152).

Only a few examples of the application of LC-ESI-MS to proteins have thus far been reported (54,153). The use of LC-ESI-MS for analysis of protein enzymatic digests has attracted great interest (153), particularly because sufficient sensitivity exists to allow on-line MS/MS of separated polypeptides (e.g., tryptic fragments). Generally, such analyses are conducted in several steps, involving an initial LC/MS separation used to identify enzymatic fragments and to determine detailed MS/MS scans for a subsequent separation. Conventional triple quadrupole instrumentation currently provides insufficient sensitivity for useful on-line MS/MS of proteins; however, the ion trap mass spectrometer should provide superior performance for such applications. An advantage of LC separations currently is that relatively low buffer or salt concentrations are generally employed, leading to a sensitivity advantage over capillary zone electrophoresis (CZE) (but not necessarily capillary isotachopheresis) at equivalent flow rates. The higher flow rate for LC separations will often allow much better "trace" analysis than CZE separations, even though the latter generally would require much less sample, and will likely produce the lowest absolute mass (but not molar) detection limits.

The applications of CZE (one form of CE) are also expanding rapidly, and a number of commercial instruments are now available. The first CZE-MS was based on an ESI interface developed at our laboratory (146,147). Following this initial work with CZE-MS, we reported an improved interface using a flowing sheath liquid electrode (26), the combination of capillary isotachopheresis (CITP) with MS (154,155), and CE-MS/MS (155,156). More recently, other researchers have reported similar interfaces (153,157-159). CE-MS interface designs have also been reported based on CF-FAB mass spectrometry (160-163). However, the ESI methods appear to offer clear advantages in most cases because of better sensitivity, reduced background, and interface designs that do not require long transfer lines or incur a pressure drop across the capillary (69,164,165). Perhaps the most significant advantage of the ESI interface to CE is the applicability to higher-molecular-weight compounds that are impractical by CF-FAB methods (37,166).

Peptides are easily amenable to CZE-MS analysis with low, even subfemtomole, detection limits. High-efficiency separations have been demonstrated, generating over 250,000 theoretical plates. Complex mixtures generated from tryptic digestion of large proteins are well suited to CZE-MS analysis. Such doubly charged tryptic peptides generally fall within the m/z range of quadrupole mass spectrometers. The resolving power of these methods is illustrated in Fig.

2.24, which shows a UV electropherogram (top), obtained in conjunction with a CZE-MS separation of a tryptic digest of tuna cytochrome *c* in a 50 mM acetate buffer (at pH 6.1). On-column UV detection at the middle of the CZE capillary for our instrumentation provides a "preview" of ESI-MS detection at twice the separation time (Fig. 2.24). Shown in the bottom four panels of Fig. 2.24 are single-ion electropherograms for two charge states of two tryptic fragments. The individual peaks shown are <2–3 sec in width at half height and indicate a separation efficiency corresponding to more than 4×10^5 theoretical plates. Experience to date indicates that nearly all tryptic fragments can be effectively detected by ESI-MS methods and that tryptic fragments not detected are generally "lost" by reaction or adsorption on surfaces before the analysis. Full utilization of the power of these methods will depend on concomitant improvements in the earlier stages of sample handling and preparation.

The analysis of proteins by CZE-MS is challenging because of the well-established difficulties associated with protein interactions with capillary surfaces. It is unlikely that one capillary or buffer system will be ideal for all protein separations, but rather (as for LC separations) procedures optimized for specific classes of proteins will have to be developed. Most CZE-ESI-MS separations require the ionic strength of the buffer to be about 10^2 greater than that of the sample to prevent degradation of the separation (from perturbation of the local electric field in the capillary). Detection sensitivity for proteins is generally lower than that for small peptides because of the greater distribution of charge states.

Figure 2.25 shows a separation of three myoglobins obtained on an uncoated 50- μm i.d. fused silica capillary of 80 cm length. The separation was obtained in 10 mM TRIS buffer at pH 8.3 with CE electric field strength of 120 V/cm. Approximately 100 fmol per component was injected onto the capillary column. Figure 2.25a shows the UV trace for the separation, and Figs. 2.25b and 2.25c show two single-ion electropherograms (m/z 861 and 893, respectively) from MS detection for the same separation. The resolution of the mass spectrometer was too low to separate the 19^+ molecular ion of horse myoglobin (M_r 16,951) from that for sheep myoglobin (M_r 16,923), and both species were detected at m/z 893 (Fig. 2.25c). Whale myoglobin (M_r 17,199) was detected at m/z 861 and carried 20+ charges. The ion at m/z 617 (not shown) represents the heme group of the myoglobins and clearly remains associated with the protein during CZE separation. Because the heme is not covalently bound to these proteins, it is labile under the acidic sheath conditions used for ESI-MS.

For targeted compound analysis, where a single ion or mass can be monitored continuously, detection of very sharp peaks (<1 sec in width) is readily accomplished without substantial broadening caused by the interface. Peak widths for CZE-MS of proteins can be sufficiently narrow to challenge or exceed scanning capabilities of quadrupole mass spectrometers, particularly when signal intensities are low. Recent work has shown that "full-scan" spectra

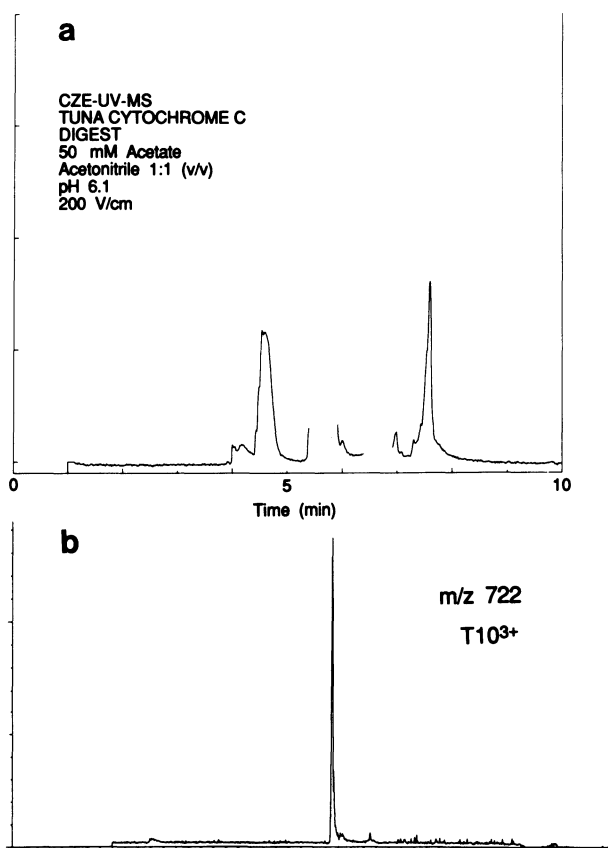


Figure 2.24. Ultraviolet (210-nm) (a) and selected single-ion electropherograms (b–e) for the CZE–MS separation of the products of a tryptic digest of tuna cytochrome *c*.

can be obtained for subfemtomole injections of standard proteins when using small diameter capillaries (167). Improved full scan spectra can also be obtained using a reduced elution speed method involving programmed changes in CE field strength (168). Obtaining full-scan spectra for fast or high-resolution separations will benefit from more sensitive ion trapping or array-based instrumentation, particularly used in conjunction with these new methods (167,168).

Capillary isotachopheresis or displacement electrophoresis is an attractive complement to CZE and has several advantages in combination with mass spectrometry (154,164). CITP is amenable to low-concentration samples, where the amount of solution is relatively large, whereas CZE is ideal for minute quantities of solution. Detection limits of approximately 10^{-11} M have been demonstrated by CITP/ESI–MS for quaternary phosphonium salts, and substantial improve-

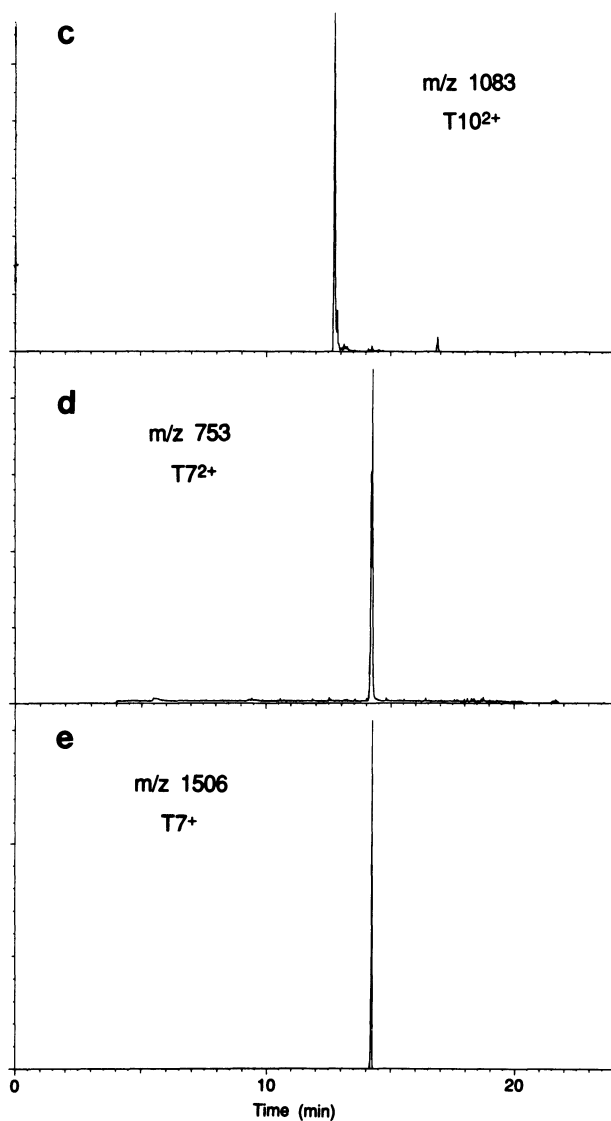


Figure 2.24. (Continued)

ments appear feasible (154). Sample sizes that can be amenable to CITP are also much greater (>100-fold) than for CZE because CITP results in the concentration of analyte bands, in contrast to the inherent dilution with CZE. Analytes elute in CITP as bands, where the length of the analyte band provides information regarding analyte concentration. Most importantly, however, CITP provides

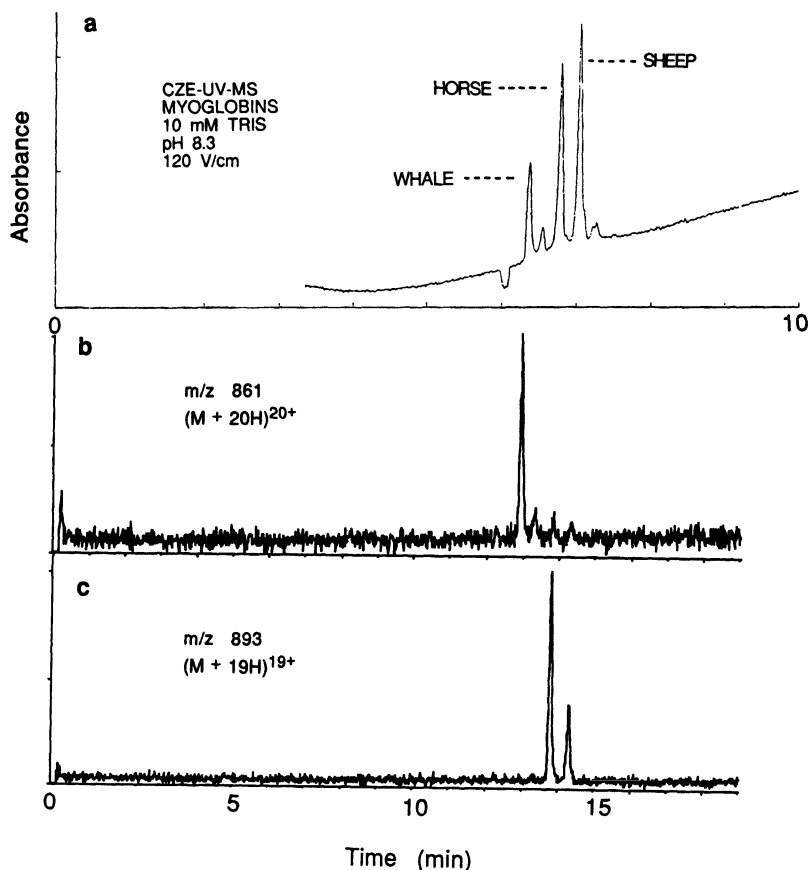


Figure 2.25. Ultraviolet (a) and single-ion electropherograms [for $m/z = 861$ (b) and $m/z 893$ (c)] for the CZE-MS separations of three myoglobins.

a relatively pure analyte band to the ESI source without the large concentration of a supporting electrolyte demanded by CZE. This latter characteristic circumvents the principal disadvantage of CZE/ESI-MS, the effect of supporting electrolyte constituents on ESI sensitivity. Thus, whereas the development of CITP separations is generally more difficult, and less guidance is currently available, CITP/MS has the potential of allowing much greater sensitivities (and analyte ion currents), facilitating combined MS/MS experiments. CITP in combination with CZE also has potential for sample concentration from larger sample injections.

6. CONCLUSIONS

With the emergence and rapid expansion of biochemical and biotechnology-related fields, improved analytical methodologies are becoming vital. Electrospray ionization–mass spectrometry has already been proved a sensitive analytical method for a variety of biomolecular classes and may offer a basis for rapid and efficient sequencing methods when combined with capillary electrophoresis and tandem mass spectrometry. The capability to examine various noncovalent associations by ESI will likely open broad new areas of application. Increasing interest in ESI–MS is reflected by the number of presentations at the annual American Society for Mass Spectrometry (ASMS) Conference. Eight papers were presented on the topic of ESI–MS (and ion spray–MS) at the Annual Conference in 1988. At the 1992 meeting, 228 contributions were presented involving ESI, many of which dealt with a variety of biochemical applications. Interfaces of ESI to other types of mass spectrometers, offering advantages over quadrupole instruments, are currently being developed. At this time, the most confident prediction is that the next few years will bring an improved level of understanding and a broader range and number of applications of ESI–MS.

SUMMARY

The application of electrospray ionization–mass spectrometry (ESI–MS) for the analysis of biomolecules, and particularly polypeptides and proteins, has been reviewed. ESI–MS has provided new capabilities by allowing molecular weight determination of proteins extending to over 100 kDa using methods largely adaptable to conventional mass spectrometers. The relationship between higher-order protein structure and the ESI distribution of molecular ion charge states has been discussed based on a wide range of recent experimental studies. Sequence information can be obtained from dissociation of multiply charged molecules, but interpretation becomes more difficult, and the extent of sequence information that can be obtained from conventional tandem mass spectrometric (MS/MS) methods decreases as molecular weight increases. However, it is possible to obtain structurally informative fragmentation from proteins extending to at least 66 kDa. A potentially important role for these methods may involve the rapid determination of changes or variation in protein structure (e.g., posttranslational modifications). Another attribute of ESI–MS is its ready interfacing with high-resolution “nanoscale” liquid chromatography and capillary electrophoresis separation methods. Recent progress in the development of such combined methods for application to proteins has been described.

ACKNOWLEDGMENTS. We thank the Director, Office of Health and Environmental Research, U.S. Department of Energy for support of this research through contract DE-AC06-76RLO 1830. Pacific Northwest Laboratory is operated by Battelle Memorial Institute. The authors thank C. J. Barinaga, R. R. Ogorzalek Loo, K. J. Light-Wahl, M. Busman, A. L. Rockwood, B. E. Winger, and H. R. Udseth for discussions and contributions to the work covered in this review.

REFERENCES

1. Bose, G. M., 1745, *Recherches sur la Cause et sur la Véritable Théorie de l'Électricité*, Wittenberg.
2. Zeleny, J., 1917, *Phys. Rev.* **10**:1-6.
3. Dole, M., Mack, L. L., Hines, R. L., Mobley, R. C., Ferguson, L. D., and Alice, M. B., 1968, *J. Chem. Phys.* **49**:2240-2249.
4. Mack, L. L., Kralik, P., Rheude, A., and Dole, M., 1970, *J. Chem. Phys.* **52**:4977-4986.
5. Chapman, S., 1937, *Phys. Rev.* **64**:184-190.
6. Clegg, G. A., and Dole, M., 1971, *Biopolymers* **10**:821-826.
7. Gieniec, J., Mack, L. L., Nakamae, K., Gupta, C., Kumar, V., and Dole, M., 1984, *Biomed. Mass Spectrom.* **11**:259-268.
8. Teer, C., and Dole, M., 1975, *J. Polymer Sci. Phys.* **13**:985.
9. Yamashita, M., and Fenn, J. B., 1984, *J. Phys. Chem.* **88**:4451-4459.
10. Aleksandrov, M. L., Gall, L. N., Krasnov, V. N., Nikolaev, V. I., Pavlenko, V. A., and Shkurov, V. A., 1984, *Dokl. Akad. Nauk SSSR* **277**:379-383.
11. Aleksandrov, M. L., Gall, L. N., Krasnov, V. N., Nikolaev, V. I., Pavlenko, V. A., Shkurov, V. A., Baram, G. I., Gracher, M. A., Knorre, V. D., and Kusner, Y. S., 1984, *Bioorg. Khim.* **10**:710-712.
12. Yamashita, M., and Fenn, J. B., 1984, *J. Phys. Chem.* **88**:4671-4675.
13. Aleksandrov, M. L., Besuklandnikov, P. V., Grachev, M. A., Elyakova, L. A., Zyyaginsteva, T. N., Kondratsev, V. M., Kusner, Y. S., Mirgorodskaya, O. A., and Fridlyansky, G. V., 1986, *Bioorg. Khim.* **12**:1689-1692.
14. Aleksandrov, M. L., Baram, G. I., Gall, L. N., Krasnov, N. V., Kusner, Y. S., Mirgorodskaya, O. A., Nikolaev, V. I., and Shkurov, V. A., 1985, *Bioorg. Khim.* **11**:700-705.
15. Aleksandrov, M. L., Baram, G. I., Gall, L. M., Grachev, M. A., Knorre, V. D., Krasnov, N. V., Kusner, Y. S., Mirgorodskaya, O. A., Nikolaev, V. I., and Shkurov, V. A., 1985, *Bioorg. Khim.* **11**:705-708.
16. Whitehouse, C. M., Dreyer, R. N., Yamashita, M., and Fenn, J. B., 1985, *Anal. Chem.* **57**:675-679.
17. Aleksandrov, M. L., Kondratsev, V. M., Kusner, Y. S., Mirgorodskaya, O. A., Podtelezhnikov, A. V., and Fridlyanskü, G. V., 1988, *Bioorg. Khim.* **14**:852-857.
18. Wong, S. F., Meng, C. K., and Fenn, J. B., 1988, *J. Phys. Chem.* **92**:546-550.
19. Meng, C. K., Mann, M., and Fenn, J. B., 1988, *Z. Phys. D.* **10**:361-368.
20. Loo, J. A., Udseth, H. R., and Smith, R. D., 1988, *Biomed. Environ. Mass Spectrom.* **17**:411-414.
21. Loo, J. A., Udseth, H. R., and Smith, R. D., 1988, *Rapid Commun. Mass Spectrom.* **2**:207-210.
22. Covey, T. R., Bonner, R. F., Shushan, B. I., and Henion, J. D., 1988, *Rapid Commun. Mass Spectrom.* **2**:249-256.

23. Karas, M., and Hillenkamp, F., 1988, *Anal. Chem.* **60**:2299–2301.
24. Smith, R. D., Barinaga, C. J., and Udseth, H. R., 1989, *J. Phys. Chem.* **93**:5019–5022.
25. Smith, R. D., and Barinaga, C. J., 1990, *Rapid Commun. Mass Spectrom.* **4**:54–57.
26. Smith, R. D., Barinaga, C. J., and Udseth, H. R., 1988, *Anal. Chem.* **60**:1948–1952.
27. Smith, R. D., Udseth, H. R., 1992, in *Capillary Electrophoresis* (N. A. Guzman, ed.), Marcel Dekker, New York.
28. Hail, M., Mylchreest, I., and Seta, K., 1991, in: *39th ASMS Conference on Mass Spectrometry and Allied Topics*, Nashville, American Society for Mass Spectrometry, East Lansing, MI.
29. Michelson, D., Shorey, J. D., Kiraoka, K., and Kudaka, I., 1990, *Rapid Commun. Mass Spectrom.* **4**:519–526.
30. Ikonomou, M. G., Blades, A. T., and Kebarle, P., 1991, in: *39th ASMS Conference on Mass Spectrometry and Allied Topics*, Nashville, American Society for Mass Spectrometry, East Lansing, MI.
31. Allen, M., and Lewis, I. A. S., 1991, *U.S. Patent 4,999,493*.
32. Lee, E. D., and Henion, J. D., 1988, in: *36th ASMS Conference on Mass Spectrometry and Allied Topics*, San Francisco, pp. 1308–1309, American Society for Mass Spectrometry, East Lansing, MI.
33. Bruins, A. P., Covey, T. R., and Henion, J. D., 1987, *Anal. Chem.* **59**:2642–2646.
34. Fenn, J. B., Mann, M., Meng, C. K., Wong, S. F., and Whitehouse, C. M., 1990, *Mass Spectrom. Rev.* **9**:37–70.
35. Shen, S., Nohmi, T., and Fenn, J. B., 1991, in: *39th ASMS Conference on Mass Spectrometry and Allied Topics*, Nashville, American Society for Mass Spectrometry, East Lansing, MI.
36. Vestal, M. L., and Allen, M. H., 1991, in: *39th ASMS Conference on Mass Spectrometry and Allied Topics*, Nashville, American Society for Mass Spectrometry, East Lansing, MI.
37. Smith, R. D., Loo, J. A., Edmonds, C. G., Barinaga, C. J., and Udseth, H. R., 1990, *Anal. Chem.* **62**:882–898.
38. Chowdhury, S. K., Katta, V., and Chait, B. T., 1990, *Rapid Commun. Mass Spectrom.* **4**:81–87.
39. Ogorzalek Loo, R. R., Loo, J. A., Udseth, H. R., Fulton, J. L., and Smith, R. D., 1992, *Rapid Commun. Mass Spectrom.* **6**:159–165.
40. Rockwood, A. L., Busman, M., and Smith, R. D., 1992, *J. Phys. Chem.* **96**:2397–2400.
41. Meng, C. K., McEwen, C. N., and Larsen, B. S., 1990, *Rapid Commun. Mass Spectrom.* **4**:147–150.
42. Meng, C. K., McEwen, C. N., and Larsen, B. S., 1990, *Rapid Commun. Mass Spectrom.* **4**:151–155.
43. Meng, C. K., McEwen, C. N., Larsen, B. S., Whitehouse, C. M., and Fenn, J. B., 1990, in: *Biological Mass Spectrometry* (Burlingame, A. L., McCloskey, J. A., eds.), Elsevier, New York, p. 147.
44. Larsen, B. S., and McEwen, C. N., 1991, *J. Am. Soc. Mass Spectrom.* **2**:205–211.
45. Lee, E. D., Shumate, B., Radolovich, G., Clench, M., and Lewis, C., 1990, in: *38th ASMS Conference on Mass Spectrometry*, Tucson, American Society for Mass Spectrometry, East Lansing, MI.
46. Clench, M., Lewis, C., Lee, E., Radolovich, G., and Shumate, C., 1990, in: *38th ASMS Conference on Mass Spectrometry*, Tucson, American Society for Mass Spectrometry, East Lansing, MI.
47. Dobberstein, P., Giessmann, U., and Schroeder, E., 1991, in: *39th ASMS Conference on Mass Spectrometry and Allied Topics*, Nashville, American Society for Mass Spectrometry, East Lansing, MI.
48. Bateman, R. H., Major, H. J., and Woolfitt, A. R., 1991, in: *39th ASMS Conference on Mass Spectrometry and Allied Topics*, Nashville, American Society for Mass Spectrometry, East Lansing, MI.

49. Gallagher, R. T., Chapman, J. R., and Mann, M., 1990, *Rapid Commun. Mass Spectrom.* **4**:369–372.
50. Musselman, B., Tamura, J., Cody, R. B., and Kassel, D. B., 1991, in: *39th ASMS Conference on Mass Spectrometry and Allied Topics*, Nashville, American Society for Mass Spectrometry, East Lansing, MI.
51. Kassel, D. B., Cody, R. B., and Musselman, B. D., 1991, in: *39th ASMS Conference on Mass Spectrometry and Allied Topics*, Nashville, American Society for Mass Spectrometry, East Lansing, MI.
52. Boyle, J. G., Whitehouse, C. M., and Fenn, J. B., 1991, *Rapid Commun. Mass Spectrom.* **5**:400–405.
53. Van Berkel, G. J., Glish, G. L., and McLuckey, S. A., 1990, *Anal. Chem.* **62**:1284–1295.
54. McLuckey, S. A., Van Berkel, G. J., Glish, G. L., Huang, E. C., and Henion, J. D., 1991, *Anal. Chem.* **63**:375–383.
55. Schwartz, J. C., Syka, J. E. P., and Jardine, I., 1991, in: *39th Annual ASMS Conference on Mass Spectrometry and Allied Topics*, Nashville, American Society for Mass Spectrometry, East Lansing, MI.
56. Voyksner, R. D., and Lin, H. Y., 1991, in: *39th Annual ASMS Conference on Mass Spectrometry and Allied Topics*, Nashville, American Society for Mass Spectrometry, East Lansing, MI.
57. Voyksner, R. D., Lin, H. Y., and Pack, T., 1991, in: *39th Annual ASMS Conference on Mass Spectrometry and Allied Topics*, Nashville, American Society for Mass Spectrometry, East Lansing, MI.
58. Henry, K. D., Williams, E. R., Wang, B. H., McLafferty, F. W., Shabanowitz, J., and Hunt, D. F., 1989, *Proc. Natl. Acad. Sci. U.S.A.* **86**:9075–9078.
59. Henry, K. D., and McLafferty, F. W., 1990, *Org. Mass Spectrom.* **25**:490–492.
60. Henry, K. D., Quinn, J. P., and McLafferty, F. W., 1991, *J. Am. Chem. Soc.* **113**:5447–5449.
61. Hofstadler, S. A., and Laude, D. A., 1992, *Anal. Chem.* **64**:569–572.
62. Mann, M., Meng, C. K., and Fenn, J. B., 1989, *Anal. Chem.* **61**:1702–1708.
63. Feng, R., Konishi, Y., and Bell, A. W., 1991, *J. Am. Soc. Mass Spectrom.* **2**:387–401.
64. Loo, J. A., Edmonds, C. G., Udseth, H. R., and Smith, R. D., 1990, *Anal. Chem.* **62**:693–698.
65. Bojesen, G., 1987, *J. Am. Chem. Soc.* **109**:5557–5558.
66. Chait, B. T., Chowdhury, S. K., and Katta, V., 1991, in: *39th ASMS Conference on Mass Spectrometry and Allied Topics*, Nashville, American Society for Mass Spectrometry, East Lansing, MI.
67. Moore, W. T., Suter, M. J. F., and Caprioli, R. M., 1991, in: *39th ASMS Conference on Mass Spectrometry and Allied Topics*, Nashville, American Society for Mass Spectrometry, East Lansing, MI.
68. Katta, V., and Chait, B. T., 1991, *J. Am. Chem. Soc.* **113**:8534–8535.
69. Edmonds, C. G., Loo, J. A., Barinaga, C. J., Udseth, H. R., and Smith, R. D., 1989, *J. Chromatogr.* **474**:21–37.
70. Puett, D., 1973, *J. Biol. Chem.* **248**:4623–4634.
71. Loo, J. A., Ogorzalek Loo, R. R., Light, K. J., Edmonds, C. G., and Smith, R. D., 1992, *Anal. Chem.* **64**:81–88.
72. Peters, T, Jr., 1985, in: *Advances in Protein Chemistry*, Vol. 37 (Anfinsen, C. B., Edsall, J. T., and Richards, F. M., eds.), pp. 161–245. Academic Press, San Francisco.
73. Brown, W. M., Dziegielewska, K. M., Foreman, R. C., and Sanders, N. R., 1989, *Nucleic Acids Res.* **17**:10495.
74. Weinstock, J., and Baldwin, G. S., 1988, *Nucleic Acids Res.* **16**:9045.
75. Loo, J. A., Edmonds, C. G., and Smith, R. D., 1991, *Anal. Chem.* **63**:2488–2499.

76. Hirayama, K., Akashi, S., Furuya, M., and Fukuhara, K., 1990, *Biochem. Biophys. Res. Commun.* **173**:639–646.
77. Geisow, M. J., Green, B. N., and Hutton, T., 1991, in: *Techniques in Protein Chemistry II* (Villafranca, J. J., ed.), pp. 567–572. Academic Press, San Diego.
78. Briggs, J., and Panfili, P. R., 1991, *Anal. Chem.* **63**:850–859.
79. Garnick, R. L., Solli, N. J., and Papa, P. A., 1988, *Anal. Chem.* **60**:2546–2557.
80. Van Dorselaer, A., Bitsch, F., Green, B., Jarvis, S., Lepage, P., Bischoff, R., Kolbe, H. V. J., and Roitsch, C., 1990, *Biomed. Environ. Mass Spectrom.* **19**:692–704.
81. Witkowska, H. E., Green, B. N., and Smith, S., 1990, *J. Biol. Chem.* **265**:5662–5665.
82. Smith, J. B., Thevenon-Emeric, G., Smith, D. L., and Green, B., 1991, *Anal. Biochem.* **193**:118–124.
83. Smith, J. B., Miesbauer, L. R., Leeds, J., Smith, D. L., Loo, J. A., Smith, R. D., and Edmonds, C. G., 1991, *Int. J. Mass Spectrom. Ion Proc.* **111**:229–245.
84. Chowdhury, S. K., and Chait, B. T., 1990, *Biochem. Biophys. Res. Commun.* **173**:927–931.
85. Green, B. N., Oliver, R. W. A., Falick, A. M., Shackleton, C. H. L., Roitman, E., and Witkowska, H. E., 1990, in: *Biological Mass Spectrometry* (A. L. Burlingame and J. A. McCloskey, eds.), Elsevier, Amsterdam, pp. 129–146.
86. Shackleton, C. H. L., Falick, A. M., Green, B. N., and Witkowska, H. E., 1991, *J. Chromatogr.* **562**:175–190.
87. Light, K. J., Loo, J. A., Edmonds, C. G., Smith, R. D., Witkowska, H. E., and Shackleton, C. H. L., 1991, in: *39th ASMS Conference on Mass Spectrometry and Allied Topics*, Nashville, American Society for Mass Spectrometry, East Lansing, MI.
88. Spellman, M. W., 1990, *Anal. Chem.* **62**:1714–1722.
89. Burlingame, A. L., Millington, D. S., Norwood, D. L., and Russell, D. H., 1990, *Anal. Chem.* **62**:268R–303R.
90. Loo, J. A., Edmonds, C. G., Smith, R. D., Lacey, M. P., and Keough, T., 1990, *Biomed. Environ. Mass Spectrom.* **19**:286–294.
91. Hemling, M. E., Roberts, G. D., Johnson, W., Carr, S. A., and Covey, T. R., 1990, *Biomed. Environ. Mass Spectrom.* **19**:677–691.
92. Huddleston, M. J., Bean, M. F., Barr, J. R., and Carr, S. A., 1991, in: *39th ASMS Conference on Mass Spectrometry and Allied Topics*, Nashville, American Society for Mass Spectrometry, East Lansing, MI.
93. Conboy, J. J., and Henion, J. D., 1991, in: *39th ASMS Conference on Mass Spectrometry and Allied Topics*, Nashville, American Society for Mass Spectrometry, East Lansing, MI.
94. Gillice-Castro, B. L., Bourell, J. H., and Stults, J. T., 1991, in: *39th ASMS Conference on Mass Spectrometry and Allied Topics*, Nashville, American Society for Mass Spectrometry, East Lansing, MI.
95. Covey, T., and Shushan, B., 1990, in: *38th ASMS Conference on Mass Spectrometry and Allied Topics*, Tucson, American Society for Mass Spectrometry, East Lansing, MI.
96. Lisek, C., Kolodziej, D., Leimgruber, N., Toren, P., Hecht, R., Howard, S., Welply, J., and Allen, M., 1991, in: *39th ASMS Conference on Mass Spectrometry and Allied Topics*, Nashville, p. MP74.
97. Smith, R. D., Loo, J. A., Barinaga, C. J., Edmonds, C. G., and Udseth, H. R., 1990, *J. Am. Soc. Mass Spectrom.* **1**:53–65.
98. Creighton, T. E., 1984, *Proteins, Structures and Molecular Principles*, W. H. Freeman, New York.
99. Chowdhury, S. K., Katta, V., and Chait, B. T., 1990, *J. Am. Chem. Soc.* **112**:9012–9013.
100. Loo, J. A., Ogorzalek Loo, R. R., Udseth, H. R., Edmonds, C. G., and Smith, R. D., 1991, *Rapid Commun. Mass Spectrom.* **5**:101–105.
101. McDonald, C. C., Phillips, W. D., and Glickson, J. D., 1971, *J. Am. Chem. Soc.* **93**:235–246.

102. Feng, R., and Konishi, Y., 1991, in: *39th ASMS Conference on Mass Spectrometry and Allied Topics*, Nashville, American Society for Mass Spectrometry, East Lansing, MI.
103. Timasheff, S. N., 1970, *Acc. Chem. Res.* **3**:62.
104. Franks, R., and Eagland, D., 1975, *CRC Crit. Rev. Biochem.* **3**:165.
105. Vijay-Kumar, S., Bugg, C. E., and Cook, W. J., 1987, *J. Mol. Biol.* **194**:531–544.
106. Rechsteiner, M., ed., 1988, *Ubiquitin*, Plenum Press, New York.
107. Herskovits, T. T., Gadgebeku, B., and Jallet, H., 1970, *Biol. Chem.* **245**:2599.
108. Wilkinson, K. D., and Mayer, A. N., 1986, *Arch. Biochem. Biophys.* **250**:390–399.
109. Katta, V., Chait, B. T., 1991, *Rapid Commun. Mass Spectrom.* **5**:214–217.
110. DeMeys, P., Ciu, J. L., Shymko, R. M., Kaplan, B. E., Bell, G. I., Whittaker, R., 1990, *J. Mol. Endocrinol.* **4**:409–416.
111. Ganem, B., Li, Y.-T., and Henion, J. D., 1991, *J. Am. Chem. Soc.* **113**:6294.
112. Li, Y.-T., Ganem, B., and Henion, J., 1991, *J. Am. Chem. Soc.* **113**:7818–7819.
113. Sui, K. W. M., Gardner, G. J., and Berman, S. S., 1989, *Org. Mass Spectrom.* **24**:931–942.
114. Edlund, P. O., Lee, E. D., Henion, J. D., and Budde, W. L., 1989, *Biomed. Environ. Mass Spectrom.* **18**:233–240.
115. Covey, T. R., Bruins, A. P., and Henion, J. D., 1988, *Org. Mass Spectrom.* **23**:178–186.
116. McLuckey, S. A., Van Berkel, G. J., and Glish, G. L., 1991, *39th ASMS Conference on Mass Spectrometry and Allied Topics*, Nashville, American Society for Mass Spectrometry, East Lansing, MI.
117. Stults, J. T., and Marsters, J. C., 1991, in: *39th ASMS Conference on Mass Spectrometry and Allied Topics*, Nashville, American Society for Mass Spectrometry, East Lansing, MI.
118. Craig, A. G., Engstrom, A., Bennich, H., and Kamensky, I., 1987, in: *35th ASMS Conference on Mass Spectrometry and Allied Topics*, Denver, pp. 528–529, American Society for Mass Spectrometry, East Lansing, MI.
119. Lacey, M. P., and Keough, T., 1989, *Rapid Commun. Mass Spectrom.* **3**:323–328.
120. Zhao, S., Somayajula, K. V., Sharkey, A. G., Hercules, D. M., Hillenkamp, F., Karas, M., and Ingendoh, A., 1991, *Anal. Chem.* **63**:450–453.
121. Cantor, C. R., and Schimmel, P. R., 1980, *Biophysical Chemistry*, W. H. Freeman, San Francisco.
122. Barinaga, C. J., Edmonds, C. G., Udseth, H. R., and Smith, R. D., 1989, *Rapid Commun. Mass Spectrom.* **3**:160–164.
123. Roepstorff, P., and Fohlman, J., 1984, *Biomed. Mass Spectrom.* **11**:601.
124. Biemann, K., 1988, *Biomed. Environ. Mass Spectrom.* **16**:99–111.
125. Martin, S. A., and Biemann, K., 1987, *Int. J. Mass Spectrom. Ion Proc.* **78**:213–228.
126. Hunt, D. F., Yates, J. R. III, Shabanowitz, J., Winston, S., and Hauer, C. R., 1986, *Proc. Natl. Acad. Sci. U.S.A.* **83**:6233–6237.
127. Locke, M., and McIver, R. T., 1983, *J. Am. Chem. Soc.* **105**:4226–4232.
128. McLuckey, S. A., Glish, G. L., and Van Berkel, G. J., 1991, in: *39th ASMS Conference on Mass Spectrometry and Allied Topics*, Nashville, American Society for Mass Spectrometry, East Lansing, MI.
129. McLuckey, S. A., Glish, G. L., and Van Berkel, G. J., 1991, *Anal. Chem.* **63**:1971–1978.
130. McLuckey, S. A., Van Berkel, G. J., and Glish, G. L., 1990, *J. Am. Chem. Soc.* **112**:5668–5670.
131. McLuckey, S. A., Van Berkel, G. J., and Glish, G. L., 1990, *38th ASMS Conference on Mass Spectrometry and Allied Topics*, Tucson, pp. 1134–1135, American Society for Mass Spectrometry, East Lansing, MI.
132. Hartman, K. N., Lias, S., Ausloos, P., Rosenstock, N. M., Schroyer, S. S., Schmidt, C., Martinson, D., and Milne, G. W. A., 1979, *A Comparison of Gas Phase Basicity and Proton Affinity Measurements*, NBSIR 79-1777, National Bureau of Standards, Washington.

133. Smyth, D. G., Stein, W. H., and Moore, S., 1963, *J. Biol. Chem.* **238**:227.
134. Montelione, G. T., and Scheraga, H. A., 1989, *Acc. Chem. Res.* **22**:70.
135. Loo, J. A., Edmonds, C. G., and Smith, R. D., 1990, *Science* **248**:201–204.
136. Loo, J. A., Udseth, H. R., and Smith, R. D., 1989, *Anal. Biochem.* **179**:404–412.
137. Rockwood, A. L., Busman, M., and Smith, R. D., 1991, *Int. J. Mass Spectrom. Ion Proc.* **111**:103–129.
138. Biemann, K., and Scoble, H. A., 1987, *Science* **237**:992–998.
139. Dixon, J. W., and Sarkar, B., 1974, *J. Biol. Chem.* **249**:5872–5877.
140. Bunker, D. L., and Wang, F. M., 1977, *J. Am. Chem. Soc.* **99**:7457–7459.
141. Vötsch, W., Wagner, H. A., and Anderer, F. A., 1980, *Comp. Biochem. Physiol.* **66B**:87–91.
142. Jardine, I., Hail, M., Lewis, S., Zhou, J., Schwartz, J., and Whitehouse, C. M., 1990, in: *38th ASMS Conference on Mass Spectrometry and Allied Topics*, Tucson, pp. 16–17, American Society for Mass Spectrometry, East Lansing, MI.
143. Mann, M., 1990, *Org. Mass Spectrom.* **25**:575–587.
144. Ikononou, M. G., Blades, A. T., and Kebarle, P., 1990, *Anal. Chem.* **62**:957–967.
145. Raffaelli, A., and Bruins, A. P., 1991, *Rapid Commun. Mass Spectrom.* **6**:269–275.
146. Olivares, J. A., Nguyen, N. T., Yonker, C. R., and Smith, R. D., 1987, *Anal. Chem.* **59**:1230–1232.
147. Smith, R. D., Olivares, J. A., Nguyen, N. T., and Udseth, H. R., 1988, *Anal. Chem.* **60**:436–441.
148. Lee, E. D., Mück, W., Henion, J. D., and Covey, T. R., 1988, *J. Chromatogr.* **458**:313–321.
149. Lee, E. D., Mück, W., Henion, J. D., and Covey, T. R., 1989, *Biomed. Environ. Mass Spectrom.* **18**:253.
150. Covey, T. R., Huang, E. C., and Henion, J. D., 1991, *Anal. Chem.* **63**:1193–1200.
151. Huang, E. C., and Henion, J. D., 1991, *Anal. Chem.* **63**:732–739.
152. Hail, M., Lewis, S., Jardine, I., Liu, J., and Novotny, M., 1990, *J. Microcol. Sep.* **2**:285–292.
153. Hunt, D. F., Alexander, J. E., McCormack, A. L., Martino, P. A., Michel, H., Shabanowitz, J., Sherman, N., Moseley, M. A., Jorgenson, J. W., and Tomer, K. B., 1991, in: *Techniques in Protein Chemistry II* (J. J. Villafranca, ed.), Academic Press, San Diego, pp. 441–454.
154. Udseth, H. R., Loo, J. A., and Smith, R. D., 1989, *Anal. Chem.* **61**:228–232.
155. Smith, R. D., Fields, S. M., Loo, J. A., Barinaga, C. J., Udseth, H. R., and Edmonds, C. G., 1990, *Electrophoresis* **11**:709–716.
156. Edmonds, C. G., Loo, J. A., Fields, S. M., Barinaga, C. J., Udseth, H. R., and Smith, R. D., 1990, in: *Biological Mass Spectrometry* (A. L. Burlingame and J. A. McCloskey, eds.), Elsevier, Amsterdam, p. 77.
157. Hail, M., Schwartz, J., Mylchreest, I., Seta, K., Lewis, S., Zhou, J., Jardine, I., Liu, J., and Novotny, M., 1990, in: *38th ASMS Conference on Mass Spectrometry and Allied Topics*, Tucson, p. 353, American Society for Mass Spectrometry, East Lansing, MI.
158. Moseley, M. A., Deterding, L. J., Tomer, K. B., and Jorgenson, J. W., 1991, *Anal. Chem.* **63**:109.
159. Lee, E. D., Mück, W., Henion, J. D., and Covey, T. R., 1989, *Biomed. Environ. Mass Spectrom.* **18**:253–257.
160. Moseley, M. A., Deterding, L. J., Tomer, K. B., and Jorgenson, J. W., 1989, *J. Chromatogr.* **480**:197–206.
161. Caprioli, R. M., Moore, W. T., Martin, M., DaGue, B. B., Wilson, K., and Moring, S., 1989, *J. Chromatogr.* **480**:247–257.
162. Reinhoud, N. J., Schroder, E., Tjaden, U. R., Niessen, W. M. A., Ten Noever de Brauw, M. C., and Van der Greef, J., 1990, *J. Chromatogr.* **516**:147–155.
163. Moseley, M. A., Deterding, L. J., Tomer, K. B., and Jorgenson, J. W., 1990, *J. Chromatogr.* **516**:167–173.

164. Smith, R. D., Loo, J. A., Barinaga, C. J., Edmonds, C. G., and Udseth, H. R., 1989, *J. Chromatogr.* **480**:211–232.
165. Smith, R. D., Loo, J. A., Edmonds, C. G., Barinaga, C. J., and Udseth, H. R., 1990, *J. Chromatogr.* **516**:157–165.
166. Loo, J. A., Jones, H. K., Edmonds, C. G., Udseth, H. R., and Smith, R. D., 1989, *J. Microcol. Sep.* **1**:223–229.
167. Wahl, J., Udseth, H. R., and Smith, R. D., *Anal. Chem.* Submitted.
168. Goodlett, D. R., Wahl, J., Udseth, H. R., Smith, R. D., *Anal. Chem.* Submitted.

The Analysis of Muscle Relaxants by Mass Spectrometric Methods

Diane Rindgen and Paul Vouros

1. INTRODUCTION

The introduction of curare in 1942 (1) generated a great interest in the chemistry and pharmacology of a class of compounds known as neuromuscular blocking agents. Curare, a generic term for several South American arrow poisons, has enjoyed a long and romantic history (2). It has been used for many years by the Indians living in the regions surrounding the Amazon and Orinoco Rivers for killing wild animals for food. Only tribal witch doctors possessed the knowledge of the preparation of curare. Following the discovery of the American continent, early explorers became interested in this compound and brought samples of the native preparations to Europe for evaluation.

The related compounds in use today act by interfering with the transmission of nerve impulses at the skeletal neuromuscular junction and are used in the operating room and intensive care units as an adjunct to anesthesia to induce muscle relaxation and to facilitate mechanical ventilation. Neuromuscular blocking agents are subdivided based on their mechanism of action. The competitive or stabilizing agents include *d*-tubocurarine, the active constituent of curare, and the synthetic derivatives pancuronium and vecuronium. Succinylcholine and decamethonium are examples of depolarizing agents. Structural differences exist between the two classes of compounds. The competitive agents are generally

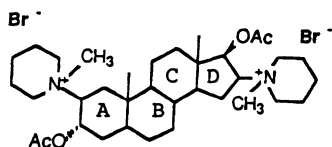
Diane Rindgen and Paul Vouros • Department of Chemistry and The Barnett Institute of Chemical Analysis and Materials Science, Northeastern University, Boston, Massachusetts 02115.

bulky, rigid molecules, whereas the depolarizing compounds exhibit a more flexible structure allowing for free bond rotation. Neuromuscular blocking agents act on the acetylcholine receptors of skeletal muscle cells. The mechanism of action is determined by the characteristic structural features of each. In general, many of the synthetic neuromuscular blocking agents mimic the structural features of the transmitter acetylcholine in that they contain at least two sites of potential positive charge (quaternary nitrogen atoms) separated by a lipophilic bridging structure. These structural characteristics are thought to be the principal reason for the binding of these drugs to cholinergic receptors (3).

The nicotinic acetylcholine receptors of skeletal muscle cells are transmitter-gated ion channels. The acetylcholine receptor is a glycoprotein consisting of five transmembrane polypeptides that define an internally located channel (4). Binding sites for acetylcholine are located on two identical subunits. Following nerve stimulation, acetylcholine is released into the synaptic cleft. The neurotransmitter binds to the pentameric receptor, inducing a conformational change that opens the ion channel. This action results in a large influx of sodium ions, causing a membrane depolarization that leads to muscle contraction. The competitive neuromuscular blocking agents interrupt the neurotransmitter action of acetylcholine by binding at the cholinergic receptor sites. The mechanism of action of the depolarizing agents is different. Initially, these muscle relaxants mimic the action of acetylcholine by opening ion channels, causing membrane depolarization. However, the duration of depolarization is longer because of the persistence of these agents at the neuromuscular junction. This process is followed by a block of neuromuscular transmission and paralysis (2).

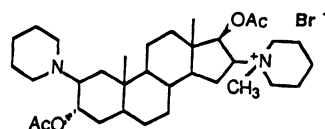
Pancuronium bromide ($3\alpha,17\beta$ -diacetoxy- $2\beta,16\beta$ -dipiperidino- 5α -androstande dimethobromide) (Fig. 3.1, structure **I**) is one of a series of neuromuscular blocking agents in current clinical use. This compound is a bisquaternary ammonium steroid synthesized in 1964 (5). It possesses five times the potency of *d*-tubocurarine and has fewer side effects (6). Vecuronium bromide (Fig. 3.1, structure **II**) is the monoquaternary analogue of pancuronium with a potency equal to or slightly greater than that of pancuronium (7). Pancuronium and vecuronium are both metabolized in the body. Approximately 5 to 25% of an injected dose of pancuronium is deacetylated to the 3-hydroxy, 17-hydroxy, or 3,17-dihydroxy derivative (8). The 3-hydroxy derivative is the most abundant and the most potent of the metabolites. Metocurine iodide (dimethyl-*d*-tubocurarine) (Fig. 3.1, structure **III**), a nonsteroidal blocking agent, is a synthetic derivative of *d*-tubocurarine that is three times as potent in man (2).

Pharmacokinetic studies of neuromuscular blocking agents necessitate the development of accurate, reliable, sensitive, and selective assays. The action of these compounds can be affected by certain disease states and concurrent drug therapy. For example, the anticonvulsant drugs phenytoin and carbamazepine can



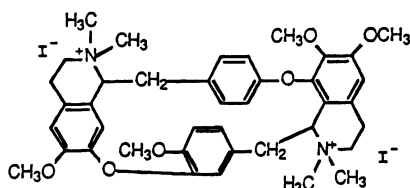
Pancuronium bromide

I



Vecuronium bromide

II



Metocurine iodide

III

Figure 3.1. Structures of pancuronium bromide (I), vecuronium bromide (II), and metocurine iodide (III).

induce liver drug-metabolizing enzymes and alter the effects of the neuromuscular junction (9,10). Resistance to the neuromuscular effects of these compounds has also been demonstrated (11). Quantitative analytical assays capable of detecting parent compounds and metabolites are necessary to characterize the variable responses to these compounds in the clinical setting. The analysis of neuromuscular blocking agents poses a challenge in part because of the polar, nonvolatile nature of the compounds coupled with the lack of chromophoric groups for spectroscopic detection in the case of the steroidal muscle relaxants. The nonsteroidal compounds, however, contain chromophoric moieties, making the use of spectroscopic techniques a viable alternative for their detection.

Limitations exist with much of the current methodology used for the analysis of neuromuscular blocking agents. For example, assays that lack selectivity cannot differentiate between parent compounds and metabolites. These compounds are typically present at low nanogram levels in biological fluids, and

these levels may be further reduced in the presence of other exogenous compounds. Thus, a clear need exists for accurate and sensitive assays. Analytical methods based on mass spectrometry offer the necessary selectivity and sensitivity for the evaluation of neuromuscular blocking agents. Utilization of different ionization modes together with tandem mass spectrometry can provide powerful approaches for the evaluation of the pharmacokinetic properties of these compounds. Such techniques are discussed in the following sections.

2. CHEMICAL ANALYSIS

2.1. Other Analytical Techniques

2.1.1. Steroidal Compounds

A number of analytical assays have been developed over the years for the analysis of the steroidal muscle relaxants, but, for the most part, they suffer from a lack of sensitivity and/or specificity. The original assay for steroidal neuromuscular blocking agents consisted of a fluorometric analysis of their complexes with rose bengal (12–15). These analyses, however, were nonspecific because the complex formed with rose bengal did not differentiate between the parent and all its metabolites. For vecuronium bromide and its metabolites, a normal-phase HPLC assay was developed. Separation was achieved with a mixture of methanol, aqueous ammonia, and ammonium chloride as the eluent (16). With UV detection at 215 nm, detection limits of 50 ng/ml in plasma could be achieved. This assay could not be readily adapted to the more polar bisquaternary compounds because the required modifications of the mobile phase increased the base-line absorbance beyond a usable level.

An assay for steroidal neuromuscular blocking agents using ion-pair extraction and gas chromatography (GC) with nitrogen-sensitive detection was recently developed by Furuta *et al.* (17). Deacetylated metabolites were determined by chemical derivatization designed to increase the volatility of the metabolites. The salts undergo thermal dealkylation in the injection port of the GC, and, as a result, compounds with identical demethylation products such as pancuronium and vecuronium or related metabolites could not be distinguished. For example, Segredo *et al.* (18) reported on the occurrence of a prolonged neuromuscular blockade after the termination of long-term administration of vecuronium. The observed condition was attributed to the accumulation of the active metabolite, 3-deacetylvecuronium. The specificity of the analytical method was questioned in a subsequent editorial letter (19), and in a reply (20), the original authors acknowledged the advantages of a mass spectrometric detector for identification of the metabolite and confirmed its identity by GC/MS.

2.1.2. Nonsteroidal Compounds

Development of high-performance liquid chromatography (HPLC) assays for the benzylisoquinoline neuromuscular blocking agents, i.e., *d*-tubocurarine and metocurine, was prompted by the poor specificity of the previously used radioimmunoassay methods, which could not distinguish between parent drug and metabolites (21). *d*-Tubocurarine and related metabolites were separated by reversed-phase ion-pair chromatography with isocratic elution using water-methanol-dibutylamine phosphate as the mobile phase (22). This method was used to study benzylisoquinoline neuromuscular blocking agents in biological fluids, including the pharmacokinetics of metocurine in phenytoin-treated rabbits. The average clearance in the phenytoin group was significantly higher compared to the controls (2.26 ± 0.48 versus 1.69 ± 0.31 liters/min per kg) (J. A. J. Martyn, unpublished data). The half-lives were 83 ± 22 min and 100 ± 17 min, respectively (J. A. J. Martyn, unpublished data). These preliminary data suggest that the pharmacokinetic parameters are enhanced in the phenytoin group even for a drug with minimal hepatic clearance.

Preliminary evidence on the metabolism of *d*-tubocurarine and metocurine has been obtained using the abovementioned HPLC assay. Following catheterization of the bile duct of the rabbit, bile was sampled before and for 6 hr after the intravenous dose (0.5 mg/kg) of *d*-tubocurarine. Figure 3.2 shows three chromatograms. The bottom trace (a) shows passage of the mobile phase only (retention time 2.5 min) through the HPLC column. The middle trace (b) is a chromatogram of bile (retention time 3.5 min) collected 5 min after intravenous injection of *d*-tubocurarine. No *d*-tubocurarine (retention time 8 min) was detected in that sample. Trace c shows the appearance of *d*-tubocurarine in the bile and a new peak, a possible metabolite (retention time 4.0 min), appearing 30 min following the intravenous *d*-tubocurarine dose. This metabolite persisted in the bile until the end of the sampling period. Metocurine, used as the internal standard, appeared at 10 min in traces b and c (J. A. J. Martyn, unpublished data).

2.2. Mass Spectrometric Techniques

2.2.1. Fundamental Ion Chemistry of Neuromuscular Blocking Agents

2.2.1a. *Chemical Ionization.* Baker *et al.* (23,24) have conducted a detailed study of the mass spectrometric properties of many of the relevant neuromuscular blocking agents, and information relating structural features to fragmentation patterns has been generated. Chemical ionization (CI) and fast atom bombardment (FAB) have been evaluated. The CI mass spectra of pancuronium bromide and vecuronium bromide are shown in Fig. 3.3 along with the

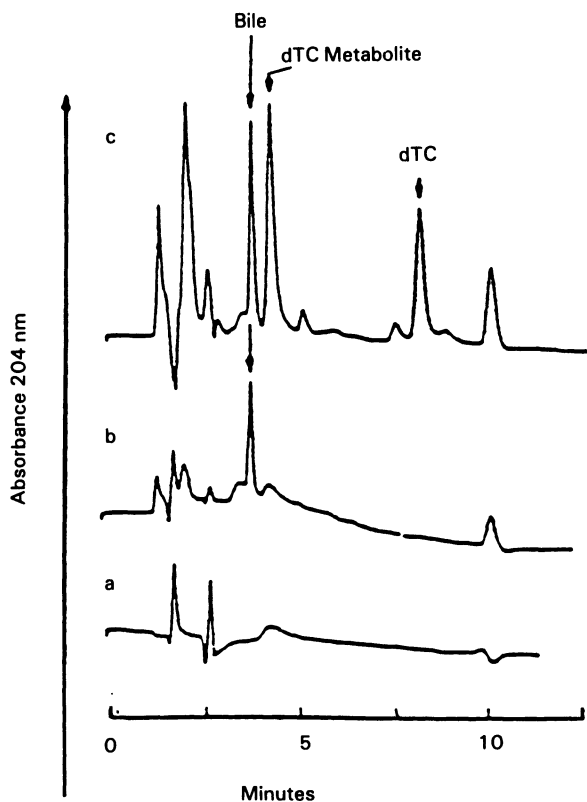


Figure 3.2. Chromatogram of *d*-tubocurarine and possible metabolite. See text for explanation.

isotopically labeled [$^2\text{H}_3$]3-acetyl analogue of pancuronium and the [$^2\text{H}_3$]17-acetyl analogue of vecuronium (23). Pancuronium and vecuronium undergo thermal dealkylation as mentioned previously, followed by protonation to yield identical molecular species with identical CI mass spectra. In general, fragmentation is a result of eliminations associated with the acetyl or piperidyl groups. The CI fragmentations are summarized in Fig. 3.4 and are confirmed by metastable transitions (magnetic/electric, *B/E*, linked scans) as indicated (23). It should be noted that the structures in Fig. 3.4 are drawn to indicate the position(s) of cleavage and are not necessarily the most stable forms of the ion. Initial elimination of acetic acid occurs from the 3 position to produce the ion of m/z 483. The initial loss of acetic acid from the A ring is also confirmed by the appearance of the m/z 486 peak in the spectrum of the [$^2\text{H}_3$]17-acetyl vecuronium analogue (Fig. 3.3d). Additional fragmentations initiated from the CI protonation of the A ring are shown in Fig. 3.4.

The stereochemical orientation of the piperidyl and acetyl groups with respect to one another on the A and D rings provides a basis for understanding the strong preference for fragmentation from groups positioned on the A ring. The two groups are located *cis* to each other on the D ring, and this feature leads to formation of a hydrogen bridge between the two functionalities following protonation (Fig. 3.5) (23). This ion is quite stable. In contrast, the 2 β -piperidyl and 3 α -acetyl groups on the A ring are *trans* and relatively far apart from each other. Protonation results in a quaternary ammonium or oxonium ion that can be eliminated as shown in Fig. 3.5. This rationale is consistent with that proposed by Longevialle *et al.* (25) to explain the tendency for H₂O elimination from steroidal amino alcohols during CI. McCloskey (26,27) and Weinkam (28) have also observed functional group interactions that allow proton sharing during CI. Fragmentations originating from D ring protonation are shown in Fig. 3.6 (23). Unique to this sequence is the loss of methane observed from *m/z* 483, generating the ion of *m/z* 467. This decomposition presumably results from loss of the 18-angular methyl group along with an adjacent hydrogen.

A fragmentation process involving the apparent concerted loss of dehydropiperidine and acetic acid from the A ring is indicated in the B/E linked-scan experiments. The normal spectrum of [²H₃]3-acetylpancuronium bromide (Fig. 3.3c) shows ions resulting from the same process, which appears to be a remote-charge-site-directed dissociative event. A proposed mechanism is shown in Fig. 3.7 (23), involving a six-membered molecular rearrangement. This mechanism is consistent with molecular models, which show that a hydrogen located α to the piperidyl nitrogen can approach within bonding distance to the ester oxygen when ring A is in the boat conformation. The subsequent loss of the second acetic acid molecule produces the ion of *m/z* 340.

The principal metabolic pathway for these compounds is deacetylation at the 3 and 17 positions (8). The CI spectra of 3-deacetyl and 17-deacetylvecuronium bromide have been obtained (Fig. 3.8) (23). The fragmentation patterns generally follow those of the acetylated compounds. Thermal elimination of methylbromide is followed by successive losses of water, acetic acid, and piperidine.

The CI fragmentation behavior of pipecuronium bromide has also been investigated (Fig. 3.9a) (24). Pipecuronium bromide is a bisquaternary ammonium steroid like its dipiperidino analogue pancuronium. Pipecuronium generates a methane CI spectrum with a base peak at *m/z* 573, which results from thermal dealkylation followed by protonation. A B/E linked-scan analysis of this ion produces several product ions; the most prominent is *m/z* 513 (Fig. 3.9b). This ion corresponds to the loss of acetic acid analogous to that observed with pancuronium bromide. The proposed fragmentation mechanism for the *m/z* 573 \rightarrow *m/z* 415 transition involves the simultaneous elimination of dehydropiperazine from the 2 position and acetic acid from the 3 position. This six-membered ring rearrangement has been suggested for pancuronium (23).

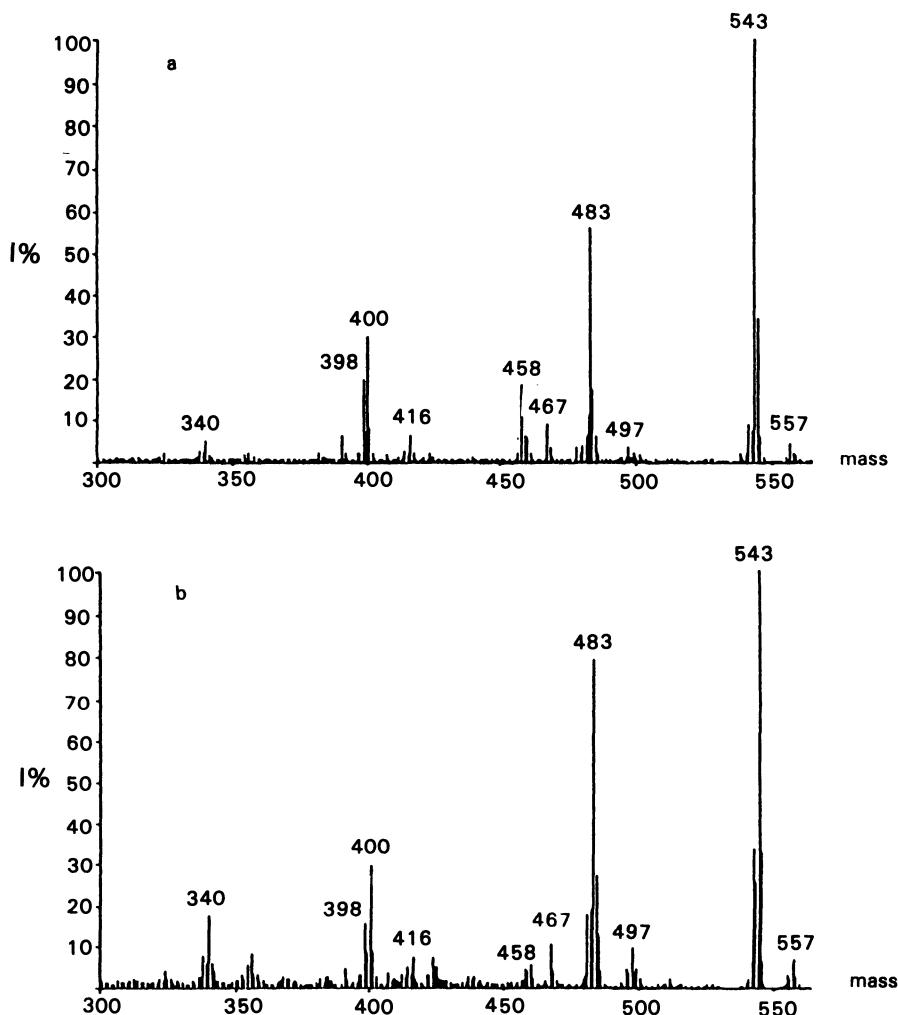


Figure 3.3. Methane chemical ionization (CI) spectra of (a) pancuronium bromide, (b) vecuronium bromide.

The CI mass spectrometric properties of several of the nonsteroidal neuromuscular blocking agents have also been investigated. Unlike the steroidal neuromuscular blocking agents, metocurine has a strong chromophore in the UV spectrum, which facilitates its analysis by conventional HPLC, as previously indicated. Mass spectrometry can, however, play a key role in identifying metabolites or characterizing the structures of unknown byproducts of the drug. Linked-scan MS in the *B/E* mode provides a suitable approach for this purpose.

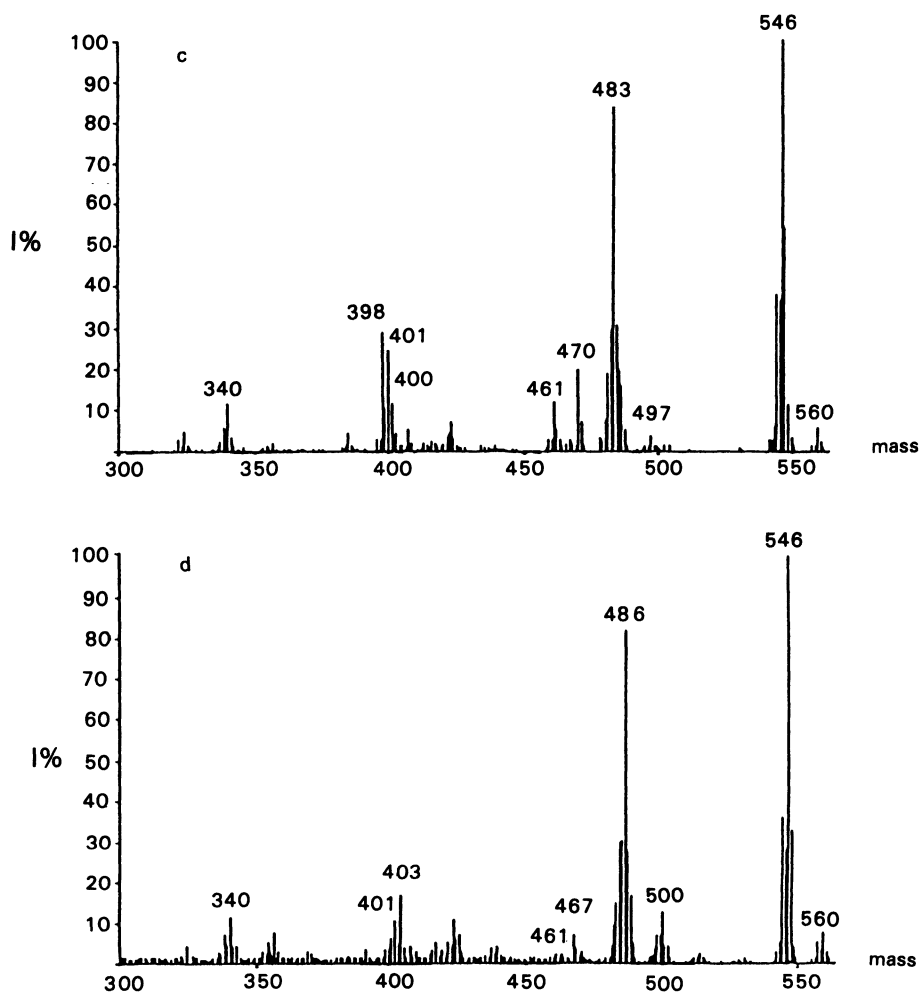


Figure 3.3. (Continued) (c) $[^2\text{H}_3]3\text{-acetylpancuronium}$, and (d) $[^2\text{H}_3]17\text{-acetylvecuronium}$ obtained from the moving-belt interface. [From Baker *et al.* (23). Copyright 1989 John Wiley & Sons, Ltd. Reprinted with permission.]

For example, the conventional CI mass spectrum of metocurine iodide (Fig. 3.10a) (24) shows little more than the peak at m/z 623, which corresponds to the protonated free base produced from the thermal dealkylation of the salt. On the other hand, a host of fragment ions derived directly from the m/z 623 becomes prominent in the linked-scan spectrum (Fig. 3.10b). The m/z 312 ion is interesting from the standpoint of fragmentation processes. A proposed fragmentation mechanism is indicated in Fig. 3.11 (24). Cleavage of the benzyl bonds produces

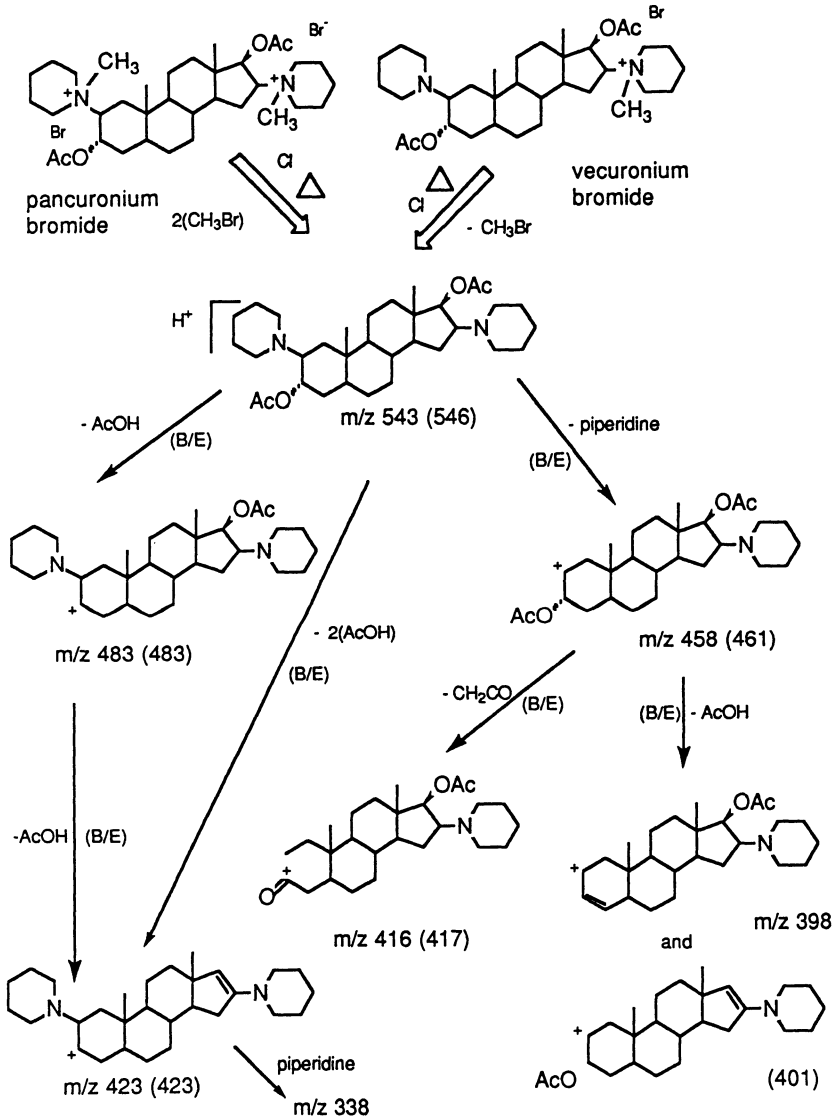


Figure 3.4. Methane chemical ionization fragmentation mechanism based on protonation of the A ring. Corresponding mass of $[\text{}^2\text{H}_3]\text{3-acetylpancuronium}$ in parentheses. [From Baker *et al.* (23). Copyright 1989 John Wiley & Sons, Ltd. Reprinted with permission.]

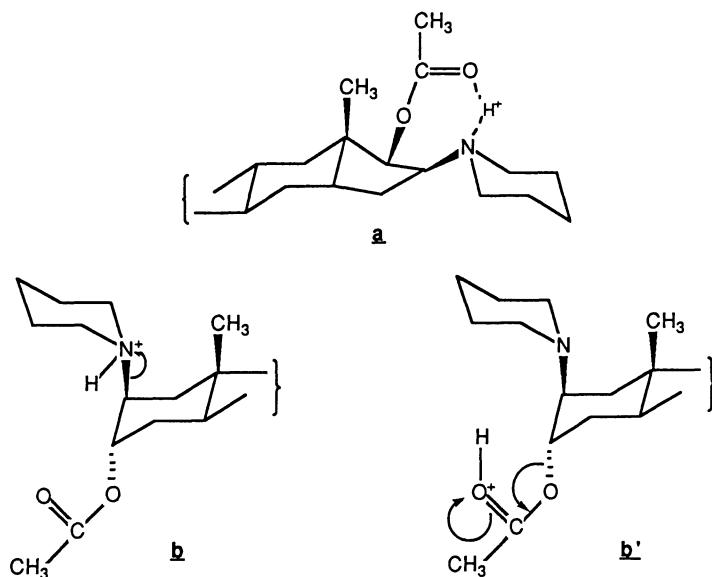


Figure 3.5. Positions of hydrogen attachment on dealkylated pancuronium based on the orientations of the piperidyl and acetyl groups on the D ring (a) and A ring (b, b'). [From Baker *et al.* (23). Copyright 1989 John Wiley & Sons, Ltd. Reprinted with permission.]

two isobaric fragments of mass 311 Da. Each of these fragments may cyclize to form a neutral or an m/z 312 ion, depending on which fragment retains the proton.

Atracurium besylate (Fig. 3.12a) (24) is a neuromuscular blocking agent of intermediate duration that is also in clinical use (10). The CI mass spectrum of this compound shows a base peak at m/z 358 (Fig. 3.12b). Loss of the counterions and the chain connecting the two ring systems followed by protonation results in the formation of this ion. The linked-scan (B/E) spectrum of m/z 358 is shown in Fig. 3.12c. Fragmentation of this ion produces m/z 327, which is formed by loss of a methoxy group (31 Da), and the ion of m/z 206 (Fig. 3.13). The m/z 213 ion (Fig. 3.12b) is believed to result from fragmentation of the other product of thermal decomposition, namely, the two besylates connected by the aliphatic chain.

2.2.1b. Fast Atom Bombardment. The FAB properties of pancuronium and vecuronium bromide have also been investigated (23). Figure 3.14 (23) shows the FAB spectra for both compounds and the labeled analogues, [²H₃]3-acetylpancuronium and [²H₃]17-acetylvecuronium. An initial loss of halide is observed, resulting in an ion of highest mass m/z 651 for pancuronium and m/z 557

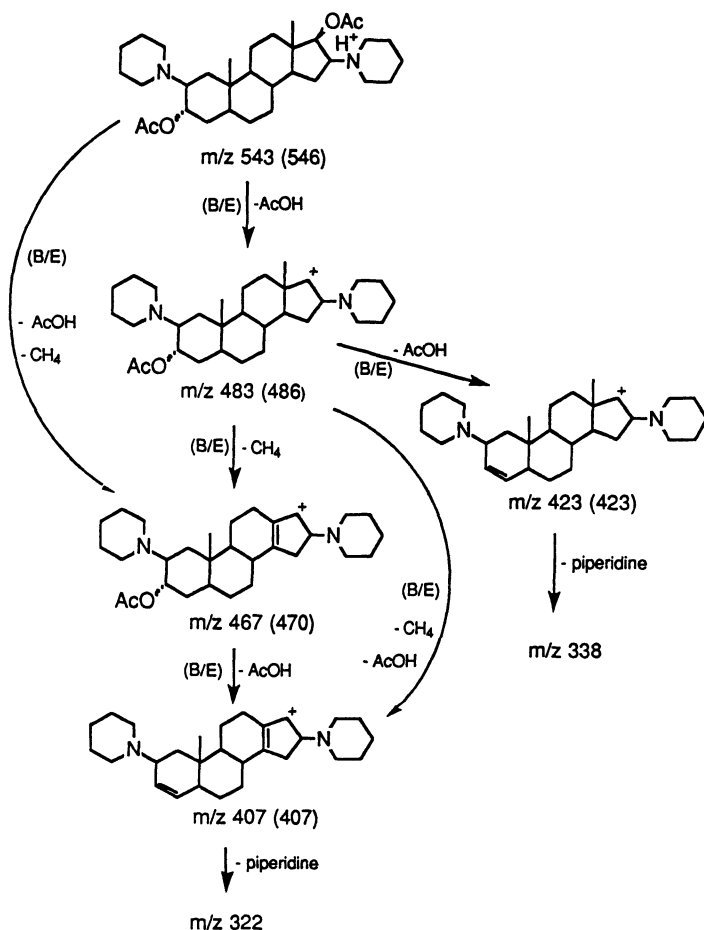


Figure 3.6. Chemical ionization (CH₄) fragmentations initiated by D ring protonation. Corresponding mass of [2H₃]3-acetylpancuronium in parentheses. [From Baker *et al.* (23). Copyright 1989 John Wiley & Sons, Ltd. Reprinted with permission.]

for vecuronium. The *m/z* 651 ion of pancuronium undergoes subsequent loss of methylbromide to yield *m/z* 557. Linked-scan (B/E) data confirm the relationship between *m/z* 651, 557, and the base peak *m/z* 472 in the pancuronium spectrum (Fig. 3.15) (23). These unique metastable transitions can be used to differentiate pancuronium in the presence of vecuronium. The origin of the initial bromide loss, A versus D ring, was determined by obtaining the FAB spectrum of [2-N-C²H₃]piperidylpancuronium. The spectrum of this compound reveals an

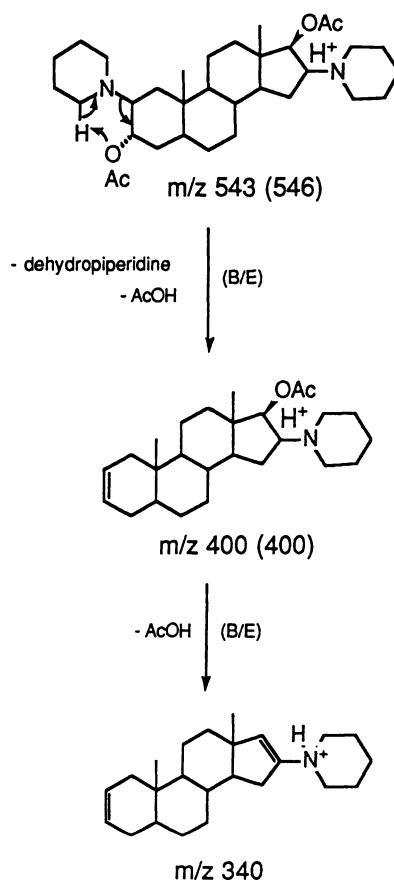


Figure 3.7. Mechanism for concerted elimination of 2 β -piperidyl and 3 α -acetyl observed for pancuronium and vecuronium under chemical ionization (CH_4) conditions. Corresponding mass of [$^2\text{H}_3$]3-acetylpancuronium in parentheses. [From Baker *et al.* (23). Copyright 1989 John Wiley & Sons, Ltd. Reprinted with permission.]

initial loss of bromide to produce the ion of m/z 702 (Fig. 3.16) (23). This process results in a stable quaternary ammonium ion bearing an N-methylpiperidine on the D ring. Loss of $\text{C}^2\text{H}_3\text{I}$ from the A ring yields m/z 557.

The formation of m/z 414 from m/z 557 proceeds via two routes. One route involves the concerted elimination of dehydropiperidine and acetic acid, which is analogous to the combined loss of 143 Da observed under CI conditions (Fig. 3.7) (23). The second pathway involves elimination of piperidine followed by loss of 58 Da. Analysis of the spectrum of 3-deuterioacetylpancuronium bromide indicates that this loss involves the methyl group of the 3-acetyl function. Therefore, this fragmentation event probably involves the loss of CH_3COCH_3 via some extensive rearrangement process.

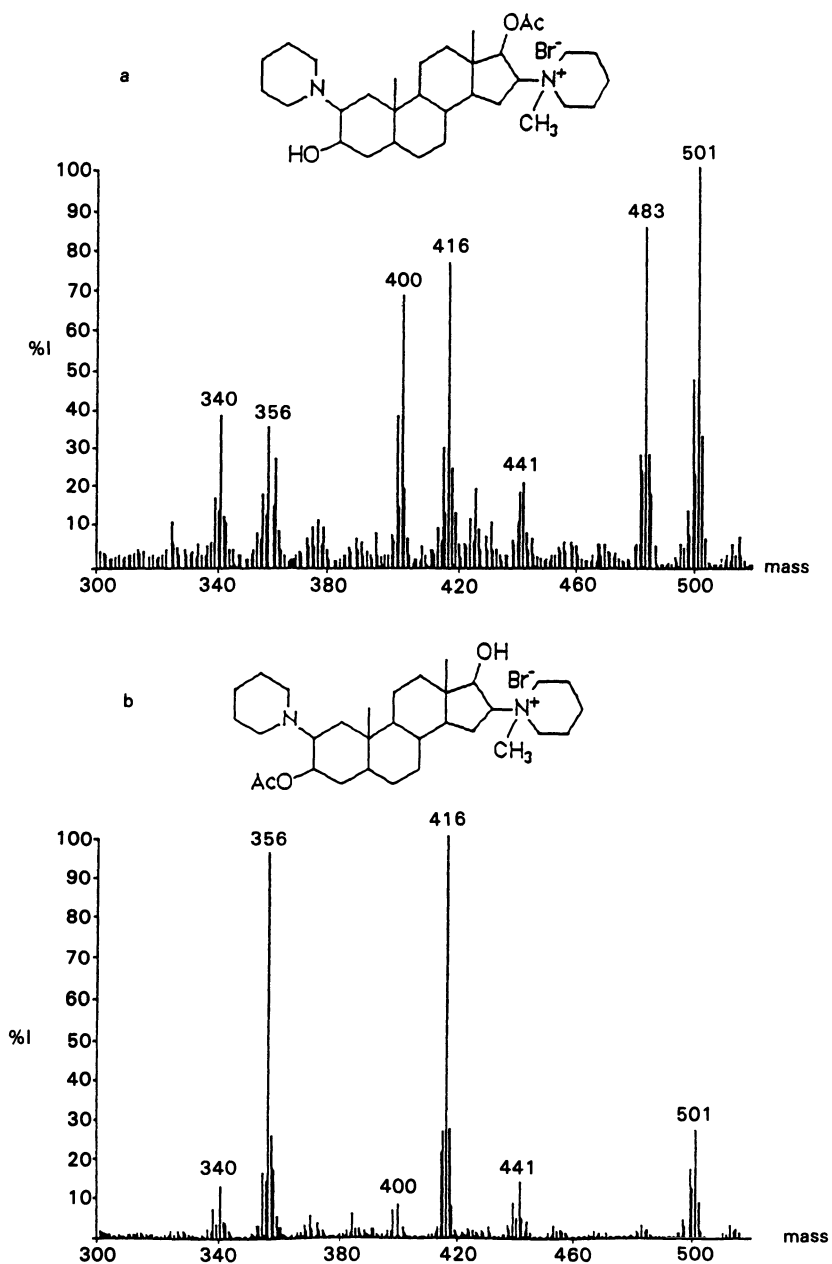


Figure 3.8. Methane chemical ionization (CI) spectra of (a) 3-deacetylvecuronium bromide and (b) 17-deacetylvecuronium bromide. [From Baker *et al.* (23). Copyright 1989 John Wiley & Sons, Ltd. Reprinted with permission.]

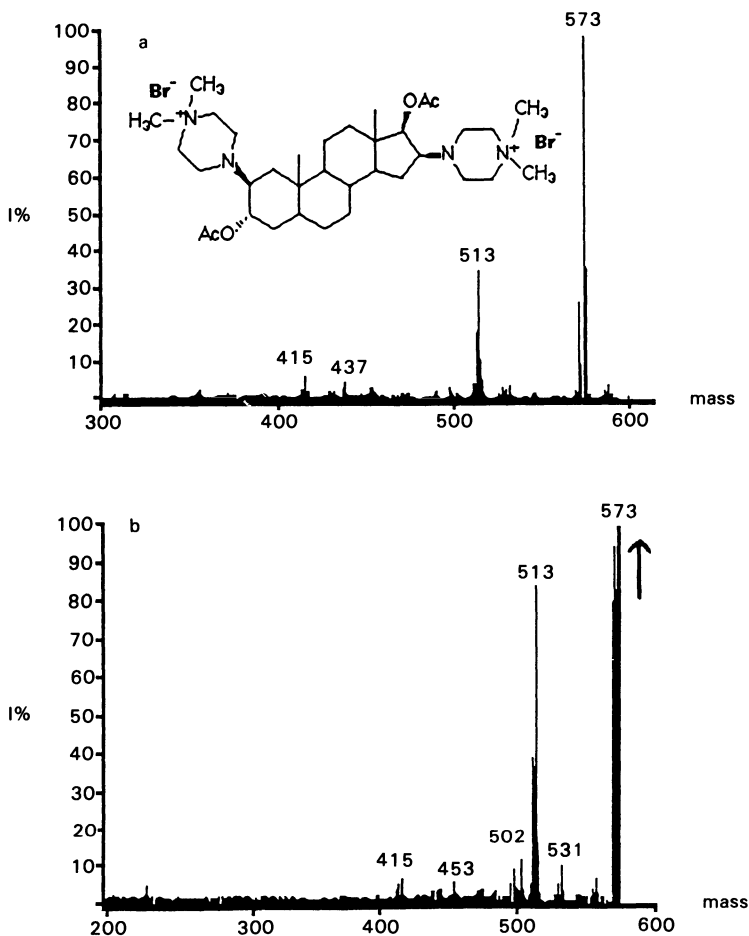


Figure 3.9. Pipecuronium bromide (A) structure and methane chemical ionization (CI) spectrum and (b) linked-scan (B/E) of m/z 573. [From Baker *et al.* (24). Copyright 1990 John Wiley & Sons, Ltd. Reprinted with permission.]

2.2.2. Assay Development Utilizing Mass Spectrometry

In view of the low specificity of fluorometric methods and the poor sensitivity of HPLC techniques, Castagnoli *et al.* (29) examined the utility of mass spectrometry for quantitation of neuromuscular blocking agents. That work represented one of the earlier efforts using mass spectrometry in a quantitative mode. The authors used direct insertion probe CI mass spectrometry for the determination of serum levels of these neuromuscular blocking agents. Their method is based on the thermolytic N-demethylation reaction, which occurs

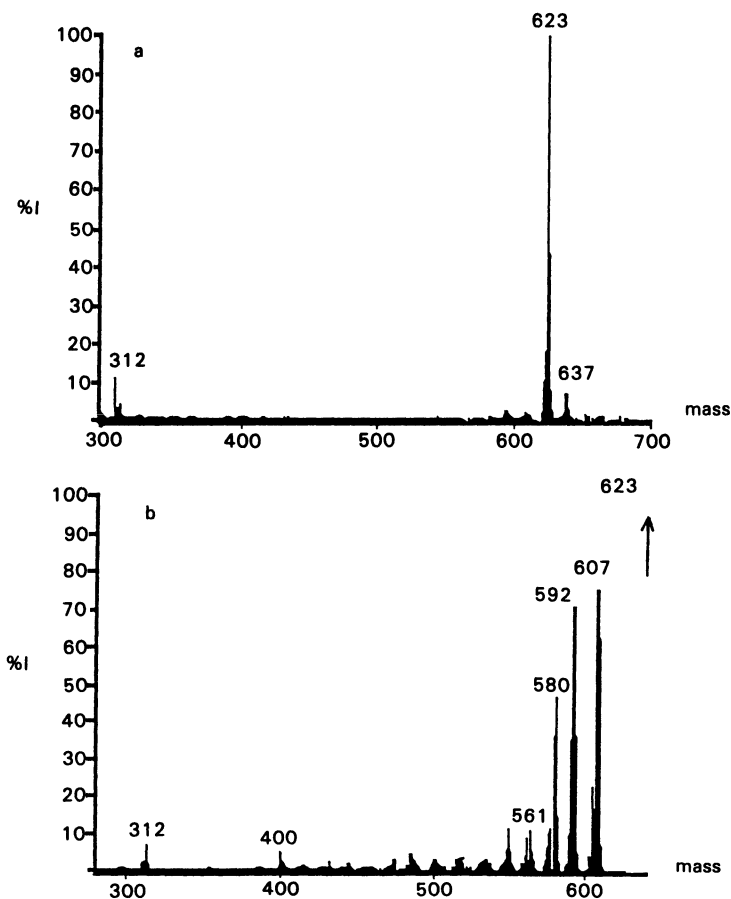


Figure 3.10. Metocurine iodide (a) methane chemical ionization (CI) spectrum and (b) linked-scan (B/E) of m/z 623. [From Baker *et al.* (24). Copyright 1990 John Wiley & Sons, Ltd. Reprinted with permission.]

when vecuronium or pancuronium salts are pyrolyzed. The resulting free base is protonated during CI to yield an ion of m/z 543, as discussed previously. A problem with that method, however, is its inability to distinguish between pancuronium and vecuronium because they both yield the same bisamine on heating in the mass spectrometer source. No reference to metabolites was made in that work. In addition, the mass spectrometric analysis time was relatively long. The extraction residue was dissolved in the appropriate organic solvent and the resulting solution transferred to the mass spectrometer probe tip. The solvent was evaporated, and impurities were removed by placing the probe in the ion cham-

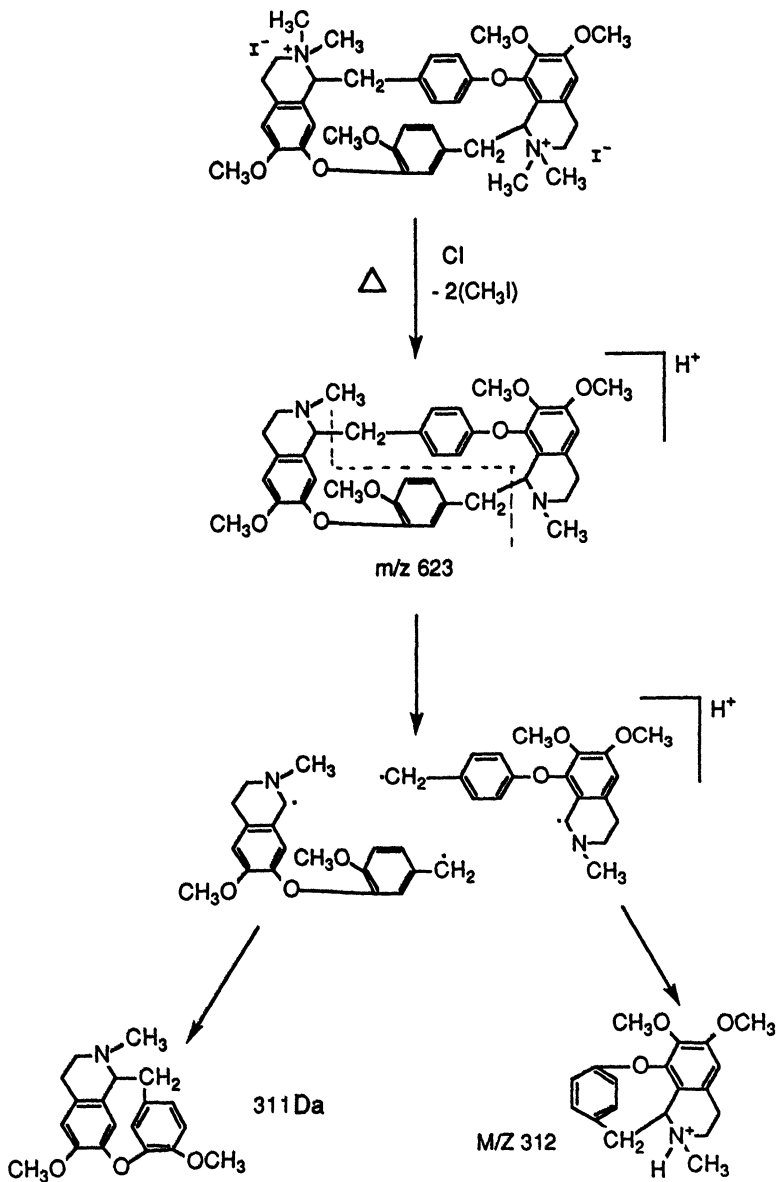


Figure 3.11. Chemical ionization (CH_4) fragmentation mechanism for metocurine iodide. [From Baker *et al.* (24). Copyright 1990 John Wiley & Sons, Ltd. Reprinted with permission.]

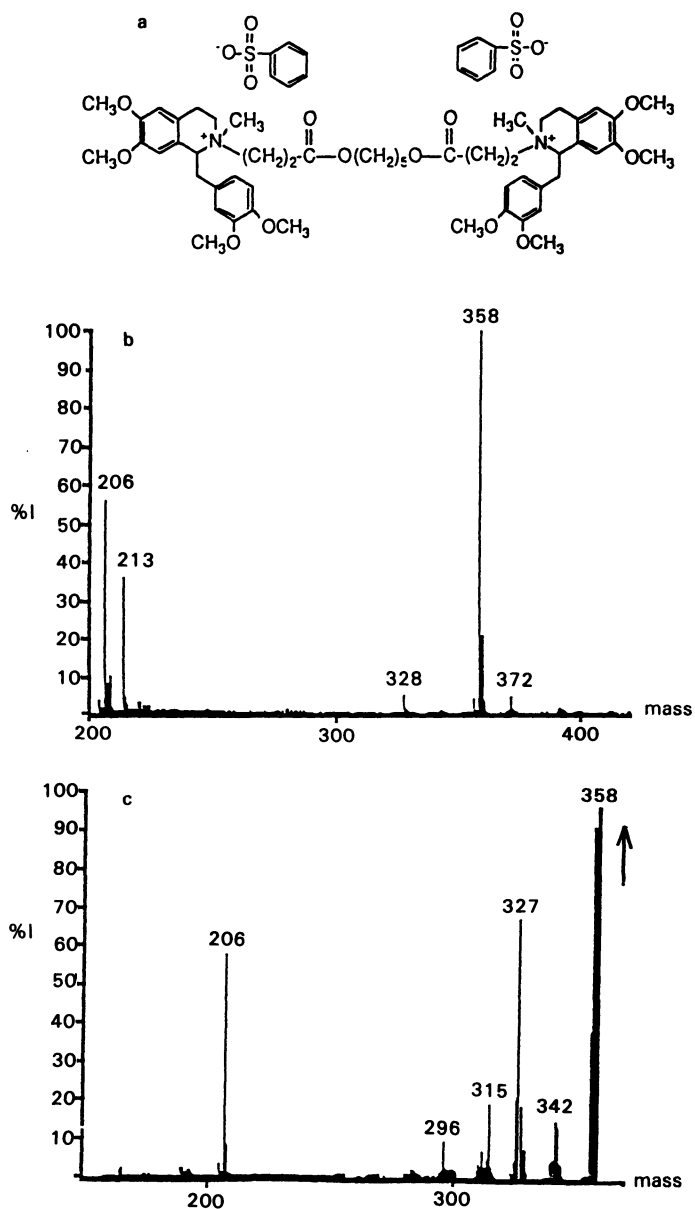


Figure 3.12. Atracurium besylate (a) structure, (b) methane chemical ionization (CI) spectrum, and (c) linked-scan (*B/E*) of *m/z* 358. [From Baker *et al.* (24). Copyright 1990 John Wiley & Sons, Ltd. Reprinted with permission.]

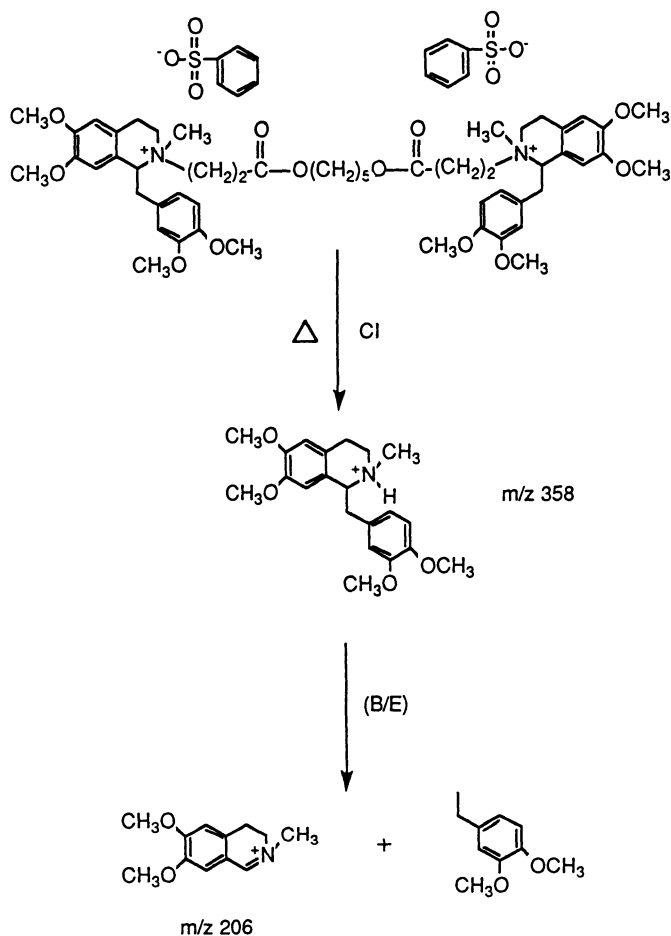


Figure 3.13. Chemical ionization (CH_4) fragmentation mechanism for atracurium besylate. [From Baker *et al.* (24). Copyright 1990 John Wiley & Sons, Ltd. Reprinted with permission.]

ber and heating the source to 145–150°C. The sample was held at this temperature for 0.5–3 min to remove impurities that interfered with the mass of interest. The source temperature was then increased to 165–170°C, where the thermolytic demethylation products were detected. This work focused on quantitative assay development using selected ion monitoring (SIM).

Evaluation of the CI fragmentation behavior of pancuronium bromide shows useful metastable transitions from the protonated free base, m/z 543, that are sufficiently selective to permit identification and quantitation of the drug in

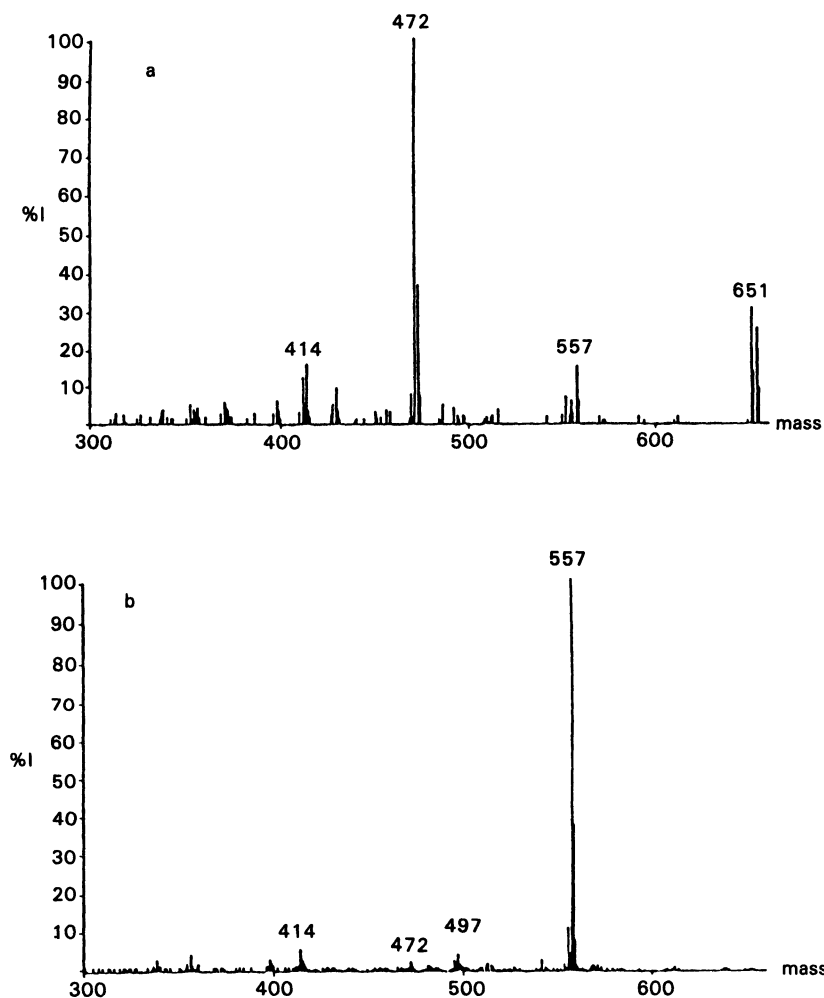


Figure 3.14. Fast atom bombardment (FAB) spectra of (a) pancuronium bromide, (b) vecuronium bromide.

plasma and urine by linked-scan B/E (Fig. 3.17) (30). The procedure takes advantage of the selective metastable transition m/z 543 \rightarrow m/z 483, which involves the elimination of acetic acid from the A ring (Fig. 3.4). The selectivity and specificity of the linked-scan method have permitted analysis of plasma samples following simple extraction in methylene chloride (30). A hexadeuterated analogue was used as an internal standard with concurrent monitoring of the analogous transition m/z 549 \rightarrow m/z 486 (Fig. 3.18). Pancuronium was quantified to levels as low as 1 ng/ml of plasma.

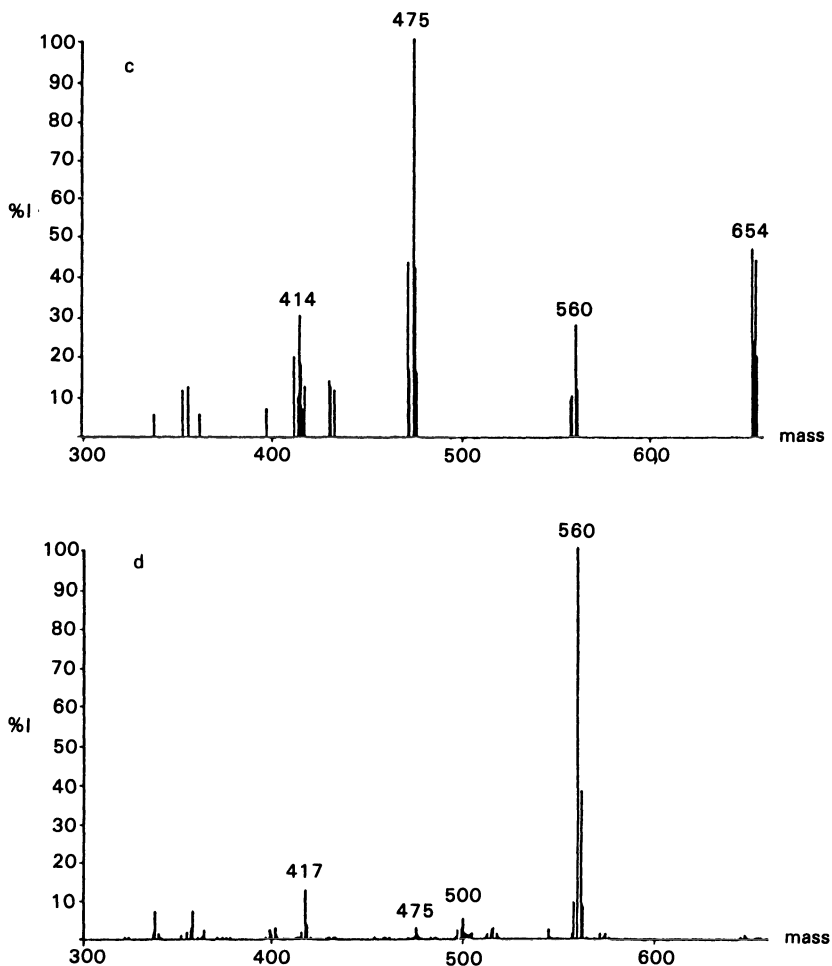


Figure 3.14. (Continued) (c) $[^2\text{H}_3]3\text{-acetylpancuronium}$, and (d) $[^2\text{H}_3]17\text{-acetylvecuronium}$ obtained from the moving-belt surface in a matrix-free environment. [From Baker *et al.* (23). Copyright 1989 John Wiley & Sons, Ltd. Reprinted with permission.]

In accordance with the need for methodology that provides for rapid analysis and large sample throughput, the moving-belt liquid chromatography/mass spectrometry (LC/MS) interface (Fig. 3.19) was used for introduction of extract aliquots into the mass spectrometer. This interface provides a convenient inlet for introduction of samples into the mass spectrometer at a very rapid rate. The quaternary ammonium compounds are dealkylated at the flash vaporizer and introduced into the MS ion source as the free bases. In this way, the belt interface acts effectively as a flow injection inlet, and a single determination can be done

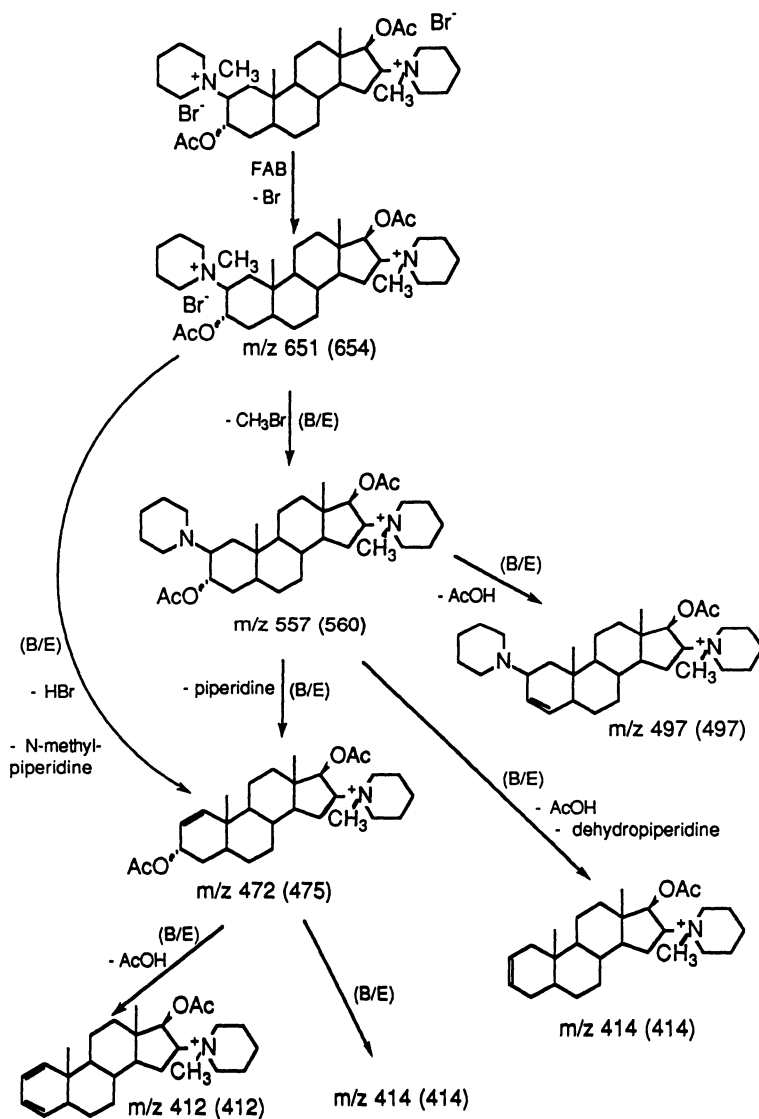


Figure 3.15. Fast atom bombardment (FAB) fragmentations of pancuronium bromide. Corresponding mass of $[^2\text{H}_3]$ 3-acetylpancuronium in parentheses. [From Baker *et al.* (23). Copyright 1989 John Wiley & Sons, Ltd. Reprinted with permission.]

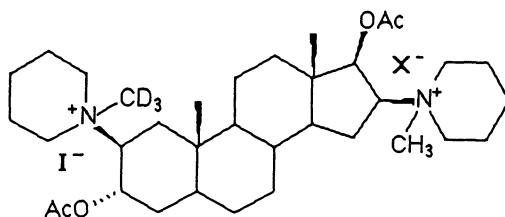
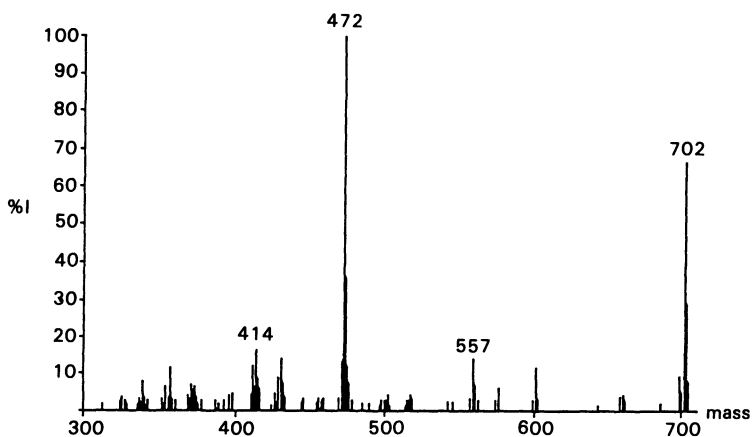


Figure 3.16. Fast atom bombardment (FAB) spectrum and structure of [2-N-C₂H₃]piperidylpancuronium (X⁻ = Br⁻). [From Baker *et al.* (23). Copyright 1989 John Wiley & Sons, Ltd. Reprinted with permission.]

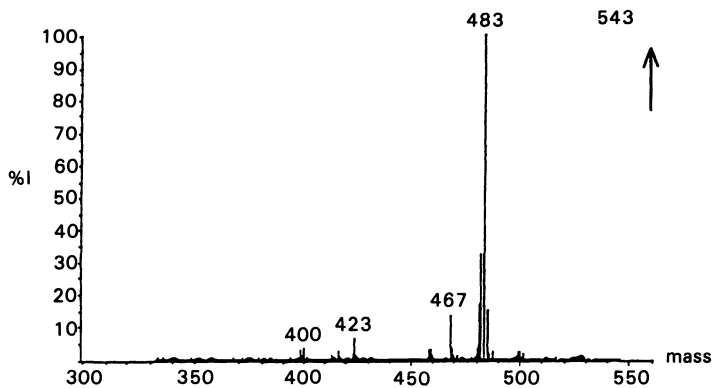


Figure 3.17. Linked-scan (B/E) spectrum of pancuronium bromide. [From Baker *et al.* (30). Copyright 1990 John Wiley & Sons, Ltd. Reprinted with permission.]

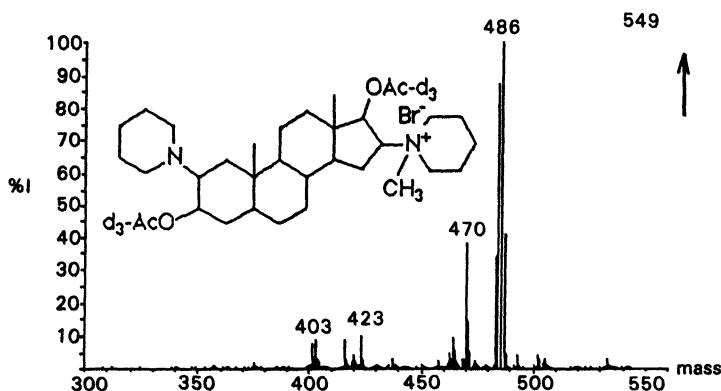


Figure 3.18. Linked-scan (B/E) spectrum and structure of hexadeuteriovecuronium. [From Baker *et al.* (30). Copyright 1990 John Wiley & Sons, Ltd. Reprinted with permission.]

in less than a minute. A complete pharmacokinetic curve for the drug of interest may be completed in less than 2 hr after initial sample isolation. This assay has been tested in two patients (30). A concentration–time curve in the two patients who received pancuronium is shown in Fig. 3.20. An interesting observation is the persistence of similar plasma concentrations of the drug in each of the patients at 0.75 to 1.0 hr after its administration. This phenomenon may be related to enterohepatic recirculation of the steroidal neuromuscular blocking agents, which heretofore may not have been observed because of poor assay techniques.

As discussed previously, CI does not distinguish between pancuronium and vecuronium, and this assay by itself reflects the combined contributions of the two drugs. In view of the possible metabolism of pancuronium to vecuronium, methodology is needed to differentiate between the two analytes. The utility of FAB/MS has been demonstrated previously. Continuous-flow fast atom bombardment/mass spectrometry (CF-FAB/MS) offers an additional alternative for differentiation between pancuronium and vecuronium. Figure 3.21 compares the positive-ion CF-FAB mass spectra of the two compounds. Sensitivity in the low nanogram range was demonstrated for vecuronium by Schubert *et al.* (Fig. 3.22) (31). Detection limits were further reduced by selected ion monitoring (m/z 557) and use of an internal standard. As mentioned previously, for pancuronium and vecuronium, the ion of highest mass is formed by loss of Br^- from the salt. For pancuronium, this loss results in a unique bromine-containing doublet at m/z 651/653. In principle, either ion in the doublet could be used to quantify pancuronium without interference from vecuronium. However, even better selectivity and sensitivity for pancuronium can be generated by consideration of the metastable transition m/z 651 \rightarrow m/z 472, which involves the loss of hydrogen

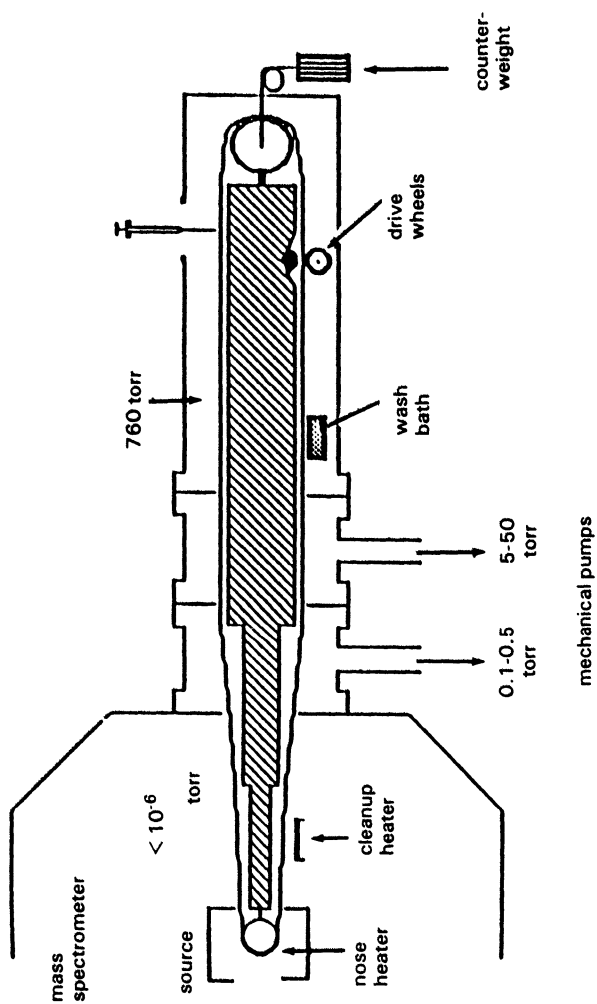


Figure 3.19. Moving-belt liquid chromatography/mass spectrometry (LC/MS) interface. [Reprinted with permission from T. R. Baker, Ph.D. thesis, 1990, Northeastern University, Boston, Mass.]

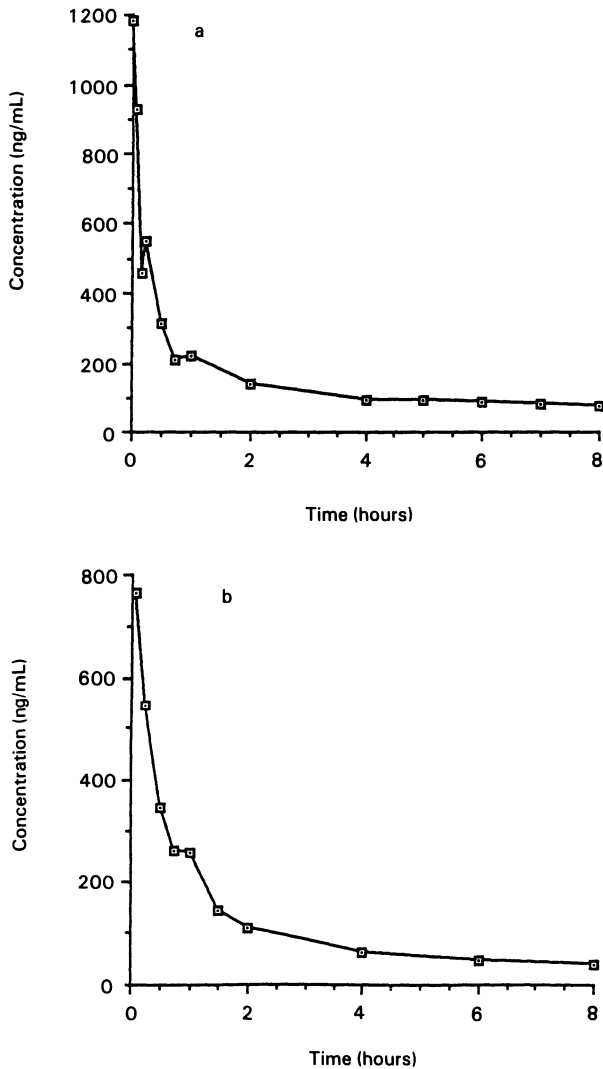


Figure 3.20. Clearance of pancuronium bromide from the plasma of (a) patient 1 and (b) patient 2. [Reprinted with permission from T. R. Baker, Ph.D. thesis, 1990, Northeastern University, Boston, Mass.]

bromide and N-methylpiperidine from m/z 651 (Fig. 3.15). Two single transition-monitoring profiles of repeat injections of 20 ng each are shown in Fig. 3.23. The indicated excellent reproducibility and signal-to-noise ratio are suggestive of a fragmentation process with high analytical utility.

Although CF-FAB can clearly be definitive in identifying and quantifying

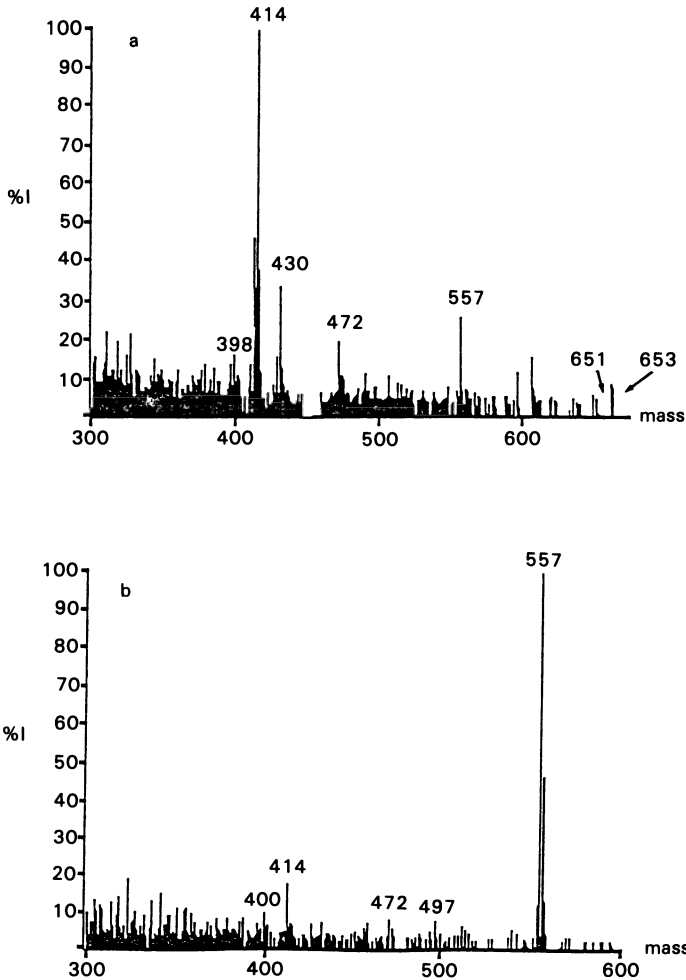


Figure 3.21. Continuous-flow fast atom bombardment (CF-FAB) spectra of (a) pancuronium bromide (50 ng) and (b) vecuronium bromide (40 ng). [Reprinted with permission from T. R. Baker, Ph.D. thesis, 1990, Northeastern University, Boston, Mass.]

pancuronium in the presence of vecuronium, the reverse does not necessarily hold true. This inability results from the considerable overlap in the spectra of the two compounds at the lower-mass end, e.g., m/z 557, 472, and 414. Electrospray ionization (ESI) holds considerable promise for selective detection of vecuronium in the presence of pancuronium. Examination of the ESI spectra of the two compounds (Fig. 3.24) reveals qualitative and quantitative differences. The spectrum of vecuronium has a well-defined peak at m/z 558, which corre-

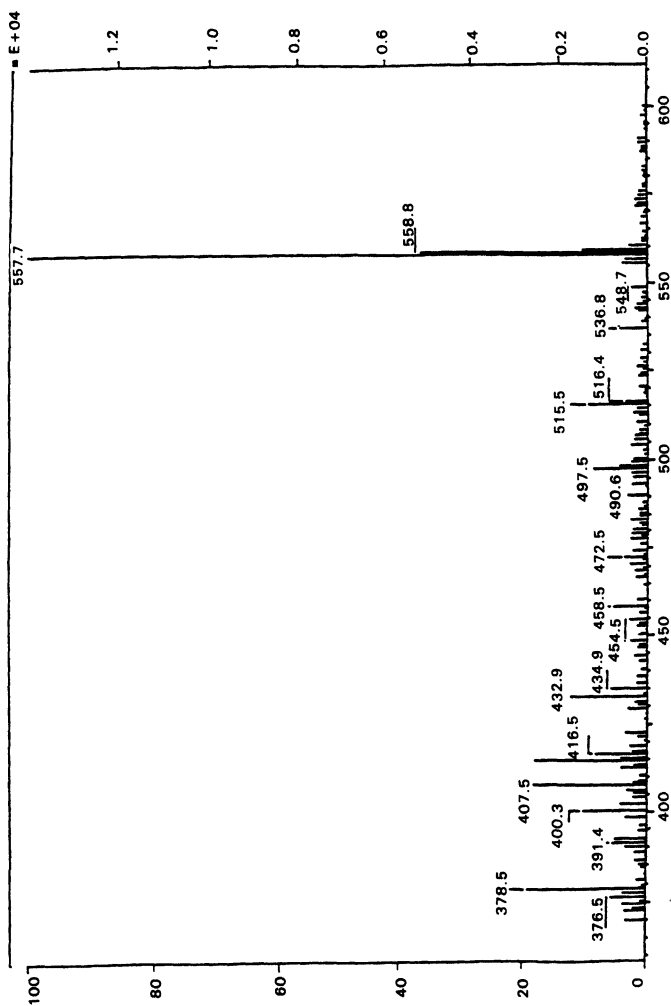


Figure 3.22. Demonstration of detection capabilities of continuous-flow fast atom bombardment (CF-FAB) for low nanogram quantities of vecuronium bromide (1.6 ng). [Reprinted from Schuber *et al.* (31), with permission from the author.]



Figure 3.23. Duplicate 20-ng injections of pancuronium using continuous-flow fast atom bombardment (CF-FAB) with single metastable transition monitoring (m/z 651 \rightarrow m/z 472). [Reprinted with permission from T. R. Baker, Ph.D. thesis, 1990, Northeastern University, Boston, Mass.]

sponds to the loss of the bromide counterion. In addition, the spectrum shows the doubly charged species at m/z 279 and a third unique peak at m/z 250. On the other hand, the ESI spectrum of pancuronium is dominated by the doubly charged ion at m/z 287. The potential for deconvolution of vecuronium from pancuronium by ESI is clearly evident from these data.

3. CONCLUSIONS

Despite their bisquaternary ammonium centers and their apparent non-volatile nature, the neuromuscular blocking agents are amenable to MS analysis by classical vapor-phase (EI, CI) as well as the more modern (FAB, ESI) methods of ionization. Because the compounds are of relatively low molecular weight, it is possible to vaporize them as the free bases via thermal dealkylation. This process is typical of quaternary alkyl ammonium salts. The free bases may be ionized by EI or, as discussed here for the neuromuscular blocking agents, by CI. Alternatively, the presence of two cationic centers in the molecules makes them ideal for ionization by FAB or ESI. Thus far, little work has been done using the later technique.

To date, CI techniques have been utilized effectively to assay the steroidal neuromuscular blocking agents in plasma or urine using either conventional SIM or tandem MS. Even though SIM of the protonated free base has provided a workable approach for assaying these compounds, the method lacks adequate specificity when used in conjunction with the direct insertion probe. To be more effective, this approach would require additional sample cleanup for the removal of interferences. In contrast, high-performance MS techniques, e.g., tandem mass

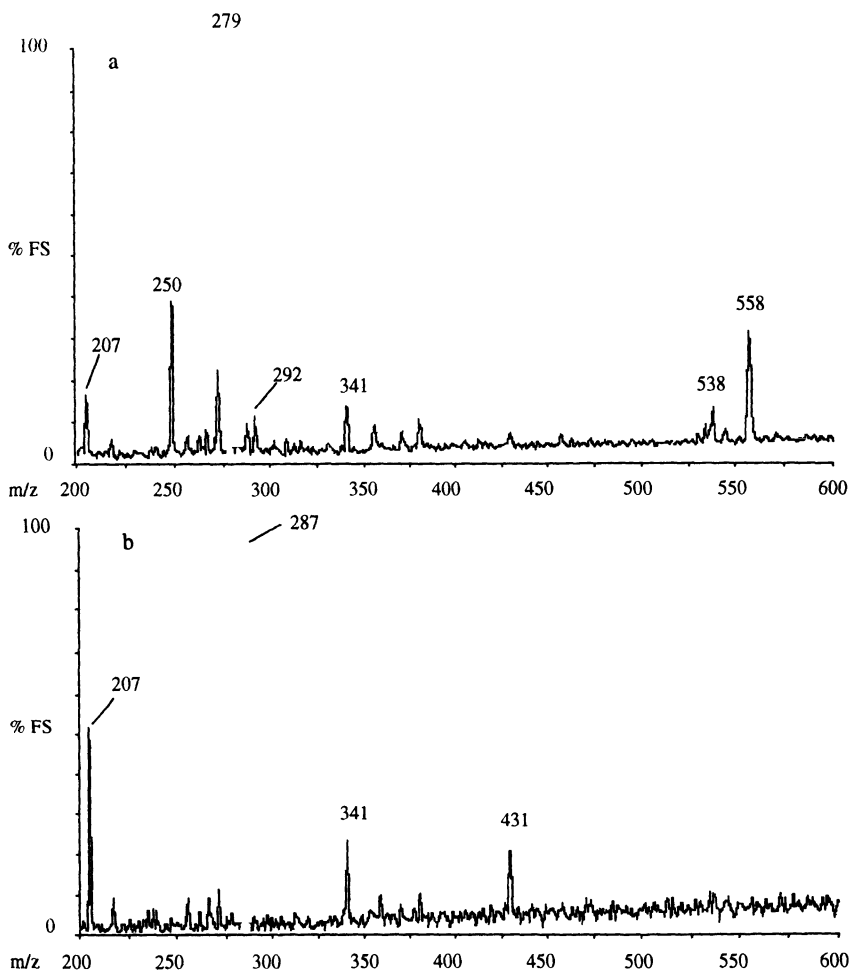


Figure 3.24. Electrospray ionization (ESI) mass spectra of (a) vecuronium bromide and (b) pancuronium bromide obtained on the VG BIO-Q.

spectrometry, can overcome many of the limitations that currently exist with the analytical methodology available for detection and quantitation of neuromuscular blocking agents. Initially, it is necessary to gain an understanding of the fundamental ion chemistry of these compounds using different ionization modes. The potential analytical utility of unique transitions can then be determined from the critical evaluation of this information. Single- and multiple-transition monitoring are techniques that provide the high level of selectivity and sensitivity necessary

for analysis of drugs in complex biological matrices. The use of the linked-scan method was demonstrated for the analysis of pancuronium in plasma and can be applied to the quantitative determination of other neuromuscular blocking agents in biological fluids. Rapid analysis can be achieved through use of the moving-belt LC/MS interface. This sample introduction system acts effectively as a flow injection inlet and is able to transport extracts into the mass spectrometer at a rapid rate.

As stated previously, FAB and ESI of neuromuscular blocking agents have both been explored to a limited degree. Further development of these techniques could lead to simpler and more definitive approaches for quantitation of muscle relaxants in biological fluids. Both methods may be readily adapted to introduction via flow injection and quantitation by MS/MS in order to generate large volumes of accurate pharmacokinetic data efficiently and rapidly. Moreover, they can be coupled to liquid chromatography and capillary electrophoresis to allow for on-line separation and sample cleanup prior to mass spectrometric analysis. This mode of sample introduction into the MS could possibly eliminate the need for the liquid-liquid extraction procedures currently used for sample isolation. Thus, FAB or ESI coupled with tandem mass spectrometry represent newer approaches in the continuing search for rapid, reliable, sensitive, and accurate analytical methods for evaluation of neuromuscular blocking agents.

REFERENCES

1. Griffith, H. R., and Johnson, G. E., 1942, The Use of Curare in General Anesthesia, *Anesthesiology* **3**:418–420.
2. Taylor, P., 1985, Neuromuscular Blocking Agents, in: *The Pharmacological Basis of Therapeutics*, 7th ed. (Gilman, A. G., Goodman, L. S., Rall, T. W., Murad, F., eds.), pp. 222–235. Macmillan, New York.
3. Miller, R. D., and Savarese, J. J., 1986, Pharmacology of Muscle Relaxants and Their Antagonists, in: *Anesthesia*, Vol. 2, 2nd ed. (Miller, R. D., ed.), pp. 889–943. Churchill Livingstone, New York.
4. Alberts, B., Bray, D., Lewis, J., Raff, M., Roberts, K., and Watson, J. D., 1989, *Molecular Biology of the Cell*, 2nd ed., pp. 319–321, Garland, New York.
5. Buckett, W. R., Marjoribanks, C. E. B., Marwick, F. A., and Morton, M. B., 1968, The Pharmacology of Pancuronium Bromide (Org.NA97), a New Potent Steroidal Neuromuscular Blocking Agent, *Br. J. Pharmacol. Chemother.* **32**:671–682.
6. Baird, W. L. M., and Reid, A. M., 1967, The Neuromuscular Blocking Properties of a New Steroid Compound, Pancuronium Bromide, *Br. J. Anaesth.* **39**:775–780.
7. Miller, R. D., Rupp, S. M., Fisher, D. M., Cronnelly, R., Fahey, M. R., and Sohn, Y. J., 1984, Clinical Pharmacology of Vecuronium and Atracurium, *Anesthesiology* **61**:444–453.
8. Miller, R. D., Agoston, S., Booij, L. H. D. J., Kersten, U. W., Crul, J. F., and Ham, J., 1978, The Comparative Potency and Pharmacokinetics of Pancuronium and Its Metabolites in Anesthetized Man, *J. Pharmacol. Exp. Ther.* **207**:539–543.
9. Roth, S., and Ebrahim, Z. Y., 1987, Resistance to Pancuronium in Patients Receiving Carbamazepine, *Anesthesiology*, **66**:691–693.

10. Ornstein, E., Matteo, R. S., Schwartz, A. E., Silverburg, P. A., Young, W. L., and Diaz, J., 1987, The Effect of Phenytoin on the Magnitude and Duration of Neuromuscular Block Following Atracurium or Vecuronium, *Anesthesiology*, **67**:191–196.
11. Martyn, J. A. J., Goldhill, D. R., and Goudsouzian, N. G., 1986, Clinical Pharmacology of Muscle Relaxants in Patients with Burns, *J. Clin. Pharmacol.* **26**:680–685.
12. Kersten, U. W., Meijer, D. K. F., and Agoston, S., 1973, Fluorimetric and Chromatographic Determination of Pancuronium Bromide and Its Metabolites in Biological Materials, *Clin. Chim. Acta* **44**:59–66.
13. Tanaka, K., Hioki, M., and Shindo, H., 1974, Determination of Pancuronium Bromide and Its Metabolites in Human Urine by Dye-Extraction Method—Relation between the Extractability and Structure of Quaternary Ammonium Ions, *Chem. Pharm. Bull.* **22**(11):2599–2606.
14. Buzello, W., 1974, The Colorimetric Determination of Pancuronium and Its Desacetyl Derivatives in the Human Body Fluids, *Anaesthesist* **23**:443–449.
15. Kinget, R. D., and Michoel, A. J., 1976, Thin-Layer Chromatography of Pancuronium Bromide and Its Hydrolysis Products, *J. Chromatogr.* **120**:234–238.
16. Paanakker, J. E., and Van de Laar, G. L. M., 1980, Determination of Org NC45 (A Myoneural Blocking Agent) in Human Plasma Using High-Performance Normal-Phase Liquid Chromatography, *J. Chromatogr.* **183**:459–466.
17. Furuta, T., Canfell, P. C., Castagnoli, K. P., Sharma, M. L., and Miller, R. D., 1988, Quantitation of Pancuronium, 3-Desacetylpancuronium, Vecuronium, 3-Desacetylvecuronium, Pipecuronium and 3-Desacetylpipecuronium in Biological Fluids by Capillary Gas Chromatography Using Nitrogen-Sensitive Detection, *J. Chromatogr.* **427**:41–53.
18. Segredo, V., Matthay, M. A., Sharma, M. L., Gruenke, L. D., Caldwell, J. E., and Miller, R. D., 1990, Prolonged Neuromuscular Blockade after Long-Term Administration of Vecuronium in Two Critically Ill Patients, *Anesthesiology* **72**:566–570.
19. Agoston, S., 1991, Paralysis after Long-Term Administration of Vecuronium, *Anesthesiology* **74**:792–793.
20. Segredo, V., and Sharma, M., 1991, [A Reply to S. Agoston.] *Anesthesiology* **74**:793–794.
21. Horowitz, P. E., and Spector, S., 1973, Determination of Serum *d*-Tubocurarine Concentration by Radioimmunoassay, *J. Pharmacol. Exp. Ther.* **185**:94–100.
22. Annan, R. S., Kim, C., and Martyn, J. A. J., 1990, Measurement of *d*-Tubocurarine Chloride in Human Urine Using Solid-Phase Extraction and Reversed-Phase High-Performance Liquid Chromatography with Ultraviolet Detection, *J. Chromatogr.* **526**:228–234.
23. Baker, T. R., Vouros, P., and Martyn, J. A. J., 1989, Mass Spectrometry of Pancuronium Bromide and Related Quaternary Ammonium Steroids Using the Moving Belt LC/MS Interface, *Org. Mass Spectrom.* **24**:723–732.
24. Baker, T. R., Vouros, P., and Martyn, J. A. J., 1990, Mass Spectrometry of Various Neuromuscular Blocking Agents, *Org. Mass Spectrom.* **25**:131–134.
25. Longevialle, P., Milne, G. W., and Fales, H. M., 1973, Chemical Ionization Mass Spectrometry of Complex Molecules. XI. Stereochemical and Conformational Effects in the Isobutane Chemical Ionization Mass Spectra of Some Steroidal Amino Alcohols, *J. Am. Chem. Soc.* **95**:6666–6669.
26. Wilson, M. S., and McCloskey, J. A., 1975, Chemical Ionization Mass Spectrometry of Nucleosides. Mechanisms of Ion Formation and Estimations of Proton Affinity, *J. Am. Chem. Soc.* **97**:3436–3444.
27. Dzidic, I., and McCloskey, J. A., 1971, Influence of Remote Functional Groups in the Chemical Ionization Mass Spectra of Long-Chain Compounds, *J. Am. Chem. Soc.* **93**:4955–4956.
28. Weinkam, R. J., 1974, The Importance of Intramolecular Associations in the Chemical Ionization Mass Spectra of Monoenoic and Monoepoxy Fatty Acid Methyl Esters, *J. Am. Chem. Soc.* **96**:1032–1037.

29. Castagnoli, K. P., Shinohara, Y., Furuta, T., Nguyen, T. L., Gruenke, L. D., Miller, R. D., and Castagnoli, N., 1986, Quantitative Estimation of Quaternary Ammonium Neuromuscular Blocking Agents in Serum by Direct Insertion Probe Chemical Ionization Mass Spectrometry, *Biomed. Environ. Mass Spectrom.* **13**:327–332.
30. Baker, T. R., Vouros, P., Rindgen, D., and Martyn, J. A. J., 1990, Mass Spectrometric Assay for Determination of Pancuronium and Vecuronium in Biological Fluids Utilizing the Moving Belt Introduction System, *Biomed. Environ. Mass Spectrom.* **19**:69–74.
31. Schubert, R., Schroeder, E., and Jacobs, P., 1988, Applications of Continuous Flow FAB Mass Spectrometry for the Study of Drug Metabolism, *Proceedings of the 36th ASMS Conference on Mass Spectrometry and Allied Topics*, San Francisco, CA, June 5–10, 1988, pp. 151–152.

Quantitative Analytical Mass Spectrometry of Endogenous Neuropeptides in Human Pituitaries

Dominic M. Desiderio

1. INTRODUCTORY COMMENTS AND OVERVIEW

The objective of this chapter is to describe mass spectrometric (MS) methodology for the qualitative and quantitative analysis of neuropeptides in human pituitary tissue. Those analytical data are required for a variety of different studies, including the elucidation of the basic molecular mechanisms involved in tumor formation (1). Most of the concepts underlying the instrumentation and analytical methods used for quantitative analytical MS and MS/MS have been discussed in previous publications (2–6). Recent developments in analyzing several different neuropeptide systems in the human pituitary are described in this chapter (7–13).

Several different neuropeptide products that derive metabolically from pro-enkephalin A and proopiomelanocortin (POMC) precursors have been analyzed separately and together in human pituitaries-postmortem controls and post-surgical tumors. The accurate quantification of a peptide in a tissue is important because the amount of an endogenous peptide reflects the ratio of its synthesis to degradation; thus, defects in those two metabolic processes will be reflected in the amount of a peptide.

Dominic M. Desiderio • Departments of Neurology and Biochemistry, Charles B. Stout Neuroscience Mass Spectrometry Laboratory, University of Tennessee–Memphis, Memphis, Tennessee 38163.

Fast atom bombardment (FAB) ionization was used to analyze methionine enkephalin (ME = YGGFM) (7,9) and β -endorphin (BE_{1-31,human} = YGGMTSEKSQTPLVTLFKNAIKNAYKKGE) in human control pituitaries and pituitary tumors (10,12). The BE and ME were measured together by MS/MS methods (8). The novel finding in those studies was that the BE content was significantly lower in tumor tissues versus controls, indicating an altered metabolism of the POMC system. An alteration in the metabolism of a neuropeptide system could involve the biosynthesis of the precursors and neuropeptide, defects in the transport of peptide from the cell body of the neuron to the presynaptic region, the metabolism of the neuropeptide to inactive metabolites, an alteration in the enzymes used for the biosynthesis and degradation of peptides, or a combination of those factors. This chapter describes the experimental details of those MS measurements.

One objective of this chapter and of this book is to expand the concept of clinical MS, which generally has meant the use of an MS instrument located in, for example, a clinical chemistry laboratory to provide the routine analyses for a hospital or other clinical setting (14,15). This book expands that concept by describing a wider range of analyses used to elucidate clinically relevant questions and compound types.

This chapter reviews the use of MS and MS/MS techniques to analyze qualitatively and quantitatively ME and BE neuropeptides extracted from human tissues, using the specific example of human pituitaries. Figure 4.1 defines the terms that are used in this chapter. Qualitative analysis means structure elucidation of an unknown compound; for nucleotides, saccharides, and peptides that term means the determination of the sequence of the constituent monomeric nucleosides, sugars, and amino acids, respectively. Quantitative analysis involves the use of an internal standard (such as a stable isotope-incorporated compound); production of a molecular ion species such as the M^+ , MH^+ , or $(M-H)^-$ ion; selected ion monitoring (SIM) of a fragment or molecular ion; or using a tandem MS method (MS/MS) to link together and monitor the transition $MH^+ \rightarrow$ fragment ion. That MS/MS method, known as multiple reaction monitoring (MRM), increases significantly the molecular specificity of the quantitative measurements (3,4).

It is important to place qualitative analysis into the overall context of research being performed on the MS of peptides. Several reviews (16–18) and most of the chapters in a recent book (4) describe in detail the use of MS to determine the amino acid sequence of synthetic and biological peptides. However, very few data are available for the MS quantification of peptides in human tissues and fluids. Quantitative measurements with a high level of molecular specificity are needed in several different clinical areas and in basic, cellular, and clinical neuroscience research. Toward that end, this chapter addresses specifically the qualitative and quantitative analysis of opioid peptides extracted from

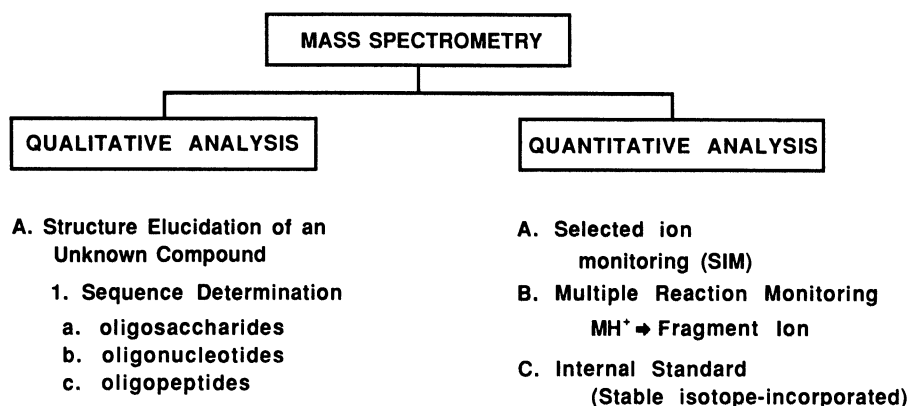


Figure 4.1. Schematic definition of the terms used in qualitative and quantitative analytical mass spectrometry.

postmortem control pituitaries and from postsurgical pituitary tumor tissues. Finally, MS is described as one important component in a multifaceted analytical system to measure peptides. That system also uses several other different techniques such as two-dimensional reversed-phase high-performance liquid chromatography (RP-HPLC) in different elution modes (isocratic, gradient) and with different analytical column-packing materials possessing different physicochemical characteristics [octadecylsilyl (ODS), synthetic hydrocarbon polymer] to purify neuropeptides, receptor assay (RRA) to measure the receptor-binding characteristics of a peptide (19), and radioimmunoassay (RIA) to measure the binding of the peptide to an antibody (5,6,9,20–24).

2. QUALITATIVE ANALYTICAL MASS SPECTROMETRY

The bulk of the scientific literature that illustrates the development and use of MS for the qualitative analysis of peptides deals with synthetic peptides to demonstrate the principles, utility, and range of application of a new instrumental method (25,26) or the determination of the amino acid sequence of an unknown peptide (4,27) or protein fragment (28,29) from nanomole to picomole amounts of purified peptide. Bioengineering of peptides and proteins is another developing area where MS provides significant analytical support (30). Thus, the bulk of the published MS data is qualitative analytical MS, and it can be predicted with confidence that most of the MS data to be published in the future will also continue to be qualitative.

Historically, the use of electron ionization (EI) MS was one of the first examples of the determination of the amino acid sequence of a naturally occur-

ring peptide, fortuitine (31), and of chemically reduced peptides (32). The study of the hypothalamic thyrotropin-releasing hormone, TRH (33,34), was one of the first uses of MS to elucidate the amino acid sequence of a naturally occurring brain peptide. For example, 300,000 sheep hypothalami were processed and chromatographically purified to produce a sufficient amount of TRH for qualitative analysis. That elucidation of the TRH amino acid sequence introduced the era of modern molecular neuroendocrinology. More recent applications of MS to sequence peptides have been reviewed (4,16–18). This chapter reviews the quantitative analysis of endogenous opioid peptides in the human pituitary, concomitantly using the amino acid sequence of the peptide to optimize the molecular specificity of the measurement.

3. QUANTITATIVE ANALYTICAL MASS SPECTROMETRY

The objective of many areas of neuroscience research is to analyze, quantify, and subcellularly localize a peptide in biological tissues and fluids (35,36). Several different analytical techniques are used for that purpose, but they do not possess the high level of molecular specificity that is required for unambiguous quantitative analysis. For example, because HPLC, cDNA, *in situ* hybridization (37), mRNA measurement, RIA, RRA, and immunohistochemical analyses cannot determine the amino acid sequence of a peptide (3,4), it is clear that the molecular specificity of all of those methods is limited (9). The lack of molecular specificity of those analytical techniques, in conjunction with the inherent complexity involved in a typical multistep metabolic pathway of peptides (see the example of the POMC neuropeptide system in Fig. 4.2) leads in some cases to potentially conflicting results (38).

Molecular specificity is the hallmark and experimental objective of the qualitative and quantitative MS analytical methods described in this chapter. Specifically, the ultimate goal of this research program is to determine the amino acid sequence of each endogenous peptide every time that the peptide is quantified in a biological matrix (7–13). That goal represents a significant advancement over every other published measurement method. Although that goal may be difficult to attain in some cases, it is nonetheless crucial to do so because of the need for increased molecular specificity. The following example will clarify the nature and extent of the problem. If an unknown peptide contains m amino acids, then it is possible to construct 20^m different peptides. For example, 20^5 or 3,200,000 different pentapeptides are possible. The goal of qualitative analytical MS is to elucidate the one correct amino acid sequence out of those 3,200,000 possible sequences. For example, if the peptide is methionine enkephalin (ME = YGGFM), then the amino acid sequence Tyr-Gly-Gly-Phe-Met must be estab-

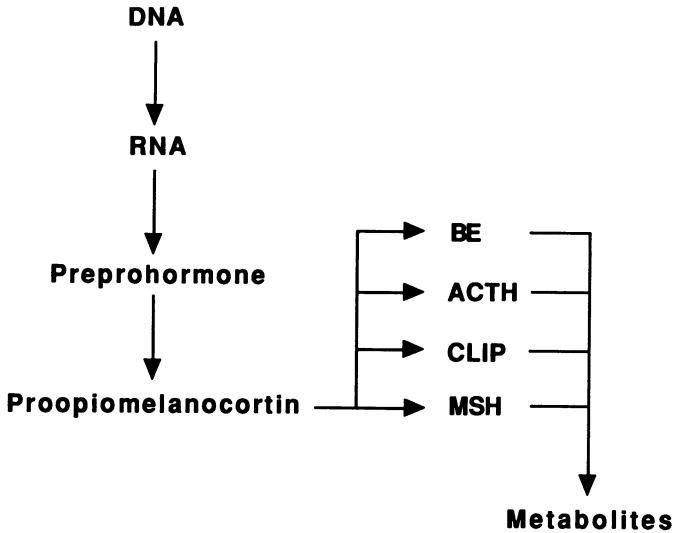


Figure 4.2. Schematic representation of the metabolism of the proopiomelanocortin (POMC) neuropeptide system (BE, β -endorphin; ACTH, adrenocorticotrophic hormone; CLIP, corticotropin-like intermediate peptide; MSH, melanocyte-stimulating hormones).

lished experimentally each time that the peptide is quantified in a biological tissue or fluid (7).

On the other hand, if qualitative and quantitative amino acid analysis data are available for a peptide, and thus it is known that n specific amino acids are present in the peptide, then a much smaller number, $n!$, of different peptides could be constructed. For a pentapeptide with five different amino acids, $5!$ or 120 different amino acid sequences could be constructed. Qualitative analytical MS/MS is one of only three experimental methods that can elucidate the amino acid sequence of a peptide; sequenators (gas phase and liquid phase) and x-ray crystallography are the other two methods.

Those types of analytical and mathematical computations must always be considered each time a compound that consists of different monomer units such as a peptide (monomer = amino acid), nucleotide (nucleoside), or saccharide (sugar) has been detected or quantified in a biological matrix.

The first step in performing any quantification is to extract that peptide from a biological matrix. Separation techniques have been developed in this laboratory to extract neuropeptides from brain tissue, tooth pulp tissue, and cerebrospinal fluid (lumbar and ventricular fluid). A basic principle of chromatography underlies much of the discussion in this chapter (2). For example, if chromatographic resolution were infinite, then no detector would be required because the peptide

of interest would be isolated completely from every other component in that biological matrix. To date, that objective has not been attained, and the probability is low that it can or ever will be attained.

If, on the other hand, the molecular specificity of the detector were infinite, then no chromatographic resolution would be required because the response of the detector would correspond only to that unique analyte. That goal has not been attained either; however, significant experimental strides are being made toward achieving that objective because of the optimal molecular specificity that can be achieved by state-of-the-art MS/MS (and MSⁿ) techniques (4,39–41).

The production of the protonated molecule ion, MH⁺ (see ref. 42 for nomenclature of MH⁺), of a peptide is an important first step to indicate the presence of the peptide in a biological matrix. Of course, that MH⁺ ion is a necessary but not sufficient experimental datum to quantify a peptide with a high level of molecular specificity. The reason the MH⁺ ion is insufficient to quantify a peptide relates to the *n!* concept described above. However, the MH⁺ ion data may be experimentally useful because some peptides do not produce any amino acid sequence-determining fragment ions. For example, in electrospray MS (ES–MS), the (M + 4H)⁴⁺ of BE and the (M + 2H)²⁺ ion of substance P (SP = RPKPQQFFGLM-NH₂) are stable, and no fragment ions were observed for femtomole amounts of those synthetic peptides (see Electrospray Ionization, p. 151).

Therefore, a link among several different experimental parameters, including RP-HPLC retention time (gradient and isocratic elution; ODS and polymer analytical columns), MH⁺ ion, and a metastable transition connecting the MH⁺ ion with one or more unique amino acid sequence-determining fragment ions is needed each time the peptide is quantified in a biological extract.

Finally, the accuracy, recovery, and molecular specificity of peptide quantification are optimized by using an appropriate internal standard, which consists of the synthetic peptide of interest where stable isotopes are incorporated to increase the mass of the MH⁺ ion by at least 4–5 Da. For ES ions such as the (M + 4H)⁴⁺ of BE, 30 to 40 stable isotopes are required. By considering the metabolism, hydrophobicity, and HPLC separation characteristics of the particular peptide under study, experience demonstrates that deuterated peptides are the best internal standards (7).

4. BASIC PRINCIPLES OF THE ANALYTICAL METHOD

The following analytical scheme (see Fig. 4.3) has been developed over the past decade and is the basis in our laboratory for the analysis of peptides in human tissues and fluids.

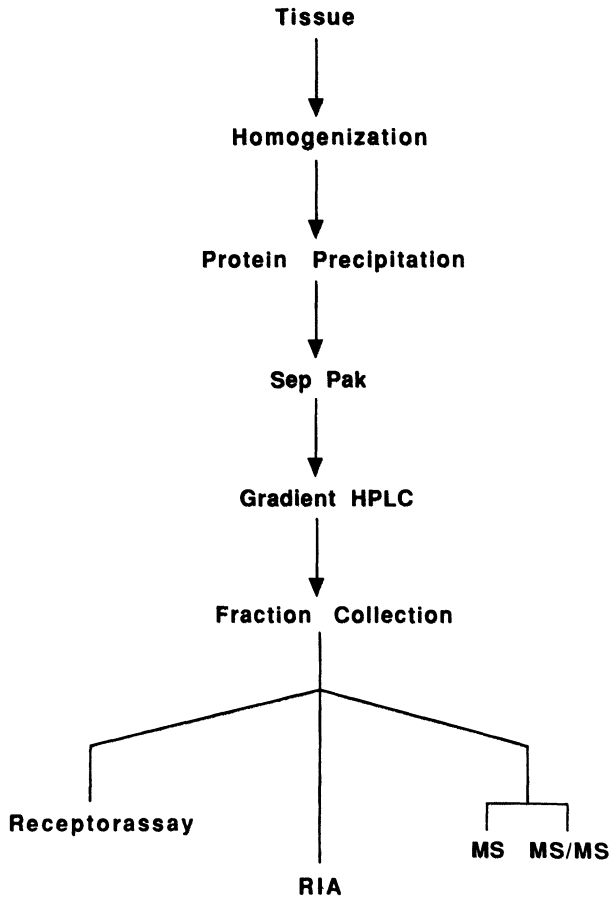


Figure 4.3. Analytical system used to collect, purify, and measure peptides in biological tissues and fluids.

4.1. Tissue Acquisition

It is important to collect the postsurgical or postmortem pituitary tissue immediately and to freeze the sample as rapidly as possible. For example, the tissue can be collected directly into acetic acid, and the tube placed into liquid nitrogen to avoid any enzyme-mediated production of peptides from precursors and to avoid enzyme degradation of peptides to inactive metabolites. Various enzyme inhibitors could be added to the sample, but that step is of limited utility because all potential enzymes that could degrade endogenous peptides and precursors are not known.

In the case of the analysis of postmortem human tissue, ethical and legal factors mitigate against immediate sample acquisition. That limitation must be taken into consideration because time is an important parameter for peptide studies. Some data (43) indicated that peptide-like immunoreactivity remains intact for up to 72 hr post-mortem. The expression of another labile molecule, POMC mRNA, was measured in 56 postmortem human pituitaries; the average postmortem delay was 18.5 ± 13.2 (s.d) hr with a range of 2–66 hr (44). Furthermore, tissue differences exist in neuropeptidergic processing of a precursor (45).

4.2. Extraction

Acidification protonates and stabilizes peptides and also precipitates proteins. Tissues are homogenized in acetic acid (1 M) (unless precursors are to be studied, in which case tissue is frozen without acid and homogenization is done in water), and the sample is centrifuged to remove cell debris and precipitated proteins. Recovery studies indicate that $85 \pm 5\%$ ($n = 3$) of [^3H]ME was recovered after these steps (9). It is important in any recovery study to allow a sufficient amount of incubation time for the exogenous radiolabeled peptide to experience the same microenvironment in the biological matrix as the endogenous peptide. For example, if a tritiated compound were added and extracted immediately, then that short equilibrium time could produce an artificially high level of recovery. Also, care must be exercised against the back-exchange of ^3H from a labile position in the molecule. Furthermore, radioiodinated peptides, although possessing a high level of specific radioactivity, have a very different hydrophobicity and molecular size and thus may not behave as the peptide being studied (46). Even stronger arguments extend to Bolton–Hunter labeled peptides (47,48), where a radioiodinated amino acid is synthesized to the N terminus of the peptide. Thus, experiments with iodinated and Bolton–Hunter conjugated peptides must be interpreted with caution.

The supernatant of the tissue extract is eluted through a previously prepared octadecylsilyl (ODS) Sep-Pak (49). Water-soluble solutes (salts, saccharides) are eluted with water, and the peptide–buffer ion-pair complex that remains on the ODS surface is eluted with a bolus of a high percentage of acetonitrile (7).

4.3. Reversed-Phase High-Performance Liquid Chromatography

HPLC in the reversed-phase mode (RP-HPLC) is a fast and efficient method to separate peptides from each other and from other cellular constituents (5,6). A volatile buffer (50) uses formic acid titrated to pH 3.15 with triethylamine to produce triethylamine formate (TEAF). Buffer volatility minimizes interference with subsequent RIA, RRA, and MS measurements.

The RP-HPLC detector is an important component in our comprehensive analytical scheme, and several different types of detectors are used. We use off-line RP-HPLC before MS analysis. For example, detection at 200 nm measures the ultraviolet (UV) absorption of the peptide bond. However, UV sensitivity is insufficient to detect endogenous neuropeptides (\leq pmol); because, generally, only nanomole amounts of peptides can be detected with UV, although synthetic somatostatin demonstrated a sensitivity at the femtomole level (50).

The HPLC analytical column packing (ODS, synthetic hydrocarbon polymer) and the elution mode (gradient, isocratic) can be used in various combinations to optimize chromatographic resolution and the MS analysis that follows. For example, the low level of silica that solubilizes in an ODS analytical column interferes with the FAB ionization of a peptide: FAB is an ionization process that is sensitive to surface activity and relative hydrophobicity properties of the matrix and peptide. Therefore, it is best first to use an ODS gradient elution of the Sep-Pak peptide-rich fraction to separate peptides over a wide range of size and hydrophobicity, followed by isocratic elution on a polymer column to further purify a selected gradient peak (7,9,13,21). That order of experimental manipulations takes advantage of the change in the composition of the solid matrix on which chromatographic separation is performed. For example, switching from an ODS to a polymer column for the final, pre-MS chromatographic step improved significantly the peak purity, minimized matrix interference, and improved the FAB-MS behavior of ME extracted from a human pituitary (7).

The data in Fig. 4.4 demonstrate this two-stage HPLC process. The RP-HPLC chromatographic separation of peptides in one human pituitary (no internal standard added) (7) is shown in Fig. 4.4A, which is the UV trace of the gradient elution of pituitary tissue from an ODS column. An aliquot of the fraction collected in the region of the ME elution (arrow) was subjected to FAB-MS, and the resulting spectrum is shown in Fig. 4.4B (MH^+ for ME: m/z 574). The signal-to-noise ratio of the ion at m/z 574 was low, unacceptable for subsequent qualitative and quantitative analysis of ME, and indicated the need for a second stage of HPLC analysis. Thus, the remaining fraction was purified isocratically on a polymer column (Fig. 4.4C) and analyzed by FAB-MS (Fig. 4.4D). The final signal-to-noise ratio of the m/z 574 ion in Fig. 4.4D is much improved and is sufficient for subsequent MS/MS analysis (see Scan Modes, below).

4.4. Fast Atom Bombardment Ionization

FAB is an effective method to ionize biological peptides (10,25,51-53), and liquid secondary-ion mass spectrometry (SIMS) using cesium ions (Cs^+) is preferred to ionize peptides with a molecular weight (M.W.) greater than about 4000 (54). The FAB matrix must possess appropriate hydrophobicity, solubility,

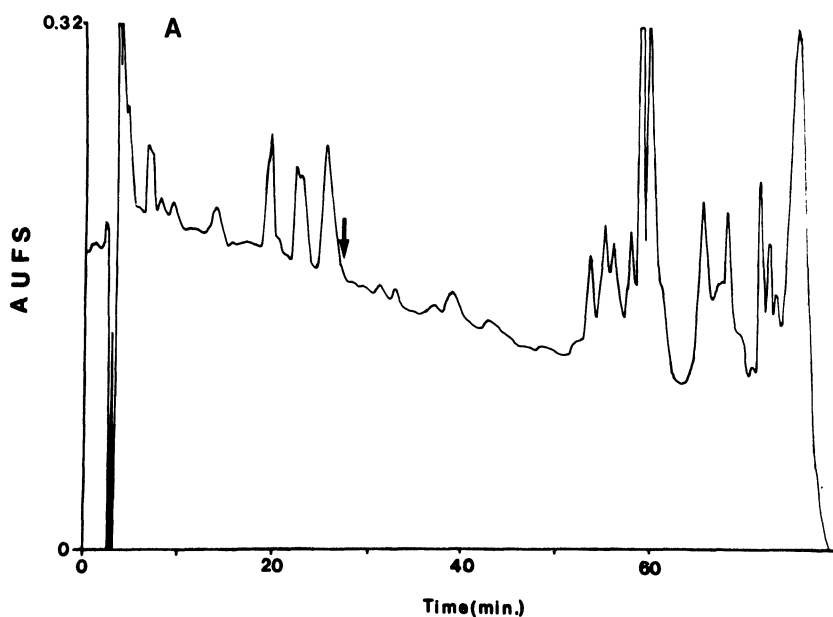


Figure 4.4. Reversed-phase HPLC chromatography of one human pituitary (no IS added); the arrow denotes ME retention time. [Reprinted with permission from Kusmierz *et al.* (7). Copyright 1990 American Chemical Society.] (A) ODS, gradient elution.

and pH characteristics to enhance the detection of the neuropeptides of interest (55). Glycerol, α -thioglycerol, dithiothreitol/dithioerythritol (DTT/DTE), or 3-nitrobenzylalcohol (NBA) are appropriate matrices from which peptides can be desorbed (56–58). In general, 200 nl of matrix is deposited onto the probe tip, and a methanol solution of the sample is deposited over it. Solvent is removed in the vacuum lock, and the probe tip is introduced into the FAB beam. Xenon (59) is an appropriate gas to use in FAB (generally 6 at 6 kV).

4.5. Scan Modes

For qualitative analysis, a complete product-ion scan of the peptide is required to determine the amino acid sequence of the peptide. In a human pituitary tissue extract, this step is possible because a sufficient amount (nanomoles) of a peptide such as ME is present (7). When only very low levels of endogenous peptides exist in a given tissue or fluid (20,60), a scan over a narrow mass range to bracket the MH^+ ion is the only information that can be obtained.

A full linked-field scan at a constant B/E ratio (B = magnetic field; E = electrical field) of the MH^+ ion of the peptide as the precursor ion collects all of

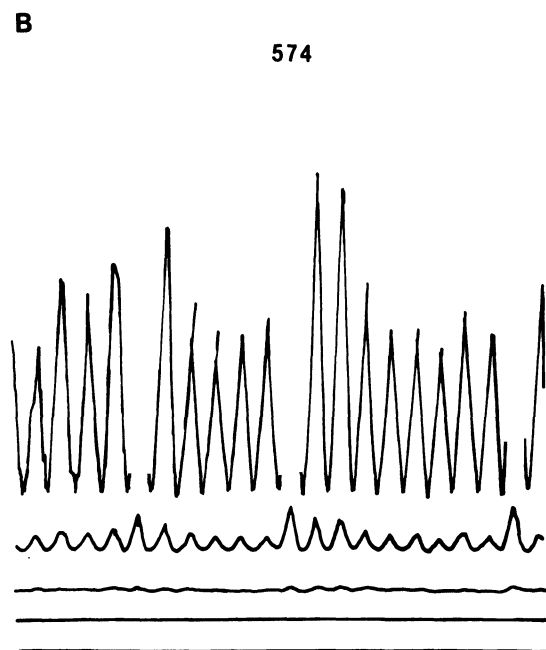


Figure 4.4. (Continued) (B) FAB-MS analysis of the ME MH^+ ion at m/z 574 in the fraction collected at the ME elution from the gradient profile in A.

the amino-acid-sequence-determining product ions and unambiguously determines the amino acid sequence of the peptide. This process has been achieved in one human pituitary for the first time for ME (7) and for BE, as BE_{20-24} (12).

Figure 4.5 contains the linked-field, constant- B/E product-ion scans obtained on a Finnigan MAT 731 mass spectrometer of (Fig. 4.5A) 100 ng synthetic ME, (Fig 4.5B) 50% of a pituitary tissue extract (from Fig. 4.4D; no internal standard), and (Fig. 4.5C) the glycerol matrix. The fragmentation scheme in Fig. 4.6 rationalizes the genesis of the ions found in the two product-ion spectra (Figs. 4.5A and B). These data are important to demonstrate that the multiple steps of chromatographic separations actually yield an HPLC fraction (Fig. 4.4C) that contains the specific pentapeptide ME (the amino-acid-sequence-determining fragment ions from a FAB-MS product-ion spectrum were obtained to demonstrate that the peptide was YGGFM), and therefore that the human pituitary tissue contains ME. Of course, such a step might appear to be a trivial experiment, but in fact this corroboration and proof of amino acid sequence has never been performed before, especially for each and every peptide analyzed.

In both of those product-ion spectra from the precursor ion of m/z 574 (Fig. 4.5A,B), amino-acid-sequence-determining fragment ions (refs. 61 and 62 for

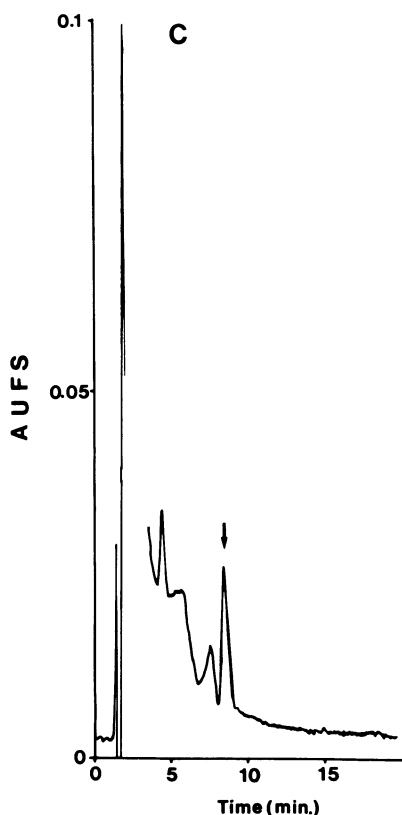


Figure 4.4. (Continued) (C) Polymer, isocratic (16% CH_3CN) elution of the fraction collected at the ME elution in A.

nomenclature) occur at m/z 425 (B_4), 411 (Y''_4), 397 (A_4), 354 (Y''_3), 297 (Y''_2), and 278 (B_3) (Fig. 4.6) (*cf.* ref. 52). Those two equivalent product-ion spectra verify for the first time the ME amino acid sequence YGGFM in an extract from a single human pituitary.

In another study, BE was similarly quantified using the tryptic peptide BE_{20-24} (NAIK) (12). Figure 4.7 contains the linked-field scan at constant B/E of the precursor ion at m/z 558. Those data were obtained on a VG 7070E-HF mass spectrometer. The qualitative equivalence of that product-ion spectrum to the corresponding spectrum of synthetic BE_{20-24} (Fig. 4.8) confirms the amino acid sequence NAIK for the endogenous peptide. The insert in Fig. 4.8 rationalizes the fragmentation pattern of the pentapeptide BE_{20-24} .

To increase by several orders of magnitude the detection sensitivity for quantifying a peptide while maintaining optimal molecular specificity, the MRM

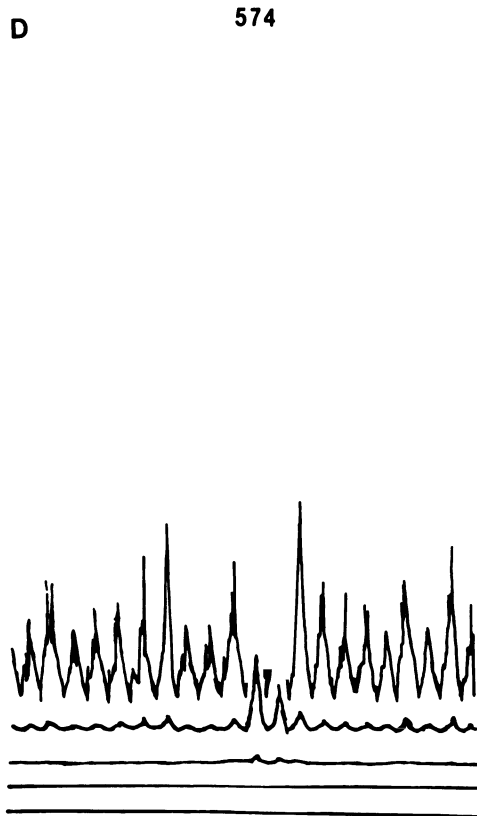


Figure 4.4. (Continued) (D) FAB-MS analysis of the ME MH^+ ion at m/z 574 in the fraction collected from the isocratic profile in C.

mode was used to monitor the metastable transition that links the selected precursor ion with a unique product ion (3,4,41). The MH^+ ion is always the best precursor ion to use (it has the highest ion current in a FAB spectrum, and it contains all of the amino acids in the peptide) in conjunction with a specific and unique amino-acid-sequence-determining fragment ion. For example, for ME, the transition $MH^+ \rightarrow YGGF^+$ (m/z 574 \rightarrow 425) (see Fig. 4.5A) was monitored to quantify ME, and the transition $MH^+ \rightarrow NAI^+$ (m/z 558 \rightarrow 299) (see Fig. 4.8) was monitored for BE (see discussion below). Therefore, MRM links together the precursor and product ions and increases significantly the molecular specificity of the quantitative analysis of the peptide. In a product-ion spectrum, where the product ion intensity is normally $<10\%$ of the MH^+ intensity (52), chemical noise is reduced significantly, and the analytically important signal-to-noise ratio increases.

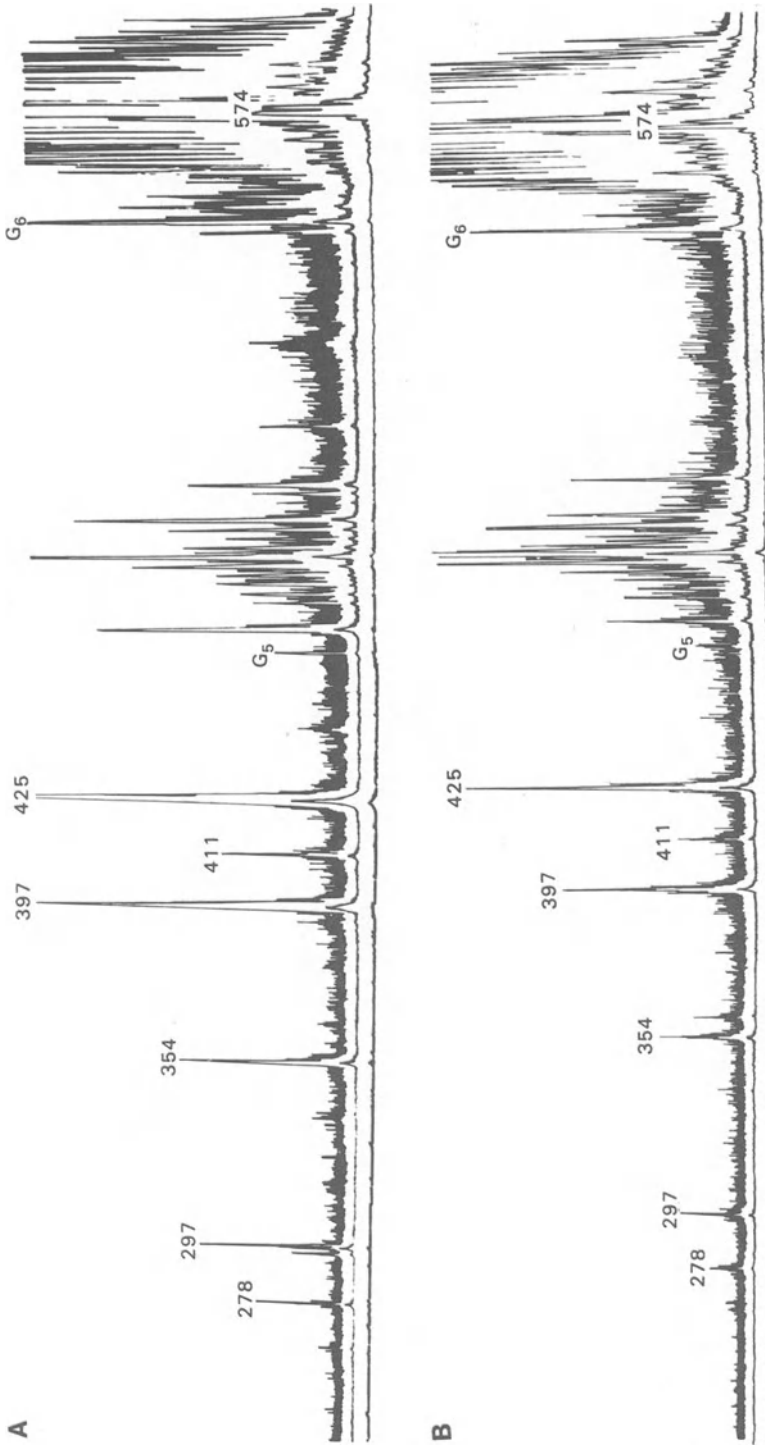


Figure 4.5. Production spectra of ME. The precursor ion is m/z 574 in all three production spectra. [Reprinted with permission from Kusmierz *et al.* (7). Copyright 1990 American Chemical Society.] (A) Synthetic ME (100 ng). (B) One pituitary tissue extract (no IS) (see Fig. 4.4D).

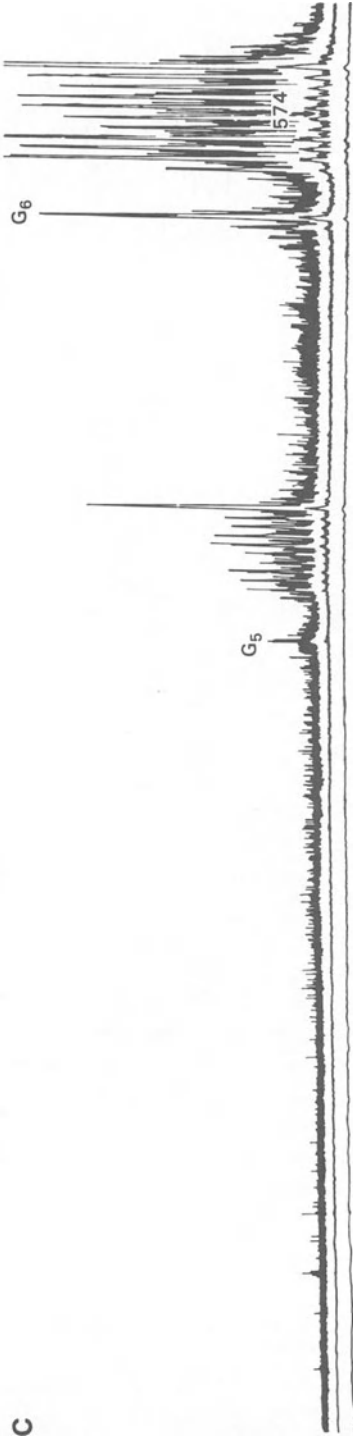


Figure 4.5. (Continued) (C) Glycerol matrix only.

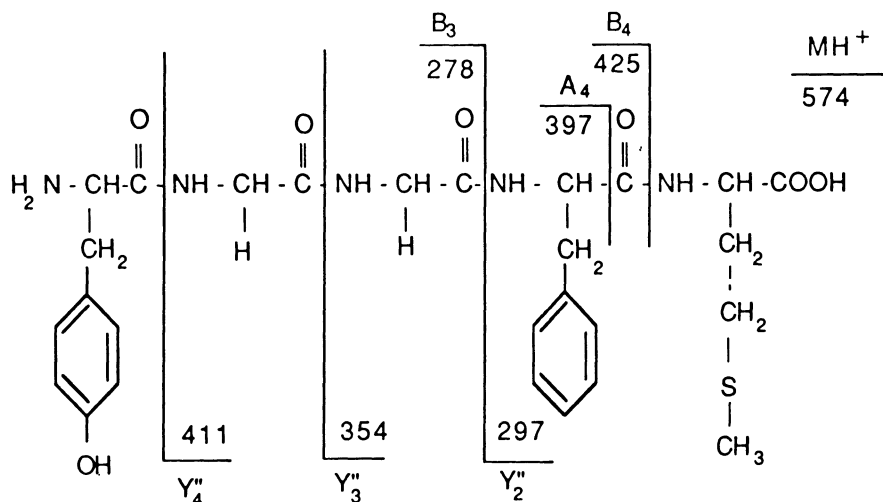


Figure 4.6. Observed fragmentation pattern and ion nomenclature for ME. [Reprinted with permission from Kusmierz *et al.* (7). Copyright 1990 American Chemical Society.]

4.6. Internal Standard

A deuterated peptide is the most appropriate type of internal standard to use because it possesses virtually the same chromatographic, desorption, ionization, and fragmentation characteristics as the corresponding peptide and also because all fragment ions containing the stable isotopes increase by the corresponding number of mass units. Thus, an internal standard will compensate for recovery losses during the extraction of the peptide and the MS measurement process. The location of the stable isotopes in the peptide is an important factor and is chosen as a function of the fragmentation pattern of the peptide and of the product ion that is selected for quantification. YGG-[$^2\text{H}_5$ -F]M and NAI[$^2\text{H}_4$ -I]K have been used to quantify endogenous ME and BE, respectively. Empirically, the ratio of the deuterated internal standard peptide to the endogenous peptide should be within the range of about 1 : 4 to 4 : 1 (12). The deuterated internal standard also helps to improve the recovery of the endogenous compound from a biological matrix because of the greater amount of that chemical entity (endogenous peptide plus equivalent internal standard).

4.7. Calibration Curves

The calibration curve for quantifying a peptide is constructed from data obtained by analyzing a series of sequentially diluted solutions of synthetic peptide, each containing a constant amount of the deuterated internal standard.

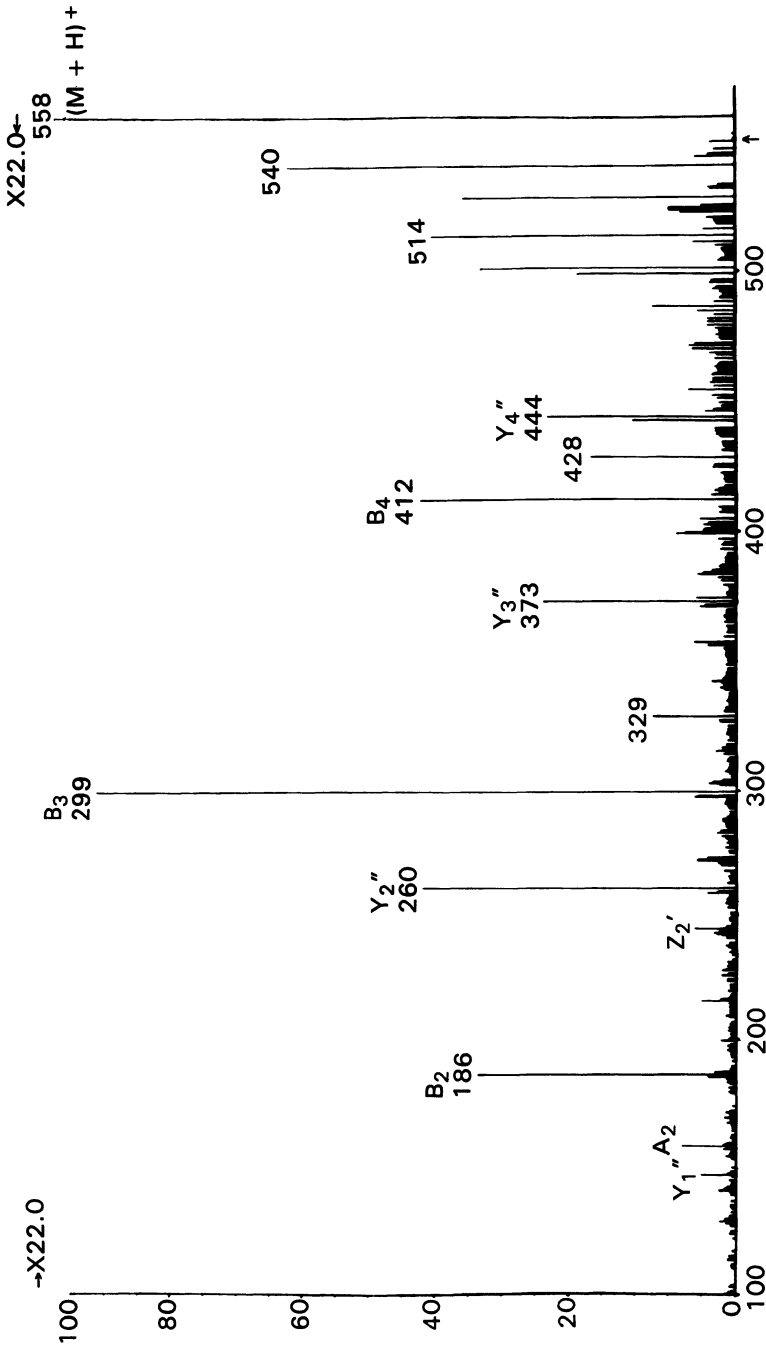


Figure 4.7. The product-ion spectrum of the m/z 558 ion from a tryptic fragment of an extract of pituitary B. The BE-containing fraction was trypsinized, and the tryptic fragment NAIHK, after isocratic RP-HPLC purification, was used to obtain this production spectrum. [From Dass *et al.* (12). Reprinted with permission from John Wiley and Sons Ltd. Copyright 1991 John Wiley and Sons Ltd.]

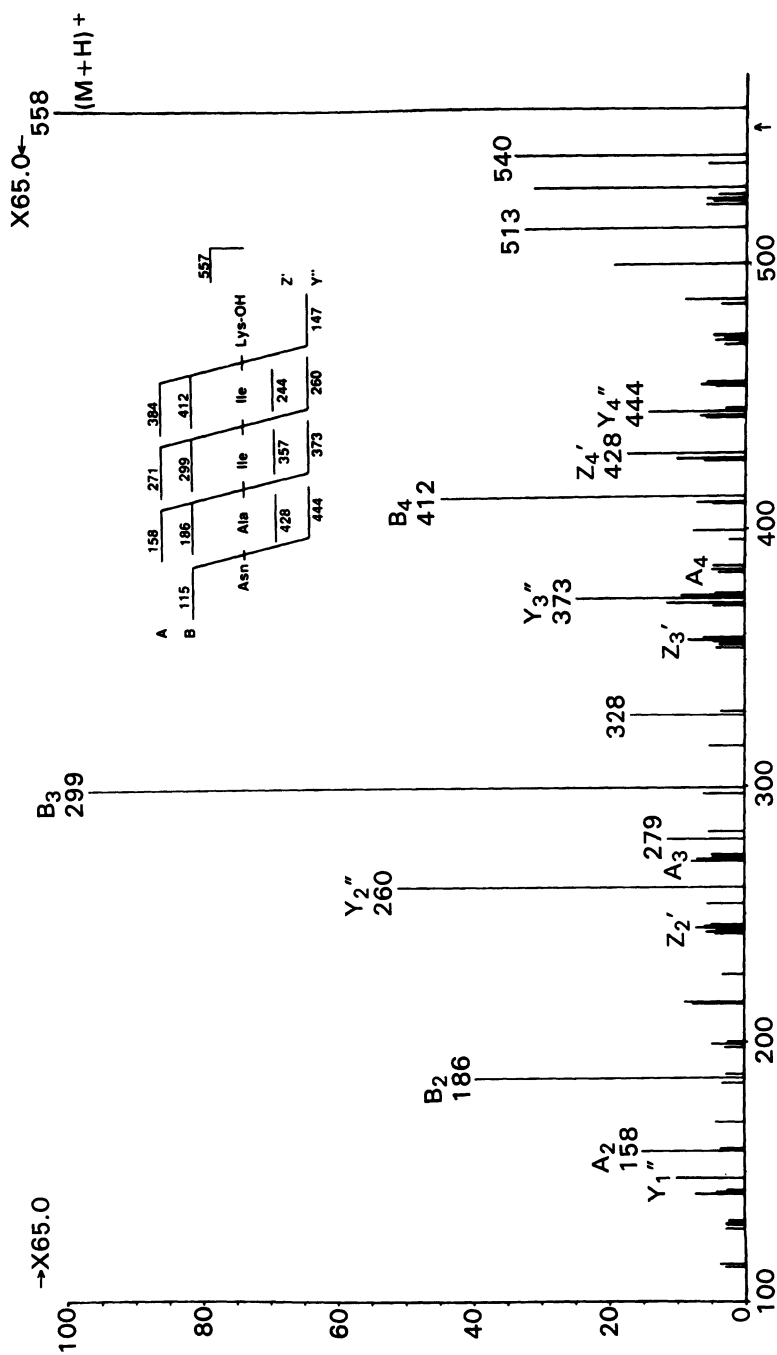


Figure 4.8. The B/E linked-field scan of the MH^+ ion at m/z 558 of synthetic NAIHK. [From Dass *et al.* (12). Reprinted with permission from John Wiley and Sons Ltd. Copyright 1991 John Wiley and Sons Ltd.]

MRM measures the transition for the endogenous peptide and the transition for the internal standard. The ratio is obtained for those two measurements, and the amount of endogenous peptide is calculated by multiplying that ratio by the amount of deuterated peptide that was added to the biological extract.

4.8. Electrospray Ionization

FAB ionization has been used for most of the peptide quantitation studies discussed in this chapter. However, FAB ionization has several important experimental limits: the mass spectrum consists of a mixture of spectra because of the matrix and the compound of interest; the matrix interacts chemically with peptides (63); irradiation effects occur (51,53); mutual suppression of ionization occurs when multiple analytes are present in the matrix; the relative hydrophobicity of the matrix to analyte plays a crucial role in analyte desorption and ionization; and redox reactions can occur (55).

Electrospray ionization (EI) MS (26; Mann and Fenn, Chapter 1, this volume; Smith *et al.*, Chapter 2, this volume) is a recent development that is useful for the fast and facile ionization of large polar molecules such as proteins and enzymes and overcomes some of the limitations of FAB. Electrospray analysis of neuropeptides has also demonstrated a high level of detection sensitivity (11), although multiply charged species, such as $(M + 4H)^{4+}$ of BE and $(M + 2H)^{2+}$ of SP do not fragment readily to provide sequence ions (unpublished data). For example, Fig. 4.9 contains the triple sector quadrupole (TSQ) MS/MS spectrum of the transition between the MH^+ of ME and the product ion at m/z 397 (A_4). The data have a signal-to-noise ratio of 3 : 1 and correspond to the injection of

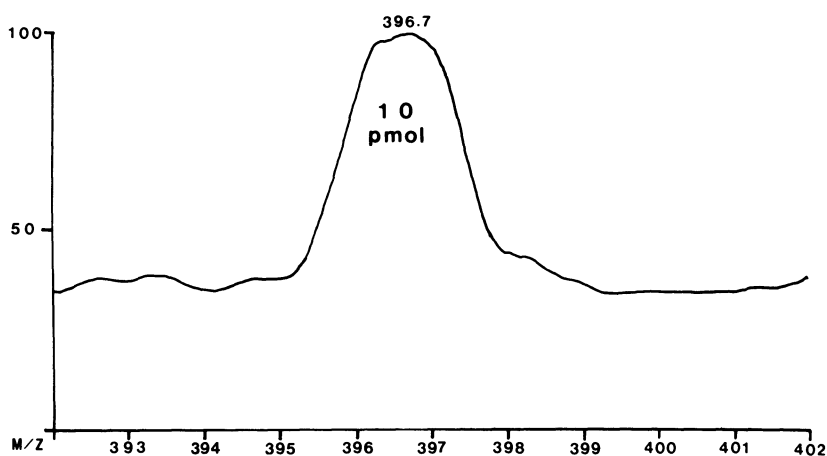


Figure 4.9. Electrospray spectrum of the transition $MH^+ \rightarrow 397$ from synthetic ME.

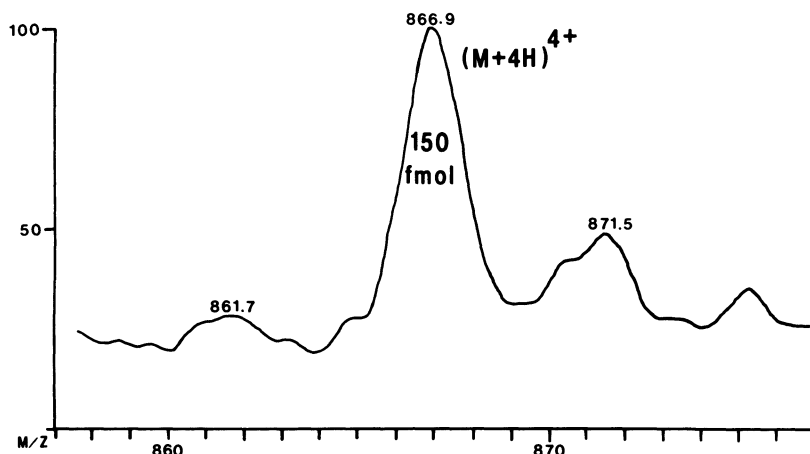


Figure 4.10. Electrospray spectrum of the $(M + 4H)^{4+}$ ion from synthetic BE_{1-31m} human.

10 pmol (5.7 ng) of synthetic ME. Figure 4.10 contains the ES spectrum of the $(M + 4H)^{4+}$ ion of BE (150 fmol), and Fig. 4.11 the $(M + 2H)^{2+}$ ion of SP (150 fmol). These ES-MS-MS and ES-MS data represent the current limits of detection sensitivity for those three neuropeptides.

5. EXAMPLES OF MEASUREMENTS OF OPIOID PEPTIDES IN A SINGLE HUMAN PITUITARY

5.1. Method Development: Measurement of ME in 11 Human Pituitaries

Once it was determined that ME (= YGGFM) and BE (as BE₂₀₋₂₄ = NAIK) were present in pituitary tissue extracts, ME and BE were quantified in each pituitary using the stable isotope-incorporated internal standards [²H₅]ME and [²H₄]BE, respectively (7). The calibration data for the MH⁺ ion from a series of solutions of synthetic ME yielded the best-fit regression line with the equation: ratio [²H₀/²H₅]ME = 0.00101 × (ME, ng) + 0.019. One microgram of [²H₅]ME was added to each solution of decreasing amounts of ME. Table 4.1 contains the measurements of ME in 11 individual human pituitary extracts. The MH⁺ and MRM (MH⁺ → YGGF⁺) data demonstrate that, because of extensive HPLC purification, the two methods yield similar quantitative values. The MRM data are, however, more specific.

The MH⁺ data averaged to 31.9 ± 11.0 (s.e.m.) and the MRM data to 26.7 ± 9.2 (s.e.m.) pmol ME/mg protein. The coefficients of variation of these two

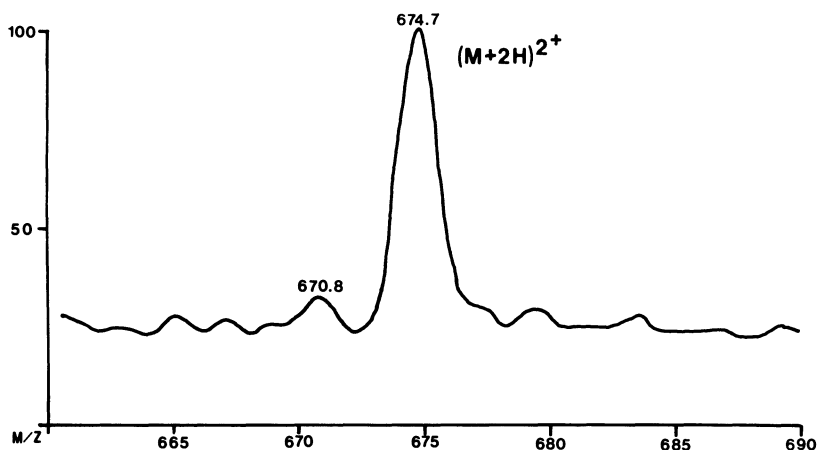


Figure 4.11. Electrospray spectrum of the $(M + 2H)^{2+}$ ion from synthetic SP.

measurement methods (114%) do not reflect the reproducibility of the analytical measurement but rather reflect the biological variation usually obtained for human tissue measurements. The coefficient of variation for the analytical measurement itself was 2–5% (7). Approximately 52 pmol of ME was on the FAB probe tip during MH^+ quantification, and approximately three times more, or

Table 4.1
FAB-MS Analysis of ME in 11 Human Pituitaries
 Based on MH^+ and MRM
 ($MH^+ \rightarrow YGGF^+$) Data

Sample	MH^+	MRM
A	23.8	20.2
B	9.5	8.0
C	22.9	22.1
D	8.4	4.4
E	54.5	41.6
F	133.5	109.4
G	21.4	15.1
H	38.9	42.5
I	17.5	14.2
J	10.9	7.5
K	9.1	8.4
Mean \pm s.e.m.	31.9 \pm 11.0	26.7 \pm 9.2

Data given as picomoles ME per milligram protein. One microgram $[^2H_5]ME$ was added to each pituitary sample; MRM monitored the transition $MH^+ \rightarrow YGGF^+$. [Reprinted with permission from Kusmierz *et al.* (7). Copyright 1990 American Chemical Society.]

about 156 pmol ME, was on the tip during the acquisition of the corresponding product ion spectrum.

5.2. Pituitaries: Control versus Tumors

In another experiment designed to elucidate the molecular mechanism involved in tumor formation, ME and BE were measured in a set of control pituitaries and in pituitary tumor tissues (8). The hypothesis of that study is that multiple neuropeptide systems are involved in tumor formation, a covariance or coregulation of the production of two peptides occurs, and a metabolic defect occurs in the neuropeptide system (Fig. 4.2) in tumor formation. Table 4.2 contains the measurements of ME and BE in eight controls, and Table 4.3 contains the measurements in five tumors. The MRM method was used to measure the neuropeptides.

The amount of ME in controls was 75.2 ± 29.6 (s.e.m.), and in tumors 25.0 ± 7.6 pmol ME/mg protein. The amount of BE in controls was 132.5 ± 22.3 , and in tumors 36.0 ± 14.8 pmol BE/mg protein. The ratio of the POMC to the proenkephalin A peptide, BE/ME, was greater than 1 in all controls except number 5. That ratio was less than 1 for three of the tumors.

A statistically significant difference ($p = 0.004$) was found for the amount of BE, which derives from the POMC (BE-containing) system, in the tumor data. That difference indicates that either a down-regulation or an increased level of degradation of the POMC peptide has occurred; a combination of those two factors is possible. Thus, it appears that the absolute amount of neuropeptides and the relative amounts of neuropeptide systems may be two important factors in the formation of tumors in the human pituitary. That study is being expanded

Table 4.2
Measurement of ME and BE by FAB-MS-MRM in Postmortem
Human Pituitary Controls

Pituitary	ME	BE	BE/ME
1	151.7	180.9	1.2
2	28.0	88.5	3.2
3	66.5	71.8	1.1
4	251.8	181.5	0.7
5	30.8	88.9	2.9
6	19.9	241.8	12.1
7	27.6	71.9	2.6
8	25.2	134.6	5.4
Mean \pm s.e.m.	75.2 ± 29.6	132.5 ± 22.3	3.6

Measurements are given as picomoles peptide per milligram protein. [Reprinted with permission from Kusmierz *et al.* (7). Copyright 1990 American Chemical Society.]

Table 4.3
Measurement of ME and BE by FAB-MS-MRM
in Postsurgery Human Pituitary Tumor Tissue

Tumor	ME	BE	BE/ME
9	13.3	4.5	0.3
10	33.1	1.1	0.03
11	48.9	38.0	0.8
12	5.5	61.3	11.2
13	24.2	75.2	3.1
Mean \pm s.e.m.	25.0 \pm 7.6	36.0 \pm 14.8	3.1

Measurements are given as picomoles peptide per milligram protein. [Reprinted with permission from Kusmierz *et al.* (7). Copyright 1990 American Chemical Society.]

to increase the number of measurements (the ME data were nearly significant), to separate tumors into nonsecreting and hormone-secreting (ACTH, GH, TSH, FSH, prolactin), and to include the measurement of other neuropeptide systems such as tachykinins (SP).

FAB-MS had been used in another study to confirm the MH⁺ ion of SP (confirmed by Edman sequencing) in a metastatic ileal carcinoid tissue (64).

These MS measurements of neuropeptides in the pituitary can be compared with other studies that used different analytical methods. For example, the presence and properties of different BE-related peptides in the human pituitary were studied (65). BE-like immunoreactivity (BE-li) was measured in CSF before and after removing an ACTH-secreting tumor in Cushing's disease, and the amount of BE-li increased significantly from 9.2 \pm 1.3 fmol BE-li/ml CSF to 17.9 \pm 3.1 fmol/ml ($p < 0.05$) after tumor resection (66). The ME-like receptor activity remained unchanged.

The BE-li was measured in a rare BE-containing pituitary adenoma (67), and ME-li and BE-li in a subset of thyrotrophs and in a microadenoma (68).

In situ hybridization histochemistry was used to analyze the expression of the POMC gene in 56 human postmortem pituitaries (44). A patchy pattern of mRNA hybridization was observed in the anterior lobe; no hybridization was observed in the posterior lobe. No significant effect was observed for postmortem delay (between 25 and 66 hr), gender, age (22–103 years), or cause of death. That type of analysis indicates the expression of a gene but cannot provide information on the amino acid sequence of the final posttranslationally modified neuropeptide. The MS method does convey that sequence information.

Although it is important to study a selected peptide, it is also important to analyze the relationship between that peptide and its precursor (69–71). In the human trigeminal system (calcified tissue of teeth), the amount of free ME was compared to the amount of ME released by enzyme treatment (trypsin, carbox-

ypeptidase B) of precursors (70). Approximately ten times more ME-like receptor activity from precursor was found compared to the amount of free ME. Preliminary data on the analysis of ME-containing peptides in postmortem human pituitaries have indicated the presence of several areas of immunoreactivity that might indicate the precursor forms (21).

Biological fluids contain very low levels of peptides. We have analyzed neuropeptide-li in human lumbar (20) and ventricular CSF, but the small amount of peptide (femtomoles) contained in CSF precludes the use of the MRM methods with our current MS instruments. State-of-the-art MS instruments may achieve that level of sensitivity. On the other hand, tissues such as tooth pulp (22–24), calcified tooth (70), caudate nucleus and hypothalamus (72), thalamus (73), spinal cord (74), and the pituitary and seven selected brain regions (hypothalamus, caudate nucleus, midbrain, amygdala, thalamus, pons–medulla, and hippocampus) (19) contain higher levels of peptide, and some are amenable to quantification by MS methods. Furthermore, as shown above, product-ion scans, MH^+ , and MRM measurements can all be performed on a fraction of one human pituitary extract (7).

5.3. Electrospray

As mentioned above, ES offers several significant advantages for the quantitative analysis of biological peptides (11). For example, the ES mass spectrum of synthetic leucine enkephalin (LE = YGGFL) is shown in Fig. 4.12; the MH^+ ion occurs at m/z 556 (11). The ES spectrum of synthetic $BE_{1-31, human}$ is shown in Fig. 4.13 and contains an abundant $(M + 5H)^{5+}$ ion. We and others have shown that the number of charges that a peptide can carry during EI relates to the number of positive charges in the peptide. For example, Table 4.4 collects data from the ES mass spectra of the neuropeptides that we have studied and correlates the number of basic amino acids with the relative abundance of the MH^+ ions (11).

Methionine enkephalin was quantified by ES–MS in three human pituitaries using the MH^+ data of endogenous ME compared to the internal standard, $[^2H_5]^4Phe$ -ME. The amounts found were 9.1, 8.2, and 4.7 pmol ME/mg protein. Intact BE was quantified by ES–MS, using the ion current attributable to the $(M + 5H)^{5+}$ ion. Compared to an external calibration curve obtained by analyzing solutions of synthetic BE over the range 5 fmol to 50 pmol, the amount in one human pituitary was 660 fmol BE/mg protein.

6. CONCLUSIONS

The details of the basic principles of, and the experimental data resulting from, the quantitative analytical MS measurement of opioid peptides in human

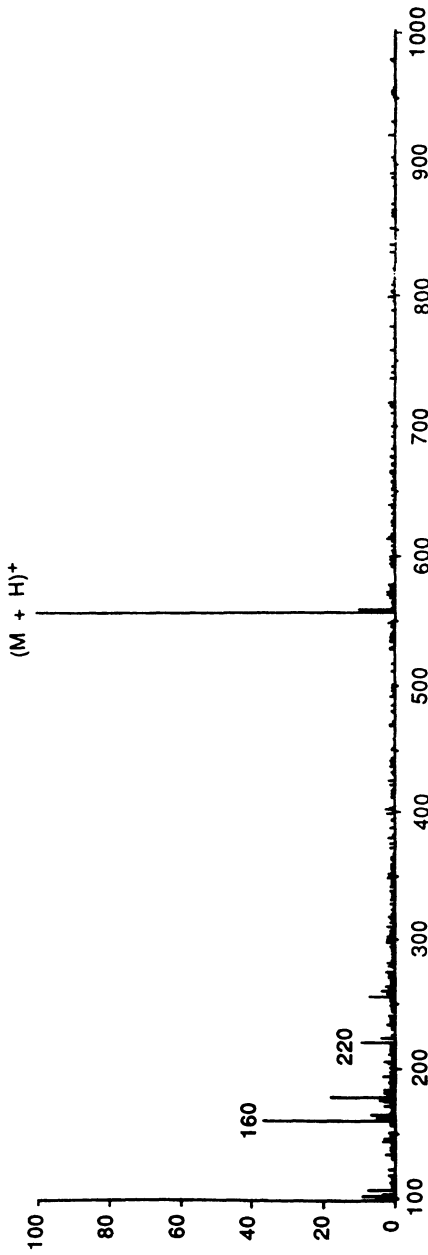


Figure 4.12. The ES spectrum of synthetic LE. The MH^+ ion is at m/z 556. [From Dass *et al.* (11). Reprinted with permission from Elsevier Science Publishing Co., Inc., from Electrospray mass spectrometry for the analysis of opioid peptides and for the quantification of endogenous methionine enkephalin and β -endorphin, by Dass *et al.*, *Journal of the American Society for Mass Spectrometry*, Vol. 2, pp. 149–156. Copyright 1991 by the American Society for Mass Spectrometry.]

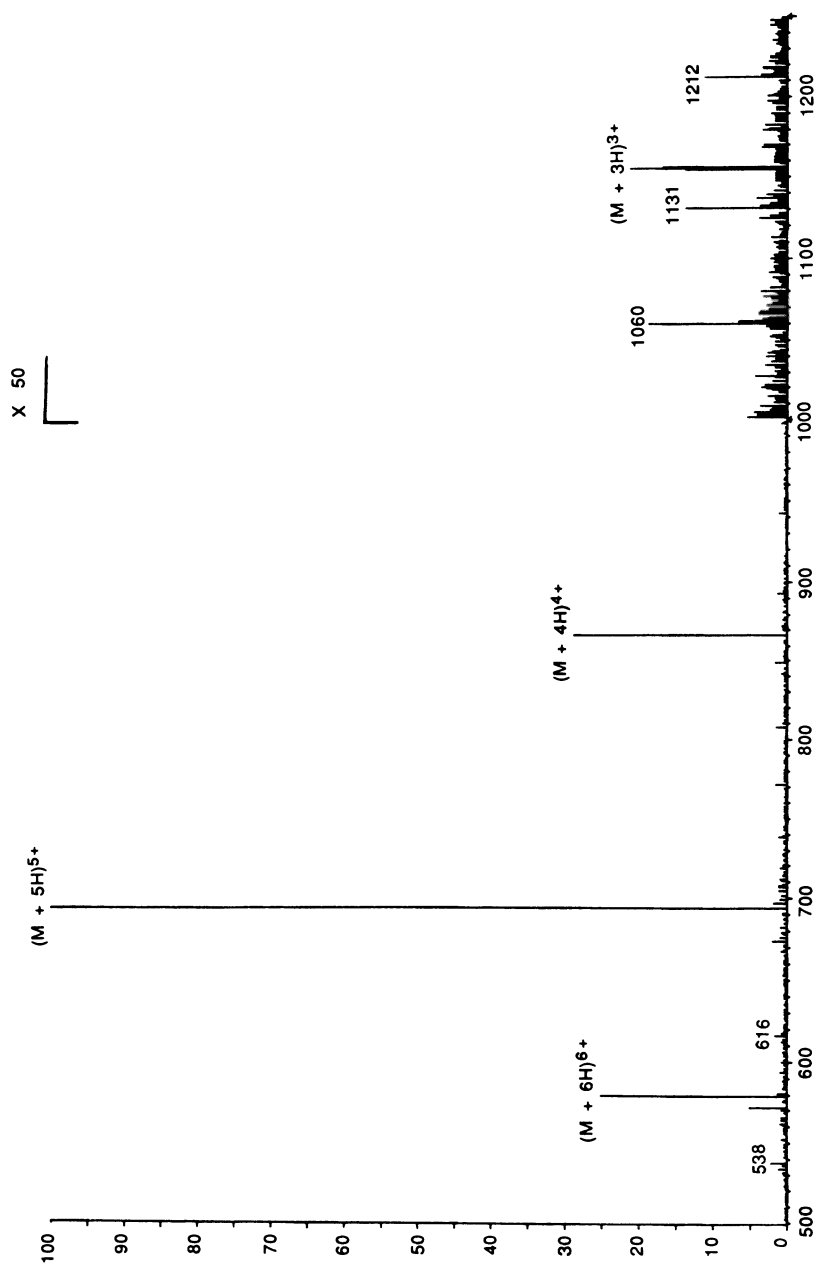


Figure 4.13. The ES spectrum of synthetic BE 1-31, human. The $[M + 3H]^3+$, $[M + 4H]^4+$, $[M + 5H]^5+$, and $[M + 6H]^6+$ ions are at m/z 1156, 867, 694, and 578, respectively. [Reprinted with permission from Elsevier Science Publishing Co., Inc., from Electro spray mass spectrometry for the analysis of opioid peptides and the quantification of endogenous methionine enkephalin and β -endorphin, by Dass *et al.*, *Journal of the American Society for Mass Spectrometry*, Vol. 2, pp. 149-156. Copyright 1991 by the American Society for Mass Spectrometry.]

Table 4.4
ES Mass Spectra of Synthetic Neuropeptides

Neuropeptide	Number of basic amino acid residues	Relative abundance of					
		(M + H) ⁺	(M + 2H) ²⁺	(M + 3H) ³⁺	(M + 4H) ⁴⁺	(M + 5H) ⁵⁺	(M + 6H) ⁶⁺
LE	0	100	—	—	—	—	—
ME	0	100	—	—	—	—	—
ME-Lys-Lys	2	4	100	—	5	—	—
Dynorphin A ₁₋₈	2	<1	100	—	8	—	—
Dynorphin A ₁₋₉	3	<1	12	100	—	—	—
Dynorphin A ₁₋₁₀	3	<1	17	100	—	—	—
Dynorphin A ₁₋₁₃	5	—	3	67	100	—	—
Dynorphin A ₁₋₁₇	5	—	1	15	100	<1	—
Dynorphin B ₁₋₁₃	3	—	5	100	3	—	—
β-Endorphin ₁₋₃₁	5	—	—	1	29	100	26

From (11).

pituitaries have been discussed in this chapter. These studies are significant because molecular specificity is an important experimental parameter needed to elucidate molecular mechanisms in tumor formation in the human pituitary. This section summarizes briefly some of the pertinent experimental aspects of this novel method of peptide measurement.

6.1. *Detection Sensitivity*

Radioimmunoassay is the analytical method used in most laboratories around the world to measure biological peptides. The detection sensitivity of RIA is generally at the femtomole level. Some literature reports suggest that the molecular specificity of RIA is very high and, furthermore, that no chromatographic separation is needed before measuring a peptide. That claim is not supported by experimental data (9); RIA cannot provide any primary structure (amino acid sequence) information (3,4) because it is based only on secondary structural characteristics (71). Only protein-protein intermolecular factors are involved in antibody-antigen interactions. HPLC with RIA (using either polyclonal or monoclonal antibodies) cannot overcome that limitation. Those limitations of RIA are understood readily once the molecular steps in an immunoassay are rationalized. For example, an antibody generally is raised to a peptide-carrier molecule complex such as thyroglobulin-ME₂₃ (75) because ME itself is not inherently immunogenic. Thus, specificity toward the carboxy terminus of ME is lost. In another example, enzymoimmunologic measurements indicated a ratio of six SP molecules per bovine serum albumin carrier molecule (48). In any event, direct amino acid sequence data cannot be obtained from any type of immune-based measurement.

6.2. *Nomenclature*

The multiplicity of nomenclature that appears in the literature of RIA measurements must also be discussed. For example (using ME as an example), "methionine enkephalin-like immunoactivity" (ME-li) is the only datum obtained from an RIA measurement. The incorrect term "immunoreactive methionine enkephalin" (ir-ME) is used frequently. However, that term implies erroneously that ME (= YGGFM) was measured. Clearly, amino acid data must be provided before that claim can be made. Similar arguments are applied to the term "ME immunoreactivity." The term "methionine enkephalin" has only one meaning—the amino acid sequence Tyr-Gly-Gly-Phe-Met is known. Thus, peptide-li is the only accurate term to be used for all RIA measurements (76).

Similar arguments extend to the use of receptors to measure peptides; for

example, for ME the term “methionine enkephalin-like receptor activity” should be used (9,19,71).

6.3. Molecular Specificity

Because of the need for molecular specificity, the ionization characteristics and the MS fragmentation behavior of each and every neuropeptide to be studied in a biological tissue by ES, FAB-MS, MS/MS, or MRM methods must be studied first in great detail (41,51-53). Because a wide range of peptide molecular weights and polarities must be studied, all ionization and instrumental techniques must be used for this problem. Various peptides have different pH, hydrophobicity, and hydrophilicity properties, and FAB-MS is not always the optimal ionization method. Thus, ES-MS/MS will be a powerful adjunct method for neuropeptide analysis.

6.4. Endogenous Neuropeptide Systems

New data are emerging from this laboratory that identify the molecular mechanisms involved in tissue pathophysiologies such as anterior pituitary tumor formation. For example, the ratio of ME and BE has been measured to determine whether an abnormal relationship exists between the expression of two different neuropeptide genes, proenkephalin A (ME) and POMC (BE), in human pituitary tumor tissues (7). This type of finding is important because, up until now, most tumors have been detected and characterized only because they hypersecrete a particular hormone (ACTH, GH, FSH, TSH, prolactin, etc.). On the other hand, the mass spectrometric data described above did indicate an altered metabolism of the proenkephalin A and POMC neuropeptide systems. The absolute amounts of two neuropeptides (ME, BE) differed between the controls and tumors, and the relative amounts of the two neuropeptide systems (proenkephalin A, POMC) also varied.

In other studies, mass spectrometry was used to quantify the amount of ME released by *in vitro* enzymolysis of a precursor molecule in the human trigeminal system (70) and in the bovine cornea (71). In the control human trigeminal system, calcified tooth tissue contains more than ten times more ME remaining within its precursor form(s) compared to the free native pentapeptide. Those data indicate the importance of investigating entire neuropeptidergic systems and the interaction between different systems.

ACKNOWLEDGMENTS. The author gratefully acknowledges the financial support of NIH (GM 26666, DRR 01651); the scientific collaboration of several colleagues (G. Fridland, C. Dass, J. Kusmierz, J. Lovelace, P. Tinsley, L.

Greene, and J. T. Robertson); the editorial assistance of G. Fridland and C. Dass; and the typing assistance of D. Reid and V. Antwine.

REFERENCES

1. Odell, W. D., and Nelson, D. H. (eds.), 1984, *Pituitary Tumors*, Futura, Mt. Kisco, NY.
2. Desiderio, D. M., 1983, in: HPLC and MS of biologically important peptides, *Advances in Chromatography*, Vol. 22 (J. C. Giddings and P. Brown, eds.), Marcel Dekker, New York, pp. 1–36.
3. Desiderio, D. M., 1984, *Analysis of Neuropeptides by Liquid Chromatography and Mass Spectrometry*, Elsevier, Amsterdam.
4. Desiderio, D. M. (ed.), 1991, *Mass Spectrometry of Peptides*, CRC Press, Boca Raton, FL.
5. Fridland, G. H., and Desiderio, D. M., 1986, Profiling of neuropeptides using gradient reversed-phase high-performance liquid chromatography with novel detection methodologies, *J. Chromatogr.* **379**:251–268.
6. Desiderio, D. M., and Fridland, G., 1986, in: *Mass Spectrometry in Biomedical Research* (S. Gaskell, ed.), John Wiley & Sons, New York, pp. 443–458.
7. Kusmierz, J. J., Sumrada, R., and Desiderio, D. M., 1990, Fast atom bombardment mass spectrometric quantitative analysis of methionine enkephalin in human pituitary tissues, *Anal. Chem.* **62**:2395–2400.
8. Kusmierz, J. J., Dass, C., and Desiderio, D. M., 1991, Mass spectrometric measurement of β -endorphin and methionine enkephalin in human pituitaries—tumors and post-mortem controls, *Int. J. Mass Spectrom. Ion Proc.* **111**:247–262.
9. Lovelace, J. L., Kusmierz, J. J., and Desiderio, D. M., 1991, Analysis of methionine enkephalin in human pituitary by multi-dimensional RP-HPLC, radioreceptorassay, radioimmunoassay, FAB–MS, and FAB–MS–MS, *J. Chromatogr.* **530**:235–252.
10. Dass, C., Fridland, G. H., Tinsley, P. W., Killmar, J. T., and Desiderio, D. M., 1989, Characterization of β -endorphin in human pituitary by fast atom bombardment mass spectrometry of trypsin-generated fragments, *Int. J. Peptide Protein Res.* **34**:81–87.
11. Dass, C., Kusmierz, J. J., Desiderio, D. M., Jarvis, S. A., and Green, B. N., 1991, Electrospray mass spectrometry for the analysis of opioid peptides and for the quantification of endogenous methionine enkephalin and β -endorphin, *J. Am. Soc. Mass Spectrom.* **2**:149–156.
12. Dass, C., Kusmierz, J. J., and Desiderio, D. M., 1991, Mass spectrometric quantification of endogenous β -endorphin, *Biol. Mass Spectrom.* **20**:130–138.
13. Desiderio, D. M., Kusmierz, J. J., Zhu, X., Dass, C., Hilton, D., and Robertson, J. T., 1992, Increased protachykinin, POMC, and proenkephalin A peptides in human pituitary tumors, *Biol. Mass Spectrom.* (Submitted).
14. Lawson, A. M., Lim, C. K., and Richmond, W. (eds.), 1980, *Current Developments in the Clinical Applications of HPLC, GC, and MS*, Academic Press, London.
15. Lawson, A. M. (ed.), 1989, *Mass Spectrometry*, W. de Gruyter, Berlin.
16. Biemann, K., and Martin, S. A., 1987, Mass spectrometric determination of the amino acid sequence of peptides and proteins, *Mass Spectrom. Rev.* **6**:1–76.
17. Biemann, K., 1990, in: Sequencing of peptides by tandem mass spectrometry and high-energy collision-induced dissociation, *Methods in Enzymology*, Vol. 193 (J. A. McCloskey, ed.), Academic Press, New York, pp. 455–479.
18. Stults, J. T., 1990, in: Peptide sequencing by mass spectrometry, *Biomedical Applications of Mass Spectrometry* (C. H. Suelter and J. T. Watson, eds.), Wiley–Interscience, New York, pp. 145–201.

19. Takeshita, H., Desiderio, D. M., and Fridland, G., 1986, Metabolic profiling of opioid peptides in canine pituitary and selected brain regions using HPLC with a RRA detector, *Biomed. Chromatogr.* **1**:126–139.
20. Liu, D., Dass, C., Wood, G., and Desiderio, D. M., 1989, Opioid and tachykinin peptides, and their precursors and precursor-processing enzymes, in human cerebrospinal fluid. *J. Chrom.* **500**:395–412.
21. Lovelace, J. L., 1991, *Characterization of Proenkephalin A in the Human Pituitary Gland*, Thesis, University of Tennessee, Memphis.
22. Walker, J. A., Tanzer, F. S., Harris, E. F., Wakelyn, C., and Desiderio, D. M., 1987, The enkephalin response in human tooth pulp to orthodontic force, *Am. J. Orthodont. Dentofac. Orthop.* **92**:9–16.
23. Parris, W. G., Tanzer, F. S., Fridland, G. H., Harris, E. F., Killmar, J., and Desiderio, D. M., 1989, Effects of orthodontic force on methionine enkephalin and substance P concentrations in human pulpal tissue, *Am. J. Orthodont. Dentofac. Orthop.* **95**:479–489.
24. Robinson, Q. C., Killmar, J. T., Desiderio, D. M., Harris, E. F., and Fridland, G., 1989, Immunoreactive evidence of β -endorphin and methionine enkephalin-Arg-Gly-Leu in human tooth pulp, *Life Sci.* **45**:987–992.
25. Barber, M., Bordoli, R. S., Sedgwick, R. D., Tyler, A. N., and Whalley, E. T., 1981, Fast atom bombardment mass spectrometry of bradykinin and related compounds, *Biomed. Mass Spectrom.* **8**:337–342.
26. Whitehouse, C. M., Dreyer, R. N., Yamashita, M., and Fenn, J. B., 1985, Electrospray interface for liquid chromatographs and mass spectrometers, *Anal. Chem.* **57**:675–679.
27. Hunt, D. F., Krishnamurthy, T., Shabanowitz, J., Griffin, P. R., Yates, J. R., Martino, P. A., McCormack, A. L., and Hauer, C. R., 1991, Peptide sequence analysis by triple quadrupole and quadrupole fourier transform mass spectrometry, in: *Mass Spectrometry of Peptides* (D. M. Desiderio, ed.), CRC Press, Boca Raton, FL, pp. 139–158.
28. Walz, D. A., Wider, M. D., Snow, J. W., Dass, C., and Desiderio, D. M., 1988, The complete amino acid sequence of porcine gastrotropin, and ileal protein which stimulates gastric acid and pepsinogen secretion, *J. Biol. Chem.* **263**:14189–14195.
29. Johnson, R. S., and Biemann, K., 1987, The primary structure of thioredoxin from *Chromatium vinosum* determined by high-performance tandem mass spectrometry, *Biochemistry*, **26**:1209–1214.
30. Scoble, H. A., and Martin, S. A., 1990, Characterization of recombinant proteins, in: *Methods of Enzymology*, Vol. 193 (J. A. McCloskey, ed.), Academic Press, New York, pp. 519–536.
31. Lederer, E., 1968, Mass spectrometry of natural and synthetic peptide derivatives, *Pure Appl. Chem.* **17**:489–517.
32. Biemann, K., Gapp, F., and Seibl, J., 1959, Application of mass spectrometry to structure problems. I. Amino acid sequence in peptides, *J. Am. Chem. Soc.* **81**:2274.
33. Burgus, R., Dunn, T. F., Desiderio, D. M., Ward, D. N., Vale, W., and Guillemin, R., 1970, Characterization of ovine hypothalamic hypophysiotrophic TSH-releasing factor, *Nature* **226**:321–325.
34. Desiderio, D. M., Burgus, R., Dunn, T. F., Ward, D. N., Vale, W., and Guillemin, R., 1971, The primary structure of the hypothalamic hypophysiotropic thyroid stimulating hormone releasing factor of ovine origin, *Org. Mass Spectrom.* **5**:221–228.
35. Emson, P. C. (ed.), 1983, *Chemical Neuroanatomy*, Raven Press, New York.
36. Krieger, D. T., Brownstein, M. J., and Martin, J. B. (eds.), 1983, *Brain Peptides*, Wiley-Interscience, New York.
37. Valentino, K. L., Eberwine, J. H., and Barchas, J. D. (eds.), 1987, *In situ Hybridization*, Oxford University Press, New York.
38. Wessel, H. B., 1990, Dystrophin: A clinical perspective, *Pediatr. Neurol.* **6**:3–12.

39. McLafferty, F. W. (ed.), 1983, *Tandem Mass Spectrometry*, John Wiley & Sons, New York.
40. Busch, K. L., Glish, G. L., and McLuckey, S. A., 1988, *Mass Spectrometry/Mass Spectrometry: Techniques and Applications of Tandem Mass Spectrometry*, VCH Publishers, New York.
41. Desiderio, D. M., 1986, FAB-MS/MS study of two neuropeptides, dynorphins 1-7 and 1-13, *Int. J. Mass Spectrom. Ion Proc.* **74**:217-233.
42. Bursey, M. M., 1991, Comment to readers: Style and the lack of it, *Mass Spectrom. Rev.* **10**:1-2.
43. Sagar, S. M., Beal, M. F., Marshall, P. E., Landis, D. M. D., and Martin, J. B., 1984, Implications of neuropeptides in neurological diseases, *Peptides* **5**:255-262.
44. Mengod, G., Vivanco, M. M., Christnacher, A., Probst, A., and Palacios, J. M., 1991, Study of pro-opiomelanocortin mRNA expression in human postmortem pituitaries, *Mol. Brain Res.* **10**:129-137.
45. Liston, D., Patey, G., Rossier, J., Verbanck, P., and Vanderhaeghen, J. J., 1984, Processing of proenkephalin is tissue-specific, *Science* **225**:734-737.
46. Grouselle, D., Tixier-Vidal, A., and Pradelles, P., 1982, A new improvement of the sensitivity and specificity of radioimmunoassay for thyroliberin, application to biological samples, *Neuropeptides* **3**:29-44.
47. Bolton, A. E., and Hunter, W. M., 1973, The labeling of proteins to high specific radioactivities by conjugation to a ^{125}I -containing acylating agent, *Biochem. J.* **133**:529-539.
48. Couraud, J. Y., Frobert, Y., Conrath, M., Renzi, D., Grassi, J., Drapeau, G., Regoli, D., and Pradelles, P., 1987, Monoclonal antibodies to substance P: Production, characterization of their fine specificities, and use in immunocytochemistry, *J. Neurochem.* **49**:1708-1719.
49. Higa, T., and Desiderio, D. M., 1989, Optimizing recovery of peptides from an octadecylsilyl (ODS) cartridge, *Int. J. Peptide Protein Res.* **33**:250-255.
50. Desiderio, D. M., and Cunningham, M. D., 1981, Triethylamine formate buffer for HPLC-FDMS of oligopeptides, *J. Liq. Chromatogr.* **4**:721-733.
51. Dass, C., and Desiderio, D. M., 1987, Fast atom bombardment mass spectrometry analysis of opioid peptides, *Anal. Biochem.* **163**:52-66.
52. Dass, C., and Desiderio, D. M., 1989, Characterization of neuropeptides by fast atom bombardment and *B/E* linked-field scan techniques, *Int. J. Mass Spectrom. Ion Proc.* **92**:267-287.
53. Dass, C., 1991, Applications of mass spectrometry for characterization of neuropeptides, in: *Mass Spectrometry of Peptides* (D. M. Desiderio, ed.), CRC Press, Boca Raton, FL, pp. 327-345.
54. Aberth, W., Straub, K. M., and Burlingame, A. L., 1982, Secondary ion mass spectrometry with cesium ion primary beam and liquid target matrix for analysis of bioorganic compounds, *Anal. Chem.* **54**:2029-2034.
55. Busch, K. L., 1991, Sample preparation and matrix selection for analysis of peptides by FAB, in: *Mass Spectrometry of Peptides* (D. M. Desiderio, ed.), CRC Press, Boca Raton, FL, pp. 173-200.
56. Gower, J. L., 1985, Matrix compounds for fast atom bombardment mass spectrometry, *Biomed. Mass Spectrom.* **12**:191-196.
57. Tolun, E., Dass, C., and Desiderio, D. M., 1987, Trace level measurement of enkephalin peptides at the attomole/femtomole level by FAB-MS, *Rapid Commun. Mass Spectrom.* **1**:77-79.
58. de Pauw, E., 1990, Matrix selection for liquid secondary ion and fast atom bombardment mass spectrometry, in: *Methods in Enzymology*, Vol. 193 (J. A. McCloskey, ed.), Academic Press, New York, pp. 201-214.
59. Martin, S. A., Costello, C. E., and Biemann, K., 1982, Optimization of experimental procedures for fast atom bombardment mass spectrometry, *Anal. Chem.* **54**:2362-2368.
60. Ahmed, M. S., Randall, L. W., Sibai, B., Dass, C., Fridland, G., Desiderio, D. M., and Tolun,

- E., 1987, Identification of dynorphin 1–8 in human placenta by mass spectrometry, *Life Sci.* **40**:2067–2076.
61. Roepstorff, P., and Fohlman, J., 1984, Proposal for a common nomenclature for sequence ions in mass spectra of peptides, *Biomed. Mass Spectrom.* **11**:601.
 62. Biemann, K., 1990, in: *Methods in Enzymology*, Vol. 193 (J. A. McCloskey, ed.), Academic Press, New York, pp. 886–887.
 63. Dass, C., and Desiderio, D. M., 1988, Particle beam-induced reactions between peptides and liquid matrices, *Anal. Chem.* **60**:2723–2729.
 64. Roth, K., Makk, G., Beck, O., Faull, K., Tatemoto, K., Evans, C., and Barchas, J., 1985, Isolation and characterization of substance P, substance P 5–11, and substance K from two metastatic ileal carcinoids, *Reg. Peptides* **12**:185–199.
 65. Vuolteenaho, O., Leppaluoto, J., Hoyhtya, M., and Hirvonen, J., 1983, Beta-endorphin-like peptides in autopsy pituitaries from adults, neonates, and fetuses, *Acta Endocrinol.* **102**:27–34.
 66. Furui, T., Kageyama, N., Kuwayama, A., Nakao, K., and Fukushima, M., 1981, Increase of β -endorphin in cerebrospinal fluid after removal of ACTH-secreting pituitary adenomas, *Pain* **11**:127–132.
 67. Trouillas, J., Girod, C., Sassolas, G., Vitte, P., Claustrat, B., Perrin, G., Lheritier, M., Fischer, C., and Dubois, M., 1984, A human β -endorphin pituitary adenoma, *J. Clin. Endocrinol. Metab.* **58**:242–249.
 68. Roth, K., and Krause, J., 1990, Substance P is present in a subset of thyrotrophs in the human pituitary, *J. Clin. Endocrinol. Metab.* **71**:1089–1095.
 69. Panula, P., and Lindberg, I., 1987, Enkephalins in the rat pituitary gland: Immunohistochemical and biochemical observations, *Endocrinology* **121**:48–58.
 70. Tanzer, F. S., Tolun, E., Fridland, G. H., Dass, C., Killmar, J., Tinsley, P. W., and Desiderio, D. M., 1988, Methionine-enkephalin peptides in human teeth, *Int. J. Peptide Protein Res.* **32**:117–122.
 71. Tinsley, P. W., Fridland, G. H., Killmar, J. T., and Desiderio, D. M., 1989, Purification, characterization and localization of neuropeptides in the cornea, *Peptides* **9**:1373–1379.
 72. Yamada, S., and Desiderio, D. M., 1982, Measurement of endogenous neuropeptides in canine caudate nuclei and hypothalami with high performance liquid chromatography and field desorption mass spectrometry, *Anal. Biochem.* **127**:213.
 73. Desiderio, D. M., and Yamada, S., 1982, Measurement of endogenous leucine enkephalin in canine thalamus by HPLC and FD–MS, *J. Chromatogr.* **239**:87–95.
 74. Desiderio, D. M., and Yamada, S., 1983, FDMS measurement of picomole amounts of leucine enkephalin in canine spinal cord tissue, *Biomed. Mass Spectrom.* **10**:358–360.
 75. Gros, C., Pradelles, P., Rouget, C., Bepoldin, O., Dray, F., Fournie-Zaluski, M. C., Roques, B. P., Pollard, H., Llorens-Cortes, C., and Schwartz, J. C., 1978, Radioimmunoassay of methionine- and leucine-enkephalins in regions of rat brain and comparison with endorphins estimated by a radioreceptorassay, *J. Neurochem.* **31**:29–39.
 76. Merchenthaler, I., Maderdrut, J. L., Altschuler, R. A., and Petrusz, P., 1986, Immunocytochemical localization of proenkephalin-derived peptides in the central nervous system of the rat, *Neuroscience* **17**:325–348.

Neurotransmitters

Kym F. Faull

1. INTRODUCTION

Neurotransmitters are chemical agents that mediate the transmission of nerve impulses across the synaptic cleft between adjacent nerve cells. They are essential components of the peripheral and central nervous systems (CNS), and their role as the chemical messengers responsible for transsynaptic information transfer has excited biologists ever since their role in mammalian physiology was recognized.

1.1. History of the Recognition of Neurotransmitters

The discovery of the involvement of chemicals in neuronal communication dates to the beginning of this century from observations made by T. R. Elliott, who found that “adrenalin” simulated the effects of electrical stimulation of sympathetic nerves (1,2) and put forward a hypothesis attributing to adrenalin the function of a chemical transmitter for sympathetic nerve impulses [cited by Dale (3)]. However, the demonstration 17 years later by Otto Loewi of the release of a compound following stimulation of the vagus nerve is most often cited as providing the first compelling evidence for chemical neurotransmission (4). In the same year Cannon and Uridil (5) described the properties of a factor originating in the liver that accelerated the beat of the denervated heart. The compounds discovered by Loewi and Cannon and Uridil have subsequently been identified as acetylcholine and norepinephrine, respectively, the first two neurotransmitters to receive extensive investigation. A debate about the mode of information transfer

Kym F. Faull • The Neuropsychiatric Institute and Department of Psychiatry and Biobehavioral Sciences, UCLA School of Medicine, Los Angeles, California 90024.

in the CNS followed, which centered on the relative importance of chemical versus purely electrical communication for the rapid transfer of signals (6,7). Chemical neurotransmission emerged as the overwhelmingly important mode for one reason: the results from electrical recording of nerve cell activity following microiontophoretic application of compounds were incompatible with purely electrical neurotransmission (8).

Two other milestones in this story are worthy of note. The first is the discovery in 1946, independently by von Euler in Sweden and Holtz in Germany, of norepinephrine as a natural constituent of mammalian tissues (3), and the second is Marthe Vogt's bioassay measurements of the concentrations of "sympathin" (actually norepinephrine plus epinephrine) in the mammalian CNS under normal conditions and following the administration of drugs (9). The observations by Vogt had significant implications for our understanding of the role of these compounds in brain function because for the first time attention was drawn to their markedly different concentrations in different regions of the mammalian brain, and the results showed that the tissue concentrations were influenced by centrally acting drugs. Since that time the complexity of the nervous system has become increasingly apparent as more neurotransmitters have been discovered and their receptors have been characterized. The focus of this chapter is on mass spectrometry and neurotransmitters (with emphasis on the CNS systems), but before discussing this subject some important features of the nervous system are described in general terms to lay the necessary background.

1.2. Neurotransmitters and Their Role in Information Transfer

Synaptic transmission is the most common form of communication in the mammalian nervous system. However, areas of the nervous system exist in which other forms of intercellular communication are important [such as gap junctions and electrotonic (ephaptic) transmission], although these modes are not confined solely to neurons. Synaptic transmission is confined to neurons, and the feature that distinguishes neurons from other cell types is that they are electrically excitable. When stimulated, a wave of depolarization of the cell membrane travels along the length of the neuron. It is thought that when this wave reaches the nerve terminal, voltage-gated calcium channels open in the cell membrane, resulting in an influx of calcium ions from the extracellular compartment. The ensuing rise in intracellular calcium ion concentration triggers the release of neurotransmitters into the extracellular compartment between adjacent nerve cells known as the synapse (for a recent review, see ref. 10).

The classical idea is that the neurotransmitters are localized in the presynaptic terminal in membrane-bound vesicles, which deposit their contents into the synapse by exocytosis. This model is established for the biogenic amines (the catecholamines, serotonin, and acetylcholine) and the neuropeptides. Initially, it

was thought that the amino acid neurotransmitters were an exception to this rule because attempts to demonstrate their localization in membrane-bound vesicles were unsuccessful. However, recent results have shown that glutamate is enriched in rat brain cortex synaptic vesicles and that glutamate is taken up into cortex vesicles in an ATP-dependent and sodium-independent manner. Should similar findings hold true for the other amino acid neurotransmitters, the classical idea of neurotransmitter localization in membrane-bound vesicles will be extended to another important class of these compounds (see refs. 11 and 12 and references cited therein).

Following release, the neurotransmitters diffuse through the extracellular compartment (synaptic cleft) and are available for recognition by any of a variety of receptors that are located on the extracellular membranes of adjacent postsynaptic neurons. In the case of excitatory neurotransmitters, binding to the receptor results in hypopolarization of the postsynaptic neuron, which can initiate a wave of electrical depolarization in the cell. In the case of inhibitory neurotransmitters, binding to the receptor results in hyperpolarization of the postsynaptic neuron with consequent inhibition of electrical excitation that might otherwise have occurred. Some receptors are also located on the outside surface of the presynaptic neuron, and binding to these receptors is thought to be one mechanism involved in the regulation of neurotransmitter release. Other mechanisms exist for regulating neurotransmitter concentration in the synaptic cleft. One is the active reuptake of neurotransmitter into the presynaptic terminal. This mechanism may be a general one for controlling synaptic concentrations of neurotransmitters because it is well established for the catecholamines and serotonin, and evidence exists that it may also be important for acetylcholine, histamine, the amino acid transmitters, and some neuropeptides including thyrotropin-releasing hormone, substance P, and enkephalin. Degradative enzymes in the extracellular compartment rapidly degrade neurotransmitters, and the activity of acetylcholinesterase and peptidases are two such examples that are thought to be particularly important for regulating the synaptic concentrations of acetylcholine and neuropeptides, respectively.

Although useful for illustrative purposes, cartoons of neurons such as the one shown in Fig. 5.1 greatly simplify the geography of the arrangement of cells in the nervous system. A more realistic impression of the complexity of this cellular environment, and the relative sizes of the cellular processes and the synapse, are obtained from electron micrographs, typical examples of which are shown in Fig. 5.2. The neurons occur in close proximity to a variety of other cell types, most notably glia and Schwann cells. For a long time, glia were thought mainly to provide physical support for the neurons and also to have some role in the supply of nutrients. This idea is now changing because new results indicate that glia may also be involved in neurotransmitter processing. Some enzymes involved in neurotransmitter biosynthesis are expressed by glia, and some neuro-

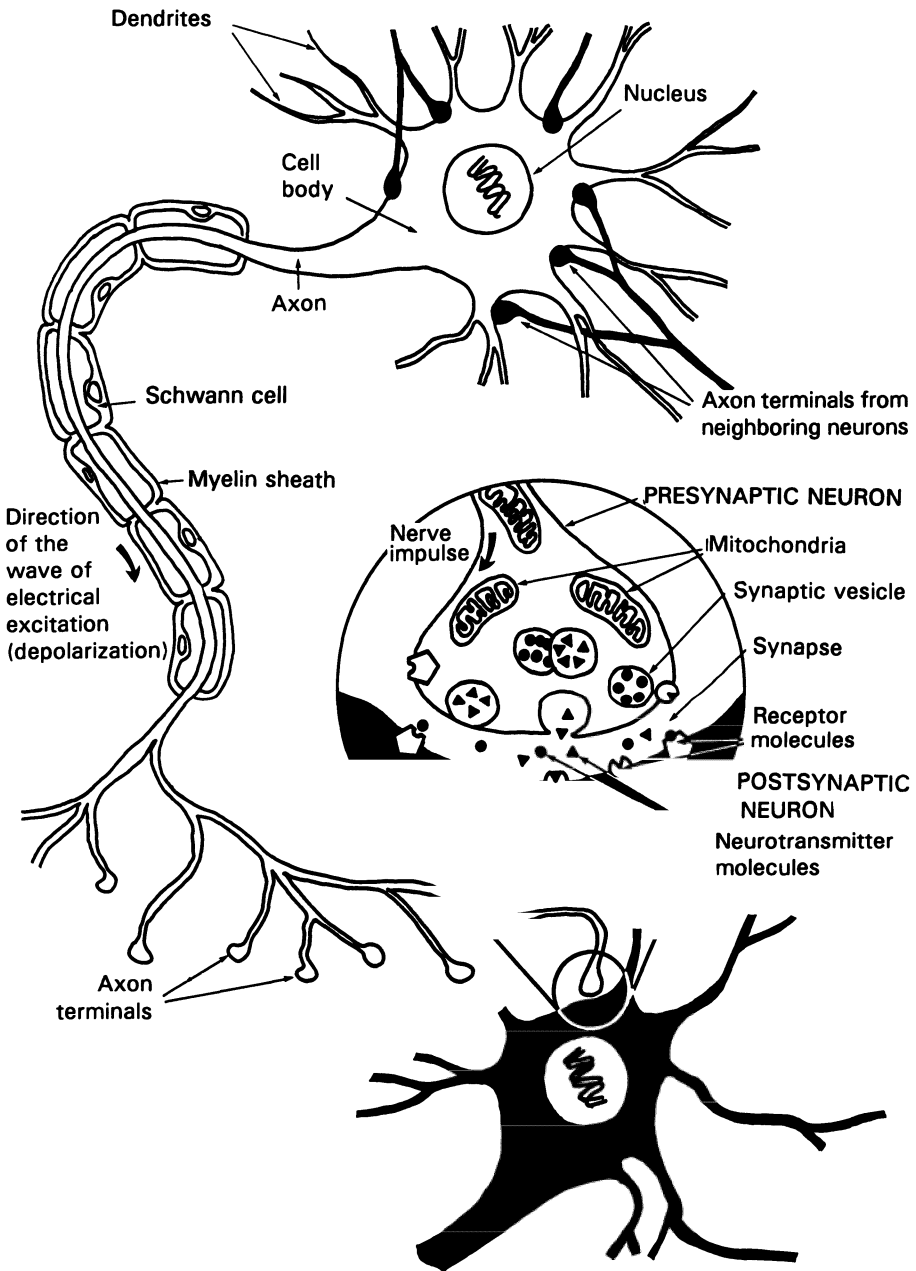


Figure 5.1. Cartoon of a neuron with an expanded view of the principal features of the synaptic cleft.

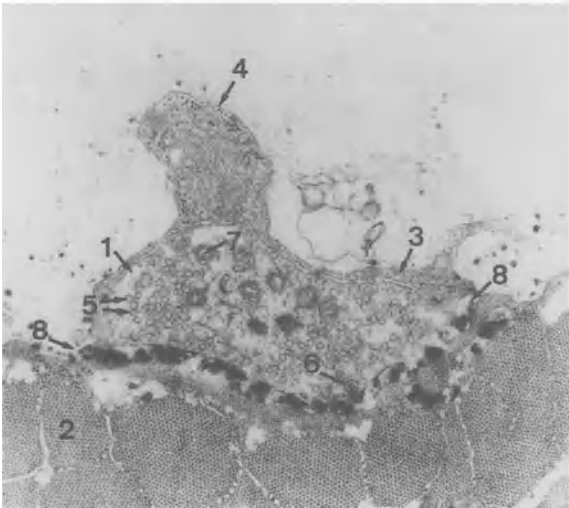
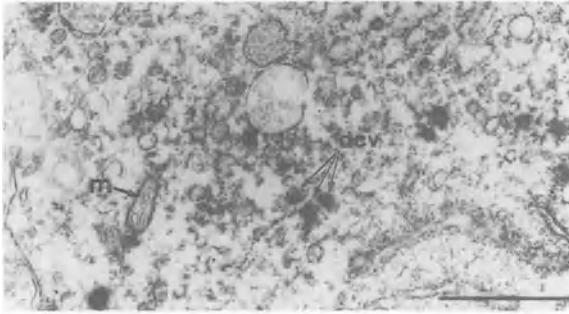
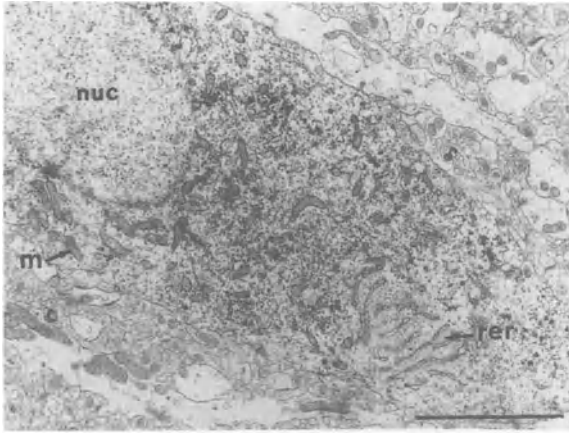
transmitter receptors may be also located on the surfaces of glia. Furthermore, intercellular communication between glia, and between glia and neurons, occurs as a result of connections made via gap junctions. The Schwann cells wrap around neuronal axons and form a myelin sheath that enhances the speed with which the wave of depolarization travels down the axon.

1.3. Characteristics of Synaptic Vesicles

Electron microscopic and biochemical examinations have led to the recognition of several morphologically distinct types of synaptic vesicles in neurons. These vesicles vary in size, abundance, and in the electron density of their contents. The electron-lucent uniformly sized organelles are thought to contain predominantly classical neurotransmitters, and the larger dense-core, less-abundant vesicles are thought to contain predominantly neuropeptide transmitters. One hypothesis has been that the small electron-lucent vesicles may be involved in short-range communication between adjacent nerve cells, whereas the large dense-core vesicles may be involved in long-range communication between neurons. Convincing immunocytochemical evidence now exists to support the existence of subpopulations of vesicles that contain a classical neurotransmitter and a neuropeptide in the same vesicle. An example of colocalization of this type is that of serotonin and substance P in large dense-core vesicles in the raphe nuclei and dorsal horn of the spinal cord. In addition, ample evidence exists to refute the long-standing notion (attributed to the English electrophysiologist Sir Henry Dale) that each neuron contains only one type of neurotransmitter. Examples of colocalization of different neurotransmitters within the same neuron include dopamine and cholecystinin in some midbrain neurons and acetylcholine and vasoactive intestinal polypeptide in the salivary gland. More recent electron microscopic examinations with antisera directed against amino acid conjugates have revealed characteristic vesicles in nerve terminals that contain abundant stores of glutamate, aspartate, glycine, and taurine (11).

1.4. Anatomic Localization

The anatomic localization of neurotransmitters has been, and still is, the subject of close examination, and elegant techniques have been developed for their cellular localization in thin tissue sections using immunologic and fluorescent approaches. The different neurotransmitters have distinct but overlapping anatomic and neuroanatomic distributions. Despite the fact that they are localized in high concentrations within the neuron, bulk tissue concentrations are much lower, and this factor creates problems for their isolation and identification. When expressed in comparable units, the various neurotransmitters show an enormous range of tissue concentration, which varies across three orders of



magnitude (Table 5.1). In tissues that are predominantly composed of nerve terminals, where neurotransmitters are most concentrated, the descending order of bulk tissue concentrations is: amino acids \gg acetylcholine $>$ the catecholamines and serotonin $>$ neuropeptides. Although a proportion of glutamate, aspartate, and glycine would be in a general metabolic pool for use in other aspects of cellular metabolism such as protein synthesis, it is thought that the bulk tissue content of these compounds in the region of the nerve terminals is in the neurotransmitter pool. The order of tissue concentrations of the various compounds has implications for the subject of this volume because it is in the area of neuropeptide identification that mass spectrometry has much to offer, but neuropeptides have the lowest bulk tissue concentration.

1.5. The Correlation between Sites of Release and Receptor Density

Taken as a whole, the available data show that for most systems a reasonable match exists between brain regions where neurotransmitter release is thought to occur (i.e., areas of relatively high neurotransmitter concentration and/or neurotransmitter reuptake activity) and the density of appropriate receptors. However, the opportunity to confirm this arrangement of molecules in the synapse awaits techniques with adequate spatial resolution and sensitivity and specificity for localization of neurotransmitters and their receptors. It is interesting to speculate how newer imaging techniques, such as static secondary-ion mass spectrometry, might in the future be used to help answer this question with molecular specificity (for a preliminary account of this type of work see refs. 13 and 14). There has, however, been increasing discussion about the neuroanatomic mismatch that exists between some neurotransmitters and their receptors. This mismatch is not confined to one class of neurotransmitter and is apparent, for example, in the case of serotonin (15,16) and some of the neuropeptides including neuropeptide Y (17,18). Provided these apparent mismatches do not disappear with the discovery of as yet unrecognized receptor subtypes, they could imply that in some brain regions neurotransmitters are

Figure 5.2. Electron micrographs of various neuron-containing tissues. (Top) Ultrastructural immunoperoxidase labeling of neurotensin in the central nucleus of the rat amygdala, showing the unlabeled nucleus (nuc), rough endoplasmic reticulum (rer), and mitochondria (m) in a neuron that contains dense localized cytoplasmic labeling for the peptide (the dark spots; bar = 10 μ m). (Middle) The neurotensin localization in A is primarily in large dense-cored vesicles (dcv) that can be seen more clearly in this higher magnification of the same section (bar = 2 μ m). (Bottom) Micrograph of a transverse section through the frog neuromuscular junction showing a nerve terminal (1) and muscle fibers (2) in cross section. The nerve terminal is surrounded by Schwann cell processes (3) with a portion of the Schwann cell visible (4). The nerve terminal is filled primarily with clear synaptic vesicles (5, approx 200 nm in diameter) with a few large dense-cored vesicles (6) and some mitochondria (7). The synaptic cleft (8) is stained for acetylcholinesterase, leaving a dense precipitate.

Table 5.1
Concentrations of Some Important Neurotransmitters in Brain Tissue

Compound	Tissue	Concentration (nmol/g tissue)	Species (sacrifice method)	Reference
Dopamine	Whole brain	4.8	Rat (anesthesia)	105
	Substantia nigra	11.0	Rat (decapitation)	106
	Caudate nucleus	48.6	Rat (decapitation)	106
	Hypothalamus	3.9	Rat (decapitation)	107
	Putamen	11.6	Human (autopsy)	107
	Caudate	8.7	Human (autopsy)	107
	Whole brain	1.6	Rat (anesthesia)	105
	Locus coeruleus	5.9	Rat (decapitation)	106
	Hypothalamus	12.2	Rat (decapitation)	106
	Hypothalamus	4.3	Human (autopsy)	107
Norepinephrine	Olfactory tubercule	1.6	Human (autopsy)	107
	Thalamus	1.0	Human (autopsy)	107
	Whole brain	2.3	Rat (anesthesia)	105
	Hypothalamus	4.8	Rat (decapitation)	108
	Raphe	3.4	Rat (decapitation)	108
	Cerebellum	0.4	Rat (decapitation)	107
	Substantia nigra	2.7	Human (autopsy)	109
	Olfactory tubercule	2.0	Human (autopsy)	107
	Putamen	1.4	Human (autopsy)	107
	Serotonin	Whole brain	1.0	Human (autopsy)
Hypothalamus		2.3	Rat (anesthesia)	105
Raphe		4.8	Rat (decapitation)	108
Cerebellum		3.4	Rat (decapitation)	108
Substantia nigra		0.4	Rat (decapitation)	107
Olfactory tubercule		2.7	Human (autopsy)	109
Putamen		2.0	Human (autopsy)	107
Whole brain		1.4	Human (autopsy)	107
Hypothalamus		2.3	Rat (anesthesia)	105
Raphe		4.8	Rat (decapitation)	108

Glutamate	Cortex	9767	Rat (microwave irradiation)	109
	Hippocampus	15626	Rat (microwave irradiation)	109
	Striatum	12294	Rat (microwave irradiation)	109
	Substantia nigra	11672	Rat (microwave irradiation)	109
GABA	Cortex	1276	Rat (microwave irradiation)	109
	Hippocampus	2058	Rat (microwave irradiation)	109
	Striatum	2184	Rat (microwave irradiation)	109
	Substantia nigra	3557	Rat (microwave irradiation)	109
Acetylcholine	Cingulate cortex	18.4	Rat (microwave irradiation)	110
	Medial frontoparietal cortex	20.1	Rat (microwave irradiation)	110
	Lateral frontoparietal cortex	27.2	Rat (microwave irradiation)	110
	Olfactory cortex	50.5	Rat (microwave irradiation)	110
Leucine enkephalin	Caudate putamen	0.05	Rat (decapitation)	111
	Globus pallidus	0.57	Rat (decapitation)	111
Methionine enkephalin	Caudate putamen	0.05	Rat (decapitation)	111
	Globus pallidus	0.57	Rat (decapitation)	111
Neuropeptide Y	Frontal cortex	0.015	Rat (decapitation)	112
	Parietal cortex	0.014	Rat (decapitation)	112
	Hippocampus	0.012	Rat (decapitation)	112
	Paraventricular nucleus	5.5	Rat (CO ₂ inhalation)	113

The list includes representatives from most classes of compounds that have been established as having a neurotransmitter function. Where necessary, the data were adapted for uniformity in concentration units; calculations for the data in references 111–113 were made assuming 1 g of tissue is equivalent to 0.11 g of protein. Abbreviation: GABA, γ -aminobutyric acid.

released in areas of low receptor density where they may have a “neurohumoral-like” effect. In this way, the neurotransmitter would have pervasive effects on a larger volume of brain tissue than might result from release in areas of high receptor density. It is possible to imagine how such a system could be involved in the initiation and maintenance of synchronicity in activity of groups of neurons. However, one problem with such a concept concerns neurotransmitter dilution; for example, at remote recognition sites would there be sufficient concentrations of the neurotransmitter to produce a response?

1.6. The Relationship between Neurotransmitters and Clinical Medicine

Neurotransmitters are a critical component of all organisms that possess a nervous system. Therefore, it is not surprising that a large number of human diseases, which have diverse clinical manifestations and encompass most medical disciplines, involve impaired neurotransmitter function. These diseases include, among others, neurological, psychiatric, cardiovascular, endocrinological, and metabolic diseases and encompass diseases that are thought to arise from exclusively environmental causes, diseases that arise exclusively from inherited defects, and diseases in which environment and heredity are etiological factors. Therefore, great interest exists at the basic science, preclinical, and clinical levels to develop methods for obtaining reliable measures of neurotransmitter activity. This objective is a thorny problem. Because neurons are embedded in tissues that contain several cell types, where they occupy a small fraction of the total tissue mass, it is currently not possible in a clinical setting to obtain an accurate and direct measure of neurotransmitter release in a specific tissue. In the future, *in vivo* imaging approaches with radiolabeled drugs may be helpful in this regard, but at the moment the concentrations of the compounds and/or their metabolites in body fluids (plasma, cerebrospinal fluid, and urine) are the only measurements that can be made. Although these measures are valuable, particularly for measuring the response to therapeutic drugs, they lack anatomic precision. Furthermore, because many neurotransmitters are used by other cells in the body as endocrine and paracrine factors and as hormones (see later), the concentrations of the parent compound and its metabolites will reflect release by all these routes and will not be solely a measure of release from the neurotransmitter pool *per se*. In basic and preclinical research, other methods can be used to obtain more direct and anatomically precise estimates of neurotransmitter activity, for example, bulk tissue concentrations and concentrations in the extracellular fluids as measured by *in vivo* dialysis (19,20) and voltammetry (21).

In the case of certain rare neuroendocrine tumors, measurement of circulating levels or urinary excretion rates of some of these compounds is clinically diagnostic. Pheochromocytoma, for example, is a tumor of the adrenal medulla

that results in excessive production of catecholamines, and diagnosis of this disease is achieved by quantification of epinephrine and norepinephrine and their metabolites in urine. Intestinal carcinoid tumors, which secrete large amounts of serotonin into the circulation, are often discovered by an elevated urinary excretion of the serotonin metabolite 5-hydroxyindoleacetic acid, and repeated quantitative determination of the urinary metabolite has been used for many years as the principal laboratory test for both diagnosis of serotonin overproduction and for treatment follow-up. Other examples of diseases of this type include endocrinopathies that affect carbohydrate metabolism, water, and electrolyte balance and ectopic endocrinopathies that result in hypersecretion of peptides. Diagnosis of these rare conditions relies increasingly on measurement of circulating levels of specific neurohormones, including glucagon, somatostatin, vasoactive intestinal polypeptide, serotonin and its metabolite 5-hydroxyindoleacetic acid, pancreatic polypeptide, cholecystokinin, and adrenocorticotrophic hormone (22). The measurement of circulating concentrations is usually done by conventional techniques and generally does not involve mass spectrometry. Radioimmunoassay is used in the case of the peptides, although FAB mass spectrometry has been used to identify the peptides produced by some of these tumors (23). Chemical, electrochemical, and fluorescence procedures coupled to liquid chromatography are commonly used for serotonin and its metabolite.

Whereas the pattern of neurotransmitter dysfunction in a particular disease may be known from the results of preclinical research, this information is often not useful clinically because of the lack of *in vivo* measures that reflect neurotransmitter release from distinct anatomic sites. Three examples of this type have been selected for discussion because they highlight the numerous opportunities that exist for diagnostic applications of analytical technology in this area of research.

Idiopathic Parkinson disease is a progressive neurodegenerative disease with mid-age onset. It is thought to be environmentally caused with no demonstrably inherited component, and the disease results from marked degeneration of the dopaminergic nigrostriatal system, with associated but less marked degeneration of the noradrenergic and serotonergic systems in a variety of limbic and neocortical areas of the brain and spinal cord. At death, a virtually complete loss of dopamine has occurred in the substantia nigra and striatum (24), which normally is responsible for approximately 50% of brain dopamine metabolism. Despite the magnitude of the dopamine lesion, no reliance is placed on neurotransmitter measurements, and diagnosis of the disease is made on the basis of cognitive and motor impairments. Autopsy examination for confirmation of the loss of the dopamine cells in the substantia nigra is done only in select instances to confirm the diagnosis.

Basic research in Parkinson disease nevertheless presents a fascinating challenge to the analytical chemist. The observations concerning 1-methyl-4-phe-

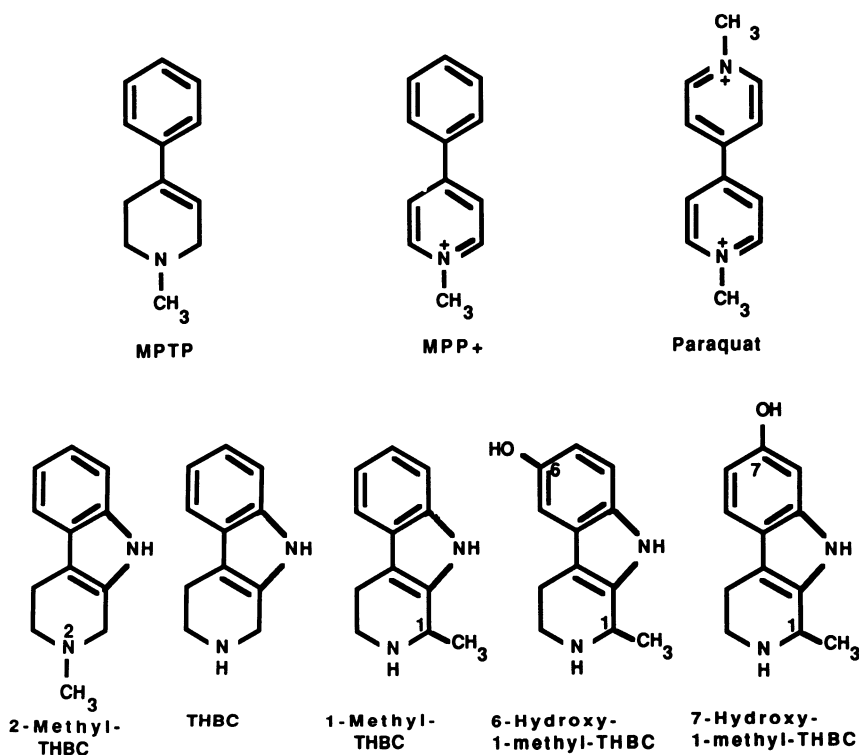


Figure 5.3. Structural formulas of 1-methyl-4-phenyl-1,2,3,6-tetrahydropyridine (MPTP) and some chemical analogues (THBC, tetrahydro-β-carboline, also known as tryptoline).

nyl-1,2,3,6-tetrahydropyridine (MPTP, Fig. 5.3), a byproduct in the synthesis of meperidine derivatives, gained the attention of the research community since the realization that it caused chronic, irreversible parkinsonism in humans following intravenous administration (25,26). Identification of MPTP as a toxic contaminant in illicit drug samples was made by GC/EI-MS analysis of samples collected on site. Studies in rodents and nonhuman primates, in addition to investigations of affected humans, have since shown that MPTP causes a selective lesion of the nigrostriatal pathway not unlike that seen in idiopathic Parkinson disease. The neuronal death is thought to be the result of the effects of a metabolite (MPP⁺, Fig. 5.3) that has affinity for the dopamine reuptake system and is thereby concentrated within dopaminergic neurons. The inhibition of mitochondrial NADH oxidation caused by MPP⁺ is thought eventually to result in cell death (for reviews see refs. 27 and 28).

Hitherto it had been thought unlikely that a peripherally administered agent could cause cell loss with this degree of neuronal selectivity. Because of the

clinical/behavioral/neurochemical and neuroanatomic similarities, MPTP neurotoxicity has since been used as a model of idiopathic Parkinson disease. In addition, these observations have sparked debate about the possibility that the disease is caused by an environmental toxin that over time accumulates in the nigrostriatal pathway, eventually resulting in lesioning of the nigrostriatal tract (29,30). For example, attempts have been made to find an association between the occurrence of this disease and centers of industrial activity that might be expected to be concentrated sources of heterocyclic nitrogen-containing compounds that, on the basis of structural similarity to MPTP, could conceivably produce such a clinical result. Structural similarity between MPTP and certain herbicides including paraquat, and between MPTP and certain tetrahydro- β -carbolines (Fig. 5.3) have sparked discussion about the possible role of these compounds in some cases of idiopathic Parkinson disease. In this regard, particular attention has focused on N-methylated-tetrahydro- β -carboline derivatives (31–34), which are semirigid tricyclic analogues of MPTP. On the basis of GC/MS evidence, one member of this group has been reported to occur naturally in the mammalian brain (35).

Following emergence of the MPTP story, attention was focused on a parkinsonism–dementia complex prevalent on the Pacific island of Guam. The original description of this disease was made in 1961 (36,37), and a relationship between the trend in incidence rates of the disease and the changing patterns of use of cycad seeds as a source of flour before and since World War II had long drawn attention to the possibility of a toxin in the seeds that was responsible for the condition. This possibility was greatly strengthened by the fact that the natives of the island who used the cycad seeds were aware that the material was toxic and extensively washed it to remove the toxic properties before use. In 1987, it was reported that β -N-methylamino-L-alanine (BMAA, Fig. 5.4), an unusual amino acid that occurs in cycad seeds in low concentration, causes symptoms not unlike those of the affected natives on Guam when administered to cynomolgus monkeys (38). If results of ongoing investigations confirm the suspected role of BMAA in causing the disease, then a likely mode of action of the toxin is via disruption of the amino acid neurotransmitter systems because BMAA is a potent stereospecific glutamate antagonist with the property of eliciting convulsions in acutely intoxicated rodents (for review see ref. 39). It seems likely that the parkinsonism–dementia complex of Guam is another example of a neurological disease created by an environmental toxin. MPTP neurotoxicity and Guam dementia complex have clinical similarities to idiopathic Parkinson disease, thus strengthening the argument that idiopathic Parkinson disease is also caused by some type of insidious environmental toxin. Regardless of the source of the presumed toxin, proof of this hypothesis will require the identification of the active agent(s), and this task is almost assuredly going to involve careful analytical work in which mass spectrometry could be used to great effect.

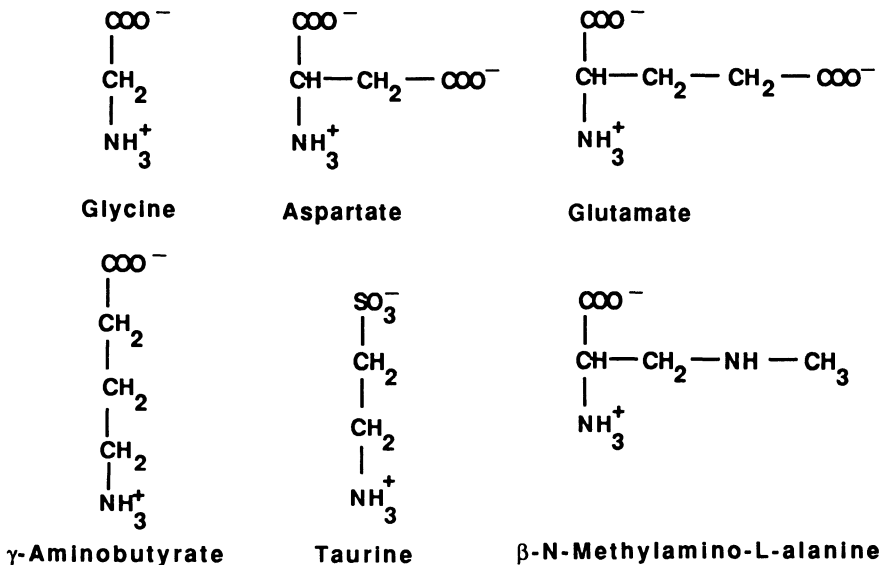


Figure 5.4. Structures of the amino acid neurotransmitters and β -N-methylamino-L-alanine.

Huntington chorea is another progressive neurodegenerative disease with mid-age onset. This disease is inherited in an autosomal dominant fashion and results in selective degeneration of basal ganglia structures, mainly the striatum including the globus pallidus and substantia nigra, with relative sparing of the nucleus accumbens. Although postmortem studies have shown loss of enkephalin- and γ -aminobutyric-acid-containing cells, followed by loss of dynorphin- and later substance-P-containing cells, with sparing of somatostatin and neuropeptide Y colocalized in the same cell group, clinical diagnosis is again made without reference to neurotransmitter function.

Perhaps a more poignant example that bears on the point that measures of neurotransmitter function are not often used clinically is that of Alzheimer disease. This malady is another progressive neurodegenerative disease that appears to involve environmental and inherited causative factors, strikes in mid- to old age, and is of growing concern in Western society because its prevalence is increasing as the population ages. Neurochemical investigations have revealed that the disease involves widespread CNS neuronal degeneration because many systems are affected, but with particularly marked deterioration of the acetylcholine system. Yet, clinical diagnosis does not rely on measurements of neurotransmitter function, and the disease can only be diagnosed with certainty at autopsy from examination of brain tissue for the presence of proteinaceous plaques and neurofibrillary tangles. In the foreseeable future, it is hoped that pharmacological approaches will emerge for the arrest and/or prevention of this disease. Such

developments will add to the already existing need for a reliable early in vivo clinical test for diagnosis of the disease and for assessment of disease progression.

2. CHEMICAL NATURE OF NEUROTRANSMITTERS

As already mentioned, neurotransmitters do not encompass one particular class of molecules, and a given molecule can be used by neurons as a neurotransmitter and by other cells in the body as a hormone, endocrine, or paracrine factor. Examples of this fact include norepinephrine, which behaves as a neurotransmitter in the CNS and as a hormone in the general circulation following release from the adrenal medulla. Serotonin also acts as a neurotransmitter in the CNS, but 80% of the serotonin in the body is confined to the enterochromaffin cells in the gut, where it is important in the regulation of gut motility. Dopamine is an important neurotransmitter in several areas of the brain and is also released by the hypothalamus into the hypophyseal portal circulation, where it is thought to have a hormonal role regulating prolactin release by the pituitary. Histamine is thought to be a neurotransmitter in the CNS and is also an important mediator in hypersensitivity reactions (such as asthma and allergic reactions) in which it is released from tissue mast cells and circulating basophils. Many of the neuropeptides were originally discovered in the tissues of the gastrointestinal tract, where it is thought they have a hormonal function regulating gut motility and acid secretion, and it has often been realized subsequently that the same compounds are used as neurotransmitters in the nervous system, where their bulk tissue concentrations are much lower. Also, atrial natriuretic factors are synthesized by the heart and released into the bloodstream for the hormonal regulation of homeostasis, but the same factors are also present in the brain, where they are thought to modulate various cardiovascular parameters.

It is a daunting task to prepare a list of the compounds that are known to be, or thought likely to be, neurotransmitters in the mammalian nervous systems. First, any such list will quickly become incomplete, as new candidate neurotransmitters are continually emerging. Second, a demarcation exists between the relatively few compounds that have been unequivocally demonstrated to act as neurotransmitters and many others that, by inference, are thought likely to have such a role. Unequivocal demonstration of a neurotransmitter role would include evidence of neuronal biosynthesis, presynaptic localization, release, receptor recognition and response, and reuptake and/or metabolism. Third, a large number of compounds are thought to be involved in this process, and many belong to the growing list of neuropeptides. Neurotransmitters cover a diverse range of compounds with widely differing chemical structures and biochemical properties and include quaternary amines (acetylcholine), secondary amines (epi-

nephri- ne, melatonin), primary amines (dopamine, norepinephrine, serotonin, and histamine), gases (nitric oxide), amino acids (γ -aminobutyric acid, glutamate, glycine, aspartate, taurine), nucleosides (adenosine), and the neuropeptides. Fourth, it is debatable if such a list should include so-called *neuromodulators*, which is a term coined to describe those compounds that are thought to influence neurotransmitter activity without having a strict neurotransmitter function (40). The present discussion has been limited to compounds that are thought to have a neurotransmitter function and to a few related compounds of interest.

2.1. *Comparison between the Nonpeptide and Peptide Neurotransmitters*

Without meaning to imply that the distinction has any fundamental biological significance, but merely for the sake of simplicity, the discussion of the various compounds involved in neurotransmission has been divided into nonpeptide and peptide neurotransmitters, and the compounds of principal interest are listed in Tables 5.2 and 5.3, respectively. Nevertheless, it is instructive to compare these two categories in a general sense. The nonpeptides are smaller, with molecular weights less than 300, and at physiological pH they are either zwitterionic, as in the case of the amino acid neurotransmitters, or cationic, as in the case of acetylcholine, the catecholamines, serotonin, adenosine, the trace amines, and the alkaloids. The neuropeptides range in size from two amino acid residues in the case of N-acetylaspartylglutamate (molecular weight 292, neurotransmitter role unproven but suspected at the present time) and three amino acid residues in the case of thyrotropin-releasing hormone (molecular weight 362) to more than 30 amino acid residues; for example, the human forms of β -endorphin and neuropeptide Y have 31 and 36 amino acid residues with monoisotopic molecular weights of 3464 and 4267, respectively.

2.2. *Neurotransmitter Biosynthesis and Processing*

It is also interesting to compare the biosynthesis of the peptide and nonpeptide neurotransmitters. The nonpeptide neurotransmitters are biosynthesized as the result of several enzymatic reactions. The biosynthetic rate can be controlled at the level of gene transcription and translation of the messenger RNA encoding the biosynthetic enzymes as well as at the individual biosynthetic steps. On the other hand, the neuropeptides are typically biosynthesized as large preproproteins (preprohormones) that are cleaved by proteolytic enzymes into the proproteins (prohormones), which are then further cleaved to yield the active compound(s). Therefore, the opportunities for controlling the rate of neuropeptide biosynthesis include control at the level of transcription of the gene and transla-

Table 5.2
The Nonpeptide Neurotransmitters and Related Compounds

Classical neurotransmitters	Alkaloids
Catecholamines	Morphinans
Dopamine	Morphine
Norepinephrine	Codeine
Epinephrine	6-Acetylmorphine
Indoleamines	Thebaine
Serotonin	Tetrahydro- β -carbolines (tryptolines)
Melatonin	Tetrahydro- β -carboline
Acetylcholine	1-Methylethyltetrahydro- β -carboline
Histamine	Harmane
Amino acid neurotransmitters	Tetrahydro-isoquinolines
γ -Aminobutyric acid	Salsolinol
Glutamate	Salsolinol-1-carboxylic acid
Aspartate	Salsoline
Glycine	Salsoline-1-carboxylic acid
Taurine	
Nucleosides	
Adenosine	
Gases	
Nitric oxide	
Trace amines	
β -Phenethylamine	
<i>para</i> -Tyramine	
<i>meta</i> -Tyramine	
Tryptamine	
Octopamine	

tion of the messenger RNA encoding the preproprotein and the peptidases responsible for the cleavage reactions, and control of the rate of the individual proteolytic cleavage steps. Although the sequence of events is quite different in the two situations, in both, multiple places exist where control mechanisms can operate, and arguments that the peptide neurotransmitters are more proximal to genomic regulation seem ill-placed.

3. MASS SPECTROMETRIC CHARACTERIZATION OF NEUROTRANSMITTERS

The value of mass spectrometry in biomedical research in general, and specifically in the field of neurotransmitters, is well known but nevertheless worth repeating. It comes from a combination of factors. Of the physical tech-

Table 5.3
Known or Presumed Mammalian
Peptide Neurotransmitters

Atrial natriuretic factors
 N-Acetylaspartylglutamate (NAAG)
 Calcitonin-gene related peptides
 Calcitonin
 Calcitonin-gene related peptide (CGRP)
 Cholecystokinins (CCK) and CCK-releasing factors
 CCK₈
 CCK₅₆
 Corticotropin-releasing factor (CRF)
 Delta sleep factor
 Diazepam binding inhibitor (DBI)
 Galanin
 Gastrin-releasing peptide and related peptides
 Gastrin
 Glucagon
 Gonadotropin-releasing hormone
 Growth hormone-releasing hormone
 Insulin
 Leuteinizing hormone-releasing hormone (LHRH)
 Neuropeptide Y (NPY)
 Neurotensin
 Opioid peptides
 Prodynorphin products
 Pro-enkephalin products
 Pro-opiomelanocortin products
 Pancreatic polypeptide
 Peptide H1
 Peptide YY
 Proressorphysin
 Vasopressin
 Prooxyphysin
 Oxytocin
 Secretin
 Sleep-promoting factor (FSu) and related muramyl peptides
 Somatostatin
 Tachykinin peptides
 Substance P
 Substance K/neurokinin A
 Neuromedin K/neurokinin B
 Thyrotropin-releasing hormone (TRH)
 Vasoactive intestinal polypeptide (VIP) and related peptides

Some of the precursors code for more than one biologically active neuropeptide. In perhaps the most extreme example, more than 20 peptides from the mammalian CNS have now been isolated with the N-terminal opioid sequence Tyr-gly-gly-phe-x (YGGF_x); these are all carboxy-terminal extensions of methionine enkephalin and leucine enkephalin, the sequences of which are contained within the three precursor molecules prodynorphin, proenkephalin, and proopiomelanocortin (114).

niques available for obtaining structurally relevant information, mass spectra can be recorded on less than 0.1% of the material that is required for obtaining NMR spectra. Although mass spectrometry usually compares less favorably in terms of sensitivity with immunologically based techniques (e.g., radioimmunoassay), the superior specificity gained from precise mass measurement is often a significant advantage, particularly when distinction between similar molecular structures is required. Mass measurements are routinely made with ± 0.5 -Da accuracy at low resolution and with ± 0.002 -Da accuracy at high resolution. The specificity of mass spectrometric measurement can be further enhanced by considering the ratio of intensity of the various ions in the spectrum (e.g., ratio of molecular to fragment ion intensity) and by measuring the product ions that result from dissociation of a selected precursor ion (e.g., product ions resulting from collisionally activated dissociation of the molecular ion in the tandem mass spectrometric mode). The mass spectrometer can be used as a universal detector (with some practical limitations) that is capable of detecting and identifying all the known types of molecules involved in neurotransmission. This absence of restrictions is in sharp contrast to other procedures for determining these structures and is particularly valuable for resolving issues of posttranslational modification of neuropeptides. Also, of real practical importance is the ability to couple mass spectrometers directly to separation systems including gas, liquid, and supercritical fluid chromatographs and capillary zone electrophoretographs. In this way, structural information can be obtained for the components of complex mixtures and impure extracts without the need for the preparation of pure samples. An additional benefit that usually results from coupling to a chromatographic device is that the sample is presented to the instrument in a more concentrated form than can otherwise be easily achieved, and this concentration of the sample further improves the limits of detection over that which can be obtained from off-line sample introduction methods.

Developments in computer techniques and improved coupling to chromatography and, most significantly, in ionization modes have improved the limits of detection and vastly extended the mass range of the molecules that can be analyzed. The recent development of electrospray ionization (described in Chapters 1 and 2 in this volume) offers the promise of even greater sensitivity of detection with an increased effective mass range for the compounds of interest.

3.1. The Nonpeptide Neurotransmitters

The utility of mass spectrometry in biomedical research really blossomed after the technique was interfaced to gas chromatography. This coupling occurred in the 1960s, by which time most of the classical neurotransmitters had already been identified. The major impact of the technique, therefore, has been in the GC/MS mode (and in some more recent instances in the LC/MS mode) as a

sensitive and specific analytical tool for precise quantitative determinations. These applications are important, and GC/MS assays of these compounds are considered the “gold” standard against which the results from other assays are compared.

In order to be applicable to GC/MS, a molecule must be sufficiently volatile, nonpolar, and thermally stable for passage through the chromatographic column. Few biological molecules meet these requirements in and of themselves. Accordingly, chemical derivatization is necessary. However, the difficulty of chemically derivatizing in high yield the compound of interest when present in trace amounts in a crude extract should not be underestimated. Because of the problems associated with derivatization, and because of the time required for chromatographic separation, chemical ionization was thought to have special promise when it was developed in the early 1970s. The reason for this expectation was the hope that the simple spectra produced during chemical ionization would have sufficient inherent specificity for the identification and quantification of targeted compounds in complex extracts from direct analysis by solid-probe techniques. The advantage of obviating the requirement for gas chromatographic separation would be elimination of the usual need for derivatization and shortening of the analysis time. Because the specificity that can be obtained from unit-resolved protonated molecules produced by the CI source is insufficient for the analysis of complex extracts, this hope did not materialize except in a few isolated circumstances such as the quantification of plasma free fatty acids and amino acids (41,42). However, the subsequent development of tandem mass spectrometry revitalized this hope, and in many instances it has been shown to be a viable practical alternative for the direct analysis of targeted compounds in complicated mixtures using electron impact and chemical ionization conditions (43,44). However, attempts to use the same approach for the direct analysis of neurotransmitters and related compounds in brain tissue extracts have not been universally successful. The failure is restricted to instances in which it has been necessary to use the ultrahigh sensitivity that is available under electron-capture ionization conditions with perfluorinated derivatives. Because of limitations in the number of low-energy electrons available for capture in the chemical ionization source, chromatographic separation is still an essential component of the analytical process for resolution of the various electron-capturing compounds in the derivatized extracts (45,46).

An unexpected requirement for chromatographic separation prior to mass spectrometry also emerged during the identification of morphine in extracts of mammalian brain. In this case, the material was concentrated from several kilograms of bovine brain, and it behaved on HPLC indistinguishably from authentic morphine. However, attempts to confirm the identification by solid-probe electron-impact mass spectrometry of the HPLC-purified material (trifluoroacetic acid salt) were unsuccessful, despite the fact that authentic morphine (HCl salt)

gave a characteristic mass spectrum with adequate sensitivity (R. W. Barrett and K. F. Faull, unpublished results). A subsequent attempt to confirm the suspected identification using GC/MS of the trifluoroacetyl derivative was successful (47), and in retrospect it was concluded that the solid-probe experiment inexplicably failed because of interference from low-level trace impurities in the biological sample. This problem is not confined to morphine because a similar example of the need for chromatographic separation prior to mass spectrometry when working with relatively pure extracts has also been observed during the isolation of reticuline from plant sources (K. F. Faull, unpublished observations).

3.1.1. The Catecholamines and Indoleamines and Their Metabolites

The development and application of GC/MS approaches for the identification and quantification of the catecholamines and indoleamines (Fig. 5.5) have been extensively described elsewhere (48,49). A wide repertoire of sample preparation and derivatization schemes is available for isolating these compounds from tissues and body fluids free of protein, water, and inorganic salts and for converting them to thermally stable derivatives suitable for gas chromatographic separation and mass spectrometric detection. Efforts have continued to refine these methods to further improve their reliability and sensitivity. Limits of detection in the range of 6–60 fmol per injection have now been reported (50,51). Although several steps are usually involved in sample preparation, final yields in excess of 70% can be achieved. However, given the expense and relative complexity of mass spectrometric instrumentation, an understandable trend has occurred toward the development of simpler, less expensive methods for quantification of these compounds.

Of particular note has been the successful development of reverse-phase HPLC with electrochemical detection (HPLC/EC) for quantification of compounds with catechol, phenol, or substituted indole moieties. HPLC/EC has reached an impressive level of accuracy, simplicity, sensitivity, and speed because the analyses are usually done under isocratic conditions. This technique is now the most widely used method for the quantification of the catecholamines, serotonin, and their acidic metabolites. Limits of detection down to 10 fmol per injection can be achieved, but the practical figure for the routine analysis of samples is probably ten times higher. The alcoholic metabolites pose a problem for HPLC because they are not always easily resolved from the solvent front in systems that elute the other compounds of interest in a reasonable period of time. For this reason, GC/MS is still the preferred method for quantification of 3-methoxy-4-hydroxyphenylethylene glycol (MHPG), the principal CNS metabolite of epinephrine and norepinephrine. GC/MS of course retains an advantage in that it can be used with stable-isotope-labeled molecules to study the pharmacokinetics of the compounds of interest. A recent example of such an application

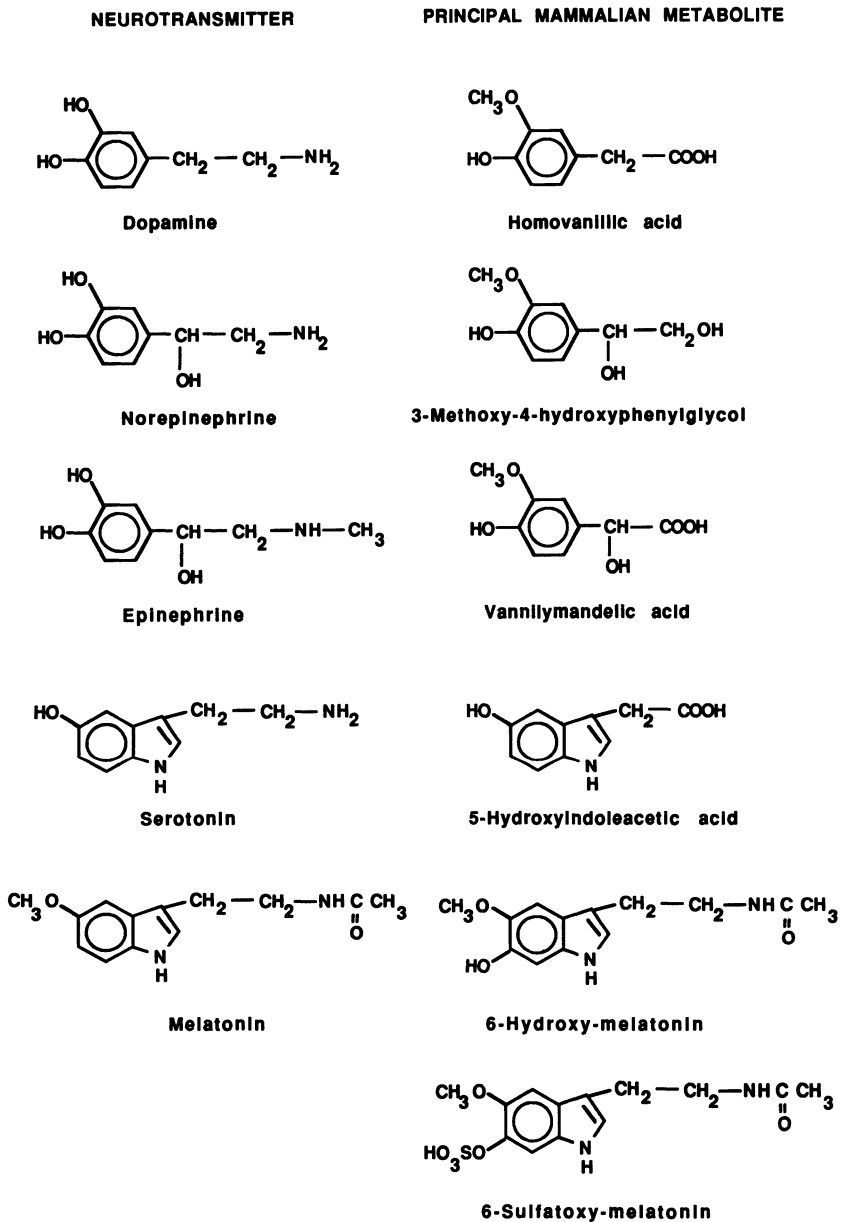


Figure 5.5. Structures of the catecholamine and indoleamine neurotransmitters and their corresponding mammalian metabolites. Epinephrine and norepinephrine are converted to two principal metabolites, 3-methoxy-4-hydroxyphenylglycol (MHPG) and vanillylmandelic acid. MHPG is the principal CNS metabolite. MHPG is converted in part to vanillylmandelic acid outside the brain. Melatonin is converted to 6-hydroxy- and then to 6-sulfatoxymelatonin, which is excreted in the urine and accounts for the bulk of melatonin turnover.

was the demonstration of the rapid movement of MHPG across the blood–CSF barrier in squirrel monkeys intravenously administered [$^2\text{H}_3$]MHPG (52). The results of this study showed that the plasma and cervical CSF pools of this metabolite reach concentration equilibrium within 30 min of a disturbance of the plasma concentration. This finding, which follows earlier work by Kopin and colleagues (53), has important implications when CSF MHPG concentrations are used as an indirect index of CNS norepinephrine activity.

Melatonin deserves special comment. Attempts to develop radioimmunoassays to measure plasma melatonin concentrations in the 1970s and early 1980s were unsuccessful. The development of a reliable method for measuring plasma melatonin concentrations by GC/electron capture MS using the spirocyclic derivative formed following treatment with pentafluoropropionic anhydride was a significant advance in the field (54) and enabled measurements down to low femtomoles per milliliter of plasma. Sensitivity in this range is essential because daytime (nadir) circulating levels of this compound are around 5 fmol/ml. The methods developed by Markey and co-workers were expanded to include the melatonin metabolite 6-hydroxymelatonin (55) and serotonin (56), and they remain the methods of reference for these compounds. More recently the radioimmunosassays have been improved to the point that they now produce quantitative results comparable to those produced by GC/MS. Because the RIA procedure is simpler, it is possible to conveniently process large numbers of samples, and it is now finding acceptance as a valid method.

3.1.2. Acetylcholine

GC/MS has been used successfully for the quantitative measurements of acetylcholine and choline, its biochemical precursor (Fig. 5.6), and is the preferred method for these measurements. The most commonly used approach, perfected by Jenden and co-workers, involves demethylation of the quaternary amine to form the corresponding tertiary amine. Demethylation is achieved either chemically with sodium benzenethiolate (57) or by direct pyrolysis of the quaternary ammonium salt (58). Choline can be measured in the same assay but must first be esterified with an acyl halide prior to demethylation. The demethylated products can be analyzed by CG/MS with either electron-impact (59) or chemical ionization (60). To some extent, the GC/MS approach for measuring acetylcholine has also been replaced by an HPLC approach. In the HPLC method, detection is achieved by use of a postcolumn immobilized-enzyme reactor, which, via the combined activity of acetylcholinesterase and choline oxidase, produces betaine and hydrogen peroxide (Fig. 5.6), which is then detected amperometrically at a downstream platinum electrode (61). The HPLC method has increased in popularity since it was first introduced because minimum sample preparation is involved and aqueous solutions can be analyzed directly. This

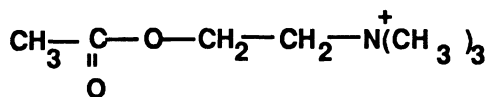
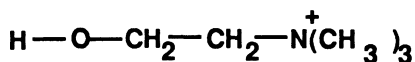
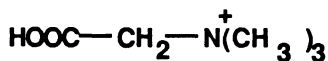
**Acetylcholine****Choline****Betaine**

Figure 5.6. Structures of acetylcholine, choline, and betaine.

method is finding application in conjunction with dialysis experiments for in vivo measurements of the extracellular concentrations of choline and acetylcholine.

3.1.3. Amino Acids

Numerous GC/MS methods have been developed for the analysis of amino acids, and many of these methods could be used for the quantitative measurement of the amino acid neurotransmitters (Fig. 5.4). The procedures most commonly used to derivatize amino acids in preparation for gas chromatography are based on formation of the carboxylic acid alkyl ester followed by perfluoroacylation of the remaining functional groups. Analyses based on such protocols are routine, and the resolution attainable using capillary columns is probably unmatched by any other method, a factor that is an advantage when working with complex biological mixtures. One notable application of GC/MS occurred in the mid-1970s when a controversy over the occurrence of γ -aminobutyric acid in human lumbar CSF was resolved with the unequivocal identification of the N-pentafluoropropionyl methyl ester in derivatized CSF extracts (62). Efforts continue to develop a single reaction procedure for preparing volatile amino acid derivatives. In this regard, the most useful of these procedures is probably formation of the N(O)-dimethyl-*tertiary*-butylsilyl derivatives via a single-step reaction with dimethyl-*tertiary*-butylsilyltrifluoroacetamide (63).

However, the simplicity and sensitivity of procedures based on HPLC with detection of fluorescent derivatives, formed by either pre- or postcolumn chemical derivatization, have been perfected to a high level of reliability, and these techniques are enjoying widespread use in neurotransmitter research as the methods of choice for quantification of the amino acid neurotransmitters (for repre-

sentative references see refs. 64–66). Nevertheless, mass spectrometry is still a useful tool in this field. GC/MS, for example, is being used in elegant experiments for measuring amino acid neurotransmitter fluxes and the pathways of nitrogen transfer in isolated brain synaptosomal preparations and cultured astrocytes with ^{15}N and ^{13}C stable-isotope-labeled precursors (67–71). As with all experiments of this type, care must be taken to assure that the precursor load, which approximately matches the pool size of the unlabeled precursor, does not overwhelm the system. In contrast, similar experiments with radioisotope-labeled substrates would involve administration of precursor quantities that would have no detectable effect on tissue pool size.

3.1.4. Histamine

There has been increasing interest in measuring plasma histamine levels in various clinical conditions and in response to a variety of antihistamine drugs and in measuring the concentrations of histamine and its metabolites in CSF and brain tissue extracts to estimate histamine neurotransmitter activity. The concern for reliable methodology for clinical measurements in this field prompted a recent external quality control study in Europe (72,73) in which the results from GC/MS, enzymatic, fluorometric, radioimmunoassay, and HPLC assays were compared. Several GC/MS methods have now been developed for histamine and its predominant metabolites N^{τ} -methylhistamine, N^{τ} -methyimidazole acetic acid, and imidazole acetic acid (Fig. 5.7). These methods were initially geared toward optimizing the sensitivity that could be obtained with electron impact ionization (74–76), but in order to achieve greater sensitivity recent developments have focused on exploiting electron-capture ionization of fluorinated derivatives (77,78). The electron-capture methods can achieve 1–10 fmol/injection limits of detection for histamine and the major CNS metabolite N^{τ} -methylhistamine with excellent precision and reliability.

3.1.5. The Trace Amines

These amines constitute a group of compounds (Fig. 5.8) of obscure physiological significance that are found in mammalian brain in relatively low abundance of not more than 50 pmol/g. It is doubtful if they behave in the CNS as neurotransmitters, and a role in some form of neuromodulation is considered a possibility. More often they are ignored on the basis of their low tissue concentrations, despite the fact that their metabolites are present in brain tissue and CSF in about the same concentrations as the metabolites of the catecholamines and serotonin, suggesting a high turnover rate. Furthermore, they have been repeatedly implicated in various psychiatric and neurological illnesses. Because of the need to distinguish clearly among these compounds and the more abundant and

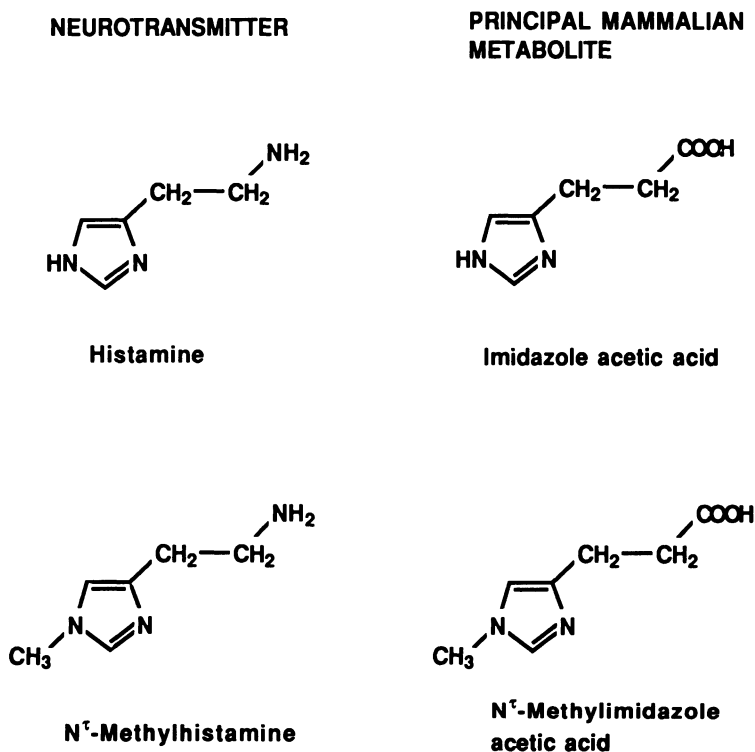


Figure 5.7. Structures of histamine and N^m-methylhistamine and their principal mammalian metabolites.

structurally related catechol- and indoleamines, the identification and quantification of the trace amines and their metabolites is virtually exclusively in the domain of mass spectrometry. In contrast to the catecholamines and serotonin, HPLC/EC has not been very useful for these compounds because of their unfavorable electrochemical characteristics. The compounds with an unsubstituted aromatic ring are transparent in their native form at electrochemical detectors, and the higher working electrode voltages required for detection of the mono-substituted compounds increase the chances of mistaken identity.

The work of Boulton and co-workers has been particularly thorough in the application of mass spectrometry to the identification and quantification of these compounds (79). They have developed methods for identification and quantification of the parent amines (β -phenethylamine, tryptamine, *meta*- and *para*-tyramine, the octopamines, and synephrine) as the dansyl derivatives, after thin-layer chromatographic separation and by electron-impact ionization followed by selected ion monitoring of the molecular ions at low and high mass spectrometric

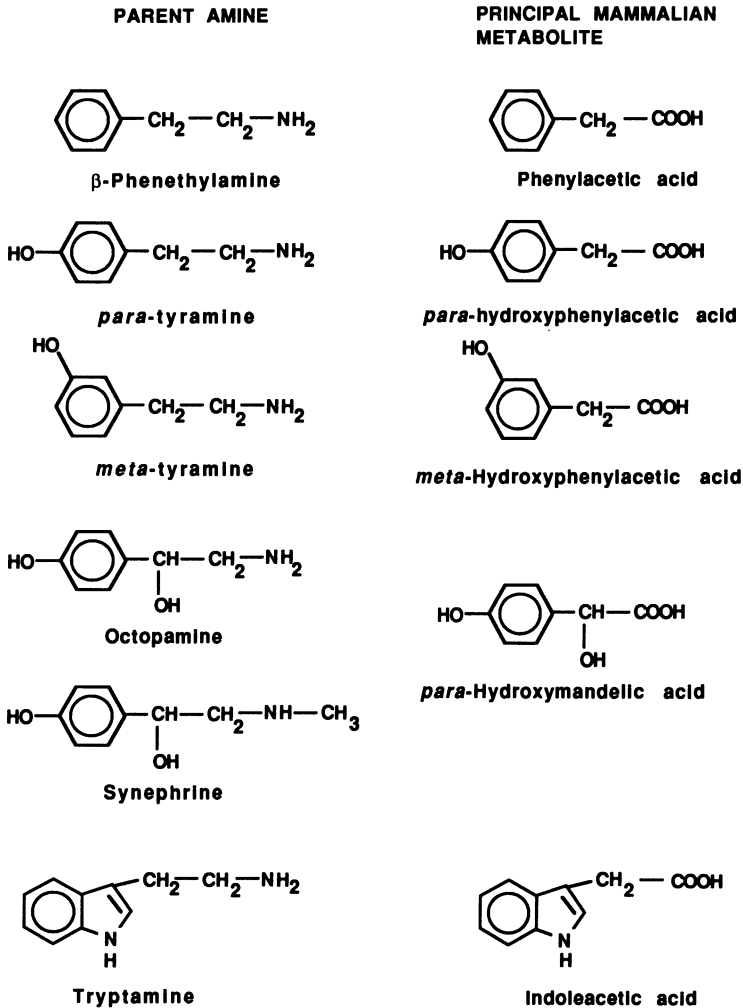


Figure 5.8. Structures of some of the trace amines and their principal mammalian metabolites. *para*-Hydroxymandellic acid would be the principal metabolite of octopamine and synephrine.

resolution. Deuterated internal standards are used for quantification, and the method offers sensitivity of about 1 pmol/g of tissue. In the case of tryptamine and β -phenethylamine the analysis can be done by GC/electron-capture mass spectrometry of the N-acetylpentafluoropropionyl or N-acetylpentafluorobenzoyl derivatives with limits of detection down to 10 fmol/g of tissue. Furthermore, Boulton and co-workers have perfected methods for the simultaneous analysis of a wide range of acidic and neutral metabolites (up to 12) as the methylpen-

tafluoropropionyl or trifluoroethylpentafluoropropionyl derivatives using GC/MS, with sensitivities in the 1- to 100-pmol range.

3.1.6. *Morphinan, Tetrahydro- β -Carboline, and Tetrahydroisoquinoline Alkaloids*

These alkaloids constitute three interesting groups of compounds that have been the focus of recurring investigation with regard to the mammalian CNS. Traditionally, they are thought of as being derived exclusively from plant sources. However, convincing mass spectrometric evidence has been collected showing unequivocally that they occur naturally in the mammalian CNS, although their physiological significance and origin (i.e., whether they are biosynthesized by mammals or whether they are of dietary origin) is unclear. Although it is premature to suggest that these compounds have a neurotransmitter function in the mammalian CNS, it is appropriate that they be mentioned in the present context because of their close chemical and/or pharmacological relationship to known mammalian neurotransmitters and because of the important use that has been made of mass spectrometry in their identification.

Morphine is legendary because of its antidiarrhetic, euphoric, addictive, and analgesic properties, and traditionally it is the prototypical ligand for the μ opioid receptor type. Historically, it had been thought that morphine and its relatives (Fig. 5.9) occur naturally only in a few species of the genus *Papaver* (Asian poppy). However, morphine, codeine, and 6-acetylmorphine have been identified in extracts of mammalian brain by GC/MS of their trifluoroacetyl derivatives, and thebaine has also been identified by GC/MS from the same source (for a recent review see ref. 80). It has also been shown that mammals can execute some of the same steps in morphine biosynthesis as the opium poppy. These results challenge the dogma that these alkaloids occur naturally only in the plant kingdom and invite speculation that mammals biosynthesize these compounds. This rationale has led to the suggestion that endogenous morphine alkaloids have a physiological function in mammals.

The tetrahydro- β -carbolines (Fig. 5.3, tryptolines) and tetrahydroisoquinolines (Fig. 5.10, TIQs) are the classes of compounds that arise from Pictet-Spengler condensations between carbonyl compounds and indoleamines and catecholamines, respectively. Their occurrence in mammals has long been contentious. Originally, speculation concerned formation from catecholamines (such as dopamine) or indolethylamines (such as serotonin and tryptamine) and aldehydes (such as acetaldehyde and formaldehyde) via a reaction that has favorable rate constants at physiological pH and temperature. The neuropharmacological effects of these compounds are diverse and include hallucinations, monoamine oxidase inhibition, inhibition of biogenic amine reuptake, attenuation of monoamine release, and inhibition of cholinesterase.

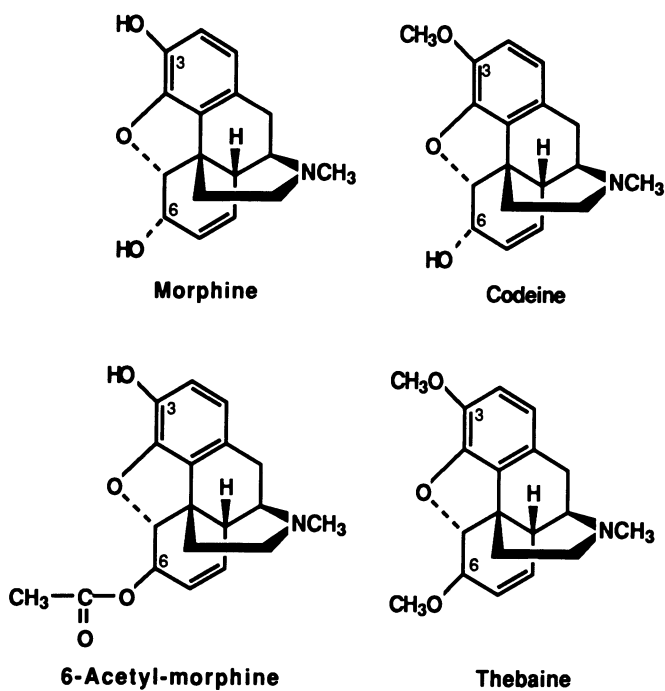


Figure 5.9. Structures of the morphinan alkaloids that have been identified in extracts of mammalian tissues.

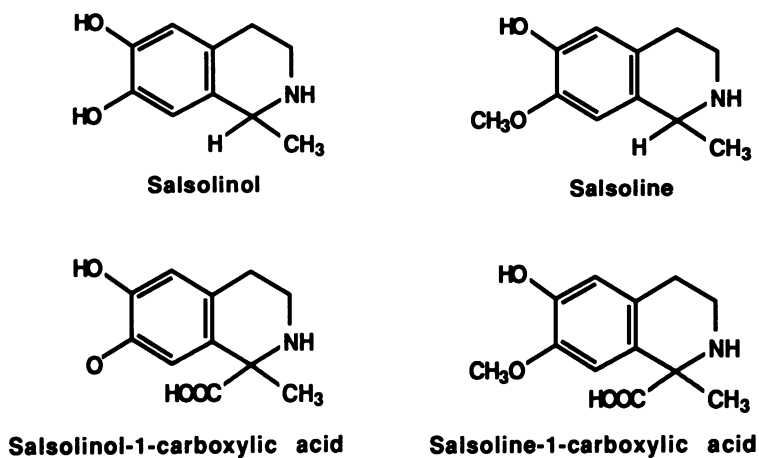


Figure 5.10. Structures of the tetrahydroisoquinoline alkaloids that have been identified in extracts of mammalian tissues.

The identification of these compounds in tissue extracts has relied principally on mass spectrometry. Radioimmunoassays have not been used because of difficulty raising antibodies that do not cross-react with structurally similar and more abundant catecholamines and indoleamines. It has now been convincingly demonstrated that some members of these classes of compounds, and at least one β -carboline, occur endogenously in mammals. The evidence is most compelling for tetrahydro- β -carboline (THBC) and 1-methyl-THBC in brain, lung, plasma, and urine; 6-hydroxy-1-methyl-THBC in liver, kidney, plasma, and urine; 7-hydroxy-1-methyl-THBC in urine; harman (a structurally related β -carboline) in brain, lung, and platelets; and salsolinol, salsoline, and their 1-carboxylic acid derivatives in brain (81–85). The majority of these claims have relied on characterization by GC/MS of perfluoroacyl derivatives, which have excellent GC properties and characteristic mass spectra under electron-impact and electron-capture conditions (86).

Earlier concerns that the condensation products were formed during sample preparation by condensation between endogenous catecholamines and indoleamines and aldehydes liberated during tissue homogenization or introduced in laboratory solvents have now been dispelled. This clarification has largely been achieved through the use of aldehyde-free reagents, aldehyde-trapping systems, and most convincingly through the application of mass spectrometry in conjunction with stable isotope-labeled amines and aldehydes. Apart from providing virtually unequivocal evidence of structural identification, mass spectrometry allows the addition of ^2H - or ^{13}C -labeled amines or aldehydes at the time of sample preparation, thus providing an automatic check on the production of labeled condensation products during sample preparation (87–89).

3.2. *The Peptide Neurotransmitters*

The neuropeptides are generally less than 40 amino acids in length and are synthesized in precursor form (the preproprotein), which is generally between 60 and 300 amino acids in length. The preproprotein has a signal or leader sequence located at the N terminus, which is thought to be crucial for insertion of the prohormone into the lumen of the endoplasmic reticulum and thus for routing through the Golgi apparatus for eventual packaging into secretory granules. The preproprotein also has spacers flanking the regions encoding the biologically active neuropeptide sequence(s). During translation, the signal sequence is proteolytically removed from the nascent polypeptide. During the packaging process, or in the secretory granules, the prohormone is cleaved to yield the biologically active compound(s). Some neuropeptide precursors contain a single copy of a neuropeptide sequence; other neuropeptide precursors contain multiple copies of a neuropeptide sequence; and some precursors also contain copies of multiple neuropeptides. It has been demonstrated repeatedly that differential

mechanisms exist for activation of multifunctional biosynthetic precursors in various tissues. Furthermore, the spacer region(s) on the preproprotein may code for a biologically relevant peptide(s). The sites of cleavage of the precursor are dictated by specific amino acid sequences, for which a set of basic amino acids is the most common site of precursor cleavage (90).

The most logical way to list the known and suspected peptide neurotransmitters is in families according to sequence homology and prohormone precursor commonality. The list given in Table 5.3 of peptides found in the mammalian CNS is not intended to be complete but should provide a sense of the variety of peptides that are thought to be important.

For a complete treatment of the subject of mass spectrometry of peptides, the reader is referred to recent publications that provide extensive and up-to-date coverage of the field (91,92). Applications of mass spectrometry for molecular weight determination and sequence determination and quantification of neuropeptides are specifically covered by Barofsky *et al.* (93), Feistner *et al.* (94), and Desiderio (Chapter 4, this volume). Only a few specific points of particular interest are covered here. Historically, one of the most useful mass spectrometric techniques for peptide analysis was permethylation and electron impact ionization of samples introduced via the conventional solids probe (for a recent review see ref. 95). This approach gives excellent molecular weight and sequence information on small peptides, but with increasing chain length the volatility of the molecules declines, and most importantly there is decreasing intensity of the higher-mass and structurally significant ions in the mass spectra so that the practical limit for this technique is about ten or so residues. Nevertheless, this method was used to assist in sequence determination of some of the hypothalamic releasing factors and was crucial for sequencing the first of the opioid peptides, methionine enkephalin and leucine enkephalin (96). FAB mass spectrometry largely superseded this technique because intense signals in the molecular ion region could be obtained from underivatized peptides with molecular weights up to and exceeding 3000. Among biomedical mass spectroscopists, FAB found increasing application for molecular weight determination, sequencing, and quantification of biologically important peptides. Plasma desorption-time-of-flight mass spectrometry (PD-TOF-MS) has also been applied to this area of research. In a direct comparison between FAB on a sector instrument and PD-TOF-MS for the analysis of the neuropeptide profile from bovine pituitary extracts, PDMS was found to have between five and ten times superior sensitivity (97). However, the advantage of superior accuracy of mass measurement obtained on the sector instrument can sometimes be important, especially for distinguishing between molecules with similar molecular weights, such as amidated species, which differ by 1 molecular weight unit from the nonamidated molecule. Despite the obvious utility of mass spectrometry for structural determination, the proportion of publications that rely on these measurements is still

relatively small. Nevertheless, the further improvements in sensitivity and mass range anticipated with electrospray should result in even more widespread appreciation and use of mass spectrometry in this field.

3.2.1. *Posttranslational Modification of Neuropeptides*

Mass spectrometry is particularly useful for determination of posttranslational modifications of neuropeptides (98). Posttranslational modification is a prominent feature of neuropeptide processing. It is thought that its purpose is to provide protection for the peptide from cleavage by peptidases and to change or remove biological activity of the peptide. A number of different covalent modifications are known to occur, including N-acetylation, N- and O-linked glycosylation, phosphorylation, sulfation, hydroxylation, and conversion of N-terminal glutamic acid to pyroglutamic acid. One prevalent chemical motif among peptide neurotransmitters is that of C-terminal α -amidation. At least 24 known mammalian peptide hormones and neuropeptides possess this functionality (99). In the late 1970s Mutt and co-workers developed a chemical assay for screening for peptides with the C-terminal amide structure in tissue extracts, a strategy that resulted in the isolation and identification of four new compounds of hormonal or neurotransmitter interest (100–102). The molecular signatures produced by C-terminal amidation and other posttranslation modifications can be readily identified from molecular weight measurements (98). For example, amidation, acetylation, sulfation, and pyroglutamic acid formation produce mass changes of -1 , $+42$, $+80$, and -18 Da, respectively. A general feature of mass spectrometry is that no implicit assumptions need be made concerning the type of modification that is involved, and this advantageous absence of restrictions is in sharp contrast to traditional wet chemistry procedures for determining structure modifications.

Flanagan and co-workers have exploited this advantage of mass spectrometry by developing a method for screening for peptides containing the pyroglutamic acid residue (103). This method is based on searching for molecules that undergo a mass loss of 111 Da following treatment with pyroglutamate aminopeptidase. Using this strategy, they were able to detect, isolate, and sequence a novel pyroglutamate-containing peptide from bovine adrenomedullary chromaffin vesicles.

3.2.2. *Peptide Charting*

The number of neuropeptide systems and the multiple forms of some of the compounds pose a problem to understanding the interrelationships among the different compounds. Because of its speed, specificity, and sensitivity, mass spectrometry can be used to advantage here. For example, the combination of molecular weight determination and partial sequence determination is sufficient

to characterize complex neuropeptide profiles such as those obtained from HPLC analysis of neuroendocrine tissues (93,97). Preliminary results suggest that electrospray mass spectrometry with on-line HPLC will considerably extend, with superior sensitivity, the molecular weight range of compounds that can be characterized in this way (94).

Finally, in relation to a possible neurotransmitter role, interest is growing in the class of N-terminal-blocked small peptides such as N-acetylaspartylglutamate and the related amino acid derivative N-acetylaspartic acid (NAA). These compounds are abundant components of neurons. Zollinger *et al.* (104) have developed a GC/MS method based on formation of the trimethyl ester of N-acetylaspartylglutamate for accurate quantification of this compound in tissue perfusates.

ACKNOWLEDGMENTS. Appreciation is extended to several colleagues for providing advice on various aspects of this chapter, including Drs. Benito Anton, Christopher Evans, and Gregory Bass. The electron micrographs shown in Fig. 5.2 were kindly provided by V. E. Bayer and V. M. Pickel (Figs. 5.2A,B) and by A. D. Grinnell (Fig. 5.2C). Preparation of this chapter was supported in part from grants from the National Institute of Drug Abuse (NIDA 05010) and the Alcoholic Beverage Medical Research Foundation.

REFERENCES

1. Elliott, T. R., 1904, On the innervation of the ileo-colic sphincter, *J. Physiol.* **31**:157–168.
2. Elliott, T. R., 1905, The action of adrenalin, *J. Physiol.* **32**:401–467.
3. von Euler, U. S., 1956, *Noradrenaline. Chemistry, Physiology, Pharmacology and Clinical Aspects*, Charles C. Thomas, Springfield, IL.
4. Loewi, O., 1921, Uber humorale Ubertnagbarkeit de Herznervenwirkung, *Pflugers Arch. Ges. Physiol.* **189**:239–242.
5. Cannon, W. B., and Uridil, J. E., 1921, Studies on the conditions of activity in endocrine glands. VIII Some effects on the denervated heart of stimulating the nerves of the liver, *Am. J. Physiol.* **58**:353–364.
6. Eccles, J. C., 1949, A review and restatement of the electrical hypotheses of synaptic excitatory and inhibitory action, *Arch. Sci. Physiol.* **3**:567–584.
7. Dale, H. H., 1954, The beginnings and prospects of neurohumoral transmission, *Pharmacol. Rev.* **6**:7–13.
8. Eccles, J. C., 1953, *The Neurophysiological Basis of Mind*, Clarendon Press, Oxford.
9. Vogt, M., 1954, The concentration of sympathin in different parts of the central nervous system under normal conditions and after the administration of drugs, *J. Physiol.* **123**:451–481.
10. Sudhof, T. C., and Jahn, R., 1991, Proteins of synaptic vesicles involved in exocytosis and membrane recycling, *Neuron* **6**:665–677.
11. Clements, J. R., Magnusson, K. R., and Beitz, A. J., 1990, Ultrastructural description of glutamate-, aspartate-, taurine-, and glycine-like immunoreactive terminals from five rat brain regions, *J. Elec. Microsc. Tech.* **15**:49–66.

12. Kelly, R. B., 1991, A system for synapse control, *Nature* **349**:650–651.
13. John, C. M., Chakel, J. A., Schueler, B., and Odom, R. W., 1991, Time-of-flight secondary ion mass spectrometry and ion-image analysis of biological surfaces, in: *Proceedings of the 39th ASMS Conference on Mass Spectrometry and Allied Topics*, Nashville, May 19–24, pp. 27–28, American Society of Mass Spectrometry, East Lansing, MI.
14. Grimm, C. C., Short, R. T., and Todd, P. J., 1991, A wide-angle secondary ion probe for organic ion imaging, *J. Am. Soc. Mass Spectrom.* **2**:362–371.
15. Pazos, A., Probst, A., and Palacios, J. M., 1987, Serotonin receptors in the human brain. III. Autoradiographic mapping of serotonin-1 receptors, *Neuroscience* **21**:97–122.
16. Paxos, A., Probst, A., and Palacios, J. M., 1987, Serotonin receptors in the human brain. IV. Autoradiographic mapping of serotonin-2 receptors, *Neuroscience* **21**:123–129.
17. Brown, M. R., 1990, Peptide biology: Past, present, and future, *Ann. N.Y. Acad. Sci.* **579**:8–16.
18. Fuxe, K., Agnati, L. F., Harfstrand, A., Zoli, M., von Euler, G., Grimaldi, R., Merlo Pich, E., Bjelke, B., Eneroth, P., Benfenati, F., Cintra, A., Zini, I., and Martire, M., 1990, On the role of neuropeptide Y in information handling in the central nervous system in normal and physiopathological states: Focus on volume transmission and neuropeptide Y/ α_2 receptor interactions, *Ann. N.Y. Acad. Sci.* **579**:28–67.
19. Maidment, N. T., Brumbaugh, D. R., Rudolph, V. D., Erdelyi, E., and Evans, C. J., 1989, Microdialysis of extracellular endogenous opioid peptides from rat brain *in vivo*, *Neuroscience* **33**:549–557.
20. Maidment, N. T., and Evans, C. J., 1991, Measurement of extracellular neuropeptides in the brain: Microdialysis linked to solid-phase radioimmunoassays with subfemtomole limits of detection, in: *Microdialysis in the Neurosciences* (T. E. Robinson and J. B. Justice, Jr., eds.), Elsevier, New York, pp. 275–303.
21. Maidment, N. T., Martin, K. F., Ford, A. P. D. W., and Marsden, C. A., 1990, *In vivo* voltammetry: the use of carbon fibre electrodes to monitor amines and their metabolites, in: *NeuroMethods*, Vol. 14: *Neurophysiological Techniques* (A. A. Boulton, G. B. Baker, and C. H. Vanderwolf, eds.), Humana Press, Clifton, NJ.
22. Friesen, S. R., 1987, Update on the diagnosis and treatment of rare neuroendocrine tumors, *Surg. Clin. North Am.* **67**:379–393.
23. Roth, K. A., Makk, G., Beck, O., Faull, K., Tatemoto, K., Evans, C. J., and Barchas, J. D., 1985, Isolation and characterisation of substance P, substance P 5–11, and substance K from two metastatic ileal carcinoids, *Regul. Peptides* **12**:185–199.
24. Hornykiewicz, O., 1982, Imbalance of brain monoamines and clinical disorders, *Prog. Brain Res.* **55**:419–429.
25. Davis, G. C., Williams, A. C., Markey, S. P., Ebert, M. H., Caine, E. D., Reichert, C. M., and Kopin, I. J., 1979, Chronic parkinsonism secondary to intravenous injection of meperidine analogues, *Psychiatr. Res.* **1**:249–254.
26. Langston, J. W., Ballard, P., Tetrud, J. W., and Irwin, I., 1983, Chronic parkinsonism in humans due to a product of meperidine analogue synthesis, *Science* **219**:979–980.
27. Kopin, I. J., and Markey, S. P., 1989, MPTP toxicity: Implications for research in Parkinson's disease, *Ann. Rev. Neurosci.* **11**:81–96.
28. Stern, Y., 1990, MPTP-induced parkinsonism, *Prog. Neurobiol.* **34**:107–114.
29. Calne, D. B., and Langston, J. W., 1983, Aetiology of Parkinson's disease, *Lancet* **2**:1457–1459.
30. Barbeau, A., 1984, Etiology of Parkinson's disease: A research strategy, *Can. J. Neurol. Sci.* **11**:24–28.
31. Ohkubo, S., Hirano, T., and Oka, K., 1985, Methyltetrahydro- β -carbolines and Parkinson's disease, *Lancet* **1**:1272–1273.

32. Testa, B., Naylor, R., Costall, B., Jenner, P., and Marsden, C. D., 1985, Does an endogenous methylpyridinium analogue cause Parkinson's disease? *J. Pharm. Pharmacol.* **37**:679–680.
33. Collins, M. A., and Neafsey, E. J., 1985, β -Carboline analogues of N-methyl-4-phenyl-1,2,5,6-tetrahydropyridine (MPTP): Endogenous factors underlying idiopathic parkinsonism? *Neurosci. Lett.* **55**:179–184.
34. Booth, R. G., Trevor, A., Singer, T. P., and Castagnoli, N., Jr., 1989, Studies on semirigid tricyclic analogues of the nigrostriatal toxin 1-methyl-4-phenyl-1,2,5,6-tetrahydropyridine, *J. Med. Chem.* **32**:473–477.
35. Barker, S. A., Harrison, R. E. W., Monti, J. A., Brown, G. B., and Christian, S. T., 1981, Identification and quantification of 1,2,3,4-tetrahydro- β -carboline, 2-methyl-1,2,3,4-tetrahydro- β -carboline, and 6-methoxy-1,2,3,4-tetrahydro- β -carboline as *in vivo* constituents of rat brain and adrenal gland, *Biochem. Pharmacol.* **30**:9–17.
36. Hirano, A., Kurland, L. T., Krooth, R. S., and Lessel, S., 1961, Parkinsonism–dementia complex, an endemic disease on the island of Guam. I. Clinical features, *Brain* **84**:642–661.
37. Hirano, A., Malamud, N., and Kurland, L. T., 1961, Parkinsonism–dementia complex, an endemic disease on the island of Guam. II. Pathological features, *Brain* **84**:662–679.
38. Spencer, P. S., Nunn, P. B., Hugon, J., Ludolph, A. C., Ross, S. M., Roy, D. N., and Robertson, R. C., 1987, Guam amyotrophic lateral sclerosis–parkinsonism–dementia linked to a plant excitant neurotoxin, *Science* **237**:517–522.
39. Kurland, L. T., 1988, Amyotrophic lateral sclerosis and Parkinson's disease complex on Guam linked to an environmental neurotoxin, *Trends Neurosci.* **11**:51–54.
40. Barchas, J. D., Akil, H., Elliott, G. R., Holman, R. B., and Watson, S. J., 1978, Behavioral neurochemistry: Neuroregulators and behavioral states, *Science* **200**:964–973.
41. Mee, J., Korth, J., and Halpern, B., 1976, Rapid and quantitative blood analysis for free fatty acids by chemical ionization mass spectrometry, *Anal. Lett.* **9**:1075–1083.
42. Mee, J. L., Korth, J., Halpern, B., and James, L. B., 1977, Rapid and quantitative blood amino acid analysis by chemical ionization mass spectrometry, *Biomed. Mass Spectrom.* **4**:178–181.
43. Brotherton, H. O., Johnson, J. V., and Yost, R. A., 1983, Determination of drugs in blood serum by mass spectrometry/mass spectrometry, *Anal. Chem.* **55**:549–553.
44. Johnson, J. V., and Yost, R. A., 1985, Tandem mass spectrometry for trace analysis, *Anal. Chem.* **57**:758A–768A.
45. Johnson, J. V., Yost, R. A., and Faull, K. F., 1984, Tandem mass spectrometry for the trace determination of tryptolines in crude brain extracts, *Anal. Chem.* **56**:1655–1661.
46. Johnson, J. V., 1984, *Tandem Mass Spectrometry for the Identification and Quantitation of Tryptolines (Tetrahydro-beta-carbolines) in Rat Brain Extracts*, Ph.D. Thesis, University of Florida, Gainesville.
47. Weitz, C. J., Lowney, L. I., Faull, K. F., Feistner, G., and Goldstein, A., 1986, Morphine and codeine from mammalian brain, *Proc. Natl. Acad. Sci. U.S.A.* **83**:9784–9788.
48. Faull, K. F., and Barchas, J. D., 1983, Negative-ion mass spectrometry fused-silica capillary gas chromatography of neurotransmitters and related compounds, in: *Methods of Biochemical Analysis*, Vol. 29 (D. Glick, ed.), John Wiley & Sons, New York, pp. 325–383.
49. Faull, K. F., and Barchas, J. D., 1983, Analysis of catecholamines and their metabolites by combined gas chromatography–mass spectrometry, in: *Methods in Biogenic Amine Research* (S. Parvez, T. Nagatsu, I. Nagatsu, and H. Parvez, eds.), Elsevier/North Holland Medical Press, Amsterdam/New York, pp. 189–236.
50. Scriba, G. K. E., Borchardt, R. T., Zirrolli, J. A., and Fennessey, P. V., 1988, Selected-ion monitoring gas chromatographic–mass spectrometric analysis of catecholamines: Enhancement of sensitivity by a simple clean-up step on Sephadex G-10, *J. Chromatogr.* **433**:31–40.
51. Chang, S. Y., Moore, T. A., Devaud, L. L., Taylor, L. C. E., and Hollingsworth, E. B., 1991,

- Analysis of rat brain microdialysate by gas chromatography–high-resolution selected ion monitoring mass spectrometry, *J. Chromatogr.* **562**:111–118.
52. Faull, K. F., Pascoe, N., Maddaluno, J. M., Greene, K. A., and Wiener, S., 1990, Passage from MHPG from plasma to CSF in a non-human primate, *J. Neurosci. Res.* **27**:533–540.
 53. Kopin, I. J., Gordon, E. K., Jimerson, D. C., and Polinsky, R. J., 1984, Relationship between plasma and cerebrospinal fluid levels of 3-methoxy-4-hydroxyphenylglycol, *Science* **219**:73–75.
 54. Lewy, A. J., and Markey, S. P., 1978, Analysis of melatonin in human plasma by gas chromatography negative chemical ionization mass spectrometry, *Science* **201**:741–743.
 55. Tetsuo, M., Markey, S. P., Colburn, R. W., and Kopin, I. J., 1981, Quantitative analysis of 6-hydroxymelatonin in human urine by gas chromatography–negative chemical ionization mass spectrometry, *Anal. Biochem.* **110**:208–215.
 56. Markey, S. P., Colburn, R. W., and Johanessen, J. N., 1981, Efficient extraction and mass spectrometric assay of serotonin in biological fluids, *Biomed. Mass Spectrom.* **8**:301–304.
 57. Jenden, D. J., Hanin, I., and Lamb, S. I., 1968, Gas chromatographic microestimation of acetylcholine and related compounds, *Anal. Chem.* **40**:125–128.
 58. Szilagyi, P. I. A., Schmidt, D. E., and Green, J. P., 1968, Microanalytical determination of acetylcholine, other choline esters, and choline by pyrolysis gas chromatography, *Anal. Chem.* **40**:2009–2013.
 59. Hammar, C.-G., Hanin, I., Holmstedt, B., Kitz, R. J., Jenden, D. J., and Karlen, B., 1968, Identification of acetylcholine in fresh rat brain by combined gas chromatography–mass spectrometry, *Nature* **220**:915–917.
 60. Hanin, I., and Skinner, R. F., 1975, Analysis of microquantities of choline and its esters utilizing gas chromatography–chemical ionization mass spectrometry, *Anal. Biochem.* **66**:568–583.
 61. Potter, P. E., Meek, J. L., and Neff, N. H., 1983, Acetylcholine and choline in neuronal tissue measured by HPLC with electrochemical detection, *J. Neurochem.* **41**:188–194.
 62. Faull, K. F., DoAmaral, J. R., Berger, P. A., and Barchas, J. D., 1978, Mass spectrometric identification and selected ion monitoring quantitation of gamma-aminobutyric acid (GABA) in human lumbar cerebrospinal fluid, *J. Neurochem.* **31**:1119–1122.
 63. MacKenzie, S. L., Tenaschuk, D., and Fortier, G., 1987, Analysis of amino acids by gas–liquid chromatography as *tert*.-butyldimethylsilyl derivatives. Preparation of derivatives in a single reaction, *J. Chromatogr.* **387**:241–253.
 64. Ishida, Y., Fujita, T., and Asai, K., 1981, New detection and separation method for amino acids by high-performance liquid chromatography, *J. Chromatogr.* **204**:143–148.
 65. Blankenship, D. T., Krivanek, M. A., Ackerman, B. L., and Cardin, A. D., 1989, High-sensitivity amino acid analysis by derivatization with *o*-phthaldehyde and 9-fluorenylmethyl chloroformate using fluorescence detection: Applications in protein structure determination, *Anal. Biochem.* **178**:227–232.
 66. Farrant, M., Zia-Gharib, F., and Webster, R. A., 1987, Automated pre-column derivatization with *o*-phthalaldehyde for the determination of neurotransmitter amino acids using reverse-phase liquid chromatography, *J. Chromatogr.* **417**:385–390.
 67. Yudkoff, M., Nissim, I., and Pleasure, D., 1988, Astrocyte metabolism of [¹⁵N]glutamine: Implications for the glutamine–glutamate cycle, *J. Neurochem.* **51**:843–850.
 68. Yudkoff, M., Zaleska, M. M., Nissim, I., Nelson, D., and Erecinska, M., 1989, Neuronal glutamine utilization: Pathways of nitrogen transfer studied with [¹⁵N]glutamine, *J. Neurochem.* **53**:632–640.
 69. Erecinska, M., Zaleska, M. M., Nissim, I., Nelson, D., Dagani, F., and Yudkoff, M., 1988, Glucose and synaptosomal glutamine metabolism: Studies with [¹⁵N]glutamate, *J. Neurochem.* **51**:892–902.
 70. Kapetanovic, I. M., Yonekawa, W. D., and Kupferberg, H. J., 1987, Determination of 4-

- aminobutyric acid, aspartate, glutamate, and glutamine and their ^{13}C stable-isotopic enrichment in brain tissue by gas chromatography–mass spectrometry, *J. Chromatogr.* **414**:265–274.
71. Kapetanovic, I. M., Yonekawa, W. D., and Kupferberg, H. J., 1990, Use of stable isotopes and gas chromatography–mass spectrometry in the study of different pools of neurotransmitter amino acids in brain slices, *J. Chromatogr.* **500**:387–394.
 72. Oosting, E., Neugebauer, E., Keyzer, J. J., and Lorenz, W., 1990, Determination of histamine in human plasma: The European external quality control study 1988, *Clin. Exp. Allergy* **20**:349–357.
 73. Neugebauer, E., Keyzer, J., Oosting, E., and Lorenz, W., 1990, Reliability of current techniques for histamine determination in human plasma: The European external quality control study 1988, *Agents Actions* **30**:274–277.
 74. Hough, L. B., Khandelwal, J. K., Morrishow, A. M., and Gree, J. P., 1981, An improved GCMS method to measure *tele*-methylhistamine, *J. Pharmacol. Meth.* **5**:143–148.
 75. Khandelwal, J. K., Hough, L. B., and Green, J. P., 1984, Regional distribution of the histamine metabolite, *tele*-methylimidazoleacetic acid, in rat brain: Effects of pargyline and probenecid, *J. Neurochem.* **42**:519–522.
 76. Mallet, A. I., and Rendell, N. B., 1988, Analysis of N^{τ} -methyl imidazole acetic acid by electron impact gas chromatography/mass spectrometry, *Biomed. Mass Spectrom.* **17**:275–279.
 77. Murray, S., O'Malley, G., Taylor, I. K., Mallet, A. I., and Taylor, G. W., 1989, Assay for N^{τ} -methylimidazoleacetic acid, a major metabolite of histamine, in urine and plasma using capillary column gas chromatography-negative ion mass spectrometry, *J. Chromatogr.* **491**:15–25.
 78. Payne, N. A., Zirrolli, J. A., and Gerber, J. G., 1989, Analysis of histamine and N^{τ} -methylhistamine in plasma by gas chromatography-negative ion-chemical ionization mass spectrometry, *Anal. Biochem.* **178**:414–420.
 79. Boulton, A. A., Durden, D. A., and Davis, B. A., 1989, Isolation, separation and analysis in neurochemistry: Trace amines and acids as an illustrative example, *J. Chromatogr.* **488**:129–143.
 80. Faull, K. F., 1992, Mammalian morphine alkaloids: Identification and possible *in vivo* biosynthesis, in: *The Biological Basis of Substance Abuse and its Therapy* (S. G. Korenman and J. D. Barchas, eds.), Oxford University Press, Oxford.
 81. Collins, M. A., Ung-Chun, N., Cheng, B. Y., and Pronger, D., 1990, Brain and plasma tetrahydroisoquinolines in rats: Effects of chronic ethanol intake and diet, *J. Neurochem.* **55**:1507–1514.
 82. Beck, O., and Faull, K. F., 1986, Concentrations of the enantiomers of 5-hydroxymethyltryptoline in mammalian urine: Implications for *in vivo* biosynthesis, *Biochem. Pharmacol.* **35**:2636–2639.
 83. Beck, O., Repke, D. B., and Faull, K. F., 1986, 6-Hydroxymethyltryptoline is naturally occurring in mammalian urine: Identification by combined chiral capillary gas chromatography and high resolution mass spectrometry, *Biomed. Environ. Mass Spectrom.* **13**:469–472.
 84. Bosin, T. R., and Faull, K. F., 1988, Measurement of beta-carbolines by high performance liquid chromatography with fluorescence detection, *J. Chromatogr.* **428**:229–236.
 85. Bosin, T. R., Borg, S., and Faull, K. F., 1989, Harman in rat brain, lung and human CSF: Effect of alcohol consumption, *Alcohol* **5**:505–511.
 86. Faull, K. F., and Beck, O., 1986, Quantification of neurotransmitters and related compounds by electron capture chemical ionization GC–MS, in: *Mass Spectrometry in Biomedical Research* (S. Gaskell, ed.), John Wiley & Sons, pp. 403–421.
 87. Barker, S. A., Harrison, R. E., Brown, G. B., and Christian, S. T., 1979, Gas chromatographic/mass spectrometric evidence for the identification of 1,2,3,4-tetrahydro- β -carboline as an *in vivo* constituent of rat brain, *Biochem. Biophys. Res. Commun.* **87**:146–154.
 88. Faull, K. F., Holman, R. B., Elliott, G. R., and Barchas, J. D., 1982, Tryptolines: Artifact or

- reality. A new method of analysis using GC/MS, in: *Beta-Carbolines and Tetrahydroisoquinolines* (E. Usdin, F. Bloom, and J. D. Barchas, eds.), Alan R. Liss, New York, pp. 135–154.
89. Peura, P., Johnson, J. V., Yost, R. A., and Faull, K. F., 1989, The concentrations of tryptoline and methtryptoline in rat brain, *J. Neurochem.* **52**:847–852.
 90. Dores, R. M., McDonald, L. K., Steveson, T. C., and Sei, C. A., 1990, The molecular evolution of neuropeptides: Prospects for the '90s, *Brain Behav. Evol.* **36**:80–99.
 91. Desiderio, D. M. (ed.), 1990, *Mass Spectrometry of Peptides*, CRC Press, Boca Raton, FL.
 92. McCloskey, J. A. (ed.), 1990, *Methods in Enzymology, Vol. 193: Mass Spectrometry*, Academic Press, San Diego.
 93. Barofsky, D. F., Geistner, G. J., Faull, K. F., and Roepstorff, P., 1989, Peptide charting applied to studies of precursor processing in endocrine tissues, in: *Mass Spectrometry of Peptides* (D. M. Desiderio, ed.), CRC Press, Boca Raton, FL, pp. 348–365.
 94. Feistner, G. J., Barofsky, D. F., Evans, C. J., Faull, K. F., and Roepstorff, P., 1990, Charting of rat pituitary peptides by plasma desorption and electrospray ionization mass spectrometry, in: *Methods and Mechanisms for Producing Ions from Large Molecules* (K. Standing, ed.), Plenum Press, NATO ASI Science Series, New York, 45–53.
 95. Rose, K., 1990, Analysis of permethylated peptides by mass spectrometry, in: *Mass Spectrometry of Peptides* (D. M. Desiderio, ed.), CRC Press, Boca Raton, FL, pp. 316–323.
 96. Hughes, J., Smith, T. W., Kosterlitz, H. W., Fothergill, L. A., Morgan, B. A., and Morris, H. R., 1975, Identification of two related pentapeptides from the brain with potent opiate agonist activity, *Nature* **258**:577–579.
 97. Feistner, G. J., Hojrup, P., Evans, C. J., Barofsky, D., Faull, K. F., and Roepstorff, P., 1989, Mass spectrometric charting of bovine posterior/intermediate pituitary peptides, *Proc. Natl. Acad. Sci. U.S.A.* **86**:6013–6017.
 98. Andrews, P. C., and Dixon, J. E., 1989, Application of fast atom bombardment mass spectrometry to posttranslational modification of neuropeptides, *Methods Enzymol.* **168**:72–103.
 99. Barchas, J. D., Tatemoto, K., Faull, K. F., Evans, C. J., Valentino, K. L., and Eberwine, J. H., 1987, The search for neuropeptides, in: *Psychopharmacology: The Third Generation of Progress* (H. Y. Meltzer, ed.), Raven Press, New York, pp. 437–447.
 100. Tatemoto, K., and Mutt, V., 1981, Isolation and characterization of the intestinal peptide porcine PHI (PHI-27) a new member of the glucagon–secretin family, *Proc. Natl. Acad. Sci. U.S.A.* **78**:6603–6607.
 101. Tatemoto, K., and Mutt, V., 1980, Isolation of two novel candidate hormones using a chemical method for finding naturally occurring polypeptides, *Nature* **285**:417–418.
 102. Tatemoto, K., Efendic, S., Mutt, V., Makk, G., Feistner, G. J., and Barchas, J. D., 1987, Isolation and structure of pancreastatin, a novel pancreatic peptide that inhibits insulin secretion, *Nature* **324**:476–478.
 103. Flanagan, T., Taylor, L., Poulter, L., Viveros, O. H., and Diliberto, E. J., Jr., 1990, *Cell. Mol. Neurobiol.* **10**:507–523.
 104. Zollinger, M., Amsler, U., and Brauchli, J., 1990, Quantification of N-acetylaspartylglutamate, an N-terminal blocked dipeptide neurotransmitter candidate, in brain slice superfusates by gas chromatography–mass spectrometry, *J. Chromatogr.* **532**:27–36.
 105. Matsumoto, M., Togashi, H., Yoshioka, M., Morii, K., Hirokami, M., Tochihiro, M., Ikeda, T., Saito, Y., and Saito, H., 1990, Significant correlation between cerebrospinal fluid and brain levels of norepinephrine, serotonin and acetylcholine in anesthetised rats, *Life Sci.* **48**:823–829.
 106. Bacopoulos, N. G., and Bhatnagar, R. K., 1977, Correlation between tyrosine hydroxylase activity and catecholamine concentration or turnover in brain regions, *J. Neurochem.* **29**:639–643.

107. Wester, P., Bergstrom, U., Eriksson, A., Gezelius, C., Hardy, J., and Winblad, B., 1990, Ventricular cerebrospinal fluid monoamine transmitter and metabolite concentrations reflect human brain neurochemistry in autopsy cases, *J. Neurochem.* **54**:1148–1156.
108. Mefford, I. N., and Barchas, J. D., 1980, Determination of tryptophan and metabolites in rat brain and pineal tissue by reverse-phase high-performance liquid chromatography with electrochemical detection, *J. Chromatogr.* **181**:187–193.
109. Miller, J. M., Jope, R. S., Ferraro, T. N., and Hare, T. A., 1990, Brain amino acid concentrations in rats killed by decapitation and microwave irradiation, *J. Neurosci. Methods* **31**:187–192.
110. Scremin, O. U., and Jenden, D. J., 1991, Time-dependent changes in cerebral choline and acetylcholine induced by transient global ischemia in rats, *Stroke* **22**:643–647.
111. Zamir, N., Weber, E., Palkovits, M., and Brownstein, M., 1984, Differential processing of prodynorphin and proenkephalin in specific regions of the rat brain, *Proc. Natl. Acad. Sci. U.S.A.* **81**:6886–6889.
112. Wahlestedt, C., Blendy, J. A., Kellar, K. J., Heilig, M., Widerlov, E., and Ekman, R., 1990, Electroconvulsive shocks increase the concentration of neocortical and hippocampal neuropeptide Y (NPY)-like immunoreactivity in the rat, *Brain Res.* **507**:65–68.
113. McKibbin, P. E., Rogers, P., and Williams, G., 1991, Increased neuropeptide Y concentrations in the lateral hypothalamic area of the rat after the onset of darkness, *Life Sci.* **48**:2527–2533.
114. Evans, C. J., Hammond, D. L., and Frederickson, R. C. A., 1988, The opioid peptides, in: *The Opiate Receptors* (G. W. Pasternak, ed.), The Humana Press, Clifton, NJ, pp. 23–71.

Cannabinoids

David J. Harvey

1. INTRODUCTION

The cannabinoids form a group of terpene-related compounds unique to the plant *Cannabis sativa* L., the source of the drug marijuana. To date, some 70 of these compounds have been identified (1), the major ones having the structures shown in Fig. 6.1. Of these, delta-9-tetrahydrocannabinol (delta-9-THC, I) is the major psychoactive constituent, cannabidiol (CBD, II) is its biosynthetic precursor, and cannabinol (CBN, III) is generally regarded as a chemical degradation product (2). Most of the major cannabinoids possess a pentyl chain, but the complexity of cannabinoid mixtures arises from the presence of lower homologues, of which the propyl series is the best known (3). Methyl (4) and butyl (5) cannabinoids have also been reported, but in low concentration. An interesting feature of the relative abundance of all of the cannabinoids is their dependence on geographical origin and age. Plants grown in temperate regions tend to have low THC contents, whereas those originating in tropical regions contain high concentrations of this cannabinoid. In addition, the relative concentration of the homologues displays a strong regional bias with, for example, propyl cannabinoids being particularly abundant in samples originating from the Indian subcontinent. Further complexity is imparted by the fact that most natural cannabinoids contain a carboxylic acid group either at C-2 (named acid A, IV) or at C-4 (acid B, V). This group is labile, is lost when the drug is smoked, and presents problems when analysis is performed by gas chromatography.

Although marijuana has been used by man for its euphoric effects for several millennia, its mechanism of action is by no means fully understood. Indeed, it is only in the last few years that a specific receptor for delta-9-

David J. Harvey • Department of Pharmacology, University of Oxford, Oxford OX1 3QT, England.

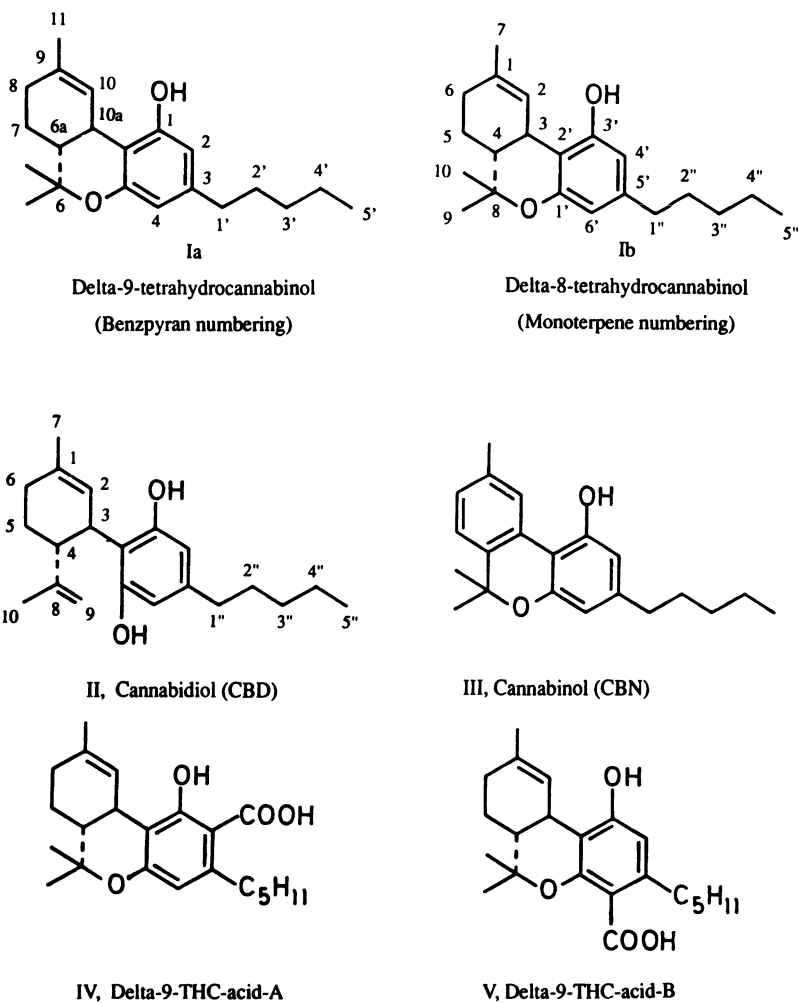
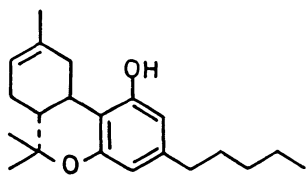
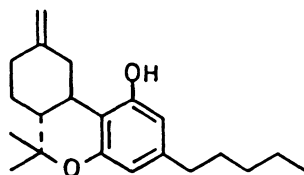


Figure 6.1. Structures of the major cannabinoids from *Cannabis sativa* L.

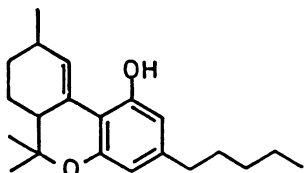
tetrahydrocannabinol has been found in the brain (6). Action at this receptor, however, by no means accounts for all of the drug's effects, particularly its long-term adverse effects (7). Effects are more commonly attributed to the drug's high lipid solubility, which both causes accumulation in fatty tissues and affects the structure of cell membranes. As a direct consequence of the drug's lipid solubility, it has proved difficult to determine pharmacokinetic parameters because the drug's concentration in blood drops to levels too low to be measured within a few hours of drug administration. Thus, only highly sensitive and specific tech-



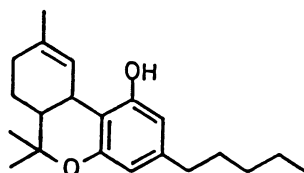
VI, Delta-8-THC



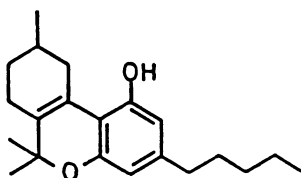
VII, Delta-9(11)-THC



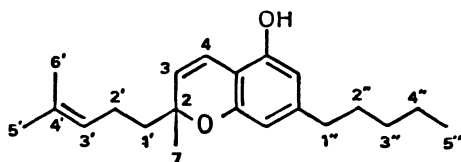
VIII, Delta-10-THC



IX, 6a(10a)-trans-delta-9-THC



X, Delta-6a(10a)-THC

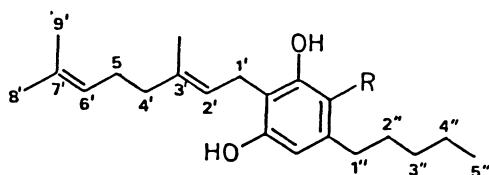


XI, Cannabichromene (CBC)

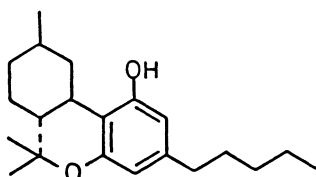
Figure 6.1. (Continued)

niques such as mass spectrometry are appropriate for measurement. A further consequence of the drug's lipophilic nature is its rapid and extensive metabolism by enzymes of the mixed-function oxidase system. This metabolism gives as many as 100 identified metabolites from some of the major cannabinoids (8,9).

From an analytical point of view, therefore, the cannabinoids present a considerable challenge. With natural cannabinoid mixtures, it is necessary to separate and identify many closely related structures with due regard to the unstable nature of the cannabinoid acids. Similar constraints apply to the metabo-



XII, Cannabigerol (CBG)



XIII, Hexahydrocannabinol

Figure 6.1. (Continued)

lites, with the additional problem that many of these compounds accumulate in fatty tissues or are excreted in the feces. However, it is the quantification of these compounds that perhaps presents the greatest challenge, because very low concentrations have to be measured in complex biological matrices. Fortunately, with suitable derivatization, most of the cannabinoids and their metabolites are ideally suited to analysis by GLC and GC/MS, and this chapter concentrates on the development of various techniques for obtaining qualitative and quantitative information using these methods.

2. MASS SPECTROMETRIC CHARACTERISTICS OF NATURAL CANNABINOIDS

If mass spectrometry is to be used to identify new cannabinoids or metabolites, it is essential that fragmentation mechanisms of characterized compounds are fully defined so that the areas of the molecule giving rise to specific fragment ions are understood. This information is particularly important when, for example, identifying the position of a metabolically added substituent. Fortunately, it has been found that many derivatives, such as the TMS ethers, have little effect on the general fragmentation patterns, which are usually directed by charge

localization at a site remote from the derivatized function. Several studies have addressed cannabinoid fragmentation using a combination of deuterium labeling and comparisons of spectra between homologues, and the pathways responsible for the major fragment ions of most cannabinoids are now fairly well understood (10).

2.1. Tetrahydrocannabinols

Although delta-9-THC appears to be the only isomer to occur naturally in any abundance, several other, synthetic compounds have been well studied, both mass spectrometrically and pharmacologically. These compounds include delta-8-THC (VI), a cannabinoid with equivalent psychoactivity to the delta-9 isomer, the inactive, exocyclic delta-11-isomer (VII), and delta-6a,10a-THC (X). A number of minor compounds such as delta-10-THC (VIII) and the 6a,10a-*cis,trans* isomers (IX) have also received some attention. The spectra of these compounds tend to contain fragment ions at common masses, but with considerably different relative abundances (11). All of the compounds give prominent molecular ions, with that from delta-9-THC being the base peak in the spectrum of the free cannabinoid (Fig. 6.2) and of its TMS ether (Fig. 6.3) (12). The $[M - 15]^+$ ions are the result of loss of the C-11 carbon atom or one of the *gem*-methyl groups. The very favorable loss of a *gem*-methyl group from delta-6a,10a-THC (X) and the consequent formation of an aromatic species accounts for the high abundance of this ion (base peak) in its spectrum. In contrast to this loss, the abundant $[M - 15]^+$ ion in the spectrum of delta-9-THC appears to arise predominantly by loss of the C-11 methyl group, as shown by deuterium labeling; a hydrogen rearrangement and formation of a conjugated ion (*a*), as depicted in Fig. 6.4, has been proposed to account for this fragment (12). It is supported by the relatively low abundance of this ion in the spectra of isomers such as delta-8-THC, where such a rearrangement is not possible. The mass spectra of the TMS derivatives of the THC's are similar, with only a very minor contribution to the $[M - 15]^+$ ion being from a TMS group.

A retro-Diels–Alder reaction accounts for the formation of the abundant ion at m/z 246 (*b*) in the spectrum of delta-8-THC and its derivatives (Fig. 6.5). Loss of CH_3 from this ion results in a contribution to the ion at m/z 231 (*c*). However, deuterium labeling shows a substantial retention of the methyl group from C-11, implying the existence of at least another pathway involving rearrangement (13). These ions are weaker in the spectrum of delta-9-THC, where they must be formed by another mechanism because the retro-Diels–Alder reaction does not result in loss of a fragment. More abundant in the spectrum of this isomer is the ion at m/z 243 [315 (*d*, Fig. 6.6)] in the spectrum of the TMS derivative, which appears to be produced by loss of the entire pentyl chain. This ion is not seen in the spectrum of the other isomers, implying some involvement of the double

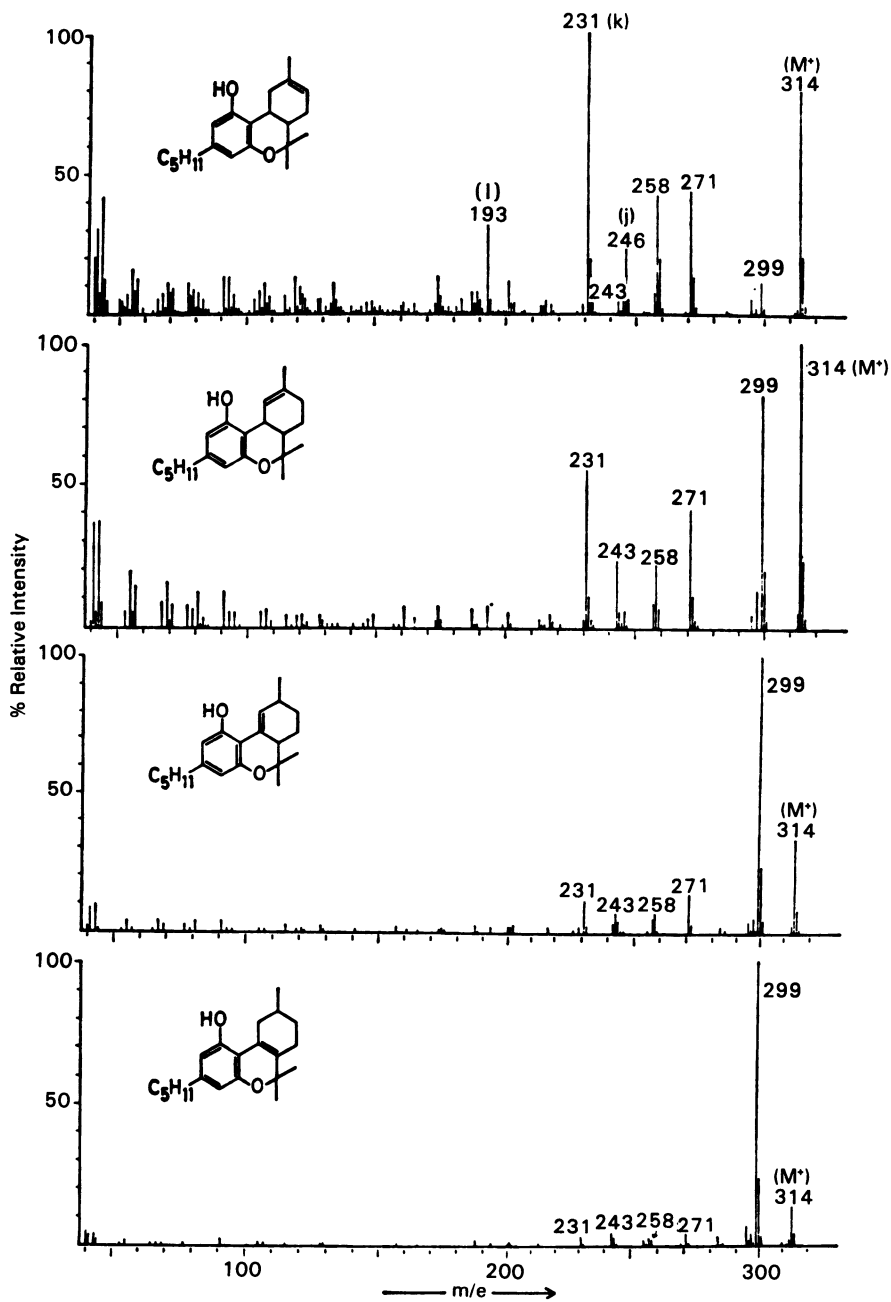


Figure 6.2. Mass spectra of (from top to bottom) delta-8-THC, delta-9-THC, delta-10-THC, and delta-6a(10a)-THC (11). [Reproduced with permission from Pergamon Press Ltd.]

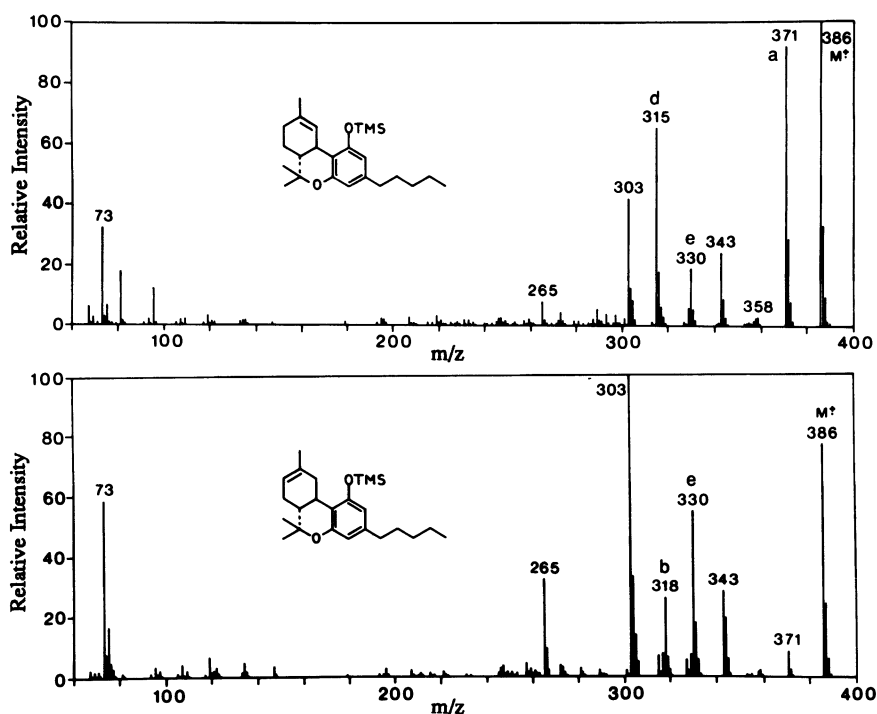


Figure 6.3. Mass spectra (25 eV) of the TMS derivatives of delta-9-THC (top) and delta-8-THC (bottom) (12). [Reproduced with permission from John Wiley & Sons, Ltd.]

bond. A more common fragmentation of the side chain of all THC isomers and other cannabinoids is the rearrangement depicted in Fig. 6.7, involving migration of a C-3' hydrogen atom to the phenyl ring to yield the prominent ion at $[M - 56]^+$ (e, Fig. 6.7).

2.2. Cannabinol

The mass spectrum of this cannabinoid and its derivatives is relatively simple (Fig. 6.8) with a molecular ion of about 20% relative abundance and a base peak corresponding to $[M - 15]^+$. This latter ion is produced by loss of a *gem*-methyl group in an analogous manner to the corresponding loss in the fragmentation of delta-6a,10a-THC to give an aromatic species. The only other ion whose relative abundance exceeds 1% is that at $[M - 72]^+$; this ion appears to have lost carbon atoms from the pentyl chain.

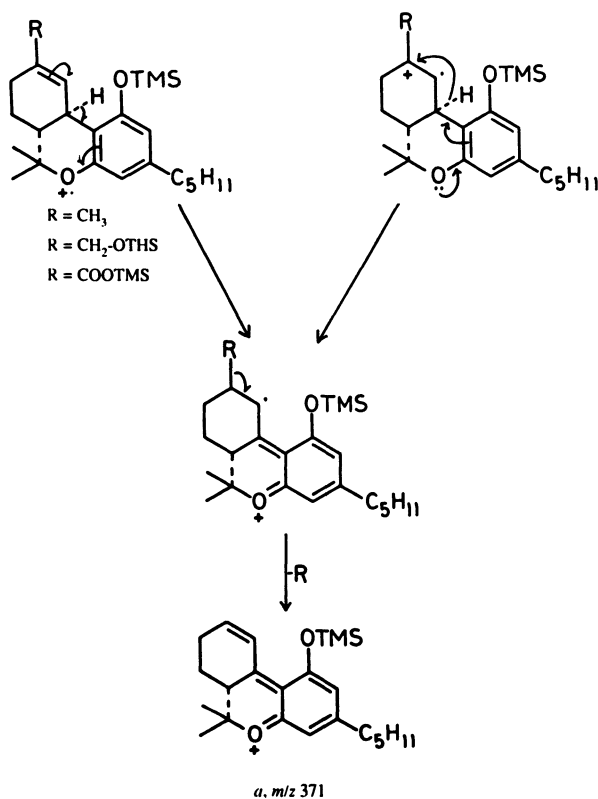


Figure 6.4. Proposed mechanism for the formation of the $[M - 15]^+$ ion in the mass spectrum of delta-9-THC.

2.3. Cannabidiol

The spectra of this compound and of its TMS ether (Fig. 6.9) are more interesting. The base peak in the spectrum of the TMS ether (m/z 390, *f*) is the result of a retro-Diels–Alder fragmentation (Fig. 6.10) (14). In the spectrum of the underivatized compound, this ion loses a further methyl radical to give the base peak at m/z 231, for which a cyclic structure has been proposed. Another prominent ion in the spectrum of the TMS ether is the tropylium ion at m/z 337 (*g*, Fig. 6.10).

2.4. Minor Cannabinoids

Fewer studies have been performed on the fragmentation of these compounds. Most appear to give relatively simple spectra. Cannabichromene (CBC,

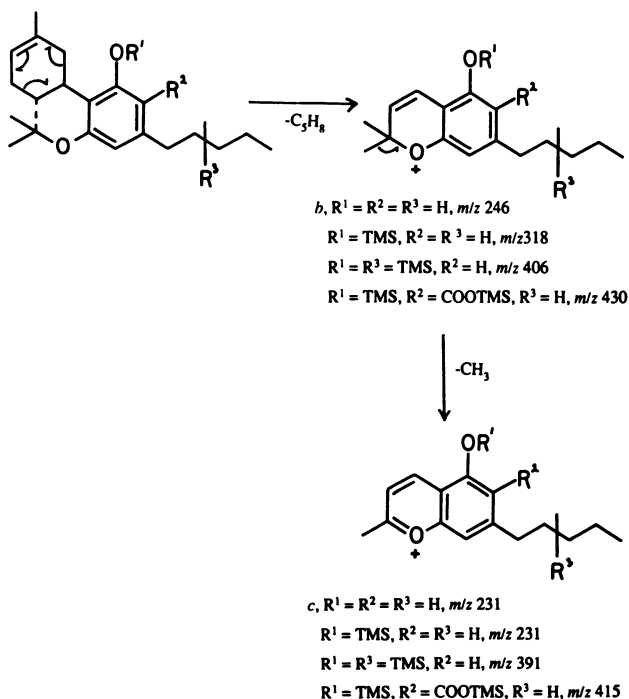


Figure 6.5. Retro-Diels–Alder fragmentation of delta-8-THC and its derivatives.

XI, Fig. 6.1) TMS ether, for example, gives a spectrum with a very abundant chromenyl ion (m/z 303) produced by loss of the methylpentenyl chain and little else (15). Cannabigerol (CBG, XII) gives essentially only four ions of which the tropylium ion is the base peak. The other ions are formed by cleavages of the unsaturated chain between the double bonds (16). The spectrum of the tetrahydro derivative of CBG (TMS derivative) contains essentially only two significant fragment ions: the tropylium ion and the side-chain cleavage ion of the type

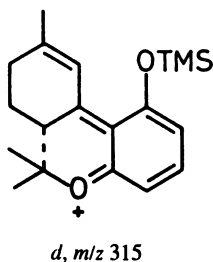


Figure 6.6. Structure of the ion at m/z 315.

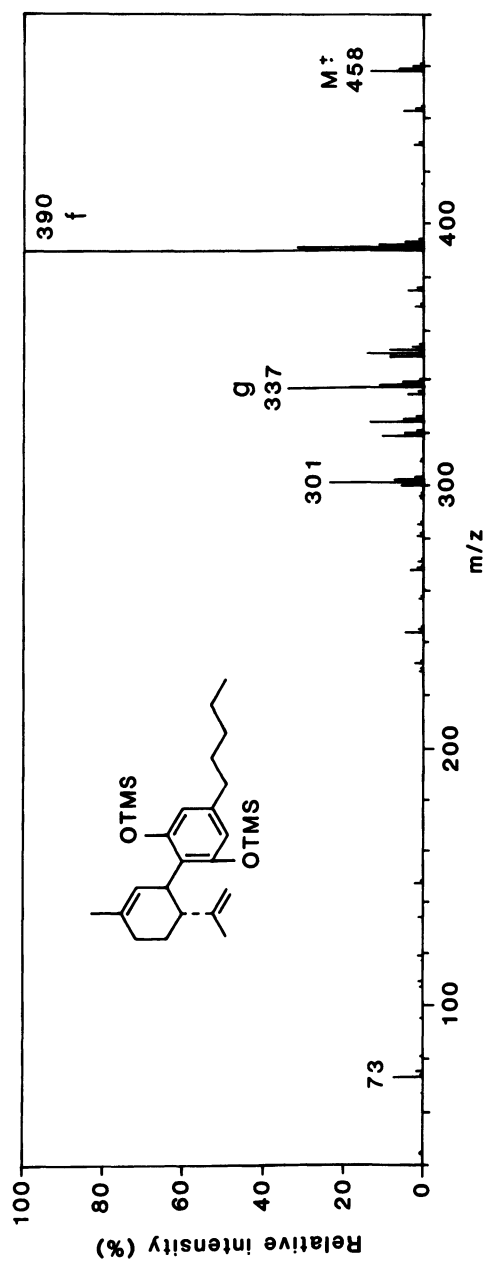


Figure 6.9. Mass spectrum (25 eV) of the TMS derivative of CBD (10). [Reproduced with permission from John Wiley & Sons, Ltd.]

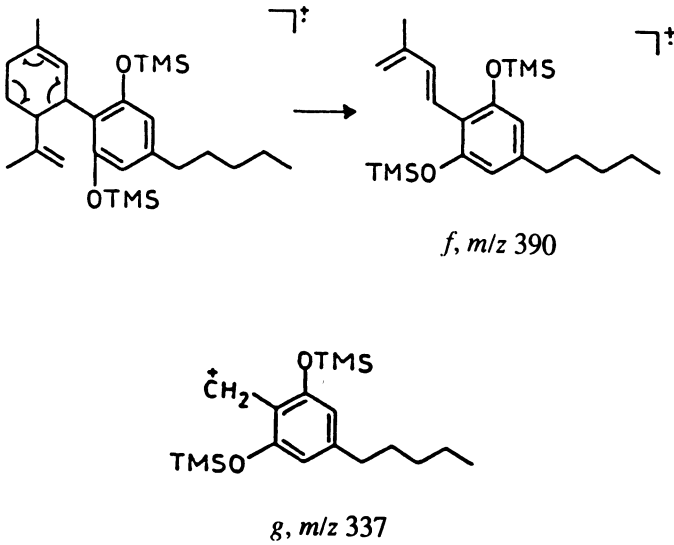


Figure 6.10. Major fragment ions in the mass spectrum of the TMS derivative of CBD.

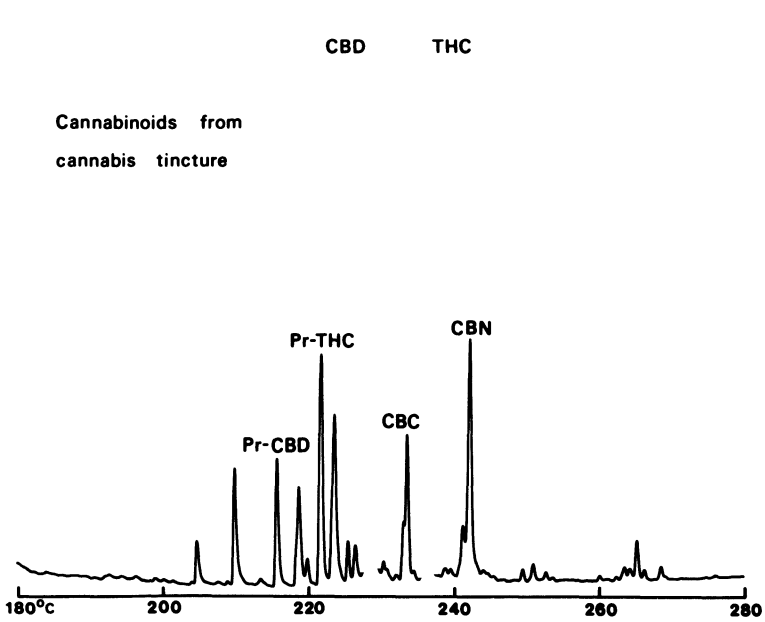


Figure 6.11. Separation of natural cannabinoids as TMS derivatives on an OV-1 fused-silica capillary column.

hence separation of most cannabinoids, it is also possible to effect separation of many of these constituents on lower-resolution columns by variation of the derivative. This variation is the result of the presence of mono- and dihydroxylation among the major compounds. If, instead of trimethylsilylation, the derivatization is changed to triethylsilylation, a greater relative retention increment will be imparted to the dihydroxylated cannabinoids such as CBD and CBG than to the monohydroxylated compounds (19). Thus, these compounds will be moved to higher-temperature regions of the chromatogram. By the use of tributylsilyl derivatives, it is possible to effect complete separation of these groups of compounds, as shown in Fig. 6.12. The mass spectrometric fragmentation of these derivatives is similar to that of the TMS derivatives (20), although the higher homologues produce additional ions because of loss of alkenes from the alkylsilyl moiety.

Derivatization can be used not only to affect chromatographic retention times but also to direct mass spectrometric fragmentation into structurally informative pathways. This change in fragmentation can be illustrated with the cannabinoid acids of type A, which do not give useful spectra (Fig. 6.13). These spectra are dominated by the ion at $[M - 15]^+$ (*h*) formed by loss of a methyl radical from a TMS group and stabilized by cyclization, as shown in Fig. 6.14. This cyclization localizes the charge at a site remote from the terpene ring and inhibits further fragmentation. However, changing the derivative to a cyclic alkane boronate can be used to restore the typical fragmentation pattern of the parent cannabinoid, as shown in Fig. 6.15 for delta-9-THC acid A (21). This pattern results from the charge being relocated from the boronate group to the same area of the molecule to that occurring in the parent compound.

Another property of cannabinoid mass spectra that has been utilized for structural elucidation of natural cannabinoids is the different appearance potentials of the fragment ions (22). If the relative abundance of the ions is plotted against ionization potential in the 10- to 20-eV region, a series of characteristic curves for the different cannabinoids is obtained as shown in Fig. 6.16. Although characteristically different for each cannabinoid, these curves are very similar for different homologues of a given cannabinoid, enabling the presence of these homologues to be confirmed in the mixture (23,24).

4. CANNABINOID METABOLITES

Most cannabinoids are good substrates for the cytochrome P-450 mixed-function oxidases and are initially metabolized by hydroxylation at many sites. The resulting alcohols are further transformed by such reactions as oxidation to acids, conjugation with glucuronic acid, and β -oxidation as illustrated by the metabolic scheme for delta-9-THC shown in Fig. 6.17. A feature of the metabo-

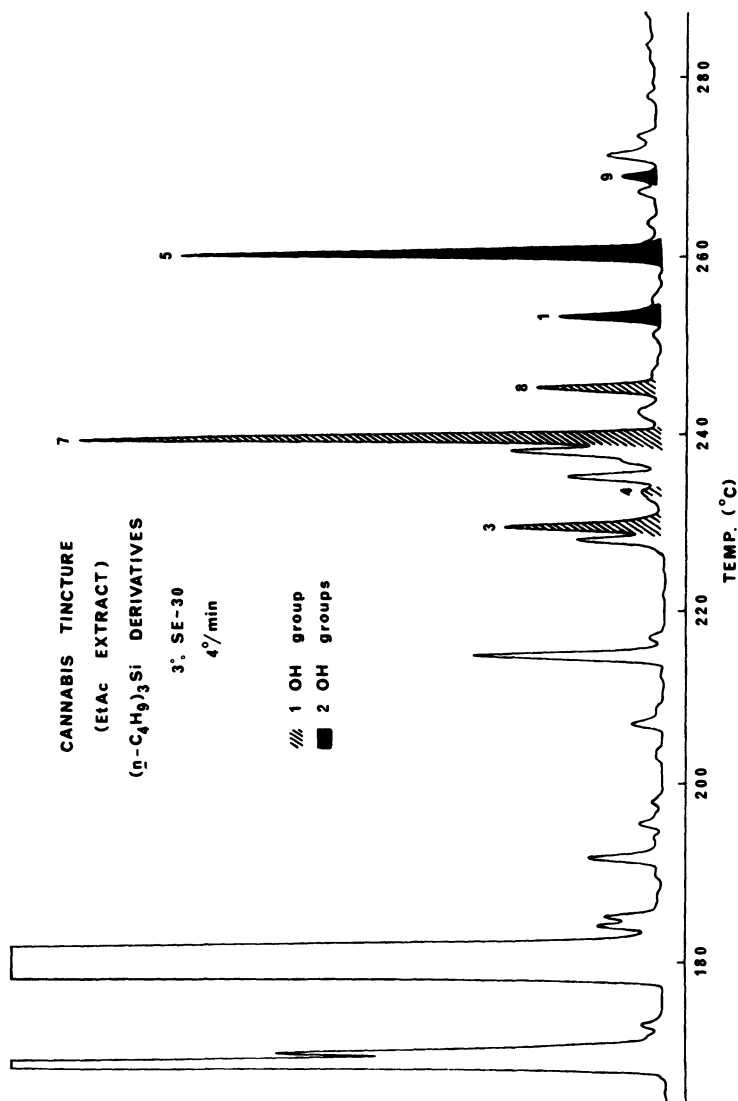


Figure 6.12. Separation of natural cannabinoids on an SE-30 packed column as tributylsilyl derivatives (19). [Reproduced with permission from Elsevier Scientific Publishers.]

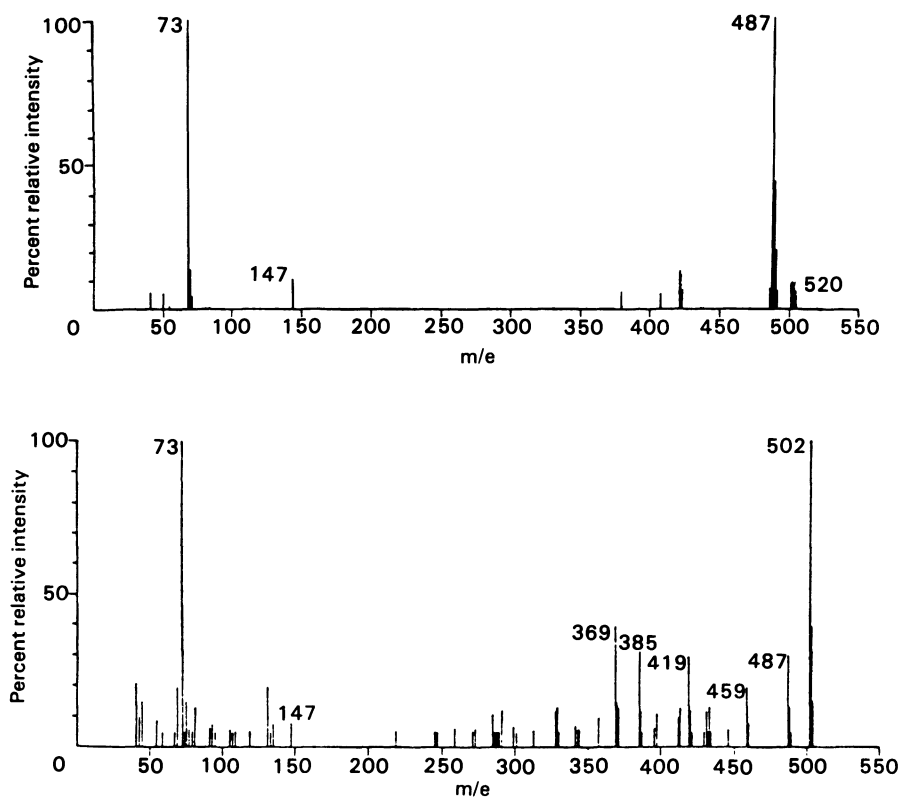


Figure 6.13. Mass spectra of the TMS derivatives of delta-9-THC acid-A (top) and delta-9-THC acid-B (bottom). From Billets, S., El-Feraly, F., Fetterman, P.S., and Turner, C. E., 1976, *Org. Mass Spectrom.*, 11:741–751. [Reproduced with permission from John Wiley & Sons, Ltd.]

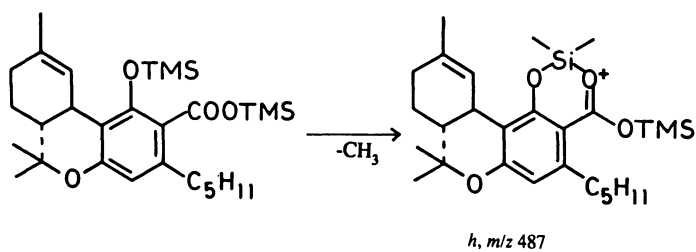


Figure 6.14. Mechanism for the formation and stabilization of the $[M - 15]^+$ ion in the mass spectrum of delta-9-THC acid-A TMS derivative.

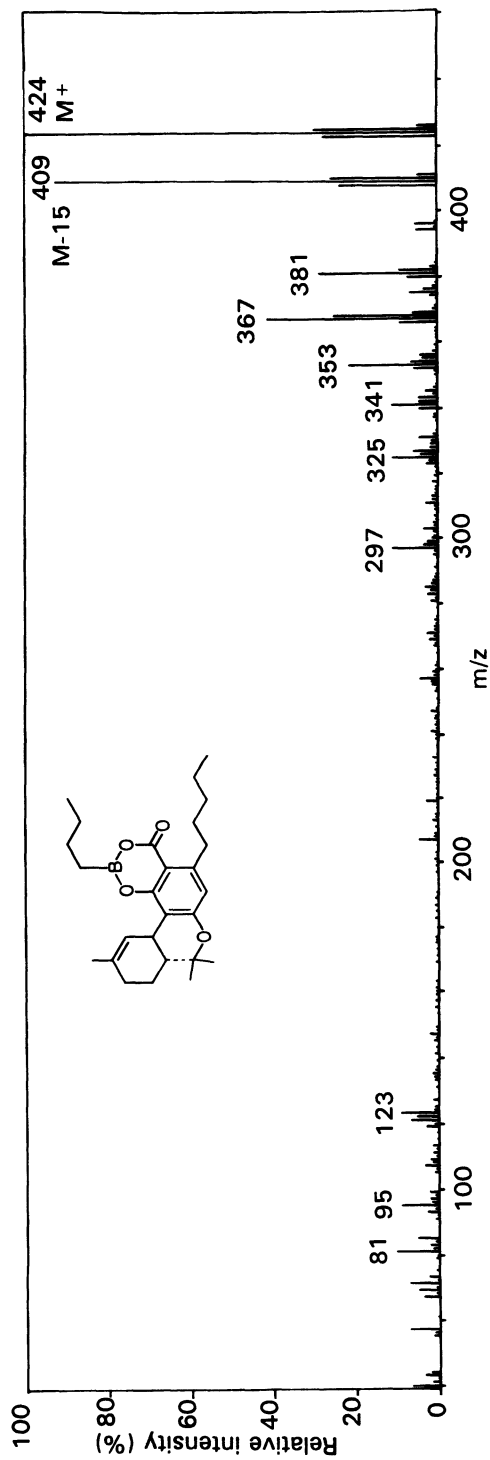


Figure 6.15. Mass spectrum (25 eV) of the cyclic *n*-butane boronate derivative of delta-9-THC acid-A showing the presence of ions yielding structural information (21). [Reproduced with permission from John Wiley & Sons, Ltd.]

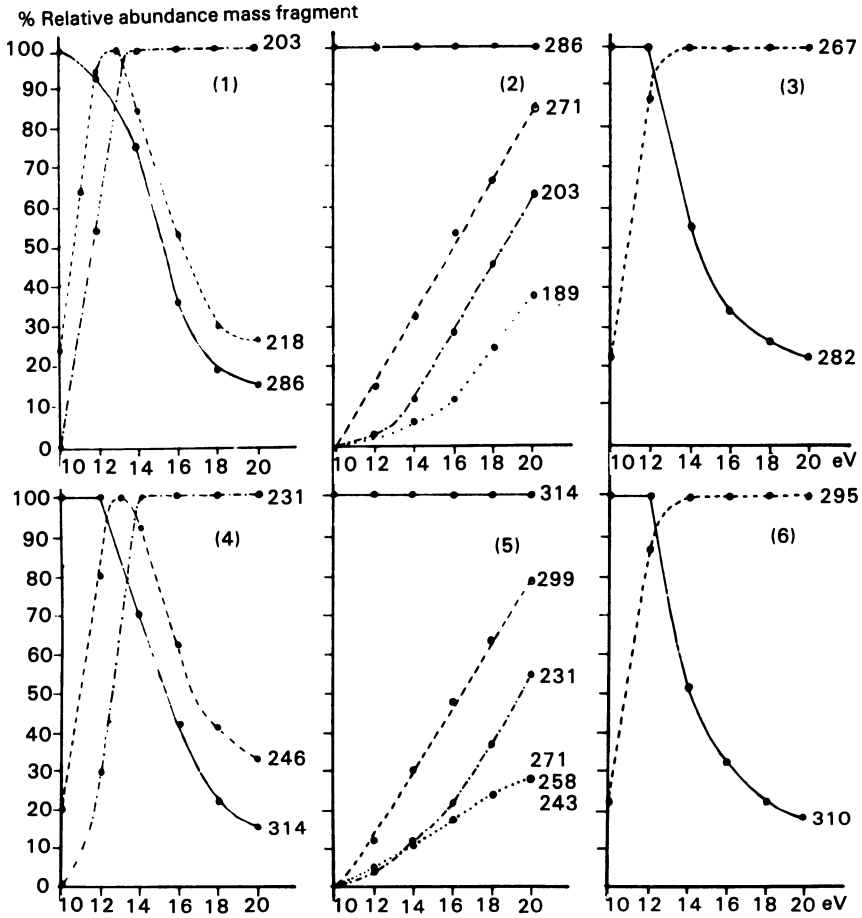


Figure 6.16. Plots of ion abundance as a function of electron energy for some major cannabinoids and their propyl homologues. 1, propyl-CBD; 2, propyl-delta-9-THC; 3, propyl-CBN; 4, CBD; 5, delta-9-THC; 6, CBN (22). [Reproduced with permission from Elsevier Scientific Publishers.]

lism of these compounds is the appearance of a large number of metabolites containing biotransformations at multiple sites. This multiple biotransformation results in a very complex metabolic profile necessitating very considerable separation and mass spectrometric identification at low levels. The early studies on these compounds (25,26) were performed with urine extracts or with microsomal hydroxylations. The former medium, however, only contains the terminal, acidic products of metabolism, whereas the microsomal experiments give only the early hydroxy metabolites. In our studies (27), we have preferred to obtain a more complete profile by examining metabolites in whole livers of animals treated intraperitoneally with the drugs.

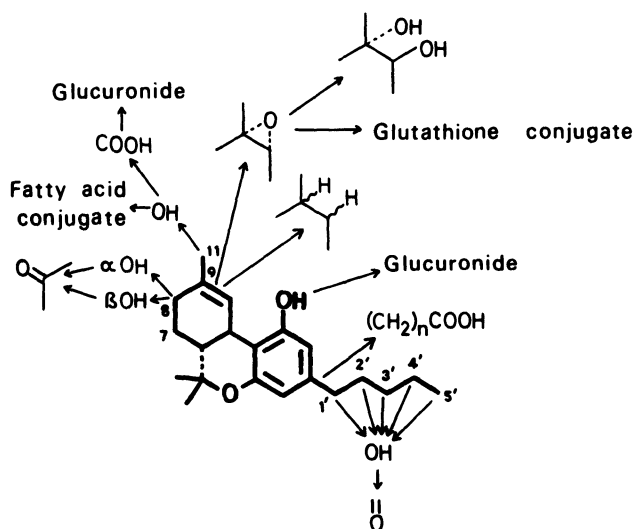


Figure 6.17. Diagram showing the major metabolic pathways for delta-9-THC.

4.1. General Method for the Identification of Hepatic Metabolites

Animals were treated with reasonably high concentrations of the drugs (typically 50–100 mg/kg) and allowed to metabolize these drugs for up to 1 hr. The animals were then killed, and the livers removed. The strategy adopted for metabolite extraction (28) was to use as little chemical clean-up as possible in order to avoid losses of minor and reactive metabolites and to rely on the separating power of the gas chromatograph to separate the metabolites and the specificity of the mass spectrometer, combined with the use of a number of different chemical derivatives and stable isotope labeling, to identify them.

The first extraction stage employed ethyl acetate because this polar solvent has been shown to be capable of dissolving a wide range of lipid-like molecules even when they are substituted with several hydroxy and acid groups. However, large quantities of neutral lipid, mainly triglycerides and cholesterol, are also extracted and need to be removed. Because the cannabinoids are lipophilic molecules without an ionizable nitrogen atom, the common techniques of acid and base partition are inappropriate, and the best approach proved to be the use of gel filtration in the form of chromatography on Sephadex LH-20. Chloroform was used as the eluting solvent for the neutral and monohydroxy cannabinoids, and an increase in polarity by the addition of 10% methanol was used to recover the more highly substituted metabolites including acids and glucuronide conjugates. Details are given in Fig. 6.18.

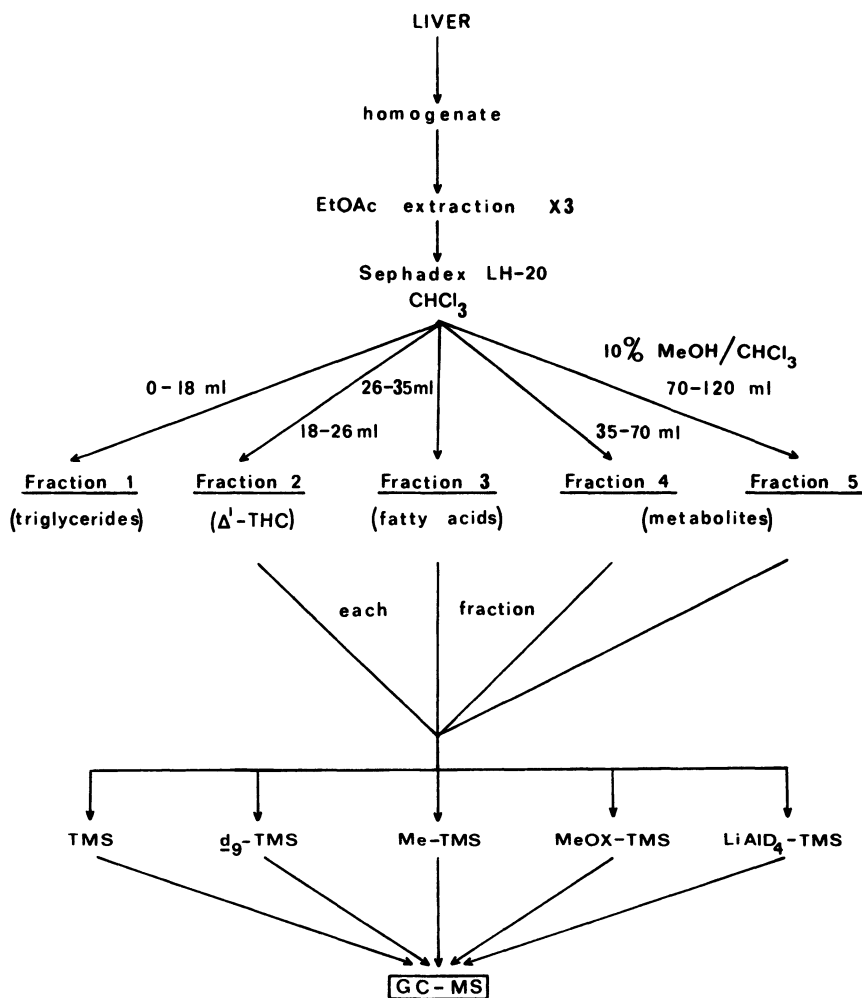


Figure 6.18. Extraction scheme for cannabinoids in liver.

The metabolite-containing fractions were converted into various derivatives for examination by GC/MS. TMS derivatives were used routinely, and the difference in mass between TMS and the perdeuterio-TMS ($[^2\text{H}_9]\text{TMS}$) derivatives gave the number of TMS groups and hence the number of added hydroxy or acid groups in the metabolite. Methyl esters were prepared using diazomethane in order to identify carboxylic acids, and methyloximes were used to identify carbonyl compounds. Occasionally other derivatives such as cyclic alkane boronates were used to confirm the presence of *cis*-diols, and TMS formation under different conditions was used to reveal the presence of sterically hindered hy-

droxy groups. The 9 α -hydroxy group is particularly hindered and only trimethylsilylated with prolonged heating with trimethylsilylimidazole. Consequently, it is possible to prepare mixed TMS and [$^2\text{H}_9$]TMS derivatives by performing a dual derivatization reaction under different conditions with the two reagents. This system enables fragmentation of dihydroxy metabolites containing a 9 α -hydroxy group to be studied in detail because it is possible to determine the order in which OTMS groups are lost as trimethylsilanol (17).

4.1.1. Use of Deuterium Labeling for Metabolite Identification

In addition to the use of perdeuterio-TMS derivatives to determine the number of metabolic hydroxy and acid groups in a molecule and for defining fragmentation pathways, there have been a number of additional uses of deuterium labeling for obtaining structural and mechanistic information with the cannabinoids. These uses involve both the preparation of labeled derivatives and studies with labeled cannabinoids (29,30).

4.1.1a. Isotope Doublet Technique. The first task when examining the GLC profile of separated metabolites is to identify which peak in the complex chromatogram is produced by a metabolite and which represents a residual endogenous constituent. This differentiation is important because it has been found that some metabolites gave spectra that are very similar to natural lipids. This is illustrated in Fig. 6.19, which shows the mass spectrum of 1-monopalmitin and the major monohydroxy metabolite of delta-9-THC. Not only do the compounds have very similar GLC retention times and mass spectra, but both have the same molecular weight and form *bis*-TMS derivatives. It is clear from Fig. 6.19 that differences do exist between the spectra; monopalmitin does not produce a molecular ion, and the spectrum contains an acylium ion at m/z 239. However, in the absence of reference spectra it would be very easy to assume that monopalmitin was a metabolite of delta-9-THC. A convenient way around this problem is to use the isotope-doublet technique. The animal is treated with a 1 : 1 mixture of the drug and a variant labeled with a stable isotope, and the resulting spectra are examined to see which contain the consequent doublet peaks. For delta-9-THC, the use of [$1',1',2',2'-^2\text{H}_4$]delta-9-THC is convenient and the resulting spectrum for the partially labelled 11-hydroxy metabolite is shown in Fig. 6.19. Care must be taken, however, to allow for the fact that one or more deuterium atoms may be replaced metabolically and that, if so, metabolic switching from a primary kinetic isotope effect may result in an altered metabolic profile. Deuterium can also be lost by exchange. It would be safer to use another stable isotope such as ^{13}C , but even here, carbon-carbon bond cleavage may result in loss of the label.

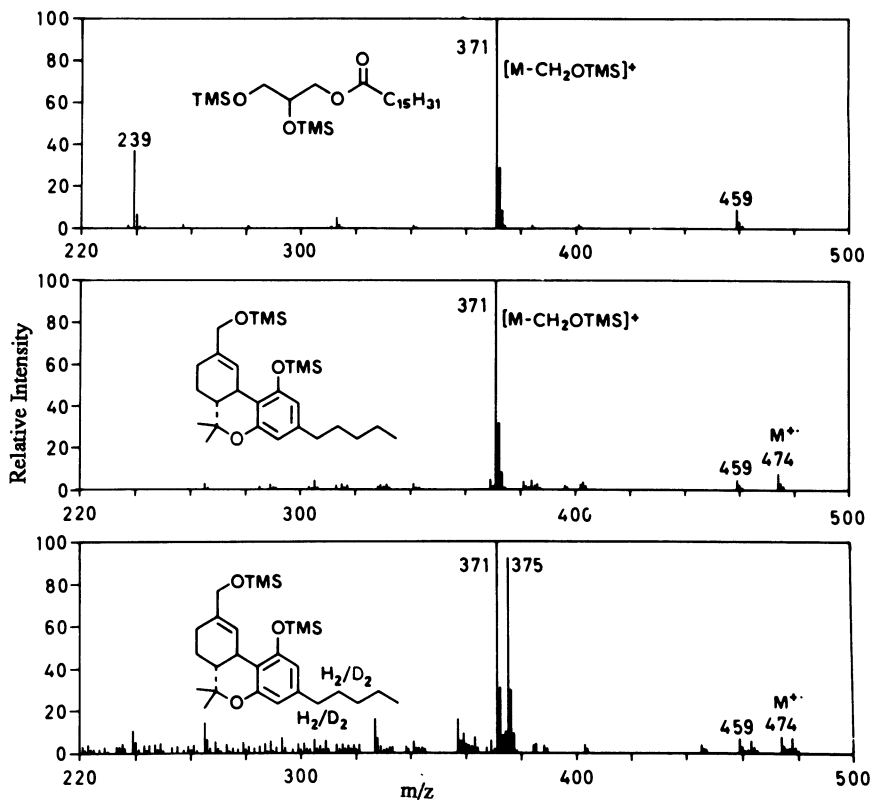


Figure 6.19. Mass spectra (25 eV) of the TMS derivatives of (a) 1-monopalmitin, (b) 11-hydroxy-delta-9-THC, and (c) a 1:1 mixture of 11-hydroxy-delta-9-THC and its [1',1',2',2'- $^2\text{H}_4$] analogue (30). [Reproduced with permission from John Wiley & Sons, Ltd.]

4.1.1b. Reduction with Lithium Aluminium Deuteride. Once the metabolites have been located and their functional groups determined, the next task is to determine the location of those groups. This step is one where a detailed knowledge of the fragmentation of the individual parent cannabinoids is valuable because many of the fragment ions present in the parent spectrum are also present in the spectra of the metabolites, with the appropriate mass shift depending on the nature of the functional group. In a few cases, reference compounds are available or can be conveniently synthesized. However, in view of the complexity of the metabolic profiles, it would be impractical to synthesize all suspected metabolites because synthesis in this area is not easy. In order to overcome this difficulty, we have attempted to use stable isotope labeling to link metabolites in different oxidation states and to show common positions of substitution. Within a

metabolic fraction, several metabolites are usually found with common positions of substitution but with the substituents in different oxidation states. Thus, for example, for an alcohol, the derived carbonyl compound and a carboxylic acid may be present. If the metabolic fraction is reduced with lithium aluminium deuteride, both oxidized metabolites are converted back to the alcohol, resulting in one peak in the gas chromatogram. However, the spectrum of this alcohol will consist of different isotopic variants depending on the source of the alcohol. Natural alcohols will contain no added deuterium, those produced by reduction of a carbonyl compound will contain one deuterium atom, and those resulting from reduction of an acid will contain two. By observing the isotopic distribution in the molecular ion cluster, it is possible to determine not only which higher oxidized metabolites were present but also their relative abundances.

An example of this approach is shown in Fig. 6.20 (30), which shows the mass spectrum of the 7,11-dihydroxy metabolite of delta-8-THC as its TMS derivative. The ion at m/z 562 is the molecular ion of the metabolic alcohol. That at m/z 563, containing one deuterium atom, results from reduction of an oxo metabolite, whereas the major ion at m/z 564 is produced by reduction of a hydroxy acid (7-hydroxy-delta-8-THC-11-oic acid). The elevated abundance of the ion at m/z 565 shows that 7-oxo-delta-8-THC-11-oic acid was also present in the extract.

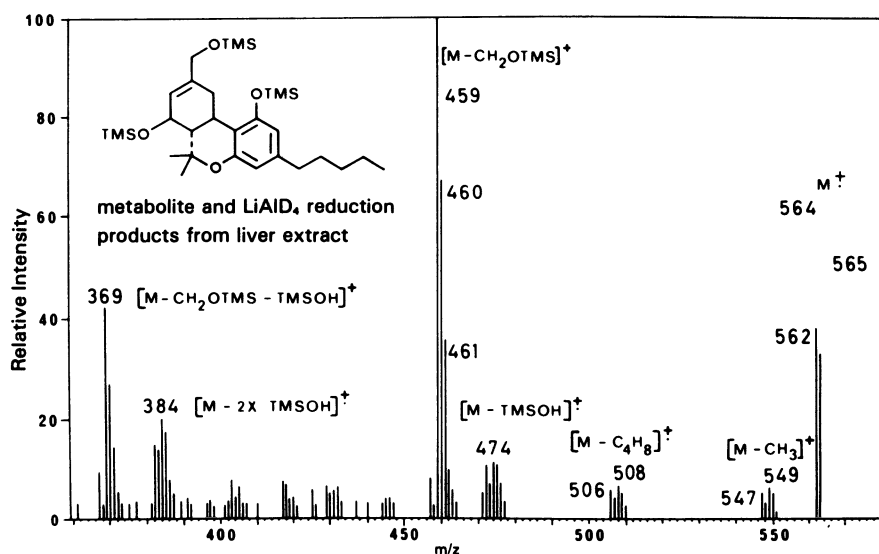


Figure 6.20. Mass spectrum (upper mass region, 25 eV) of the TMS derivative of 7 β ,11-dihydroxy-delta-8-THC obtained by lithium aluminium deuteride reduction of metabolites of delta-8-THC produced by the mouse (30). [Reproduced with permission from The Institute of Petroleum.]

4.1.1c. Stereospecific Loss of Deuterium as a Probe of Stereochemistry.

As described below, many THC metabolites hydroxylated on the terpene ring produce similar spectra with the dominant metabolite-related ion being $[M - \text{TMSOH}]^+$. The presence of this ion does not provide much evidence on the position of substitution. However, because it is formed by the abstraction of a TMSO group and a hydrogen atom, location of the abstracted hydrogen atom can be used to deduce information on the location, and particularly the stereochemistry, of the derivatized hydroxy group. This result is because the abstracted hydrogen is usually positioned at the 3 or 4 position relative to the hydroxy group and must be able to approach to within 3.2 Å for interaction to occur. This distance usually implies a *cis*-diaxial interaction. In the THC series, an obvious candidate for labeling is the hydrogen at C-10a because this hydrogen atom is axial and suitably placed to be abstracted by OTMS groups at C-7 and C-9. Indeed, it was found that, in the fragmentation of 7-hydroxy- δ -8-THC, this atom was quantitatively eliminated during formation of the abundant $[M - \text{TMSOH}]^+$ ion, whereas in the 7 β -hydroxy isomer, where the OTMS group is equatorial and remote from the 10a-hydrogen, the $[M - \text{TMSOH}]^+$ ion is weak and involves mainly abstraction of hydrogen rather than deuterium (31). A similar situation exists for the 8 α -hydroxy isomer of δ -9-THC even though the hydroxy group is only pseudoaxial.

With dihydroxy metabolites containing a 9 α (axial) hydroxy group, the situation is not quite as simple because bond cleavage sometimes occurs between the carbon atoms bearing the hydroxy groups. This cleavage removes the stereochemical identity of the hydroxy groups and results in abstraction of the reactive 10a hydrogen by a hydroxy group from all isomers. This loss appears to occur with 8,9-dihydroxy-8,9-dihydro metabolites, although the 9,10-dihydroxylated compounds show the expected stereochemically specific deuterium removal. It is possible to confirm that it is the 9-OTMS group of the 9,10-dihydroxy metabolite that is involved in the deuterium abstraction by specific TMS/[²H₉]TMS labeling as described above. 9,11-Dihydroxy metabolites also display aberrant behavior because the major initial fragmentation is loss of the 11-CH₂OTMS group. However, the stereospecificity can be restored by preparation of the cyclic alkane boronate derivatives, as shown in Fig. 6.21. In these spectra, the ion at *m/z* 299 (*i*) is more abundant from the fragmentation of the 9 α -hydroxy isomer and clearly involves specific abstraction of deuterium by the mechanism shown in Fig. 6.22. Only a limited amount of deuterium is lost during fragmentation of the other isomer. The relative positions of the groups are shown in Fig. 6.23.

Another example of the successful use of this approach is provided by the spectra of the two C-9 isomers of HHC-11-oic acid. The spectra, shown in Fig. 6.24, are very similar, with the main difference being in the relative abundance of the ion at *m/z* 372, which is more abundant in the spectrum of the C-9-axial

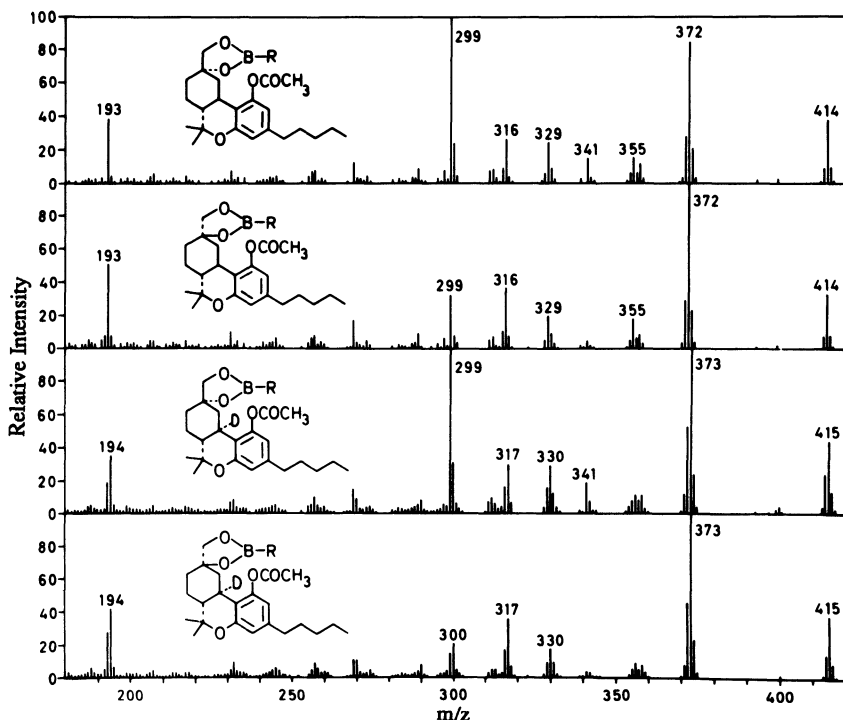


Figure 6.21. Mass spectra (25 eV) of the cyclic methane boronate/acetate derivatives of epimeric 9 α - and 9 β ,11-dihydroxy-HHCs and their [10a- 2 H] analogues (30). [Reproduced with permission from The Institute of Petroleum.]

isomer than in the other spectrum. This ion is formed by loss of the carboxylic acid group together with a hydrogen atom. That this atom is the 10a-hydrogen, shown by deuterium labeling, confirms that this fragmentation only occurs to any extent in the axial isomer.

4.1.2. Use of Computer Processing to Identify Metabolites

Figure 6.25a shows the metabolic total ion current profile of delta-9-THC metabolites extracted from mouse liver by the scheme shown in Fig. 6.18 and appearing in fraction 5. Most of the peaks in the center of the chromatogram are produced by metabolites. This separation was performed on an SE-30 packed column, and it is apparent that several of the peaks contain more than one constituent. Computer algorithms, such as the Biller-Biemann algorithm, are now available that allow the apparent resolution of this column to be improved. One of these programs works by examining each ion in each spectrum and

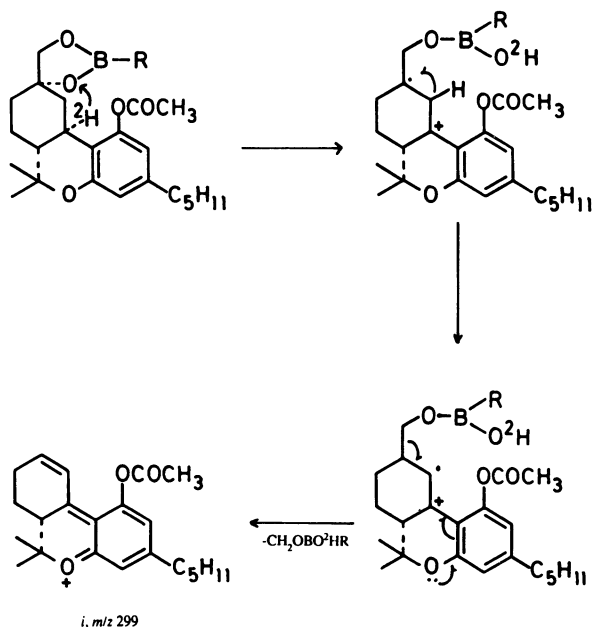


Figure 6.22. Fragmentation mechanism for the formation of the ion at m/z 299 in the spectra of the cyclic methane boronate/acetate derivatives of 9,11-dihydroxy-HHC.

comparing its absolute abundance with the corresponding ion in the preceding spectrum. If a drop in abundance is detected, then the ion is flagged in the earlier spectrum. The chromatogram plotted using only the flagged ions shows considerably enhanced resolution, as shown in Fig. 6.25b (32,33). It is clear from this figure that some of the composite peaks from Fig. 6.25a have been deconvoluted into as many as three individual metabolites. The mass spectrum of each constit-

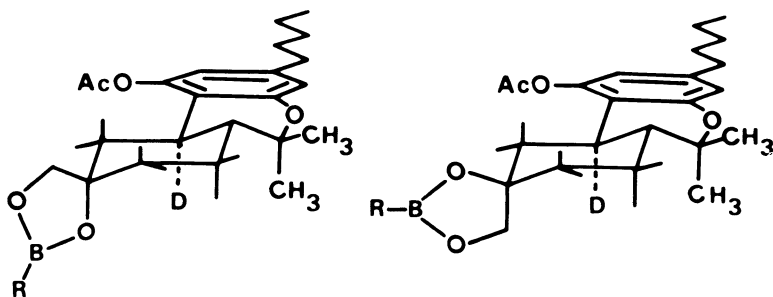


Figure 6.23. Diagram showing the relative positions of the cyclic methane boronate ring and 10a-hydrogen atom in isomers of 9,11-dihydroxy-HHC.

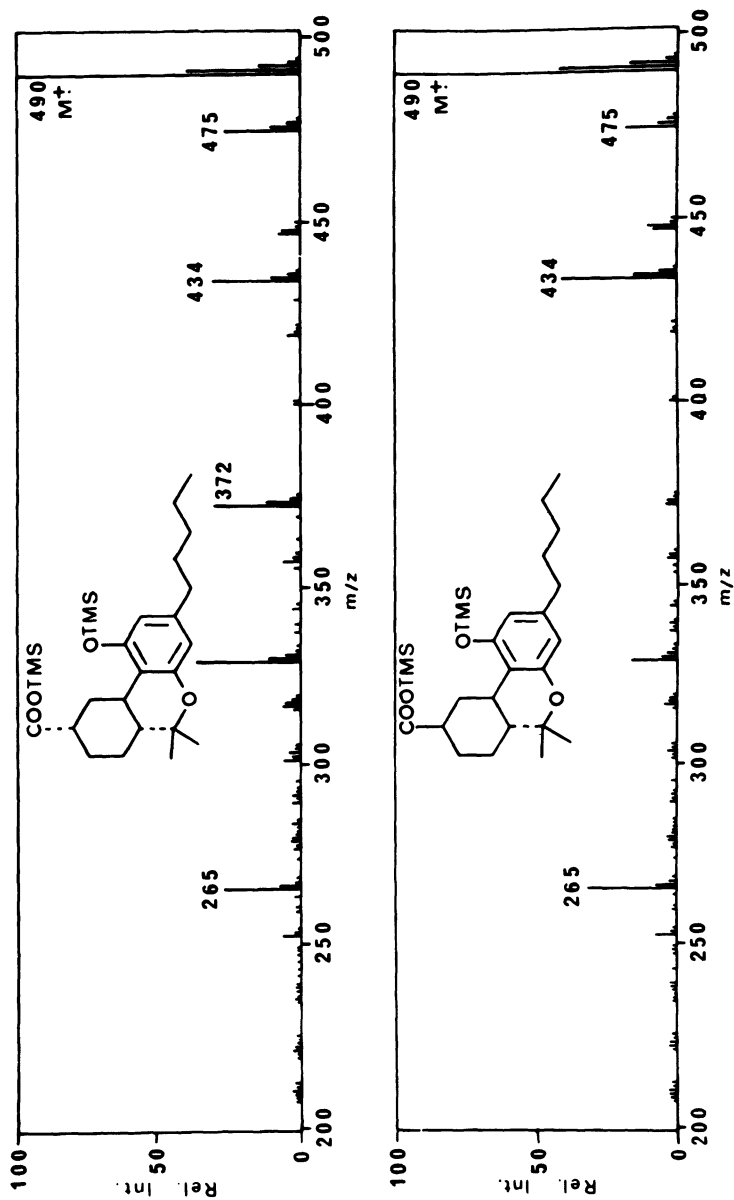


Figure 6.24. Mass spectra (25 eV) of the TMS derivatives of epimeric HHC-11-oic acids (30). [Reproduced with permission from the Institute of Petroleum.]

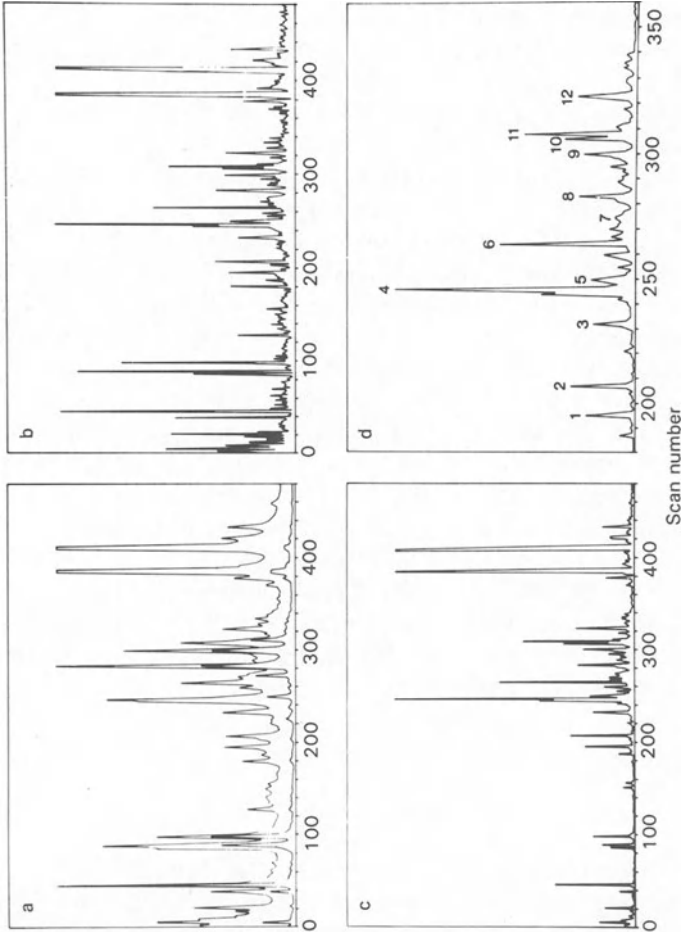


Figure 6.25. (a) Total-ion chromatogram of metabolites of delta-9-THC (TMS derivatives) extracted from mouse liver and single-ion chromatogram of m/z 145. (b) Computer-enhanced chromatogram (see text) of the metabolites shown in Fig. 6.23a. (c) Limited-ion chromatogram (m/z 300–700) of the metabolites shown in b. (d) Expansion of the metabolite region of the chromatogram shown in c. Major peaks are: (1) 8 α -hydroxy-delta-9-THC; (2) 11-hydroxy-delta-9-THC; (4) delta-9-THC-11-oic acid; (6) 8 α -hydroxy-delta-9-THC-11-oic acid; (8) 2'-hydroxy-delta-9-THC-11-oic acid; (9) 2'-8 α -dihydroxy-delta-9-THC-11-oic acid; (11) 3'- and 4'-hydroxy-delta-9-THC-11-oic acid; 3'- and 4'-8 α -dihydroxy-delta-9-THC-11-oic acid (33). [Reproduced with permission from Biomedical Publications.]

uent can be obtained by plotting only the flagged ions. The method, however, suffers from several drawbacks such as the necessity for different mass ions to be present in the constituents of the GLC peak to be deconvoluted. Further enhancement in the profile can be obtained by utilizing the fact that, whereas most ions in the spectra of THC metabolites occur at masses higher than m/z 300, those for residual biological compounds present in the liver occur at lower masses. Thus, if only ions above m/z 300 are used when plotting the chromatogram, a much better signal/noise ratio will be obtained, as illustrated in Fig. 6.25c. Figure 6.25d shows an expansion of the region of the chromatogram containing the metabolites.

Single-ion chromatograms are frequently used to identify GLC peaks produced by compounds with a specific structural feature. As discussed below, hydroxylation of the basic cannabinoid molecules gives rise to specific diagnostic fragment ions. Single-ion plots of these ions may be used to identify metabolites with these specific structural features. A plot of the ion at m/z 145, diagnostic, as described below, of metabolites possessing a 2'-hydroxy function, is shown superimposed on the total ion chromatogram in Fig. 6.25a and highlights those metabolites containing this hydroxy group. Again, false-positive results must be taken into account. These false positives will arise from any compound of a different type that happens to produce an ion of the same mass even if by an unrelated mechanism. In Fig. 6.25a, two such sets of compounds are found. The peaks in the 0–100 region are produced by fatty acids, whereas those toward the high-temperature end of the chromatogram are derived from bile acids. Identification of metabolites, particularly those occurring in low abundance, can be made by plotting ions known or suspected to be present in the spectrum of the metabolite and checking that they all maximize in the same mass spectrometric scan and occur in the correct abundance ratio. For complex mixtures this process often provides an easier method than attempting to sort out the ions from several compounds appearing in a single scan.

4.2. Metabolic Studies on Specific Cannabinoids

4.2.1. Tetrahydrocannabinols

Metabolism of the THC_s has received more attention than that of the other cannabinoids, and mass spectrometry has been used from the earliest study. The major sites of hydroxylation are the allylic positions of the terpene ring and any position of the pentyl side chain (Fig. 6.19). The relative concentration of the metabolites shows considerable species dependence, as illustrated for the monohydroxy metabolites of delta-11-THC (Fig. 6.26) recorded in a microsomal incubation. Each hydroxy metabolite gives rise to an abundant and diagnostic fragment ion, making identification reasonably straightforward. These ions also

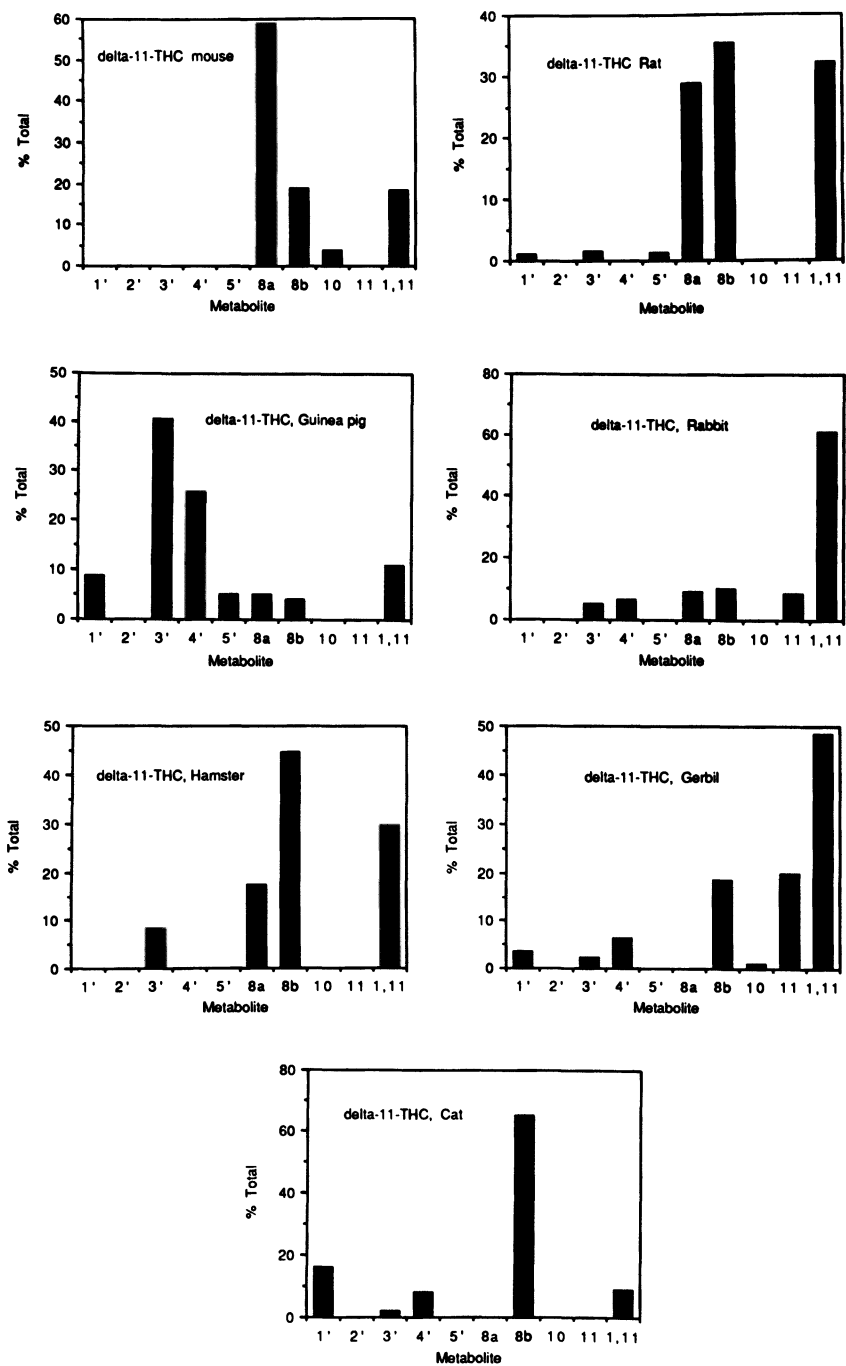


Figure 6.26. Histograms showing the variation in relative abundance of monohydroxy metabolites of delta-11-THC in various species.

appear in the spectra of metabolites containing more than one metabolic transformation.

4.2.1a. Electron Impact-Induced Fragmentation. The mass spectrum of the TMS derivative of the major metabolite of delta-9-THC, 11-hydroxy-delta-9-THC (Fig. 6.19), contains a very abundant ion at m/z 371, formed by loss of the C-11 $\text{CH}_2\text{-OTMS}$ group. Cleavage of the bond adjacent to the unsaturated site is not energetically favorable, and thus the rearrangement shown in Fig. 6.4 involving ionization of the double bond, hydrogen migration to C-9, and a radical-induced cleavage has been proposed (10,34). 8α -Hydroxylation is characterized by an abundant loss of trimethylsilanol caused, as described above, by the facile abstraction of the allylic 10a-hydrogen atom by the trimethylsilyloxy group. In the fragmentation of the 8β isomer, where this reaction is not possible, the base peak is produced by the ion at $[\text{M} - 131]^+$ (*k*). A mechanism for its formation is suggested in Fig. 6.27.

Fragmentation of the corresponding metabolites of delta-8-THC is considerably different on account of the facile retro-Diels–Alder fragmentation and the more isolated position of the double bond (10,34). Thus, the spectrum of the TMS derivative of 11-hydroxy-delta-8-THC lacks the abundant $[\text{M} - \text{CH}_2 - \text{OTMS}]^+$ ion of the delta-9 isomer but, instead, is dominated by the retro-Diels–Alder ion at m/z 303, which has lost the metabolic substituent. The spectrum of

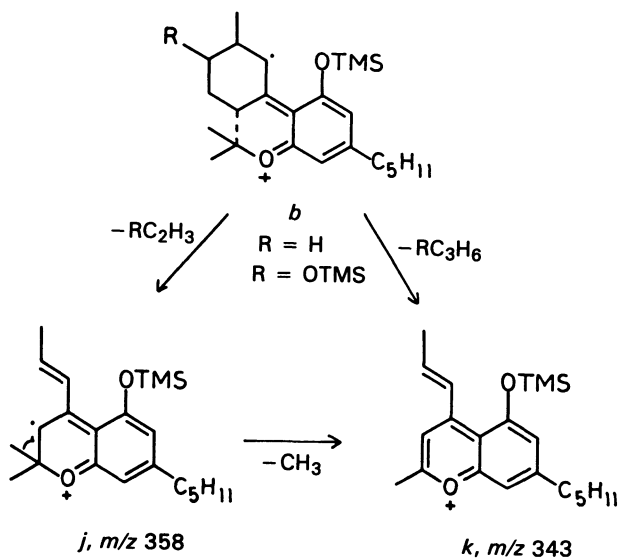


Figure 6.27. Proposed mechanism for the formation of the ion at $[\text{M} - 131]^+$ in the mass spectrum of the TMS derivative of 8β -hydroxy-delta-9-THC.

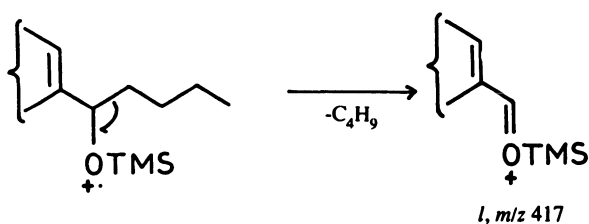


Figure 6.28. Formation of the diagnostic fragment ion at $[M - 57]^+$ from the TMS derivatives of cannabinoid metabolites containing a 1'-hydroxy group.

the 7α -hydroxy metabolite (TMS derivative), in which interaction can occur between the OTMS group and the hydrogen atom at C-10a, contains abundant ions at $[M - \text{TMSOH}]^+$ and $[M - \text{TMSOH} - \text{CH}_3]^+$ and a relatively weak molecular ion. Its 7β -hydroxy analogue, on the other hand, cannot eliminate trimethylsilanol in this manner, and consequently its spectrum contains a much more abundant molecular ion and a base peak produced by the retro-Diels–Alder cleavage.

The position of side-chain hydroxylation in these and all other cannabinoids is again easily determined because each produces its characteristic pattern of fragmentation (10,34–36). Hydroxylation in the 1' position induces an α -cleavage of the pentyl chain with loss of the terminal four carbon atoms ($[M - 57]^+$ (ion *l*, Fig. 6.28). 2'-Hydroxylation also induces an α -cleavage, but this time the charge resides with the smaller fragment to give the ion at m/z 145 (*m*) as the base peak (Fig. 6.29). The spectra of the 3'-hydroxy metabolites are dominated by an ion at $[M - 144]^+$ (*n*) that forms by the same mechanism as that resulting in the loss of 56 mass units in the fragmentation of the unsubstituted cannabinoid (Fig. 6.30). An ion at $[M - 72]^+$ (*o*) is produced by the mechanism shown in Fig. 6.31. α -cleavage to give the ion at m/z 117 (*p*) is characteristic of metabolites containing a 4'-hydroxy group (Fig. 6.32), but this ion is not nearly as abundant as the diagnostic ions in the spectra of the other metabolites. 5'-Hydroxylation does not give rise to a diagnostic ion of this type, but metabolites containing hydroxylation in this position can usually be identified by their typical GLC retention time. Fortuitously, the side-chain-hydroxylated metabolites elute

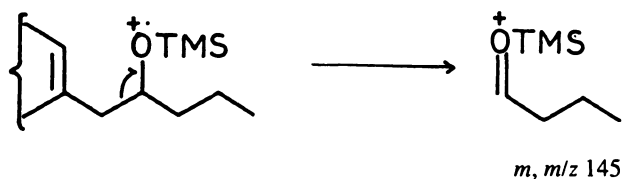


Figure 6.29. Formation of the diagnostic fragment ion at m/z 145 from the TMS derivatives of cannabinoid metabolites containing a 2'-hydroxy group.

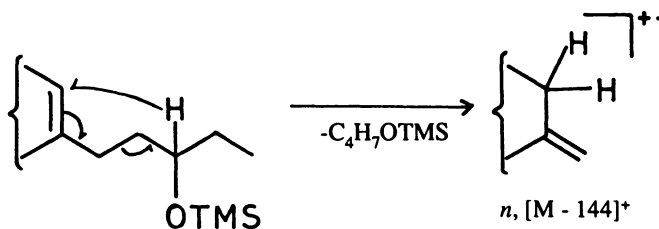


Figure 6.30. Formation of the diagnostic fragment ion at $[M - 144]^+$ from the TMS derivatives of cannabinoid metabolites containing a 3'-hydroxy group.

from most GLC columns in the order of substitution, that is, 1', 2', 3', 4', and 5'. Separation between the 3'- and 4'-hydroxy metabolites is marginal on a packed SE-30 column but much better on an OV-17 phase (37).

The mass spectra of the glucuronide conjugates of THC and some of their hydroxylated derivatives have been studied by Fenselau's group (38,39). Two sets of ions are produced from the TMS derivatives: those arising from the glucuronic acid moiety and those arising from the aglycone. The latter ions resemble those from the unconjugated compound in the spectra of the phenol O-glucuronides because of a TMS rearrangement, resulting in the parent ion of the unconjugated compound appearing in the spectrum. This ion then fragments in a strictly analogous manner to that of the unconjugated compound. This similarity not only provides a convenient method for identification of the O-glucuronides but also permits ready identification of the aglycone. Molecular ions from these compounds are very weak or nonexistent. However, ammonia CI has been used to enhance their relative abundance, but in no case have these ions been observed as the base peaks.

Another type of drug conjugate, first reported for THC and now known to be fairly common, is the formation of fatty acid esters. These esters were first isolated from adipose tissue of rats and identified by mass spectrometry as the

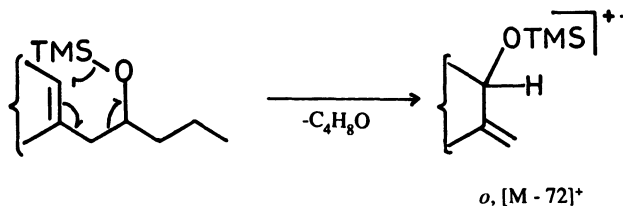


Figure 6.31. Formation of the diagnostic fragment ion at $[M - 72]^+$ from the TMS derivatives of cannabinoid metabolites containing a 3'-hydroxy group.

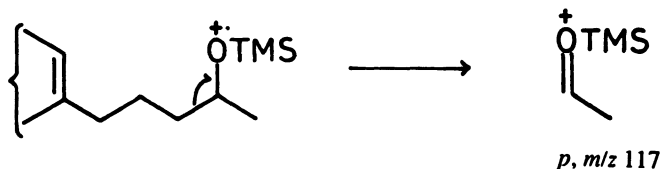


Figure 6.32. Formation of the diagnostic fragment ion at *m/z* 117 from the TMS derivatives of cannabinoid metabolites containing a 4'-hydroxy group.

conjugates of the major hydroxy metabolite, 11-hydroxy-THC (40). Their spectra are fairly simple, with the acid moiety being eliminated to give the ion at *m/z* 384 as the highest mass fragment ion of any abundance.

4.2.1b. General Method for Hydroxy-THC Identification. Hydroxylated metabolites of other isomeric THC's are not as easy to identify because reference compounds are not available. However, the reference compounds that are available, mostly of delta-8- and delta-9-THC, contain among them hydroxy groups on most positions of the basic cannabinoid structure. Conversion of these reference materials into cannabinoids with a saturated terpene ring, namely, hydroxylated HHCs, would form a reference set to which unknown metabolites could be related after similar reduction. Unfortunately, most of the common hydrogenation catalysts such as platinum oxide and palladium/charcoal cause concomitant elimination of allylic hydroxy groups, even when these groups are protected as, for example, acetates. However, rhodium on alumina appears to be milder and has been used in the prostaglandin field to accomplish this type of hydrogenation (41). This catalyst was used to synthesize 1'-, 2'-, 3'-, 4'-, 5'-, 8 α -, 8 β -, 11-, and 12-hydroxy-HHC from the appropriately hydroxylated delta-9-THC and 7 α -, 7 β -, 10 α -, and 10 β -hydroxy-HHC from the corresponding delta-8 isomers (Fig. 6.33). 2-, 4-, 6 α -, and 9-Hydroxy-HHC were synthesized by other methods. Each hydroxy-HHC gave a characteristic spectrum with, in most cases, a single diagnostic ion (41,42), which are summarized in Table 6.1. The method was validated by a reexamination of the metabolites of delta-11-THC and confirmation of the structures of the allylic alcohols.

4.2.1c. Typical in Vivo Profiles. A typical profile for the metabolites of delta-9-THC in mouse liver is shown in Fig. 6.25d (27,32). The major metabolite is produced by delta-9-THC-11-oic acid (peak 4), and the other major peaks are produced by its 8 α -hydroxy (peak 6), 2'-hydroxy (peak 8), 3'-hydroxy (peak 9), 2',8 α -dihydroxy (peak 11), and 3',8-dihydroxy (peak 12) metabolites. Minor compounds consist of the corresponding di- and trihydroxy-delta-9-THC and metabolites containing an 8 β -hydroxy group or an 8-oxy function. By con-

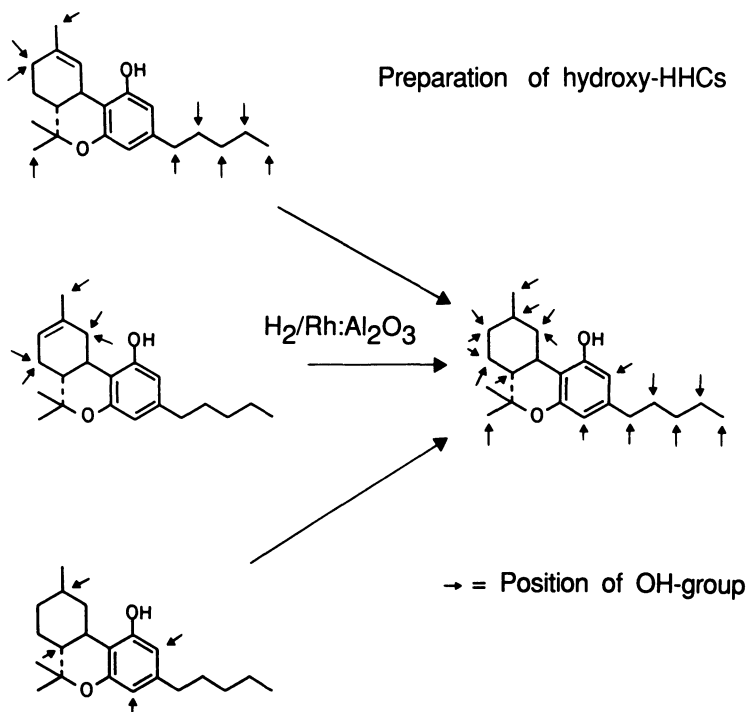


Figure 6.33. Synthesis of hydroxylated HHCs.

trast, the corresponding profile from the guinea pig is totally different (Fig. 6.34) (43). Here, the major metabolites are $8\beta,11$ -dihydroxy- Δ^9 -THC (peak 10) and products of β -oxidation of the pentyl chain (peak 41).

4.2.2. Cannabidiol

Identification of CBD metabolites by mass spectrometry is particularly simple. The major sites of metabolic attack are the pentyl chain, the terpene ring at C-6 and C-7, and the isopropenyl group. The major fragment ions seen in the spectrum of CBD TMS ether appear in most of these metabolites with suitable mass shifts and readily delineate the area of the molecule containing the metabolic transformation (44–47). Thus, a shift in mass of the base peak at m/z 390 (*f*) indicates metabolic transformation in that part of the molecule (pentyl chain, aromatic ring, and carbon atoms 1, 2, 6, or 7) not lost during the retro-Diels–Alder cleavage. A shift in the mass of the tropylium ion (m/z 337, *g*) further indicates transformation of the pentyl chain (aromatic substitution has not been observed for CBD). The ions *l*–*p*, diagnostic of the position of hydroxy substitu-

Table 6.1
Ions Diagnostic for the TMS Derivatives of Hydroxy-HHCs

Compound	Base peak	Ion structure	Other diagnostic ions
7Alpha-OH	371	[M-TMSOH-CH ₃] ⁺	157 (7), 143 (15) ^a
7Beta-OH	319	[M-157] ⁺	157 (84), 143 (93), 476 (80)
8Alpha-OH	371	[M-TMSOH-CH ₃]	No ions at 157 and 143
8Beta-OH	476	M ⁺	343 (75), 420 (30)
9Alpha-OH	386	[M-TMSOH] ⁺	371 (71)
9Beta-OH	476	M ⁺	343 (47), 371 (42), (no 420)
10Alpha-OH	461	[M-CH ₃] ⁺	143 (7)
10Beta-OH	461	[M-CH ₃] ⁺	143 (8)
11-OH (axial)	371	[M-TMSOH-CH ₃]	476 (90), 317 (79), 265 (84)
(equatorial)	476	M ⁺	265 (90)
12-OH	373	[M-CH ₂ OTHS] ⁺	
1'-OH	419	[M-C ₄ H ₉] ⁺	
2'-OH	145	C ₄ H ₈ OTMS ⁺	
3'-OH	332	[M-C ₄ H ₇ OTMS] ⁺	
4'-OH	476	M ⁺	117 (21)
5'-OH	476	M ⁺	332 (84)

^am/z and (relative abundance).

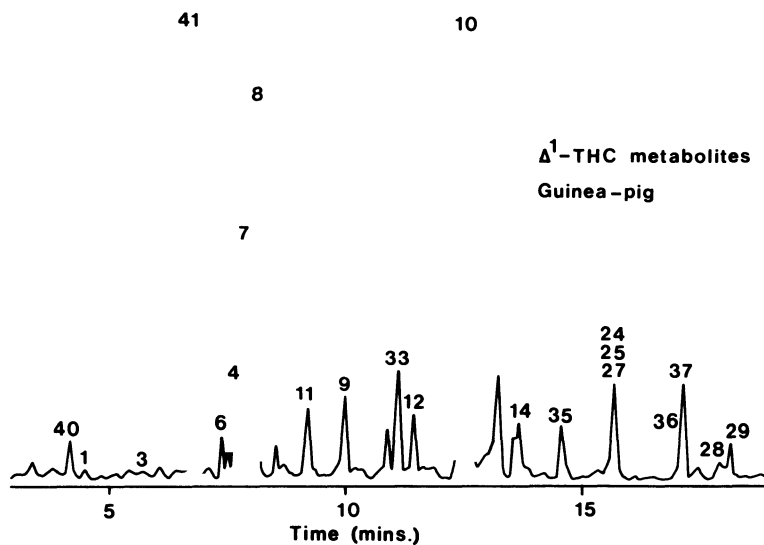


Figure 6.34. Limited-ion chromatogram (m/z 300–700) of the metabolites of delta-9-THC extracted from guinea pig liver.

tion of the side chain, are all present, although it should be noted that these ions are more prominent as eliminations from the retro-Diels–Alder than from the molecular ion. Substitution at C-7 results in an abundant loss of C-7 with its substituents, whereas hydroxylation at C-6 is characterized by an abundant retro-Diels–Alder ion and the virtual absence of the molecular ion.

Metabolism at the double bond of the isopropenyl group results in a different set of ions, although those discussed above are still present (48). Although the retro-Diels–Alder fragmentation is still dominant, charge retention is predominantly with the smaller, dihydroxylated fragment to give the ion at m/z 143 as the base peak and production of the other ions illustrated in Fig. 6.35.

Early work by Martin *et al.* (45,46) using mass spectrometry enabled many mono- and dihydroxy metabolites of CBD to be identified in microsomal preparations. Later work by Harvey and Brown (48,49) showed very extensive species variation in metabolic profiles and the formation of metabolites dihydroxylated in the isopropenyl group. This work was extended to examination of the drug's metabolism in whole liver (46) using the protocol described above for THC (Fig. 6.18). However, unlike THC, this drug was found to be much more extensively metabolized by β -oxidation, even in species such as the mouse, which does not tend to β -oxidize delta-9-THC. Several studies of the metabolism of this drug have been reported in urine with identification by GC/MS. Some 37 metabolites have been characterized in human urine (50) (Fig. 6.36) and consist of the 7-oic acid, its side-chain-hydroxylated analogues, products of β - and other oxidations of the side chain, and epoxidation of the delta-8-double bond. In the dog (51), the major oxidized metabolites are β -oxidized derivatives of 6-hydroxy- and 6-oxo-CBD together at early times after drug administration, with substantial concentrations of unusual glucose conjugates (52). The spectra of these latter compounds are similar to those of the glucuronides, but no reaction is observed with diazomethane, indicating the absence of the carboxylic acid group. In the rat (53), the drug is metabolised mainly by acid formation at C-11 and further hydroxylation in the side chain.

4.2.3. Cannabinol

As with the fragmentation of the unmetabolized cannabinoid, the spectra of most metabolites of CBN, recorded as their TMS derivatives, contain abundant $[M - 15]^+$ ions, which are often the base peaks. Indeed, metabolites such as 11-hydroxy-CBN give spectra very similar to that of CBN with the only difference being the shift of all ions by 88 mass units to higher mass (54–56). Diagnostic ions are, however, produced from side-chain-hydroxylated CBNs as described above for THC (ions $l-p$). The aromatic nature of the molecule drastically reduces the range of metabolites produced, with the result that metabolic profiles are comparatively simple.

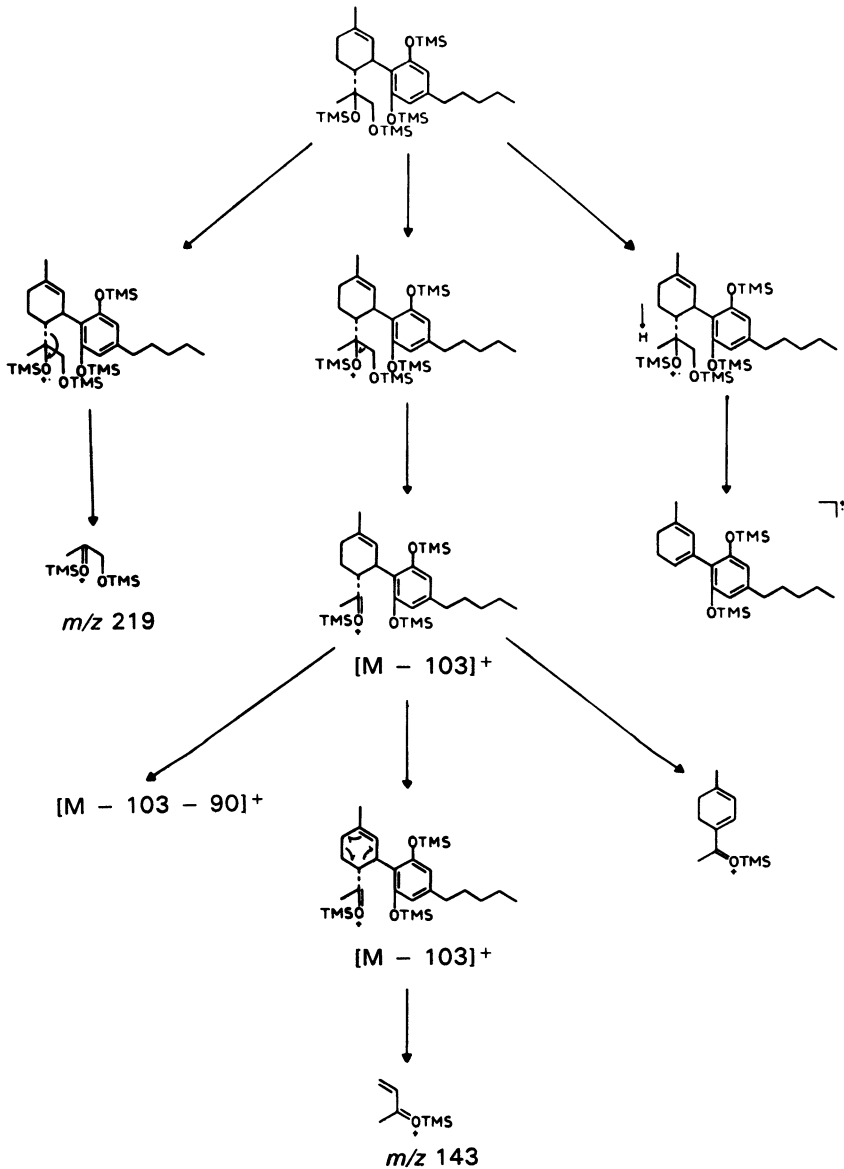


Figure 6.35. Fragmentation of CBD metabolites (TMS derivatives) containing dihydroxylation in the isopropenyl group (48). [Reproduced with permission from John Wiley & Sons, Ltd.]

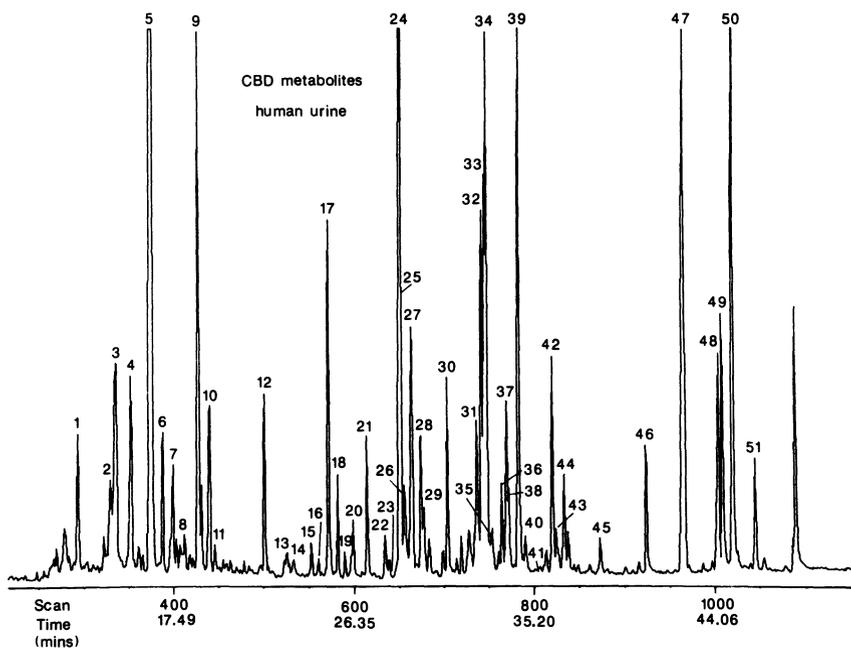


Figure 6.36. Limited-ion chromatogram (m/z 300–700) of metabolites of CBD extracted from human urine (50). [Reproduced with permission from Taylor and Francis, Ltd.]

4.2.4. Cannabichromene

Cannabichromene metabolites have only been reported from microsomal preparations and consist mainly of mono- and dihydroxylated compounds with some material produced by epoxidation and subsequent hydroxylation of the double bond (15). Little structural information is available in the spectra of the TMS derivatives because by far the major ion results from loss of the methylpropenyl chain to give the chromenyl ion (x , m/z 391, Fig. 6.37). Although the mass of this ion indicates which of the side chains is hydroxylated, other diagnostic ions are very weak or absent. In the spectrum shown in Fig. 6.37, the presence of the weak ion at $[M - 144]^+$ (m/z 330) shows the presence of a 3''-hydroxy group. However, this ion is too weak to be of any significant use. The reason for the very facile production of the chromenyl ion is the presence of the double bond in the dioxene ring. Reduction of this bond with the rhodium/alumina catalyst can prevent chromenyl ion formation and can be used to redirect fragmentation into more diagnostic pathways, as shown in Fig. 6.38 (57). Here, the diagnostic $[M - 144]^+$ ion (m/z 334) is now the base peak.

The major metabolites of CBC in most species are usually those mono-hydroxylated on the terminal allylic methyl groups of the methylpentenyl chain.

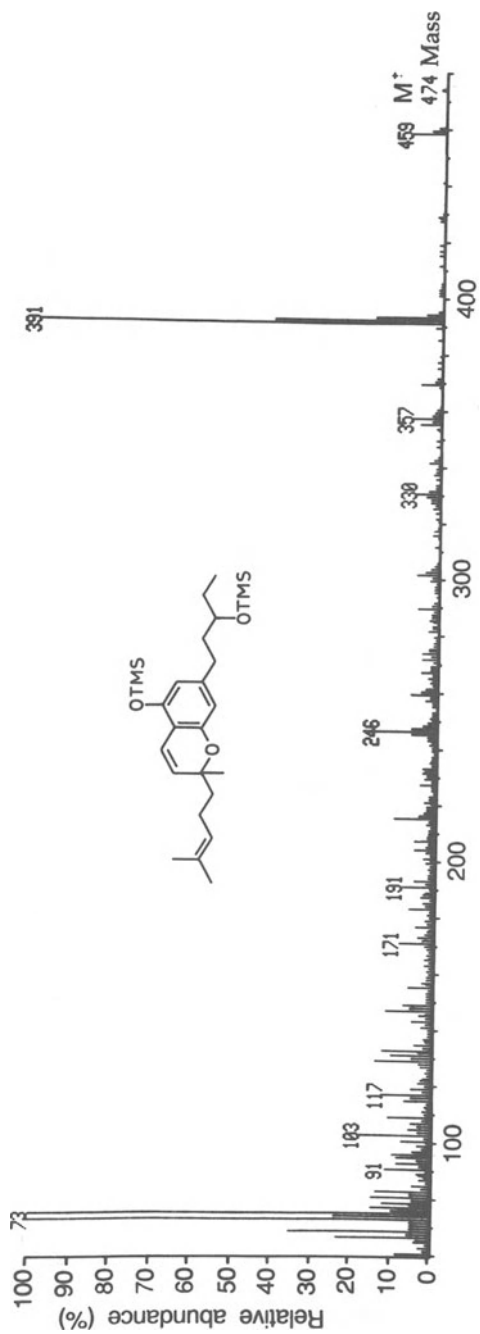


Figure 6.37. Mass spectrum of the TMS derivative of 3'-hydroxy-CBC (57). [Reproduced with permission from John Wiley & Sons, Ltd.]



Figure 6.38. Mass spectrum of the TMS derivative of 3''-hydroxy-CBC after reduction with hydrogen using a rhodium/alumina catalyst (57). [Reproduced with permission from John Wiley & Sons, Ltd.]

After hydrogenation, these positions become chromatographically equivalent, thus providing another diagnostic indicator. Deuterium labeling, combined with synthesis, has also been used to identify these metabolites (15). When these metabolites are oxidized with selenium dioxide, three oxo derivatives of CBC are produced, which, on reduction with lithium aluminium hydride, give three of the hydroxy metabolites observed *in vitro*, including the major metabolites. Base exchange of the α -hydrogens of the synthetic oxo compounds for deuterium results in a different incorporation depending on the site of the oxo group. Thus, the compounds oxidized at the terminal methyl groups incorporate two deuterium atoms, whereas that oxidized at the other (position 2) allylic position incorporates up to eight. After exchange, the oxo-CBCs were reduced with lithium aluminium deuteride rather than hydride to avoid any possible loss of deuterium, and the deuterium incorporation, although not complete, clearly differentiated between the two types of metabolite. This method has been used to confirm the structures of all three of these metabolites following *in vitro* metabolism.

4.2.5. Cannabigerol

Only one study has been reported on the metabolism of this compound (16). *In vitro*, the drug is metabolized by hydroxylation at most of the aliphatic positions. This hydroxylation causes shifts in the positions of the ions reported above for the unmetabolized molecule when hydroxylation occurs in the unsaturated chain, together with the usual range of side-chain cleavage ions (*l-p*) when hydroxylation is at this site. The major hydroxylated sites are the terminal allylic methyl groups.

5. QUANTITATIVE STUDIES

5.1. Measurement of Delta-9-THC in Physiological Fluids

The high lipophilicity of delta-9-THC results in rapid uptake of the drug by adipose and other fatty tissues. This rapid uptake causes the blood concentration to fall rapidly so that it soon drops below the detection limit of even the most sensitive analytical techniques. Consequently, the full pharmacokinetics of the drug have not yet been determined in humans. The first GC/MS method for quantification of delta-9-THC in human plasma was published by Agurell *et al.* in 1973 (58). The drug and its internal standard ($[1',1'\text{-}^2\text{H}_2]\text{delta-9-THC}$) were extracted with 1.5% isoamyl alcohol in light petroleum and concentrated by chromatography on Sephadex LH-20. No derivatization was used, but even so the drug could be measured down to 1 ng/ml. A related method was reported in the following year with $[1',1',2',2'\text{-}^2\text{H}_4]\text{delta-9-THC}$ as the internal standard,

giving a detection limit of 0.3 ng/ml (59). The use of TMS derivatization has recently improved the sensitivity of the assay to 0.01 ng/ml (60). The effect of derivatization on detection limits is shown in Fig. 6.39 (61). From these data, it is apparent that, although most derivatives improve the detection significantly, it does not appear to matter which derivative is used.

An interesting modification of the assay reported by Agurell's group allows the pharmacokinetics of THC (62) and other cannabinoids (63,64) to be measured in the blood of addicts without interference by the habitual use of the drug. This modification makes use of stable isotopes by administration of $[^2\text{H}_2]\text{THC}$ as the test compound with quantification against $[^2\text{H}_7]\text{THC}$ as the internal standard. Any THC ingested by the subject either before or after the test dose of $[^2\text{H}_2]\text{THC}$ is not seen by the mass spectrometer. The method does, however, have a drawback in that equilibration of THC with adipose tissue is a dynamic process. The administered $[^2\text{H}_2]\text{THC}$ may displace some of the unlabeled THC present in the adipose tissue as the result of earlier use, thus effectively lowering the concentration of the labeled test compound in the blood.

The major limiting factor in the ultimate sensitivity of these assays is the

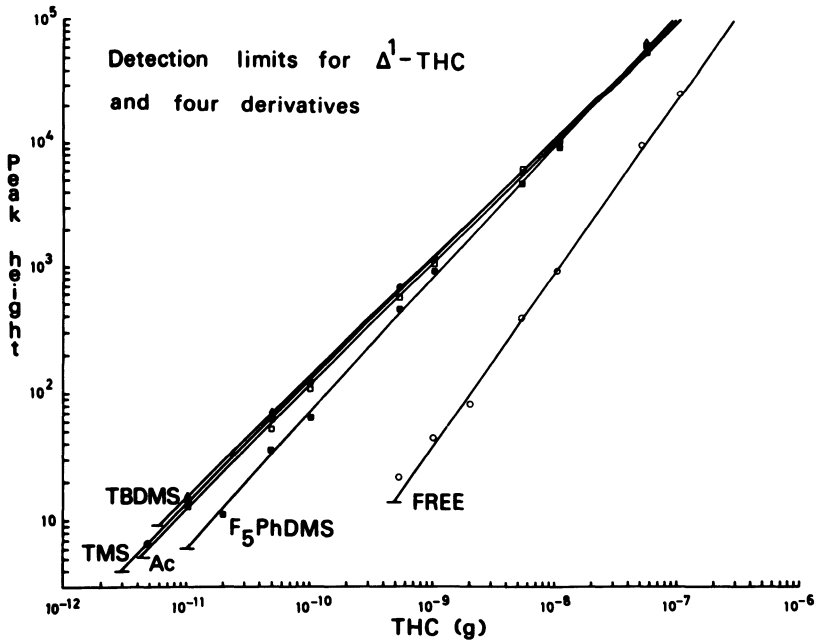


Figure 6.39. Plots of ion abundance against concentration for delta-9-THC and four of its derivatives (61). [Reproduced with permission from Pergamon Press, Ltd.]

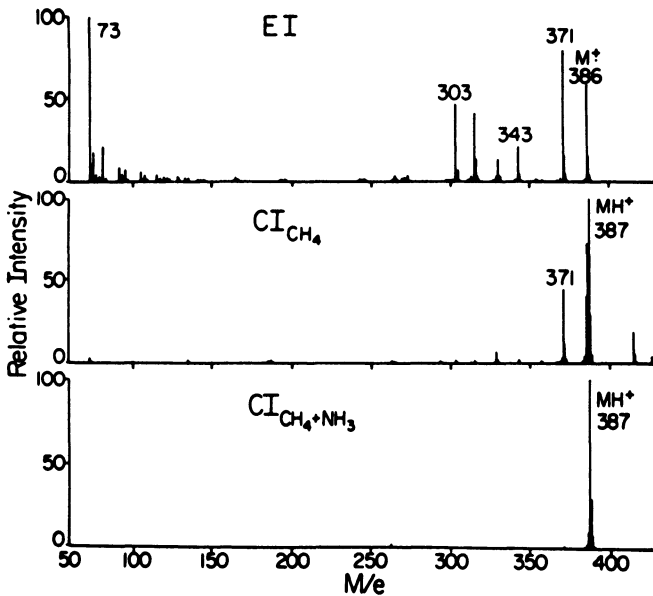


Figure 6.40. Comparison of the electron-impact and chemical ionization mass spectra of the TMS derivative of delta-9-THC (65). [Reproduced with permission from DHEW.]

signal/noise ratio, with most of the noise being from other biological molecules present in the extracts. CI mass spectrometry is one method for improving the signal/noise ratio and is the method favored by Detrick and Foltz (65). Figure 6.40 shows a comparison of the EI and both methane and methane/ammonia CI mass spectra of the TMS derivative of delta-9-THC and shows the concentration of ion current into the MH^+ ion in the latter spectrum. Although the presence of this abundant ion, in itself, does not indicate a more sensitive assay because the total ion current reflects the ion production as well as the percentage of the ion current in the ion to be monitored, for THC the use of CI appears favorable. Concentrations of 0.2 ng/ml of THC were measured. Negative CI shows even more promise. Foltz *et al.* (66) have used this technique combined with the formation of the electron-capturing TFA derivatives and capillary column separation to measure delta-9-THC and its 11-hydroxy and 11-oic acid metabolites to 0.2, 0.5, and 0.1 ng/ml, respectively. The power of negative CI to improve detection levels has been demonstrated by Hunt and Crow (67), who used the pentafluorobenzoyl derivative to detect the pure drug at the 15-fg level. The $[M - 1]^-$ ion carried 90.1% of the ion current, but, unfortunately, the technique was never developed into a method for detection of the drug in plasma.

5.2. Metastable Ion Monitoring

Two methods are available for using the mass spectrometer to improve signal/noise ratios. One is to increase the instrument resolution so that only the ion with the elemental composition of the analyte is measured, and the second is to make use of metastable transitions. We have used the second approach to develop the most sensitive assay for THC currently available with a detection limit of 0.005 ng/ml in plasma (68). The method was developed on an old VG 70/70F instrument, which was set up to monitor the ion at m/z 371 ($[M - 15]^+$) in the spectrum of the TMS derivative. The accelerating voltage was then increased from 4 to 4.16 kV in order to monitor the M^+ to $[M - CH_3]^+$ (m/z 386 to 371) transition. With the instrumentation available it was not possible to use a stable-isotope standard because, in order to focus the corresponding transition from a compound of different mass, it would have been necessary simultaneously to alter two fields. This dual alteration, however, has now been achieved by Davis with extra electronic circuitry (69). For assay with the unmodified instrument, a chromatographically separable standard was required. Isomeric THC's were found to be insufficiently separated on the packed column used for the assay, leaving CBN as the most appropriate compound. However, this cannabinoid has a mass of 4 units less than THC and is not suitable without modification. The mass difference was rectified by incorporating four deuterium atoms into the molecule (Fig. 6.41), which could then be monitored using the same transition as that from delta-9-THC.

The resulting chromatogram of the two compounds recorded at the 10-pg level is shown in Fig. 6.42a. A detection limit of 0.5 pg for pure delta-9-THC injected onto the column was recorded. The compounds were then added to plasma and extracted with hexane, a solvent chosen to optimize the differential recovery of cannabinoids and impurities. The resulting chromatogram (Fig.

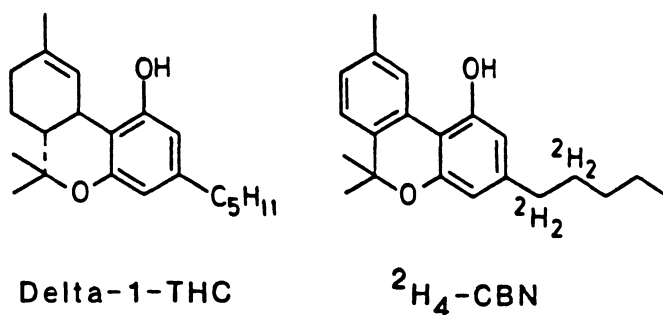


Figure 6.41. Structure of [²H₄]CBN used as the internal standard for quantification of delta-9-THC.

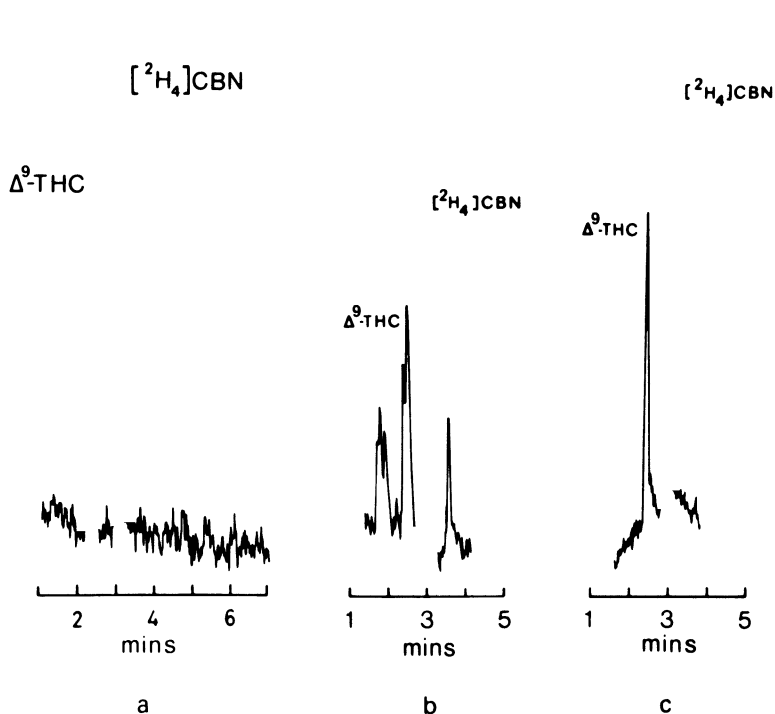


Figure 6.42. Chromatograms obtained by metastable ion monitoring of the TMS derivatives of (a) delta-9-THC (0.01 ng) and $[^2\text{H}_4]$ CBN (0.01 ng), (b) the same compounds extracted from rabbit plasma, and (c) the compounds extracted from plasma (efficiency 70%) and methylated with diazomethane prior to TMS ether formation (63). [Reproduced with permission from Academic Press, Ltd.]

6.42b), although allowing the drug to be monitored to about the 0.1-ng/ml level, did not offer any significant advantage over existing assays because a considerable amount of contamination remained. Attempts to separate the cannabinoids from this contamination by changing the chromatographic column were unsuccessful but gave changes in relative retention times suggesting that the impurities were fatty acids. Therefore, the extract was methylated with diazomethane prior to TMS ether formation, causing the impurity peaks to disappear from the chromatogram, leaving a clean base line against which THC could be measured to 0.005 ng/ml. Figure 6.42c shows the drug and its internal standard at the 0.01 ng level added to plasma and recovered with an efficiency of about 70%.

This method was subsequently used to measure the drug's pharmacokinetics in rabbits after acute and chronic administration (70). A typical trace is shown in Fig. 6.43, where it can be seen that, after chronic administration of delta-9-THC, the drug could be measured in plasma for as long as 28 days. A half-life of

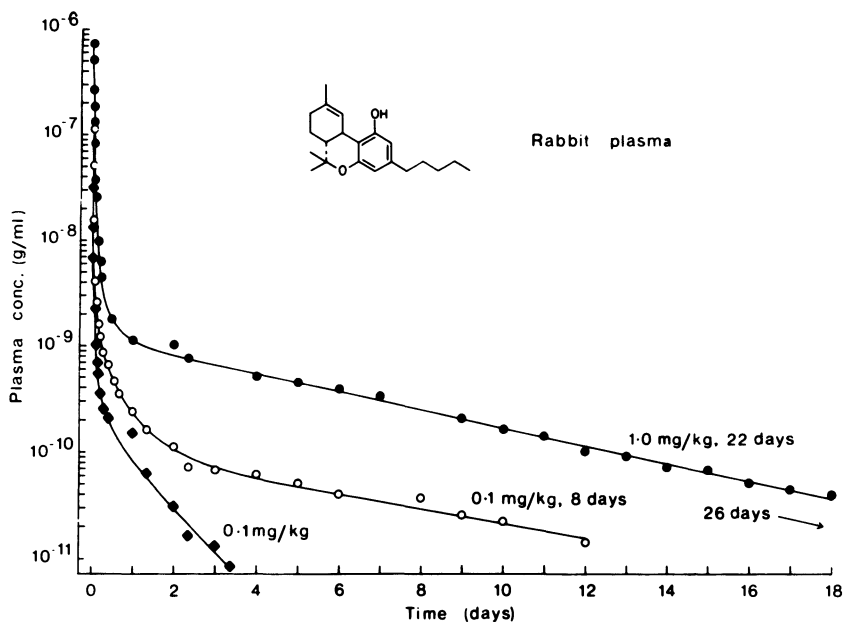


Figure 6.43. Plots of the concentration of delta-9-THC in rabbit plasma after a single 0.1 mg/kg intravenous dose (\blacklozenge), after eight daily injections of the same dose (\circ), and after 22 doses of the drug (\bullet) at a concentration of 1.0 mg/kg (63). [Reproduced with permission from Academic Press, Ltd.]

between 30 and 66 hr was recorded after a single dose; this half-life increased to 83 hr after multiple dosing.

With assays as sensitive as the one described above, it is vital to take stringent precautions to avoid contamination. All solvents used in the above assay were doubly distilled in glass, with plastics being avoided at any stage where they could be in contact with organic solvents. In a laboratory that has been handling cannabinoids for some years, general contamination is inevitable. It was found that new sample vials had to be used for sample collection and extraction in order to avoid contamination and that microliter syringes with removable needles also accumulated sufficient cannabinoid material between the needle and barrel to contaminate the sample. Cannabinoids have been reported to stick to glassware, and so all glass had to be silanized with a 10% solution of dichlorodimethylsilane followed by methanol before use.

6. CONCLUSIONS

Although trends in mass spectrometry are currently toward the use of LC/MS and desorption techniques for the analysis of nonvolatile molecules with

high molecular weights, the above examples demonstrate that GC/MS is still the most appropriate technique for small molecules, provided that they can be volatilized either before or after derivatization. It is frequently assumed, quite unjustifiably, that derivatization is difficult and complicates an assay. This assumption is not justified, at least for the cannabinoids, and, indeed, derivatization can lead to the development of useful methods for structural identification, as the above examples illustrate. Additional information can also be obtained very conveniently by use of stable-isotope labeling of the derivative and of the parent cannabinoid, which can enable much structural and mechanistic information to be obtained on extremely low concentrations of material. It is hoped that the methods discussed above will stimulate the development of similar techniques for the analysis of other drugs and biomolecules.

REFERENCES

1. Turner, C. E., ElSohly, M. A., and Boeren, E. G., 1980, Constituents of *Cannabis sativa* L., XVII: A review of the natural constituents, *J. Nat. Prods.* **43**:169–234.
2. Turner, C. E., and ElSohly, M. A., 1979, Constituents of *Cannabis sativa* L. XVI: A possible decomposition pathway of delta-1-tetrahydrocannabinol to cannabinol, *J. Heterocyclic Chem.* **16**:1667–1668.
3. Gill, E. W., 1971, Propyl homologue of tetrahydrocannabinol: Its isolation from cannabis, properties and synthesis, *J. Chem. Soc. (C)*. **1971**:579–582.
4. Vree, T. B., Breimer, D. D., van Ginneken, C. A. M., and van Rossum, J. M., 1972, Identification in hashish of tetrahydrocannabinol, cannabidiol and cannabinol analogues with a methyl side-chain, *J. Pharm. Pharmacol.* **24**:7–12.
5. Harvey, D. J., 1976, Characterization of the butyl homologues of delta-1-tetrahydrocannabinol, cannabinol and cannabidiol in samples of *Cannabis* by combined gas chromatography and mass spectrometry, *J. Pharm. Pharmacol.* **28**:280–285.
6. Matsuda, L. A., Lolait, S. J., Brownstein, M. J., Young, A. C., and Bonner, T. I., 1990, Structure of a cannabinoid receptor and functional expression of the cloned cDNA, *Nature* **346**:561–564.
7. Harvey, D. J., 1985, Marijuana '84; Summary of the session on adverse effects, in: *Marijuana '84; Proceedings of the Oxford Symposium on Cannabis* (D. J. Harvey, ed.), IRL Press, Oxford, pp. 667–670.
8. Harvey, D. J., and Paton, W. D. M., 1984, Metabolism of the cannabinoids, *Rev. Biochem. Toxicol.* **6**:221–264.
9. Harvey, D. J., 1991, Metabolism and pharmacokinetics of the cannabinoids, *Biochem. Physiol. Substance Abuse* **3**:279–365.
10. Harvey, D. J., 1985, Mass spectrometry of the cannabinoids and their metabolites, *Mass Spectrom. Rev.* **6**:135–229.
11. Claussen, U., Fehlhaber, H.-W., and Korte, F., 1966, Haschisch—XI. Massenspektrometrische Bestimmung von Haschisch-Inhaltstoffen—III, *Tetrahedron* **22**:3535–3543.
12. Harvey, D. J., 1981, The mass spectra of the trimethylsilyl derivatives of delta-1- and delta-6-tetrahydrocannabinol, *Biomed. Mass Spectrom.* **8**:575–578.
13. Boeren, E. G., Heerma, W., and Terlouw, J. K., 1976, The use of labeled analogues for the determination of mass spectrometric fragmentation mechanisms of cannabinoids. A reinvestiga-

- tion of the formation of the most abundant fragment ion $[C_{15}H_{19}O_2]$ in delta-1(8)-tetrahydrocannabinol, *Org. Mass Spectrom.* **11**:659–663.
14. Budzikiewicz, H., Aplin, R. T., Lightner, D. A., Djerassi, C., Mechoulam, R., and Gaoni, Y., 1965, Massenspektroskopie und ihre Anwendung auf strukturelle und stereochemische Probleme. LXVIII. Massenspektroskopische Untersuchung der Inhaltstoffe von Hashische, *Tetrahedron* **11**:1881–1888.
 15. Harvey, D. J., and Brown, N. K., 1992, Identification of cannabichromene metabolites by mass spectrometry: Identification of eight new dihydroxy metabolites in the rabbit, *Biomed. Environ. Mass Spectrom.* **20**:275–285.
 16. Harvey, D. J., and Brown, N. K., 1990, *In vitro* metabolism of cannabigerol in several mammalian species, *Biomed. Environ. Mass Spectrom.* **19**:545–553.
 17. Harvey, D. J., 1981, The mass spectra of the trimethylsilyl derivatives of *cis*- and *trans*-hexahydrocannabinol and their hydroxy and acid analogues, *Biomed. Mass Spectrom.* **8**:366–372.
 18. Turner, C. E., Hadley, K. W., Henry, J., and Mole, W. L., 1974, Constituents of *Cannabis sativa*, L., VII. Use of silyl derivatives in routine analysis, *J. Pharm. Sci.* **63**:1872–1876.
 19. Harvey, D. J., and Paton, W. D. M., 1975, Use of trimethylsilyl and other homologous trialkylsilyl derivatives for the separation and characterisation of mono- and di-hydroxycannabinoids by combined gas chromatography and mass spectrometry, *J. Chromatogr.* **109**:73–80.
 20. Harvey, D. J., 1977, Mass spectrometry of the triethylsilyl, tri-*n*-propylsilyl and tri-*n*-butylsilyl derivatives of some alcohols, steroids and cannabinoids, *Org. Mass Spectrom.* **12**:473–474.
 21. Harvey, D. J., 1977, Cyclic alkane boronates as derivatives for the characterisation of cannabinolic acids by combined gas chromatography and mass spectrometry, *Biomed. Mass Spectrom.* **4**:88–93.
 22. Vree, T. B., Breimer, D. D., van Ginneken, C. A. M., van Rossum, J. M., DeZeeuw, R. A., and Witte, A. H., 1971, Identification of cannabinoids in hashish by a new method of combined GC/MS, *Clin. Chim. Acta* **34**:365–372.
 23. Vree, T. B., Breimer, D. D., van Ginneken, C. A. M., and van Rossum, J. M., 1972, Identification of cannabicyclol with a propyl or pentyl side-chain by means of combined gas chromatography mass spectrometry, *J. Chromatogr.* **74**:124–127.
 24. DeZeeuw, R. A., Vree, T. B., Breimer, D. D., and van Ginneken, C. A. M., 1973, Cannabivarichromene, a new cannabinoid with a propyl side chain in cannabis, *Experientia* **29**:260–261.
 25. Nilsson, I. M., Agurell, S., Nilsson, J. L. G., Ohlsson, A., Sandberg, F., and Wahlqvist, M., 1970, Delta-1-tetrahydrocannabinol: Structure of a major metabolite, *Science* **168**:1228–1229.
 26. Nordqvist, M., Lindgren, J.-E., and Agurell, S., 1979, Acidic metabolites of delta-1-tetrahydrocannabinol isolated from rabbit urine, *J. Pharm. Pharmacol.* **31**:231–237.
 27. Harvey, D. J., Martin, B. R., and Paton, W. D. M., 1977, Identification of di- and tri-substituted hydroxy and ketone metabolites of delta-1-tetrahydrocannabinol in mouse liver, *J. Pharm. Pharmacol.* **29**:482–486.
 28. Harvey, D. J., Martin, B. R., and Paton, W. D. M., 1978, Comparative *in vivo* metabolism of delta-1-tetrahydrocannabinol (delta-1-THC), cannabidiol (CBD) and cannabinol (CBN) in several species, in: *Recent Developments in Mass Spectrometry in Biochemistry and Medicine*, Vol. 1 (A. Frigerio, ed.), Plenum Press, New York, pp. 161–184.
 29. Harvey, D. J., and Paton, W. D. M., 1979, The metabolism of deuterium-labeled analogues of delta-1-, delta-6- and delta-7-tetrahydrocannabinol and the use of deuterium labelling, in: *Recent Developments in Mass Spectrometry in Biochemistry and Medicine*, Vol. 2 (A. Frigerio, ed.), Plenum Press, New York, pp. 127–147.
 30. Harvey, D. J., and Paton, W. D. M., 1980, The use of deuterium labeling in structural and quantitative studies of tetrahydrocannabinol metabolites by mass spectrometry, *Adv. Mass Spectrom.* **8**:1194–1203.

31. Harvey, D. J., 1980, Stereospecific elimination of deuterium as a method for determining the stereochemistry of a number of metabolites of the tetrahydrocannabinols, *Biomed. Mass Spectrom.* **7**:28–34.
32. Harvey, D. J., and Paton, W. D. M., 1976, Examination of the metabolites of delta-1-tetrahydrocannabinol in mouse liver, heart and lung by combined gas chromatography and mass spectrometry, in: *Marihuana: Chemistry, Biochemistry and Cellular Effects* (G. G. Nahas, ed.), Springer-Verlag, New York, pp. 93–109.
33. Harvey, D. J., 1985, Combined gas chromatography–mass spectrometry in metabolic and pharmacokinetic studies of delta-9-tetrahydrocannabinol, in: *Pharmacokinetics and Pharmacodynamics of Psychoactive Drugs* (G. Barnett and C. N. Chiang, eds.), Biomedical Publications, Foster City, CA, pp. 456–486.
34. Harvey, D. J., 1981, The mass spectra of the trimethylsilyl derivatives of the hydroxy and acid metabolites of delta-1- and delta-6-tetrahydrocannabinol, *Biomed. Mass Spectrom.* **8**:579–588.
35. Wall, M. E., and Brine, D. R., 1976, Identification of cannabinoids and metabolites in biological materials by combined gas–liquid chromatography–mass spectrometry, in: *Marihuana: Chemistry, Biochemistry and Cellular Effects* (G. G. Nahas, ed.), Springer-Verlag, New York, pp. 51–62.
36. Binder, M., Agurell, S., Leander, K., and Lindgren, J.-E., 1974, Zur Identifikation potentieller Metabolite von Cannabis-inhaltstoffen: Kernresonanz und massenspektroskopische Untersuchungen und Seitenkettenhydroxylierten Cannabinoiden, *Helv. Chim. Acta* **57**:1626–1641.
37. Harvey, D. J., and Paton, W. D. M., 1978, Identification of six substituted 4"-hydroxy-metabolites of delta-1-tetrahydrocannabinol in mouse liver, *Res. Commun. Chem. Pathol. Pharmacol.* **21**:435–446.
38. Lyle, M. A., Pallante, S., Head, K., and Fenselau, C., 1977, Synthesis and characterization of glucuronides of cannabiniol, cannabidiol, delta-9-tetrahydrocannabinol and delta-8-tetrahydrocannabinol, *Biomed. Mass Spectrom.* **4**:190–196.
39. Pallante, S., Lyle, M. A., and Fenselau, C., 1978, Synthesis and characterization of glucuronides of 5'-hydroxy-delta-9-tetrahydrocannabinol and 11-hydroxy-delta-9-tetrahydrocannabinol, *Drug Metab. Dispos.* **6**:389–395.
40. Leighty, E. G., Fentiman, A. F., and Foltz, R. L., 1976, Long-retained metabolites of delta-9- and delta-8-tetrahydrocannabinol identified as novel fatty acid conjugates, *Res. Commun. Chem. Pathol. Pharmacol.* **14**:13–28.
41. Harvey, D. J., and Brown, N. K., 1990, A method, based on catalytic hydrogenation, for the identification of monohydroxy metabolites of isomeric tetrahydrocannabinols, *Rapid Commun. Mass Spectrom.* **4**:67–68.
42. Harvey, D. J., and Brown, N. K., 1991, Electron-impact induced fragmentation of the trimethylsilyl derivatives of monohydroxy-hexahydrocannabinols, *Biol. Mass Spectrom.* **20**:292–302.
43. Harvey, D. J., Martin, B. R., and Paton, W. D. M., 1980, Identification of *in vivo*, liver metabolites of delta-1-tetrahydrocannabinol, cannabidiol and cannabiniol produced by the guinea-pig, *J. Pharm. Pharmacol.* **32**:267–271.
44. Martin, B., Nordqvist, M., Agurell, S., Lindgren, J.-E., Leander, K., and Binder, M., 1976, Identification of monohydroxylated metabolites of cannabidiol formed by a rat liver, *J. Pharm. Pharmacol.* **28**:275–279.
45. Martin, B., Agurell, S., Nordqvist, M., and Lindgren, J.-E., 1976, Dioxygenated metabolites of cannabidiol formed by rat liver, *J. Pharm. Pharmacol.* **28**:603–608.
46. Martin, B. R., Harvey, D. J., and Paton, W. D. M., 1977, Biotransformation of cannabidiol in mice: Identification of new acid metabolites, *Drug Metab. Dispos.* **5**:259–267.
47. Harvey, D. J., Samara, E., and Mechoulam, R., 1991, Urinary metabolites of cannabidiol in dog, rat and man and their identification by GC/MS, *J. Chromatogr.* **562**:299–322.
48. Harvey, D. J., and Brown, N. K., 1990, *In vitro* metabolism of cannabidiol in the rabbit:

- Identification of seventeen new metabolites including thirteen dihydroxylated in the isopropenyl chain, *Biomed. Environ. Mass Spectrom.* **19**:550–567.
49. Harvey, D. J., and Brown, N. K., 1990, *In vitro* metabolism of cannabidiol in seven common laboratory mammals, *Res. Commun. Substance Abuse* **11**:27–37.
 50. Harvey, D. J., and Mechoulam, R., 1990, Metabolites of cannabidiol identified in human urine, *Xenobiotica* **20**:303–320.
 51. Samara, E., Bialer, M., and Harvey, D. J., 1990, Identification of urinary metabolites of cannabidiol in the dog, *Drug Metab. Dispos.* **18**:571–579.
 52. Samara, E., Bialer, M., and Harvey, D. J., 1990, Identification of glucose conjugates as the major urinary metabolites of cannabidiol in the dog, *Xenobiotica* **20**:303–320.
 53. Samara, E., Bialer, M., and Harvey, D. J., 1992, Metabolism of cannabidiol by the rat, *Eur. J. Drug Metab. Pharmacokin.* **16**:305–313.
 54. Widman, M., Nilsson, I. M., Nilsson, J. L. G., Agurell, S., and Leander, K., 1971, Metabolism of cannabis, IX, Cannabinol: Structure of a major metabolite formed in rat liver, *Life Sci.* **10**:157–162.
 55. Widman, M., Dahmen, J., Leander, K., and Petersson, K., 1975, *In vitro* metabolism of cannabinol in rat and rabbit liver, synthesis of 2"-, 3"- and 4"-hydroxycannabinol, *Acta Pharm. Suec.* **12**:385–392.
 56. Harvey, D. J., Martin, B. R., and Paton, W. D. M., 1977, *In vivo* metabolism of cannabinol by mouse and rat and a comparison with the metabolism of delta-1-tetrahydrocannabinol and cannabidiol, *Biomed. Mass Spectrom.* **4**:364–370.
 57. Harvey, D. J., and Brown, N. K., 1990, A method for structural determination of cannabinol metabolites by mass spectrometry, *Rapid Commun. Mass Spectrom.* **4**:135–136.
 58. Agurell, S., Gustafsson, B., Holmstead, B., Leander, K., Lindgren, J.-E., Nilsson, I., Sandberg, F., and Asberg, M., 1973, Quantitation of delta-1-tetrahydrocannabinol in plasma from cannabis smokers, *J. Pharm. Pharmacol.* **25**:554–558.
 59. Agurell, S., Levander, S., Binder, M., Bader-Bartfai, A., Gustafsson, B., Leander, K., Lindgren, J. E., Ohlsson, A., and Tobisson, B., 1974, Pharmacokinetics of delta-1-tetrahydrocannabinol in man after smoking: Relations to physiological and psychological effects, *Pharmacology of Marijuana* (M. C. Braude and S. Szara, eds.), Raven Press, New York, pp. 49–61.
 60. Ohlsson, A., Agurell, S., Lindgren, J.-E., and Leander, K., 1979, Improvement in the mass fragmentographic technique for quantification of tetrahydrocannabinol in human blood plasma, in: *Cannabinoid Analysis in Physiological Fluids*, ACS Symposium Series, No. 98 (J. A. Vinson, ed.), American Chemical Society, Washington, pp. 73–79.
 61. Harvey, D. J., Martin, B. R., and Paton, W. D. M., 1979, Identification and measurement of cannabinoids and their *in vivo* metabolites by gas chromatography and mass spectrometry, in: *Advances in Biosciences*, Vols. 22–23, *Marihuana, Biological Effects* (G. G. Nahas and W. D. M. Paton, eds.), Pergamon Press, Oxford, pp. 45–62.
 62. Ohlsson, A., Lindgren, J.-E., Wahlen, A., Agurell, S., Hollister, L. E., and Gillespie, H. K., 1982, Single-dose kinetics of deuterium-labelled delta-1-tetrahydrocannabinol in heavy and light cannabis users, *Biomed. Mass Spectrom.* **9**:6–10.
 63. Ohlsson, A., Lindgren, J.-E., Andersson, S., Agurell, S., Gillespie, H., and Hollister, L. E., 1984, Single dose kinetics of cannabidiol in man, in: *The Cannabinoids, Chemical, Pharmacologic and Therapeutic Aspects* (S. Agurell, W. L. Dewey, and R. E. Willette, eds.), Academic Press, Orlando, pp. 219–225.
 64. Ohlsson, A., Johansson, E., Lindgren, J.-E., Agurell, S., Gillespie, H., and Hollister, L. E., 1985, Kinetics of cannabinol in man, in: *Marihuana '84: Proceedings of the Oxford Symposium on Cannabis* (D. J. Harvey, ed.), IRL Press, Oxford, pp. 63–68.
 65. Detrick, R., and Foltz, R. L., 1976, Quantitation of delta-9-tetrahydrocannabinol in body fluids by gas chromatography/chemical ionization mass spectrometry, in: *Cannabinoid Assays in Humans* (R. E. Willette, ed.), NIDA, Rockville, MD, pp. 88–95.

66. Foltz, R. L., McGinnis, K. M., and Chin, D. M., 1983, Quantitative measurement of delta-9-tetrahydrocannabinol and two major metabolites in physiological specimens using capillary column gas chromatography and negative chemical ionization mass spectrometry, *Biomed. Mass Spectrom.* **10**:316–323.
67. Hunt, D. F., and Crow, F. W., 1978, Electron capture negative ion chemical ionization mass spectrometry, *Anal. Chem.* **50**:1781–1784.
68. Harvey, D. J., Leuschner, J. T. A., and Paton, W. D. M., 1980, Measurement of delta-1-tetrahydrocannabinol in plasma to the low picogram range by gas chromatography–mass spectrometry using metastable ion detection, *J. Chromatogr.* **202**:83–92.
69. Davis, N. W., 1989, Updating instrument control modes on a VG 7070F, *Adv. Mass Spectrom.* **11**:178–179.
70. Leuschner, J. T. A., Harvey, D. J., Bullingham, R. E. S., and Paton, W. D. M., Pharmacokinetics of delta-9-tetrahydrocannabinol in rabbits following single or multiple intravenous doses, *Drug Metab. Dispos.* **14**:230–238.

Inborn Errors of Amino Acid and Organic Acid Metabolism

Isamu Matsumoto and Tomiko Kuhara

1. INTRODUCTION

Human genes are assumed to number more than 50,000, and 4937 Mendelian inheritances are presently known (1). There are more than 500 inherited diseases in which primary defects are located in enzyme protein or nonenzyme protein. About 180 diseases are known in which a disorder of intermediary metabolism occurs as a result of a single enzyme defect. In these inherited metabolic disorders, the morbidity and mortality in the affected patients are high, and severe retardation of mental and physical development often occurs in surviving cases of some disorders. Most of these disorders are of autosomal recessive inheritance, and despite the low incidence of the homozygote of individual diseases, the overall occurrence of inherited metabolic disorders is significantly high. Several of these disorders can now be treated, if early diagnosis is successfully made, by administering a special dietary regimen that prevents severe mental retardation, life-threatening metabolic acidosis, early death, and so on, and allows normal mental and physical development. In other metabolic disorders, prenatal diagnosis becomes more important when no adequate treatment exists. Prenatal diagnosis also has significant value in preventing indiscriminate abortion when the mother has had a previous affected child.

Remarkable advances in gas chromatography–mass spectrometry (GC/MS) in the last two decades have made possible the diagnosis of metabolic disorders affecting amino acids, organic acids, fatty acids, carbohydrates, steroids, prostaglandins, vitamins, and so on.

Isamu Matsumoto and Tomiko Kuhara • Division of Human Genetics, Medical Research Institute, Kanazawa Medical University, Uchinada, Ishikawa 920-02, Japan.

The number of diagnosable diseases has been increasing rapidly year by year. The discovery of organic acidemias, the inherited metabolic disorders in which organic acids accumulate primarily in the body fluid of the patients, was facilitated by the introduction of GC and GC/MS to the medical field. Before 1966, when Tanaka *et al.* first discovered isovaleric acidemia by using GC/MS (2), only five organic acidurias were known. At present, more than 60 organic acidurias have been found. A number of review articles on the application of GC/MS in the diagnosis of organic acidurias has appeared in recent years (3–6).

Advanced chemical diagnosis using GC/MS/computer (COM) has become an important part of the routine service of selected laboratories in some countries. Our institute has been successful in applying chemical diagnosis for 115 inherited organic and amino acid disorders at present by employing a combination of GC/MS and an amino acid analyzer, and more than 910 cases and 80 inherited amino acid and organic acid metabolic diseases have been successfully identified since 1978. Among them, lactic acidosis was the most frequently found inborn organic acid metabolic error, comprising approximately 40% of the total disorders.

Chemical diagnosis of inherited metabolic disorders is critically important for correct treatment of patients; the treatment may differ depending on the underlying enzyme defect. In this chapter we attempt to review the differential chemical diagnosis of inherited aromatic and branched-chain amino acid and organic acid metabolic disorders, particularly regarding the substantial role played by mass spectrometry.

2. PROFILING PROCEDURE

2.1. Analytical Methods

Body fluids contain a wide variety of compounds including organic acids, inorganic acids, amino acids, peptides, carbohydrates, fatty acids, steroids, vitamins, minerals, nucleic acids, and so on, varying in relative quantities from very large to extremely small. In a diseased state, the levels of some compounds are elevated and/or decreased, whereas others remain in the normal range. For the analysis of a multicomponent body fluid by gas chromatography (GC), GC/MS, high-performance liquid chromatography (HPLC), amino acid analysis, and/or LC/MS, it is necessary to prepurify the specimen prior to analyzing every compound to minimize the contaminants and to keep the separation column in the best condition.

For the purpose of chemical diagnosis of metabolic disorders of amino acids and organic acids, the authors prefer to use urine as the target fluid, because urine

contains carboxylic acids with or without oxo, hydroxy, or other nonfree amino functional groups. Short-chain fatty acids, medium-chain dicarboxylic acids, and nitrogen-containing amino acid conjugates are also included in organic acids. The above compounds are relatively highly water-soluble and acidic, have a high renal clearance rate, and are often much more concentrated in the urine than in serum or other fluids. In addition, urine is the most readily available physiological fluid.

Usually, early morning urine (the first specimen of urine voided in the morning) or a random urine specimen (especially during clinical attack) is used for the analysis. Adequate or reliable 24-hr or other time-scheduled urine collection is often difficult, especially for the newborn, small children with acute illness, mentally subnormal patients, or from large numbers of ambulant normal subjects.

In some diseases, 24-hr or 8-hr urine collection has no advantage for diagnosis because the metabolism in such disorders changes quickly. For accurate chemical diagnosis, not only qualitative but also quantitative analysis is important. For the latter purpose, the concentration of organic acids should be referred to that of creatinine in the urine because the flow rate and concentration of urine may vary widely.

As a yardstick, creatinine measurement is necessary for the evaluation of urinary compounds, because the 24-hr excretion amount of creatinine in the urine of a given subject is remarkably constant from day to day. The creatinine coefficient is the 24-hr urinary creatinine expressed in terms of body size. Serum samples are also used in some cases, especially when the index compound for the diagnosis is nonpolar or relatively water-insoluble. For amino acid analysis, urine sediment is separated by centrifugation, and the urine equivalent to 0.5 mg creatinine is subjected to amino acid analysis without further treatment or derivatization.

Urinary organic acid analysis by GC or GC/MS is more complicated. The authors prefer a simple and rapid organic solvent extraction method for routine chemical diagnosis and for emergency cases. To an aliquot of the urine sample equivalent to 0.5 mg creatinine is added 20 μ g each of *n*-heptadecanoate and 3-hydroxymyristate as internal standards. The urine is acidified and extracted with diethyl ether or sometimes with ethyl acetate. The extracted organic acids are converted into trimethylsilyl derivatives and then analyzed by GC or GC/MS. The most complete extraction and reproducible recoveries of organic acids from urine have been achieved by the use of DEAE-Sephadex (7). The acids are eluted with aqueous pyridinium acetate buffer after washing in water. The eluate is concentrated by lyophilization, and the acids are subsequently derivatized. In this method, however, inorganic phosphate and sulfate, which are present in large amounts, are extracted and trimethylsilylated lest they obscure large proportions of the chromatograms.

Serum or plasma samples are usually first deproteinized with 4 volumes of ethanol, which is subsequently completely removed *in vacuo*. The residues are dissolved in water and treated thereafter like urine. The authors (8) deproteinize plasma samples with 1.5 volumes of N perchloric acid and directly subject them to organic solvent extraction.

2.2. Gas Chromatographic and Mass Spectrometric Analysis

Gas chromatographic separations for nonvolatile organic acids have been carried out with 8% butane-1,4-diol succinate (BDS), with 3% OV-1, and with 5% OV-17 on Supelcoport, on a glass capillary column coated with OV-101 and SP-2100, or with an Emulphor, a fused-silica column coated with OV-1701, SE-30, or UCON. The authors carry out the separation of nonvolatile organic acids either on a packed column filled with 3% OV-17 on Gas Chrom Q (3 m × 2 mm, 80/100 mesh), or on an MPS-50 (25 m × 0.32 mm i.d., 10 μm film thickness) fused silica capillary column. Mass spectra are recorded with a JEOL JMS D-300 system in the EI mode at a scan rate of 800 amu/sec in most of the measurements in our laboratory.

3. AMINO ACID AND ORGANIC ACID METABOLIC DISORDERS

3.1. Disorders of Aromatic Amino Acid and Organic Acid Metabolism

Two aromatic amino acids, phenylalanine and tyrosine, a hydroxylated metabolite of phenylalanine, are catabolized similarly in the first two steps, although the major metabolic pathway for phenylalanine is the conversion to tyrosine in man (Fig. 7.1). They undergo in the first step of catabolism, the vitamin-B₆-dependent transamination with 2-oxoglutarate to form the α-keto acids phenylpyruvate and 4-hydroxyphenylpyruvate, respectively. These aromatic α-keto acids are oxidized by an oxidase (*p*-hydroxyphenylpyruvate oxygenase) to give *o*-hydroxyphenylacetate and homogentisate. They also partly undergo reduction to form phenyllactate and *p*-hydroxyphenyllactate, respectively.

The most common disorders in aromatic amino acid metabolism are phenylketonuria, the tyrosinemias, and alcaptonuria.

3.1.1. Disorders of L-Phenylalanine Metabolism

Phenylketonuria (PKU) is very often encountered and is one of the most common inherited amino acid disorders. The biochemical defect in classical PKU is the inability to carry out the hydroxylation of L-phenylalanine to

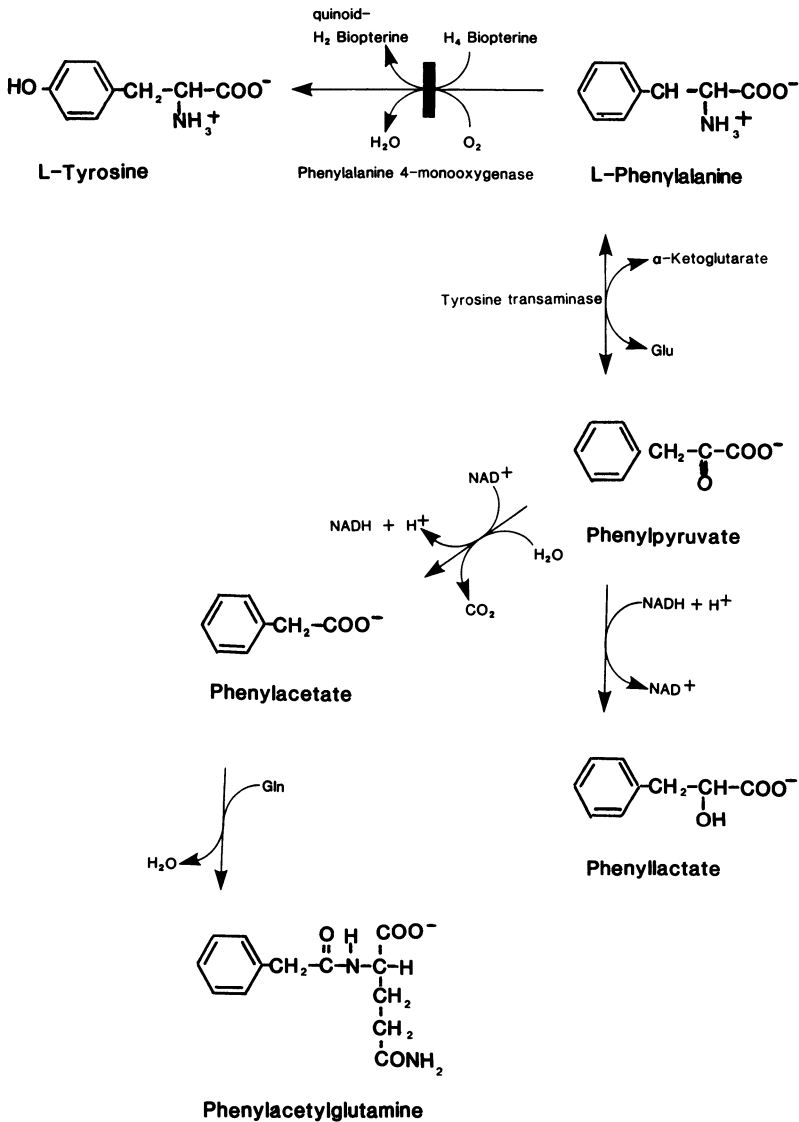


Figure 7.1. Phenylalanine metabolism and its inherited disorder, phenylketonuria (PKU).

tyrosine, which is the major metabolic route for phenylalanine in normal subjects. The enzyme catalyzing this reaction is a so-called mixed-function oxidase (phenylalanine hydroxylase).

Auerbach *et al.* and Woolf *et al.* pointed out evidence of heterogeneity in PKU. Hyperphenylalaninemia from dihydropterin synthetase deficiency and hy-

perphenylalaninemia from a defect in the synthesis of biopterin have been recognized (9). It was found by Bowden and McArthur that phenylpyruvate inhibits pyruvate decarboxylase in the brain but not in the liver. They suggested that this factor accounts for the defect in the formation of myelin and mental retardation in this disease.

The survey from the national neonatal mass screening program for seven inherited metabolic diseases in Japan in 1990 demonstrated that the incidence of phenylketonuria is about 1/80,100 and is lower than that in the United States and European countries (estimated at about 1/12,000).

*3.1.1a. Classical PKU (McKusick 261600)** L-Phenylalanine is an essential amino acid for man. Measurement of phenylalanine requirements in patients with classical PKU revealed that less than 50% of the normal dietary intake of L-phenylalanine consumed by the growing infant can be used for protein synthesis; the remainder must be oxidized primarily to tyrosine and to a much lesser extent to other metabolites. The fraction of phenylalanine intake that is disposed of by specific hydroxylation to form tyrosine increases as the growth rate declines. When hydroxylation is impaired, the rate of metabolism along the minor pathways is greatly augmented. It is the accumulation of these normal metabolites in abnormal amounts that first attracted attention to the disorders of phenylalanine metabolism. As a consequence, in blood and urine one finds phenylpyruvate, phenyllactate, *o*-hydroxyphenylacetate, and minor amounts of phenylethylamine, mandelate, and hippurate. An essential biochemical feature is the depression in plasma of tyrosine levels because of the enzyme defect. The pigmentary defects in PKU appear to arise as a consequence of phenylalanine acting as competitive inhibitor of tyrosine oxidase, the enzyme responsible for production of melanin. It is curious that, with the multiplicity of metabolites produced, the only system severely damaged in PKU is the central nervous system.

Chemical diagnosis can be made by the identification of abnormally high levels of phenylpyruvate, phenyllactate, and *o*-hydroxyphenylacetate in urine and extremely large amounts of phenylalanine in blood and urine.

Damage to the developing central nervous system may be profound if the PKU infants are not treated with a special diet and low-phenylalanine milk shortly after birth. Several studies indicate that the average loss in the development quotient during the first year of life in over 95% of untreated patients is

*All the inherited metabolic diseases since 1960 have been collected and cataloged by Victor A. McKusick, M.D. In the ninth edition, more than 5000 traits were listed that include inherited metabolic diseases, the structural gene locus for a given enzyme, and some human genes that had been cloned and fully sequenced. Most entries are arranged alphabetically by title. Entries are numbered consecutively beginning with 100100, 200100, and 300100 in the dominant, recessive, and X-linked catalogues, respectively. Because all inherited diseases reviewed in this chapter are autosomal recessive phenotype, all these diseases have as the first digit the number 2.

approximately 50 points. A consensus has thus developed that the earlier the corrective diet is instituted, the milder will be the effects on the brain.

3.1.1b. Dihydropteridine Reductase Deficiency (McKusick 261630). In contrast to classical PKU, this variant is unresponsive to prompt institution of dietary phenylalanine restriction.

Phenylalanine hydroxylase in a liver biopsy from one patient showed 20% of normal adult control values, but the dihydropteridine reductase activity of this patient was less than 1% of normal in liver, brain, and other tissues (10). This latter deficiency prevents regeneration of tetrahydrobiopterin, the cofactor for the hydroxylase reaction. Because the reductase enzyme reaction regenerates the cofactor for both tyrosine and tryptophan hydroxylase, catecholamine and serotonin synthesis is compromised as well. Patient studies are scanty, but in one patient, abnormally low levels of dopamine and serotonin were found in cerebrospinal fluid, brain, and various other tissues, whereas norepinephrine metabolites were normal. This discrepancy is at present unexplained. Although phenylalanine hydroxylase activity was lower than that of adult controls, it has not been determined whether this value represented significantly decreased activity in children.

Clinical recognition occurs because of the development of seizures, hypotonia, choreiform movements, and psychomotor retardation in patients demonstrating elevated serum phenylalanine and depressed tyrosine. These clinical symptoms are seen despite normalization of phenylalanine levels with a restricted diet.

Mass spectrometry can demonstrate that patients with this variant of hyperphenylalanemia excrete only oxidized forms of biopterin in their urine; normal children and those with phenylalanine hydroxylase deficiency predominantly excrete tetrahydrobiopterin.

However, chemical diagnosis can be made by almost the same methods as for classical PKU, and it is necessary to identify phenylpyruvate, phenyllactate, and *o*-hydroxyphenylacetate in urine, but additional analysis is required for the differential diagnosis of this PKU variant patient and the classical PKU to identify the abnormal excretion of dihydrobiopterin in the former patient.

Mass spectra of trimethylsilyl derivatives of dihydrobiopterin and tetrahydrobiopterin are shown in Fig. 7.2.

Replacement therapy with L-dopa and 5-hydroxytryptophan has been suggested as the means to circumvent the block in the synthesis of dopamine and serotonin. Ascorbate, which stabilizes tetrahydrobiopterin *in vitro*, may also have some place in the therapy.

General symptoms in affected infants with this disease in the early period are almost the same as those of classical PKU, but neurological symptoms, particularly hypotonia and delay in motor development, are recognized earlier

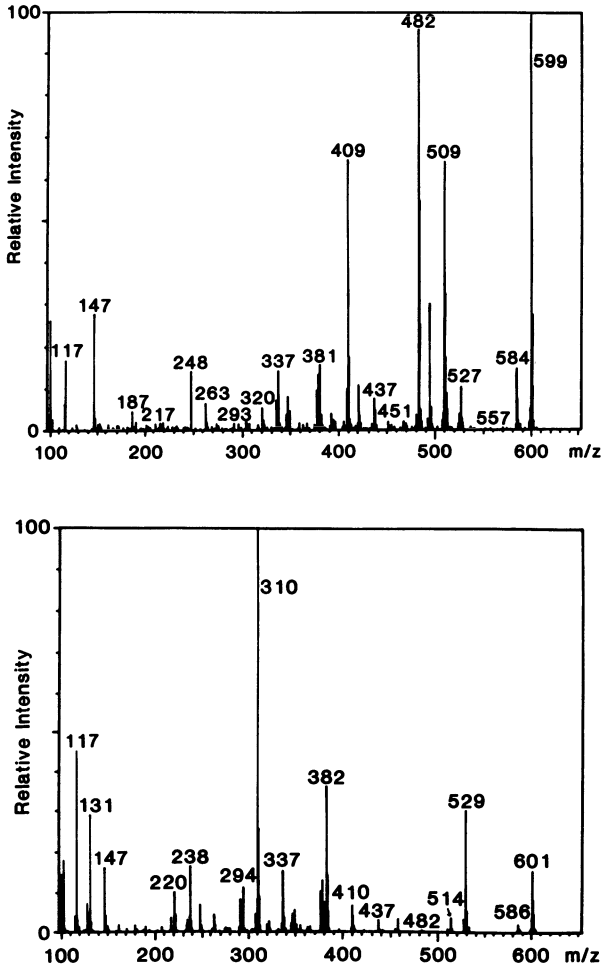


Figure 7.2. Mass spectra of dihydrobiopterin penta-TMS (top) and tetrahydrobiopterin penta-TMS (bottom).

than with classical PKU. In spite of adequate control of serum phenylalanine levels, deterioration continues unabated. Seizures have not been encountered in these patients because they have dihydrobiopterin reductase deficiency. Because tetrahydrobiopterin and dihydrobiopterin reductase are essential to the hydroxylases that synthesize dopamine, serotonin, and norepinephrine, it is not surprising that neurological symptoms are prominent in both defects. Why seizures occur in one and not in the other is at present unanswered.

3.1.2. Disorders of L-Tyrosine Metabolism

Free body fluid tyrosine is derived primarily from the conversion of dietary or endogenous phenylalanine and from peptide-bound tyrosine in proteins. A small amount of tyrosine may also be derived from nitrogen fixation by intestinal bacteria in the presence of the equivalent keto acid, *p*-hydroxyphenylpyruvate (*p*-HPPA). Tyrosine, like its precursor phenylalanine, is oxidized by tissues to fumarate and acetoacetate (Fig. 7.3). The normal catabolic pathway is impaired

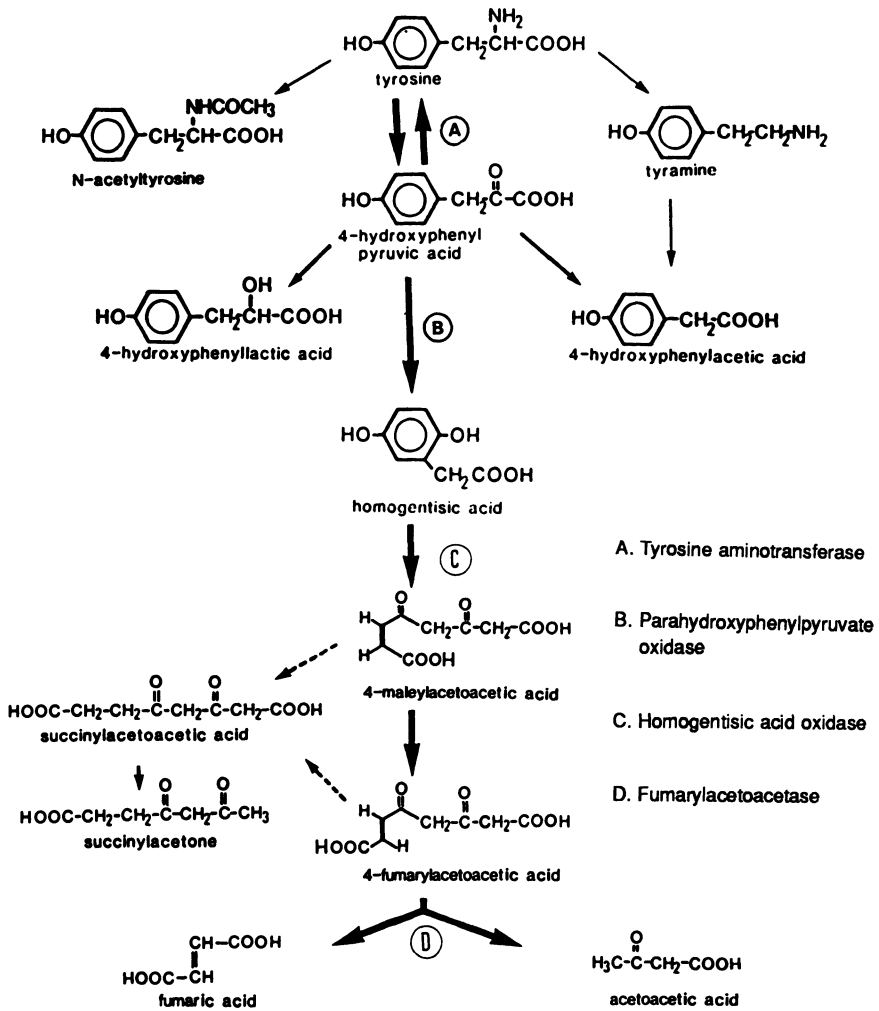


Figure 7.3. Tyrosine metabolism and its inherited disorders.

in several conditions of clinical interest. In the "Oregon type" of tyrosinemia (tyrosinemia type II), a disorder of transamination has been described in which the cytosol form of tyrosine aminotransferase is deficient. *p*-Hydroxyphenylpyruvic acid oxidase (*p*-HPPA), which catalyzes the second step in tyrosine catabolism, is affected in three diseases: transient neonatal tyrosinemia, which is of interest because it elucidates several important facets of postnatal enzyme development, tyrosinemia type III, and hereditary tyrosinemia (tyrosinemia type I), a complex disease accompanied by grave illness in which the oxidase step is impaired secondarily.

3.1.2a. Tyrosinemia Type II (McKusick 276600). Buist (11) referred to studies of a child with tyrosinemia and tyrosine transaminase deficiency but normal *p*-hydroxyphenylpyruvic acid oxidase; the phenylalanine level was normal, and *p*-hydroxyphenylpyruvate was elevated in the urine. Fellman et al. (12) reported chemical studies on the same patient. Only the mitochondrial form of tyrosine aminotransferase (TAT) was present in the liver, whereas the soluble form of TAT was lacking.

This condition is less common than the hereditary tyrosinemia described below. Several patients have been described with mental retardation, microcephaly, hyperkeratotic skin lesions, cataracts, and keratotic eye lesions (pseudoherpetic keratitis). No renal or hepatic abnormalities have been encountered. Enzymatic studies in only one of six patients demonstrated a defect of cytosolic tyrosine aminotransferase.

Chemical diagnosis can be made by the detection of N-acetyltyrosine in addition to *p*-hydroxyphenylpyruvate, *p*-hydroxyphenyllactate, and *p*-hydroxyphenylacetate, with the latter two metabolites being lower in the tyrosinemia type II patient than in cases of tyrosinemia types I and III. An extremely high level of tyrosine can be detected in blood and urine in the type II patient. This high concentration of plasma tyrosine is secreted into the intestine and metabolized to form the two metabolites last mentioned. N-Acetylation of tyrosine takes place only in the presence of a large excess of tyrosine in the type II patient and not in the other types of tyrosinemia.

3.1.2b. Transient Neonatal Tyrosinemia. Transient neonatal tyrosinemia is the most common disorder of amino acid metabolism in man. Although it occurs more frequently in premature infants than in full-term infants, it is not limited to small infants. Plasma tyrosine levels reach their apogee at the end of the first week of life and remain elevated for several weeks after birth in 0.5% of surviving infants. Because plasma tyrosine concentration in this disorder can exceed 2 mM, it is important to recognize that, although such high levels are considered harmless, some infants may manifest lethargy and obtundation during the period of elevation. The most significant feature of this disorder is its early biochemical

similarity to hereditary tyrosinemia. Hence, it is essential to make a definitive diagnosis as early as possible in order to begin dietary therapy for the hereditary form.

The enzyme defect in this disorder is seen as the diminished activity of *p*-hydroxyphenylpyruvic acid oxidase. This enzyme forms homogentisate through a complex series of reactions involving hydroxylation of the ring, migration of the pyruvyl side chain with conversion to an acetyl group, and liberation of carbon dioxide. In the premature infant the enzyme is subject to inhibition by its substrate because of the large quantities of tyrosine in the newborn diet. Relative deficiency of ascorbate in the diet and reduced amounts of enzyme in the cell contribute to decreased tyrosine clearance from the blood.

The characteristic abnormal urinary metabolites in this patient are *p*-hydroxyphenylpyruvate, *p*-hydroxyphenyllactate, and *p*-hydroxyphenylacetate in addition to tyrosine in blood and urine. However, the high levels of these abnormal metabolites will disappear within several weeks.

3.1.2c. Hereditary Tyrosinemia (Tyrosinemia Type I: McKusick 276700). Hereditary tyrosinemia represents a metabolic enigma because methionine metabolism as well as tyrosine metabolism is affected. When the disease presents in the so-called "acute" form, the course is particularly malignant. Acute presentation is characterized by the appearance of symptoms within the first 6 months of life, with death from liver failure in about 90% of patients. Failure to thrive is almost universal, whereas hepatomegaly, jaundice, vomiting, a distinctive methionine or cabbage-like odor, ascites, fever, and bleeding episodes are also seen to varying degrees. Hypoglycemia from islet cell hyperplasia has also been recorded, along with diarrhea and dyspnea.

Some patients do not present until later with a more slowly progressing form that includes failure to thrive, severe nodular cirrhosis, Fanconi syndrome, susceptibility to hypoglycemia, leukopenia, and thrombocytopenia. Many of these patients have come to the attention of the medical practitioner because of hypophosphatemic rickets secondary to the Fanconi syndrome. Patients with the chronic form have a decided proclivity to develop hepatomas. As with many inborn errors, hybrid forms exist, thus rendering a strict distinction between acute and chronic forms impractical.

In this disorder, fumarylacetoacetate hydrolase (fumarylacetoacetase), the enzyme that catalyzes the last step of tyrosine catabolism, is deficient. Linblad *et al.* (13) have isolated and identified succinylacetone (Fig. 7.4) and succinylacetoacetate, which are thought to originate from maleylacetoacetate and fumarylacetoacetate, intermediates of the tyrosine catabolic sequence, which is blocked at the final step. These authors attribute damage to liver and kidney to the accumulation of these compounds in these organs; both organs possess significant activity of an earlier enzyme in this catabolic sequence, *p*-HPPA oxidase,

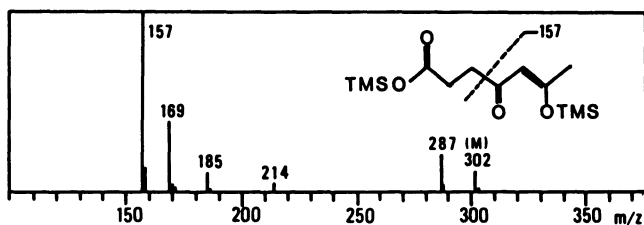


Figure 7.4. Mass spectrum (70 eV) of succinylacetone di-TMS.

which leads to maleylacetoacetate formation. Further, succinylacetone appears to be a potent inhibitor of porphobilinogen synthetase, accounting for the increased excretion of δ -aminolevulinate in the patient with hereditary tyrosinemia.

Chemical diagnosis can be made by the detection and identification of *p*-hydroxyphenylpyruvate, *p*-hydroxyphenyllactate, *p*-hydroxyphenylacetate, δ -aminolevulinate, succinylacetone, and succinylacetoacetate. Amino acids showing particular elevation include tyrosine, proline, threonine, glycine, alanine, leucine, and methionine; δ -aminolevulinate may also be elevated in urine.

3.1.2d. Tyrosinemia Type III (McKusick 276710). In one patient, the authors demonstrated (14) hypertyrosinemia without hepatic dysfunction, with normal soluble tyrosine aminotransferase and fumarylacetoacetase activities. The activity of *p*-hydroxyphenylpyruvic acid oxidase in the patient's liver was about 5% of controls: the enzyme had a high K_m for *p*-hydroxyphenylpyruvate.

The clinical picture was that of mild mental retardation. The mother also had mild mental retardation and elevated blood tyrosine level (6.1 mg/dl as compared with 11.6 mg/dl in the infant).

3.1.2c. Alcaptonuria (McKusick 203500). Alcaptonuria, or homogentisic aciduria, is the predecessor to ochronosis, the deposition of oxidized homogentisic acid pigment in connective tissue, and to spondylitis and arthropathy, the degenerative conditions that follow deposition of pigment.

Alcaptonuria is one of the four inborn errors of metabolism described by Garrod 1902 (15). It is also the first disease of man for which Mendelian recessive inheritance was proposed (15). The disease has a long history, probably because the darkening of urine, which occurs when it is exposed to air, has attracted the attention of patients for centuries. The darkening of urine on standing was attributed to increasing alkalinity and uptake of oxygen; Boedeker called the substance responsible for this finding "Alkapton"; thereafter, the condition was known as "alcaptonuria."

Alcaptonuria occurs when homogentisate is not oxidized to maleylacetoacetate. It is recognized that homogentisate is the normal intermediate formed dur-

ing the enzymatic conversion of tyrosine to fumarate and acetoacetate in the liver.

The patient's urine will darken, eventually turning black, on standing in air or with the addition of an alkali. Bile, porphyrins, myoglobin, and hemoglobin may also darken urine, thus giving a false-positive reaction. Identification of homogentisate in the urine can be made very easily by GC/MS analysis without confusion.

3.2. Disorders of Branched-Chain Amino Acid Metabolism

Leucine, isoleucine, and valine are essential amino acids in man. Figure 7.5 shows the metabolic pathways of branched-chain amino acids and disorders of

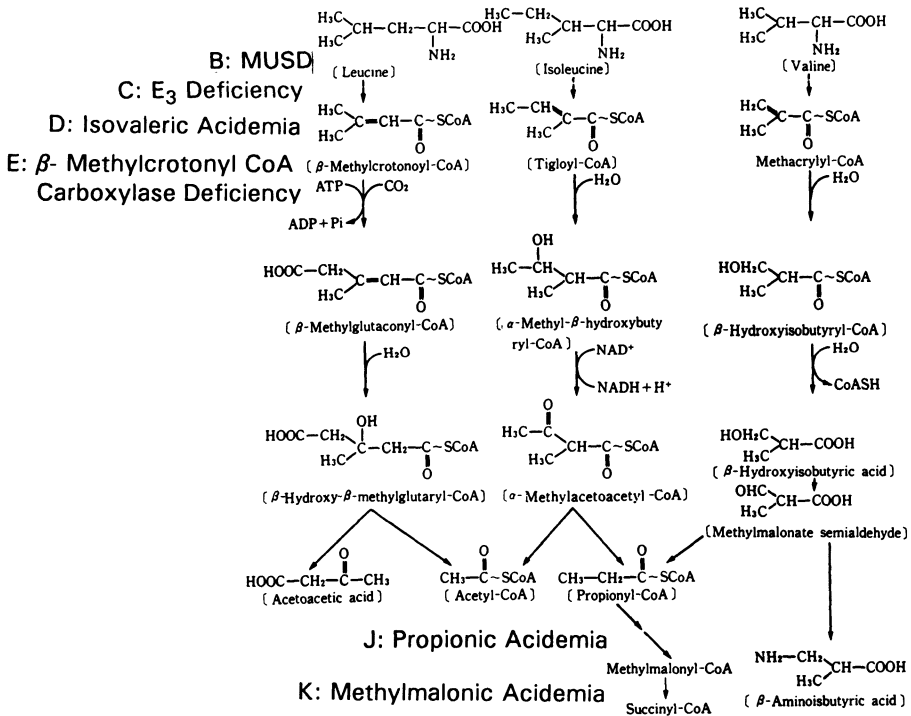


Figure 7.5. Metabolic pathway of branched-chain amino acids and some disorders. A₁, hyperleucine-hyperisoleucinemia; A₂, hypervalinemia; B, maple syrup urine disease (MSUD); C, dihydrolipoyl dehydrogenase (E₃) deficiency; D, isovaleric acidemia; E, β -methylcrotonyl-CoA carboxylase deficiency; F, β -methylglutaconyl-CoA hydratase deficiency; G, β -hydroxyisobutyryl-CoA deacetylase deficiency; H, β -hydroxy- β -methylglutaryl-CoA lyase deficiency; I, β -ketothiolase deficiency; J, propionic acidemia; K, methylmalonic acidemia.

these pathways. In the first step of the catabolism of branched-chain amino acids, they undergo transamination to give the corresponding α -keto acids by vitamin-B₆-dependent transamination with 2-oxoglutarate in the cytosol of extrahepatic tissue cells. The presence of a specific transaminase functioning for valine, which is a five-carbon amino acid, and those for leucine and isoleucine, which are six-carbon amino acids, is indicated by finding of isolated hypervalinemia (McKusick 27710) (16).

In the second step, these branched-chain α -keto acids undergo oxidative decarboxylation to yield the branched-chain acyl CoA, catalyzed by the branched-chain keto acid dehydrogenase complex, which is located on the outer surface of the inner mitochondrial membrane in a wide variety of tissues, but mainly in the liver and kidney. The nature of this enzyme complex is very similar to those of the pyruvate dehydrogenase (PDH) complex and the 2-oxoglutarate dehydrogenase complex (17). The deficiency of the first component of this complex causes branched-chain ketoaciduria or maple syrup urine disease (MSUD). The deficiency of the third component leads to multiple ketoaciduria, named dihydrolipoyl dehydrogenase (E3) deficiency (18,19). Because transamination is reversible, the branched-chain amino acids as well as their corresponding keto acids and hydroxy acids accumulate in body fluids of patients with MSUD. Because an enzyme deficiency at any step after oxidative decarboxylation, an irreversible reaction, does not cause persistent and significant branched-chain amino acidemia, the analysis of organic acids is essential for the chemical diagnosis of the enzyme deficiencies at any step after oxidative decarboxylation. GC/MS has proved to be most suitable for this purpose.

After transamination and oxidative decarboxylation, the degradative pathway of leucine is distinct from those of valine and isoleucine, and enzyme deficiencies at every step of these pathways are known and are described below. Leucine, a ketogenic amino acid, yields acetoacetate and acetyl CoA, which are further degraded in the tricarboxylic acid cycle in healthy man. No specific enzyme deficiency after the first two steps in the degradation of valine is known at present. For isoleucine, a late error is known: β -ketothiolase deficiency. Isoleucine and valine are major precursors of propionyl CoA and methylmalonyl CoA, whose metabolism is affected in propionic acidemia and methylmalonic aciduria, very common organic acidemias that are associated with secondary lactic acidosis. Thus, special attention has been paid to these disorders of amino acid metabolism by many researchers.

3.2.1. Maple Syrup Urine Disease (McKusick 248600)

As is true for most other amino acids, the initial metabolic step in the catabolism of the three branched-chain amino acids (leucine, isoleucine, and valine) is transamination. In MSUD, this initial transamination occurs normally,

but the second step, oxidative decarboxylation, is impaired. The decarboxylation of the three branched-chain amino acids is catalyzed by one multienzyme complex, branched-chain α -keto acid dehydrogenase complex (EC 1.2.4.4),* consisting of three components: E_1 (composed of two α subunits and two β subunits), E_2 , and E_3 (composed of two subunits). Deficiency of either E_1 , E_2 , or E_3 components causes a defect in the oxidative decarboxylation of the three branched-chain α -keto acids. As a result of the enzymatic defect, the keto-acid derivatives accumulate in plasma, urine, red cells, and cerebrospinal fluid. And because the transamination of branched-chain amino acids, which is the step immediately preceding oxidative decarboxylation, is reversible, as described before, three branched-chain amino acids also accumulate in body fluids.

In addition, alloisoleucine is often found increased in this disease, occurring as a result of enolization and subsequent reamination of 2-keto-3-methylvalerate. The odor of maple syrup, after which MSUD was named, is proved to be caused by 2-keto-3-methylvalerate, the transamination product of isoleucine (20).

Affected infants with the classical form of MSUD (21) usually appear normal for the first few days of life; symptoms arise somewhere between 3 and 5 days of age. As is characteristic of all the organic acidemias, symptoms are nonspecific, with the babies appearing listless and having poor appetites. The development of a high-pitched, unpleasant cry is indicative of CNS toxicity. In quick succession, other neurological symptoms appear, including loss of tendon and Moro reflexes, wandering eye movement, and periods of extreme flaccidity and hypotonicity altering with opisthotonos. Convulsions may appear during this time, and respiratory disturbances and coma may supervene. The symptoms worsen rapidly, and the patient becomes acutely ill, may suffer intercurrent infections, and usually dies within the first year of life unless treated with low-branched-chain-amino-acid milk. Even if the patient survives longer than 1–2 years, severe brain damage is often the result. The appearance of the odor that has given the disease its name occurs simultaneously with the earliest onset of neurological symptoms. It can be detected in urine, sweat, and ear wax and is so prominent that the discerning observer cannot help but notice it. Hence, one cannot overstate the importance of smelling the urine and breath of any child appearing to have sepsis neonatorum. Warming a urine that has been refrigerated may be necessary to encourage volatilization of the acids and metabolites.

By conventional mass screening, blood leucine concentration is measured by Guthrie's method. However, as discussed later, E_3 deficiency is sometimes misdiagnosed as MSUD. In order to avoid such a risk, chemical diagnosis of MSUD should be made by the analyses of organic acids in the urine of the patient by GC/MS in addition to an amino acid analysis. Urinary concentrations of

*Each enzyme has an EC number, which is assigned by the Nomenclature Committee of the International Union of Biochemistry (IUB).

leucine, isoleucine, and valine are extremely high, especially leucine, and three 2-keto acids, 2-ketoisocaproate, 2-keto-3-methylvalerate, and 2-ketoisovalerate, are excreted in huge amounts. These 2-keto acids give the unusual odor described earlier.

We analyzed the TMS derivatives of urinary acids of a patient with intermittent MSUD by using a column packed with 3% OV-17 and detected 2-hydroxyisovalerate, 2-hydroxyisocaproate, and 2-ketoisocaproate, but not 2-keto-3-methylvalerate or 2-hydroxy-3-methylvalerate. In E_3 deficiency, which is almost indistinguishable from intermittent MSUD, 2-ethylhydracrylate is detectable (22). Although the chromatographic resolution and the sensitivity for the detection of 2-oxo acids with a branch at the 3-carbon are low when simple trimethylsilylation and packed columns are employed, this method affords enough information for the chemical diagnosis of MSUD, saving approximately one-half of the analysis time.

3.2.2. Dihydrolipoyl Dehydrogenase Deficiency (McKusick 246900)

Pyruvate, which is produced by the glycolytic pathway from glucose, directly from phosphoenolpyruvate, or from alanine or other glycogenic amino acids, is metabolized to acetyl CoA through oxidative decarboxylation by the pyruvate dehydrogenase (PDH) complex (EC 1.2.4.1) or to oxaloacetate by pyruvate carboxylase. The molecular weight of the bovine heart PDH complex is 8.5 million, made up of 30 units of E_1 , 60 units of E_2 , and six units of E_3 . The E_1 unit is an $\alpha_2\beta_2$ tetramer with 41 and 36 kDa for α and β , respectively. The E_2 is a monomer that gives an apparent molecular weight of 74,000 on SDS polyacrylamide gel electrophoresis. The E_3 dihydrolipoyl dehydrogenase is a dimer whose subunit molecular weight is 55,000. Moreover, E_1 is inactivated through phosphorylation by PDH kinase. Pyruvate phosphate decarboxylase, which is dephosphorylated by PDH phosphate phosphatase, becomes active. The latter two, therefore, are concerned with the regulation of PDH activity. Figure 7.6 shows the oxidative decarboxylation of pyruvate to acetyl CoA, 2-ketoglutarate to succinyl CoA, and 2-oxoisovalerate, 3-methyl-2-oxovalerate, and 2-oxoisocaproate to isobutyryl CoA, 2-methylbutyryl CoA, and isovaleryl CoA, respectively.

The frequency of inherited PDH complex deficiency is relatively high in patients with lactic acidosis. However, dihydrolipoyl dehydrogenase (E_3) deficiency is very rare and was first described by Haworth *et al.* in 1976 (17) in three siblings of a Canadian Indian family, all of whom were mentally retarded and had seizures, other neurological signs, and chronic lactic acidosis. Lactate, pyruvate, alanine, glutamate, and proline levels in the blood were increased. Large amounts of pyruvate and 2-oxoglutarate were excreted in the urine. Two of them had hypoglycemia when fasting. The activities of pyruvate and 2-oxoglutarate

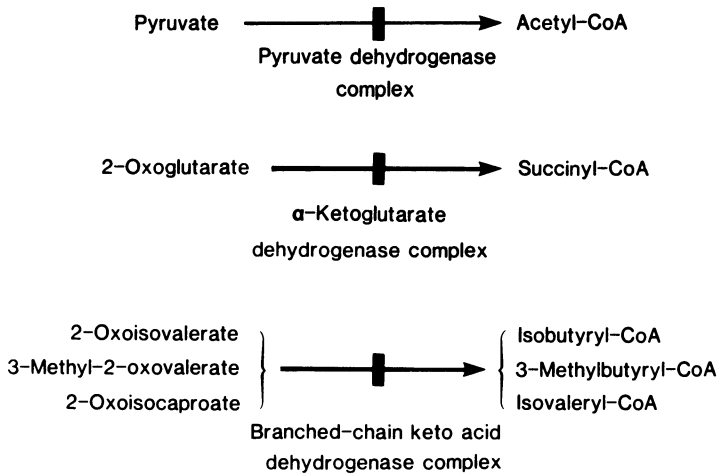


Figure 7.6. Oxidative decarboxylation of pyruvate, 2-ketoglutarate, and branched-chain 2-keto acids.

dehydrogenase complexes in the cultured fibroblasts from one of the siblings were very low. On the basis of this fact, Haworth *et al.* (17) suggested that pyruvate and 2-oxoglutarate dehydrogenase complexes were damaged in the patients. The year after Haworth's report, Robinson *et al.* first discovered that a PDH complex deficiency patient had very low enzyme activity of E₃ (19). The patient was a boy with progressive neurological deterioration and persistent metabolic acidosis. The blood levels of pyruvate, lactate, 2-oxoglutarate, and branched-chain amino acids such as leucine, isoleucine, and valine were increased (23). He sometimes demonstrated hypoglycemia. The patient had developed normally until 8 weeks of age, when he began to have irregular labored respiration marked with inspiratory stridor. He tended to be lethargic and very loose-limbed.

Because E₃ is a common element in human pyruvate, 2-oxoglutarate, and the branched-chain keto acid dehydrogenase complexes (Fig. 7.7), its deficiency affects the conversions of pyruvate to acetyl CoA, of 2-oxoglutarate to succinyl CoA, and of branched-chain keto acids to the corresponding acyl CoA. Thus, pyruvate, lactate, alanine, 2-oxoglutarate, 2-hydroxyglutarate, glutamate, and branched-chain keto acids, their reduced hydroxy acid forms, and branched-chain α -amino acids all accumulate in body fluids.

Based on the urinary organic acid profiles obtained by GC/MS, the authors have made chemical diagnoses of two cases of E₃ deficiency, a 6-month-old boy who had been suspected to have MSUD (24) and a 5-month-old boy with Leigh's syndrome (25). Only a few cases with E₃ deficiency have been described, and their diagnoses have so far been based on E₃ activity. The first case was a boy of

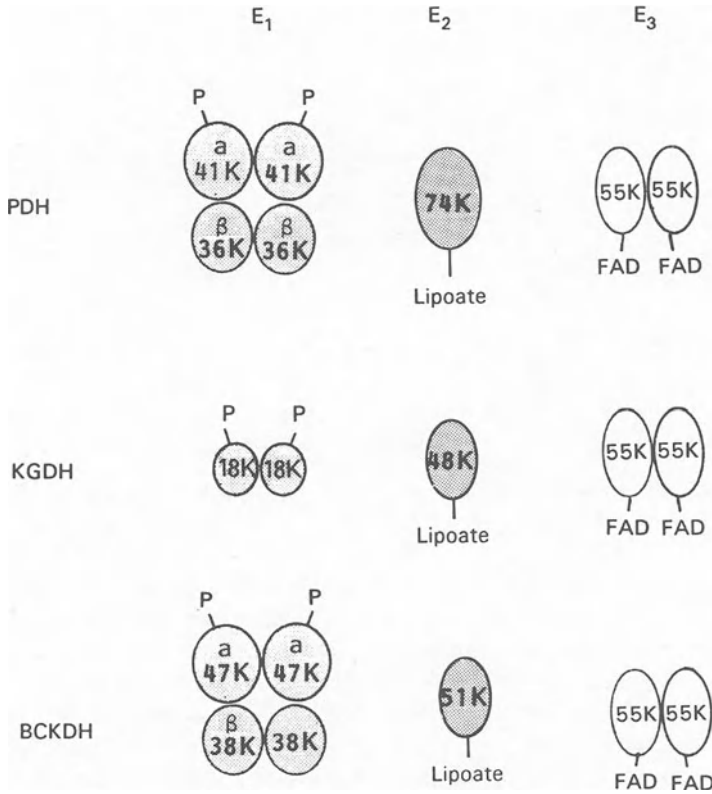


Figure 7.7. Subunit structure of PDH complex, 2-ketoglutarate dehydrogenase complex, and branched 2-keto acid dehydrogenase complex.

nonconsanguineous Japanese parents. By the neonatal screening test based on the Guthrie test on the fifth day of life, he was found to have a high blood leucine level and was suspected of MSUD. But the leucine value at this time was not as high as that of classical MSUD, and he was left on normal milk until 4 months of age, when he had the first severe clinical episode.

Thereafter, he was transferred among a few neighborhood hospitals and finally, at 7 months of age, was admitted to Kurume University Hospital.

The reconstructed ion current chromatogram (RIC) of the TMS derivatives of organic acids in the urine from the patient on admission are shown in Fig. 7.8. Large quantities of lactate (m/z 219, M-CH₃), 2-hydroxybutyrate, 2-hydroxyisovalerate derived from valine (m/z 145, M-COOTMS), 2-hydroxyisocaproate (m/z 159, M-COOTMS) derived from leucine, 2-hydroxyglutarate, and 2-oxoglutarate (m/z 347, M-CH₃) were detected. Markedly increased excretion of 2-

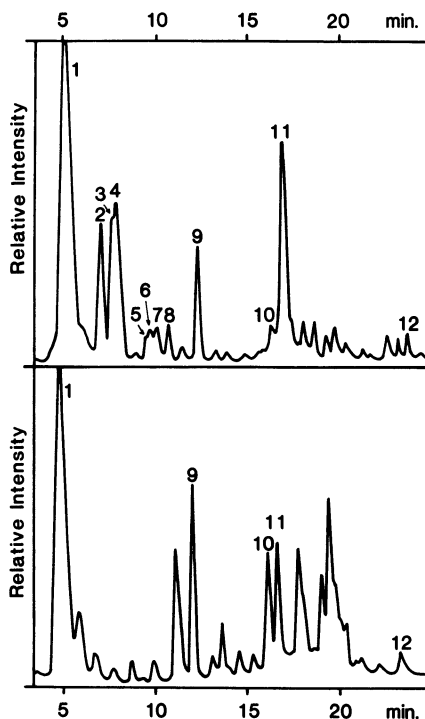


Figure 7.8. Reconstructed ion chromatogram of urinary organic acids in a patient with E_3 deficiency. During a clinical episode on ordinary milk (top) and after restriction of branched-chain amino acid ingestion (bottom). Peaks: 1, lactate; 2, 2-hydroxybutyrate; 3, 2-hydroxyisovalerate; 4, 3-hydroxybutyrate; 5, 2-hydroxyisocaproate and 2-ethylhydracrylate; 6, acetoacetate (isomer 1); 7, 2-oxoisocaproate; 8, acetoacetate (isomer 2); 9, succinate and fumarate; 10, 2-hydroxyglutamate; 11, 2-oxoglutarate; 12, internal standard (IS).

oxoisovalerate, 2-oxoisocaproate, 3-methyl-2-oxovalerate, corresponding hydroxy acids, and branched-chain amino acids are known for patients with MSUD. The amounts of urinary 2-hydroxyisovalerate, 2-hydroxyisocaproate, and 2-oxoisocaproate in this patient were elevated far more than those in normal children or in patients with other diseases, less than those in classical MSUD, and comparable to those in intermittent MSUD.

As a result of restriction of the ingestion of branched-chain amino acids, serum branched-chain amino acid levels were lowered to the normal range, and urinary branched-chain hydroxy acids and branched-chain keto acids were undetectable. The lactate levels, however, remained elevated (24). Although the 2-oxoglutarate level was lowered by restriction of the ingestion of branched-chain amino acids, it was still elevated significantly in the urine (Fig. 7.8). This observation strongly suggests that branched-chain keto acids inhibit the 2-oxoglutarate dehydrogenase complex in humans. Severe ketosis was never observed in these patients with E_3 deficiency. However, they were slightly ketotic during episodes.

It was shown that acetyl CoA accumulation causes the inhibition of pyruvate dehydrogenase, leading to lactate and α -ketoglutarate accumulation. A

high-carbohydrate diet was recommended (24) because it prevents an increased supply of acetyl CoA from lipids.

The second case (25) was a boy whose blood leucine concentration, when examined by using the neonatal mass screening test, was found to be normal. The infant developed normally until 4 months of age but became acutely sick after the age of $4\frac{1}{2}$ months. He was very loose-limbed and developed tonic-clonic convulsions. Metabolic acidosis was found, and computerized tomography revealed progressive loss of density of the basal ganglia bilaterally, indicative of Leigh's syndrome. He became lethargic, developed anuria, and died at 5 months of age. Serum levels of leucine, isoleucine, valine, proline, alanine, and glutamine were greatly elevated. The urinary organic acid profile was very similar to that in the first case, so the authors concluded that patient was E_3 deficient. We also emphasize that an accurate and rapid diagnosis of E_3 deficiency can be best made by employing GC/MS analysis of urinary acids. More time-consuming enzyme studies should then be carried out to provide a better comparative data base.

As noted in several cases, most patients with E_3 -deficiency develop normally until several months of age. Deterioration, however, proceeds rapidly once the clinical signs appear. Therefore, it is necessary to make an accurate and rapid diagnosis of this disorder to differentiate it from E_1 deficiency in the PDH complex or from MSUD, a deficiency of E_1 in the branched-chain keto acid dehydrogenase complex, and it is critical to see that patients receive adequate and appropriate treatment.

Branched-chain amino acid restriction appears partly effective for E_3 deficiency (24). Patients with deficiency of E_1 in the PDH complex also exhibit chronic lactic acidemia but are treated to some extent with a diet comparatively rich in fat (26), because there is no defect in the utilization through the TCA cycle of acetyl CoA produced by β -oxidation of fatty acid. Treatment with pharmacological doses of lipoic acid, biotin, riboflavin, and thiamine was not effective in most cases of E_3 deficiency.

3.2.3. Isovaleric Acidemia (McKusick 243500)

Following the decarboxylation of the three branched-chain 2-keto acids, the metabolic products, isovaleryl CoA, 2-methylbutyryl CoA, and isobutyryl CoA are dehydrogenated to form 3-methylcrotonyl CoA, tiglyl CoA, and methacrylyl CoA, respectively. Unlike the decarboxylation reaction, the enzymes catalyzing the dehydrogenation reaction in each of the substrates is different. Novel research work done with GC/MS by Tanaka *et al.* (2) indicated that isovaleryl CoA dehydrogenase accepts only isovaleryl CoA as a substrate. Diminished or absent isovaleryl CoA dehydrogenase activity was suggested to be the cause of isovaleric acidemia because serum 3-methylcrotonate did not increase despite the

increase of isovalerate, and leucine loading during remission caused a large increase of isovalerate. Figure 7.9 shows the metabolic pathway of leucine and the feedback inhibition by end-products of leucine, acetoacetate, and 3-hydroxybutyrate of 3-methylcrotonyl CoA carboxylase and 3-methylglutaconyl CoA hydratase.

The other evidence for isovaleryl CoA dehydrogenase deficiency is that the other short-chain fatty acids do not accumulate in serum or urine, suggesting that isovaleryl CoA dehydrogenase is a very specific dehydrogenase and is responsible for this acidemia (27,28), the first organic acidemia discovered using GC/MS (2). As a consequence of the defect of isovaleryl CoA dehydrogenase, excessive isovaleric acid accumulates in the blood. The concentration during an episode can reach 100–500 times greater than normal but is lowered to three to four times the normal level during remission. A relatively minor pathway utilized for acyl CoA conjugation with glycine assumes major importance in the disposition of isovaleric acid. Indeed, during periods of acute exacerbation and remission, isovalerylglycine is rapidly cleared by the kidney and is persistently found in the urine. The other characteristic metabolite peculiar to isovaleric acidemia is 3-hydroxyisovalerate, which is found only during episodes when free isovalerate is heavily accumulated in the body (29).

The general symptoms associated with this disease are those characteristic

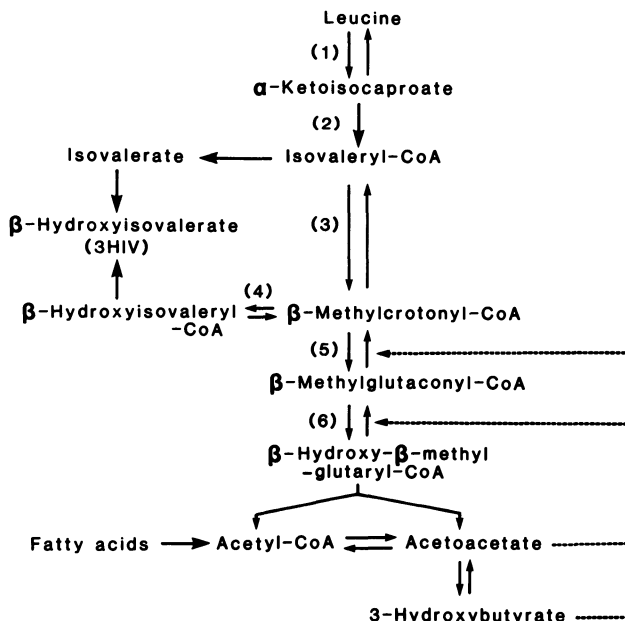


Figure 7.9. Metabolic pathway of leucine.

of all of the organic acidemias, save for the presence of the distinctive odor of “sweaty feet” imparted by isovalerate (2). Whereas small amounts of this acid accumulate in these individuals even during periods of remission, it is only during periods of clinical deterioration that large amounts are found in urine, blood, sweat, saliva, and cerumen (ear wax). Ketoacidosis is common in this disease, and it is associated with vomiting and CNS depression that progresses to coma. Milder, later-occurring cases may be associated with slow mental development rather than these acute symptoms; the spectrum of clinical presentation can vary widely.

At present, more than 60 cases of isovaleric acidemia have been reported. In the authors’ laboratory, six cases were chemically diagnosed by using GC/MS. The hereditary transfer is autosomal recessive. The true incidence is difficult to assess, probably because some cases that occur acutely in the newborn and lead to early death are not recognized, and also because other, non-GC/MS methods for the diagnosis in laboratories are not as reliable.

Chemical diagnosis of isovaleric acidemia is mostly performed by demonstrating the massive urinary excretion of isovalerylglycine. Trimethylsilylation of glycine conjugates gives two derivatives separable on GC, mono-TMS and di-TMS (Fig. 7.10). The relative peak ratio of the two differs on each injection (30). Methylation with diazomethane is preferred (31), and synthesis of acylglycines and mass spectra of methyl esters of isovalerylglycine and other acylglycines of biological interest have been reported (32).

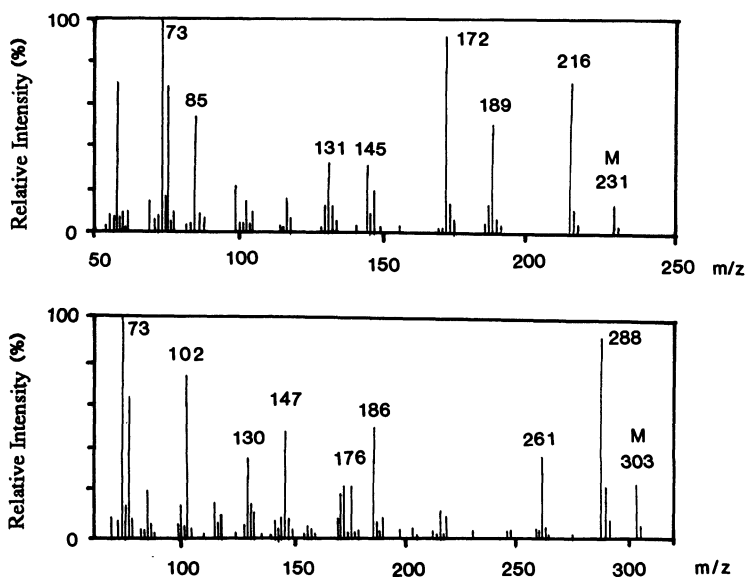


Figure 7.10. Mass spectra (70 eV) of isovalerylglycine mono-TMS (top) and di-TMS (bottom).

3.2.4. β -Ketothiolase Deficiency (McKusick 203750)

This abnormality of isoleucine catabolism has been reported in three families by Daum and colleagues in 1971 (33). The patient in the first family was a 6-year-old boy with recurrent ketoacidosis from 17 months of age. Some of his episodes had necessitated parenteral fluid and alkali therapy in the hospital; others ameliorated spontaneously. In spite of these recurrent setbacks, the physical and mental development of the patient was normal. But in a second family with three affected siblings, they found that one had normal psychomotor development, another died at 1 year of age during an episode, and another showed distinct psychomotor retardation from repeated ketoacidotic attacks (34). GC/MS analysis of the urinary acids as their TMS derivatives revealed massive urinary excretion of 2-methyl-3-hydroxybutyrate. Tiglylglycine (Fig. 7.11), 2-methylacetoacetate, and its decarboxylation product, butanone, were also noted in their urine. 3-Hydroxybutyrate was detected only when the patient was acidotic. 2-Methyl-3-hydroxybutyrate was excreted at a rate of more than 1 g/g creatinine during acidosis, whereas the level was lowered to 250–1000 mg during remission.

Mamer and Tjoa (35) found butanone, acetone, and 2-ethylhydracrylate in the urine of a patient in acidotic periods. The last-mentioned acid is presumed to arise from L-isoleucine by an alternative pathway via *R(L)*-2-oxo-3-methylvalerate (36).

GC/MS analysis of urinary organic acids always demonstrates the increased concentrations of lactate, 3-hydroxybutyrate, acetoacetate, 2-methyl-3-hydroxy-

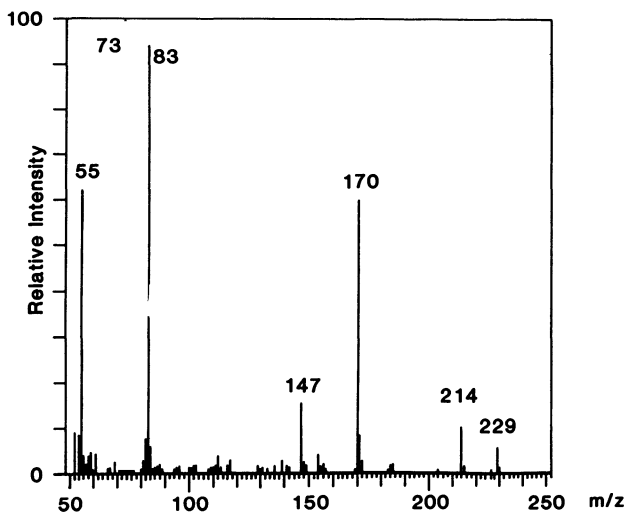


Figure 7.11. Mass spectrum (70 eV) of tiglylglycine mono-TMS.

butyrate, 2-methylacetoacetate, 3-hydroxyisovalerate, and tiglylglycine. Apparently, the high serum concentration of salicylate resulted from acetoacetate.

The symptoms and the onset of this disease differ, depending on the different types of the enzyme. At present, three different β -ketothiolases are known to exist in mammalian systems: (1) mitochondrial short-chain 3-ketoacyl CoA thiolase (EC 2.3.1.9), which can thiolize 2-methylacetoacetyl CoA and acetoacetyl CoA, the activity being stimulated by K^+ ; (2) a mitochondrial general-specificity β -ketothiolase (EC 2.3.1.16), which can thiolize long and medium straight-chain β -ketoacyl CoA; and (3) a cytosolic acetoacetyl CoA thiolase (EC 2.3.1.9), which is found in liver and brain and functions for the biosynthesis of steroids and fatty acids. A deficiency of the mitochondrial short-chain β -ketoacyl CoA thiolase causes massive urinary excretion of 2-methylacetoacetic acid and 2-methyl-3-hydroxybutyric acid, which are catabolic intermediates of isoleucine. In the degradation of fatty acids via β -oxidation, mitochondrial general-specificity β -ketothiolase is thought to play an important role, although the deficiency in humans is not known at present. This enzyme also thiolizes acetoacetyl CoA, but to a lesser extent. Sixteen cases from 11 families have been described to date. Most cases with β -ketothiolase deficiency were caused by the lack of mitochondrial short-chain β -ketoacyl CoA thiolase activity, whereas only two cases reported had deficient activity of cytosolic β -ketothiolase. Because cytosolic β -ketothiolase catalyzes the first committed step of cholesterol synthesis *de novo*, deficiency of this enzyme produces severe neurological symptoms by impairing myelination, altering membrane function, and reducing steroid hormone levels.

The authors also discovered with GC/MS a case with β -ketothiolase deficiency by analyzing the urinary acids of a 23-month-old boy who had been vomiting and had low consciousness and tachypnea (37). The serum ketone body test on admission was strongly positive, and apparent serum salicylate was recognized. The blood glucose level was normal, and blood gases were normalized shortly after glucose and bicarbonate administration. Consciousness was restored and ketone bodies disappeared only after 20 hr of treatment. The urinary metabolite profiles of the patient were compared under different clinical conditions.

During an episode, large amounts of 2-methyl-3-hydroxybutyrate and 2-methylacetoacetate were detected, but the quantity of ketone bodies (3-hydroxybutyrate and acetoacetate) was much larger than that of 2-methyl-3-hydroxybutyrate and 2-methylacetoacetate, and that of lactate was remarkably elevated (100 times that of the control). Tiglylglycine was also detected. Propionic acidemia was completely ruled out because methylcitrate and 3-hydroxypropionate, which are characteristic of propionic acidemia, were not found. After this case was chemically diagnosed as β -ketothiolase deficiency, enzymological studies with fibroblasts showed the lack of mitochondrial short-chain- β -ketoacyl CoA thiolase. The urinary organic acid profile studies of the patient during

remission showed complete disappearance of ketone bodies, and the quantities of 2-methyl-3-hydroxybutyrate and 2-methylacetoacetate, although still high, were remarkably less than those during an episode.

3.2.5. β -Methylcrotonyl CoA Carboxylase Deficiency (McKusick 210200)

The fourth step in the catabolism of branched-chain amino acids is the carboxylation of 3-methylcrotonyl CoA by 3-methylcrotonyl CoA carboxylase (EC 6.4.1.4), a biotin-dependent carboxylase, to give 3-methylglutaconyl CoA. The deficiency of this enzyme causes 3-methylcrotonylglycinuria.

3-Methylcrotonylglycinuria was first reported by Eldjarn *et al.* (38) with a 4½-month-old Norwegian girl from parents of a consanguineous marriage. From the second week of life, feeding difficulties, including choking, appeared. No growth retardation was recognized, but her motor development was greatly retarded for her age. Large amounts of 3-hydroxyisovalerate and 3-methylcrotonylglycine were excreted in her urine.

3-Hydroxyisovalerate detected in her urine is produced by enoyl hydratase (crotonase) hydration of 3-methylcrotonyl CoA. 3-Methylcrotonylglycine is the glycine conjugate of 3-methylcrotonyl CoA catalyzed by glycine-N-acylase. The mass spectrum of 3-methylcrotonylglycine mono-TMS is shown in Fig. 7.12.

The general symptoms associated with this disease are severe hypotonia, atrophy of skeletal muscles, absence of deep tendon reflexes, and fibrillation of the tongue.

Two forms of 3-methylcrotonyl CoA carboxylase deficiency have been

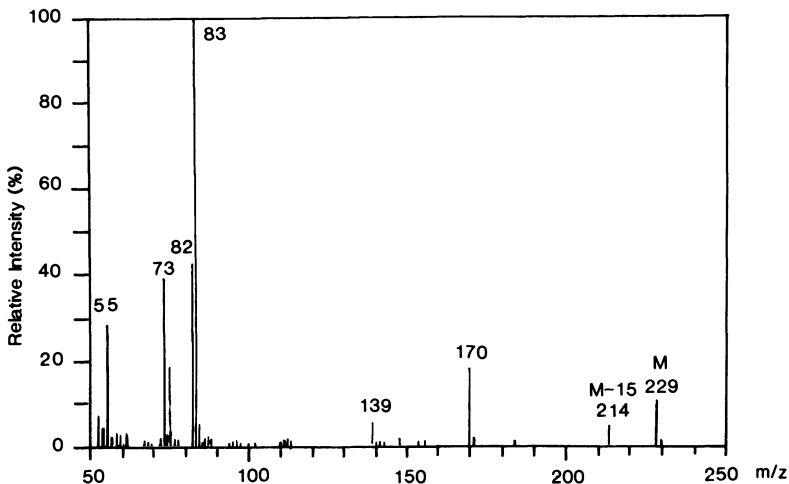


Figure 7.12. Mass spectrum (70 Ev) of 3-methylcrotonylglycine mono-TMS.

reported: the biotin-responsive and the nonresponsive forms. More than 20 cases with defective 3-methylcrotonyl CoA carboxylase have been reported to date, but the majority of these patients appear to be biotin-responsive. In the biotin-responsive patients, the activity of all three mitochondrial carboxylases is deficient, as discussed later in “multiple carboxylase deficiency.”

In the case described by Bartlett *et al.* (39), levels of three branched-chain amino acids and urinary medium-chain dicarboxylates (adipate, suberate, and sebacate) were also elevated in plasma during episodes, but only urinary levels of 3-hydroxyisovalerate and 3-methylcrotonylglycine remained greatly elevated during remission.

Chemical diagnosis can be made by the detection of large amounts of 3-hydroxyisovalerate, 3-methylcrotonylglycine, lactate, and 2-oxoglutarate in the urine.

3.2.6. 3-Methylglutaconic Aciduria (McKusick 250950)

3-Methylglutaconic aciduria is a rare, inherited metabolic disorder in which 3-methylglutaconate and 3-methylglutarate are increased in the urine. There are at least three known types of 3-methylglutaconic aciduria, which differ clinically and biochemically from each other. In MG type I, the activity of 3-methylglutaconyl-CoA hydratase (EC 4.2.1.18), a specific enzyme involved in leucine catabolism, is deficient, and the only significant clinical symptom is retarded speech development. In contrast, in type II and III the activity of 3-methylglutaconyl-CoA hydratase is normal in fibroblasts, no specific enzyme defect has yet been identified, and the metabolites' concentrations are lower than in type I. Type II is clinically characterized by a congenital cardiomyopathy, neutropenia, short stature, recurrent infection, and normal cognitive development. The type III includes progressive neurological impairment and retarded psychomotor development. The authors have made chemical diagnosis of type II for a 6-year-old boy and of type III for a 6-month-old male infant. Recently, the authors found the first two healthy adults with 3-methylglutaconic aciduria during the study of toxemia of pregnancy (40). The origin of 3-methylglutaconic aciduria in these healthy women is unclear. The addition of these cases may, however, contribute to an understanding of the heterogeneity of this metabolic disorder.

3.2.7. Propionic Acidemia (McKusick 232000)

Propionyl CoA is a catabolic intermediate of isoleucine, valine, methionine, threonine, and odd-numbered fatty acids but not of leucine. Propionyl CoA is carboxylated to give D-methylmalonyl CoA by propionyl CoA carboxylase. D-Methylmalonyl CoA is possibly nonenzymatically racemized to L-meth-

ylmalonyl CoA, which is then converted to succinyl CoA by methylmalonyl CoA mutase. Succinyl CoA enters the citric acid cycle and is completely oxidized. Propionyl CoA carboxylase (PCC) requires biotin as a coenzyme, as do other carboxylases. Propionic acidemia, as first reported by Hommes *et al.* (41), has autosomal recessive inheritance caused by a deficiency of PCC.

Affected infants are generally normal at birth but develop vomiting, lethargy, and hypotonia, progressing to coma within the first week or so of life. As in most of the members of these diseases, there is a predictably severe ketoacidosis. Respiratory compensation with hyperventilation is often a prominent finding. Subsequent neurological deterioration may result in seizures and apneic episodes. Occasionally, infants and older children present with a somewhat different clinical picture. In such a case, failure to thrive, hypertonia, and occasional seizures are the prominent findings, and the acidosis is variable and peripheral in importance.

Hsia *et al.* (42) demonstrated the defect in propionate catabolism with leukocytes from a male patient, and deficiency of PCC activity was first demonstrated in cultured fibroblasts in 1971 (43). Since then, more than 30 cases with PCC deficiency have been reported.

In patients with propionic acidemia, propionyl CoA undergoes metabolic changes that facilitate transport from the mitochondria: β -oxidation to give 3-hydroxypropionate (44), glycine conjugation of propionyl CoA or of its precursor tiglyl CoA (45), condensation with oxaloacetate to give methylcitrate (46), condensation with acetyl CoA to give 3-hydroxyvalerate (47) and 3-oxovalerate (48), and condensation with another propionyl CoA to give 2-methyl-3-hydroxyvalerate and 2-methyl-3-oxovalerate (48,49). The minor metabolites 3-ethyl-3-hydroxyglutarate (50,51), 2-methylbutyrylglycine (52), 2-methylacetoacetate (52), 3-hydroxy-2-methylbutyrate (52), 2-methylacetoacetate (52), 3-hydroxy-2-methylbutyrate (52), 2-methylglutaconate (53), propionyl carnitine (54), and 2-hydroxy-2-methylsuccinate (55) have been reported. More recently, the methyl branched-chain dicarboxylates 3-methyladipate, 4-methylpimerate, 4-methylsuberate, pimelate, and azelate have been identified in the amniotic fluid of a fetus with propionic acidemia, and concentrations much higher than those of the amniotic fluid were found in the urine of neonates with propionic acidemia and methylmalonic acidemia (56). In Fig. 7.13, the mass spectrum of methylcitric acid tetra-TMS is shown.

Propionic acidemia produces characteristic urinary organic acid profiles. The diagnosis is based on the detection of these propionyl-CoA-derived metabolites rather than propionate. However, the profiles of the patients are not simple, and they differ depending on their clinical condition at the time of analysis, age, and so on. Chemical diagnosis of propionic acidemia is more difficult than for other organic acidemias and can be facilitated by GC/MS. The authors have also chemically diagnosed 27 cases in Japan.

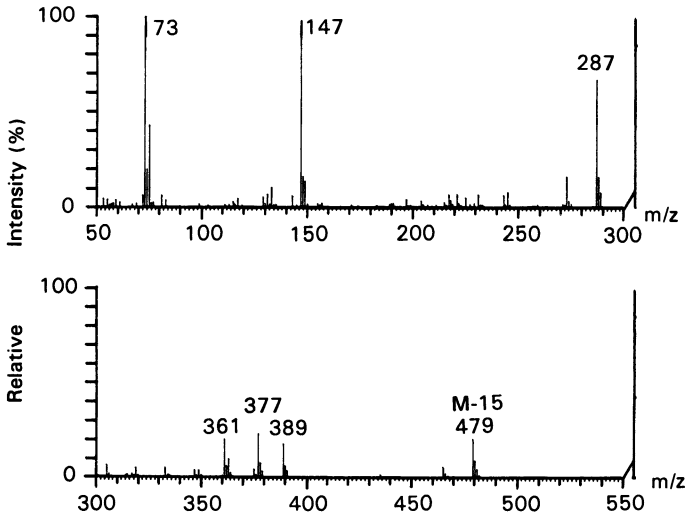


Figure 7.13. Mass spectrum (70 eV) of methylcitric acid tetra-TMS.

Kuhara *et al.* compared the urinary acid profiles during a clinical episode and remission in an 8-month-old girl with propionic acidemia (57). Only methylcitrate and 2-methyl-3-oxovalerate were detected under clinically favorable conditions (Fig. 7.14).

During episodes of clinical decompensation, however, the patient excreted increased amounts of all the metabolites associated with this disorder. In addition to ketone bodies, four acetyl CoA precursors increased during clinical episodes: glutarate, a catabolic intermediate of lysine; 3-hydroxyisovalerate and 3-methylglutaconate, catabolic intermediates of leucine; and lactate. Metabolism of propionyl CoA in propionic acidemia patients seems to proceed via normal acetyl CoA metabolism except for glycine conjugation and β -oxidation. Methylcitrate is formed in the same manner that citrate is formed from acetyl CoA and oxalacetate. 3-Oxovalerate and 3-hydroxyvalerate appear to be produced by a mechanism similar to that for formation of ketone bodies from acetyl CoA. The authors suggested that the mechanism that lowers mitochondrial acetyl CoA levels also serves to lower mitochondrial propionyl CoA levels by preventing competitive inhibition by acetyl CoA of the metabolism of propionyl CoA.

3-Hydroxyvalerate, 3-oxovalerate, and 3-ethyl-3-hydroxyglutarate were found in the urine of patients with propionic acidemia or methylmalonic acidemia only during ketotic episodes (50). Thus, these homologues of ketone bodies and the intermediates of ketone bodies may be formed as follows. (1) Catalyzed by a thiolase (EC 2.3.1.9), one molecule of propionyl CoA and one molecule of acetyl CoA condense to give 3-oxovaleryl CoA. (2) Catalyzed by 3-hydroxy-3-methylglutaryl CoA synthase, 3-oxovaleryl CoA condenses with another acetyl

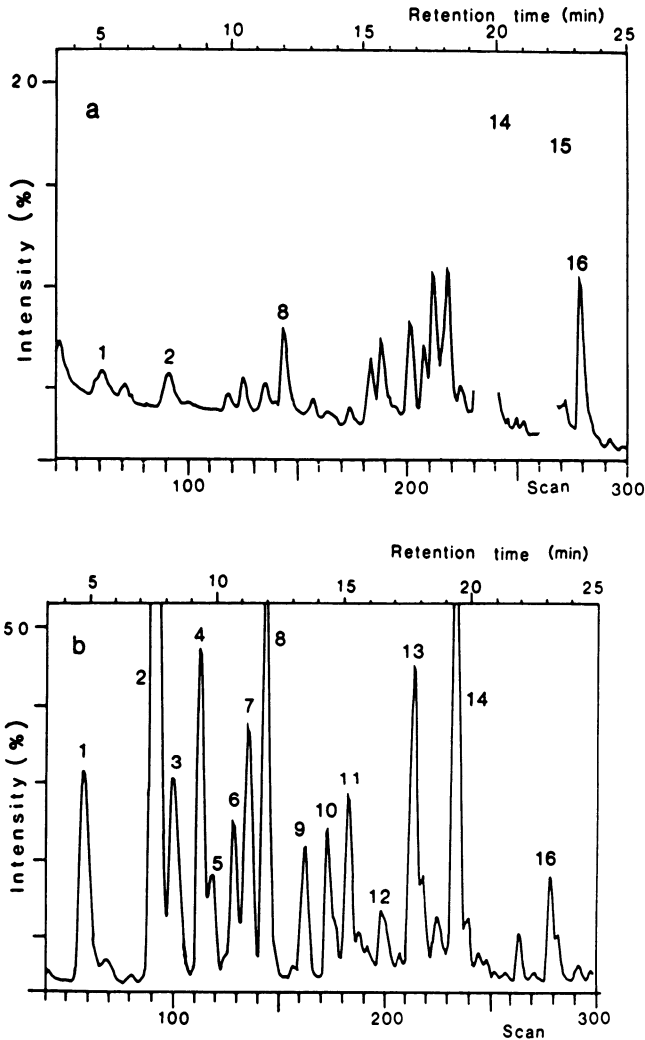


Figure 7.14. Reconstructed ion chromatogram of urinary organic acids in a patient with propionic acidemia under clinically favorable conditions (a) and during a clinical episode (b). 1, lactate; 2, 3-hydroxypropionate; 3, 3-hydroxy-2-methylbutyrate and 3-hydroxyisovalerate; 4, 3-hydroxyvalerate; 5, 3-hydroxy-2-methylvalerate; 6, 3-oxovalerate (isomer 1); 7, 3-oxovalerate (isomer 2) and 2-methyl-3-oxovalerate (isomer 1); 8, 2-methyl-3-oxovalerate (isomer 2); 9, glutarate; 10, 3-methylglutaconate (isomer 1); 11, 3-methylglutaconate (major, isomer 2) and adipate (minor); 12, 3-hydroxy-3-ethylglutarate; 13, tiglylglycine; 14, methylcitrate; 15, pantothenate; 16, IS.

CoA to give 3-hydroxy-3-ethylglutaryl CoA. (3) 3-Hydroxy-3-ethylglutaryl CoA is cleaved to 3-oxovalerate and acetyl CoA, which is catalyzed by 3-hydroxy-3-methylglutaryl CoA lyase (EC 4.1.3.4). (4) 3-Hydroxyvalerate is formed from 3-oxovalerate by 3-hydroxybutyrate dehydrogenase (EC 1.1.1.30).

Affected persons who are not placed on a protein-restricted diet develop mental retardation and seizures and die at an early stage, although some of them are not seriously ill (58). Because the quantity of protein in breast milk is less than that in cow's milk, the disease occurs later for patients on breast milk.

Propionic acidemia is also called ketotic hyperglycinuria and has two forms: a biotin-responsive form (59) and a biotin-nonresponsive form. It has been demonstrated that three loci that are biotin responsive (*bio*), *pccA* and *pccBC*, are present in PCC.

As described above, organic acid profiles of propionic acidemia are very complicated. Depending on the clinical condition of the patient, methylcitrate and 3-hydroxypropionate are always the best markers for the chemical diagnosis of propionic acidemia (60).

3.2.8. Methylmalonic Acidemia (*McKusick 251000, 251100, 251110, 251120*)

In 1967, Oberholzer *et al.* (61) and Stokke *et al.* (62) reported cases of critically ill infants with profound metabolic ketoacidosis and developmental retardation with large accumulations of methylmalonate in the blood and urine. Hematological or neurological symptoms of cobalamin defect were not found in these infants, and they failed to respond to administration of cobalamin. Nevertheless, they excreted much more methylmalonate than persons with pernicious anemia. Rosenberg *et al.* (63) and Mahoney *et al.* (64) proved that the fall of mutase activity in these two examples was caused by an adenosylcobalamin synthesis deficiency.

Methylmalonic acidemia is very frequently found as a genetic metabolic error (65,66). From biochemical considerations, it became clear that methylmalonic acidemia occurs in the six following forms: (a) complete mutase apoenzyme deficiency (*mut*^o); (b) partial apoenzyme deficiency (*mut*⁻); (c) mitochondrial IF cobalamin reductase (*cbl A*) deficiency; (d) mitochondrial cob(1)alamin adenosyltransferase (*cbl B*) deficiency; (e) adenosylcobalamin (*Ado cbl*) synthesis deficiency by abnormal cytosolic metabolism of cobalamins (*cbl C*); and (f) methylcobalamine (*Me cbl*) synthesis deficiency by abnormal cobalamin D (*cbl D*) cytosolic metabolism.

In the authors' laboratory, 49 cases of methylmalonic acidemia have been found, and the majority have been clarified as complete or partial mutase apoenzyme deficiency (*mut*^o or *mut*⁻) with a few examples of adenosylcobalamin synthesis deficiency. Matsui *et al.* (67) examined 45 out of 100 persons affected

by the mutase deficiency type of methylmalonic acidemia and reported that 15 patients were mut° , 5 mut^{-} , 14 cbl A , and 11 cblB and that the male/female ratio of each form was about the same.

A large accumulation of methylmalonate is found in the blood and urine of patients with methylmalonic acidemia. The excretion within 24 hr from a normal adult or child is 5 mg, whereas that from the methylmalonic acidemia patient is 240–570 mg. In addition, plasma concentration in the affected patient reaches 2.6–34 mg/dl, although it is not detectable in a normal subject. Therefore, GC is useful for detecting methylmalonate and for clinical diagnosis. Since propionyl CoA carboxylation is reversible, a high accumulation of methylmalonate may cause accumulation of propionate and its related byproducts in the blood and excretion in the urine. A marked tendency to high accumulation is recognized as the condition gets worse, and in addition to the majority of methylmalonate, various other abnormal metabolites were excreted in the urine.

3.3. Disorders of Multienzyme Defects

3.3.1. Glutaric Acidemia Type II (McKusick 231680)

In 1976, Prezyremble *et al.* reported the first case of glutaric aciduria type II in a boy whose birth was normal but had metabolic acidosis and hypoglycemia (24 mg/dl) from the age of 16 hr (68). Despite intravenous infusion of glucose and bicarbonate, an extremely low blood glucose level of 5 mg/dl and extremely severe metabolic acidosis were seen in the patient. A strong odor of “sweaty feet” and hypothermia (32°C) were recognized, and the case ended in epilepsy and death after 70 hr.

High levels of glutarate, ethylmalonate, adipate, suberate, sebacate, and unsaturated dicarboxylates with eight or ten carbons were detected in the urine. Glutaric aciduria type I is recognized as a disease with high levels of excretion of glutarate, the glutarate pathway of which is inhibited, and the patient with this disease excretes large quantities of glutaconate and 3-hydroxyglutarate. Because the type of metabolic deficiency in the patient was apparently different from that of type I, his disease was named glutaric aciduria type II. After that, other cases of this disease were reported and reviewed by Niederweizer (69), Sweetman *et al.* (70), and Gregersen (71).

Figure 7.15 demonstrates the RIC chromatogram of the authors' patient at the age of 2 days whose clinical symptoms and profile of urinary organic acids are similar to the case reported by Prezyremble *et al.* (68) and diagnosed as glutaric aciduria type II.

Mantagos *et al.* (72) reported on ethylmalonic–adipic aciduria, which causes vomiting, spasm, coma associated with hypoglycemia and acidosis, and urinary excretion of ethylmalonate, adipate, and hexanoylglycine. Goodmann *et*

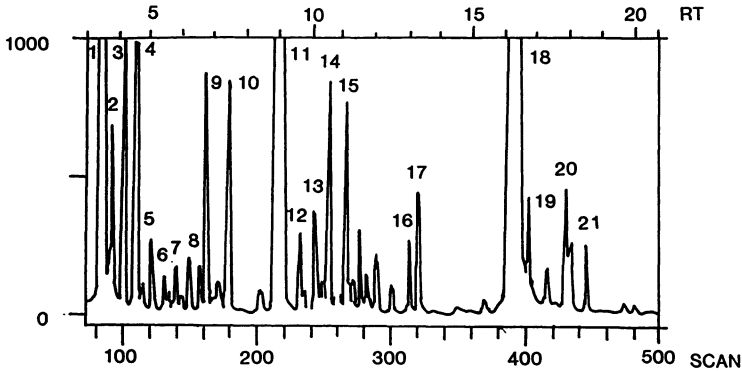


Figure 7.15. Reconstructed ion chromatogram of urinary organic acids in a patient with glutaric aciduria type II. 1, lactate; 2, unknown; 3, 2-hydroxybutyrate; 4, 2-hydroxyisovalerate and 3-hydroxybutyrate; 5, unknown; 6, 2-hydroxyisocaproate; 7, acetoacetate (I); 8, acetoacetate (II); 9, ethylmalonate; 10, succinate, fumarate, and 5-hydroxyhexanoate; 11, glutarate; 12, malate; 13, unknown; 14, adipate; 15, 2-hydroxyglutarate; 17, suberate and monounsaturated suberate; 18, 4-hydroxyphenyllactate; 19, IS₁ (3-hydroxymyristate); 20, hippurate; 21, IS₂ (heptadecanoate).

al. (73) also reported on a similar case and noted the similarity between it and glutaric aciduria type II, but lacking lactic acidosis.

3.3.2. Multiple Carboxylase Deficiency (McKusick 253260, 253270)

Multiple carboxylase deficiency is a deficiency of complex enzymes—pyruvate carboxylase, propionyl CoA carboxylase, and 3-methylcrotonyl CoA carboxylase—all of which require biotin as a coenzyme (Fig. 7.16). The first case was reported as 3-methylcrotonylglycinuria by Gompertz *et al.* (74). The patient was a 5½-month-old son of unrelated parents and whose sister was in good health. He had persistent vomiting, extensive skin rash, and severe metabolic ketoacidosis. Urinary levels of 3-methylcrotonylglycine, 3-hydroxyisovalerate, and tiglylglycine were detected. Administration of D-biotin (10 mg/day) achieved notable improvement of the clinical symptoms. Therefore, this disease was presumed to be biotin-dependent 3-methylcrotonyl CoA carboxylase deficiency, which was proved by examination of leukocytes. Chalmers *et al.* (75) again analyzed the urine of the patient. Among the organic acids that showed unusual high levels, 3-hydroxyisovalerate (10,000 mg/g creatinine), 3-methylcrotonylglycine (4000 mg/g creatinine), 3-hydroxypropionate (4000 mg/g creatinine), methylcitrate (1000 mg/g creatinine), and 3-hydroxy-*n*-valerate (4000 mg/g creatinine) were remarkably elevated. Because the latter three compounds are abnormal components that are characteristic of propionyl CoA carboxylase deficiency, and propionate concentration in the urine was 100 mg/g

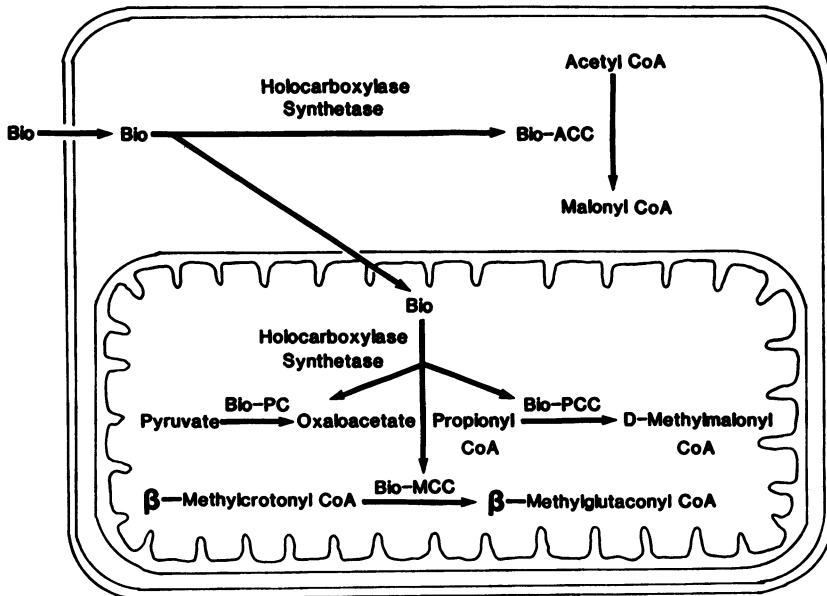


Figure 7.16. Schematic enzyme defect in a patient with multiple carboxylase deficiency.

creatinine, it became clear that propionyl CoA carboxylase in the patient was also deficient.

It was later proven with this patient's cultured skin fibroblasts that 3-methylcrotonyl CoA carboxylase and propionyl CoA carboxylase were deficient (76). Sweetman *et al.* (77) and Weyler *et al.* (78) presumed it to be a deficiency of holocarboxylase synthetase (EC 6.3.4.10/11), and Chalmers *et al.* (75) confirmed it by demonstrating a high excretion of lactate in the patient's urine. Multiple carboxylase deficiency was also reported by Saunders *et al.* (79) and Lehnert *et al.* (80).

The case the authors studied (81) was that of a 6-year-old girl who had had severe vomiting, metabolic acidosis, and eruptions around the eyes, mouth, and vulvar mucous membrane since 1 year and 9 months of age. Thereafter, infection caused continuous episodes of lactic acidosis, vomiting, and eruption. The urinary organic acids at the 12th admission in December, 1982 were analyzed by GC/MS. The most outstanding abnormal peaks (Fig. 7.17) were lactate and 3-hydroxybutyrate, with acetoacetate and 3-methylcrotonylglycine following them. Additionally, 2-hydroxybutyrate, 3-hydroxyisovalerate, 3-hydroxyvalerate, 3-oxovalerate, urea, 2-methyl-3-oxovalerate, adipate, and 4-hydroxyphenylacetate were detected in large amounts.

Several causes of this disease are known: (a) biotin deficiency; (b) deficiency of biotinidase, which acts on utilization and reutilization of biotin; (c) fall of

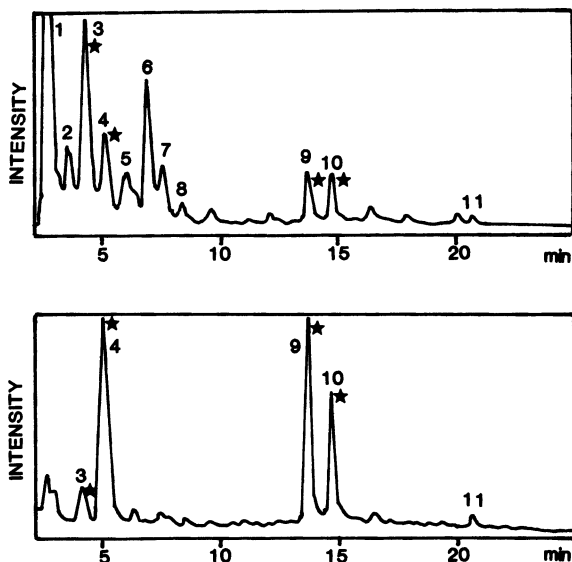


Figure 7.17. Reconstructed ion chromatogram of organic acids in a patient with multiple carboxylase deficiency during a clinical episode (top) and under remission (bottom). 1, lactate; 2, 2-hydroxybutyrate; 3, 3-hydroxybutyrate and 3-hydroxypropionate; 4, 3-hydroxyisovalerate; 5, acetoacetate and 3-hydroxyvalerate; 6, acetoacetate; 7, 3-oxovalerate and urea; 8, 2-methyl-3-oxovalerate; 9, 3-methylcrotonylglycine (2-TMS); 10, 3-methylcrotonylglycine (1-TMS) and 4-hydroxyphenylacetate; 11, heptadecanoate (IS). Star mark indicates the abnormally elevated peaks in the urinary organic acids of the patient with multiple carboxylase deficiency both during a clinical episode and under remission.

holocarboxylase synthetase apoenzyme affinity for biotin; (d) fall of synthetase activity because of abnormal holoenzyme active site; and (e) mutant carboxylase apoenzymes. Cause 3 was improbable, for it seems difficult to accept that all three apoenzymes are defective. As for the first possible cause, the authors' patient did recover following biotin administration, and her urinary organic acid profile was completely normalized. Her biotin concentration and biotinidase activity in serum also were normal. Therefore, she was diagnosed as cause 2, holoenzyme error.

4. PROBLEMS UNDERLYING THE CHEMICAL DIAGNOSIS

As stated above, enzyme deficiencies in the metabolism of aromatic and branched-chain amino acids come in many varieties and are encountered frequently among the inherited metabolic diseases. Irregularities in the mitochondrial electron transport system are also found with relatively high frequency. The

carboxylase apoenzymes require biotin as a cofactor for their activity. Thus, biotinidase deficiency appears as a multiple carboxylase deficiency. Similarly, the primary defect in the transfer of an electron between a common electron-transferring flavoprotein (EFT) and coenzyme Q causes multiple acyl-CoA dehydrogenase deficiencies. These multienzyme deficiencies exhibit very complicated and highly varied clinical features and biochemical characteristics. In addition, as in propionic acidemia or methylmalonic acidemia, profiles can vary greatly depending on pathological conditions and on the age of patients (57,82). Moreover, foods containing medium-chain triglycerides, drugs, alcohol intake, menstrual period, and the patient's living environment may have powerful influence.

Common metabolites are often found elevated in several related diseases and may closely coelute on GC/MS analysis, which makes the analysis more complex and difficult. Diagnosis with only GC can sometimes be very ambiguous, and this test should perhaps be used as only a first screen, with GC/MS for confirmation. Because citric acid cycle compounds are not easily extracted by diethyl ether, ethyl acetate is recommended (83). It is also very important to avoid introduction of contaminants such as phthalates and plasticizers (84).

Although there are many problems, as indicated above, and diagnosis with GC/MS alone is difficult and sometimes insufficient, the number of inherited amino acid and organic acid disorders diagnosable by GC/MS alone is increasing steadily, and it has become possible to diagnose with GC/MS most of the metabolic disorders of the aromatic, branched-chain, and many other amino acids and their acidic metabolites. The determination of enzymatic activity is most reliable for the diseases that are hard to diagnose with only GC/MS. Often, enzyme assay using substrates labeled with radioisotopes is essential because of the small quantity of biopsy samples.

5. CONCLUSION

Advanced GC/MS methodology made the rapid, precise, and differential chemical diagnosis of inherited aromatic and branched-chain amino acid and organic acid disorders possible. Furthermore, inherited multienzyme deficiencies, such as glutaric aciduria type II and multiple carboxylase deficiencies, can also be diagnosed by GC/MS.

ACKNOWLEDGMENTS. The authors are indebted to Dr. Orval A. Mamer, Professor of McGill University, for valuable comments and discussion. We also thank Drs. Toshihiro Shinka, Yoshito Inoue, and Masahiro Matsumoto for their assistance in the preparation of this manuscript.

REFERENCES

1. McKusick, V. A., 1990, A guide to use of MIMC Mendelian inheritance in man, in: *Mendelian Inheritance in Man*, 9th ed., The Johns Hopkins University Press, Baltimore, p. xiii.
2. Tanaka, K., Budd, M. A., Efron, M. L., and Isselbacher, K. J., 1966, Isovaleric acidemia. A new genetic defect of leucine metabolism, *Proc. Natl. Acad. Sci. U.S.A.* **56**:236–242.
3. Jellum, E. J., 1977, Profiling of human body fluids in healthy and diseased states using gas chromatography and mass spectrometry, with special reference to organic acids, *J. Chromatogr.* **143**:427–462.
4. Goodman, S. I., and Markey, S. P., 1981, *Diagnosis of Organic Acidemias by Gas Chromatography–Mass Spectrometry*, Alan R. Liss, New York.
5. Chalmers, R. A., and Lawson, A. M., 1982, *Organic Acids in Man*, Chapman and Hall, London.
6. Matsumoto, I., and Kuhara, T., 1987, Gas chromatography–mass spectrometry for chemical diagnosis of the inherited metabolic diseases—differential chemical diagnosis of lactic acidosis, *Mass Spectrom. Rev.* **6**:77–134.
7. Chalmers, R. A., and Watts, R. W. E., 1972, The quantitative extraction and gas–liquid chromatographic determination of organic acids in urine, *Analyst* **97**:958–967.
8. Matsumoto, I., Kuhara, T., Tetsuo, M., Yoshino, M., Ito, M., Takahira, H., and Hara, K., 1975, The variations of the lipids in diabetes mellitus patients. Detection of ethylstearate and ethylpalmitate in the serum of diabetic patients, *J. Kurume Med. Assoc.* **38**:479–486.
9. Auerbach, V. H., DiGeorge, A. M., and Carpenter, G. G., 1967, Phenylalaninemia: A study of the diversity of disorders which produce elevation of blood concentrations of phenylalanine, in: *Amino Acid Metabolism and Genetic Variation* (W. L. Nyhan, ed.), McGraw-Hill, New York, pp. 11–68.
10. Smith, I., Clayton, B. E., and Wolf, O. H., 1975, New variant of phenylketonuria with progressive neurological illness unresponsive to phenylalanine restriction, *Lancet* **1**:1108–1111.
11. Buist, N., 1967, Phenylketonuria and related problems, in: *Amino Acid Metabolism and Genetic Variation* (W. L. Nyhan, ed.), McGraw-Hill, New York, p. 117.
12. Fellman, J. H., Vanbellinghen, P. J., Jones, R. T., and Koler, R. D., 1969, Soluble and mitochondrial forms of tyrosine aminotransferase: Relationship to human tyrosinemia, *Biochemistry* **8**:615–622.
13. Lindbladt, B., Lindstedt, S., and Steen, G., 1977, On the enzymatic defects in hereditary tyrosinemia, *Proc. Natl. Acad. Sci. U.S.A.* **74**:4641–4645.
14. Endo, F., Kitano, A., Uehara, I., Nagata, N., Matsuda, I., Shinka, T., Kuhara, T., and Matsumoto, I., 1983, Four-hydroxyphenylpyruvic acid oxidase deficiency with normal fumarylacetoacetase: A new variant form of hereditary hypertyrosinemia, *Pediatr. Res.* **17**:92–96.
15. Garrod, A. E., 1902, The incidence of alkaptonuria: A study in chemical individuality, *Lancet* **2**:1616–1620.
16. Dancis, J., Hutzler, J., Tada, K., Wada, Y., Morikawa, T., and Arakawa, T., 1964, Hypervalinemia: A defect in valine transamination, *Pediatrics* **39**:813–472.
17. Haworth, J. C., Perry, T. L., Blass, J. P., Hansen, S., and Urquhart, N., 1976, Lactic acidosis in 3 sibs due to defect in both pyruvate dehydrogenase and alpha-ketoglutarate dehydrogenase complexes, *Pediatrics* **58**:564–572.
18. Robinson, B. H., Taylor, J., and Sherwood, W. G., 1977, Deficiency of dihydrolipoyl dehydrogenase (a component of the pyruvate and α -ketoglutarate dehydrogenase complexes): A cause of congenital chronic lactic acidosis in infancy, *Pediatr. Res.* **11**:1198–1202.
19. Robinson, B. H., Taylor, J., Kahler, S. G., and Kirkman, H. N., 1981, Lactic acidemia,

- neurological deterioration and carbohydrate dependence in a girl with dihydrolipoyl dehydrogenase deficiency, *Eur. J. Pediatr.* **136**:35–39.
20. Snyderman, S. E., Norton, P. M., Roitman, E., and Holt, L. E., 1964, Maple syrup urine diseases, with particular reference to dietotherapy, *Pediatrics* **34**:454–472.
 21. Dancis, J., and Levitz, M., 1978, Abnormalities of branched-chain amino acid metabolism, in: *The Metabolic Basis of Inherited Disease* (J. B. Stanbury, J. B. Wyngarden, and D. S. Fredrickson, eds.), McGraw-Hill, New York, pp. 397–410.
 22. Kuhara, T., Shinka, T., Inoue, Y., Matsumoto, M., Yoshino, M., Sakaguchi, Y., and Matsumoto, I., 1983, Studies of urinary organic acid profiles of a patient with dihydrolipoyl dehydrogenase deficiency, *Clin. Chim. Acta* **133**:133–140.
 23. Taylor, J., Robinson, B. H., and Sherwood, W. G., 1978, A defect in branched-chain amino acid metabolism in a patient with congenital lactic acidosis due to dihydrolipoyl dehydrogenase deficiency, *Pediatr. Res.* **12**:60–62.
 24. Sakaguchi, Y., Yoshino, M., Aramaki, S., Yoshida, I., Yamashira, F., Kuhara, T., Matsumoto, I., and Hayashi, T., 1986, Dihydrolipoyl dehydrogenase deficiency: A therapeutic trial with branched-chain amino acid restriction, *Eur. J. Pediatr.* **145**:271–274.
 25. Kuhara, T., Inoue, Y., Shinka, T., Matsumoto, M., Matsumoto, I., Yoshino, M., and Okada, S., 1984, Chemical diagnosis of dihydrolipoyl dehydrogenase deficiency, *J. Inher. Metab. Dis. [Suppl.]* **2**(7):115–116.
 26. Stromme, J. H., Borud, O., and Moe, P. J., 1976, Fatal lactic acidosis in a newborn attributable to a congenital defect of pyruvate dehydrogenase, *Pediatr. Res.* **10**:62–66.
 27. Rhead, W. J., and Tanaka, K., 1980, Demonstration of a specific mitochondrial isovaleryl-CoA dehydrogenase deficiency in fibroblasts from patients with isovaleric acidemia, *Proc. Natl. Acad. Sci. U.S.A.* **77**:580–583.
 28. Tanaka, K., Orr, J. C., and Isselbacher, K. J., 1968, Identification of β -hydroxyisovaleric acid in the urine of a patient with isovaleric acidemia, *Biochim. Biophys. Acta* **152**:638–641.
 29. Gregersen, N., Keiding, K., and Kolvraa, S., 1979, N-Acylglycines: Gas chromatographic mass spectrometric identification and determination in urine by selected ion monitoring, *Biomed. Mass Spectrom.* **6**:439–443.
 30. Ando, T., and Nyhan, W. L., 1970, A simple method for detecting isovalerylglycine in urine of patients with isovaleric acidemia, *Clin. Chem.* **16**:420–422.
 31. Ramsdell, H. S., and Tanaka, K., 1977, Gas chromatographic studies of twenty metabolically important acylglycines, *Clin. Chim. Acta* **74**:109–114.
 32. Ramsdell, H. S., Baretz, B. H., and Tanaka, K., 1977, Mass spectrometric studies of twenty-one metabolically important acylglycines, *Biomed. Mass Spectrom.* **4**:220–225.
 33. Daum, R. S., Lamm, P. H., Mamer, O. A., and Scriver, C. R., 1971, A “new” disorder of isoleucine catabolism, *Lancet* **2**:1289–1290.
 34. Daum, R. S., Scriver, C. R., Mamer, O. A., Delvin, E., Lamm, P., and Goldman, H., 1973, An inherited disorder of isoleucine catabolism causing accumulation of α -methylacetoacetate and α -methyl- β -hydroxybutyrate, and intermittent metabolic acidosis, *Pediatr. Res.* **7**:149–160.
 35. Mamer, O. A., and Tjoa, S. S., 1974, 2-Ethylhydracrylic acid: A newly described urinary organic acid, *Clin. Chim. Acta* **55**:199–204.
 36. Mamer, O. A., Tjoa, S. S., Scriver, C. R., and Klassen, G. A., 1976, Demonstration of a new mammalian isoleucine catabolic pathway yielding an R series of metabolites, *Biochem. J.* **160**:417–426.
 37. Hiyama, K., Sakura, N., Matsumoto, T., and Kuhara, T., 1986, Deficient β -ketothiolase activity in leucocytes from a patient with 2-methylacetoacetic aciduria, *Clin. Chim. Acta* **155**:189–194.
 38. Eldjarn, L., Jellum, E., Stokke, O., Pande, H., and Waaler, P. E., 1970, β -hydroxyisovaleric acidemia and β -methylcrotonylglycinuria: A new inborn error of metabolism, *Lancet* **2**:521–522.

39. Bartlett, K., Bennett, M. J., Hill, R. P., Lashford, L. S., Pollit, R. J., and Worth, H. G. J., 1984, Isolated biotin-resistant 3-methylcrotonyl CoA carboxylase deficiency presenting with life-threatening hypoglycemia, *J. Inher. Metab. Dis.* **7**:182.
40. Kuhara, T., Matsumoto, I., Saiki, K., Takabayashi, H., and Kuwabara, S., in press, 3-Methylglutaconic aciduria in two adults, *Clin. Chim. Acta*.
41. Hommes, F. A., Kuipers, J. R. G., Elema, J. D., Jansen, J. F., and Jonxis, J. H. P., 1968, Propionicacidemia, a new inborn error of metabolism, *Pediatr. Res.* **2**:519–524.
42. Hsia, Y. E., Scully, K. J., and Rosenberg, L. E., 1969, Defective propionate carboxylation in ketotic hyperglycinemia, *Lancet* **1**:757–758.
43. Hsia, Y. E., Scully, K. J., and Rosenberg, L. E., 1971, Inherited propionyl CoA carboxylase deficiency in ketotic hyperglycinemia, *J. Clin. Invest.* **50**:127–130.
44. Ando, T., Rasmussen, K., Nyhan, W. L., and Hull, D., 1972, 3-Hydroxypropionate: Significance of β -oxidation of propionate in patient with propionic acidemia and methylmalonic acidemia, *Proc. Natl. Acad. Sci., U.S.A.* **69**:2807–2811.
45. Rasmussen, K., Ando, T., Nyhan, W. L., Hull, D., Cotton, D., Kilroy, A. W., and Wadlington, W., 1972, Excretion of tiglylglycine in propionic acidemia, *J. Pediatr.* **81**:970–972.
46. Ando, T., Rasmussen, K., Wright, J. M., and Nyhan, W. L., 1972, Isolation and identification of methylcitrate, a major metabolic product of propionate in a patient with propionic acidemia, *J. Biol. Chem.* **247**:2200–2204.
47. Stokke, O., Jellum, E., Eldjarn, L., and Schnitler, R., 1973, The occurrence of β -hydroxy-n-valeric acid in a patient with propionic and methylmalonic acidemia, *Clin. Chim. Acta* **45**:391–401.
48. Matsumoto, I., Shinka, T., Kuhara, T., Oura, T., Yamamoto, H., Hase, Y., Aoki, H., Isshiki, G., and Tada, K., 1978, Investigation of unusual metabolites in the urine of a patient with propionic acidemia, in: *Recent Developments in Mass Spectrometry in Biochemistry and Medicine*, Vol. 1 (A. Frigerio, ed.), Plenum Press, New York, pp. 203–216.
49. Truscott, R. J. W., Pullin, C. J., Halpern, B., Hammond, J., Haan, E., and Danks, D. M., 1979, The identification of 3-keto-2-methylvaleric acid and 3-hydroxy-2-methylvaleric acid in a patient with propionic acidemia, *Biomed. Mass Spectrom.* **6**:294–300.
50. Kuhara, T., Inoue, Y., Shinka, T., Matsumoto, I., and Matsumoto, M., 1983, Identification of 3-hydroxy-3-ethylglutaric acid in urine of patients with propionic acidemia, *Biomed. Mass Spectrom.* **10**:629–632.
51. Pollitt, R. J., 1983, The occurrence of substituted 3-methyl-3-hydroxyglutaric acids in urine in propionic acidemia and in β -ketothiolase deficiency, *Biomed. Mass Spectrom.* **10**:253–257.
52. Sweetman, L., Weyler, W., Nyhan, W. L., Cespedes, C., Loria, A. R., and Estrada, Y., 1978, Abnormal metabolites of isoleucine in a patient with propionyl-CoA carboxylase deficiency, *Biomed. Mass Spectrom.* **5**:198–207.
53. Duran, M., Bruinvis, L., Ketting, D., Kamerling, J. P., Wadman, S. K., and Schutgens, R. B. H., 1982, The identification of (*E*)-2-methylglutaconic acid, a new isoleucine metabolite, in the urine of patients with β -ketothiolase deficiency, propionic acidemia and methylmalonic acidemia, *Biomed. Mass Spectrom.* **9**:1–5.
54. Donato, S. D., Rimoldi, M., Garavaglia, B., and Uziel, G., 1984, Propionylcarnitine excretion in propionic and methylmalonic acidurias: A cause of carnitine deficiency, *Clin. Chim. Acta* **139**:13–21.
55. Greter, J., Lindstedt, S., Seeman, H., and Steen, G., 1980, 2-Hydroxy-2-methylsuccinic acid—a urinary metabolite in propionyl CoA carboxylase deficiency, *Clin. Chim. Acta* **106**:103–106.
56. Jakobs, C., Dorland, L., Sweetman, L., Duran, M., Nyhan, W. L., and Wadman, S. K., 1984, Identification of methyl-branched chain dicarboxylic acids in amniotic fluid and urine in propionic and methylmalonic acidemia, *Pediatr. Res.* **18**:1185–1191.

57. Kuhara, T., Shinka, T., Matsuo, M., and Matsumoto, I., 1982, Increased excretion of lactate, glutarate, 3-hydroxyisovalerate and 3-methylglutaconate during clinical episodes of propionic acidemia, *Clin. Chim. Acta* **123**:101–109.
58. Wolf, B., Paulsen, E. P., and Hsia, Y. E., 1979, Asymptomatic propionyl CoA carboxylase deficiency in a 13-year-old girl, *J. Pediatr.* **95**:563–565.
59. Hillman, R. E., Keating, J. P., and Williams, J. C., 1978, Biotin-responsive propionic acidemia presenting as the rumination syndrome, *J. Pediatr.* **92**:439–441.
60. Duran, M., Gompertz, D., Bruinvis, L., Ketting, D., and Wadman, S. K., 1978, The variability of metabolite excretion in propionic acidemia, *Clin. Chim. Acta* **82**:93–99.
61. Oberholzer, V. G., Levin, B., Burgess, E. A., and Young, W. F., 1967, Methylmalonic aciduria. A new inborn error of metabolism leading to chronic metabolic acidosis, *Arch. Dis. Child.* **42**:492–504.
62. Stokke, O., Eldjarn, L., Norum, K. R., Steen-Johnsen, J., and Halvorsen, S., 1967, Methylmalonic acidemia. A new inborn error of metabolism which may cause fatal acidosis in the neonatal period, *Scand. J. Clin. Lab. Invest.* **20**:313–328.
63. Rosenberg, L. E., Lilljeqvist, A. C., Hsia, Y. E., and Rosenbloom, F. M., 1969, Vitamin B₁₂ dependent methylmalonic aciduria. Defective metabolism in cultured fibroblast, *Biochem. Biophys. Res. Commun.* **37**:607–614.
64. Mahoney, M. J., Rosenberg, L. E., Mudd, S. H., and Uhelendorf, B. W., 1971, Defective metabolism of vitamin B₁₂ in fibroblast from children with methylmalonic aciduria, *Biochem. Biophys. Res. Commun.* **44**:375–381.
65. Inoue, Y., Kuhara, T., Shinka, T., Matsumoto, M., Matsumoto, A., Matsumoto, I., Mizuno, T., and Itagaki, Y., 1982, Application of gas chromatography–mass spectrometry–computer for the diagnosis of methylmalonic acidemia, *Proc. Jpn. Soc. Med. Mass Spectrom.* **7**:211–214.
66. Matsumoto, I., 1984, Novel application of mass spectrometry for the diagnosis of inherited metabolic diseases, *Mass Spectros.* **32**:79–96.
67. Matsui, S. M., Mahoney, M. J., and Rosenberg, L. E., 1983, The natural history of the inherited methylmalonic acidemias, *N. Engl. J. Med.* **308**:857–861.
68. Przyremble, H., Wendel, U., Becker, K., Bremer, H. J., Bruinvis, L., Ketting, D., and Wadman, S. K., 1976, Glutaric aciduria type II: Report on a previously undescribed metabolic disorder, *Clin. Chim. Acta* **66**:227–239.
69. Niederweizer, A., Steinmann, B., Exner, U., Neuheiser, F., Redweik, U., Wang, M., Rampini, S., and Wendel, U., 1983, Multiple acyl-CoA dehydrogenation deficiency (MADD) in a boy with nonketotic hypoglycemia, hepatomegaly, muscle hypotonia and cardiomyopathy, *Helv. Paediatr. Acta* **38**:9–26.
70. Sweetman, L., Nyhan, W. L., Trauner, D. A., Merritt, T. A., and Singh, M., 1980, Glutaric aciduria type II, *J. Pediatr.* **96**:1020–1026.
71. Gregersen, N., 1985, Acyl-CoA dehydrogenation disorders, *Scand. J. Clin. Invest.* **45**(Suppl. 174):1–60.
72. Montagos, S., Genel, M., and Tanaka, K., 1979, Ethylmalonic–adipic aciduria: *In vivo* and *in vitro* studies indicating deficiency of activities of multiple acyl-CoA dehydrogenases, *J. Clin. Invest.* **64**:1580–1589.
73. Goodman, S. I., McCabe, E. R. B., Fennessey, P. V., and Mace, J. W., 1980, Multiple acyl-CoA dehydrogenase deficiency (glutaric aciduria type II) with transient hypersarcosinemia and sarcosinuria; possible inherited deficiency of an electron transfer flavoprotein, *Pediatr. Res.* **14**:12–17.
74. Gompertz, D., Draffan, G. H., Watts, J. L., and Hull, D., 1971, Biotin-responsive β -methylcrotonylglycinuria, *Lancet* **2**:22–24.
75. Chalmers, R. A., Lawson, A. M., and Watts, R. W. E., 1974, Studies on the urinary acidic

- metabolites excreted by patients with β -methylcrotonylglycinuria, propionic acidemia and methylmalonic acidemia, using gas-liquid chromatography and mass spectrometry, *Clin. Chim. Acta* **52**:43-51.
76. Bartlett, K., and Gompertz, D., 1976, Combined carboxylase defect: Biotin-responsiveness in cultured fibroblasts, *Lancet* **2**:804.
 77. Sweetman, L., Bates, S. P., Hull, D., and Nyhan, W. L., 1977, Propionyl-CoA carboxylase deficiency in a patient with biotin-responsive 3-methylcrotonylglycinuria, *Pediatr. Res.* **11**:1144-1147.
 78. Weyler, W., Sweetman, L., Maggio, D. C., and Nyhan, W. L., 1977, Deficiency of propionyl-CoA carboxylase and methylmalonyl-CoA carboxylase in a patient with methylcrotonylglycinuria, *Clin. Chim. Acta* **76**:321-328.
 79. Saunders, M., Sweetman, L., Robinson, B., Roth, K., Cohn, R., and Gravel, R. A., 1979, Biotin responsive organic aciduria. Multiple carboxylase defects and complementation studies with propionic acidemia in cultured fibroblasts, *J. Clin. Invest.* **64**:1695-1702.
 80. Lehnert, W., Niederhoff, H., Junker, A., Saule, H., and Frasch, W., 1979, A case of biotin-responsive 3-methylcrotonylglycine- and 3-hydroxyisovaleric aciduria, *Eur. J. Pediatr.* **132**:107-114.
 81. Shinka, T., Kuhara, T., Inoue, Y., Matsumoto, I., Tanaka, S., Nagao, M., and Hiromitsu, S., 1982, Gas chromatography-mass spectrometric analysis of urinary organic acids in a patient with multiple carboxylase deficiency presenting with huge lactic aciduria, *Proc. Jpn. Soc. Med. Mass Spectrom.* **7**:207-210.
 82. Jakobs, C., Sweetman, L., Wadman, S. K., Duran, M., Saudubray, J. M., and Nyhan, W. L., 1984, Prenatal diagnosis of glutaric aciduria Type II by direct chemical analysis of dicarboxylic acids in amniotic fluid, *Eur. J. Pediatr.* **141**:153-157.
 83. Sengers, R. C. A., Stadhouders, A. M., and Trijbels, J. M. F., 1984, Mitochondrial myopathies: Clinical, morphological and biochemical aspects, *Eur. J. Pediatr.* **141**:192-207.
 84. Ende, M., and Spitteller, G., 1982, Contaminants in mass spectrometry, *Mass Spectrom. Rev.* **1**:29-62.

Carnitine and Acylcarnitines in Metabolic Disease Diagnosis and Management

David S. Millington and Donald H. Chace

1. INTRODUCTION AND BACKGROUND

The biochemical functions of carnitine are reviewed, especially as they apply to metabolic disease states. Although mass spectrometry has played a major role in the biochemical assessment of L-carnitine therapy, those details are considered beyond the scope of this chapter; however, a brief outline is given here.

1.1. Biochemical Role of Carnitine

L-Carnitine (3-hydroxy-4-aminobutyrobetaine) plays a vital role in the mitochondrial β -oxidation of fatty acids by acting as a transporter of acyl groups across mitochondrial membranes (1). The essential components in the intramitochondrial β -oxidation system are depicted in Fig. 8.1 (2). Free fatty acids are activated in the cytosol to the coenzyme A thioesters (acyl CoA) and conjugated with carnitine by the long-chain carnitine acyltransferase, also known as carnitine palmitoyl transferase (CPT). This enzyme is located on the inner surfaces of the outer and inner mitochondrial membranes and for distinction is labelled CPT-I and CPT-II, respectively. A tranlocase enables the acylcarnitines to cross the inner membrane, where CPT-II reforms the acyl-CoA and regenerates carnitine. Successive cycles of β -oxidation are carried out by a closely

David S. Millington and Donald H. Chace • Division of Genetics and Metabolism, Department of Pediatrics, Duke University Medical Center, Durham, North Carolina 27710.

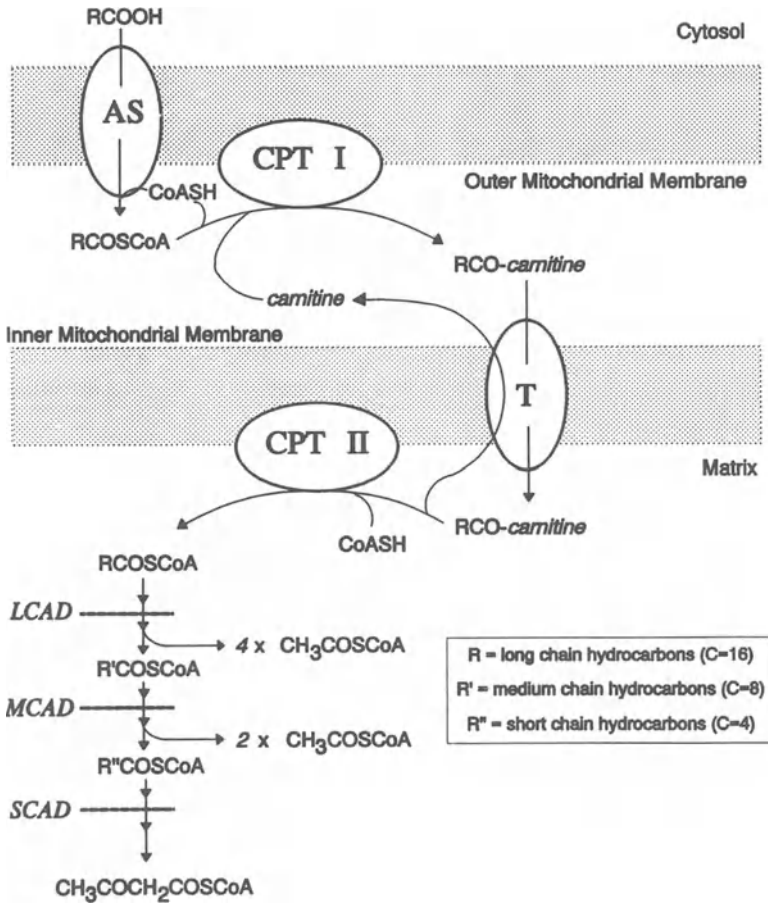


Figure 8.1. System of enzymes involved in the transport and β -oxidation of fatty acids in the mitochondrion. Abbreviations: AS, acyl CoA synthetase; CPT, carnitine palmitoyl transferase; T, acylcarnitine translocase; LCAD, MCAD, SCAD, long-, medium-, and short-chain acyl CoA dehydrogenase, respectively.

coupled system of enzyme complexes, of which the acyl CoA dehydrogenases are essential components. Three systems exist with overlapping chain-length specificities—long-chain (LCAD), medium-chain (MCAD), and short-chain (SCAD)—whose preferred substrates are palmitoyl CoA, octanoyl CoA, and butyryl CoA, respectively. One of the major products of β -oxidation, acetyl-coA, is transported out of the mitochondrion as a carnitine conjugate formed by the enzyme carnitine acetyltransferase (CAT).

Defects have been identified and characterized in many of these enzymes,

including CPT-II (3). In disorders of fatty acid and branched-chain amino acid catabolism affecting the mitochondrial enzymes, the potential exists for accumulation of abnormal acyl CoA intermediates. These compounds can exhibit toxicity by inhibiting other essential enzymes; they also sequester the limited pool of coenzyme A in the mitochondrion. Carnitine plays an important role in the transport of these undesirable intermediates out of the mitochondrion using the carnitine acyltransferases. The ratio of "bound" carnitine (acylcarnitine) to free carnitine in plasma reflects the acyl CoA to free CoASH ratio, and the ratio is usually elevated in patients with this type of metabolic disorder (4). The secondary biochemical role of carnitine is therefore one of detoxification, which applies when there is an accumulation of abnormal acyl CoA.

1.2. Carnitine Deficiency

L-Carnitine is biosynthesized from protein-bound lysine residues and stored mostly in muscle tissue (5). The major dietary sources are meat and dairy products. Normal plasma concentrations of carnitine are relatively stable at 46 ± 10 nmol/ml, of which about 15% is O-acylated, mostly as acetylcarnitine (4). The plasma free carnitine concentration is thought to reflect the tissue level and is considered abnormally low when its value is less than about 20 nmol/ml. Carnitine deficiency can cause myopathy, hypotonia, hypoglycemia, and other symptoms (6). A condition known as "primary" carnitine deficiency has been described (6,7), the mechanism of which is unknown. In inherited disorders of fatty acids and branched-chain amino acid catabolism involving mitochondrial enzyme defects, carnitine deficiency can develop "secondary" to the main defect, again by mechanisms not fully understood (4). Secondary carnitine deficiency can also result from long-term parenteral nutrition (8) and from the prolonged use of valproic acid for control of seizures (9).

1.3. Carnitine Therapy

Carnitine deficiency is corrected or alleviated by dietary supplementation with L-carnitine, aimed at restoration of normal plasma free carnitine concentration (10). In the metabolic disorders, carnitine therapy has an additional role, namely, the removal of cytotoxic acyl CoA intermediates by conjugation and excretion as acylcarnitines (11,12). Restoration of the free carnitine-to-acylcarnitine ratio toward normal is the goal in this case and usually requires higher doses of carnitine. The effectiveness of carnitine replacement therapy can be judged from the reversal of symptoms associated with carnitine deficiency and reduced incidence of metabolic decompensation. Once correctly diagnosed and treated, the prognosis for most affected patients is greatly improved. The efficacy and safety of L-carnitine supplementation have been investigated by research

studies using high-dose intravenous carnitine (12) and stable-isotope-labeled carnitine (13). Mass spectrometry (MS) has been used extensively in these studies, both to assess the fate of the labeled carnitine (13) and to measure the concentrations of important metabolites. These studies have shown that exogenous carnitine exchanges rapidly with the mitochondrial pool of carnitine and acylcarnitine and that although the excretion of abnormal acylcarnitines increases with the dose, there was no evidence for enhanced turnover of fatty acids or other toxic effect (12). Intravenous carnitine is useful in the treatment of acute episodes of metabolic decompensation, and oral maintenance doses reduce the frequency and the severity of episodes (12,14). Carnitine is now widely used as an adjunct to dietary therapy for the long-term management of patients with metabolic disorders.

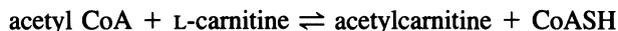
1.4. Role of Mass Spectrometry

Until the application of fast atom bombardment mass spectrometry (FAB-MS) in 1984 (15), no specific methods existed for the analysis of intact acylcarnitines. Since then, numerous additional methods have been developed. Some of these methods and their application to acylcarnitine analysis in urine were reviewed in an earlier publication (16). The importance of mass spectrometry in this context is the diagnostic value of identifying the species of acyl groups attached to carnitine, because these species represent the acyl CoA compounds, normal or abnormal, present in mitochondria. This report considers new mass spectrometric methods and alternative methods for carnitine and acylcarnitines reported up to the present time with emphasis on analysis in blood, including the neonatal samples used for biochemical screening tests for inborn errors of metabolism. These samples are in the form of dried blood spots deposited on cards made from a special type of filter paper, known as "PKU" or "Guthrie" cards after their inventor.

2. METHODS FOR THE ANALYSIS OF CARNITINE

2.1. Enzymatic Assays

The most widely used methods for the measurement of carnitine in biological fluids are dependent on the enzyme carnitine acetyltransferase, which catalyzes the reaction:



A popular spectrophotometric assay is based on the reaction of the liberated CoASH with 5,5'-dithiobis-2-nitrobenzoic acid (DTNB), producing the thio-

phenylate ion, which absorbs at 412 nm (17). The assay is repeated after alkaline hydrolysis, enabling the quantification of free and total carnitine and hence the acylcarnitine fraction by difference. An automated version of this procedure has been described (18). The most widely used alternative method is a radioisotopic exchange (REA) assay, which uses [1-¹⁴C]acetyl CoA as the substrate for the enzyme and measures the [1-¹⁴C]acetylcarnitine produced (19). Several modifications of this method have been described (20), but the method remains labor intensive and unsuitable for automation.

2.2. Tandem Mass Spectrometric Assay

A new method recently developed in this laboratory (21) combines the principles of isotope dilution, fast-atom bombardment (FAB) ionization, and tandem mass spectrometry (MS/MS). The method is so specific that it is applied directly to a dried urine sample or to the dried supernatant from a homogenate of plasma with ethanol. The sensitivity of FAB-MS to carnitine is enhanced by esterification of the carboxylic acid function (16), with the *n*-butyl ester being the most sensitive of the *n*-alkyl series (methyl to hexanoyl). The reaction is accomplished using 3 mmol/ml HCl (or BF₃) in dry butanol (50 μl) for 10 min at 65°C, under which conditions the acid-catalyzed hydrolysis of acetylcarnitine is minimal. If the sample is not analyzed immediately, then the solvent is evaporated under nitrogen, and the specimen is redissolved in methanol : glycerol (1 : 1 v/v). This solution can be stored at 4°C for several days without affecting the result. In a triple quadrupole tandem mass spectrometer ($Q_1Q_2Q_3$), the preformed molecular cation (M^+) of the carnitine derivative (I, Fig. 8.2) is released under fast-atom bombardment (FAB). After mass selection by Q_1 and collision-induced dissociation (CID) in Q_2 , the M^+ ion loses the elements of trimethylamine and butene to give the abundant ion (II) at m/z 103 (Fig. 8.2). Further fragmentation produces the ion at m/z 85. The same fragments are produced from the M^+ ion of N-[²H₃-methyl]carnitine butyl ester, whereas the fragmentation of the M^+ ions of O-acylcarnitine butyl esters yields a base peak at m/z 85.

The specificity of the reaction giving m/z 103 is the basis of the assay. Typically, 100 μl urine or blood plasma are used for the assay, to which 20 nmol or 4 nmol N-[²H₃-methyl]carnitine is added as the internal standard, respectively. The urine is simply evaporated under N₂; plasma is deproteinized by addition of ethanol, and the supernatant is evaporated. The residue is derivatized and analyzed by FAB-MS/MS using a scan function that detects the precursors of m/z 103.

To generate the spectra shown in Fig. 8.3, Q_3 was set to transmit only m/z 103 while Q_1 was scanned over the range m/z 210–225 (1 sec/scan). Fifty continuum scans were accumulated into a single raw data file (Fig. 8.3A). After centroiding (Fig. 8.3B), the relative abundances of the m/z 221 and 218 ions

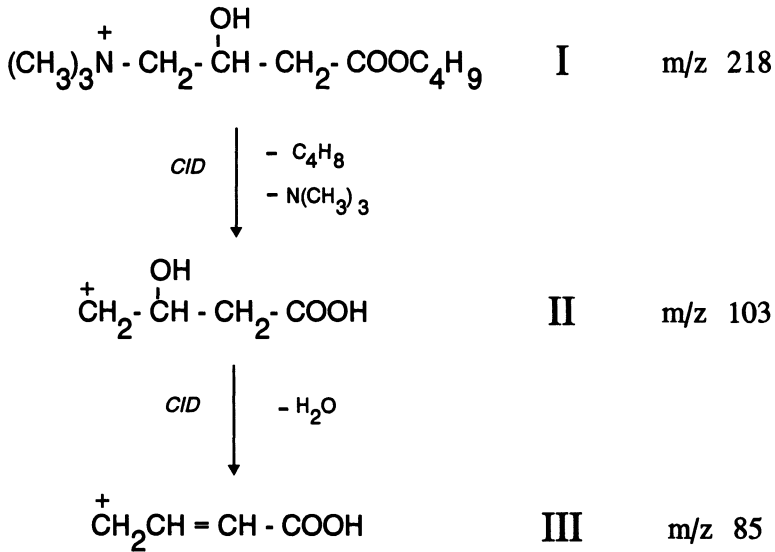


Figure 8.2. Fragmentation of the carnitine butyl ester molecular ion by CID in a triple quadrupole MS. The base peak is m/z 102, and the only other significant fragment is at m/z 85.

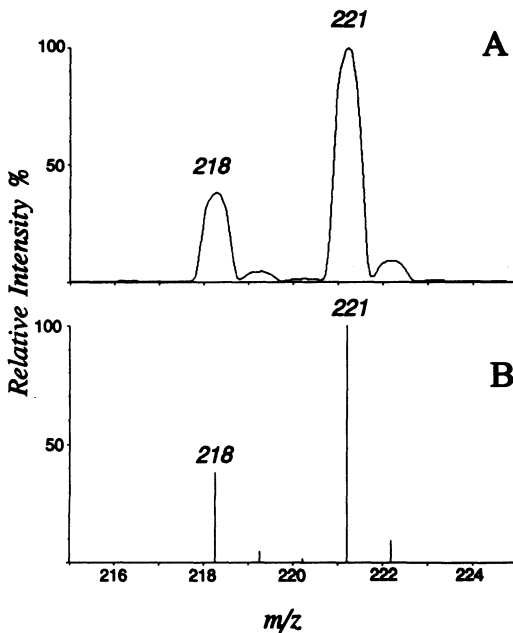


Figure 8.3. Specific detection of carnitine ($M^+ = 218$, endogenous) and N -[$^2\text{H}_3$ -methyl]carnitine ($M^+ = 221$, internal standard) as butyl esters by direct analysis of plasma using the precursors of m/z 103 scan function on a triple quadrupole mass spectrometer. The spectrum is acquired using 50 accumulated continuum spectra (A) then centroided (B) for calculation of the ratio of m/z 218 to 221.

were calculated and related to a standard curve to obtain the carnitine concentration. The analysis takes less than 2 min of instrument time, and in our hands the FAB-MS/MS method is much faster, more reliable, and more accurate than REA (21). When combined with an acylcarnitine profile, the method gives the most complete and accurate diagnostic information.

3. METHODS FOR THE ANALYSIS OF SPECIFIC ACYLCARNITINES

3.1. High-Performance Liquid Chromatographic Methods

Carnitine and its O-acyl derivatives lack a suitable chromophore for analysis by standard UV detectors. Minkler *et al.* (22) developed a reversed-phase HPLC method using 4'-bromophenacyl ester derivatives and have applied it to urine, but interference with ubiquitous organic acids is a major limitation. More successful methods have used enzyme reactions to improve selectivity. Takeyama *et al.* used carnitine acetyltransferase to form CoA derivatives from the corresponding acylcarnitines, which were then detectable by HPLC with UV detection (23). Another approach used the radioisotopic exchange of ^{14}C -labeled carnitine into the acylcarnitines using the same enzyme (24,25). The HPLC analysis was then carried out using a radioactivity detector. These methods are comparatively laborious and suffer from the lack of a specific detector. They also depend on a specific enzyme (CAT), which could give a misleading result unrepresentative of the true acylcarnitine profile. That profile is formed from a mixture of carnitine acyltransferases (20).

The first report of a HPLC-MS method was by Yergey *et al.* (26), who coupled reversed-phase chromatography of the underivatized compounds with thermospray ionization. Quantitative analysis of acylcarnitines using isotope dilution was demonstrated. This method was subsequently applied successfully to urine from patients with several metabolic disorders (27) and was instrumental in the discovery of valproylcarnitine, a novel drug metabolite (28). It was also used to characterize tiglylcarnitine in a patient with β -ketothiolase deficiency (29). This analysis necessitated chromatographic resolution of tiglylcarnitine from 3-methylcrotonylcarnitine, a possible biological isomer.

More recently, the technique of continuous-flow FAB (30) has been employed for LC/MS analysis of acylcarnitines, using microbore fused-silica columns (31,32) and standard analytical columns (33,34). This method has numerous advantages, primarily because of the inherent suitability of acylcarnitines for FAB ionization. Because of the presence of the quaternary ammonium group, acylcarnitines have higher surface activity than most other components of urine or plasma. This activity is further enhanced by esterification of the carboxyl

group (16) and exhibits predominantly molecular ion signals with little or no fragmentation (32,33). The sensitivity of LC-FAB/MS is therefore very high for acylcarnitines, with proven detection limits in the low-picomole range (34).

An example of its application is shown in Fig. 8.4, which compares the reconstructed ion current profiles from the analysis of a mixture of standards (Fig. 8.4A) with the urine of a patient with medium-chain acyl CoA dehydrogen-

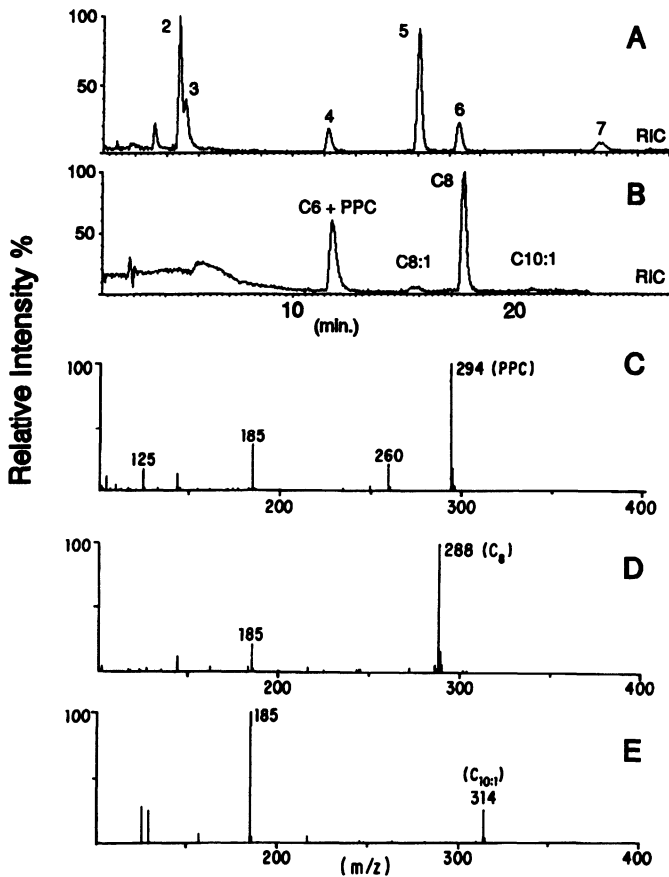


Figure 8.4. Analysis of acylcarnitines by gradient HPLC with continuous-flow FAB. A: Summed reconstructed ion-current profile of a mixture of standards (1, propionyl; 2, isobutyryl; 3, butyryl; 4, hexanoyl; 5, valproyl; 6, octanoyl; 7, decanoyl). B: Analysis of acylcarnitines in urine of patient with MCAD deficiency following a bolus of phenylpropionic acid. C: Mass spectrum of component labeled "C₆ + PPC" (PPC, phenylpropionylcarnitine), showing corresponding [M + H]⁺ ions at *m/z* 260 and 294. D: Mass spectrum of major diagnostic metabolite, octanoylcarnitine (C₈ in chromatogram B). E: Mass spectrum of minor component, *cis*-4-decenoylcarnitine (C_{10:1}).

ase (MCAD) deficiency, a defect of fatty acid oxidation (Fig. 8.4B). Representative mass spectra indicate the presence of an unresolved mixture of two components, plus the major diagnostic metabolite and a minor metabolite (Fig. 8.4C–E). This analysis was performed using a standard HPLC system with a 3.9-mm i.d. analytical column and 1 : 100 ratio stream splitting to provide the flow rate of about 10 μ l/min compatible with the MS. The system was tolerant of the solvent gradient and the 2% glycerol added to the mobile phase to provide the essential FAB matrix (34).

In practice, the resolving power of analytical HPLC columns provides marginal separation of many biological isomers such as *n*-butyryl- and isobutyrylcarnitine and is less able to resolve others such as isovaleryl- and 2-methylbutyrylcarnitine. In such cases, it is necessary to resort to other methods.

3.2. GC/MS Methods

The development of a reliable GC/MS method would enable several more laboratories to perform acylcarnitine analysis. Several methods have been reported, all having limitations. The most widely used method, developed by Roe *et al.* (35), employs alkaline hydrolysis of a purified acylcarnitine fraction and GC/MS analysis of the liberated acids as methyl or trimethylsilyl esters. This method was used to confirm the excretion of glutarylcarnitine in a patient with glutaryl CoA dehydrogenase deficiency (29) and to unequivocally identify the new metabolite, 2-*trans*-4-*cis*-decadienoylcarnitine in a patient subsequently shown to have 2,4-dienoyl-coA reductase deficiency in the liver (36). In this case, the discovery of a new metabolic defect, the first involving the oxidation of an unsaturated precursor, was dependent on the identification of a diagnostic acylcarnitine. This identification is summarized in Fig. 8.5, which shows the detection of the putative acylcarnitine in urine by FAB-MS/MS (A), the GC/MS profile of acids liberated by hydrolysis from the urine acylcarnitines (B), and the GC/MS analysis of the standard 2-*trans*-4-*cis*-decadienoic acid methyl ester (D). The mass spectrum of the target compound (Fig. 8.5C) was identical with that of the standard.

A novel and interesting method was developed by Lowes and Rose (37), involving a base-catalyzed cyclization in which the trimethylamino group is lost, but the acyl groups are retained in the resulting acyloxybutyrolactones, which can be analyzed by GC/MS. Another method has been developed, involving a mild on-column N-demethylation of acylcarnitine propyl esters and their subsequent analysis by GC/CIMS (38). Few applications of these methods have been reported, and there are no reports of the analysis of plasma acylcarnitines. Success with all GC/MS methods is dependent on multiple isotope-labeled internal standards, with the label in the acyl group. The synthesis and characterization of acylcarnitine standards are described briefly below.

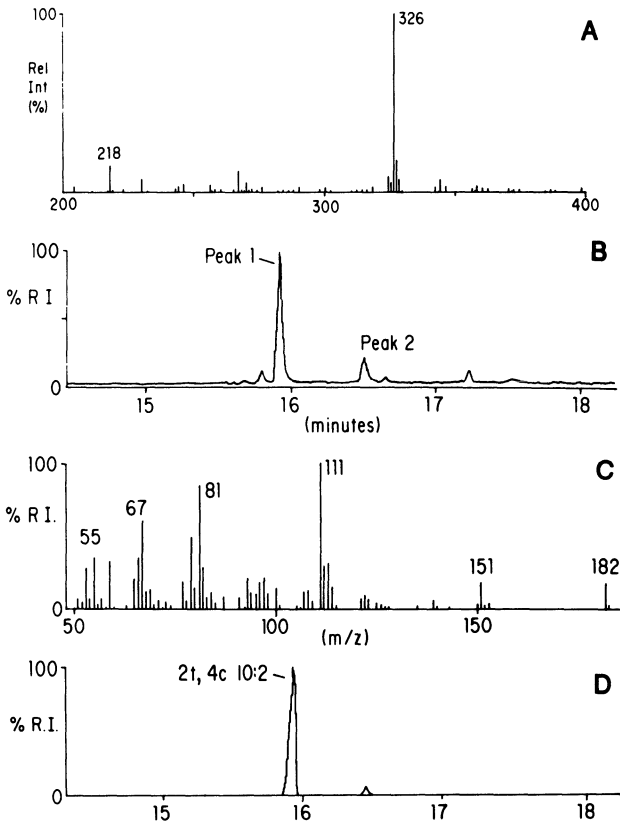


Figure 8.5. Detection and analysis of new diagnostic acylcarnitine in patient with 2,4-dienoyl CoA reductase deficiency. A: Detection of putative $C_{10:2}$ acylcarnitine methyl ester in urine by FAB-MS/MS. B: Partial RIC profile from GC/MS analysis of methylated acids hydrolyzed from acylcarnitines. C: Mass spectrum of peak 1 in chromatogram B. D: Partial GC/MS analysis of standard 2-*trans*-4-*cis*-decadienoic acid.

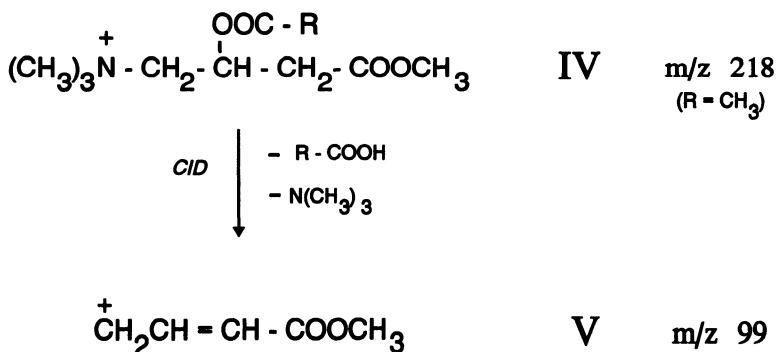
3.3. Tandem Mass Spectrometry Techniques

3.3.1. Review of Methods

The most successful method for the analysis of intact acylcarnitines is FAB-MS/MS. The earliest applications utilized a double-focusing mass spectrometer (15). The putative acylcarnitine $(M + H)^+$ signals detected by FAB-MS were identified by accurate mass (hence elemental composition) determination and by comparing their fragmentation patterns with those of authentic standards by linked-field scans at constant B/E ratio. Sensitivity was later improved by pu-

rification and methylation of the acylcarnitines, enabling characterization of diagnostic acylcarnitines in many metabolic disorders (11,12,15). The detection limit for individual species was, however, only about 50 nmol/ml, which is inadequate for plasma analysis. Furthermore, the procedure of selecting molecular ions for sequential MS/MS analysis requires too much time for routine analysis.

These limitations were effectively removed by development of an improved method using a tandem quadrupole mass spectrometer. In this instrument, all acylcarnitine methyl ester cations exhibit a signal at m/z 99 (usually the base peak) on CID (32). As shown in Fig. 8.6, this ion (V) is derived from the loss of the trimethylamino group and the acyl group from the acylcarnitine (IV). Thus, a precursor ion scan function in which Q_3 of the triple quadrupole transmits ions of m/z 99 while Q_1 is scanned from m/z 200 to 450 generates a "metabolic profile" consisting of the molecular cations of acylcarnitines with little chemical interference. The addition of sodium octylsulfate (1% v/v) to the FAB matrix increased the sensitivity and specificity to the point where acylcarnitines were easily detectable at concentrations below 0.5 nmol/ml in the equivalent of about 5 μ l urine or 2 μ l whole blood (39). The profiles of a normal plasma extract, with and without the presence of the ion-pairing reagent, are compared in Fig. 8.7A,B. The lack of chemical interference in Fig. 8.7B is remarkable considering the minimal sample work-up involved and is an excellent practical application of the ion-pair effect originally described by Ligon (40).



Acetyl	R = -CH ₃	<i>m/z</i> 218
Propionyl	R = -CH ₂ -CH ₃	<i>m/z</i> 232
Octanoyl	R = -(CH ₂) ₆ -CH ₃	<i>m/z</i> 302

Figure 8.6. Fragmentation of acylcarnitine methyl ester cations by CID in a triple quadrupole mass spectrometer, showing the origin of the common fragment at m/z 99.

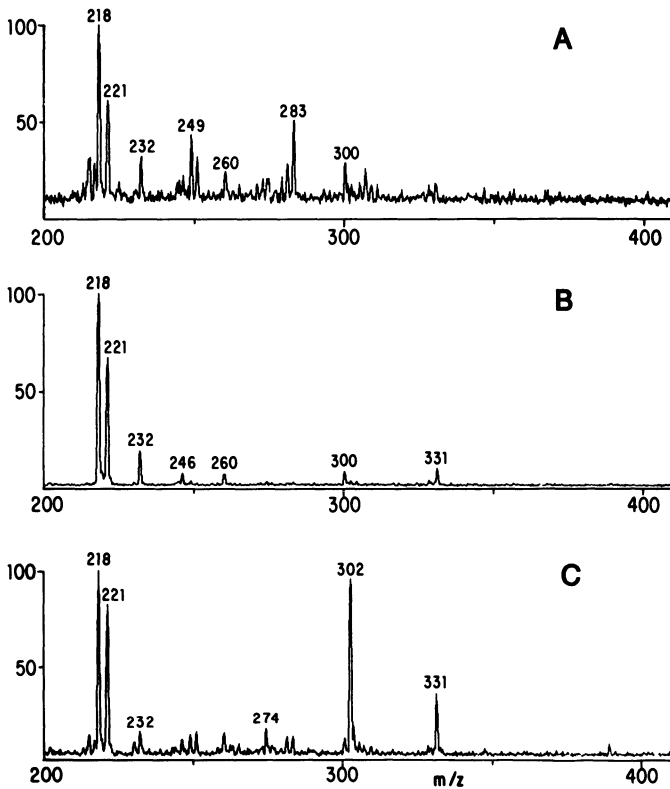


Figure 8.7. Analysis of plasma acylcarnitines by FAB-MS/MS using m/z 99 precursor ion scans. A: Normal plasma after methylation: acetylcarnitine $M^+ = m/z$ 218, internal standard $M^+ = m/z$ 221. Other acylcarnitines detected: C_3 (m/z 232), C_4 (m/z 246), C_5 (m/z 260), $C_{8:1}$ (m/z 300). B: Same analysis after addition of octyl sodium sulfate to FAB matrix, showing increase in absolute sensitivity and in specificity. C: Plasma from patient with MCAD deficiency; major diagnostic metabolite is octanoylcarnitine (m/z 302).

3.3.2. Plasma Acylcarnitine Profiles for Disease Diagnosis

The ability to generate acylcarnitine profiles in blood is a major advance in metabolic disease diagnosis. Figure 8.7C represents the plasma profile from a patient with the MCAD deficiency, the most common defect of fatty acid oxidation. The principal diagnostic metabolite, octanoylcarnitine, is clearly identified. These spectra were acquired as described for free carnitine, but without centroiding. Disease-specific profiles in the branched-chain amino acid disorders are also revealed by FAB-MS/MS analysis of plasma (see Table 8.1). Compared with urine acylcarnitine profiles, the plasma profiles are “cleaner” and much more consistent. When the carnitine flux is low, many unusual acylcarnitines appear in

Table 8.1
Diseases That Can Be Diagnosed by FAB-MS/MS
Analysis of Acylcarnitines in Blood (Confirmed
by Enzyme Assay)

Defects of fatty acid oxidation
Short-chain acyl CoA dehydrogenase deficiency ^a
Medium-chain acyl CoA dehydrogenase deficiency ^b
Long-chain acyl CoA dehydrogenase deficiency ^c
Multiple acyl CoA dehydrogenase deficiency ^c
Hydroxyacyl CoA dehydrogenase deficiency ^d
Carnitine palmitoyl transferase deficiency ^c
2,4-Dienoyl CoA reductase deficiency ^c
Disorders of branched-chain amino acid catabolism
Propionyl CoA carboxylase deficiency ^b
Methylmalonic acidemia (all types) ^c
Isovaleryl CoA dehydrogenase deficiency ^c
Methylcrotonyl CoA carboxylase deficiency ^c
β-Ketothiolase deficiency ^c
Glutaryl CoA dehydrogenase deficiency ^c
3-Hydroxy-3-methylglutaryl CoA lyase deficiency ^c

^aProven in carnitine-treated asymptomatic patient (no other sample available).

^bProven in blood spot on original Guthrie card.

^cProven in asymptomatic, untreated patient.

^dUncertain of child's status at time of sampling.

the urine, including unsaturated monocarboxylic and both saturated and unsaturated dicarboxylic species (11). These metabolites are not associated with any known pathological condition and can mask the signals from diagnostic species, leading to misinterpretation. When the carnitine flux is increased, the unusual nonspecific acylcarnitines tend to disappear, whereas the excretion of disease-specific metabolites actually increases. This phenomenon is the basis of the "carnitine load" test originally developed for diagnosis by FAB-MS/MS analysis of urine (11). Our interpretation is that the interfering metabolites are produced by local metabolism in the kidney. In any event, the availability of the plasma test has now rendered the carnitine load test obsolete.

Although the method is unable to distinguish isomeric acylcarnitines except in instruments capable of high-translational-energy CID (41), the pattern of acylcarnitines in plasma is generally specific and consistent for each metabolic disease (Table 8.1). Of most interest currently is the differential diagnosis of defects of fatty acid oxidation, because several reports have linked them to previously unexplained sudden infant deaths (42,43). The plasma acylcarnitine profiles corresponding to defects of carnitine palmitoyl transferase II, (CPT II) and several acyl CoA dehydrogenase deficiencies [multiple (MAD), medium-

chain (MCAD), long-chain (LCAD), and 3-hydroxyacyl] are compared in Fig. 8.8. These profiles are sufficiently specific to indicate the diagnosis, which would be confirmed by enzyme assay or DNA testing. These defects are difficult to recognize from organic acid profiles, because diagnostic metabolites are elevated only during clinical episodes. For LCAD deficiency and CPT-II deficiency, no specific biological markers occur in the urine. Plasma acylcarnitine analysis is therefore a valuable diagnostic technique, because a result is obtainable in minutes compared with several weeks for enzyme assays requiring cell culture.

Quantitative analysis of the acylcarnitine species is enabled by the addition of isotopically labeled internal standards to the sample before preparation and analysis. The unambiguous assignment of the signals in the MS/MS profiles as acylcarnitine M^+ ions has been confirmed by *in vivo* isotope labeling (13,32).

3.3.3. Comparison with Other Biochemical Tests

Biochemical and enzymatic tests were done on a group of 25 families affected with MCAD deficiency. Analysis of the data showed complete agreement between the PCR-based DNA test, which recognizes the most common mutation in the MCAD cDNA (45,46), and the acylcarnitine profile. The DNA test identifies carriers and homozygotes but cannot distinguish between a carrier and a compound heterozygote. The FAB-MS/MS test is positive only for disease positives; therefore, it identifies *all* MCAD-deficient patients. When combined with the DNA test, the MS test identifies the patients with new mutations (compound heterozygotes). The enzyme assay, which was performed on cultured fibroblasts (47), showed several discrepancies with the other tests (44). At the moment, enzyme assays are the accepted “gold standards” for fatty acid defects. The experience with MCAD deficiency suggests that biochemical tests and enzyme assays might be at variance in other disorders, and additional methods must be developed. Currently, DNA tests are the most definitive, when available. We are developing an *in vitro* test that involves incubation of cultured lymphoblasts with isotopically labeled precursors and the identification of labeled accumulated metabolites, including acylcarnitines and acyl CoA intermediates, using mass spectrometry. Since the earlier review of methods for acyl CoA analysis (16), new methods involving FAB with MS/MS and LC/MS have been developed (48,49).

3.3.4. Tandem MS for Neonatal Screening

Recent research in this laboratory has shown that FAB-MS/MS tests are applicable to the neonatal blood spots on the Guthrie (PKU) cards that are used to screen for inborn errors of metabolism (39,50). Current methods for large-scale screening allow for only a few tests, typically four or five, each of them indi-

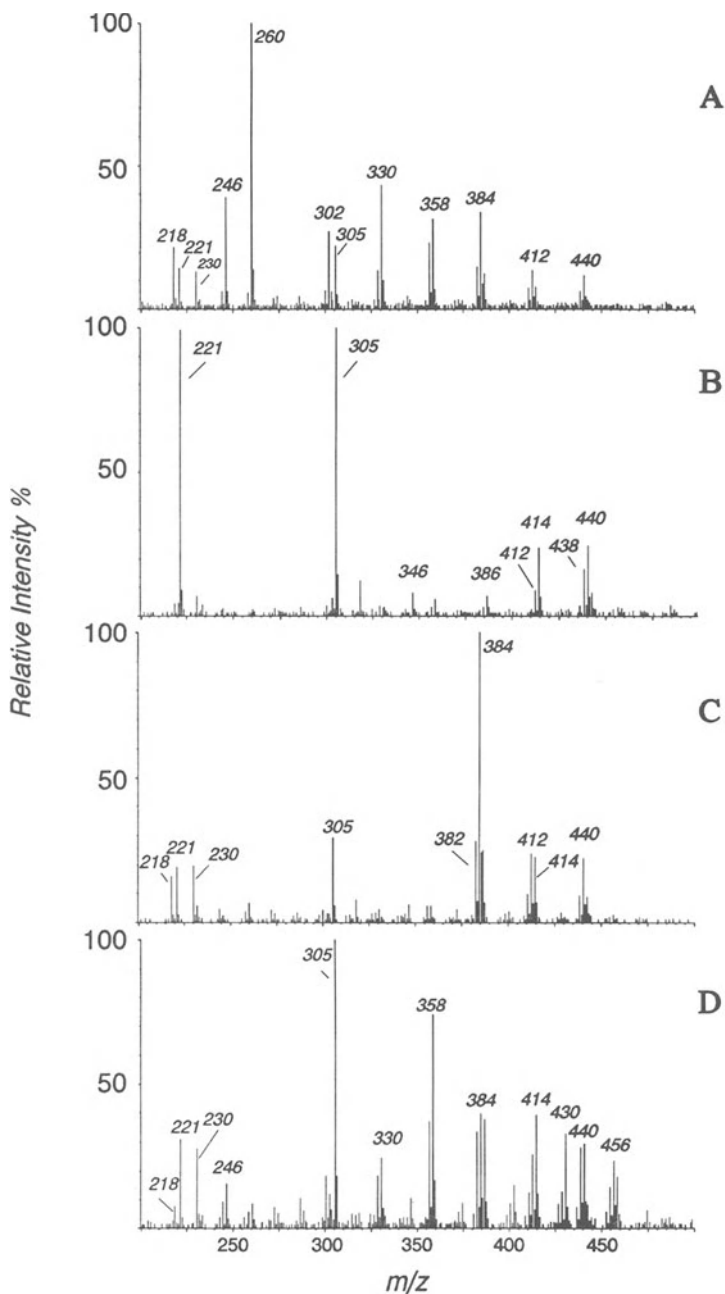


Figure 8.8. Plasma acylcarnitine profiles from patients with enzymatically confirmed defects of fatty acid oxidation. A: Multiple acyl CoA dehydrogenase deficiency, showing prominent C₄, C₅, C₈, C₁₀, C₁₂, C_{14:1}, and C_{16:1}. B: Carnitine palmitoyl transferase II deficiency, showing lack of acetyl and prominent long-chain species (C₁₆, C_{18:1}, C_{18:2}). C: Long-chain acyl CoA dehydrogenase deficiency, showing C_{14:1} as the most prominent species. D: 3-Hydroxyacyl CoA dehydrogenase deficiency, showing medium- and long-chain species, some apparently with hydroxy analogues.

vidualized for one specific metabolic disorder. The FAB-MS/MS generates metabolic profiles, analogous to the profiles generated by GC/MS analysis of groups of metabolites (such as organic acids, steroids, bile acids, and so on). Unlike GC/MS, FAB-MS/MS takes less than 1 min to perform the analysis, and rather than requiring that the different compound classes be separated chromatographically before analysis, FAB-MS/MS allows several different metabolic profiles to be generated from the same sample by applying appropriate scan functions. This concept has already been demonstrated for acylcarnitines and acylglycines in urine and acylcarnitines and amino acids in blood (39). Furthermore, the injection and analysis of samples can readily be automated such that at least 400 samples per day could be analyzed. This analysis would be accomplished using a continuous-flow FAB interface with an autoinjector as described previously (31,32).

Methods for the batched extraction of metabolites and for their derivatization and preparation for analysis by FAB-MS/MS are under development, using support from the State of North Carolina (see Acknowledgments). One of the innovative aspects of this procedure is a nitrogen dryer that uses a forced-air heating system. This device was designed and custom built for this application and is now commercially available (Grey Line Engineering, Silver Spring, MD). The system is designed to work with a batch processor that will perform the preparation of 60 samples for mass spectrometry automatically in less than 2 hr. The objective is to analyze the neonatal blood from all live births in North Carolina (currently about 100,000 per annum). This method will increase the number of diseases being screened to at least 20, when one includes amino acids and acylcarnitines (39), with the potential to add many more as additional metabolic profiles are developed. Thus far, the diagnoses of MCAD deficiency, propionic acidemia, phenylketonuria, tyrosinemia, and maple syrup urine disease have already been confirmed from blood spots on original Guthrie cards (39).

4. SYNTHESIS, CHARACTERIZATION, AND HANDLING OF STANDARDS

Relatively few acylcarnitines are commercially available, and an isotopically labeled form of free carnitine has only recently become available (Cambridge Isotopes, Woburn, MA). Researchers in this field have therefore depended largely on their own resources for the synthesis of standards. Acylcarnitines derived from straightforward monocarboxylic acids are easily synthesized by the method of Bohmer and Bremer (51). After multiple recrystallizations, the acylcarnitines are obtained as their hydrochloride salts. As such, they are extremely hygroscopic and must be kept dry to prevent decomposition and to

facilitate weighing. In our laboratory, samples are dried over P_2O_5 in a vacuum desiccator stored under dry nitrogen in screw-cap vials. The vials are kept in a desiccator over silica gel at $-70^\circ C$. The most effective method of characterizing acylcarnitines is by NMR spectroscopy (15,28), which accurately assesses the amount of free carnitine by integration of the signals for the proton at C-3 or the $N-(CH_3)_3$ signal. The corresponding signals for the free and acylcarnitines are significantly different from each other and are well resolved from other signals at 300 MHz. Except for acetylcarnitine, which is much less stable than other acylcarnitines and should be checked each time the vial is opened, it is advisable to check the NMR of the solids about once every 12 months. Solutions of acylcarnitines should be checked more often for free carnitine content, either using the isotope-dilution FAB-MS/MS method or by spectrophotometric or enzymatic assay.

5. SUMMARY

Mass spectrometry has been making significant contributions to the diagnosis of metabolic diseases for over 20 years. Acylcarnitines are an important group of diagnostic metabolites amenable to FAB-MS. Because of recent developments, FAB-MS/MS analysis of acylcarnitines in very small volumes of whole blood or plasma is now routine. It is the most satisfactory biochemical method for the differential diagnosis of disorders of fatty acid catabolism and recognizes numerous defects of branched-chain amino acid catabolism. The frequency of some of these diseases and their association with sudden unexplained death have generated interest in the development of neonatal screening tests. Such tests offer the best hope of reducing mortality and morbidity associated with metabolic disease through early diagnosis. Tandem mass spectrometry using a modern triple quadrupole mass spectrometer clearly has the potential to perform diagnostic tests using the small volumes of blood collected from newborns for existing screening programs. Compared with existing methods, it is much more versatile and less labor intensive, because most of the steps can be automated. Combined with an amino acid profile, the method will screen up to 20 different diseases. A project has begun at Duke Medical Center to develop this method for the North Carolina newborn population.

An increasing role for mass spectrometry in therapeutic and nutritional research in metabolic and other types of disease is indicated from the studies summarized in this chapter.

ACKNOWLEDGMENTS. Support for this research was provided by grants from the NICHD Division of the National Institutes of Health (Bethesda, MD, No. HD-24908), the State of North Carolina, Division of Maternal and Child Health,

Department of Environmental Health and Natural Resources (Raleigh, NC, No. C-05070), and the General Clinical Research Center Grant (No. M01-RR-30), Division of Research Resources, National Institutes of Health. We also thank Sigma-Tau Pharmaceuticals, Inc. (Gaithersburg, MD) for their generous gift of computer equipment and Fisons-VG Biotech (Altrincham, UK) for the temporary loan of a TRIO-3 tandem quadrupole mass spectrometer.

REFERENCES

1. Fritz, I. B., 1963, Carnitine and its role in fatty acid metabolism, *Adv. Lipid Res.* **1**:285–334.
2. Shulz, H., 1990, Mitochondrial β -oxidation. in: *Fatty Acid Oxidation. Clinical, Biochemical and Molecular Aspects* (K. Tanaka and P. M. Coates, eds.), Alan R. Liss, New York, pp. 23–36.
3. Roe, C. R., and Coates, P. M., 1989, Acyl-CoA dehydrogenase deficiencies. in: *The Metabolic Basis of Inherited Disease, 6th ed.* (E. R. Scriver et al., eds.), McGraw-Hill, New York, pp. 889–914.
4. Chalmers, R. A., Roe, C. R., Stacey, T. E., and Hoppel, C. H., 1984, *Pediatr. Res.* **18**:1325–1328.
5. Bremer, J., 1983, Carnitine—metabolism and functions, *Physiol. Rev.* **63**:1420–1480 (1983).
6. Irias, J. J., 1986, Genetic primary carnitine deficiency? in: *Clinical Aspects of Human Carnitine Deficiency* (P. R. Borum, ed.), Pergamon Press, New York, pp. 108–119.
7. Rebouche, C. J., and Engel, A. G., 1981, Primary systemic carnitine deficiency. I. Carnitine biosynthesis, *Neurology* **31**:813–818.
8. Helms, R. A., 1986, Possible carnitine deficiency in the neonate. in: *Clinical Aspects of Human Carnitine Deficiency* (P. R. Borum, ed.), Pergamon Press, New York, pp. 80–96.
9. Ohtani, Y., Fumino, E., and Matsuda, I., 1982, Carnitine deficiency and hyperammonemia associated with valproic acid therapy, *J. Pediatr.* **101**:782–785.
10. Novak, M., 1986, Carnitine supplementation in secondary carnitine deficiency. in: *Clinical Aspects of Human Carnitine Deficiency* (P. R. Borum, ed.), Pergamon Press, New York, pp. 216–226.
11. Roe, C. R., Millington, D. S., and Maltby, D. A., 1986, Diagnostic and therapeutic implications of acylcarnitine profiling in organic acidurias associated with carnitine deficiency. in: *Clinical Aspects of Human Carnitine Deficiency* (P. R. Borum, ed.), pp. 97–107, Pergamon Press, New York.
12. Roe, C. R., Millington, D. S., Kahler, S. G., Kodo, N., and Norwood, D. L., 1990, Carnitine homeostasis in the organic acidurias. in: *Fatty Acid Oxidation: Clinical, Biochemical and Molecular Aspects* (K. Tanaka and P. M. Coates, eds.), Alan R. Liss, New York, pp. 383–402.
13. Millington, D. S., Maltby, D. A., Gale, D. A., and Roe, C. R., 1989, Synthesis and human applications of stable isotope-labelled L-carnitine. in: *Synthesis and Applications of Isotopically Labelled Compounds. 1988.* (T. A. Baillie and J. R. Jones, eds.), Elsevier, Amsterdam, pp. 189–194.
14. Roe, C. R., Millington, D. S., Kahler, S. G., Kodo, N., and Norwood, D. L., 1991, Therapeutic applications of L-carnitine in metabolic disorders. in: *Treatment of Metabolic Diseases* (R. J. Desnick, ed.), Churchill-Livingstone, New York, pp. 69–78.
15. Millington, D. S., Roe, C. R., and Maltby, D. A., Application of high-resolution fast atom bombardment and constant B/E ratio linked scanning to the identification and analysis of acylcarnitines in metabolic disease, *Biomed. Mass Spectrom.* **11**:236–241.

16. Millington, D. S., 1986, New methods for the analysis of acylcarnitines and acyl-coenzyme A compounds. in: *Mass Spectrometry in Biomedical Research* (S. J. Gaskell, ed.), John Wiley & Sons, Chichester, pp. 97–114.
17. Marquis, N. R., and Fritz, I. B., 1964, Enzymological determination of free carnitine concentrations in rat tissues, *J. Lipid Res.* **5**:184–187.
18. Cederblad, G., Harper, P., and Lindgren, K., 1986, Spectrophotometry of carnitine in biological fluids and tissue with a Cobas Bio centrifugal analyzer, *Clin. Chem.* **32**:342–346.
19. Cederblad, G., and Lindstedt, S., 1972, A method for the determination of carnitine in the picomole range, *Clin. Chim. Acta* **37**:235–243.
20. Marzo, A., Cardace, C., Monti, N., Muck, S., and Arrigoni-Martelli, E., 1990, Review: Chromatographic and non-chromatographic assay of L-carnitine family components, *J. Chromatogr.* **527**:247–258.
21. Kodo, N., Millington, D. S., Norwood, D. L., and Roe, C. R., 1989, Quantitative assay of free and total carnitine using tandem mass spectrometry, *Clin. Chim. Acta* **186**:383–390.
22. Minkler, P. E., Ingalls, S. T., and Hoppel, C. L., 1987, Determination of total carnitine in human urine by high performance liquid chromatography, *J. Chromatogr.* **420**:385–393.
23. Takeyama, N., Takagi, D., Adachi, K., and Tanaka, T., 1986, Measurement of free and esterified carnitine in tissue extracts by high performance liquid chromatography, *Anal. Biochem.* **158**:346–354.
24. Kerner, J., and Bieber, L. L., 1983, A radioisotopic exchange method for quantitation of short-chain acid-soluble acylcarnitines, *Anal. Biochem.* **134**:459–466.
25. Schmidt-Sommerfeld, E., Penn, D., Kerner, J., and Bieber, L. L., 1989, Analysis of acylcarnitines in normal human urine with the radioisotopic exchange-high performance liquid chromatography (HPLC) method, *Clin. Chim. Acta* **181**:231–238.
26. Yergey, A. L., Liberato, D. L., and Millington, D. S., 1984, Thermospray liquid chromatography/mass spectrometry for the analysis of L-carnitine and its acyl derivatives, *Anal. Biochem.* **139**:278–283.
27. Liberato, D. J., Millington, D. S., and Yergey, A. L., 1985, Analysis of acylcarnitines in human metabolic disease by thermospray liquid chromatography/mass spectrometry. in: *Mass Spectrometry in the Health and Life Sciences* (A. L. Burlingame and N. Castagnoli, eds.), Elsevier, Amsterdam, pp. 333–348.
28. Millington, D. S., Bohan, T. P., Roe, C. R., Yergey, A. L., and Liberato, D. J., 1985, Valproylcarnitine: A novel drug metabolite identified by fast atom bombardment and thermospray liquid chromatography—mass spectrometry, *Clin. Chim. Acta* **145**:69–75.
29. Millington, D. S., Roe, C. R., and Maltby, D. A., 1987, Characterization of new diagnostic acylcarnitines in patients with β -ketothiolase deficiency and glutaric aciduria type I using mass spectrometry, *Biomed. Environ. Mass Spectrom.* **14**:711–716.
30. Caprioli, R. M., Fan, T., and Cottrell, J. S., 1986, Continuous-flow sample probe for fast atom bombardment mass spectrometry, *Anal. Chem.* **58**:1949–2951.
31. Norwood, D. L., Kodo, N., and Millington, D. S., 1988, Application of continuous-flow liquid chromatography/fast-atom bombardment mass spectrometry to the analysis of diagnostic acylcarnitines in human urine, *Rapid Commun. Mass Spectrom.* **2**:269–272.
32. Millington, D. S., Norwood, D. L., Kodo, N., Roe, C. R., and Inoue, F., 1989, Application of fast atom bombardment with tandem mass spectrometry and liquid chromatography/mass spectrometry to the analysis of acylcarnitines in human urine, blood and tissue, *Anal. Biochem.* **180**:331–339.
33. Norwood, D. L., and Millington, D. S., 1990, Analysis of metabolites of fatty acid oxidation. in: *Continuous-Flow Fast Atom Bombardment Mass Spectrometry* (R. M. Caprioli, ed.), John Wiley & Sons, Chichester, pp. 175–180.

34. Millington, D. S., Norwood, D. L., Kodo, N., Moore, R., Green, M. D., and Berman, J., 1991, Biomedical applications of high-performance liquid chromatography-mass spectrometry with continuous-flow fast atom bombardment, *J. Chromatogr.* **562**:47-58.
35. Roe, C. R., Millington, D. S., Maltby, D. A., Bohan, T. P., Kahler, S. G., and Chalmers, R. A., 1985, Diagnostic and therapeutic implications of medium-chain acylcarnitines in the medium-chain acyl-coA dehydrogenase deficiency, *Pediatr. Res.* **19**:459-466.
36. Roe, C. R., Millington, D. S., Norwood, D. L., Sprecher, H., Mohammed, B. S., Nada, M., Shulz, H., and McVie, R., 1990, 2,4-Dienoyl-coenzyme A reductase deficiency: A possible new disorder of fatty acid oxidation, *J. Clin. Invest.* **85**:1703-1707.
37. Lowes, S., and Rose, M. E., 1990, Analysis of acylcarnitines as β -acyloxybutyrolactones by gas chromatography/mass spectrometry. *Analyst* **115**:511-516.
38. Huang, Z.-H., Gage, D. A., Bieber, L. L., and Sweeley, C. C., 1991, Analysis of acylcarnitines as their N-demethylated ester derivatives by gas chromatographic-chemical ionization mass spectrometry. *Anal. Biochem.* **199**:98-105.
39. Millington, D. S., Kodo, N., Terada, N., Gale, D., and Chace, D. H., 1991, The analysis of diagnostic markers of genetic disorders in human blood and urine using tandem mass spectrometry with liquid secondary ion mass spectrometry, *Int. J. Mass Spectrom. Ion Proc.* **11**:211-228.
40. Ligon, W. V., 1990, Evaluating the composition of liquid surfaces using mass spectrometry. in: *Biological Mass spectrometry* (A. L. Burlingame and J. A. McCloskey, eds.), Elsevier, Amsterdam, pp. 61-75.
41. Gaskell, S. J., Guenat, C., Millington, D. S., Maltby, D. A., and Roe, C. R., 1986, Differentiation of isomeric acylcarnitines using tandem mass spectrometry, *Anal. Chem.* **58**:2801-2805.
42. Emory, J. L., Howat, A. J., Variend, S., and Vawter, G. F., 1988, Investigation of inborn errors of metabolism in unexpected infant death, *Lancet* **2**:29-31.
43. Howat, A. J., Bennett, M. J., Variend, S., Shaw, L., and Engel, P. C., 1985, Defects of metabolism of fatty acids in the sudden infant death syndrome, *Br. Med. J.* **290**:1771-1773.
44. Millington, D. S., Terada, N., Chace, D. H., Chen, Y.-T., Ding, J.-H., Kodo, N., and Roe, C. R., 1992, The role of tandem mass spectrometry in the diagnosis of fatty acid oxidation disorders, in: *New Developments in Fatty Acid Oxidation* (P. M. Coates and K. Tanaka, eds.), Wiley-Liss, New York, 339-354.
45. Yokota, Y., Tanaka, K., Coates, P. M., and Ugarte, M., 1990, Mutations in medium-chain acyl-coA dehydrogenase deficiency, *Lancet* **336**:748.
46. Ding, J.-H., Roe, C. R., Chen, Y.-T., Matsubara, Y., and Narisawa, K., 1990, Mutations in medium-chain acyl-coA dehydrogenase deficiency, *Lancet* **336**:748-749.
47. Hale, D. E., Stanley, C. A., and Coates, P. M., 1990, Genetic defects of acyl-CoA dehydrogenases: Studies using an electron transferring flavoprotein reduction assay. in: *Fatty Acid Oxidation: Clinical, Biochemical and Molecular Aspects* (K. Tanaka and P. M. Coates, eds.), Alan R. Liss, New York, pp. 333-348.
48. Norwood, D. L., Bus, C. A., and Millington, D. S., 1990, Combined high-performance liquid chromatographic-continuous-flow fast atom bombardment mass spectrometric analysis of acyl-coenzyme A compounds, *J. Chromatogr.* **527**:289-301.
49. Norwood, D. L., Fisher, D. L., Millington, D. S., and Aplin, R. T., 1991, Mass spectrometry of acyl-coenzyme A compounds, in: *Proceedings of the 39th ASMS Conference on Mass Spectrometry and Allied Topics, 1991, Nashville, May 19-24*, pp. 25-26.
50. Millington, D. S., Kodo, N., Norwood, D. L., and Roe, C. R., 1990, Tandem mass spectrometry: A new method for acylcarnitine profiling with potential for neonatal screening for inborn errors of metabolism, *J. Inher. Metab. Dis.* **13**:321-324.
51. Bohmer, T., and Bremer, J., 1968, Propionylcarnitine: Physiological variations *in vivo*, *Biochim. Biophys. Acta* **152**:559-567.

Platelet-Activating Factor and Related Compounds

Kunihiko Saito

1. INTRODUCTION

Platelet-activating factor (PAF) was discovered in 1972 in relation to allergic reaction as a fluid mediator released from basophils (1), and its structure was determined in 1980 as 1-alkyl(octadecyl/hexadecyl)-2-acetyl-*sn*-glycero-3-phosphocholine (2) (Fig. 9.1). Now PAF is known as a chemical mediator of allergic and inflammatory processes and is thought not to be a constituent of animal tissues but to be newly generated from inflammatory cells in response to a variety of stimuli. PAF has a variety of biological activities such as platelet activation, neutrophil activation, increasing vascular permeability, hypotension, etc. and has the strongest agonist action (10 pM) for platelet aggregation. The name, platelet-activating factor, is based on this biological activity and not on its chemical nature. On the other hand, PAF has recently been found in normal animal tissues without any exogenous or inflammatory stimuli, and its level is variable under physiological conditions (3).

Biomedically, therefore, PAF has biphasic functions. One is as a chemical mediator of allergic and inflammatory reactions, and it should be removed from the pathological region to reduce inflammation. This activity is why so many PAF inhibitors have been produced as possible antiallergic drugs, and this development is still progressing. The other function is an autacoid activity that is related to physiological reactions or physiological homeostasis. In this sense, endogenous PAF is an essential active lipid material or lipid mediator present in

Kunihiko Saito • Department of Medical Chemistry, Kansai Medical University, Moriguchi, Osaka 570, Japan.

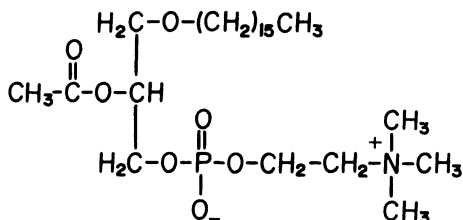


Figure 9.1. Structure of C_{16:0} PAF.

normal animal tissues. The difference between these two functions might be based on the *in situ* quantity rather than quality.

PAF is one of the molecular species of choline glycerophospholipids with chemical characteristics of an alkyl group at *sn*-1 and an acetyl group at *sn*-2; it also can be defined as a derivative of glyceryl ethers, 1-alkyl glycerols, which are chemically stable unsaponifiable lipid materials. This stability is the reason why AGEPC (acetyl glyceryl ether phosphocholine) was proposed by Hanahan *et al.* (2).

Natural glycerophospholipids are usually divided into four subclasses. For example, those of choline glycerophospholipids are (a) 1,2-diacyl, (b) 1-alkyl-2-acyl, (c) 1-alk-1'-enyl (vinyl)-2-acyl, and (d) 1,2-dialkyl GPCs (glycerophosphocholines). In mammalian tissues, however, 1,2-dialkyl GPC is not usually found. PAF is *sn*-2 acetylated 1-alkyl GPC, and two more *sn*-2 acetylated GPCs are possibly present in nature. In fact, acyl PAF (1-acyl-2-acetyl GPC) and vinyl PAF (1-alk-1'-enyl-2-acetyl GPC) have been found in animal tissues. The *sn*-1-alkyl residues and *sn*-1-acyl residues are usually 16:0, 18:0, 18:1, etc. in carbon chain length, so PAF has about ten molecular species, for example, 16:0 PAF (1-hexadecyl-2-acetyl GPC), 16:0 acyl PAF (1-hexadecanoyl-2-acetyl GPC), and 16:0 vinyl PAF (1-hexadec-1'-enyl-2-acetyl GPC) (Fig. 9.2). The identification and quantification of these molecular species in biological tissues and fluids is very important because the platelet-aggregating activity of PAF, for example, is different among these molecular species (see Table 9.1), and furthermore, platelet aggregation is not their only biological activity.

2. BIOCHEMICAL BACKGROUND

Very briefly, PAF is biosynthesized by (a) a deacylation–reacetylation (re-modeling) system or (b) *de novo*. The former method is initiated by deacylation of alkylacyl GPC with phospholipase A₂ and then acetylation by a trans-acetylase. Between these two steps an interesting intermediate *sn*-2-arachidonoyl

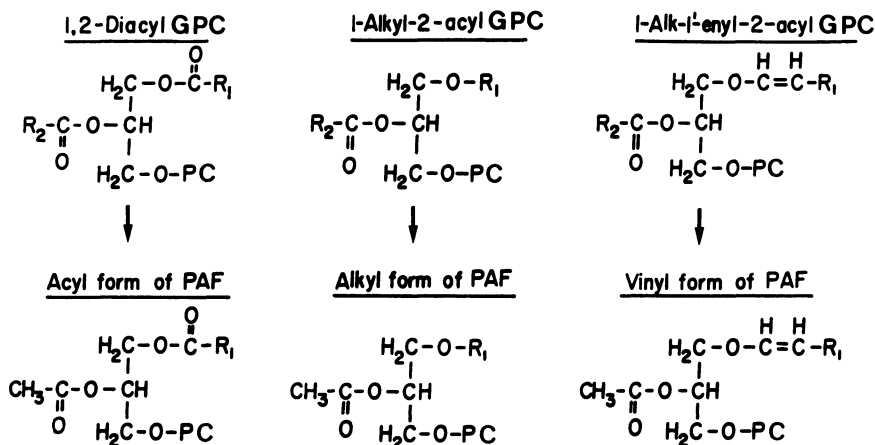


Figure 9.2. Three forms of PAF in relation to their precursors. GPC, glycerophosphocholine; PC, phosphocholine. [From Saito *et al.* (19). Reprinted with permission. Copyright 1990 Elsevier Science Publishers.]

GPC may participate, and the whole system called the PAF cycle (4,5). The 1-alkyl-2-arachidonoyl GPC can produce arachidonic acid and 1-alkyl-2-lyso GPC, lyso-PAF, by phospholipase A₂, both of which are precursors, respectively, of prostaglandins and PAFs. The latter, *de novo* system is catalyzed by 1-alkyl-2-acetylglcerol:phosphocholine transferase. Generally, the remodeling system is concerned with inflammation or allergic reactions, and the *de novo* system with physiological reactions.

The hydrolysis of PAF is catalyzed by acetylhydrolase, resulting in a formation of biologically inactive lyso-PAF. Other possible degradation enzymes corresponding to, for example, phosphoolipases C and D are not known.

3. MASS SPECTROMETRY OF PAF

Mass spectrometry (MS) is the most reliable method used in structural and quantitative analysis of PAF, and the method is rapidly improving and develop-

Table 9.1
Platelet-Aggregating Activity of 16:0 PAFs

PAF	100%
Acyl PAF	<1%
Vinyl PAF	20%

ing. Three mass spectrometric methods are discussed below. (a) GC-MS gives many fragment ions from a PAF molecule; by monitoring ions specific to the structure (SIM technique), the identification of various PAF molecular species is possible. A disadvantage is, however, that the analyte must be derivatized for GC. We usually use tBDMS (*tert*-butyldimethylsilyl) derivatives. The following diagnostic ions are chosen: $[M - 57]^+$ as an indicator for the molecular ion, $[RCO + 74]^+$ for identifying the acyl group, m/z 117 for acetyl group, $[R + 130]^+$ for alkyl group, and $[RCH:CH + 56]^+$ for vinyl group. (b) FAB-MS can directly determine the protonated molecule ion but gives fewer fragment ions. A disadvantage is that the sample to be determined must be chemically pure. (c) In MS/MS or tandem mass spectrometry, two mass spectrometers are linked in series. The precursor ion or other ion to be determined, which was produced by the first MS, is further fragmented (unimolecular or collision-induced decompositions), and the second MS collects the product ions, from which the structure of the precursor ion can be elucidated. Furthermore, from a product ion, precursor ions can be determined. The first mass spectrometer can be replaced by GC-MS or FAB-MS, and GC-MS/MS or FAB-MS/MS systems are available. This MS/MS system provides advantages because the sample is not necessarily chemically pure and the product ions derived from the precursor ion are determined, so conversely the precursor ion can be determined from each of the product ions.

For quantitation, stable isotope dilution and MS are used. Perdeuteroacetyl PAFs such as 16:0 d_3 -PAF, 17:0 d_3 -acyl PAF, and 18:0 d_3 -vinyl PAF are usual internal standards, and the analyte/internal ratio is determined. For example, $[M - 57]^+$ of tBDMS derivatives for SIM-GC-MS (6), $[M]^-$ of pentafluorobenzoyl (PFB) derivatives for GC-NICI (negative-ion chemical ionization) MS (7,8), and $[M + 1]^+$ for conventional FAB-MS, or m/z 184 and 185 for FAB-MS-MS (9) are reported. The detection limit of each method is approximately 100 pg, subpicogram, or low-picogram, respectively. Yamada *et al.* (8) reported the value of 16:0 PAF to be 10–30 pg/ml of human blood samples obtained from normal subjects between 25 and 60 years of age. Haraldsen and Gaskell (9) add simultaneously $[^3H]16:0$ PAF (10^5 dpm, 585 pg) and $[^2H_3]16:0$ PAF (100, 120, or 165 ng) to the sample to assess recovery and permit rigorous quantification.

Other analytical methods for PAF, including biological and immunologic approaches, are available. The biological method usually used is based on platelet-aggregating or serotonin-releasing activity by PAF from $[^3H]$ serotonin-loaded platelets. The sensitivity is high, but specificity is low; also, the possible presence of some endogenous inhibitors (10) must be avoided. The immunologic method has the advantage of specificity and simplicity; however, a reliable and reproducible yield of PAF antibody is rather difficult to obtain. In our experience, SPRIA (scintillation proximity radioimmunoassay) could supply comparable data to GC-MS (11). The sensitivity of SPRIA is between those of bioassay and mass spectrometry.

3.1. Gas Chromatography–MS

3.1.1. Derivatization

Usually TMS (trimethylsilyl), tBDMS, or PFB derivatives of 1-alkyl-2-acetyl-*sn*-glyceryl are used. The tBDMS derivatives provide more intense molecular ions than TMS derivatives; PFB derivatives coupled with NICI-MS provide the most sensitive mass spectrometric method (7).

3.1.2. Preparation of 1-Alkyl-2-acetyl-*sn*-glycerol

Usually phospholipase C is used for removing phosphocholine. The enzyme activity is sometimes different among preparation lots, and we use our partially purified *Bacillus cereus* culture filtrate, which is very active. To avoid acetyl migration from *sn*-2 to *sn*-3, sufficient diethyl ether should be added in the assay system.

Chemically, HF is also used to obtain 1-alkyl-2-acetyl-*sn*-glycerol (12,13), but in this case acetyl migration occurs, and 1-alkyl-2-lyso-3-acetyl-*sn*-glycerol is formed. tBDMS derivatives of these two positional isomers of 16:0 PAF show quite different fragment ions by EI-MS, and *sn*-3 tBDMS is not split at the glycerol C-C bond where *sn*-2 tBDMS is split; those two molecular ions are identical (m/z 472), and the base peaks of these isomers are m/z 57 and m/z 175, respectively. The PFB derivative of alkylacetyl glycerol coupled with NICI-MS produces an abundant molecular ion at m/z 552 and almost no fragment ions. To fully utilize this molecular ion for quantitation of PAF, Christman and Blair (13) forced the conversion of the *sn*-3 PFB derivative to its *sn*-2 isomer; the latter is thermodynamically more stable. HF sometimes catalytically splits the *sn*-2-acetyl group.

3.1.3. Mass Spectra

Figures 9.3 and 9.4 show GC–EIMS mass spectra of *sn*-3-tBDMS derivatives of 16:0 PAF and 16:0 d_3 -PAF, 16:0 vinyl PAF, and 16:0 acyl PAF, respectively (6,14,15). Ions at $[M - 57]^+$ [respectively, m/z 415, 418, 413, and 429] are clearly observed. Similarly, for hexadecyl and hexadec-1-enyl (vinyl) residues, ions at m/z 355 ($[R + 130]^+$) and m/z 353 ($[RCH:H + 130]^+$) are seen, and for acetyl and palmitoyl residues, ions at m/z 117 ($[CH_3CO + 74]^+$) and m/z 313 ($[RCO + 74]^+$) are identified. These characteristic and prominent ions are very useful for identification of individual molecular species of PAF. The quantification of each molecular species is also possible by measuring the $[M - 57]^+$ ion, but FAB-MS and CINI-MS, for example, which give more intensive molecular ions, are better.

Figure 9.5 shows isopropylidene, di-TMS, and di-tBDMS derivatives of

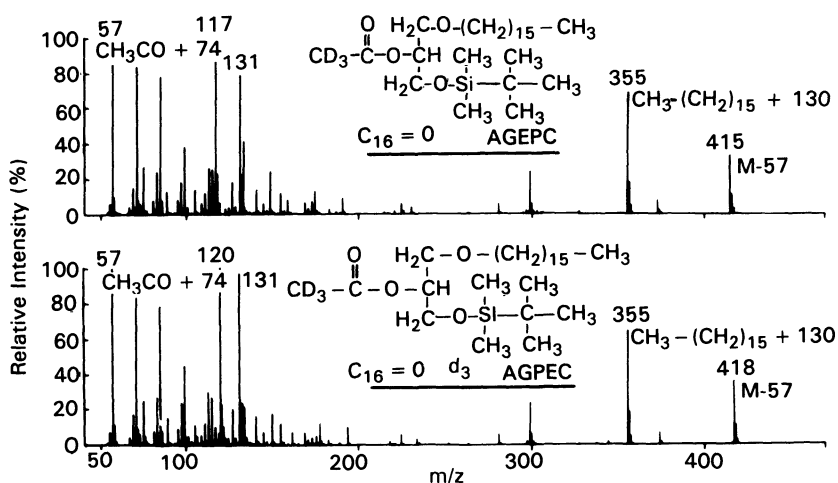


Figure 9.3. Mass spectra of tBDMS derivatives of 16:0 PAF and 16:0 d₃-PAF. [From Satouchi *et al.* (16). Reprinted with permission.]

1-O-hexadecylglycerol, chmyl alcohol, which is the most important constituent of PAF.

3.1.4. Selected Ion Monitoring of GC-EI-MS

Figure 9.6 shows the SIM trace of *sn*-3 tBDMS derivatives of PAF and acyl PAF prepared from stimulated human polymorphonuclear leukocytes (PMN)

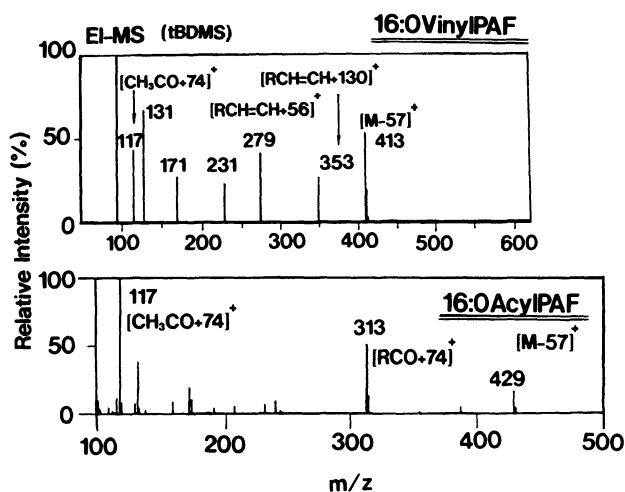


Figure 9.4. Mass spectra of tBDMS derivatives of 16:0 vinyl PAF and 16:0 acyl PAF.

(16). All molecular species can be monitored by the *sn*-2 acetyl residue, m/z 117 ($[\text{CH}_3 \text{CO} + 74]^+$). From comparison of their retention times with those of standards, as well as monitoring $[\text{M} - 57]^+$, six molecular species in the four peaks are identified as 16:0 PAF (m/z 415), 16:0 acyl PAF (m/z 429), 18:1 PAF (m/z 441), 18:0 PAF (m/z 443), 18:1 acyl PAF (m/z 455), and 18:0 acyl PAF (m/z 457), in order of their elutions. Ions at m/z 120, 418, and 446, corresponding to perdeuteroacetyl residue, 16:0 d_3 PAF, and 17:0 d_3 -acyl PAF, respectively, are used for internal standards. The absence of odd-numbered PAF was confirmed by separately remonitoring the derivative of each PAF and acyl PAF, which had been separated by TLC in hexane : diethyl ether (9 : 1, v/v).

Similarly, Fig. 9.7 shows *sn*-3 tBDMS derivatives of PAF and acyl PAF present in rat uterus. The 16:0 PAF, 16:0 d_3 -PAF, and 18:1 PAF shown in the left panel and 16:0 acyl PAF, 17:0 d_3 -acyl PAF, 18:1 acyl PAF, and 18:0 acyl PAF shown in the right panel are identified and quantified (Table 9.2).

Figure 9.8 shows the presence of 16:0 vinyl PAF in perfused rat and guinea pig hearts. The ion at m/z 413 indicates $[\text{M} - 57]^+$ of the *sn*-3 tBDMS derivative of 16:0 vinyl PAF, hexadec-1-enyl(vinyl)acetyl GPC, which has an identical retention time to the authentic perdeuteroacetyl derivative. When the sample was pretreated with 0.1 N HCl/90% methanol for 30 min, the peak corresponding to 16:0 vinyl PAF disappeared. Because the vinyl linkage is very acid-labile, any

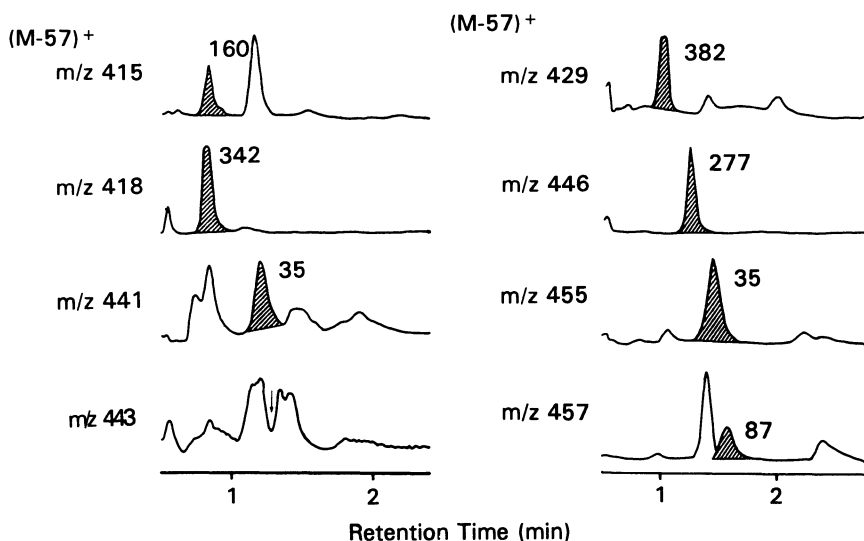


Figure 9.7. SIM traces of tBDMS derivatives of PAF (left) and acyl PAF (right) from rat uterus. The arrow shows the position of authentic 18:0 PAF. [From Yasuda *et al.* (16). Reprinted with permission. Copyright 1988 John Wiley & Sons, Ltd.]

Table 9.2
The PAF Content of Rat Uterus

	PAF (ng/mg P)	PAF (mol/10 ⁶ mol PL)
PAF		
16:0	28.4	1.7
18:0	—	—
18:1	6.2	0.4
Acyl PAF		
16:0	119.9	6.9
18:0	36.6	2.0
18:1	13.9	0.8

P, lipid phosphorus; PL, phospholipids.

acidic condition should be avoided to prepare the vinyl PAF, as will be discussed below. The content of 16:0 vinyl PAF is 46.4 ng/mg lipid phosphorus (17).

3.2. Fast Atom Bombardment MS

Fast atom bombardment (FAB) is a surface ionization technique and liquid-matrix-assisted or particle-induced desorption, and the analysis greatly depends on the nature of the matrix or contaminant salts. Figure 9.9 shows the FAB mass spectra of 16:0 PAF, 16:0 acyl PAF, and 16:0 vinyl PAF. The spectra are rather simple, and $[MH]^+$ and m/z 184 are the major ions. However, it should be noted that the compound with identical $[MH]^+$ ion or with same ion at m/z 184 is not a

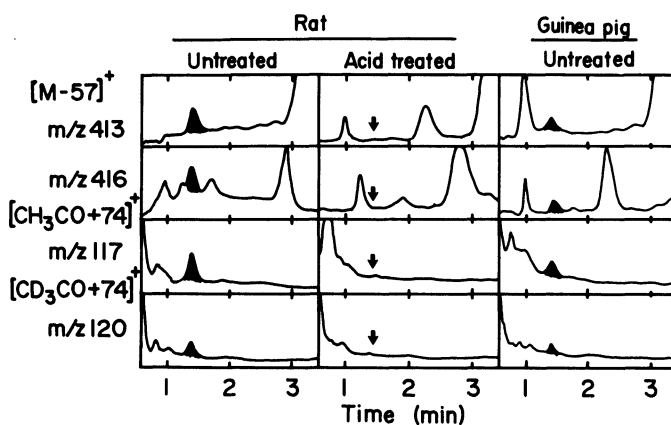


Figure 9.8. SIM traces of a tBDMS derivative of vinyl PAF from rat heart and guinea pig heart. [From Nakayama and Saito (17). Reprinted with permission.]

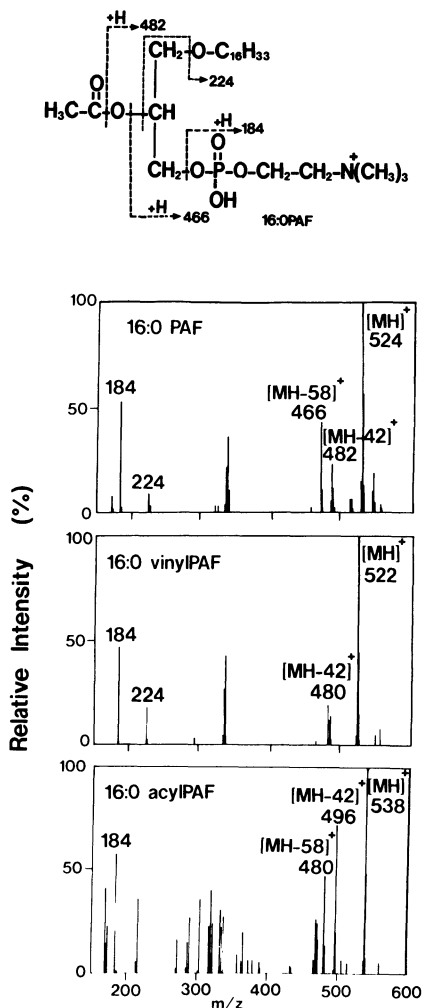


Figure 9.9. Positive FAB-MS spectra of 16:0 PAF, 16:0 vinyl PAF, and 16:0 acyl PAF. Matrix, triethanolamine.

single compound; for example, the ion at m/z 524 corresponds to $[MH]^+$ of 16:0 PAF, 15:0 acyl PAF, 18:0 lyso-PC, and 19:0 lyso-PAF, as shown in Table 9.3. To identify each molecular species, some other methods (such as MS/MS) or chemical treatments are necessary.

3.3. Fast Atom Bombardment MS/MS

Figure 9.10 shows FAB-MS/MS spectra of molecular ions of 16:0 PAF at m/z 524 $[MH]^+$ and its tBOMS derivative at m/z 415 $[M - 15]^+$. The deri-

Table 9.3
Protonated Molecule Ion $[M + 1]^+$ of PAF and Related Phospholipids

m/z 524	m/z 538	m/z 552	m/z 550
16:0 PAF	17:0 PAF	18:0 PAF	18:0 Vinyl PAF
15:0 Acyl PAF	16:0 Acyl PAF	17:0 Acyl PAF	18:1 PAF
18:0 Lyso-PC ^a	19:0 Lyso-PC	20:0 Lyso-PC	17:1 Acyl PAF
19:0 Lyso-PAF	20:0 Lyso-PAF	21:0 Lyso-PAF	20:1 Lyso-PC
			21:1 Lyso-PAF

^aPC = 1,2-diacyl GPC.

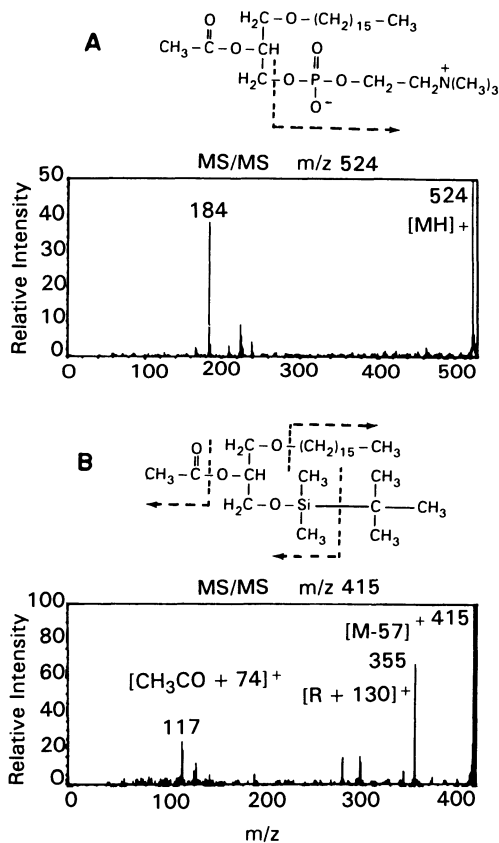


Figure 9.10. MS/MS spectra of $[MH]^+$ ion at m/z 524 of 16:0 PAF (A) and $[M - 57]^+$ ion at m/z 355 of tBDMS derivatives of 16:0 PAF (B), which are obtained in positive-ion-mode FAB-MS. [By courtesy of Finnigan MAT (1988).]

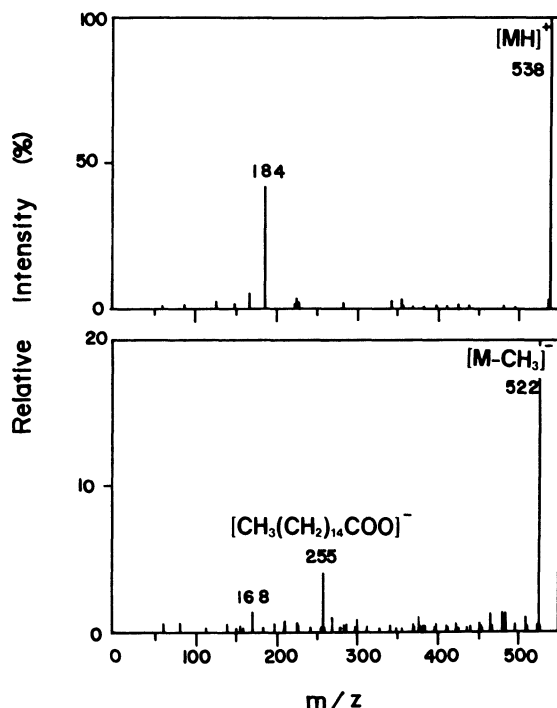


Figure 9.11. MS/MS spectra of $[MH]^+$ ion at m/z 538 of 16:0 acyl PAF obtained in positive-ion-mode FAB-MS (upper) and $[M - 15]^-$ ion at m/z 522 of 16:0 acyl PAF obtained in negative-ion-mode FAB-MS (lower).

vatized sample shows the ions based on the constituent hexadecyl and acetyl groups, whereas the underivatized one gives the ion at m/z 184 based on phosphocholine only in addition to $[MH]^+$. As mentioned above, it is impossible to identify the sample with m/z 524 $[MH]^+$ as pure 16:0 PAF from this upper spectrum. Figure 9.11 shows the MS/MS spectra of 16:0 acyl PAF. The positive and negative FAB-MS/MS data are complementary.

Choline glycerophospholipids obtained from stimulated human neutrophils were analyzed by Kayganich and Murphy (18), as shown in Fig. 9.12. They intended to analyze the arachidonate-containing molecular species of choline glycerophospholipids, which are biomedically interesting species. All kinds of molecular species are shown in Fig. 9.12A, and Fig. 9.12C shows the parent molecular species derived from the product arachidonic acid with m/z 303. The arachidonate-containing molecular species thus identified are shown in Table 9.4 with their relative abundances. Figure 9.12B shows the oleate-containing molecular species.

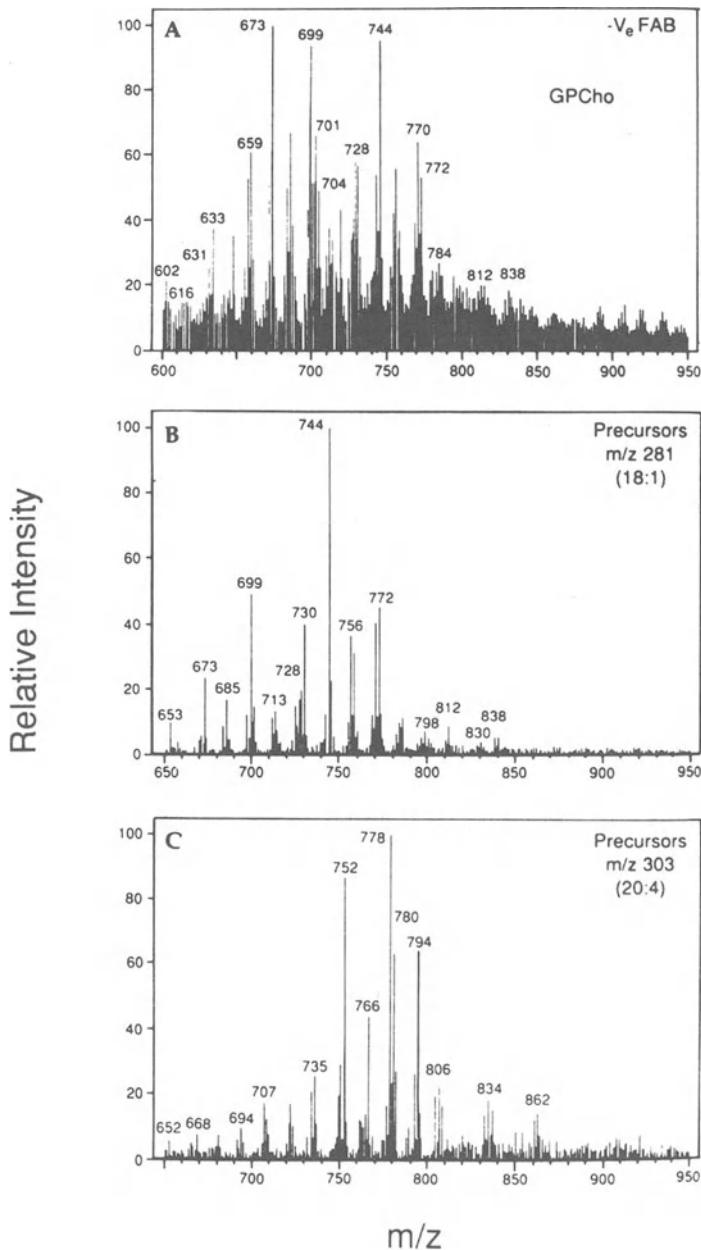


Figure 9.12. Negative FAB-MS and MS/MS spectra obtained from the cholineglycerophospholipids isolated from human neutrophils. (A) High-mass negative ions produced from the mixture of cholineglycerophospholipids molecular species. (B) Precursors of m/z 281, corresponding to those ions arising from molecular species that contain esterified oleic acid (18:1). (C) Precursors of m/z 303, corresponding to those ions arising from molecular species that contain esterified arachidonic acid (20:4). [Reprinted by permission of Elsevier Science Publishing Co., Inc., from Molecular species analysis of arachidonate-containing glycerophosphocholines by tandem mass spectrometry, by Kayganich and Murphy. *Journal of the American Society for Mass Spectrometry*, Vol. 2, pp. 45–54. Copyright 1991 by the American Society for Mass Spectrometry.]

Table 9.4
Molecular Species of Arachidonate-Containing Choline
Glycerophospholipids from Human Neutrophils^a

FAB/CID ^a	Precursors of <i>m/z</i> 303	Relative abundance of precursors of <i>m/z</i> 303 (%)
18:0a/20:4	794	64
18:1a/20:4	792	27
18:0e/20:4	780	62
18:1e/20:4	778	100
16:0a/20:4	766	40
16:0e/20:4	752	86
16:0p/20:4	750	30
20:1e/20:4	806	22
20:0e/20:4	808	16
22:1e/20:4	834	18

^aa, acyl; e, alkyl; p, vinyl.

Reprinted by permission of Elsevier Science Publishing Co., Inc., from Kayganich and Murphy (19). Copyright 1991 by the American Society for Mass Spectrometry.

4. PREPARATION OF PAF FROM ANIMAL TISSUES

The PAF content in animal tissues or cells is very minute, particularly endogenous PAF. In blood, the PAF level is comparable to that of a hormone. Figure 9.13 indicates (a) that the amount of PAF produced in stimulated leukocytes is 1000 times more than that of endogenous PAF in normal tissues, (b) that

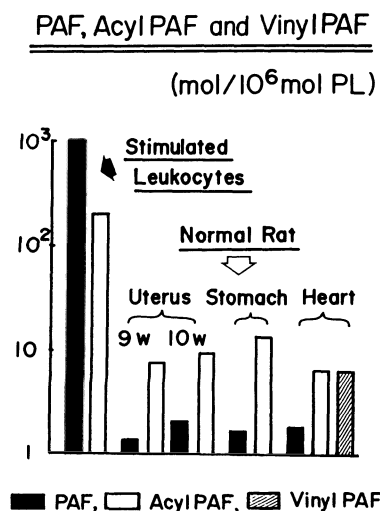


Figure 9.13. Comparison of PAF level in stimulated human leukocytes and normal rat tissues. [From Saito *et al.* (19). Reprinted with permission. Copyright 1991 Elsevier Science Publishers.]

PAF is produced more than acyl PAF in the leukocytes, but in normal tissues less PAF is produced than acyl PAF and vinyl PAF, and (c) that the level of endogenous PAF in normal tissues is less than 10 mol per 10^6 mol of mother tissue phospholipids (19). Therefore, the preparation of PAF is somewhat complicated and needs some lipid techniques.

The experimental procedures used in our laboratory for PAF analysis are as follows.

4.1. A Combination of Column Chromatography and Thin-Layer Chromatography

Briefly, total lipids were extracted (20) and applied to a silica AR CC-7 column. After elution of the simple lipids with chloroform, the phospholipids were eluted with methanol. The phospholipids were separated by TLC on silica gel H plates with a solvent mixture of chloroform : methanol : water (65 : 36 : 6 by volume). The lipid located between acyl lyso-GPC and sphingomyelin was extracted. The lipid was separated by TLC in methanol : water (2 : 1 by volume), where PAF migrated to R_f 0.5 and more lipophilic lipids remained at the origin. To determine the recovery of PAF, an internal standard of 16:0 [^3H]PAF was added to the total lipids extracted, and the bioassay was carried out at each step of purification. The recovery is usually 80%. The PAF is usually a mixture of PAF, acyl PAF, and sometimes even vinyl PAF; to separate that mixture further, it must be converted to the tBDMS derivatives, for example, and applied to TLC in a hexane : diethyl ether mixture (9 : 1, by volume), where vinyl PAF migrates fastest and acyl PAF slowest. Again, the vinyl linkage is very acid labile, and acidic condition should be avoided. As an example, the preparation of PAF from rat uterus is shown in Fig. 9.14 (15).

4.2. High-Performance Liquid Chromatography

As reviewed by Blank *et al.* (21), HPLC is a very powerful chromatographic separation method. Total lipids are separated by silica HPLC, and PAF is eluted between acyl lyso-GPE and acyl lyso-GPC. The PAF is further analyzed, for example, by reversed-phase HPLC (Fig. 9.15) or mass spectrometry.

4.3. Procedures for Vinyl PAF from Rat Heart

As mentioned above, because vinyl PAF is very acid-labile, modified procedures are needed (17,22). Total lipids were extracted from perfused rat hearts with saline; 16:0 d_3 -PAF was applied to an alumina column and eluted with chloroform : methanol (1 : 1, v/v). The choline-containing glycerophospholipids were separated by TLC in chloroform : methanol : 1 N aqueous

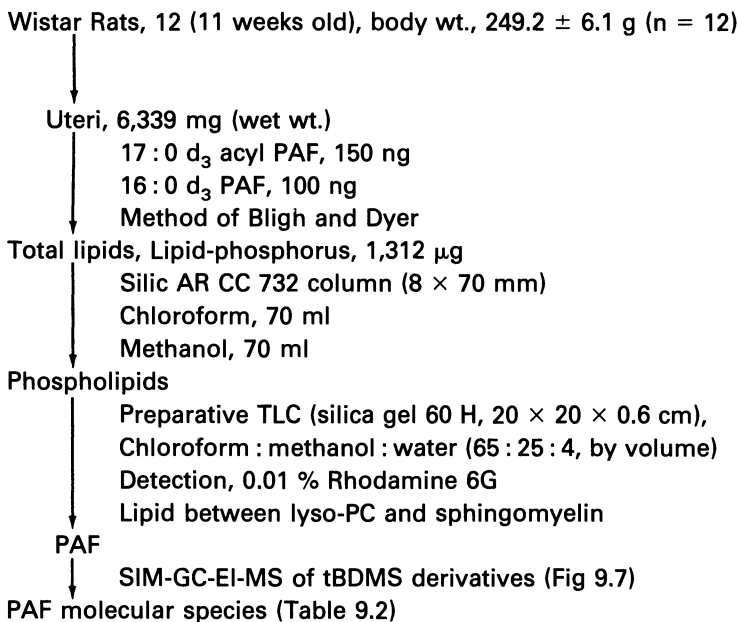


Figure 9.14. Experimental procedure to isolate PAF from rats.

NH₄OH : water (65 : 35 : 4 : 2 by volume), and the lipid located between lyso-PC and sphingomyelin was applied to reversed-phase HPLC (Fig. 9.15). The point of these procedures is to avoid silicic acid column chromatography and normal-phase HPLC containing phosphoric acid as a solvent and to use the ammonia-alkaline developing solvent for TLC.

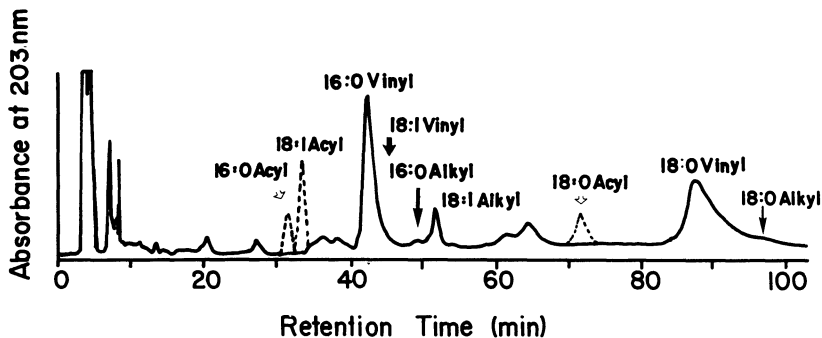


Figure 9.15. Separation of a mixture of acyl PAFs and vinyl PAFs by reversed-phase HPLC. [Modified from Nakayama and Saito (17), with permission.]

5. DISCUSSION

Glycerophospholipids have been understood in relation to cellular boundaries and membrane fluidity, but recently a new concept, lipid mediators or active lipids, has been opened by the discovery of prostaglandins and leukotrienes, inositol phospholipids and signal transduction, and PAF. Platelet-activating factors is the first example of a biologically active glycerophospholipid, and it may lead to diseases in two ways (23). PAF is a well-known chemical mediator of inflammation or allergy, but it still remains to be determined what kind of allergic disease may be closely or definitely related to PAF. Nevertheless, many exogenous PAF antagonists have been reported, some structurally related, such as CV-3988, ONO-6240, U66985, and SRI63441, and others unrelated, for example, Kadzurenon, BN52021, L652,731, and WEB2086. The development of highly effective antiinflammatory drugs is expected.

However, the effect of a PAF antagonist on allergic and inflammatory processes is to decrease the abnormally elevated PAF content to a more normal level, not to deplete PAF completely in tissues or cells, lest a disturbance of homeostasis results. This situation is just like the case of antipyretics, which work to reduce a pathologically high body temperature to about 37°C. Another role of PAF in disease might be related to an imbalance in the autacoid system, because PAF may play a physiological or pathophysiological role; some suggestive evidence is available. For example, by influencing Ca^{2+} fluxes, PAF may participate in neuronal development and degeneration (24). Water immersion stress in a rat induces a decrease in the endogenous level of PAF in the stomach, which may lead to ulcer formation (25). Following oophorectomy, the PAF level in rat uterus decreases to about one-third after 10 days, but administration of estradiol restores the level completely. The $\text{PGF}_{2\alpha}$ level of the uterus is

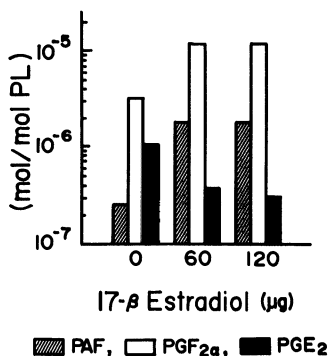


Figure 9.16. Response of rat uterine PAF and PGs to estradiol. [From Nakayama *et al.* (26). Reprinted with permission. Copyright 1991 Elsevier Science Publishers.]

Table 9.5
PAF in Blood

Animal	Disease	PAF content	Control	Method	Reference
Human	Normal		0.01–0.03 ng/ml	GC-NICI-MS	37
	Anaphric patient	N.D.	0.2 ng/ml	Bioassay	38
	Cold urticaria	0.06 ng/ml	N.D.	Bioassay	39
	Decompensated cirrhosis	0.78 ng/ml	0.2 ng/ml	Bioassay	40
	Disseminated intravascular coagulation syndrome (DIC)	0.2 ng/ml	0.005 ng/ml	GC-NICI-MS	41
Rabbit	Drug-induced allergy	0.02 ng/ml	0.001 ng/ml	Bioassay	42
	Septicemia	0.7 ng/ml	0.17 ng/ml	Bioassay	43
	Normal		0.2 ng/ml	Bioassay	38
Rat	Cationic human IgG-induced glomerulonephritis	10.5 ng/ml	2.5 ng/ml	Bioassay	44
	Endotoxin shock	2.5 ng/ml	0.1 ng/ml	Bioassay	45
	Endotoxin shock	13.7 ng/ml	4.3 ng/ml	Bioassay	46
	Nephrectomy	N.D.	1.8 ng/ml	Bioassay	38

N.D., not detectable.

Table 9.6
PAF in Body Fluid

Animal	Body fluid	Disease	PAF content	Method	Reference
Human	Amniotic fluid	Labor	0.06 ng/ml	Bioassay	47
	Ascitic fluid	Before the onset of labor	N.D.		
		Decompensated cirrhosis	1.69 ng/ml	Bioassay	40
	Bronchoalveolar lavage fluid	Bronchial asthma	1.36 ng/ml	Bioassay	48
		Emphysema	N.D.		
	Cerebrospinal fluid	Bronchial asthma	0.46 ng/ μ mol PL	Bioassay	49
		Bacterial meningitis	51.5 ng/ml	Bioassay	50
		Control	8.4 ng/ml		
	Pleural fluid	Empyema	0.89 ng/ml	Bioassay	51
		Lung cancer, pulmonary edema	N.D.		
		Eosinophilic pneumonia	0.18 ng/ml		
	Saliva	Upper respiratory infection	3.27 ng/ml		
		Normal	0.25 ng/ml	GC-NICI-MS	52
Urine	Lupus glomerulonephropathy	450 ng/24-hr urine	Bioassay	53	
	Normal	53 ng/24-hr urine			
	Pyuria	0.005–7 ng/ml	Bioassay	54	
Bovine	Semen (spermatozoa)	Normal	N.D.		
	Semen (spermatozoa)	Normal	0.3 ng/ 10^8 cells	Bioassay	55
	Semen (spermatozoa)	Normal	0.96 ng/ μ mol PL	Bioassay	56
Rabbit	Semen (spermatozoa)	Normal	0.2 ng/ 10^8 cells	Bioassay	57

PL, phospholipids.

Table 9.7
PAF in Tissue

Animal	Tissue	Disease	PAF content	Control	Method	Reference
Human	Breast	Carcinoma	2.6 ng/ μ mol PL	0.3 ng/ μ mol PL	Bioassay	58
	Skin	Psoriatic scale	5-30 ng/g.w.w.		GC-MS, bioassay	59
Baboon	Thymus			35.1 ng/g.w.w.	Bioassay	60
	Myocardium	Myocardial infarction	0.5-6.2 ng/g.w.w.	22.8 ng/g.w.w.	Bioassay	61
Bovine	Brain			N.D.	GC-MS	62
Guinea pig	Skin	UV erythema	0.4 ng/g.w.w.		Bioassay	63
Rabbit	Uterus	Pregnancy	19.8 ng/g.w.w.	1.2 ng/g.w.w.	Bioassay	64
Rat	Hindpaw	Carrageenin-induced edema	13.1 ng/rat	5.8 ng/rat	Bioassay	65
	Kidney	Endotoxin shock	12.8 ng/rat	2.2 ng/rat	Bioassay	46
Rat	Lung	Endotoxin shock	312.3 ng/rat	32.3 ng/rat	Bioassay	46
	Stomach	Ulcer (antrum)	3.2 ng/g.w.w.	8.1 ng/g.w.w.	Bioassay	25
	Uterus			0.73 ng/ μ mp; ;	GC-MS	16

g.w.w., gram wet weight of tissue.

ten times greater than that of PAF and changes quite parallel with PAF, but PGE₂ decreases as shown in Fig. 9.16 (26).

The biomedical significance of acyl PAF, which is widely distributed in normal tissues, and vinyl PAF is still unknown, although the PMN adhesion activity of 16:0 acyl PAF is about 40% of that of 16:0 PAF (27). 1-O-Alkyl-2-O-N-carbamoyloxy-*sn*-glycero-3-phosphocholine (C-PAF) (28) is biologically active and resistant to PAF acetylhydrolase activity, which enables it to be used for PAF study *in vivo*. Interestingly, a significant amount of PAF, mainly 16:0 PAF, is present in two species of slug, *Incilaria bilineta* and *Incilaria fruhstorferi*, and the content was markedly increased by treatments such as the injection of dimethylsulfoxide (29).

Biochemically, arachidonate-containing choline glycerophospholipids are putative precursors of PAF and PG. The molecular species of these phospholipids obtained from human neutrophils were recently analyzed by MS/MS (Fig. 9.12). The relationship between these lipid mediators and arachidonic acid is examined by depleting arachidonic acid or replacing it with fish oil or perilla oil, which is rich in eicosapentaenoic acid or linolenic acid (18:3, *n*-3) (30–35).

The methodology of mass spectrometry is rapidly developing, and Cole and Enke (36) report the complete and rapid characterization of phospholipid content of lipid extracts based on positive-ion neutral-loss scans and negative-ion product scans.

The PAF levels in various physiological and pathological materials are listed in Tables 9.5–9.7.

ACKNOWLEDGMENTS. This study was supported in part by a Grant-in-Aid for Scientific Research (63480132) from the Ministry of Education, Science and Culture of Japan and by the Science Research Promotion Fund from the Japan Private School Promotion Foundation (1991). The author wishes to thank Dr. T. Horii, Miss A. Namikawa, and Miss S. Unezaki for their help in preparing this manuscript.

REFERENCES

1. Benveniste, J., Henson, P. M., and Cochrane, C. G., 1972, Leukocyte-dependent histamine release from rabbit platelets: The role of IgE, basophils and a platelet-activating factor, *J. Exp. Med.* **136**:1356–1377.
2. Hanahan, D. J., Demopoulos, C. A., Liehr, J., and Pinckard, R. N., 1980, Identification of platelet-activating factor isolated from rabbit basophils as acetyl glyceryl ether phosphorylcholine, *J. Biol. Chem.* **255**:5514–5516.
3. Saito, K., Nakayama, R., Yasuda, K., Sugatani, J., and Satouchi, K., in: *Platelet-Activating Factor and Diseases* (K. Saito and D. J. Hanahan, eds.), International Medical Publishers, Tokyo, pp. 19–35.

4. Chilton, F. H., Ellis, J. M., Olson, S. C., and Wykle, R. L., 1984, 1-O-Alkyl-2-arachidonoyl-*sn*-glycero-3-phosphocholine, *J. Biol. Chem.* **259**:12014–12019.
5. Snyder, F., 1987, in: *Platelet-Activating Factor and Related Lipid Mediators* (F. Snyder, ed.), Plenum Press, New York, pp. 89–113.
6. Satouchi, K., Oda, M., Yasunaga, K., and Saito, K., 1983, Application of selected ion monitoring to determination of platelet-activating factor, *J. Biochem.* **94**:2067–2070.
7. Ramesha, C. S., and Pickett, W. C., 1986, Measurement of sub-picogram quantities of platelet activating factor (AGEPC) by gas chromatography/negative ion chemical ionization mass spectrometry, *Biomed. Environ. Mass Spectrom.* **13**:107–111.
8. Yamada, K., Asano, O., Yoshimura, T., and Katayama, K., 1988, Highly sensitive gas chromatographic–mass spectrometric method for the determination of platelet-activating factor in human blood, *J. Chromatogr.* **433**:243–247.
9. Haroldsen, P. E., and Gaskell, S. J., 1989, Quantitative analysis of platelet activating factor using fast atom bombardment/tandem mass spectrometry, *Biomed. Environ. Mass Spectrom.* **18**:439–444.
10. Nakayama, R., Yasuda, K., and Saito, K., 1987, Existence of endogenous inhibitors of platelet-activating factor (PAF) with PAF in rat uterus, *J. Biol. Chem.* **262**:13174–13179.
11. Sugatani, J., Lee, D. Y., Hughes, K. T., and Saito, K., 1990, Development of a novel scintillation proximity radioimmunoassay for platelet-activating factor measurement: Comparison with bioassay and GC/MS techniques, *Life Sci.* **46**:1443–1450.
12. Clay, K. L., Murphy, R. C., Andres, J. L., Lynch, J. M., and Henson, P. M., 1984, Structure elucidation of platelet activating factor derived from human neutrophils, *Biochem. Biophys. Res. Commun.* **121**:815–825.
13. Christman, B. W., and Blair, I. A., 1989, Analysis of platelet activating factor in human saliva by gas chromatography/mass spectrometry, *Biomed. Environ. Mass Spectrom.* **18**:258–264.
14. Nakayama, R., Yasuda, K., Satouchi, K., and Saito, K., 1988, in: 1-O-Hexadec-1'-enyl-2-acetyl-*sn*-glycero-3-phosphocholine and its biological activity, *Biochem. Biophys. Res. Commun.* **151**:1256–1261.
15. Satouchi, K., Oda, M., and Saito, K., 1987, 1-Acyl-2-acetyl-*sn*-glycero-3-phosphocholine from stimulated human polymorphonuclear leukocytes, *Lipids* **22**:285–287.
16. Yasuda, K., Satouchi, K., Nakayama, R., and Saito, K., 1988, Acyl type platelet-activating factor in normal rat uterus determined by gas chromatography mass spectrometry, *Biomed. Environ. Mass Spectrom.* **16**:137–141.
17. Nakayama, R., and Saito, K., 1989, Presence of 1-O-alk-1'-enyl-2-O-acetyl glycerophosphocholine (vinyl form of PAF) in perfused rat and guinea pig hearts, *J. Biochem.* **105**:494–496.
18. Kayganich, K., and Murphy, R. C., 1991, Molecular species analysis of arachidonate containing glycerophosphocholines by tandem mass spectrometry, *J. Am. Soc. Mass Spectrom.* **2**:45–54.
19. Saito, K., Nakayama, R., Yasuda, K., Satouchi, K., and Sugatani, J., 1990, in: *Biological Mass Spectrometry* (A. L. Burlingame and J. A. McCloskey, eds.), Elsevier, Amsterdam, pp. 527–547.
20. Kates, M., in: *Techniques of Lipidology*, 2nd rev. ed., Elsevier, Amsterdam, pp. 100–111.
21. Blank, M. L., Robinson, M., and Snyder, F., 1987, in: *Platelet-Activating Factor and Related Lipid Mediators* (F. Snyder, ed.), Plenum Press, New York, pp. 33–52.
22. Creer, M. H., Pastor, C., Corr, P. B., Gross, R. W., and Sobel, B. E., 1985, Quantification of choline and ethanolamine phospholipids in rabbit myocardium, *Anal. Biochem.* **144**:65–74.
23. Saito, K., and Hanahan, D. J. (eds.), 1989, *PAF and Diseases*, International Medical Publishers, Tokyo.
24. Kornecki, E., and Ehrlich, Y. H., 1988, Neuroregulatory and neuropathological actions of the ether-phospholipid platelet-activating factor, *Science* **240**:1792–1794.
25. Sugatani, J., Fujimura, K., Miwa, M., Mizuno, T., Sameshima, Y., and Saito, K., 1989,

- Occurrence of platelet-activating factor (PAF) in normal rat stomach and alteration of PAF level by water immersion stress, *FASEB J.* **3**:65–70.
26. Nakayama, R., Yasuda, K., Okumura, T., and Saito, K., 1991, Effect of 17 β -estradiol on PAF and prostaglandin levels in oophorectomized rat uterus, *Biochim. Biophys. Acta* **1085**:235–240.
 27. Smiley, P. L., Stremler, K. E., Prescott, S. M., Zimmerman, G. A., and McIntyre, T. M., 1991, Oxidatively fragmented phosphatidylcholines activate human neutrophils through the receptor for platelet-activating factor, *J. Biol. Chem.* **266**:11104–11110.
 28. O'Flaherty, J. T., Redman, J. F., Jr., Schmitt, J. D., Ellis, J. M., Surles, J. R., Marx, M. H., Piantadosi, C., and Wykle, R. L., 1987, 1-O-Alkyl-2-N-methylcarbamyl-glycerophosphocholine: A biologically potent, nonmetabolizable analog of platelet-activating factor, *Biochem. Biophys. Res. Commun.* **147**:18–24.
 29. Sugiura, T., Ojima, T., Fukuda, T., Satouchi, K., Saito, K., and Waku, K., 1991, Occurrence of platelet-activating factor in slugs, *J. Lipid Res.* **32**:1795–1803.
 30. Ramesha, C. S., and Pickett, W. C., 1986, Platelet-activating factor and leukotriene biosynthesis is inhibited in polymorphonuclear leukocytes depleted of arachidonic acid, *J. Biol. Chem.* **261**:7592–7595.
 31. Ramesha, C. S., and Pickett, W. C., 1986, Metabolism of platelet-activating factor by arachidonic acid-depleted rat polymorphonuclear leukocytes, *J. Biol. Chem.* **261**:15519–15523.
 32. Sperling, R. I., Robin, J.-L., Kylander, K. A., Lee, T. H., Lewis, R. A., and Austen, K. F., 1987, The effects of *n*-3 polyunsaturated fatty acids on the generation of platelet-activating factor-acether by human monocytes, *J. Immunol.* **139**:4186–4191.
 33. Croft, K. D., Codde, J. P., Barden, A., Vandongen, R., and Beilin, L. J., 1988, Effect of dietary fish oils on the formation of leukotriene B₄ and B₅, thromboxane and platelet activating factor by rat leukocytes, *Clin. Exp. Pharmacol. Physiol.* **15**:517–525.
 34. Triggiani, M., Connell, T. R., and Chilton, F. H., 1990, Evidence that increasing the cellular content of eicosapentaenoic acid does not reduce the biosynthesis of platelet-activating factor, *J. Immunol.* **145**:2241–2248.
 35. Horii, T., Satouchi, K., Kobayashi, Y., Saito, K., Watanabe, S., Yoshida, Y., and Okuyama, H., 1991, Effect of dietary linolenate on platelet-activating factor production in rat peritoneal polymorphonuclear leukocytes, *J. Immunol.* **147**:1607–1613.
 36. Cole, M. J., and Enke, C. G., 1991, Direct determination of phospholipid structures in microorganisms by fast atom bombardment triple quadrupole mass spectrometry, *Anal. Chem.* **63**:1032–1038.
 37. Yamada, K., Asano, O., Yoshimura, T., and Katayama K., 1988, Highly sensitive gas chromatographic-mass spectrometric method for the determination of platelet-activating factor in human blood, *J. Chromatogr.* **433**:243–247.
 38. Caramelo, C., Fernandez-Gallardo, S., Marin-Cao, D., Inarrea, P., Santos, J. C., Lopez-Novoa, J. M., and Crespo, M. S., 1984, Presence of platelet-activating factor in blood from humans and experimental animals. Its absence in anephric individuals, *Biochem. Biophys. Res. Commun.* **120**:789–796.
 39. Grandel, K. E., Farr, R. S., Wanderer, A. A., Eisenstadt, T. C., and Wasserman, S. I., 1985, Association of platelet-activating factor with primary acquired cold urticaria, *N. Engl. J. Med.* **313**:405–409.
 40. Caramelo, C., Fernandez-Gallardo, S., Santos, J. C., Inarrea, P., Sanchez-Crespo, M., Lopez-Novoa, J. M., and Hernando, L., 1987, Increased levels of platelet-activating factor in blood from patients with cirrhosis of the liver, *Eur. J. Clin. Invest.* **17**:7–11.
 41. Sakaguchi, K., Masugi, F., Chen, Y.-H., Inoue, M., Ogihara, T., Yamada, K., and Yamatsu, I., 1989, Direct evidence of elevated levels of circulating platelet-activating factor in a patient with disseminated intravascular coagulation syndrome, *J. Lipid Med.* **1**:171–173.

42. Lazanas, M., Demopoulos, C. A., Tournis, S., Koussissis, S., Labrakis-Lazanas, K., and Tsarouhas, X., 1988, *Arch. Dermatol. Res.* **280**:124–126.
43. Diez, F. L., Nieto, M. L., Fernandez-Gallardo, S., Gijon, M. A., and Crespo, M. S., 1989, Occupancy of platelet receptors for platelet-activating factor in patients with septicemia, *J. Clin. Invest.* **83**:1733–1740.
44. Camussi, G., Pawlowski, I., Saunders, R., Brentjens, J., and Andres, G., 1987, Receptor antagonist of platelet activating factor inhibits inflammatory injury induced by in situ formation of immune complexes in renal glomeruli and in the skin, *J. Lab. Clin. Med.* **110**:196–206.
45. Doebber, T. W., Wu, M. S., Robbins, J. C., Choy, B. M., Chang, M. N., and Shen, T. Y., 1985, Platelet activating factor (PAF) involvement in endotoxin-induced hypotension in rats. Studies with PAF-receptor antagonist Kadsurenone, *Biochem. Biophys. Res. Commun.* **127**:799–808.
46. Chang, S-W., Feddersen, C. O., Henson, P. M., and Voelkel, N. F., 1987, Platelet-activating factor mediates hemodynamic changes and lung injury in endotoxin-treated rats, *J. Clin. Invest.* **79**:1498–1509.
47. Billah, M. M., and Johnston, J. M., 1983, Identification of phospholipid platelet-activating factor (1-O-alkyl-2-acetyl-sn-glycero-3-phosphocholine) in human amniotic fluid and urine, *Boichem. Biophys. Res. Commun.* **113**:51–58.
48. Stenton, S. C., Court, E. N., Kingston, W. P., Goadby, P., Kelly, C. A., Duddridge, M., Ward, C., Hendrick, D. J., and Walters, E. H., 1990, Platelet-activating factor in bronchoalveolar lavage fluid from asthmatic subjects, *Eur. Respir. J.* **3**:408–413.
49. Horii, T., Okazaki, H., Kino, M., Kobayashi, Y., Satouchi, K., and Saito, K., 1991, Platelet-activating factor detected in bronchoalveolar lavage fluids from an asthmatic patient, *Lipids* **26**:1292–1296.
50. Ardit, M., Manogue, K. R., Caplan, M., and Yogev, R., 1990, Cerebrospinal fluid cachectin/tumor necrosis factor- α and platelet-activating factor concentrations and severity of bacterial meningitis in children, *J. Infect. Dis.* **162**:139–147.
51. Oda, M., Satouchi, K., Ikeda, I., Sakakura, M., Yasunaga, K., and Saito, K., 1990, The presence of platelet-activating factor associated with eosinophil and/or neutrophil accumulations in the pleural fluids, *Am. Rev. Respir. Dis.* **141**:1469–1473.
52. Christman, B. W., and Blair, I. A., 1989, Analysis of platelet activating factor in human saliva by gas chromatography/mass spectrometry, *Biomed. Environ. Mass Spectrom.* **18**:258–264.
53. Sanchez-Crespo, M., Inarrea, P., Alvarez, V., Alonso, F., Egido, J., and Hernando, L., 1983, Presence in normal human urine of a hypotensive and platelet-activating phospholipid, *Am. J. Physiol.* **244**:F706–F711.
54. Ikeda, I., Oda, M., Sakakura, M., and Yasunaga, K., 1991, Presence of platelet-activating factor in pyuria in humans, *Lipids* **26**:1333–1335.
55. Minhas, B. S., Robertson, J. L., Kumar, R., Dodson, M. G., and Ricker, D. D., 1991, The presence of platelet-activating factor-like activity in human spermatozoa, *Fertil. Steril.* **55**:372–376.
56. Parks, J. E., Hough, S., and Elrod, C., 1990, Platelet activating factor activity in the phospholipids of bovine spermatozoa, *Biol. Reprod.* **43**:806–811.
57. Kumar, R., Harper, M. J. K., and Hanahan, D. J., 1988, Occurrence of platelet-activating factor in rabbit spermatozoa, *Arch. Biochem. Biophys.* **260**:497–502.
58. Pitton, C., Lanson, M., Besson, P., Fetissoff, F., Lansac, J., Benveniste, J., and Bougnoux, P., 1989, Presence of PAF-acether in human breast carcinoma: Relation to axillary lymph node metastasis, *J. Natl. Cancer Inst.* **81**:1298–1302.
59. Mallet, A. I., and Cunningham, F. M., 1985, Structural identification of platelet-activating factor in psoriatic scale, *Biochem. Biophys. Res. Commun.* **126**:192–198.

60. Salem, P., Denizot, Y., Pitton, C., Dulioust, A., Bossant, M.-J., Benveniste, J., and Thomas Y., 1989, Presence of PAF-acether in human thymus, *FEBS* **257**:49–51.
61. Annable, C. R., McManus, L. M., Carey, K. D., and Pinckard, R. N., 1985, Isolation of platelet-activating factor (PAF) from ischemic baboon myocardium, *Fed. Proc.* **44**:1271.
62. Tokumura, A., Kamiyasu, K., Takauchi, K., and Tsukatani, H., 1987, Evidence for existence of various homologues and analogues of platelet activating factor in a lipid extract of bovine brain, *Biochem. Biophys. Res. Commun.* **145**:415–425.
63. Calignano, A., Cirino, G., Meli, R., and Persico, P., 1988, Isolation and identification of platelet-activating factor in UV-irradiated guinea pig skin, *J. Pharmacol. Methods* **19**:89–91.
64. Angle, M. J., Jones, M. A., McManus, L. M., Pinckard, R. N., and Harper, M. J. K., 1988, Platelet-activating factor in the rabbit uterus during early pregnancy, *J. Reprod. Fert.* **83**:711–722.
65. Hwang, S., Lam, M.-H., Li, C.-L., and Shen T.-Y., 1986, Release of platelet activating factor and its involvement in the first phase of carrageenin-induced rat foot edema, *Eur. J. Pharmacol.* **120**:33–41.

Index

- Acetic acid, 39, 191
Acetoacetate, 267, 271, 272, 277, 279, 282, 291
 levels in amino acid disorders, 281
Acetoacetyl CoA thiolase, 282
Acetonitrile, 54, 85, 140
 as liquid sheath solvent for electrospray source, 39
Acetyl CoA, 272, 274, 275, 277, 278, 279, 285, 288
 metabolism, 286
N-Acetylaspartylglutamate (NAAG), 184
Acetylcholine, 100, 167, 168, 169, 171, 173, 175, 183
 biological activity, 181
 MS detection, 189–190
 receptors, 100
Acetylcholinesterase, 169, 173, 189
N-Acetyltyrosine, 267, 268
Acyl CoA, 275, 279
Acyl CoA dehydrogenase
 deficiency, 293
Acyl CoA synthetase
 role in β -oxidation, 300
Acylcarnitine translocase, 300
Acylcarnitines, 299, 301, 302
 detection, 303, 305–315
Adenosylcobalamin synthesis
 deficiency, 288
Adipate, 284, 289, 291
Adrenalin, 167
Adrenocorticotrophic hormone (ACTH), 137, 155, 161, 177
Aeroelectrospray (AES) ionization, 5
Aerospray (AS) ionization, 4, 5, 6
Alanine, 270, 274, 275, 278
Alcaptonuria, 262, 270–271
Alloisoleucine, 273
Alzheimer disease, 180
Amino acid analysis
 detection methods,
 GC/MS, 260, 273, 275, 278
 MS detection, 190–191
Amino acids
 function as neurotransmitters, 171, 173, 180
 metabolic disorders affecting, 259, 260, 262–289
 γ -Aminobutyric acid (GABA), 175, 180, 182, 183, 190
 δ -Aminolevulinate, 270
 α -Amylase
 ES mass spectra, 15, 25
Arachidonic acid, 321, 339
Arginine, 45, 47, 60, 64, 77
 ES mass spectrometry of compounds containing, 19
 proton affinities, 67, 72
Arthropathy, 270
Ascorbate, 265, 269
Asparagine, 47, 60, 63, 79
Aspartate, 60
 function as neurotransmitters, 171, 173, 180
Atmospheric pressure ion evaporation (APIE), 6; *see also* Aerospray ionization
Atracurium besylate, 109, 116
Atrial natriuretic factors, 184
Azelate, 285
Basophils, 181, 319
Betaine, 190
Bile, 103, 271
Bile acids, 234
Bilirubin, 49
Biopterin, 264, 265
Biopterine, 263
Biotin, 278
Biotin-dependent carboxylase deficiency, 283, 284, 285, 291, 292, 293

- Biotinidase
 deficiency, 291, 292, 293
- Branched-chain keto acid dehydrogenase complex, 275, 276, 278
- Butane-1,4-diol succinate (BDS), 262
- Butanone, 281
- Calcitonin, 184
- Calcitonin-gene related peptide (CGRP), 184
- Cannabichromene (CBC), 215, 244–247
- Cannabidiol (CBD), 207, 214, 217, 219, 223
 fragmentation, 218, 219
 metabolism, 240–243
- Cannabinoids, 207, 209, 220
 fragmentation, 211, 216
 GC/MS analysis, 210, 216–219, 225, 241, 253
 GLC analysis, 210, 216, 226, 234, 237, 238
 mass spectra, 221, 222
 structure, 208–209
- Cannabinol (CBN), 207, 223
 mass spectrum, 213
 metabolism, 242–244, 250
- Capillary electrophoresis (CE), 39, 85, 91, 129
- Capillary electrophoresis-mass spectrometry (CE-MS), 41
 interface design, 85
- Capillary electrophoresis-MS/MS, 86, 91
- Capillary isotachopheresis (CITP), 86, 88
- Capillary isotachopheresis/ESI-MS, 88, 90
- Capillary isotachopheresis-MS, 86, 88, 90
- Capillary zone electrophoresis (CZE), 12, 30, 86, 89, 90
 neurotransmitter detection by, 185
- Capillary zone electrophoresis-ESI-MS, 87, 90
- Capillary zone electrophoresis-MS, 86, 87, 88, 89
- Carbamazepine, 101
- β -Carboline, 196
- Carboxypeptidase B, 155–156
- Carnitine
 biochemical functions, 299, 301
 deficiency, 301–302
 detection
 enzymatic, 302–303, 312, 315
 GC/CIMS, 307
 GC/MS, 307, 314
 HPLC, 305–307
 LC/MS, 305, 306, 312
 mass spectrometry, 299, 302
- Carnitine (*cont.*)
 detection (*cont.*)
 PCR-based DNA tests, 312
 tandem mass spectrometry, 303–305, 308–315
- Carnitine acetyltransferase, 302, 305
- Carnitine acyltransferase (CAT), 299, 300, 301
- Carnitine palmitoyl transferase (CPT), 299, 311; *see also* CAT
- Catechol, 187, 192
- Catecholamines, 168, 169, 171, 173, 174, 177, 182, 183, 194, 265
 biological activity, 181
 detection methods, 177, 187, 191, 192
 MS detection, 187–189, 191
- Charged “residue model” (CRM), 2, 19, 22
- Chemical ionization (CI), 186
 mass spectrometry, 103–129, 249, 307
 direct insert probe, 113
 of neuromuscular blocking agents, 127
- Cholecystokinin, 171, 177, 184
- Cholesterol, 224
 synthesis, 282
- Choline, 190
 MS detection, 189
- Choline glycerophospholipids, 339
- Choline oxidase, 189
- Cholinesterase, 194
- Coenzyme Q, 293
- Coenzyme A thioesters
 role in β -oxidation, 299, 300, 301; *see also* Acyl CoA
- Collision-induced dissociation (CID), 59, 64, 303, 309, 322
 role of Coulombic forces in, 72, 82
 spectra, 57
 for melittin, 65, 66, 67, 68, 69
 for ribonuclease A, 73
 for serum albumins, 82, 83
- Collision-induced dissociation (CID)-tandem mass spectra, 70
- Computerized tomography, 278
- Conalbumin
 ES mass spectra for, 15, 25
- Continuous-flow fast atom bombardment/mass spectrometry (CFFAB-MS), 122, 124, 125, 126
 interface on triple quadrupole MS, 85, 86
- Corona, 11, 41
- Corticotropin releasing factor (CRF), 184

- Corticotropin-like intermediate peptide (CLIP), 137
- Creatinine, 261, 281, 290
- Curare, 99
- Cushing's disease, 155
- Cyclosporin A, 19
- Cysteine, 45, 46, 47, 53, 61
- Cytochrome C, 45, 48, 54, 57, 59, 87
 ES mass spectrum, 28
- Cytochrome-P450, 219
- Decamethonium, 99
- Dehydropiperazine, 105
- Dehydropiperidine, 105, 111
- Delta sleep factor, 184
- Diazepam binding inhibitor (DBI), 184
- Diazomethane, 225, 242, 251
- Diethyl ether, 261, 293
- Dihydrobiopterin, 265, 266
- Dihydrolipoyl dehydrogenase (E_3)
 deficiency, 271, 272, 273, 274, 275–278
- Dihydropteridine reductase, 265–266
- Dihydropterin synthetase
 deficiency, 263
- Dimethylsulfoxide, 339
- Direct insert probe CI mass spectrometry, 113
- Dithioerythritol (DTE), 142
- Dithiothreitol (DTT), 45, 46, 47, 53, 142
- l-dopa, 265
- Dopamine, 171, 174, 180, 181, 182, 183, 265, 266
- Dynorphin, 159, 180
- Electrohydrodynamic (EH) ionization, 4
- Electron capture ionization, 191, 196
- Electron impact ionization, 191, 192, 196, 197
- Electron transferring flavoprotein (EFT), 293
- Electrospray, 1, 2, 8; *see also* Electrospray ionization
- Electrospray ionization (ESI), 1, 18, 19, 41, 127, 135, 185
 as ionization method for mass spectrometry, 1, 2, 3–6, 8
 efficiency, 14–16
 factors affecting charge state distribution, 56
 negative-ion mode, 41
 positive-ion mode, 39, 41
 source, 39–41
 operation of, in combination with atmospheric vacuum interface, 41–43
- Electrospray ionization-mass spectrometry (ESI-MS), 1, 2, 7, 16, 17, 19, 37, 84, 151–152
 charged droplet formation, 8–13, 32
 combination with ion-trap mass analysis, 26
 combination with liquid chromatography, 38, 199
 coupling with high-resolution capillary electrophoresis, 39–41
 detection of,
 neuromuscular blocking agents, 127
 neuropeptides, 138, 159
 interpretation of mass spectra, 15, 26–30, 32
 mechanisms of ion formation, 19–20
 molecular weight determinations using, 43–64
 multiple charging, 13–14, 24, 32, 38, 57, 59
 negative-ion spectra of proteins, 56, 57, 58–64
 of biomolecules, 3, 19, 38, 63, 91
 operational conditions, 1, 5, 6–7, 30–32
 positive-ion spectra of proteins, 45–52, 56, 60, 64
 process, 7–30
 sensitivity, 18–19
- ESI-tandem mass spectrometry (ESI-MS/MS), 9, 64–90, 129, 152, 161
- β -Endorphin (BE), 134, 137, 138, 143, 144, 148–150, 154, 156, 161, 182
 EI-MS, 151, 152, 156, 158, 159
 FAB-MS, 154, 155
 MS/MS detection, 134
- Enkephalin, 169, 180
- Enoyl hydratase, 283
- Epinephrine, 168, 177, 183
 biological activity, 181
 metabolites, 187, 188
- Estradiol, 335
- Ethyl acetate, 261, 293
- Ethylhydraclrylate, 274, 277, 281
- Ethylmalonate, 289
- Fanconi syndrome, 269
- Fast atom bombardment (FAB), 3, 19, 29
 of neuromuscular blocking agents, 103, 109–111, 127, 129
 of neuropeptides, 141–142

- Fast atom bombardment mass spectrometry (FAB-MS), 122, 154, 155, 197; *see also* Continuous-flow fast atom bombardment/mass spectrometry (CFFAB-MS)
- continuous flow for LC-MS, 305, 306, 314
 - detection of,
 - carnitines, 302, 303, 305–308, 310–312, 314, 315
 - neuropeptides, 153, 161, 177
- Fast atom bombardment mass spectrometry–mass spectrometry (FAB/MS-MS), 129
- Fast ion bombardment (FIB), 3, 6; *see also* secondary ion mass spectrometry
- Fatty acids, 49, 279
- biodegradation, 282
 - inherited disorders, 301
 - metabolic disorders affecting, 259
 - β-oxidation, 278, 299
 - role of acetoacetyl CoA in biosynthesis of, 282
- Field desorption (FD) ionization, 4
- Fourier-transform ion cyclotron resonance (FTICR), 16, 26, 32, 43, 45, 84
- Fumarate, 267, 277
- Fumarylacetoacetate, 267, 269, 270
- Fumarylacetoacetate hydrolase, 267, 269
- Galanin, 184
- Gas chromatography (GC), 102
- diagnostic applications, 260, 261
- Gas chromatography-EIMS, 323, 324–326
- for detection of MPTP, 178
- Gas chromatography-MS, 307, 314
- carnitine detection by, 307, 314
 - diagnostic applications, 260, 261, 271, 272, 273, 275, 278, 285
 - metabolic disorder diagnosis by, 259, 278–282, 293
 - neurotransmitter detection by, 179, 185–187, 189, 191, 194, 196, 199
- Gas chromatography/electron capture MS, 189, 193
- Gas chromatography-NICI (negative-ion chemical ionization), 322, 336
- Gel filtration, 224
- Gel electrophoresis, 29, 45
- Glucagon, 177
- Glucuronides, 219, 224, 242
- Glutaconate, 289
- Glutamate, 46, 60, 63, 175, 274, 275, 278
- function as neurotransmitters, 171, 173, 180, 183
 - proton affinities, 67, 72
- Glutarate, 289
- Glutaric aciduria, 288, 289, 293
- Glutaric acidemia type II, 289–290
- Glutathione conjugates, 224, 238
- O-Glycanase, 52
- Glycans, 49
- Glycerol, 142, 147
- Glycerophospholipids, 320, 321, 335
- Glycine, 270, 278
- function as neurotransmitters, 171, 173, 180
- Glycoproteins, 29
- structural analysis, 51
- N-Glycosidase F (PNGase F), 52
- Gonadotropin-releasing hormone, 184
- Gramicidin S
- ESMS, 16, 17, 19
- Growth hormone-releasing hormone, 184
- Guam dementia complex, 179
- Guthrie test
- for neonatal screening, 276, 302, 312, 314
- Hemoglobin, 48, 51, 271
- Hereditary tyrosinemia, 268, 269–270
- High performance liquid chromatography (HPLC), 30, 103, 106, 113, 190, 191, 199, 305–307
- reverse phase, 135, 138, 139, 140–141, 142, 152, 160, 187, 305
 - elution methods, 135, 138, 141
- HPLC with electrochemical detection (HPLC/EC), 187, 192
- Higher-order mass spectrometry, 43
- Higher-order Tyndall spectra (HOTS), 11
- Histamine, 169
- biological activity, 181
 - detection, 191
 - metabolites, 192
- Histidine, 45, 60, 77, 79
- proton affinities, 67
- Holocarboxylase synthetase, 291, 292
- Homogentisate, 262, 267, 269, 270
- identification by GC/MS, 271
- Homogentisic acid oxidase, 267

- Human growth hormone, 45, 51
Human FK binding protein, 57
Huntington's chorea, 180
 β -Hydroxyisobutyryl-CoA deacylase deficiency, 271
p-Hydroxyphenyllactate, 262, 267, 268, 270
p-Hydroxyphenylpyruvate (p-HPPA), 267, 268, 270
p-Hydroxyphenylpyruvate (p-HPPA) oxidase, 268, 269, 270
p-Hydroxyphenylpyruvate (p-HPPA) oxygenase, 262
3-Hydroxypropionate, 282, 285, 290
 as a marker for propionic acidemia, 288
3-Hydroxyvalerate, 285, 286, 288, 290
- Immunosuppressant FK 506, 57
Indoleamines, 183, 192, 194, 196
 MS detection, 187–189
Inositol phospholipids, 335
Insulin, 56, 60, 184
 ESI mass spectra, 15, 25, 58, 62
 γ -Interferon, 51
Interleukin-2, 51
Ion evaporation model (IEM)
 for ion formation, 2, 4, 20
Ion trap mass spectrometers (ITMS), 64, 72, 84, 85, 86
Ionspray technique (IS), 5, 12
Isobutyryl CoA, 274, 275, 278
Isoleucine, 271–275, 278, 284
 catabolism, abnormality in, 281, 282
Isotope doublet technique, 226
Isovaleric acidemia, 260, 271, 278–280
Isovaleryl CoA, 274, 275, 278, 279
Isovaleryl-CoA dehydrogenase, 278, 279
Isovalerylglycine, 279, 280
 mass spectra, 280
- α -Keto acid dehydrogenase complex, 273
Ketoacidosis, 280, 281, 285, 288, 290
Ketoaciduria, 272; *see also* Maple syrup urine disease
Ketoglutarate, 263, 274, 277
Ketoglutarate dehydrogenase complex, 275, 276
 β -Ketoacyl CoA, 282
 β -Ketothiolase, 281–283
 deficiency, 272, 305
- Ketone bodies, 282, 283, 286
Ketosis, 277
Ketotic hyperglycinuria, 288; *see also* Propionic acidemia
- α -Lactalbumin, 45, 46
 ESI-MS, 46
Lactate, 274, 275, 276, 277
 catabolic intermediates of, 286
 levels in amino acid disorders, 284, 291
Lactate dehydrogenase, 48
Lactic acidemia, 278
Lactic acidosis, 274, 290, 291
 incidence, 260
Laser desorption (LD), 1, 3, 12, 26
Laser desorption-MS, 29
Laser desorption (LD) ionization, 33
Leigh's syndrome, 278
Leucine, 270, 271, 272, 274, 275, 276, 278, 284
 catabolic intermediates, 286
Leucine enkephalin, 156, 157, 159, 175
Leukotrienes, 335
Leuteinizing hormone-releasing hormone (LHRH), 184
Lipoic acid, 278
Liquid secondary ion mass spectrometry (LSIMS), 3
Liquid chromatography (LC), 7, 12, 85, 91;
 see also High performance liquid chromatography
 interface with mass spectrometers using ESI, 85, 86
Liquid chromatography (LC)-MS
 cannabinoid detection, 252
 carnitine detection, 305, 306, 312
 moving-belt LC/MS, 119, 123, 129
 neurotransmitter detection by, 185
 organic aciduria detection by, 260
 packed capillary LC, coupled to MS, 86
 protein separation, 86
Lithium aluminium deuteride, 227–228
Long-chain acyl CoA dehydrogenase (LCAD), 300
Lysine, 45, 46, 47, 60, 64, 67, 72
 multiple charging, 77
Lysozyme, 37, 54, 57, 58
 ES mass spectra for, 15, 25
 multiple charging, 38

- Magnetic sector analyzers, 3, 25, 32, 38
- Maple syrup urine disease (MSUD), 271, 272–274, 275, 276, 277, 278, 314
- Mass spectrometry (MS), 85, 136, 190, 213, 221, 222, 280, 323
- carnitine detection, 299, 302
 - catecholamine detection, 187–189, 191
 - neuropeptide detection, 140
 - quadrupole: *see* quadrupole mass spectrometers
 - sequence determination by, 134, 135, 137, 138, 139, 142
- Mass spectrometers, time-of-flight (TOF) instruments, 26, 32
- Matrix-assisted laser desorption/ionization (MALDI), 38, 60
- Medium-chain acyl CoA dehydrogenase (MCAD), 300, 306, 307, 310
- Melanin, 264
- Melanocyte-stimulating hormone (MSH), 137
- Melatonin, 182, 183, 188, 189
- Melittin
- CID spectra for, 65, 66, 67, 68, 69
 - ESI-MS/MS for, 64–72
- Meperidine, 178
- Messenger RNA
- for neurotransmitter biosynthesis, 182–183
 - measurements, for peptide detection, 136, 140
- Metastable ion monitoring, 251
- Methanol, 41, 142
- as liquid sheath solvent for electrospray source, 39
- Methionine enkephalin (ME), 134, 136, 148, 156, 160, 161, 175
- EI-MS, 151, 153
 - ES-MS, 156, 159
 - FAB-MS, 134, 142, 143, 145, 153, 154, 155
 - fragmentation pattern, 148
- Methionine, 270, 284
- metabolism, 269
- 3-Methoxy-4-hydroxyphenylethylene glycol (MHPG), 187, 188, 189
- Methoxyethanol
- as liquid sheath solvent for electrospray source, 39, 41
- 1-Methyl-4-phenyl-1,2,3,6-tetrahydropyridine (MPTP), 178, 179
- β -N-Methylamino-L-alanine (BMAA), 179, 180
- Methylcitrate, 282, 283, 285, 286, 290
- as a marker for propionic acidemia, 288
- Methylcobalamine synthesis
- deficiency, 288
- 3-Methylcrotonyl CoA carboxylase, 283, 284, 290, 291
- deficiency, 283–284
- 3-Methylcrotonylglycine, 284, 290, 291
- mass spectrum, 283
- β -Methylglutaconyl-CoA, 271, 291
- Methylglutaconyl-CoA hydratase, 278, 284
- deficiency, 271
- Methylmalonic acidemia, 271, 272, 285, 286, 288–289, 293
- Methylmalonyl CoA, 271, 272, 284, 291
- Methylmalonyl CoA mutase, 285
- Methylpentafluoropropionyl derivatives, 193–194
- Metocurine, 100, 101, 103, 106, 107, 114, 115
- Mixed function oxidase, 209, 210, 263
- Monoamine oxidase, 194
- Morphinan, 183
- MS detection, 194–196
- Morphine, 183, 186, 187, 194
- Multiple carboxylase deficiency, 284, 290–292, 293
- Multiple reaction monitoring (MRM), 134, 135, 144
- for neuropeptide detection, 145, 151, 152, 154, 155, 156, 161
- Myoglobin, 16, 45, 48, 56, 87, 271
- negative-ion ESI spectrum, 57, 60
- Neuraminidase, 52
- Neurokinin, 184
- Neuromedin K, 184
- Neuromuscular blocking agents
- analytical methods for evaluation, 102–103
 - competitive, 99, 100
 - mass spectrometric techniques, 103–127
- Neuropeptide Y, 173, 174, 180, 182, 184
- Neuropeptides, 133, 168, 169, 173, 176, 182
- post-translational modification, 198
- Neurotensin, 173, 184
- Neurotransmitters, 172–180
- biological function, 168–171

- Neurotransmitters (*cont.*)
 chemical characterization, 181–182
 MS characterization, 183–199
- Nitric oxide, 182
- 3-Nitrobenzylalcohol (NBA), 142
- Norepinephrine, 167, 168, 174, 177, 182,
 183, 265, 266
 biological activity, 181
 metabolites, 187, 188
- Nuclear magnetic resonance
 carnitine detection by, 315
 of neurotransmitters, 185
 protein conformational changes, determina-
 tion of, 52, 185, 315
- Ochronosis, 270
- Octopamine, 183, 192, 193
- Opioid peptides, 134, 156, 184
- Oregon type tyrosinemia: *see* Tyrosinemia type II
- Ovalbumin, 51
- Oxaloacetate, 274, 285, 286, 291
- β -Oxidation, 278, 282, 300
 of cannabinoids, 219, 242
 role of Acyl CoA in, 299, 300, 301
 role of carnitine in, 299
- 2-Oxoglutarate dehydrogenase complex, 272,
 275, 277
- Oxygen
 as a scavenger of free electrons, 11
- Oxytocin, 184
- Pancuronium, 99, 100, 101, 103–111, 114,
 122, 124
 CFFAB spectra, 125, 127
 CI fragmentation, 110, 117
 ESI-MS spectra, 128, 129
 FAB spectra, 118, 119, 120, 121
- Parkinson disease, 177, 178, 179
- Parkinsonism-dementia complex, 179
- Peptide mapping
 by LC/MS/MS, 52
- Pernicious anemia, 288
- β -Phenethylamine, 183, 192, 193
- Phenylalanine, 262, 267
 levels in metabolic disorders, 263–265, 266
 268
 metabolism, 263
- Phenylalanine hydroxylase, 263, 265
- Phenylketonuria (PKU), 262–265, 302, 312,
 314
 incidence, 264
- Phenyllactate, 262, 263, 264, 265
- Phenylpyruvate, 262, 263, 264, 265
- Phenytol, 100, 103
- Phosphocholine, 323
- Phosphoenolpyruvate, 274
- Phospholipase A₂, 320, 321
- Phospholipase C, 321, 323
- Phospholipase D, 321
- Pimelate, 285
- Pipecuronium bromide, 105, 113
- Piperidine, 105, 111
- Plasma desorption-time-of-flight mass spec-
 trometry (PD-TOF-MS), 191
- Plasma desorption (PD), 3, 19, 60
- Platelet-activating factor (PAF), 319
 biological activities, 319, 320, 335, 339
 detection methods
 biological, 322
 column chromatography, 333, 334
 FAB-MS, 322, 323, 327–328, 329, 330,
 331
 GC/MS, 322, 323–327, 338
 HPLC, 333, 334
 mass spectrometry, 321–332
 MS/MS, 322, 328–332
 inhibitors, 319
- Poly (ethylene glycols) (PEGs), 3, 14, 18, 21,
 38
- Polystyrene sulfonates, 60
- Porphobilinogen synthetase, 270
- Porphyryns, 271
- Product-ion spectra, 142, 143, 145
 of enkephalins, 146, 147, 149, 150
- Proenkephalin A, 133, 154, 161
- Proinsulin, 46, 52
 ESI-MS spectra, 46
- Prolactin, 155, 161, 181
- Proline, 66, 67, 270, 274, 278
- Proopiomelanocortin (POMC) neuropeptide
 system, 133, 134, 136, 137, 140, 154,
 155, 161
- Propionic acidemia, 271, 272, 282, 284–288,
 293, 314
- Propionyl CoA, 271, 272, 284, 285, 286, 291
 carboxylation, 289
 β -oxidation, 285, 286

- Propionyl CoA carboxylase (PCC), 284, 285, 290, 291
- Prostaglandins, 335
metabolic disorders affecting, 259
- Protoporphyrin IX heme cofactor, 60
- Pyroglutamic acid, 198
- Pyruvate, 274, 275, 291
- Pyruvate carboxylase, 274, 290
- Pyruvate decarboxylase, 264
- Pyruvate dehydrogenase (PDH) kinase, 274
- Pyruvate dehydrogenase (PDH) complex, 272, 274, 275, 276, 277, 278
- Pyruvate phosphate decarboxylase, 274
- Pyruvate phosphate phosphatase, 274
- Quadrupole analyzers
low resolution, 45
- Quadrupole mass spectrometers, 5, 38, 42; *see also* Triplequadrupole mass spectrometers
- Quadrupole ion-trap MS (ITMS), 26, 43, 64, 72, 84, 85
- Quadrupole mass filter, 3, 24, 32
- Quinones, 18
- Radioimmunoassays (RIA), 103
neuropeptide detection using, 135, 136, 139, 140, 160, 176
neurotransmitter detection using, 185, 189, 191, 196
scintillation proximity radioimmunoassay (SPRIA), 322
- Radioisotopic exchange assay (REA), 303
- Rayleigh limit, 6, 8, 11, 42
- Receptor assay (RRA)
for neuropeptides, 135, 136, 139, 140
- Reconstituted ion current chromatogram (RIC), 276, 277, 288, 289
- Retro-Diels-Alder fragmentation, 211, 214, 215, 236, 240, 242
- Reversed-phase high-performance-LC: *see* High performance liquid chromatography, reverse phase
- Reversed-phase ion pair chromatography, 103
- Riboflavin, 278
- Ribonuclease A, 73–76
CID product ion mass spectra, 73, 76
ESI mass spectra of, 73, 75
MS/MS spectra of, 74, 75
- Ribonuclease B, 51
- Sebacate, 284, 289
- Secondary lactic acidosis, 272
- Secondary-ion mass spectrometry (SIMS), 6, 141, 173
- Secretin, 184
- Selected ion monitoring (SIM), 117, 122, 127, 134, 135, 192
for PAF detection, 322, 324–327
- Sepsis neonatorum, 273
- Serotonin, 168, 169, 171, 173, 174, 182, 183, 194, 265, 266
biological activity, 181
detection, 177, 187, 191, 192
- Serum albumins, 76–84
CID mass spectra of, 82, 83
CID interfaced with MS/MS, 77, 80
ESI-MS, 49, 53, 63, 76, 78, 79, 82–84
HPLC analysis, 79
tandem MS, 80, 81
- Short-chain acyl CoA dehydrogenase (SCAD), 300
- Sleep-promoting factor (FSu), 184
- Solid probe electron-impact mass spectrometry, 186
- Somatostatin, 177, 180, 184
- Stable isotope labeling, 224, 227, 250, 253
- Steroids
acetoacetyl CoA in biosynthesis, 282
metabolic disorders affecting, 259
- Suberate, 284, 289
- Substance K, 184
- Substance P, 169, 171, 180, 184
- Succinyl CoA, 271, 274, 275, 285
- Sulfur hexafluoride
as a scavenger of free electrons, 11, 41
- Sympathin, 168
- Synephrine, 192, 193
- Tachykinins (SP), 153, 155
- Tandem mass spectrometry (MS/MS), 5, 37, 43, 64, 70, 80, 81, 86, 134
capillary electrophoresis/MS-MS: *see* Capillary electrophoresis/MS-MS
carnitine detection using, 303–305, 307, 308–31
CID/MS-MS: *see* Collision-induced dissociation-tandem mass spectra
ESI/MS-MS: *see* ESI-tandem mass spectrometry

- Tandem mass spectrometry (MS/MS) (*cont.*)
 neuromuscular blocking agents, detection of,
 using, 127, 128, 129
 neuropeptide detection using, 139, 141
 neurotransmitter detection using, 185, 186
 triple quadrupole: *see* Triple quadrupole tan-
 dem mass spectrometers
- Taurine
 function as neurotransmitter, 171, 180
- Taylor cones, 8, 9, 10
- Tetra- β -carboline
 MS detection, 194–196
- Tetrahydro- β -carbolines, 179, 183
- Tetrahydrobiopterin, 265, 266
- Tetrahydrocannabinol (THC), 207, 208, 211
 mass spectra, 212–213, 221, 222, 226, 228,
 233
 metabolism, 219, 224, 234–240, 247–
 250
 pharmacological effects, 207, 208
- Tetrahydroisoquinoline (TIQ) alkaloids
 MS detection, 194–196
- Tetrahydropteridine reductase, 265–266
- Thebaine, 183, 194
- Thermally induced dissociation (TID), 66–67
 of melittin, 71
- Thermospray (TS) ionization, 4, 5, 6, 7, 41,
 305
- Thiamine, 278
- Thioesterase II, 51
- Thioredoxin, 44
- Threonine, 270, 284
- Thyrotropin-releasing hormone (TRH), 136,
 169, 182, 184
- Tiglylglycine, 281, 282, 290
- Total-ion chromatograms, 233, 234
- Trace amines
 function as neurotransmitters, 191–194
- Transacetylase, 320
- Transfer RNA, 60
- Transferrin, 51
- Transient neonatal tyrosinemia, 268–269
- Trifluoroacetic acid, 12, 85, 186, 187
- Triple quadrupole mass spectrometers, 85, 86,
 87
- Triple quadrupole tandem mass spectrometer,
 303, 304, 309, 315
- Triple sector quadrupole (TSQ) MS/MS, 151
- Trypsin, 51, 155
- Tryptamine, 183, 192, 193, 194
- Tryptophan
 proton affinities, 67, 72
- Tryptophan hydroxylase, 265
- d*-Tubocurarine, 99, 100, 103
- Tyramine, 183, 267
- Tyrosine, 61, 262, 263, 270
 depressed levels in PKU, 264, 265
 disorders in metabolism, 267–271
- Tyrosine aminotransferase (TAT), 267, 268,
 270
- Tyrosine oxidase, 264
- Tyrosine transaminase, 263
 deficiency, 268
- Tyrosinemia, 262, 314
 type I, 268; *see also* Hereditary tyrosinemia
 type II, 268
 type III, 268, 270
- Ubiquitin, 54
 ESI mass spectra, 55
- Urea, 291
- Valine, 271, 272, 274, 275, 276, 278, 284
- Valproic acid, 301
- Vasoactive intestinal polypeptide (VIP), 171,
 177, 184
- Vasopressin, 184
- Vecuronium, 99, 100–104, 106, 107, 109,
 110, 122
 CFFAB spectra, 125, 126
 CI fragmentation, 112, 114
 ESI-mass spectra, 128
 FAB spectra, 118, 119
- Vitamins
 metabolic disorders affecting, 259
- X-ray crystallography, 52, 137
- Xenon, 142
- Zein, 37